

SMTDA 2010

**International Conference on
Stochastic Modeling Techniques and Data Analysis**

8 - 11 of June 2010 Chania Crete Greece

Proceedings



<http://www.smta.net>

Long memory based approximation of filtering in non linear switching systems

Noufel Abbassi and Wojciech Pieczynski

CITI Department, CNRS UMR 5157, Telecom SudParis,
Evry, France
e-mail : Wojciech.Pieczynskii@it-sudparis.eu
e-mail : Noufel.Abbassi@it-sudparis.eu

Abstract: In this paper we consider conditionally Gaussian state space models with Markovian switches and we propose a new method of approximating the optimal solution by the use of Markov chains hidden with long memory noise. We show through experiments that our method can be more efficient than the classical particle filter based approximation.
Keywords: Conditionally Gaussian state space model, Markov switching, Markov chains hidden with long memory noise, Expectation-Maximization, Iterative conditional estimation.

1 Introduction

Let $X_1^N = (X_1, \dots, X_N)$, $R_1^N = (R_1, \dots, R_N)$ and $Y_1^N = (Y_1, \dots, Y_N)$ be three sequences of random variables. Each X_n and Y_n take their values from \mathbb{R} , while each R_n takes its values from a finite set of switches $\Omega = \{\omega_1, \dots, \omega_K\}$. The sequences X_1^N and R_1^N are hidden and the sequence Y_1^N is observed. For each $n = 1, \dots, N$ we will denote by $p(r_n | y_1^n)$ the distribution of R_n conditional on $Y_1^n = y_1^n$, and we will denote by $E[X_n | r_n, y_1^n]$ the expectation of X_n conditional on $(R_n, Y_1^n) = (r_n, y_1^n)$. We deal with the classical problem of filtering, which consists of computation of $p(r_{n+1} | y_1^{n+1})$ and $E[X_{n+1} | r_{n+1}, y_1^{n+1}]$ with a reasonable complexity. We consider the following classical partly non linear model:

$$R_1^N \text{ is a Markov chain; } \quad (1.1)$$

$$X_{n+1} = F_n(R_{n+1})X_n + H_n(R_{n+1})W_{n+1} ; \text{ and } \quad (1.2)$$

$$Y_n = G_n(R_n, X_n) + K(R_n)Z_n. \quad (1.3)$$

where $X_1, W_2, \dots, W_N, V_1, \dots, V_N$ are independent Gaussian variables, and for each $n = 1, \dots, N$, $F_n(R_n)$, $H_n(R_n)$, $G_n(R_n)$, $K_n(R_n)$ are real numbers depending on switches. Such models are of interest in numerous situations (Cappe

et al. (2005), Costa et al. (2005), Zoeter and Heskes (2006)), among others. However, it has been well known since (Tugnait (1982)) that exact filtering and smoothing are not feasible with linear - or even polynomial - complexity in time in such models, and different approximations must be used. Many papers deal with this approximation problem and a rich bibliography can be seen in (Andrieu et al. (2003), Cappe et al. (2005), Costa et al. (2005), Zoeter and Heskes (2006)), among others.

The problem lies in the fact that the distribution of (R_1^N, Y_1^N) is not easy to manage and, in particular, does not allow one to compute the conditional probabilities $p(r_n | y_1^n)$ with a reasonable complexity. In fact, we have

$$p(x_{n+1}, r_{n+1} | y_1^{n+1}) = p(r_{n+1} | y_1^{n+1}) p(x_{n+1} | r_{n+1}, y_1^{n+1}), \quad (1.4)$$

where the probabilities $p(x_{n+1} | r_{n+1}, y_1^{n+1})$ can be recursively computed with a Kalman filter once they have been classically approximated by Gaussian densities, and the probabilities $p(r_{n+1} | y_1^{n+1})$ have to be approximated. Then they are approximated with different methods among which particle filtering is widely used (Andrieu et al. (2003)). The aim of this paper is to propose an alternate approximation of the distribution of (R_1^N, Y_1^N) based on the two following models. The first one is the very classical hidden Markov chain (HMM) model, in which $p(r_n | y_1^n)$ are computable with the classical recursive “forward” procedure. The second one is the recent Markov chain hidden with the long-memory noise (HMM-LMN) (Lanchantin et al. (2008)), in which $p(r_n | y_1^n)$ are computable too. In these two models we propose an original recursive parameter estimation method based on the general “Iterative Conditional Estimation” (ICE) procedure, which implies the possibility of partially unsupervised filtering.

Finally, we will consider the model (1.1)-(1.3) in which the distribution of (R_1^N, Y_1^N) will be approximated either by an HMM or an HMM-LMN distribution.

2 Filtering switches in hidden Markov models

Let (R_1^N, Y_1^N) be the classical HMM, whose distribution is of the form

$$p(r_1^N, y_1^N) = p(r_1) p(y_1 | r_1) \prod_{n=1}^{N-1} p(r_{n+1} | r_n) p(y_{n+1} | r_{n+1}). \quad (2.1)$$

The conditional probabilities $p(r_{n+1} | y_1^{n+1})$ are then computed from $p(r_n | y_1^n)$ by

$$p(r_{n+1}|y_1^{n+1}) = \frac{p(y_{n+1}|r_{n+1}) \sum_{r_n \in \Omega} p(r_{n+1}|r_n) p(r_n|y_1^n)}{\sum_{r_{n+1} \in \Omega} p(y_{n+1}|r_{n+1}) \sum_{r_n \in \Omega} p(r_{n+1}|r_n) p(r_n|y_1^n)} \quad (2.2)$$

Let us consider the following distribution, called a «partially» Markov distribution (Lanchantin et al. (2008)):

$$p(r, y) = p(r_1) p(y_1|r_1) \prod_{n=1}^{N-1} p(r_{n+1}|r_n) p(y_{n+1}|r_{n+1}, y_1^n) \quad (2.3)$$

One can see how the model (2.3) extends the classical HMM (2.1) : the former is obtained setting $p(y_{n+1}|r_{n+1}, y_1^n) = p(y_{n+1}|r_{n+1})$ in the latter. However, similarly to (2.2) one has

$$p(r_{n+1}|y_1^{n+1}) = \frac{p(y_{n+1}|r_{n+1}, y_1^n) \sum_{r_n \in \Omega} p(r_{n+1}|r_n) p(r_n|y_1^n)}{\sum_{r_{n+1} \in \Omega} p(y_{n+1}|r_{n+1}, y_1^n) [\sum_{r_n \in \Omega} p(r_{n+1}|r_n) p(r_n|y_1^n)]} \quad (2.4)$$

3 Parameter estimation

In the classical HMM with Gaussian noise the model parameters are usually estimated with the classical “Expectation-Maximization” (EM) algorithm. They can also be estimated by the “Iterative Conditional Estimation” (ICE) algorithm, which is another iterative parameter estimation method. For fixed N both EM and ICE provide a sequence of parameters $\theta^0, \theta^1, \dots, \theta^m$, where the vector of parameters θ contains the distribution of (R_1, R_2) , which defines the distribution of the stationary Markov chain R_1^N , K means and K variances defining the K Gaussian distributions $p(y_n|r_n = \omega_1), \dots, p(y_n|r_n = \omega_k)$, which are identical for each $n=1, \dots, N$.

ICE provides the next θ^{q+1} from the current θ^q and $y_1^N = (y_1, \dots, y_N)$. For $j, k=1, \dots, K$, let $p_{jk} = p(r_1 = \omega_j, r_2 = \omega_k)$ and let μ_j, σ_j^2 be the common mean and the variance of the Gaussian distributions $p(y_1|r_1 = \omega_j), \dots, p(y_N|r_N = \omega_j)$. The next values $p_{jk}^{q+1}, \mu_j^{q+1}, (\sigma_j^{q+1})^2$ are obtained from the current θ^q and $y_1^N = (y_1, \dots, y_N)$ in the following way. The parameters p_{jk}^{q+1} are given by

$$p_{jk}^{q+1} = \frac{1}{n} \sum_{r=1}^{n-1} p(r_i = \omega_j, r_{i+1} = \omega_k | y_1^n, \theta^q), \quad (3.1)$$

where $p(r_i = \omega_j, r_{i+1} = \omega_k | y_1^N, \theta^q)$ are classically computed with the “forward” and “backward” recursions. To obtain μ_j^{q+1} , $(\sigma_j^{q+1})^2$, one samples $r_1^{N,q} = (r_1^q, \dots, r_N^q)$ according to $p(r_1^N | y_1^N, \theta^q)$ and one sets

$$\mu_j^{q+1} = \frac{\sum_{i=1}^N y_i 1_{[r_i = \omega_j]}}{\sum_{i=1}^N 1_{[r_i = \omega_j]}} \quad (3.2)$$

$$(\sigma_j^{q+1})^2 = \frac{\sum_{i=1}^N (y_i - \mu_j^{q+1})^2 1_{[r_i = \omega_j]}}{\sum_{i=1}^N 1_{[r_i = \omega_j]}} \quad (3.3)$$

EM provides the next θ^{q+1} from the current θ^q and $y_1^N = (y_1, \dots, y_N)$ in the following way. The next parameters p_{jk}^{q+1} are given by (3.1), exactly as in the case of ICE. The next μ_j^{q+1} , $(\sigma_j^{q+1})^2$ are computed with

$$\mu_j^{q+1} = \frac{\sum_{i=1}^N p(r_i = \omega_j | y_1^N, \theta^q) y_i}{\sum_{i=1}^N p(r_i = \omega_j | y_1^N, \theta^q)} \quad (3.4)$$

$$(\sigma_j^{q+1})^2 = \frac{\sum_{i=1}^N p(r_i = \omega_j | y_1^N, \theta^q) (y_i - \mu_j^{q+1})^2}{\sum_{i=1}^N p(r_i = \omega_j | y_1^N, \theta^q)} \quad (3.5)$$

Let us notice that there is a stochastic aspect in the sequence produced by ICE, while the sequence related to EM is deterministic. This can make EM more sensitive to the initialization θ^0 than ICE. However, numerous comparisons between EM and ICE have been performed and, on the whole, in the case of classical HMM with Gaussian noise they provide similar results (Benmiloud and Pieczynski (1995)).

We propose the following adaptive parameter estimation method, based on EM or ICE. Let $\hat{\theta}^n$ be the parameter obtained from y_1^n . Then $\hat{\theta}^{n+1}$ is obtained from y_1^{n+1} by applying EM (or ICE) and using $\hat{\theta}^n$ as the initial value. Thus one obtains a sequence $\hat{\theta}^0, \hat{\theta}^1, \dots, \hat{\theta}^N$, each $\hat{\theta}^n$ being estimated from y_1^n . The computation of

$p(r_{n+1}|y_1^{n+1})$ from $p(r_n|y_1^n)$ using (2.2) is then unsupervised and is performed in two steps:

- (i) compute $\hat{\theta}^{n+1}$ with EM (or ICE) from y_1^{n+1} using $\hat{\theta}^n$ as initialization;
- (ii) compute $p(r_{n+1}|y_1^{n+1})$ from $p(r_n|y_1^n)$ using (2.2) and $\hat{\theta}^{n+1}$.

Thus for each $n=1, \dots, N-1$ one has to perform a finite number, defined in some way, of EM or ICE iterations.

In the following section these methods will be called “adaptive EM (AEM) and adaptive ICE (AICE).

Let us return to the « partially » Markov distribution defined by (2.3) and let us consider the following particular case. One considers K Gaussian distributions $p^1(y_1^N), \dots, p^K(y_1^N)$ which are used to define the distributions $p(y_{n+1}|r_{n+1}, y_1^n)$ in (2.3): for each $n=1, \dots, N-1$ and $k=1, \dots, K$, $p(y_{n+1}|r_{n+1}=\omega_k, y_1^n)$ is the conditional Gaussian distribution given by the Gaussian distribution $p^k(y_1^{n+1})$, which is the marginal distribution of the Gaussian distribution $p^k(y_1^N)$. Besides, for each $k=1, \dots, K$, $p^k(y_1^N)$ is defined by the mean vector $M^k=(m^k, \dots, m^k)$ and a variance-covariance matrix $\Gamma^k=[\gamma_{ij}^k]_{1 \leq i, j \leq N}$, with

$$\gamma_{ij}^k = \sigma_k^2(1+|i-j|)^{-a_k} \quad (3.5)$$

The distribution of such a model, which will be called in the following HMM with “long memory noise” (HMM-LMN), is then defined by the parameters p_{ij} , which give the distribution of the Markov chain X , and K triplets $(m^1, \sigma_1^2, a_1), \dots, (m^K, \sigma_K^2, a_K)$. HMM-LMN has been recently proposed in (Lanchantin et al. (2008)) and an extension of ICE, which is not trivial, to the HMM-LMN context has been described and successfully tested. As above, we propose using this ICE to estimate the parameters in an “adaptive” manner. One has the same two steps as above:

- (i) compute $\hat{\theta}^{n+1}$ with ICE from y_1^{n+1} using $\hat{\theta}^n$ as initialization;
- (ii) compute $p(r_{n+1}|y_1^{n+1})$ from $p(r_n|y_1^n)$ using (2.4) and $\hat{\theta}^{n+1}$.

4 Experiments

Let us consider an HMM with two classes $\Omega = \{\omega_1, \omega_2\}$. The distribution of R_1^N is defined by $p(r_1 = \omega_1) = p(r_1 = \omega_2) = 0.5$ and the transitions $p(r_{n+1} = \omega_1 | r_n = \omega_2) = p(r_{n+1} = \omega_2 | r_n = \omega_1) = \rho$. The two Gaussian noise distributions are $N(\mu_1, \sigma_1^2) = N(-1/2, 1/2)$, $N(\mu_2, \sigma_2^2) = N(1/2, 1/3)$. We consider $N = 200$ for the sample size and the results for four different values of ρ are presented for each

case in Table 1. An example of the evolution with respect to n of the estimation with AEM and AICE of ρ (for the true $\rho = 0.2$) is presented in Figure 1.

It is difficult to compare AEM and AICE as they are very sensitive to the initialization and give very stochastic results for small n . However, in all experiments performed they are of similar efficiency when n increases.

ρ	0.1	0.2	0.3	0.4
EM $\hat{\rho}$	0.10	0.19	0.36	0.51
ICE $\hat{\rho}$	0.09	0.18	0.39	0.52
EM τ	8.5%	6.8%	9.0%	17.1%
ICE τ	13.0%	6.0%	11.3%	22.0%

Tab. 1. Estimates of ρ and error ratio τ of unsupervised adaptive filtering.

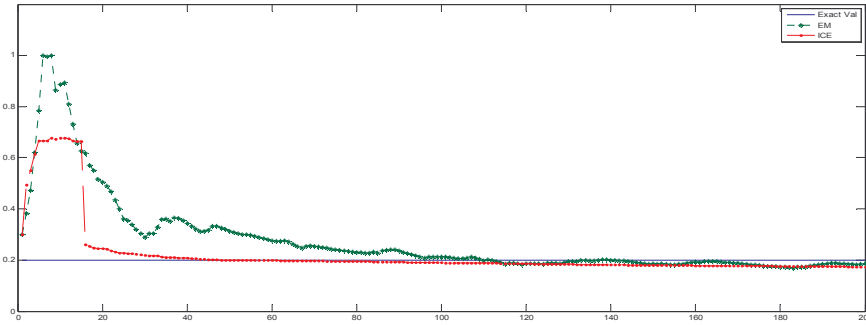


Fig. 1. Evolution with n of the estimation with AEM and AICE of ρ .

Let us now consider the case of data simulated with the model (1.1)-(1.3) and filtered by three methods. The first one is the method based on the particle filter (Andrieu et al. (2003), Doucet et al. 2001)). The second one is based on HMM, and the third one on HMM-LMN. As ρ has to be known in the particle filter based method, we also assume it to be known in the other two methods; however, let us underline the fact that it could be estimated which is an advantage of the HMM and HMM-LMN based methods over the particle filter based one.

True parameters are $N(\mu_1, \sigma_1^2) = N(-1/2, 1/2)$, $N(\mu_2, \sigma_2^2) = N(1/2, 1/3)$, $F(\omega_1) = -0.25$, $F(\omega_2) = 0.25$, $G(\omega_1) = -2$, $G(\omega_2) = 2$, $H(\omega_1) = 0.1$, $H(\omega_2) = 0.5$, $K(\omega_1) = 0.5$, $K(\omega_2) = 1$. The squared error is given by

$$\varepsilon = \sqrt{\frac{1}{200} \sum_{j=1}^{200} (x_j - \hat{x}_j)^2} \quad (4.1)$$

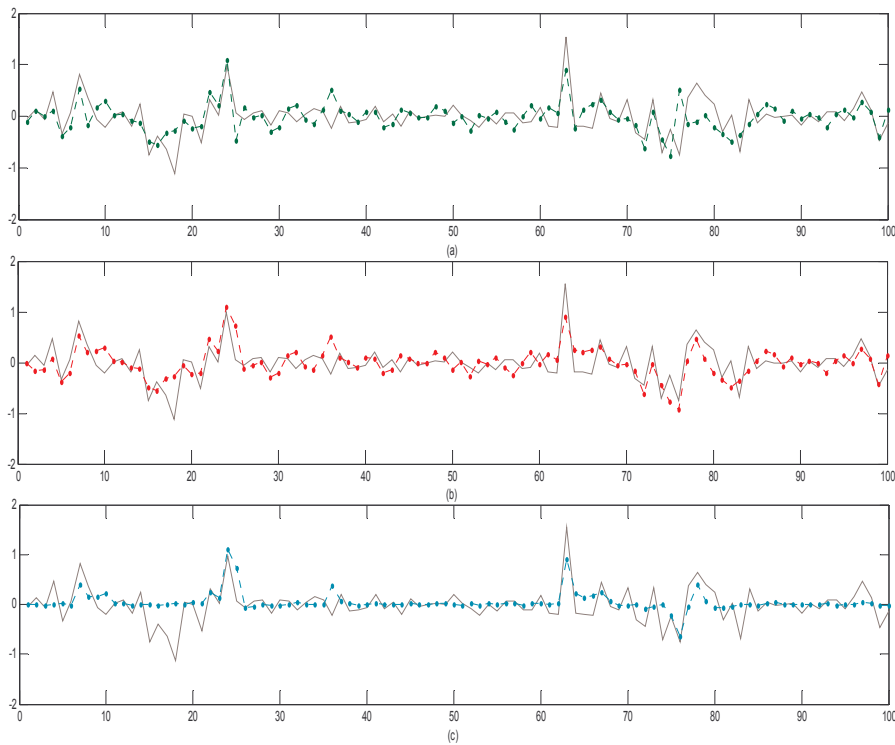


Fig. 2. Data simulated according to the model (1.1)-(1.3) with $\rho = 0.01$ and the true parameters related to Tab. 2.(continuous line) (a) : particle filter (500 particles sampled) based filtering ; (b) HMM-LMN based filtering, and (c) : HMM based filtering.

ρ	0.1	0.40	0.80
	Error ratio τ		
Particle Filter	17.0%	31.7%	37.0%
HMM-LMN	13.3%	27.3%	27.5%
HMM	29.0%	32.0%	37.3%
	Squared error ε		
Particle Filter	0.0273	0.16	0.19
HMM-LMN	0.0211	0.09	0.11
HMM	0.0301	0.12	0.13

Tab. 2. Error ratio τ of unsupervised adaptive segmentation and squared error ε (4.1) in the case of data simulated with the model (1.1)-(1.3). $\rho = 0.1$ is given for the three methods, means and variances in HMM and HMM-LMN are estimated with AICE.

According to the results presented in Table 2 and other similar results obtained, one can say that, on the whole, an HMM-LMN based method is the most efficient, while the Particle Filter based method works better than the HMM based one.

5 Conclusion

In this paper we considered the problem of optimal filtering in the conditionally Gaussian state space models with Markovian switches given by (1.1)-(1.3). We presented two original methods of approximation of the distribution of the couple (R_1^N, Y_1^N) , where $R_1^N = (R_1, \dots, R_N)$ is the random chain of switches and $Y_1^N = (Y_1, \dots, Y_N)$ is the random chain of observations. In the first one this distribution is approximated by the classical hidden Markov model (HMM) distribution, and in the second one it is approximated by a recent Markov model hidden with a “long memory noise” model (HMM-LMN) (Lanchantin et al. 2008). In these two models the parameters can be estimated by the “adaptive” methods also proposed in the paper. Using these two approximations makes the exact filtering possible with a reasonable complexity. The two related filtering methods have then been compared to the classical Particle Filter based approximation. Different experiments showed that the HMM-LMN based methods take the upper hand over the Particle Filter based ones, while the efficiency of the latter is, roughly speaking, similar to the efficiency of the HMM based methods.

As perspective, let us mention further comparisons of our methods with some recent models based exact filtering, as the method proposed in (Pieczynski (2008)).

6 References

- [1] Andrieu, C., Davy, C. M., and Doucet, A., Efficient particle filtering for jump Markov systems. Application to time-varying autoregressions, *IEEE Trans. on Signal Processing*, 51, 7, 1762-1770 (2003).
- [2] Benmiloud, B. and Pieczynski, W., Estimation des paramètres dans les chaînes de Markov cachées et segmentation d'images, *Traitement du Signal*, 12, 5, 433-454 (1995).
- [3] Cappé, O., Moulines, E., and Ryden, T., *Inference in hidden Markov models*, Springer, Series in Statistics, Springer (2005).
- [4] Costa, O. L. V., Fragoso, M. D., and Marques R. P., *Discrete time Markov jump linear systems*, New York, Springer-Verlag (2005).
- [5] Derrode, S., and Pieczynski, W., Signal and image segmentation using pairwise Markov chains, *IEEE Trans. on Signal Processing*, 52, 9, 2477-2489 (2004).
- [6] Doukhan, P., Oppenheim, G., and Taqqu, M. S., *Long-Range Dependence*, Birkhauser, 2003.
- [7] Doucet, A., Gordon, N. J., and Krishnamurthy, V., Particle filters for state estimation of Jump Markov Linear Systems, *IEEE Trans. on Signal Processing*, 49, 3, 613-624 (2001).
- [8] Lanchantin, P., Lapuyade-Lahorgue, J., and Pieczynski, W., Unsupervised segmentation of triplet Markov chains with long-memory noise, *Signal Processing*, 88, 5, 1134-1151 (2008).
- [9] Pieczynski, W., Exact calculation of optimal filter in semi-Markov switching model, (IASC 2008), December 5-8, Yokohama, Japan (2008).
- [10] Ristic, B., Arulampalam, S., and Gordon, N., *Beyond the Kalman Filter - Particle filters for tracking applications*, Artech House, Boston, MA (2004).
- [11] Tugnait, J. K., Adaptive estimation and identification for discrete systems with Markov jump parameters, *IEEE Trans. on Automatic Control*, AC-25, 1054-1065 (1982).
- [12] Zoeter, O., and Heskes, T., Deterministic approximate inference techniques for conditionally Gaussian state space models, *Statistical Computation*, 16, 279-292 (2006).

Telecenters through Wireless Technology near a Base camp of Mt. Everest of Nepal

Bimal Acharya

(PhD Candidate Tribhuvan University)

Fellow IETE, Master of Engineering (Telecom, AIT-Bangkok), B.Sc. Engineering (EEE, BUET, Dhaka)

bimal.acharya@ntc.net.np

Abstract:

Wireless communications in Nepal has expanded greatly in last decade and the number of the wireless users has grown to more than 1500 thousand. However, the distributions are more concentrated in major cities. Thus there are double challenges we are facing namely how to take telecom revolution to the rural areas especially to the mountainous villages and tourism area. This article focuses how to provide voice, email and internet services to the mountainous tourism villages: near a Base Camp of Mount Everest, the summit of world. Satellite link is presented as only one of the quick and cost effective option for providing backhaul link to this proposed project. Wireless LAN (Wi-Fi) is chosen as technology for connecting different villages or business houses or trekking camps of that area. These Telecenters is expected not only to revolutionize the system of social participation of local people by internet and communications but also attracts the foreigners for trekking. Social awareness programs including education of rural mass can be achieved in most cost effective way in the shortest possible time to an extremely larger group of rural people. Installation of Telecenters certainly improves the life styles of local people as well as facilitates the tourists.

1. Introduction

The Country Nepal is situated in South Asia, on the southern slopes of the Himalayan mountain range, and lies between India and China. Eight of the world's ten tallest peaks, including the highest Mt. Everest (8848m), are located in Nepal. Administratively, Nepal is divided into 75 districts. The lowest administrative division is the Village Development Committee (VDC) of which there are 3914. The population of Nepal is estimated at around 25 million at present. Kathmandu is the capital of the country which has about 10

of the country's population. Around 80 per cent of Nepalese reside in rural areas. Presently teledensity has reached about 9 lines per 100 inhabitants including mobile, fixed terminals and PSTN lines. Telephone service is available in all 75 districts, of which all 75 have their own telephone exchange. There is still a large challenge to provide the telecommunication service in this mountainous and rural nation as around two-thirds of all telephones are in the Kathmandu area. There are more than 250 000 on the waiting list. Some 45 per cent of VDCs are waiting for telephone service. The Nepal Telecommunications Company Limited (NT) is the incumbent public telecommunications operator and, until recently, held a monopoly over PSTN in the country. Nepal Telecom (NT) is fully State-owned registered under company act of Nepal in 2005. NT started the GSM mobile service in May 1999 and had more than 700000 subscribers as of August 2007. There is another private mobile operator named Spice Cell Nepal which has distributed around 600000 GSM mobile subscribers as of August 2007. United Telecom (U-TEL) is another WLL operator in Nepal serving CDMA technology to about 100 thousand subscribers. Nepal's Internet market got a boost in mid-1999 when Internet Service Providers (ISPs) were allowed to have their own international gateways. Prices dropped to the lowest level in the South Asia region. By January 2007, more than seventy ISPs were serving some 100,000 subscribers and an estimated 200,000 users. This facility is available only at the major cities.

This paper tries to give a solution to install a Telecenters near the Base Camp of Mount Everest. Obviously, this will provide a guideline for the selection of technology and the installation procedures and the advantages and application of Telecenters at the mountainous villages. Similar installation can be carried out near the base camp of other peaks.

This endeavor hopes to contribute in the bridging of the Digital Divide in the rural areas of the mountainous villages of Nepal by establishing facilities and provides a model for developing such facilities in the rural areas.

2. Objectives

The major goals of this project are:

- To establish Telecenters infrastructure in Syangboche, Solukhumbu of Nepal using VSAT technology as a backhaul link.
- To provide ICT services (Voice, email, internet and multimedia applications) in Syangboche, Khumjung, Namche, Tyangboche, Firiche of Solukhumbu
- To connect Syangboche, Namche, Tyangboche, Firiche of Solukhumbu to a Learning Center using Broadband Wireless LAN;
- To develop human resource in the field of ICT;
- To obtain the knowledge and skill in developing e-tourism business applications
- To have an exchange of ideas between different countries of the world on tourism development
- To strengthen partnerships between developed and developing countries as well as between rural areas and urban areas and
- To promote tourism business in the trekking areas of Mount Everest
- To promote tourism business of Nepal.
- To provide VOIP, fax, email, internet to the tourists and local people
- To share social and cultural values with others
- To connect Mount Everest with the rest of the world
- To make a model Telecenters so that other rural area can take the idea

3. Project Site

The proposed project will be located in the district of Solukhumbu. It is in the East of Kathmandu. These villages are bounded on the North by the Mount Everest, on the East and west by other mountains and on the south by the River and Forest. All villages are at an altitude of more than 3000m and takes 4 to 6 hours trekking to reach from one village to other. All of these villages are in the trekking routes to the Mount Everest. One can reach Syangboche by Helicopter or by two days foot trails from Lukla. There are regular flights from Kathmandu to Lukla. It takes about 20-30 minutes by small planes.

The main business of these areas is tourism business. They run hotel business. The people of these villages rely on tourist and farming as major sources of income. All of these areas are a scenic place with small hospital, and natural sites.

Proposed sites for Telecenters:

- A. Airport building of Syangboche
- B. Buddhist Gumba of Tyangboche
- C. Three hotels of Namche
- D. High School at Namche
- E. Hotel of Firiche
- F. School of Khumjung village
- G. Hospital building of Khumjung
- H. Two Hotels of Khumjung
- I. Two for Temporary Base Camp near to the Mount Everest

4. Technology Selections:

The most important part of operating Telecenters is the connectivity. And the connectivity can be provided via various media and technologies. But the topography of the country is a major issue in this regard. It is not easy to provide connectivity to all parts of the country using a single technology or medium. For the areas with existing network and the terrain permitting, cable (copper as well as fiber) could be the better option; but for most of the remote and rural areas, radio or satellite could be the only viable option, though sometimes expensive. Copper cable, through technologies like DSL or leased lines could be affordable, and fiber could be a better option for larger bandwidth requirements. Various existing and upcoming radio technologies with continuously decreasing prices like Wi-Fi, WiMAX and Line of Sight Radio System could be used for regions not possible to be connected through cable. For this, policy decisions have to be made for deregulating the unlicensed bands used by Wi-Fi and WiMAX. The assessment of the existing services in operation and the demand and characteristics of the targeted services should be taken care of first. Here, the technological selection for reliable backhaul link is proposed as a satellite solution. Small VSAT terminals with 1.2m antenna is installed at Syangboche for connecting these Telecenters to the internet of Kathmandu and then to the world.

Local area network will be done by using un-license Wi-Fi technology for connecting Namche, Khumjung, Tyangboche, Firiche and two temporary Base Camps.

Another important requirement for the operation of Telecenters is the power provisioning. Power sources are not readily available, especially in these remote areas. Radio technology usually requires more power than cable technology, and hence the power availability also defines the suitable connectivity technology. These sites do not have reliable AC supply so the solar power system is selected as a primary source of power supply.

5. Methodology

Document Preparation -----Planning and Scheduling-----Site Survey-----Detail System Design----Finalization of network design---Procurement of Equipment-----Erecting of Poles---Installation of the system----Testing of the system---Training to the local people/community-----Preparation of local human resources---Handover of the project to the local community.

5.1. Network Layout

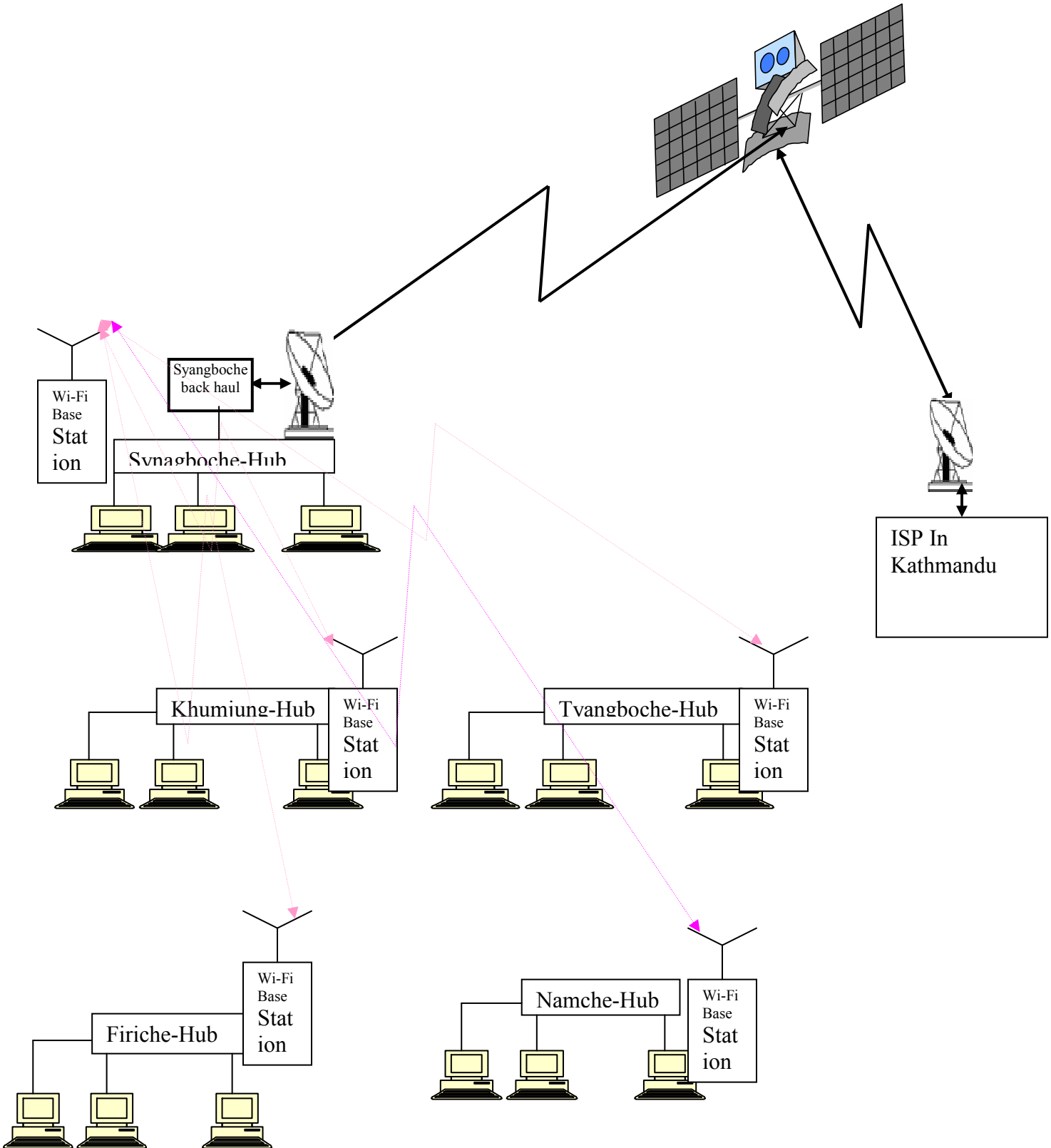


Table 1.0 List of Equipment and Accessories

S/N	Name of Sites	Name of Equipment	Specifications	Remarks
1	Syangboche	1.2m VSAT terminals	Ku band	Purchased from local ISP
2	Syangboche	2 Wi-Fi terminals with repeater stations Server computer, Hub, three directional antenna	IEEE802.11 PIV with necessary software	
3	Namche	4 Wi-Fi terminals with computer, fax, and IP phone	IEEE802.11 PIV with necessary software	One web cam for school
4	Khumjung	4 Wi-Fi terminals with computer, fax and IP phone	IEEE802.11 PIV with necessary software	1 web cam for school and 1 for hospital
5	Tyangboche	1 Wi-Fi terminals with computer, fax and IP phone	IEEE802.11 PIV with necessary software	One web cam for Gumba
6	Firiche	1 Wi-Fi terminals with computer, fax and IP phone	IEEE802.11 PIV with necessary software	One web cam for community
7	Base camp	2 Wi-Fi terminals with computer, fax and IP phone	IEEE802.11 PIV with necessary software	One web cam for tourist
Total	7 sites	14 Telecenters	2.4 GHz+10Mb/s	6 web cam

Note: Two computer servers can be placed in two different sites of Syangboche, one acting as a mirror site for web-based applications and twelve sites will be provided with computer workstations equipped with multimedia capabilities such as web cams, headsets, speakers etc, IP Phones will be provided in all sites for voice connectivity and 6 m 2” pipes will be used to mount Antenna at each sites.

6. Result and Applications:

Installation of Telecenters can provide a new dimension in every sphere of life ranging from tourism, agriculture, environment, education, medicine, space, remote sensing, weather prediction, security and all types of business in the installed area and the country. It provides not only unprecedented opportunities to solve the pressing problems of rural

masses but also offers sustained improvement in the quality of life. It enables finding innovative solutions to the many and varied practical problems, confronting the present society. Now, the society requires such an innovative solution for better management of rural problems, where development has to be very fast, highly cost effective and more efficient than earlier. ICT development is expected to revolutionize the system of social participation of people by internet, email and other means of communications. ICT enabled social awareness programme demands active participation of the people for national development especially for rural people. Education of the rural people can be achieved in a most cost effective way in the shortest possible time to an extremely larger group of people. By this method, not only we can reach larger groups of people, collect information from experienced people of world at large and implement this faster. This can provide very broad, unlimited super highway for best management at international level. Through this super highway, we can ever sell out village products and ideas to the global market and earn the good will at international level as well as earn lot of foreign exchange which could be utilized for rural development of that area.

The services of Telecenters should revolutionize rural development programme, medical applications, tele-medicine, rural health care, spreading education to poor people, rural bank etc, bringing together all the global villagers on the common platform of happy, healthy and wealthy knowledge based society. There are various issues of rural people. They have enough time compared to urban people to devote for each problem. But they do not have enough library facility, information, knowledge and education. We have large number of school teachers, college teachers in various cities who can translate the local facilities in the English such that global village concept can be achieved. Efforts have to be made to educate some local people of mountainous areas to download the information of their need about agricultural, educational, medicinal and business information of rural products. They will be able to float their queries on relevant topics. These Telecenters can help to increase the literacy rate of the rural areas. This literacy can be achieved through the internet. It should be made attractive through animation. Children's should not be forced to education. Through animation, they will be automatically attracted for education. Initially local language may be taught. Then gradually, history, geography, mathematics, science and English language can be taught.

It is truth that people of these areas are very simple and open minded. Some of these rural innovators are generously share their knowledge, innovations and practices, based on local resources, traditional knowledge and tools etc at no cost. They do not always derive the high benefits of such sharing. That is the one reason why may of them remain poor. ICT will help new generation to select the path of modern science and technology. They can store all the local and traditional resources through the internet and can be shared.

The proposed Telecenters can be utilized in the following ways and this center can make sustainable for long time by opting following options:

a) e-Learning Application:

- Conducting training coursed on computer hardware and software and applications
- Training on finding information on the Internet through search engines.
- Web page creation and web programming training.
- Remote lectures with other schools.

b) e-Governance Applications

- Access by the local government officials to other government websites.
- Possibility to communicate with other departments and officials
- Forums and dialogue between local government officials for example the officials from the Khumjung VDC can talk to the Local Development Officer of Solukhumbu.
- Geographical Information System (GIS) Integration
- Record keeping of details of local people of that VDCs

c) e-tourism Business Applications

- Record keeping of tourists and visitors
- Explore possibility of hosting services for local people and tourists.
- Provide VOIP, e-mail, internet surfing to the tourist with minimal fees.
- Possibility of utilizing e-cards

d) Offline Computer Applications

- By providing computer familiarization through training on basic computer operations and use of Office applications (MS word, Power point, Excel etc).

- By providing training on basic computer maintenance e.g. on proper use and identification of viruses distributed as e-mail attachments and through malicious websites.

e) Operation and Maintenance/ Sustainability Requirements

- Make every internet access points as Community e-Centers (CeCs). CeCs for internet surfing, educational games, software applications development, website development, content development, e-business and ICT Training. ICT Training for both hardware and software, management of CeC, etc
- ICT Training: Basic and Advance Course in Computer Education, Computer Networking Specialized application software courses, Specialized Group Training (Housewives, Elderly, Physically challenged, Farmers, Fishermen, Students, Government Employees, Businessmen, Out-of-School Youth, etc.)
- Coordinate, collaborate, cooperate and manage all these ICT activities through: A small group of concerned individuals/institutions to lead Public consultations and Activity promotion for Continuing ICT development in the villages
- Establish or create a Small Group of Telecenters Management Team
- Funding Options can be as:
 - Fees from Tourists and locals by using facility
 - Support from NGOs and INGOs
 - Support from VDCs
 - Minimum fees from Local Hotel and other business organizations

7. Conclusion and Recommendations

As a result of the implementation of this Project, selected sites will be provided with a modern wireless transmission network. They will be provided with a server computer, workstation computers, faxes and IP Phones that will be capable of delivering useful offline and online services to the recipient of the villages and tourists. Offline services such as word processing, spreadsheets, presentation and database applications are now available for the benefits of the local people. Online communications services can be utilized like sending and receiving emails, VoIP and video conferencing, as well as basic online applications like gathering information from the Internet. Various forms of e-

services can be developed; applications such as e-tourism business, e- Learning, e-Government, and e-Commerce can be learned and offered through these facilities.

This introduction of the Wireless LAN Technology in mountainous villagers opens a lot of possibilities for the advancement of the community. It will help them achieve reforms needed in education, business and governance. Similar kind of system can be duplicated in other areas of the mountainous villages and trekking areas. Final Goal should be set in such a way that Revenue should be enough to sustain the operation and maintenance of Telecenters. Telecenters are operated in non profit making basis.

8. References:

1. 2rd Anniversary souvenir, Nepal Telecom, 2006
2. 3rd Anniversary souvenir, Nepal Telecom, 2007
3. Annul report, Nepal Telecom, 2006
4. Dr. Kamilo Feher, 'Wireless Digital Communications-Modulation and Spread Spectrum, Applications' PHI, 1999.
5. IEEE Transactions in vehicular Technology
6. IEEE Transactions on Communications
7. IETE Technical review
8. Jerry D. Gibson, 'The Mobile Communications Handbook,' 2nd Edition, CRC Press in Cooperation with IEEE Press, 1999.
9. M. K. Simon et al., 'Spread Spectrum Communications', Computer Science Press, 1985
10. MIS report, Nepal Telecom, Magh 2063.
11. R Steele, 'Mobile Radio Communications,' 2nd Edition, John Wiley & Sons, 1999.
12. R. E. Ziemer, R. L. Peterson, and D. E. Borth, 'Introduction to Spread Spectrum Communications', Prentice Hall, Englewood cliffs, NJ, 1995
13. Technical journal articles.
14. Theodore S. Rappaport, "Wireless Communications: Principles and Practice, Pearson Education, 2002
15. V.K Garg, 'IS-95 CDMA and CDMA 2000', Prentice Hall,2000.

16. W.C.Y. Lee, 'Mobile Cellular Telecommunications Systems, McGraw Hill Publications, 1989.
17. www.aptsec.org
18. www.itu.int
19. www.ntc.net.np
20. www.iete.org

Performance evaluation of IP networks with differentiated services

Smail Adjabi¹, Karima Adel¹, N. Saidani², and A. Laouar²

¹ Laboratory LAMOS
University of Bejaia, Bejaia, Algeria
(e-mail: adjabi@hotmail.com)

² Department of Operations Research
University of Bejaia, Bejaia, Algeria

Abstract. The aim of this study is the mathematical modelling of the architecture with differentiation of services (DiffServ) as it is defined by the IETF workgroup with an M/G/1/N queue with multiple vacations and exhaustive service. We are interested by the evaluation of the performances of the EF (Expedited Forwarding) class of the core routers which contains the most critical packages (voice, video). For the validation of the analytical chosen model, a simulation of a simple network under DiffServ was realized with NS2. This modelling (with M/G/1/N queues) serves for the sizing of the network parameters: debit and size of buffer according to the load of the network.

Keywords: IP networks, DiffServ (differentiated services), M/G/1/N queue with multiple vacation.

1 Introduction

With the development of the multimedia applications, the IP network has to allow the deployment of these applications to guarantee its success. However these applications have specific requirements in term of QoS (Quality of service). Certain services as the vocal services need weak delay and weak jitter (variation of the crossing delays). We find many works in the literature dealing with the QoS of the real-time applications on IP networks. Our study represents one of these works which aims to the determination of the network parameters (debit and size of buffer) according to its load.

We call QoS all the mechanisms **providing a good service level to specific flows**. QoS refers to the ability of the network to transport in good conditions flows from different applications. This definition is reflected in the following technique characteristics: Availability; Bandwidth; Delay; The jitter; Loss ratio.

2 DiffServ description

Unlike the IntServ based on the booking of the resources in routers, the approach "differentiated services" tries to establish the QoS by sorting of entrant packages on the border of the network under DiffServ following various

2 S. Adjabi, K. Adel, N. saidani and A. Laouar

criteria (delay, bandwidth, address). The sorting is made at the level of the border routers. The streams of data are classified according to three categories of service (Expedited Forwarding, Assured Forwarding and Best Effort) and four classes of traffic predefined according to the performances needed for their transmission. Packages are "marked" and managed in routers by specific queues for every category or class.

In DiffServ there are border routers which are connected to border routers of other field. They take charge of the classification of entrant packages. We also find core routers which are connected to core routers or border routers of the same field. They take charge of treatment with differentiating the packages of various categories or classes.

Border routers

The structure of a border router can be divided into 4 modules [2]:

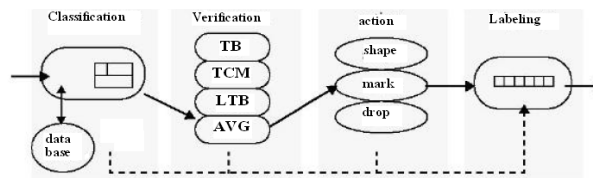


Fig. 1. Border router

- **Classification:** To treat different flows generated by users with differentiated way, the border router must first make a packet classification, which is based on the header IP.

- **Checking:** A controller is responsible for determining the level of compliance for each packet flow coming into the router. This depends mainly on the instantaneous flow behavior and the characteristics of the contract (SLA).

- **Actions (dropper & shaper):** The corrective action to be taken for non-compliant packets varies according to the service. Three penalty types can be identified:

***The elimination** is probably the most severe action, but necessary for the proper functioning of certain services.

* **The formatting** is to delay, if necessary, the flow of a stream to conform it.

- **Marker:** Before entering the network, the DSCP field (a part of header IP) of all packets that pass through the entry router is updated. It forms the DiffServ label and should not be changed by the core routers in the network.

Core routers

A PHB is the description of the delivery characteristics that will be observed by all packets containing the same DSCP. The use of a PHB or a group of

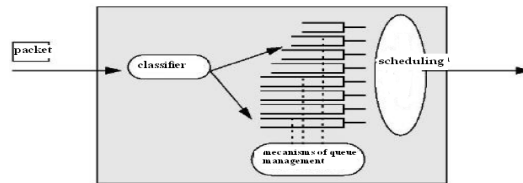


Fig. 2. Architecture of core routers.

PHB added to the packaging operations performed at the input of a field forms a DiffServ.

Diffserv defines four PHB or classes of service:

- **Expedited Forwarding (EF)** [5]: Corresponds to the maximum priority and aims to ensure bandwidth with low loss ratio, delay and jitter, achieving the flow transfer with severe time constraints like IP telephony.
- **Assured Forwarding (AF)** [1]: Groups several PHB guaranteeing delivery of IP packets with a high probability regardless of deadlines.
- **Best Effort (BE)** [6]: PHB by default.
- **Default Forwarding (DF)**: Used only for Internet streams that do not require a real-time traffic.

In each queue, a management mechanism must decide on the manner of eliminating the packets in case of congestion.

- **DropTail**; - **Random Early Discard (RED)**; - **Weighted Random Early Discard (WRED)**; - **RED with In and Out (RIO)**. Several scheduling techniques (algorithms) have been developed to control the sharing of resources between the classes of service:

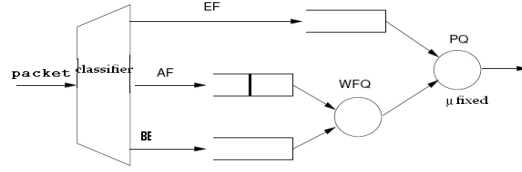
- **Fair Queueing (FQ) or Round Robin (RR) - Weighted Fair Queueing (WFQ)**. * **Generalized Processor Sharing GPS**; * **Weighted Fair Queueing (WFQ)**; * **Weighted Round Robin (WRR)**; * **Priority Queueing (PQ)**.

3 Modeling of core router

We focus on core routers of the architecture DiffServ, because the operations of these routers (queue management and scheduling), will determine network performances. We consider that our model is represented by an $M/G/1/N$ queue with multiple vacations and exhaustive service.

- Packets of the EF priority Class represent the customers of the system.
- The output link is considered as the system single server, it can get only one packet at once.
- Packets of Class EF arrive according to a Poisson process with rate λ .
- The variation of the service time is due to the packets random length and not to the server capacity, which is expressed by a general service law with probability density function $b(t)$, and cumulative distribution function $B(t)$. Let \bar{X} be the service mean time.
- The size of the queue is limited to $(N-1)$ packets.
- During the idleness period, the server begins to serve packets of other classes, which corresponds in our model to a vacation with general random duration, with probability density function $f_v(t)$, and

4 S. Adjabi, K. Adel, N. saidani and A. Laouar


Fig. 3. Model

distribution function $F_v(t)$. Let \bar{V} be the vacancy mean duration. - At the end of a vacation period, the server will not return in vacancy only when there will be no packets to serve in the EF class (multiple vacancy and comprehensive service).

The performance evaluation of the $M/G/1/N$ system with finite capacity and server vacation has been the concern of **Frey** and **Takahashi** [3]. They used the induced Markov chain method (included), where they observe the system at moments that are: either at the end of a service or at the end of a vacation period.

The state of the system at the induced points is represented by the pair (n_i, ϕ_i) , with:

- n_i : The traffic number (EF packets) in the system just after the i -th induced point;
- $\phi_i = \begin{cases} 0, & \text{If the } i\text{-th induced point corresponds to an end of period vacation;} \\ 1, & \text{If the } i\text{-th induced point corresponds to an end of service.} \end{cases}$

Consider the system in the steady state. Note by:

- $q_k, \forall k = 0, \dots, N$, the probability to be in the state $(k, 0)$;
- $r_k, \forall k = 0, \dots, (N - 1)$, the probability to be in the state $(k, 1)$;
- $f_j; j = 0, \dots, +\infty$, the probability to have j packets of the EF class in the system just after a vacation period, this probability is given by:

$$f_j = \int_0^{\infty} \frac{(\lambda t)^j}{j!} e^{-\lambda t} f_v(t) d(t), \quad j = 0, \dots, \infty. \quad (1)$$

- $\alpha_j; j = 0, \dots, +\infty$, the probability that j packets of the EF class arrive in the system during a service time, this probability is given by:

$$\alpha_j = \int_0^{\infty} \frac{(\lambda t)^j}{j!} e^{-\lambda t} b(t) d(t), \quad j = 0, \dots, \infty. \quad (2)$$

The state probabilities of the system:

$$q_k = (q_0 + r_0) f_k, \quad k = 0, \dots, (N - 1); \quad (3)$$

$$q_k = (q_0 + r_0) \sum_{k=N}^{\infty} f_k, \quad k = N; \quad (4)$$

$$r_k = \sum_{j=1}^{N+1} (q_j + r_j) \alpha_{k-j+1}, \quad k = 0, \dots, (N-2); \quad (5)$$

$$r_{N-1} = q_N + \sum_{j=1}^{N-1} (q_j + r_j) \sum_{k=N-j}^{\infty} \alpha_k, \quad k = N-1. \quad (6)$$

$$\sum_{k=0}^N q_k + \sum_{j=0}^{N-1} r_j = 1. \quad (7)$$

These state probabilities are used to get some performance parameters of the system:

- The load: $\rho_c = \frac{(1-q_0-r_0)\bar{X}}{(q_0+r_0)\bar{V}+(1-q_0-r_0)\bar{X}}$. - The offered load: $\rho = \lambda\bar{X}$.
- Blocking probability (rejection): $P_B = \frac{\rho-\rho_c}{\rho}$.
- Mean time D between successive included points: $D = (q_0 + r_0)\bar{V} + (1 - q_0 - r_0)\bar{X}$.

To determine the usual system parameters, such as the mean number of customers in the system M and the mean sojourn time W , note by:

- $Q_k = P\{k \text{ customers in the system, the server is in vacation}\}, k = 0, \dots, N;$
- $R_k = P\{k \text{ customers in the system, the server is busy}\}, k = 0, \dots, (N-1);$

The state probabilities are given by:

$$Q_k = \begin{cases} \frac{1}{\lambda D} \sum_{j=k+1}^N q_j, & k=0, \dots, (N-1); \\ 1 - \rho_c - \frac{1}{\lambda D} \sum_{j=1}^N j q_j, & k=N. \end{cases} \quad (8)$$

$$R_k = \begin{cases} \frac{1}{\lambda D} \left(r_k - \sum_{j=k+1}^N q_j \right), & k=1, \dots, (N-1); \\ \frac{\rho_c(\rho-1)}{\rho} + \frac{1}{\lambda D} \sum_{j=1}^N j q_j, & k=N. \end{cases} \quad (9)$$

In general:

$$\begin{cases} P_0 = Q_0, & j=0; \\ P_j = Q_j + R_j = \frac{r_j}{\lambda D}, & j=1, \dots, (N-1); \\ P_N = Q_N + R_N = \frac{(\rho-\rho_c)}{\rho}, & j=N. \end{cases} \quad (10)$$

6 S. Adjabi, K. Adel, N. saidani and A. Laouar

The usual parameters of the system are:

- The mean number M of packets of the EF Class in the system is:

$$M = \frac{1}{\lambda D} \sum_{j=1}^{N-1} j r_j + N \left(\frac{\rho - \rho_c}{\rho} \right). \quad (11)$$

- The mean sojourn time of a packet in the system is:

$$W = \frac{M}{\lambda(1 - P_B)}. \quad (12)$$

- The probability that the server is busy is:

$$\sum_{k=1}^N R_k = \rho_c = \rho(1 - P_N). \quad (13)$$

4 Simulation

For the validation of our analytical model, a simulation of a simple network under DiffServ was realized. For this network two types of transactions are used: a CBR (Constant Bit Rate) stream based on the UDP protocol that models audio traffic, and an FTP flow based on TCP protocol which models best-effort traffic. We focus our efforts on measuring the quality of service parameters (delay, number of lost packets) of CBR streams.

The architecture of our network consists of an UDP source, a TCP source, two border routers, a core router and a destination.

The simulation model incorporates features of DiffServ architecture. Two different queues are managed. They model different classes of service: EF and BE traffic classes. These queues are served by a scheduler Priority Queuing (PQ) where the queue of the EF class has the highest priority and the queue of the BE class has the lowest one. All DiffServ queues domain are managed by a RED mechanism, and the other queues are handled by DropTail, this latter waits for the filling of the buffers (queues) to reject the packets.

When the number of packets in the queue is equal to N , all the packets received after, are rejected. In NS2, it is sufficient to compute the number of lost packets and divide it on the simulation duration. Analytically, it corresponds to $1/\text{blocking probability}$, given in the section 3.

5 Results and interpretation

The implementation of the analytical model (section 3) with Matlab allows us to obtain the analytical results of this system, by varying:

- The arrival rate of packets of the EF priority class (Packet / ms); - The size of the system (packet); - The service law and its parameters; - The vacation

law and its parameters.

The different analytical results obtained are shown in the following tables (Table 1., Table 2. and Table 3.) with those of the simulated topology under NS2.

service		vacation		M/G/1/N		NS2	
law	para	law	para	loss	delay(W)	loss	delay
Expo	$\mu = 3$	Expo	$\mu = 1$	0.4063	0.5777	0.019	0.186
		Erlang	$\mu = 1$	0.5894	0.7514		
		Cox-2	$\mu_1 = 1$ $\mu_2 = 0.1$ $a = 0.7$	1.4684	1.9498		
Erlang	$\mu = 6$	Expo	$\mu = 0.1$	3.08×10^{-6}	0.1146		
		Erlang	$\mu = 1$	6.34×10^{-7}	0.1146		
		cox-2	$\mu_1 = 1$ $\mu_2 = 0.1$ $a = 0.7$	2.59×10^{-6}	0.1146		
cox-2	$\mu_1 = 4$ $\mu_2 = 7$ $a = 0.7$	Expo	$\mu = 1$	0.4138	0.5298		
		Erlang	$\mu = 1$	0.5459	0.6535		
		Cox-2	$\mu_1 = 1$ $\mu_2 = 0.1$ $a = 0.7$	1.2666	1.5069		

Table 1. Obtained results for N=5 and $\lambda= 3$

service		vacation		M/G/1/N		NS2	
law	para	law	para	loss	delay(W)	loss	delay
Expo	$\mu = 3$	Expo	$\mu = 1$	0.0186	0.6985	0.014	0.336
		Erlang	$\mu = 1$	0.0292	0.7147		
		Cox-2	$\mu_1 = 1$ $\mu_2 = 0.1$ $a = 0.7$	0.1097	0.8136		
Erlang	$\mu = 6$	Expo	$\mu = 1$	0	0.2583		
		Erlang	$\mu = 1$	0	0.2583		
		cox-2	$\mu_1 = 1$ $\mu_2 = 0.1$ $a = 0.7$	9.99×10^{-16}	0.2583		
cox-2	$\mu_1 = 4$ $\mu_2 = 7$ $a = 0.7$	Expo	$\mu = 0.1$	0.3559	0.8007		
		Erlang	$\mu = 1$	0.1538	0.7497		
		Cox-2	$\mu_1 = 1$ $\mu_2 = 0.1$ $a = 0.7$	0.1850	0.7908		

Table 2. Obtained results for N = 10 and $\lambda= 3$

service		vacation		M/G/1/N		NS2	
law	para	law	para	loss	delay(W)	loss	delay
Expo	$\mu = 3$	Expo	$\mu = 1$	3.18×10^{-5}	1.5227	0.004	0.404
		Erlang	$\mu = 1$	3.19×10^{-5}	1.5227		
		Cox-2	$\mu_1 = 1$ $\mu_2 = 0.1$ $a = 0.7$	1.93×10^{-4}	1.5231		
Erlang	$\mu = 6$	Expo	$\mu = 1$	0	0.5457		
		Erlang	$\mu = 1$	0	0.5457		
		cox-2	$\mu_1 = 1$ $\mu_2 = 0.1$ $a = 0.7$	0	0.5457		
cox-2	$\mu_1 = 4$ $\mu_2 = 7$ $a = 0.7$	Expo	$\mu = 1$	0.6923	1.581		
		Erlang	$\mu = 1$	0.1429	1.5962		
		Cox-2	$\mu_1 = 1$ $\mu_2 = 0.1$ $a = 0.7$	0.1429	1.5962		

Table 3. Obtained results for N = 20 and $\lambda= 3$

All the tested laws give good results for a good choice of the parameters either for the service or vacation law:

- For a considerable packet traffic (burst) of the EF Class, the occupation rate of the server is of order 1, which does not allow it to go on vacation. Therefore, we will have the independence of performance metrics of vacation time. Unlike the case when the traffic is less intense, performance metrics depend on the vacation law due to the fact that the server will have the possibility to go on vacation. The duration of this latter has a large influence on these metrics. Indeed, a long vacation period creates rise in the period and the rate of loss.
- The length of the EF queue is a parameter that also affects the loss of packets. Because a bad dimensioning of this queue may degrade the transmission of these packets with considerable losses. As can be expected more the length of the queue is long less is the number of lost packets and conversely more important is the delay, and more the length of the queue is small more we have lost packets and an acceptable delay.

6 Conclusion

We have studied quality of service parameters in a network where audio streams share resources with Best Effort traffic. We analysed two QoS parameters for audio flows : the mean delay end to end and the number of lost packets. The measurements were made in an environment with a scheduler DiffServ with strict priority PQ (Priority Queueing) by modeling with an $M/G/1/N$ queueing system with multiple vacations and exhaustive service together with a simulation under Network Simulator NS2. The presented results show that the proposed model ($M/G/1/N$ queue with vacation) allows us to evaluate the criteria of the quality of service of real time applications in a satisfactory manner for a good choice of laws parameters (service or vacation). These criteria are used for the dimensioning of the system parameters: debit and size of the buffer (queues), according to the load of the system.

References

1. Baker, F. and Heinanen, J. and Weiss, W. and Wroclawski, J. (1999). Assured Forwarding PHB Group, Standards Track, Request For Comments (RFC 2597).
2. Bernet, Y. and Blake, S. and Grossman, D. and Smith, A. (2002). An Informal Management Model for Diffserv Routers, Standards Track, Request For Comments (RFC 3444).
3. Frey, A. and Takahashi, Y. (1997). A note on a $M/G/1/N$ queue with vacation time and exhaustive service discipline, *Oper. Res. Letters*, 21, 95-111.
4. Fuin, D. (2004). Qualité de service : des réseaux IP à l'intégration dans les réseaux actifs, PhD Thesis, UFR des Sciences et Techniques de l'Université de Franche Comté, France.
5. Jacobson, V. and Nichols, K. and Poduri, K. (1999). An Expedited Forwarding PHB, Standards Track, Request For Comments (RFC 2598).
6. Hurley, P. and Le Boudec, J. Y. and Thiran, P. (1999). The Alternative Best-Effort Service, In *Proc. IEEE GLOBECOM'99*.
7. Tsolakou, E. and Nikolouzou, E. and Maniatis S. and Venieris I. (2004). Definition and Performance Evaluation of Network Services Deployed Over a Differentiated Services Network, *Journal of Network and Systems Management*, 12(4), 537-565.

Queueing Models with Periodic Input Processes

Larisa G. Afanasyeva¹ and Elena E. Bashtova²

¹ Department of Mathematics and Mechanics,
Moscow State University, Russia
(e-mail: bashtovaelena@rambler.ru)

² Department of Mathematics and Mechanics,
Moscow State University, Russia
(e-mail: afanas@mech.math.msu.su)

Abstract. Queueing systems with arrival processes having stochastic periodic intensity functions are considered. Many important queueing models have an input of this type. We prove the convergence of the interarrival times sequence to a stationary one and show how to use this property to analyze the asymptotical behaviour of many queueing systems.

Keywords: Queueing models, Periodic flows, Heavy traffic.

1 Introduction

The motivation for the investigation of queueing systems with periodic flows comes from numerous applications. Many applied problems from such areas as reliability, inventory theory, computer science, transport networks and so on, can be embedded into queueing problems for suitably selected input flow with time-dependent periodic intensity. These problems are also of theoretical interest. They are often associated with the analysis of differential and integro-differential equations with periodic coefficients. We restrict our attention to two problems, namely, the determination of conditions of a limit distribution existence and the asymptotical analysis of the queue in a heavy traffic situation. Queues with non-homogeneous Poisson arrivals were studied by many authors, see, e.g., (Harrison and Lemoine [6]). One of the main new elements in the present study is the input flow with a random intensity function.

2 Basic definitions and properties of the input flow

We consider below queueing systems with a doubly stochastic Poisson process (DSPP) as input flow. To begin with we recall the definition of a DSPP. Assume two independent stochastic processes $\{A^*(s), s \geq 0\}$ and $\{A(t), t \geq 0\}$ to be defined on a probability space $(\Omega, \mathcal{F}, \mathbf{P})$. The process $A^*(s)$ is a standard Poisson process and $A(t)$ has non-decreasing left-continuous trajectories

and $A(0) = 0$. Then doubly stochastic Poisson process is defined by the formula

$$A(t) = A^*(A(t)). \quad (1)$$

Further we assume that $A(t) = \int_0^t \lambda(y) dy$, where a random intensity function $\lambda(t)$ has nonnegative bounded trajectories.

Basic properties of DSPP are described, e.g., in (Grandell [5]). First of all let us note that interarrival times for this process form a sequence of dependent random variables even for a deterministic but nonconstant intensity function. Besides, for any nonrandom function $\lambda_0(t)$ the conditional distribution of the process $A(t)$ given $\lambda(t) = \lambda_0(t)$ coincides with the distribution of the Poisson process having the intensity function $\lambda_0(t)$.

We focus our attention on the periodic and regenerative intensity functions.

Definition 1. A stochastic process $\{V(t), t \geq 0\}$ is a periodic one with the period T if its finite-dimensional distributions are T-time-shift invariant.

Some examples will be given later on.

For a DSPP with a regenerative intensity function $\lambda(t)$ we introduce the following notation: $t_0 = 0$,

t_n is the moment of the n-th customer's arrival to the system ($n = 1, 2, \dots$),

$\{a_n = t_n - t_{n-1}\}_{n=1}^{\infty}$ is the sequence of the interarrival times,

$\{\theta_n\}_{n=1}^{\infty}$ are consecutive regeneration points of $\lambda(t, \omega)$,

$\{\tau_n = \theta_{n+1} - \theta_n\}_{n=1}^{\infty}$ are regeneration periods of $\lambda(t, \omega)$,

$\xi_n = A(\theta_{n+1}) - A(\theta_n)$ is the number of customers arriving during the n-th regeneration period.

The following result provides new opportunities for asymptotical analysis of queueing systems with a DSPP as input flow.

Without loss of generality and for the sake of brevity we can put $\theta_1 = 0$. Moreover, we write τ instead of τ_1 .

Theorem 1. *Let $\lambda(t)$ be a regenerative process and $E\tau < \infty$. There exists a stationary sequence $\{\hat{a}_k\}_{k=1}^{\infty}$ such that the sequence $\{a_{n+k}\}_{k=1}^{\infty}$ weakly converges to $\{\hat{a}_k\}_{k=1}^{\infty}$ as $n \rightarrow \infty$.*

Proof. Denote by ν_n the number of the regeneration period of $\lambda(t)$ on which the n-th jump of $A(t)$ occurs, i.e. $\nu_n = \min\{k \geq 1 : t_n \geq \theta_k\}$.

For $j = 0, 1, 2, \dots$ introduce $\zeta_j^{(n)} = t_{n+j} - \theta_{\nu_n}$ and denote by $f_n^{(m)}(x_0, x_1, \dots, x_m)$,

$x_0 < x_1 < \dots < x_m$, the density of the distribution of $(\zeta_0^{(n)}, \dots, \zeta_m^{(n)})$,

$m = 0, 1, \dots$; $f_n(x) = f_n^{(0)}(x)$.

At first we prove the following

Lemma 1. *There exists a limit*

$$\lim_{n \rightarrow \infty} f_n(x) = \frac{E\lambda(x)\mathbf{1}_{\tau > x}}{EA(\tau)}, \quad (2)$$

where $\mathbf{1}_{\tau > x}$ is the indicator of the event $\{\tau > x\}$.

Proof. In view of properties of DSPP one can see that $\{\xi_i\}_{i=1}^{\infty}$ is a sequence of i.i.d.r.v's and

$$k_j = \mathbf{P}(\xi_i = j) = \mathbf{E} \frac{\Lambda(\tau)^j}{j!} e^{-\Lambda(\tau)}.$$

From this point of view ν_n is the discrete renewal process generated by the sequence $\{\xi_i\}_{i=1}^{\infty}$, i.e. $\nu_n = \min\{k \geq 1 : \sum_{i=1}^k \xi_i \geq n\}$, $n = 1, 2, \dots$.

Denote by $\gamma_n = n - 1 - \sum_{j=1}^{\nu_n-1} \xi_j$ the defect of the renewal process generated by $\{\xi_i\}_{i=1}^{\infty}$. Moreover, γ_n is the number of customers that had entered the system on the period before the n -th customer's arrival. Set $\alpha_n(j) = \mathbf{P}(\gamma_n = j)$. In accordance with the renewal theorem (Feller [4], ch. XI) there exists a limit

$$\lim_{n \rightarrow \infty} \alpha_n(j) = \frac{1}{\mathbf{E}\Lambda(\tau)} \sum_{i=j+1}^{\infty} k_i = \alpha(j).$$

Then

$$f_n(x)dx = \sum_{j=0}^{n-1} \mathbf{P}(t_n \in (x, x+dx) | \gamma_n = j) \alpha_n(j). \quad (3)$$

The probability $\mathbf{P}(t_n \in dx | \gamma_n = j)$ is equal to the conditional probability that the n -th jump of $A(t)$ occurs on the interval $(x, x+dx)$ from the regeneration period beginning provided that its index on the period is $j+1$. This probability does not depend on n as far as $\lambda(t)$ is a regenerative process. Furthermore, for $j < n$,

$$\mathbf{P}(t_n \in dx | \gamma_n = j) = \frac{\mathbf{E} \frac{\Lambda^j(x)}{j!} e^{-\Lambda(x)} \lambda(x) \mathbf{1}_{\tau > x} dx}{\mathbf{E} \int_0^{\tau} \frac{\Lambda^j(x)}{j!} e^{-\Lambda(x)} \lambda(x) dx} = \frac{\mathbf{E} \frac{\Lambda^j(x)}{j!} e^{-\Lambda(x)} \lambda(x) \mathbf{1}_{\tau > x} dx}{\sum_{i=j+1}^{\infty} k_i} dx. \quad (4)$$

Now we complete the proof of Lemma 1 by substitution of this expression in (3) and taking a limit.

Let us return to the proof of Theorem 1. For nonnegative y_1, \dots, y_m we denote by $P_n^{(m)}(y_1, \dots, y_m)$ the distribution density of the vector $(a_n, a_{n+1}, \dots, a_{n+m})$. Taking into account Lemma 1 we have

$$\begin{aligned} P_n^{(m)}(y_1, \dots, y_m) &= \mathbf{E} \int_0^{\tau} f_n^{(m)}(x, x+y_1, \dots, x+y_m) dx = \\ &= \mathbf{E} \int_0^{\tau} f_n(x) e^{-(\Lambda(x + \sum_{j=1}^m y_j) - \Lambda(x))} \prod_{j=1}^m \lambda(x + \sum_{i=1}^j y_i) dx \xrightarrow{n \rightarrow \infty} \end{aligned}$$

$$\xrightarrow{n \rightarrow \infty} \frac{1}{\mathbb{E}A(\tau)} \mathbb{E} \int_0^\tau e^{-\Lambda(x + \sum_{j=1}^m y_j) - \Lambda(x)} \prod_{j=0}^m \lambda(x + \sum_{i=1}^j y_i) dx. \quad (5)$$

One can see that the distribution of the vector $(a_{n+s}, a_{n+s+1}, \dots, a_{n+s+m})$ has the same limit for any s . Now the weak convergence follows from the regeneration property of $\lambda(t)$.

For illustration we write the density of the one-dimensional distribution:

$$p_{\widehat{a}_k}(y) = \frac{1}{\mathbb{E}A(\tau)} \mathbb{E} \int_0^\tau e^{-\Lambda(x+y) - \Lambda(x)} \lambda(x) \lambda(x+y) dx. \quad (6)$$

It follows from regeneration property of $\lambda(t)$ that there exists a limit

$$\lim_{t \rightarrow \infty} \frac{A(t)}{t} = \lambda \quad \text{a.s. and} \quad \lambda = \frac{1}{\mathbb{E}\widehat{a}_n} = \frac{\mathbb{E}A(\tau)}{\mathbb{E}\tau}.$$

Now we consider some examples.

Example 1. In the case of deterministic periodic intensity $\lambda(t)$ with a period T the density $f(x)$ is of the form $f(x) = \lambda(x)/A(T)$.

Example 2. Let $v(t)$ be a nonnegative function on $[0, \infty)$ and $\{\tau_i\}_{i=1}^\infty$ be a sequence of i.i.d.r.v's with d.f. $F(x)$. We put $\theta_0 = 0$, $\{\theta_i = \sum_{j=1}^i \tau_j\}_{i=1}^\infty$ and $N(t) = \max\{n \geq 0 : \theta_n \leq t\}$. Intensity function $\lambda(t, \omega)$ is given by the relation $\lambda(t, \omega) = v(t - \theta_{N(t)})$. We note that process $\lambda(t)$ is a regenerative but nonperiodic one. The limit distribution of $\zeta_0^{(n)}$ is given by the formula $f(x) = v(x)\overline{F}(x) / \int_0^\infty v(y)\overline{F}(y)dy$. If $v(t) \equiv v$ we get $f(x) = \overline{F}(x)/\mathbb{E}\tau$ and this function does not depend on v .

Example 3. Let $\{\mu_{ij}(t), t \geq 0\}_{i,j=0}^M$ and $\{\lambda_i(t), t \geq 0\}_{i=0}^M$ be collections of nonnegative bounded periodic functions with period T . A control Markov chain $U(t)$ for a Markov modulated process $A(t)$, see (Asmussen [3]), is defined by infinitesimal parameters $\mu_{ij}(t)$. A stochastic intensity function $\lambda(t)$ is given by the relation

$$\lambda(t) = \sum_{i=0}^M \lambda_i(t) \mathbf{1}_{U(t)=i}. \quad (7)$$

Let us introduce a Markov chain $U_k = U(kT)$. The regeneration points $\{\theta_j\}_{j=1}^\infty$ of $\lambda(t)$ are defined as consecutive hitting times of the state $\{0\}$ by U_k , i.e. $\theta_0 = 0$, $\theta_i = \min\{kT > \theta_{i-1} : U_k = 0\}$ and $\tau_i = \theta_i - \theta_{i-1}$. One

can easily see that a Markov chain $U(t)$ has a limit periodic distribution and there exists $\lim_{k \rightarrow \infty} \mathbf{P}(U_k = j) = \pi_j$ so that $\mathbf{E}\tau = \frac{T}{\pi_0}$. In this case we have

$$f(x) = \begin{cases} \frac{\pi_0}{T} \sum_{j=0}^M P_{0j}(x) \lambda_j(x) & \text{for } x \in [0, T], \\ \frac{\pi_0}{T} \sum_{i=1}^M \mathbf{P}(\tau > kT, U_k = i) \sum_{j=0}^M P_{ij}(x - kT) \lambda_j(x - kT) & \text{for } x \in [kT, (k+1)T]. \end{cases}$$

Here $P_{ij}(y) = P(U(T+y) = j | U(T) = i)$.

Example 4. Assume a semi-Markov process $\{U(t), t \geq 0\}$ taking values $0, 1, 2, \dots$ to be defined on a probability space $(\Omega, \mathcal{F}, \mathbf{P})$. Let $\{U_n\}_{n=0}^\infty$ be its embedded Markov chain having an ergodic transition matrix $\mathbf{P} = \|P_{ij}\|$. For the process $U(t)$ let $F_{ij}(x)$ be the d.f. of the sojourn time in the state i given that the next state will be j . Let $m_{ij} = \int_0^\infty x dF_{ij}(x)$, $F_i(x) = \sum_j P_{ij} F_{ij}(x)$ and $m_i = \int_0^\infty x dF_i(x)$, moreover, $0 < m_{ij} < m < \infty$ for all i, j . Additionally suppose that a family of the functions $\{\lambda_{ij}(t), t \geq 0\}_{i,j=0}^\infty$ is defined. Let $\{s_j\}_{j=0}^\infty, s_0 = 0$, be a nondecreasing sequence of jump times for the process $U(t)$. Introduce a counting process $n(t) = \max\{k \geq 0 : s_k < t\}$. A random intensity function of DSPP is determined by the relation

$$\lambda(t) = \lambda_{U_n(t), U_{n(t)+1}}(t). \tag{8}$$

It is natural to call such a process semi-Markov modulated. If $\lambda_{ij}(t) \equiv \lambda_{ij}$ for all $i, j = 0, 1, \dots$, then the process $\lambda(t)$ is regenerative one. The regeneration points $\{\theta_n\}_{n=1}^\infty$ are the consecutive moments when the control process $U(t)$ reaches some fixed state, for example $\{0\}$. If $\lambda_{ij}(t)$ are periodic functions with period T and $F_{ij}(x)$ are distribution functions with jumps in points $\{jTn^{-1}, j, n \in \mathbf{N}\}$, then $\lambda(t)$ is a periodic regenerative process. Additionally one can see that $\lambda(t)$ is a periodic regenerative process if, e.g., $F_{0j}(x) = 1 - e^{-\mu_0 x}, j=1, 2, \dots$

For arbitrary distributions $F_{ij}(x)$ and time-dependent $\lambda_{ij}(t)$ the random intensity $\lambda(t)$ is not a regenerative process.

Theorem 1 allows us to apply traditional asymptotical methods of queueing theory to the analysis of periodic models. As illustration we give two results concerning the limit regime existence and the heavy traffic situation.

3 Existence of the limit regime.

We consider an r -server queue with FIFO queueing discipline and doubly stochastic Poisson process $A(t)$ as input flow. Service times $\{\beta_i\}_1^\infty$ are supposed to be independent random variables with a common d.f. $B(x)$ and

finite mean b . It is also assumed that the sequence $\{\beta_i\}_1^\infty$ does not depend on $A(t)$. Additionally, for the n -th customer there exists a random variable η_n which bounds its sojourn time in the system. On the expiration of the period η_n the customer leaves the system. It is possible that $\alpha = \mathbf{P}(\eta_n = \infty) > 0$, i.e. a customer may be in the system during arbitrary long time. In the case $\alpha = 1$ we get a system with unbounded sojourn time. Moreover, we suppose that η_n is a sequence of i.i.d.r.v's not depending on $\{\beta_i\}_1^\infty$ and $A(t)$.

We define the traffic coefficient as $\rho = \alpha\lambda b$. Let w_n be waiting time of the n -th customer, $W(t)$ virtual waiting time process and $q(t)$ the customers number in the system at time t .

Theorem 2. *Let $\lambda(t, \omega)$ be a regenerative process and $\mathbf{E}\tau < \infty$. Then there exists the limit*

$$\lim_{n \rightarrow \infty} \mathbf{P}(w_n \leq x) = H_1(x). \quad (9)$$

a) *If regeneration period τ has a nonlattice distribution then there exists*

$$\lim_{t \rightarrow \infty} P(W(t) \leq x) = H_2(x). \quad (10)$$

b) *If $\lambda(t, \omega)$ is a periodic process with period T and regeneration period τ has a T -lattice distribution then for any $t \geq 0$ there exists the limit*

$$\lim_{n \rightarrow \infty} P(W(nT + t) \leq x) = H(t, x) \quad (11)$$

where $H(t, x)$ is a periodic function in t .

In the case a) $H_1(x) = H_2(x)$ and in the case b)

$$H_1(x) = \frac{1}{\mathbf{E}A(\tau)} \mathbf{E} \int_0^\tau H(t, x) \lambda(t) dt \quad (12)$$

Functions $H(x)$ and $H(t, x)$ are d.f.'s iff the traffic coefficient $\rho < 1$. Otherwise they are identically zero.

Proof. Existence of the limit (9) follows from Theorem 2 and results for a queueing system with a stationary metrically transitive control sequence $\{a_n, \beta_n, \eta_n\}_{n=1}^\infty$ obtained in (Afanaseva and Martynov [1]). Furthermore, we get that $H_1(x)$ is a d.f. iff traffic coefficient $\rho < 1$. Otherwise, the sequence $\{w_n\}$ is stochastically unbounded. It means that $W(t)$ stochastically bounded iff $\rho < 1$. We note that $W(t)$ is a regenerative process. The regeneration points $\{\chi_n\}_{n=1}^\infty$ can be defined by the relations

$$\chi_n = \min\{\theta_j > \chi_{n-1} : q(\theta_j - 0) = 0\}, \quad \chi_0 = 0.$$

So, the regeneration points of $W(t)$ are the consecutive moments θ_n when the system is empty. Thus existence of the limit (10) follows from Smith's

theorem (Smith [7]). Moreover we find that $H_2(x)$ is a d.f. if $\rho < 1$ and $H_2(x) \equiv 0$ if $\rho \geq 1$.

To prove the existence of the limit (11) we note that $W(nT)$ is a regenerative process and χ_n is a sequence of its regeneration points. As above, using Smith's theorem, we establish that there exists the limit

$\lim_{n \rightarrow \infty} \mathbf{P}(W(nT) \leq x) = H(0, x)$. Furthermore, $H(0, x)$ is a d.f. iff $\rho < 1$. For $y \in [0, T]$ we consider a system S_y with DSPP input having intensity function $\lambda_y(t) = \lambda(t + y)$. Let $W_y(t)$ be a virtual waiting time process for this system and $W_y(0) = W(y)$. It is clear that $W_y(t) = W(t + y)$. Therefore there exists the limit (11).

The relation (12) one can easily obtain from (2).

Now we return to our examples.

If $\lambda(t)$ is a deterministic (non-random) periodic function (Example 1) the condition of the periodic distribution existence takes the following form $\alpha b T^{-1} \int_0^T \lambda(y) dy < 1$. This result for the case $\alpha = 1$ was obtained in (Harrison and Lemoine [6]).

For the Example 2 we have $\lambda = \int_0^\infty v(y) \bar{F}(y) dy / \int_0^\infty \bar{F}(y) dy$.

For the case of a periodic Markov modulated process (Example 3) we get $\lambda = T^{-1} \sum_{i=0}^m \int_0^T P_i(t) \lambda_i(t) dt$, where $P_i(t)$ is a periodic distribution of the control Markov chain $U(t)$.

Consider a semi-Markov modulated process (Example 4). If $\lambda(t)$ is a periodic regenerative process, we get the formula $\lambda = \sum_{i,j} \pi_i \lambda_{ij} m_{ij} m_i^{-1}$, where

$\lambda_{ij} = T^{-1} \int_0^T \lambda_{ij}(t) dt$ and π_i is a stationary distribution of the control semi-Markov process $U(t)$.

So conditions of the limit periodic regime existence can be found in the terms of the control process characteristics and the mean intensity over period.

4 Heavy traffic situation.

For queueing systems with rather complicated input flow, in particular, DSPP, it is impossible (with rare exceptions) to obtain explicit expressions of their operating characteristics such as queue length, waiting time or loss probability. Therefore we give in this section an asymptotic result for queue length in a single-server system with bounded sojourn time.

Let $\{S_\varepsilon\}$ be a family of such systems depending on parameter $\varepsilon \in (0, 1)$. The input flow for S_ε is DSPP with the intensity function

$$\lambda_\varepsilon(t) = (1 - \varepsilon) \rho^{-1} \lambda(t). \tag{13}$$

We consider the limit regime and denote by $q_\varepsilon(t)$ the customers number in S_ε at time t .

Theorem 3. *Let $\lambda(t)$ be a regenerative process, $\rho < 1$ and $\mathbf{E}\tau^{2+\delta} < \infty$, $\mathbf{E}\beta^{2+\delta} < \infty$ for some $\delta > 0$. Then*

$$\mathbf{P}(\varepsilon q_\varepsilon(t) > x) \xrightarrow{\varepsilon \rightarrow 0} e^{-2x/\sigma^2}, \quad \text{where}$$

$$\sigma^2 = \alpha\lambda \left(\frac{b_2}{b} + \frac{D(A(\tau) - \lambda\tau)}{\lambda^2 \mathbf{E}\tau} \right) \quad \text{and} \quad b_2 = \mathbf{E}\beta^2.$$

The proof is based on the theorem for queueing systems with unbounded sojourn time, obtained in (Afanaseva and Bashtova [2]) and the following fact.

Lemma 2. *Let $\tilde{q}_\varepsilon(t)$ be the customers number in the system with unbounded sojourn time and an intensity function $\lambda_\varepsilon(t)$ defined by (13). Under the Theorem 3 conditions processes $\tilde{q}_\varepsilon(t)$ and $q_\varepsilon(t)$ are asymptotically equivalent, i.e. for any fixed t*

$$\frac{\tilde{q}_\varepsilon(t)}{q_\varepsilon(t)} \xrightarrow[\varepsilon \rightarrow 0]{P} 1.$$

The proof is based on majorizing methods. It is omitted containing many technical details.

It is possible to establish some results concerning C -convergence for $q_\varepsilon(t)$. They allow us to study the asymptotical behaviour of functionals (such as supremum) on trajectories of the process under consideration.

Acknowledgement. The research was partially supported by RFBR grant 10-01-00266a.

References

1. Afanaseva, L. G., Martynov, A. V. "On ergodic properties of queueing systems with bounded sojourn times." *Probability Theory and Its Applications* 14, N1, 102–112 (1969) (in Russian)
2. Afanasyeva, L. G., Bashtova, E.E. "Limit theorems for queueing systems with doubly stochastic Poisson input (heavy traffic conditions)." *Problems of Information Transmission*, 4, N4, 81–100 (2008).
3. Asmussen, S. *Applied Probability and Queues*. John Wiley and Sons, Chichester, New York. (1987)
4. Feller, W. *An introduction to Probability Theory and Its Applications*. John Wiley and Sons, New York, London, Sydney. (1966)
5. Grandell, J. "Doubly stochastic Poisson processes." In *Lecture Notes In Mathematics*, 529 (1976).
6. Harrison, J.M., Lemoine, A.J. "Limit theorems for periodic queues." *Journal of Applied Probability* v.14, p.566–576. (1977)
7. Smith, W. L., "Regenerative stochastic processes." *Proceedings of International Congress of Mathematicians*, 2, 304–305 (1954).

Queueing Systems in Regenerative Random Environment

Larisa G. Afanasyeva² and Timopheyy N. Belorusev¹

¹ Mechanics and Mathematics Department
Moscow State University, Moscow, Russia
(e-mail: timopheyy.belorusev@gmail.com)

² Mechanics and Mathematics Department
Moscow State University, Moscow, Russia
(e-mail: afanas@mech.math.msu.su)

Abstract. In this paper we present the methods of proving ergodicity conditions for queueing models with the input flows operating in a stochastic environment. We consider two models. The first one is a single-server system with a cyclic input flow and the second one is a system with impatient customers (i.e. with the possibility of rejections). The conditions of the stochastic boundedness and necessary and sufficient ergodicity conditions are established.

Keywords: Queueing theory, Cyclic process, Regeneration, Rejection, Waiting time.

1 Introduction

We consider queueing models with the cyclic or regenerative input processes evolving in a random environment. The majority of the flows considered in queueing theory falls within this class. They also find useful applications in inventory theory, reliability theory, transportation nets, etc. To illustrate our approaches we give two models. The first of them is a single-server system with unbounded waiting time. The second model is a system with rejections.

2 Basic definitions

A stochastic process $\{X(t), t \geq 0\}$, $X(0) = 0$, on a probability space $(\Omega, \mathcal{F}, \mathbf{P})$ with nondecreasing left-continuous trajectories is called a stochastic flow. Further this process will represent either the number of the arriving customers during the time interval $[0, t)$ or their total service time. In the first case trajectories of $X(t)$ have unit jumps only.

Let $\{\theta_k, k \geq 0\}$, $\theta_0 = 0$, be a nondecreasing sequence of random variables. For $k \geq 0$ we put

$$\tau_k = \theta_{k+1} - \theta_k, \delta_k(t) = I_{[0, \tau_k)}(t), x_k(t) = [X(\theta_k + t) - X(\theta_k)]\delta_k(t),$$

$$\xi_k = x_k(\tau_k), \chi_k(\omega) = \{x_k(t), \tau_k\}, S_k = \sum_{j=1}^k (\xi_j - \tau_j), S_0 = 0.$$

Definition 1. A stochastic flow $X(t)$ is said to be cyclic if the sequence of the random elements $\{\chi_k\}_{k=1}^\infty$ is stationary and metrically transitive, $\mathbf{E} \xi_1 < \infty$, $\mathbf{E} \tau_1 < \infty$, and $\mathbf{P}(\xi_0 < \infty, \tau_0 < \infty) = 1$.

The random elements χ_k are called cycles. We remark that $X(t)$ has an intensity $\lim_{t \rightarrow \infty} X(t)/t = \mathbf{E} \xi_1 / \mathbf{E} \tau_1$ a.s.

Definition 2. A cyclic flow $X(t)$ is called regenerative if it has independent cycles.

Let $\{U(t), t \geq 0\}$ be a stochastic process on $(\Omega, \mathcal{F}, \mathbf{P})$ with values in a topological space $\{E, \mathcal{B}_E\}$.

Definition 3. A cyclic flow $X(t)$ is evolving in the random environment $\{U(t), t \geq 0\}$ if the following conditions hold:

1. The sequence $\{\theta_k\}$ consists of the Markov moments with respect to the process $U(t)$.
2. The sequence $\{\chi_k(\omega), U(\theta_k + t)\delta_k(t)\}_{k=1}^\infty$ is stationary and metrically transitive.
3. There exists a nonnegative and bounded function $f(u)$ on E such that a.s.

$$\mathbf{E}(X(t) | U(s), 0 \leq s \leq t) = \int_0^t f(U(s)) ds.$$

There is a wide range of the flows that are cyclic or regenerative. We will consider some examples below.

3 Stochastic boundedness and ergodicity conditions for cyclic systems $\mathbf{G}|\mathbf{G}|1|\infty$

Consider a single-server system S with unbounded waiting time. Let $X(t)$ be the total service time of the customers arriving during the time interval $[0, t)$ and $\rho = \mathbf{E} \xi_1 / \mathbf{E} \tau_1$. Denote by $W(t)$ the workload process.

Theorem 1. *Let $X(t)$ be a cyclic flow. If $\rho > 1$, then the process $W(t)$ is stochastically unbounded. If $\rho < 1$, then the process $W(t)$ is stochastically bounded.*

Proof. We assume $W(0) = 0$. The case $W(0) > 0$ would not bring any substantial difference. Put $W_n = W(\theta_n - 0)$ for $n = 0, 1, 2, \dots$ and introduce

$$W_n^- = [W_{n-1}^- + \xi_n - \tau_n]^+, W_n^+ = [W_{n-1}^+ - \tau_n]^+ + \xi_n, W_0^- = W_0^+ = 0. \quad (1)$$

It is easy to see that $W_n^- \leq W_n \leq W_n^+$ a.s. For $\rho > 1$ we have $W_n^- \xrightarrow{P} \infty$ as $n \rightarrow \infty$ [1], so the first assertion of the theorem is clear.

Let $\rho < 1$ and consider $\{W_n^+\}$. We can assume that $\{\xi_n, \tau_n\}$ is defined for $n = 0, \pm 1, \pm 2, \dots$ as a stationary and metrically transitive sequence. Let us denote

$$S_{-k} = \sum_{j=-k+1}^0 (\xi_j - \tau_j), \quad M_n = \max[\xi_0, \max_{1 \leq j \leq n} [\xi_{-j} + S_{-j+1}]].$$

After a series of transformations from the recurrent equations (1) we obtain $W_n^+ \stackrel{d}{=} M_n$. Since $\mathbf{E} \xi_j < \mathbf{E} \tau_j$, the limit $M = \lim_{n \rightarrow \infty} M_n$ is finite a.s. This implies the stochastic boundedness of W_n^+ , W_n , and $W(t)$.

The process $\{W_n\}$ can be stochastically bounded if $\rho = 1$ [1], however, under certain conditions it is stochastically unbounded, for instance, in $GI|GI|1|\infty$ system [2].

Corollary 1. *Let $X(t)$ be a cyclic flow in the random environment $U(t)$. Then the traffic intensity ρ is given by the relation*

$$\rho = (\mathbf{E} \tau_1)^{-1} \mathbf{E} \int_{\theta_1}^{\theta_2} f(U(s)) ds. \quad (2)$$

Proof. Since θ_n is a Markov moment with respect to $U(t)$ we get

$$\begin{aligned} \mathbf{E} X(\theta_n) &= \mathbf{E} \int_0^\infty X(y) I(\theta_n \in dy) = \mathbf{E} \int_0^\infty \mathbf{E}(X(y) I(\theta_n \in dy) | U(s), s \leq y) = \\ &= \mathbf{E} \int_0^\infty I(\theta_n \in dy) \int_0^y f(U(s)) ds = \mathbf{E} \int_0^{\theta_n} f(U(y)) dy. \end{aligned}$$

Now (2) follows from the relation $\mathbf{E} \xi_1 = \mathbf{E} X(\theta_2) - \mathbf{E} X(\theta_1)$ and definition of ρ .

Corollary 2. *Let $X(t)$ be a cyclic flow in the random environment $U(t)$. If there exists*

$$\lim_{t \rightarrow \infty} \mathbf{P}(U(t) \in A) = \pi(A) \quad (A \in \mathcal{B}_E),$$

where $\pi(A)$ is a probability measure on \mathcal{B}_E , then $\rho = \int_E f(x) \pi(dx)$.

The proof is based on the law of large numbers for stationary and metrically transitive sequences and properties of the random environment.

The problem of the proper limit distribution existence

$$\lim_{t \rightarrow \infty} \mathbf{P}\{W(t) \leq x\} = \Phi(x) \quad (3)$$

should be investigated under additional assumptions. It is easily solved for regenerative flows.

Theorem 2. *Suppose that $X(t)$ is a regenerative flow and the distribution of τ_1 has an absolutely continuous component. Then there exists the limit (3) for any initial state $W(0)$. Furthermore, $\Phi(x)$ is a distribution function iff $\rho < 1$.*

4 Ergodicity of single-server queueing systems with rejections

Let us consider a single-server queueing system S with rejections. A new customer encountering j other customers in the system stays for service with the probability f_j and leaves with the probability $1 - f_j$, where $f_j \in (0, 1]$. Service times are i.i.d.r.v.'s with an arbitrary d.f. $B(x)$ and finite mean b . The process $X(t)$ denotes the number of the customers arriving during $[0, t)$. It is a regenerative stochastic flow with unit jumps and intensity $\lambda = \mathbf{E} \xi_1 / \mathbf{E} \tau_1$. To avoid technical details we suppose that the distribution of τ_1 contains an absolutely continuous component. Let $W(t)$ be the workload process and $Q(t)$ the number of customers in the system S at time t .

Theorem 3. *Suppose $f_j > 0$, $j \geq 0$, and put $\bar{f} = \limsup_{j \rightarrow \infty} f_j$, $\underline{f} = \liminf_{j \rightarrow \infty} f_j$. There exists*

$$\lim_{t \rightarrow \infty} \mathbf{P}\{W(t) \leq x\} = \Phi(x)$$

and $\Phi(x)$ is a distribution function if

$$\lambda b \bar{f} < 1 \tag{4}$$

and $\Phi(x) \equiv 0$ if $\lambda b \underline{f} > 1$.

Proof. To begin with we prove the following

Lemma 1. *Let the sequence $\{f_j\}$ have the form*

$$f_j = \begin{cases} \alpha_1, & \text{if } j < k, \\ \alpha_2, & \text{if } j \geq k, \end{cases} \tag{5}$$

for some $k \geq 0$, $\alpha_1 > 0$, $\alpha_2 > 0$. There exists the limit (3) and $\Phi(x)$ is a distribution function if

$$\lambda b \alpha_2 < 1. \tag{6}$$

We have $\Phi(x) \equiv 0$ if

$$\lambda b \alpha_2 > 1. \tag{7}$$

Proof of Lemma 1. First suppose (6) to be fulfilled. In the case $\alpha_1 \leq \alpha_2$ the statement of the lemma is a simple corollary of Theorem 1. It is sufficient to consider a system with $\hat{f}_j = \alpha_2$ for all j . So, we assume that $\alpha_1 > \alpha_2$. Set

$W_n = W(\theta_n - 0)$, $Q_n = Q(\theta_n - 0)$. These processes are regenerative with the regeneration points $\{n_k\}$ such that $W_{n_k} = 0$. It follows from Smith's theorem [3] that limit (3) exists. Besides, we have two possibilities: $\Phi(x) \equiv 0$ or $\Phi(x)$ is a distribution function. Suppose (6) holds, but $\Phi(x) \equiv 0$, i.e. processes $W(t)$, W_n , Q_n are stochastically unbounded.

Define a family $\{\beta_j^n\}_{j=1}^\infty$, for $n = 1, 2, \dots$, of independent sequences of i.i.d.r.v.'s with the d.f. $B(x)$. Let $\{e_j^n\}_{j=1}^\infty$, for $n = 1, 2, \dots$, be a family of independent sequences of i.i.d.r.v.'s taking values 0 and 1 with the probabilities $1 - \alpha_2$ and α_2 respectively. Define

$$\gamma_n = \sum_{j=1}^{\xi_n} \beta_j^n, \quad \hat{\gamma}_n = \sum_{j=1}^{\xi_n} \beta_j^n e_j^n.$$

We introduce an event A_n that during the n th regeneration period $[\theta_{n-1}, \theta_n)$ of the process $X(t)$ the number of the customers in the system is greater than k . Since $\Phi(x) \equiv 0$, for any $\varepsilon > 0$ there exists N_ε such that for $n > N_\varepsilon$ we have

$$\mathbf{P}(\bar{A}_n) < \varepsilon. \quad (8)$$

Let us estimate

$$\begin{aligned} W_n &\leq (W_{n-1} - \tau_n + \hat{\gamma}_n)I(A_n) + ([W_{n-1} - \tau_n]^+ + \gamma_n)I(\bar{A}_n) \leq \\ &\leq (W_{n-1} - \tau_n + \hat{\gamma}_n)I(A_n) + ((W_{n-1} - \tau_n)(1 - I(\tau_n > W_{n-1})) + \gamma_n)I(\bar{A}_n) \leq \\ &\leq W_{n-1} - \tau_n + \hat{\gamma}_n + \tau_n I(\tau_n > W_{n-1})I(\bar{A}_n) + \gamma_n I(\bar{A}_n). \end{aligned}$$

Consequently,

$$\mathbf{E}W_n \leq \mathbf{E}W_{n-1} - \mathbf{E}\tau_n + \mathbf{E}\hat{\gamma}_n + \mathbf{E}\tau_n I(\tau_n > W_{n-1})I(\bar{A}_n) + \mathbf{E}\gamma_n I(\bar{A}_n). \quad (9)$$

From (8) it follows that each of the last two summands in (9) is less than εC when n is large enough, where C is a constant independent of n . Hence,

$$\begin{aligned} \mathbf{E}W_n &\leq \mathbf{E}W_{n-1} - \mathbf{E}\tau_1 + \mathbf{E}\xi_1 b \alpha_2 + \varepsilon C = \\ &= \mathbf{E}W_{n-1} + \mathbf{E}\tau_1 (\lambda b \alpha_2 - 1) + \varepsilon C < \mathbf{E}W_{n-1}. \end{aligned}$$

This fact contradicts the assertion that W_n is stochastically unbounded. Therefore, $W(t)$ and $Q(t)$ are stochastically bounded, so they are ergodic.

Now assume (7) to hold. While $Q_n \geq k$ the process W_n is minorized by a random walk with positive drift that tends to $+\infty$. Since $\alpha_1 > 0$ the process Q_n hits the range $[k, \infty)$ infinitely often. We have $\lambda b \alpha_2 = \mathbf{E}\hat{\gamma}_n / \mathbf{E}\tau_n$, so $\mathbf{P}(\hat{\gamma}_n > \tau_n) > 0$ due to (7). Therefore, W_n and Q_n are stochastically unbounded. This completes the proof.

Further we shall consider two queueing systems, namely, S with an arbitrary control sequence $\{f_j\}$ and \hat{S} with the control sequence $\{\hat{f}_j\}$ having the structure (5).

Lemma 2. *Assume $Q(0) = \widehat{Q}(0) = 0$ and $\alpha_1 \geq \alpha_2$. If $f_j \leq \widehat{f}_j$ for all $j \geq 0$, then stochastically*

$$Q(t) \leq \widehat{Q}(t) + 1, \quad t \geq 0. \quad (10)$$

If $f_j \geq \widehat{f}_j$ for all $j \geq 0$, then stochastically

$$Q(t) \geq \widehat{Q}(t) - 1, \quad t \geq 0.$$

The proof is based on the construction of a special probability space. It includes a lot of technical details and is omitted here.

Now we proceed to the proof of Theorem 3. Let (4) hold. There exists $\alpha_2 \leq 1$, so that $\bar{f} \leq \alpha_2$ and $\lambda b \alpha_2 < 1$. Therefore, there is k such that $f_j < \alpha_2$ for $j \geq k$. Consider a queueing system \widehat{S} with

$$\widehat{f}_j = \begin{cases} \alpha_1 = \max_{0 \leq j < k} f_j, & \text{if } j < k; \\ \alpha_2, & \text{if } j \geq k. \end{cases}$$

Since $\lambda b \alpha_2 < 1$, we see that \widehat{S} is ergodic according to Lemma 1. Consequently processes \widehat{W} and \widehat{Q} are stochastically bounded. The systems S and \widehat{S} satisfy the conditions of Lemma 2. In this case, stochastic inequality (10) holds. This results in the stochastic boundedness of the processes $W(t)$ and $Q(t)$. According to Smith's theorem S is ergodic.

The proof of the second part of the theorem is conducted in the same way.

Corollary 3. *Suppose there exists $\lim_{j \rightarrow \infty} f_j = f$. If $\lambda b f < 1$, then $W(t)$ is ergodic. If $\lambda b f > 1$, then $W(t) \xrightarrow{P} \infty, t \rightarrow \infty$.*

In the case $\lambda b f = 1$ both possibilities can take place depending on the sequence $\{f_j\}$. To illustrate, consider a system with the Poisson input of intensity λ and independent exponentially distributed service times with mean b . It follows from [4] that a Markov chain $Q(t)$ is ergodic iff

$$\sum_{j=1}^{\infty} \prod_{i=0}^{j-1} \frac{f_j}{f} < \infty. \quad (11)$$

Suppose $f_j = f e^{-\delta_j}$, where $\delta_j = (1 + j)^{-s}$, $s > 0$. One can easily see that (11) is fulfilled if $s \in (0, 1)$. Therefore, $Q(t)$ is ergodic in this case. If $s > 1$, then (11) does not hold, so $Q(t)$ is nonergodic.

5 Examples

Here we provide some examples of regenerative flows. From now on we assume that the process $X(t)$ denotes the number of the customers arriving during $[0, t)$ and $\lambda = \lim_{t \rightarrow \infty} X(t)/t$.

Example 1. Let $\{A(t), t \geq 0\}$, $A(0) = 0$, be a regenerative stochastic flow and $\{A(t), t \geq 0\}$ be a standard Poisson process not depending on $A(t)$. The random time substitution leads to a doubly stochastic Poisson process [5], i.e.

$$X(t) = A(\Lambda(t)).$$

Further we assume that $\Lambda(t) = \int_0^t \lambda(y) dy$, where $\lambda(y)$ is a nonnegative locally integrable bounded stochastic process named an intensity function. If $\lambda(t)$ is a regenerative stochastic process [3], then $\Lambda(t)$ and $X(t)$ are regenerative stochastic flows. Besides, $\lambda(t)$ is a stochastic environment for $X(t)$ and the function $f(u) \equiv u$.

From Corollary 2 we get $\lambda = \int_0^\infty s \pi(ds)$ if $\pi(x)$ is the stationary d.f. for $\lambda(t)$.

Example 2. For a Markov-modulated process (see [6]) the intensity function has the form

$$\lambda(t) = \sum_{k=1}^{\infty} \lambda_k I(U(t) = k),$$

where $U(t)$ is a stationary homogeneous Markov chain with a finite or countable set of states and $\{\lambda_k, k = 0, 1, 2, \dots\}$ is the collection of nonnegative numbers such that $\lambda_k \leq \lambda^* < \infty$ for any k . One can see that $U(t)$ is a stochastic environment for $X(t)$ and the function $f(s)$ is given by the relation

$$f(u) = \sum_{k=1}^{\infty} \lambda_k I(u = k).$$

Besides, $\lambda = \sum_{k=1}^{\infty} \lambda_k \pi_k$, where $\{\pi_k\}$ is a stationary distribution of the Markov chain $U(t)$.

Example 3. Assume that a stationary semi-Markov process $\{U(t), t \geq 0\}$ defined on $(\Omega, \mathcal{F}, \mathbb{P})$ takes nonnegative integer values. Let $\{\zeta_n, n = 1, 2, \dots\}$ be its embedded Markov chain having an ergodic transition matrix $P = (p_{ij})$. By $F_{ij}(x)$ we denote the d.f. of the sojourn time in the state i given that the next state will be j . Let $m_{ij} = \int_0^\infty x dF_{ij}(x)$, $F_i(x) = \sum_j p_{ij} F_{ij}(x)$, $m_i = \int_0^\infty x dF_i(x)$, $m_{ij} < m < \infty$ for all i, j . Additionally, suppose that a family of stochastic processes

$$Z = \{\{Z_{ij}^{(n)}(t), t \geq 0\}_{n=1}^\infty, i, j = 0, 1, 2, \dots\}$$

with stationary increments, not depending on $U(t)$, is defined on the same probability space. Their trajectories are nondecreasing and left-continuous functions taking nonnegative integer values. Furthermore, $Z_{ij}^{(n)}(0) = 0$. Let ν_{ij} be the intensity of $Z_{ij}^{(n)}(t)$. By $\{t_j\}_{j=0}^\infty$, $t_0 = 0$, we denote the nondecreasing sequence of the jump times for the process $U(t)$. Introduce a counting

process $N(t) = \max\{n \geq 0 : t_n \leq t\}$. For all integer $k \geq 1$ let Δ_k be the increment of the process $Z_{\zeta_{k-1}\zeta_k}^{(k)}(t)$ on the interval $[t_{k-1}, t_k)$ and let $\Delta(t)$ be the increment on the interval $[t_{N(t)}, t)$ of $Z_{\zeta_{N(t)}\zeta_{N(t)+1}}^{(N(t)+1)}(t)$. Setting $\zeta_0 = U(0)$, we define the process $X(t)$ as

$$X(t) = \sum_{k=1}^{N(t)} \Delta_k + \Delta(t).$$

We note that $X(t)$ is a regenerative flow and the regeneration points $\{\theta_j\}_{j=1}^{\infty}$ are the consecutive hitting times of some fixed state i^* by the control process $U(t)$. It is easy to see that $U(t)$ is a random environment for $X(t)$ and

$$E(X(t) | U(s), s \leq t) = \sum_{k=1}^{N(t)} \nu_{\zeta_{k-1}\zeta_k} (t_k - t_{k-1}) + \nu_{\zeta_{N(t)}\zeta_{N(t)+1}} (t - t_{N(t)}).$$

Let $\{\pi_j\}$ be a stationary distribution for the random environment $U(t)$. One can get the following relation for the intensity of $X(t)$

$$\lambda = \sum_{ij} \nu_{ij} \pi_i p_{ij} \frac{m_{ij}}{m_i}.$$

Using (4) we get the conditions of the limit distribution existence in terms of input flow characteristics.

Acknowledgement

The research is partially supported by the RFBR grant 10-01-00266a.

References

1. Loynes, R. M., "On a property of the random walks describing simple queues and dams". *J. Roy. Stat. Soc. Ser. B*, 27, 125–129 (1965).
2. Lindley, D. V., "The theory of queues with single server". *Proc. Cambirdge Phil. Soc.* 48, 277–289 (1952).
3. Smith, W. L., "Regenerative stochastic processes". *Proc. Roy. Soc. A* 232, 6–31 (1955).
4. Saaty, T. L., *Elements of Queueing Theory with Applications*, McGraw-Hill (1961).
5. Grandell, J., *Doubly Stochastic Poisson Processes*, Springer-Verlag (1976).
6. Asmussen, S., "Ladder heights and the Markov-modulated $M|G|1$ queue". *Stochastic Processes and Their Applications* 37, 313–326 (1991).

Stochastic Modeling of Web evolution

Efstathios Amarantidis, Ioannis Antoniou and Michalis Vafopoulos

PhD candidate, Aristotle University of Thessaloniki, Mathematics Department, Graduate Program in Web, Veria, Greece

Email: amartatis@yahoo.gr

Professor, Aristotle University of Thessaloniki, Mathematics Department, Graduate Program in Web, Veria, Greece

Email: iantonio@math.auth.gr

Adjunct Professor, Aristotle University of Thessaloniki, Mathematics Department, Graduate Program in Web, Veria, Greece

Email: vafopoulos@webscience.gr

Extended Abstract: In the first twenty years of its existence, the Web has proven, to have had a fundamental and transformative impact on all facets of our society. While the Internet has been introduced 20 years earlier, the Web has been its “killer” application with more than 1.5 billion users worldwide accessing more than 1 trillion web pages (excluding those that cannot be indexed, the “Deep Web”) (Googleblog 2008). Searching, social networking, video broadcasting, photo sharing, blogging and micro-blogging have become part of everyday life whilst the majority of software and business applications have migrated to the Web.

Today, the enormous impact, scale and dynamism of the Web in time and space demand more than our abilities to observe and measure its evolution process. Quantifying and understanding the Web lead to Web modeling, the backbone of Web Science research (Berners-Lee et al 2006). Web models should invest on Complexity (Antoniou et al 2000) beyond reductionism, linking structure to function and evolution (Prigogine 1999, Prigogine et al 2001, Meyers 2009). In this context, causality between events, temporal ordering of interactions and spatial distribution of Web components are becoming essential to addressing scientific questions at the Web techno-social system level.

The first steps towards understanding cyberspace involved measurements and statistics of the Internet traffic (Faloutsos et al 1999, Fabrikant et al 2002, Antoniou et al 2002 a, b, Antoniou et al 2003). The self-similar feature of the Internet was also found in the Web through preferential attachment (Barabasi et al 1999 a, b, Albert et al 1999).

Network science being a useful mathematical framework to formulate the non-reducible interdependence of Complex Systems (Prigogine 1999, Prigogine et al 2001) recently led to significant results not only in Web graph statistics, but moreover in biology (Kitano 2002), economics (Easley et al 2010) and sociology (Liljeros et al 2001). These results initiated a new understanding of Complexity in nature (Newman et al 2006).

The statistical analysis of the Web graph led to four major findings (Bonato et al 2005): on-line property (the number of nodes and edges changes with time), power law degree distribution with an exponent bigger than 2, small world property (the diameter is much smaller than the order of the graph) and many dense bipartite subgraphs.

In the light of these findings Kouroupas, Koutsoupias, Papadimitriou and Sideri proposed an economic-inspired model of the Web (KKPS model thereafter) (Kouroupas et al 2005 a, b) which explains the scale-free behavior. Web evolution is modeled as the interaction of

Documents, Users and Search Engines. The Users obtain satisfaction (Utility), when presented with some Documents by a Search Engine. The Users choose and endorse Documents with highest Utility and then the Search Engines improve their recommendations taking into account these endorsements, but not the dynamic interdependence of the Utility on the www state. Commenting on their results the authors have pointed out that (A) “more work is needed in order to define how the various parameters affect the exponent of the distribution” (of the in-degree of documents) and that (B) “increasing b (the number of endorsed documents) causes the efficiency of the algorithm to decrease. This is quite unexpected, since more user endorsements mean more complete information and more effective operation of the search engine. But the opposite happens: more endorsements per user seem to confuse the search engine.”

The purpose of this paper is to address and clarify the issues (A), (B) arising within the KKPS modeling scheme (Kouroupas et al 2005 b), through analysis and simulations and to highlight future research developments in Web modeling.

Results and Discussion

1. Concerning the dependence of the power-law exponent on the number α of recommended Documents by the Search Engine, the number k of topics and the number b of endorsed documents per User-Query, we found that the validity of the power law becomes less significant as b increases, both in the case $\alpha=b$ and in the case $\alpha \leq b$, confirming the results of Kouroupas et al [21]. Our simulations however, extended the investigation for different initial random distributions of the in-degree of Documents and for different values of α and b (Section 4).

2. In the case $\alpha=b$, Utility is useful only in terms of establishing compatibility between Utility Matrix and the Users-Queries and Documents bipartite graph, since all recommended Documents are endorsed according to the highest in-degree criterion.

3. Concerning the origin of the power law distribution of the in-degree of Documents, two mechanisms are identified in the KKPS model:

- Users-Queries endorse a small fraction of Documents presented (b).
- Assuming a small fraction of poly-topic Documents, the algorithm creates a high number of endorsements for them.

The above mechanisms are not exhaustive for the real Web graph. Indexing algorithms, crawler’s design, Documents structure and evolution should be examined as possible additional mechanisms for power law distribution.

4. Concerning the dependence of the efficiency of the search algorithm (price of anarchy [21]) on the number α of recommended Documents by the Search Engine, the number k of topics and the number b of endorsed documents per User-Query we found that the efficiency of the algorithm increases, as the number α of recommended Documents by the Search Engine, the number k of topics and the number b of endorsed Documents per User-Query increase (Section 5). Our simulations confirmed the results of Kouroupas et al [21], except the dependence on the number b of endorsed documents per User-Query where they found that “increasing b causes the efficiency of the algorithm to decrease. This is quite unexpected, since more user endorsements mean more complete information and more effective operation of the search engine. But the opposite happens: more endorsements per

user seem to confuse the search engine.” Therefore, in this case our result (Figure 7) confirmed their intuition but not their simulation.

5. According to [21] “The endorsement mechanism does not need to be specified, as soon as it is observable by the Search Engine. For example, endorsing a Document may entail clicking it, or pointing a hyperlink to it.” This hypothesis does not take into account the fundamental difference between clicking a link (browsing) and creating a hyperlink. Clicking a link during browsing is the “temporal” process called traffic of the Web sites [23]. Web traffic is observable by the website owner or administrator through the corresponding log file [24] and by third parties authorized (like search engine cookies which can trace clicking behavior [25] or malicious. On the contrary, creating a hyperlink results in a more “permanent” link between two Documents which is observable by all Users-Queries and Search Engines. Therefore, the KKPS algorithm actually examines the Web traffic and not the hyperlink structure of Documents which is the basis of the in-degree Search engine’s algorithm.

6. In this context, we remark that according to the published literature, Web traffic as well as Web content editing, are not taken into account in the algorithms of Search engines based on the in-degree (i.e. Pagerank [26]). These algorithms were built for Web 1.0 where Web content update and traffic monetization were not so significant. In the present Web 2.0 era with rapid change [27], the Web graph, content and traffic should be taken into account in efficient search algorithms. Therefore, birth-death processes for Documents and links and Web traffic should be introduced in Web models, combined with content update (Web 2.0) and semantic markup (Web 3.0 [28]) for Documents.

7. The discrimination between Users and Queries could facilitate extensions of the KKPS model in order to incorporate teleportation (a direct visit to a Document which avoids Search Engines) to a Document, different types of Users and relevance feedback between Documents and Queries [29].

8. In the KKPS model, Utility is defined to be time invariant linear function of R and D which by construction is not affecting the www state when $\alpha=b$. This is a first approximation which does not take into account the dynamic interdependence of the Utility on the www state. In reality, the evolution of the www state will change both R and D. A future extension of KKPS model should account for user behavior by incorporating Web browsing and editing preferences.

9. Lastly, it would be very useful to offer deeper insight in the Web’s business model by incorporating economic aspects in the KKPS model. This could be achieved by introducing valuation mechanisms for Web traffic and link structures and monetizing the search procedure (sponsored search [30]).

Keywords: Web science; Web modeling; scale-free networks; KKPS model; complex systems;

References

1. Albert R., Jeong H., Barabasi A.L., Diameter of the World-Wide Web, *Nature*, 401 (6749), 130 (1999).

2. Antoniou I., Reeve M., Stenning V., Information Society as a Complex System J., *Univ. Comp. Sci.* 6, 272-288 (2000).
3. Antoniou I., Ivanov Vi.V., Ivanov Valery V., Zrellov P.V., On the log-normal distribution of Network Traffic, *Physica D167*, 72-85 (2002).
4. Antoniou I., Ivanov V., Kalinovsky Yu., Kinetic model of Network traffic, *Physica A308*, 533-544 (2002).
5. Antoniou I., Ivanov Vi.V., Ivanov Valery V., Zrellov P. V., On a Statistical Model of Network Traffic, *Nucl. Instr. Meth. Phys. Res.* 4502, 768-771 (2003).
6. Barabasi A.-L., Albert R., Emergence of Scaling in Random Networks, in *Science* 286 (5439), 509 (1999).
7. Barabasi A.-L., Albert R., Jeong H., Scale-free characteristics of random networks: the topology of the world-wide web, *Physica A* 281, 69-77 (2000).
8. Berners-Lee T., Hall W., Hendler J. A., O'Hara K., Shadbolt N., Weitzner D. J., A framework for web science, in *Foundations and trends in web science*, vol. 1, issue 1. Boston: Now, (2006).
9. Bonato A., A Survey of Models of the Web Graph, in *Lecture Notes in Computer Science*, (3405), 159-172 (2005).
10. Easley D., Kleinberg J., *Networks, Crowds, and Markets: Reasoning About a Highly Connected World*, Cambridge University Press, (2010).
11. Fabrikant A., Koutsoupias E., Papadimitriou C. H., Heuristically Optimized Trade-Offs: A New Paradigm for Power Laws in the Internet, in *Lecture Notes in Computer Science*, (2380), 110-122 (2002).
12. Faloutsos M., Faloutsos P., Faloutsos C., On Power-Law Relationships of the Internet Topology, in *Computer communication review* 29 (4), 251-262 (1999).
13. Googleblog, <http://googleblog.blogspot.com/2008/07/we-knew-web-was-big.html> (2008).
14. Kitano H., Computational systems biology, *Nature*, (6912), 206-210 (2002).
15. Kouroupas G., Papadimitriou C., Koutsoupias E., Sideri M., An Economic Model of the Worldwide Web: Poster, 14th WWW Conference, (2005).
16. Kouroupas G., Koutsoupias E., Papadimitriou C. H., Sideri M., Experiments with an Economic Model of the Worldwide Web, in *Lecture Notes in Computer Science*, (3828), 46-54 (2005).
17. Liljeros F., Edling C.R., Amaral L.A., Stanley H.E., Aberg Y., The web of human sexual contacts, *Nature*, 411 (6840), 907-8 (2001).
18. Meyers R. A., *Encyclopedia of Complexity and Systems Science*, Springer, New York, (2009).
19. Newman M. E. J., Barabási A.-L., Watts D.J., *The structure and dynamics of networks*. Princeton, N.J.: Princeton University Press, (2006)
20. Prigogine I., *The End of Certainty*, Free Press, New York, 1999.
21. Prigogine I., Antoniou I., Science, Evolution and Complexity, in *Genetics in Europe*, Sommet européen Ed, 21-36 (2001).
22. Bondy J. A., Murty U. S. R., *Graph theory with applications*, The Macmillan Press Ltd., 1976.
23. Crovella M., Bestavros A., Self-Similarity in World Wide Web Traffic: Evidence and Causes, Performance Evaluation Review: a Quarterly Publication of the Special Interest Committee on Measurement and Evaluation, 24 (1), (1996) 160.

SMTDA 2010: Stochastic Modeling Techniques and Data Analysis
International Conference, Chania, Crete, Greece, 8 - 11 June 2010

24. Hallam-Baker M., Behlendorf B., Extended Log File Format, www.w3.org/TR/WD-logfile.html, retrieved January 2010
25. Attenberg J., Suel T., Pandey S., Modeling and predicting user behavior in sponsored search. Proceedings of the ACM SIGKDD International Conference on Knowledge Discovery and Data Mining (2009) 1067-1075.
26. Brin S., Page L., The anatomy of a large-scale hypertextual Web search engine, Computer Networks and ISDN Systems 30 (1-7) (1998) 107.
27. Oreilly T., What is Web 2.0: Design Patterns and Business Models for the Next Generation of Software. Communications & Strategies, No. 1, p. 17, First Quarter 2007. Available at SSRN: <http://ssrn.com/abstract=1008839> retrieved January 2010
28. J. Hendler, Web 3.0 emerging. Computer 42 (1) (2009) 111-113.
29. Jansen B. J., Spink A., Saracevic T., Real Life, Real Users, and Real Needs: A Study and Analysis of User Queries on the Web, Information Processing & Management 36 (2) (2000) 207-27.
30. Fain D. C., Pedersen J. O., Sponsored Search: A Brief History, Bulletin American Society for Information Science and Technology 32 (2) (2006) 12-13.

Simple Non-Recurrent Flow and Its Applications in the Problems of Reliability, Storage and Queueing Theory

Alexander Andronov and Jelena Revzina

Transport and Telecommunication Institute
 Lomonosova str. 1, LV-1019, Riga, Latvia
 Email: lora@mailbox.riga.lv
 Email: lana_revzina@tsi.lv

Abstract: In this paper the non-recurrent flow of arrivals is considered in a case, where interarrival times $\{X_n\}$ correspond to the Markov chain with the continuous state space $R_+ = (0, \infty)$. The conditional probability density function of X_{n+1} given $\{X_n = z\}$ is determined by means of

$$q(x | z) = q(x | X_n = z) = \sum_{i=1}^k p_i(z) h_i(x), \quad z, x \in R_+,$$

where $\{p_1(z), \dots, p_k(z)\}$ is a probability distribution, $p_1(z) + \dots + p_k(z) = 1$ for all $z \in R_+$; $\{h_1(x), \dots, h_k(x)\}$ is a family of probability density functions on R_+ .

This flow is investigated for stationary case. One is considered as the Semi-Markov process $J(t)$ on the state set $\{1, \dots, k\}$. Main characteristics are considered: stationary distribution of J and interarrival times X , correlation and Kendall tau (τ) for adjacent intervals, and so on.

Further one is considered a Markovian system on which the described flow arrives. The system has a finite or countable set of (may be multidimensional) states N_+^r with $N_+ = \{0, 1, \dots, c\}$, $c \leq \infty$. Arrival moments of the flow transfer the system from a state $i \in N_+^r$ into other state $j \in N_+^r$ with probability

$$g_{i,j}^{(v)}, \quad g_{i,0}^{(v)} + g_{i,1}^{(v)} + \dots + g_{i,c}^{(v)} = 1,$$

where v is the Semi-Markov component's J value immediately before the arrival.

Let 0 be the beginning of the new interval and w be the new value of J : $w = J(0+)$.

Between time moments of the new and the successive arrivals, a dynamic of the system is described by homogeneous Markov process $Y(t)$, $t > 0$, on the state set N_+^r with transition probabilities

$$P_{i,j}^{(w)}(t) = P\{Y(t) = j | Y(0+) = i, L(0+) = w\},$$

$$i, j \in N_+^r; w = 1, \dots, k; t \geq 0.$$

The stationary distribution and characteristics of the continuous-time process (Y, J) are considered.

Within the framework of the suggested model, various problems of reliability, storage and queues are considered.

Numerical results show that the dependence between interarrival times of the flow exercises greatly influences the efficiency characteristics of considered systems. Thus the study of stochastic models with dependencies is very important for applications.

Keywords: Semi-Markov process, Markov subordinator, stationary distribution

1 Introduction

An important element of a probabilistic model is a description of considered random variable distributions. It is supposed usually that all random variables are independent. But numerous statistical data prove the opposite. For example, it has been experimentally stated that characteristics of Internet flows are dependent ones [6, 8, 12]. Analogously, flows of insurance claims for damages have dependent structure [2-5, 12]. In the first case, a correlation between interarrivals of the claims is described by so called Markov-Additive Processes of Arrivals [11], for example for Batch Markovian Arrival Process, where a claim circulates in some Markovian network before an arrival [14]. In the second case, copulas are used usually for a description of the dependence [1, 3, 5, 10].

In our paper we wish to use natural and direct way for a description of the dependence between continue random variables X_0, X_1, \dots . We suppose that the lasts correspond a Markov chain with continue state space $(0, \infty)$ where the initial variable X_0 has the probability density function $f_0(x)$ and the distribution of any another variable X_{n+1} , $n = 0, 1, \dots$, depend from X_n only. Let each random variable X_{n+1} can have one probability density function from the family $\{h_1(x), \dots, h_k(x)\}$. The probability to have the i -th density $h_i(x)$ is a function $p_i(z)$ of fixed value $X_n = z$,

$$p_1(z) + p_2(z) + \dots + p_k(z) = 1, \quad \forall z \in (0, \infty). \quad (1)$$

Therefore the conditional density probability function for X_{n+1} is determined as

$$q(x|z) = q(x|X_n = z) = \sum_{i=1}^k p_i(z)h_i(x), \quad z, x > 0. \quad (2)$$

then random variable X_n and X_{n+1} are positively correlated, if one is the opposite order “less” then a negatively correlation has place.

The sequence X_0, X_1, \dots can be used for a description of customer flow, of service times in the queueing systems and so on. We apply one for the first case. In the next section standard analysis of such flow will be performed. Further we consider a single server queueing system with the considered flow. It allows us to investigate an influence of flow’s correlation on performance characteristics of the queueing system.

2 Flow analysis

In fact the sequence X_0, X_1, \dots can be considered as partial case of Markov renewal processes or Semi-Markov ones [7, 9, 11]. For that we use the following interpretation of the relation (2). The event $\{X_{n+1} = x\}$ given the event $\{X_n = z\}$ occurs as follows. At first it is chosen the distribution h_i with the probability $p_i(z)$. Further the value x for X_{n+1} is chosen with respect to the density $h_i(x)$. In this case we set $L_{n+1} = i$ and call it as the label of random variable X_{n+1} (Pacheco, Tang and Prabhu [11] name one the Markov component).

The distribution of the first label L_1 is calculated as

$$P\{L_1 = i\} = \int_0^{\infty} p_i(x)f_0(x)dx, \quad i = 1, \dots, k. \quad (3)$$

The sequence of labels L_1, L_2, \dots forms an embedded Markov chain with finite state space $\{1, 2, \dots, k\}$ and the transit probabilities per a step

$$P_{i,j} = P\{L_{n+1} = j | L_n = i\} = \int_0^{\infty} h_i(x)p_j(x)dx. \quad (4)$$

Obviously pair $\left(L_n, \sum_{i=0}^n X_i \right), \quad n = 1, 2, \dots$ is a Markov renewal process [11].

Additionally to the transition probability matrix $P = \{P_{i,j}\}$, the last is set usually by distribution function

$$F_{i,j}(x) = P\{X_n \leq x | L_n = i, L_{n+1} = j\} \quad (5)$$

of the holding time in state $i \in \{1, 2, \dots, k\}$ till a transition in the state j .
 In our case

$$F_{i,j}(x) = P_{i,j}^{-1} \int_0^x h_i(z) p_j(z) dz = \left(\int_0^\infty h_i(z) p_j(z) dz \right)^{-1} \int_0^x h_i(z) p_j(z) dz, x \geq 0. \quad (6)$$

Therefore a considered process is a special case of semi-Markov one with special structure of the transit probabilities (5) and the distribution of holding time (6).

It allows us to use known results of the theory. By that the final results will have more simple form than ones for the total case of semi-Markov processes.

Further we suppose that the matrix P corresponds to a finite ergodic Markov chain. Then this Markov chain has unique stationary (limiting) distribution $\pi = (\pi_1, \dots, \pi_k)^T$ that can be find as unique positive solution of the equation

$$\pi^T = \pi^T P, \quad (7)$$

satisfied the normalization condition

$$\sum_{i=1}^k \pi_i = 1. \quad (8)$$

Now it is possible to calculate the stationary probability density function of X_∞ :

$$f(x) = \frac{\partial}{\partial x} F(x) = \frac{\partial}{\partial x} P\{X_\infty \leq x\} = \sum_{i=0}^k \pi_i h_i(x), \quad x \geq 0. \quad (9)$$

Mean value and variance of X_∞ are

$$\mu = E(X_\infty) = \sum_{i=1}^k \pi_i \mu_i, \quad \sigma^2 = D(X) = \sum_{i=1}^k \pi_i (\sigma_i^2 + \mu_i^2) - \mu^2, \quad (10)$$

where

$$\mu_i = \int_0^\infty x h_i(x) dx, \quad \sigma_i^2 = \int_0^\infty (x - \mu_i)^2 h_i(x) dx. \quad (11)$$

Now our aim is calculating covariance and Kendall- τ [10] for lengths Z and X of two adjacent intervals for the stationary distribution (9) and the transition probability density (2). Firstly the bivariate density function

$$f(z, x) = \frac{\partial^2}{\partial z \partial x} F(z, x) = f(z)q(x|z) = \sum_{i=1}^k \pi_i h_i(z) \sum_{j=1}^k p_j(z) h_j(x), \quad z, x > 0. \quad (12)$$

Then

$$\begin{aligned} E(ZX) &= \int_0^\infty \int_0^\infty zx f(z, x) dx dz = \int_0^\infty \int_0^\infty zx \sum_{i=1}^k \pi_i h_i(z) \sum_{j=1}^k p_j(z) h_j(x) dx dz = \\ &= \int_0^\infty z \sum_{i=1}^k \pi_i h_i(z) \sum_{j=1}^k p_j(z) \mu_j dz = \sum_{i=1}^k \pi_i \sum_{j=1}^k \mu_j \int_0^\infty zh_i(z) p_j(z) dz. \end{aligned} \quad (13)$$

Therefore

$$\text{Cov}(Z, X) = \sum_{i=1}^k \pi_i \sum_{j=1}^k \mu_j \int_0^\infty zh_i(z) p_j(z) dz - \mu^2. \quad (14)$$

In order to calculate the Kendall- τ we consider two independent pair (Z, X) and (Z', X') with distribution (9). Then

$$\begin{aligned} P\{Z \leq Z', X \leq X'\} &= \int_0^\infty \int_0^\infty F(z, x) f(z, x) dx dz = \\ &= \int_0^\infty \int_0^\infty \sum_{i=1}^k \pi_i \sum_{j=1}^k \int_0^z h_i(w) p_j(w) dw \int_0^x h_j(v) dv \sum_{l=1}^k \pi_l h_l(z) \sum_{m=1}^k p_m(z) h_m(x) dx dz = \\ &= \sum_{m=1}^k \sum_{j=1}^k \int_0^\infty \int_0^x h_j(v) dv h_m(x) dx \int_0^\infty p_m(z) \sum_{i=1}^k \pi_i \sum_{l=1}^k \pi_l h_l(z) \int_0^z h_i(w) p_j(w) dw dz. \end{aligned} \quad (15)$$

Now the Kendall's tau can be calculated [10] as

$$\tau = 4P\{Z \leq Z', Y \leq Y'\} - 1. \quad (16)$$

3 Flow analysis: special case

Our numerical example of the considered flow is the following: $k = 2$,

$$h_1(x) = \frac{\lambda}{1 - \exp(-\lambda a)} e^{-\lambda x}, \quad h_2(x) = \frac{\lambda}{1 - \exp(-\lambda a)} e^{-\lambda(a-x)}, \quad 0 \leq x \leq a. \quad (17)$$

For probability distribution $\{p_i(z)\}$ we have two variants:

$$p_1(z) = \frac{z}{a}, \quad p_2(z) = 1 - \frac{z}{a}, \quad 0 \leq z \leq a, \quad (18)$$

and

$$\tilde{p}_1(z) = 1 - \frac{z}{a} = 1 - p_1(z), \quad \tilde{p}_2(z) = \frac{z}{a} = 1 - p_2(z), \quad 0 \leq z \leq a. \quad (19)$$

Firstly we consider the case (18). Calculations with respect to formula (4) give:

$$P_{1,1} = \int_0^a \frac{\lambda}{1 - \exp(-\lambda a)} e^{-\lambda x} \frac{x}{a} dx = \frac{1}{\lambda a(1 - \exp(-\lambda a))} [1 - e^{-\lambda a} - \lambda a e^{-\lambda a}], \quad P_{1,2} = 1 - P_{1,1},$$

$$P_{2,1} = \int_0^a \frac{\lambda}{1 - \exp(-\lambda a)} e^{-\lambda(a-x)} \frac{x}{a} dx = \frac{\lambda a e^{\lambda a} - e^{\lambda a} + 1}{\lambda a(1 - \exp(-\lambda a))} e^{-\lambda a}, \quad P_{2,2} = 1 - P_{2,1} \quad (20)$$

Now

$$\pi_1 = \frac{1}{1 - P_{1,1} + P_{2,1}} P_{2,1} = \frac{\lambda a(1 - \exp(-\lambda a))}{\lambda a(1 - \exp(-\lambda a)) + \lambda a - 2 + 2 \exp(-\lambda a) + \lambda a \exp(-\lambda a)} P_{2,1} =$$

$$= \frac{1}{2(\lambda a - 1 + \exp(-\lambda a))} [\lambda a - 1 + e^{-\lambda a}].$$

Finally,

$$\pi_1 = \frac{1}{2}, \quad \pi_2 = 1 - \pi_1 = \frac{1}{2}, \quad (21)$$

$$f(x) = \frac{1}{2} h_1(x) + \frac{1}{2} h_2(x) = \frac{\lambda}{2(1 - \exp(-\lambda a))} [e^{-\lambda x} + e^{-\lambda(a-x)}], \quad 0 \leq x \leq a. \quad (22)$$

Further we wish calculating such characteristics of the interarrival times as the expectation, variance and covariance. In order to derive these characteristics, the following values will be used:

$$\begin{aligned}\mu_1 &= \int_0^a x h_1(x) dx = \int_0^a x \frac{\lambda}{1 - \exp(-\lambda a)} e^{-\lambda x} dx = \frac{1}{\lambda(1 - \exp(-\lambda a))} (1 - e^{-\lambda a} - \lambda a e^{-\lambda a}), \\ \mu_2 &= \int_0^a x h_2(x) dx = \int_0^a x \frac{\lambda}{1 - \exp(-\lambda a)} e^{-\lambda(a-x)} dx = \frac{1}{\lambda(1 - \exp(-\lambda a))} (\lambda a + e^{-\lambda a} - 1), \\ \mu_1 - \mu_2 &= \frac{1}{\lambda(1 - \exp(-\lambda a))} (1 - e^{-\lambda a} - \lambda a e^{-\lambda a} - \lambda a - e^{-\lambda a} + 1) = \\ &= \frac{2(1 - \exp(-\lambda a)) - \lambda a(1 + \exp(-\lambda a))}{\lambda(1 - \exp(-\lambda a))} = \frac{2}{\lambda} - a \frac{1 + \exp(-\lambda a)}{1 - \exp(-\lambda a)}.\end{aligned}\quad (23)$$

Now the expected value of the interarrival time can be calculated by (10):

$$\mu = E(X) = \pi_1 \mu_1 + \pi_2 \mu_2 = \frac{1}{2} (\mu_1 + \mu_2) = \frac{1}{2} a. \quad (24)$$

In order to calculate the variance (10), at first the second moments (11) must be calculated:

$$\begin{aligned}\mu_1^{(2)} &= \int_0^a x^2 h_1(x) dx = \int_0^a x^2 \frac{\lambda}{1 - \exp(-\lambda a)} e^{-\lambda x} dx = -\frac{1}{1 - \exp(-\lambda a)} \int_0^a x^2 d e^{-\lambda x} = \\ &= -\frac{1}{1 - \exp(-\lambda a)} \left[a^2 e^{-\lambda a} - 2 \int_0^a x e^{-\lambda x} dx \right] = \frac{2\lambda^{-2}}{1 - \exp(-\lambda a)} \left[1 - e^{-\lambda a} - \lambda a e^{-\lambda a} - \frac{1}{2} (\lambda a)^2 e^{-\lambda a} \right], \\ \mu_2^{(2)} &= \int_0^a x^2 h_2(x) dx = \int_0^a x^2 \frac{\lambda}{1 - \exp(-\lambda a)} e^{-\lambda(a-x)} dx = \frac{1}{1 - \exp(-\lambda a)} e^{-\lambda a} \int_0^a x^2 d e^{\lambda x} = \\ &= \frac{1}{1 - \exp(-\lambda a)} e^{-\lambda a} \left[a^2 e^{\lambda a} - 2 \int_0^a x e^{\lambda x} dx \right] = \frac{2}{1 - \exp(-\lambda a)} \lambda^{-2} \left[1 - e^{-\lambda a} - \lambda a + \frac{1}{2} (\lambda a)^2 \right].\end{aligned}$$

Now we get

$$\mu^{(2)} = E(X^2) = \pi_1 \mu_1^{(2)} + \pi_2 \mu_2^{(2)} = 2\lambda^{-2} + \frac{1}{2} a^2 - \frac{a(1 + e^{-\lambda a})}{\lambda(1 - \exp(-\lambda a))}. \quad (25)$$

Further for the second moment (13) we have

$$\begin{aligned}
 E(ZX) &= \sum_{i=1}^2 \pi_i \sum_{j=1}^2 \mu_j \int_0^{\infty} zh_i(z) p_j(z) dz = \frac{1}{2} \left(\mu_1 \int_0^a zh_1(z) \frac{z}{a} dz + \mu_2 \int_0^a zh_1(z) \left(1 - \frac{z}{a}\right) dz \right) + \\
 &+ \frac{1}{2} \left(\mu_1 \int_0^a zh_2(z) \frac{z}{a} dz + \mu_2 \int_0^a zh_2(z) \left(1 - \frac{z}{a}\right) dz \right) = \\
 &= \frac{1}{2} \left(\mu_1 \mu_1^{(2)} \frac{1}{a} + \mu_2 \left(\mu_1 - \frac{1}{a} \mu_1^{(2)} \right) + \mu_1 \frac{1}{a} \mu_2^{(2)} + \mu_2 \left(\mu_2 - \frac{1}{a} \mu_2^{(2)} \right) \right) = \\
 &= \frac{1}{2} \left(\mu_1^{(2)} \frac{1}{a} (\mu_1 - \mu_2) + \mu_2^{(2)} \frac{1}{a} (\mu_1 - \mu_2) + \mu_2 (\mu_1 + \mu_2) \right) = \\
 &= \frac{1}{2} \left(\frac{1}{a} (\mu_1 - \mu_2) (\mu_1^{(2)} + \mu_2^{(2)}) + \mu_2 (\mu_1 + \mu_2) \right) = \frac{1}{a} (\mu_1 - \mu_2) \mu^{(2)} + \frac{1}{2} a \mu_2.
 \end{aligned}$$

Now we can calculate using previous formulas (23) – (25). Finally for the case (18)

$$Cov(Z, X) = E(ZX) - \frac{1}{4} a^2. \quad (26)$$

Let us consider the case (19). The formula (4) gives us

$$\begin{aligned}
 \tilde{P}_{i,j} &= \int_0^{\infty} h_i(x) \tilde{p}_j(x) dx = \int_0^{\infty} h_i(x) (1 - p_j(x)) dx = 1 - P_{i,j}, \quad i, j = 1, 2 \\
 \tilde{P}_{1,1} &= 1 - P_{1,1}, \quad \tilde{P}_{1,2} = 1 - P_{1,2} = P_{1,1}, \quad \tilde{P}_{2,1} = 1 - P_{2,1}, \quad \tilde{P}_{2,2} = 1 - P_{2,2} = P_{2,1}.
 \end{aligned}$$

It shows that as earlier

$$\tilde{\pi}_1 = \tilde{\pi}_2 = \frac{1}{2}.$$

Therefore for stationary distribution of the interarrival time $\tilde{f}(x)$ we have the previous expression (20) for $f(x)$. As regards the second mixed moment then

$$\begin{aligned}
 \tilde{E}(ZX) &= \sum_{i=1}^2 \pi_i \sum_{j=1}^2 \mu_j \int_0^{\infty} zh_i(z) \tilde{p}_j(z) dz = \sum_{i=1}^2 \pi_i \sum_{j=1}^2 \mu_j \int_0^{\infty} zh_i(z) (1 - p_j(z)) dz = \\
 &= (\mu_1 + \mu_2) \mu - E(ZX) = 2\mu^2 - E(ZX) = \frac{1}{2} a - E(ZX).
 \end{aligned}$$

Therefore

$$\tilde{Cov}(Z, X) = \tilde{E}(ZX) - \frac{1}{4} a^2 = \frac{1}{2} a^2 - \tilde{E}(ZX) - \frac{1}{4} a^2 = -Cov(Z, X). \quad (27)$$

Also the cases (18) and (19) give opposite correlation. Further if $\lambda \rightarrow 0$ then the distribution (22) tends to the uniform distribution on $(0, a)$, for which the covariance equals zero. Further if $\lambda \rightarrow \infty$ then as limiting distribution we have the two-point distribution $P\{X=0\} = P\{X=a\} = 1/2$, for which the correlation coefficient may be -1 ad 1 . Therefore manipulating by λ it is possible to choose the arbitrary value for the correlation coefficient.

3 Markovian system

Considered system has a finite or countable set of (may be multidimensional) states N_+^r with $N_+ = \{0, 1, \dots, c\}$, $c \leq \infty$. Arrival moments of the above-described flow transfer the system from one state $i \in N_+^r$ into other state $j \in N_+^r$. Let us consider a time moment immediately after new arrival, denote one $0+$ as a beginning of the new interval. Earlier we have denoted X as a length of the new interval and $L(0+)$ as its label. If $L(0+) = v$ then the transfer $i \rightarrow j$ takes place with probability $g_{i,j}^{(v)}$, $g_{i,0}^{(v)} + g_{i,1}^{(v)} + \dots + g_{i,c}^{(v)} = 1$. Between time moments of the new and a consequent arrivals, a dynamic of the system is described [7] by homogeneous Markov process $Y(t)$, $t > 0$, with transition probabilities

$$P_{i,j}^{(v)}(t) = P\{Y(t) = j | Y(0+) = i, L(0+) = v\}, \quad i, j \in N_+^r; \quad v = 1, \dots, k; \quad t \geq 0. \quad (28)$$

Let us suppose that the stationary distribution of the discrete-time Markov process $(Y_n, X_n, n = 0, 1, \dots)$ exists, then

$$R_j(x) = P\{Y(0+) = j, X \leq x\}, \quad r_j(x) = \frac{\partial}{\partial x} R_j(x), \quad x \geq 0, \quad i \in N_+^r. \quad (29)$$

A usual reasoning and formula (2) gives the following equations for $x \geq 0$:

$$r_j(x) = \int_0^\infty \sum_{i=0}^c \sum_{w=0}^c r_i(z) \sum_{v=1}^k p_v(z) h_v(x) P_{i,w}^{(v)}(x) q_{w,j} dz, \quad j \in N_+^r, \quad x \geq 0. \quad (30)$$

Let us denote

$$\tilde{r}_{i,v} = \int_0^\infty p_v(z) r_i(z) dz.$$

Then instead of (30) we have

$$r_j(x) = \sum_{i=0}^c \sum_{v=1}^k \tilde{r}_{i,v} h_v(x) \sum_{w=0}^c P_{i,w}^{(v)}(x) q_{w,j}, \quad j \in N_+^r, \quad x \geq 0. \quad (31)$$

Multiplying both sides of (31) by $p_m(x)$ and integrating with respect to x we get

$$\tilde{r}_{j,m} = \sum_{i=0}^c \sum_{v=1}^k \tilde{r}_{i,v} \int_0^{\infty} p_m(x) h_v(x) \sum_{w=0}^c P_{i,w}^{(v)}(x) q_{w,j} dx, \quad j, m \in N_+^r. \quad (32)$$

Denoting

$$b_{i,v,j,m} = \int_0^{\infty} p_m(x) h_v(x) \sum_{w=0}^c P_{i,w}^{(v)}(x) q_{w,j} dx \quad (33)$$

we get the system of the linear equations

$$\tilde{r}_{j,m} = \sum_{i=0}^c \sum_{v=1}^k b_{i,v,j,m} \tilde{r}_{i,v}, \quad j, m \in N_+^r. \quad (34)$$

This system may be written as the systems (7), (8). Its solution allows calculating the distribution (31).

5 Single server queueing system

A widely known queueing system is $GI/M/1/\infty$: claims arrive at a single server station in accordance with a recurrent flow. Upon arrival, the claim is immediately served if the server is free. Otherwise, one has to wait occupying one of an infinite number of places. The service time is assumed to be independent and identically exponentially distributed with intensity β .

We consider the following modification of this system. At first, instead of the recurrent, the investigated in Sections 2 and 3 flow will be used. At second, a number of the waiting places are restricted and equal to c . If all places are busy, then an arrived claim is rejected.

As earlier let us consider a time moment when a new claim arrives at the system. Now $Y(t)$ denotes a number of the claims in the system at the time moment t after a last arrival, $Y(0^-)$ - immediately before, and $Y(0^+)$ - immediately after new arrival. We are interested in the corresponding distributions.

Our special case of the general one has the following characteristics: $r = 1$, $q_{i,j} = \delta_{i,i+1}$, $i, j \in N_+ = \{0, \dots, c\}$. The transition probabilities do not depend on v and have the following expressions: $P_{0,j}(0) = \delta_{0,j}$,

$$P_{i,j}(t) = \frac{(\beta x)^{i-j}}{(i-j)!} \exp(-\beta x), \quad i = 1, \dots, c; j = 1, \dots, i; t > 0; \quad (35)$$

$$P_{i,0}(x) = \left(1 - \sum_{v=0}^{i-1} \frac{(\beta x)^v}{v!} \exp(-\beta x) \right), \quad i = 1, \dots, c; t > 0. \quad (36)$$

We have from (33) for $i = 1, \dots, c; j = 2, \dots, \min\{i + 1, c - 1\}$:

$$b_{i,v,j,m} = \int_0^a p_m(x) h_v(x) P_{i,j-1}(x) dx = \int_0^a p_m(x) h_v(x) \frac{(\beta x)^{i-j+1}}{(i-j+1)!} e^{-\beta x} dx; \quad (37)$$

for $i = c, j = c$:

$$b_{c,v,c,m} = \int_0^a p_m(x) h_v(x) (1 + \beta x) e^{-\beta x} dx \quad (38)$$

for $i = 1, \dots, c; j = 1$:

$$b_{i,v,1,m} = \int_0^a p_m(x) h_v(x) \left(1 - \sum_{w=0}^{i-1} \frac{(x\beta)^w}{w!} e^{-\beta x} \right) dx \quad (39)$$

for $i = c - 1, j = c$:

$$b_{c-1,v,c,m} = \int_0^a p_m(x) h_v(x) e^{-\beta x} dx \quad (40)$$

Note that it is easy to get explicit formulas substituting the expressions for $h_i(x)$ and $p_i(x)$ with respect to (17) – (19).

Now we use the formula (34) to calculate the distribution of the random variables $Y(0-)$ and $Y(0+)$:

$$P\{Y(0-) = j\} = P\{Y(0+) = j - 1\} = \sum_{m=1}^2 \tilde{r}_{j,m}$$

We perform a numerical analysis to evaluate various flows influence on queuing system efficiency. All three above described systems will be considered: the system $GI/M/1/\infty$ with the distribution (9) of the independent interarrival times; the analogous system with restricted number c of waiting places and dependent interarrival times with the distribution (17) and for two cases: the case (18) and the case (19). We will denote these systems as $NI/M/1/c$ and $N2/M/1/c$.

As efficiency criteria, we will use the probability not to wait for a beginning of the service and the mean value of waited claims at the time moment of a new arrival $E(Y(0-))$.

Let us give some comments. At first, we have chosen rather big value of c that gives the same results for the systems $GI/M/1/\infty$ and $GI/M/1/c$ with the infinite and restricted number of waiting places. At second, all three systems differ from each

other by the interarrival times. They are independent for the first system, and they are dependent for the rest ones. For the second system there is the following tendency: the next interarrival time will be distinguished from the previous interarrival. Note that it is a positive fact for the queueing systems because long and short interarrival times will be alternate. For the third system there is an opposite tendency: the next interarrival time will be analogous to the previous interarrival time. It has a negative influence on the queueing systems, as it is highly probable to have long series of short interarrival times.

At first we remind some necessary expressions for the system $GI/M/1/\infty$. The probability r_i that an arrived claim finds i other claims in the system is calculated by the formula:

$$r_i = (1-u)u^i, \quad i = 0, 1, \dots \quad (41)$$

where $u \in (0, 1)$ is the unique root of the equation:

$$u - \int_0^{\infty} e^{-\beta x(1-u)} f(x) dx = 0.$$

Further, we give numerical results for the following input data. The intensity of the service times $\beta = 4$, the scale parameter $a = 1$. Because the mean interarrival time equals to $\mu = a/2 = 0.5$, then the load coefficient of the server $\rho = 1/(\mu\beta) = 0.5$. The number of the waiting places for the systems with the dependent interarrival times $c = 12$. The parameter λ of the distribution (17) will be taking the following values: 0.1, 0.5, 1, 2, 3, 5, 6, and 7. The tables contain the mean number of claims $E(Y(0-))$ and the probability of the service without waiting $P\{Y(0-) = 0\}$.

Table 1. The mean number of claims in the systems $E(Y(0-))$

λ	0.1	0.5	1	2	3	5	7	9
$GI/M/1/\infty$	0.56 4	0.567	0.577	0.611	0.660	0.776	0.883	0.971
$NI/M/1/c$	0.55 9	0.539	0.523	0.508	0.506	0.521	0.539	0.556
$N2/M/1/c$	0.57 1	0.600	0.648	0.794	1.018	1.692	2.083	2.459

Table 2. The probability of the service without waiting $P\{Y(0-)=0\}$

λ	0.1	0.5	1	2	3	5	7	9

$GI/M/1/\infty$	0.639	0.638	0.634	0.621	0.602	0.563	0.531	0.507
$NI/M/1/c$	0.640	0.643	0.645	0.641	0.631	0.606	0.583	0.564
$N2/M/1/c$	0.638	0.632	0.622	0.595	0.561	0.496	0.472	0.457

Let us discuss the represented results. The system $GI/M/1/\infty$ with the recurrent input flow is a “neutral” one. The rest two systems are the opposite ones: the case (18) improves the efficiency characteristics of the service, the case (19) makes them worse. For example, if $\lambda = 2$, then the probability of the service without waiting and the mean number of claims in the system $E(Y(0-))$ consist of: for the system $GI/M/1/\infty$ 0.621 and 0.611; for the system $NI/M/1/12$ (the case (18)) 0.641, and 0.508; for the system $N2/M/1/12$ (the case (19)) 0.595 and 0.794. Note the efficiency characteristics for the case (19) deteriorate catastrophically, when the value λ increases and long series of short interarrival times is probable. It seems to us that precisely such a situation appears in the various telecommunication and financial systems.

6 Conclusions

In this paper, we have considered a model of a nonrecurrent flow, for which interarrival times can be positive or negative correlated. Such flows often appear in various telecommunication and financial systems. This flow has been used as an input flow for a single server queueing system with exponential distributed service times. Numerical results show that the dependence between interarrival times exercises great influence on efficiency characteristics of the service.

The elaborated approach gives a general tool for a construction of wide flows class with correlated interarrival times.

The article is written with the financial assistance of European Social Fund. Project Nr. 2009/0159/1DP/1.1.2.1.2/09/IPIA/VIAA/006 (The Support in Realisation of the Doctoral Programme “Telematics and Logistics” of the Transport and Telecommunication Institute).

References

1. Abegaz F., Naik-Nimbalkar U.V. Modelling statistical dependence of Markov chains via copula models, *Journal of statistical planning and inference*, 138 (4), 2008, pp. 1131-1146.
2. Breyman W., Dias A., Embrechts P. Dependence structures for multivariate high-frequency data in finance. *Quantitative Finance*, 3(1), 2003, pp. 1-16.

3. Embrechts P., Hoeing A., Juri A. Using Copulae to bind the Value-at-Risk for function of dependent risk. *Finance & Stochastic*, 7(2), 2003, pp. 145-167.
4. Embrechts P., Pucetti G. Bounds for function of dependent risk. *Finance & Stochastic*, 10, 2006, pp. 341-352
5. Embrechts P., Lindskog F., McNeil, A. *Modelling Dependence with Copulas and Applications to Risk Management* (Chapter 8). Handbook of Heavy Tailed Distributions in Finance, Amsterdam: Elsevier, 2003, pp. 329 – 384.
6. Hernandez-Campos F., Jeffay K.F, Park C., Marron J.S., Resnick S.I. Extremal dependence: Internet traffic applications. *Stochastic Models. Taylor & Francis*, 22(1), 2005, pp. 1-35.
7. Kijima M. (1997). *Markov Processes for Stochastic Modelling*. Chapman & Hall, London.
8. Kun Chan Lan, Hedemann J. On the correlation of Internet flow characteristics. *Technical report ISI-TR-574*, USC/Information Sciences Institute, July, 2003.
9. Linnios N. and Ouhbi B. (2008). Nonparametric Estimation of Integral Functionals for Semi-Markov Processes with Application in Reliability. *In Statistical Models and methods for Biomedical and Technical Systems*. F. Vonta, M.Nikulin, N. Linnios, C. Huber-Carol. Birkhauser, Boston-Basel-Berlin. 405 – 418.
10. Nelsen Roger B. *An Introduction to Copulas. Second Edition*. New York: Springer, 2006. 270 p.
11. Pacheco A., Tang L.C., Prabhu U N. Markov-Modulated process and Semiregenerative Phenomena. *World Scientific*. New Jersey, London, Singapore, 2009.
12. Zhang Y., Breslay L., Paxson V., Shenker S. On the Characteristics and Origins of Internet Flow Rates. *ACM SIGCOMM*, Pittsburgh, PA, USA. 2002.
13. Pettere G. Stochastic Risk Capital Model for Insurance Company. Applied Stochastic Models and Data Analysis: *Proceedings of the XIIth International Conference*, Chania, Crete, Greece, May 29,30,31 and June 1, 2007. Chania, 2007.
14. Dudin A., Klimenok V. Queueing systems with the correlated flows. Minsk: Belorussian State University, 2000 175 p. (in Russian).

The Research of Fractal Characteristics of the Electrocardiogram in a Real Time Mode

Valery Antonov¹, Anatoly Kovalenko², Artem Zagaynov¹, Vu Van Quang¹

¹ The St.-Peterburg State Polytechnical University,
Polytechnical st. 29, 195251, St.-Peterburg, Russia
Email: antonovvi@mail.ru

² Institute of chemistry of silicates.
Makarov quay 2, 199034, St.-Peterburg, Russia
Email: ank@isc.nw.ru

Abstract: The article presents the results of recent investigations into Holter monitoring of ECG, using non-linear analysis methods. It is shown that one of the most precise characteristics of the functional state of biological systems is the dynamical trend of correlation dimension and entropy. On the basis of this it is suggested that a complex programming apparatus be created for calculating these characteristics on line. A similar programming product is being created now with the support of RFBR. The first results of the working program, its adjustment, and further development, are also considered in the article.

Keywords: Holter monitoring, ECG, correlation dimension, Fractal analysis of temporary rows, non-linear dynamics of heart rate

1 Introduction

In 1996 the European Cardiological Society and the North American Electrophysiological Society gave recommendations on the clinical usage of the heart rate variability method (HRV) [12], and it is presently being carried out by different methods (fig. 1). Most of the HRV investigations are based on the linear measurement of cardio-rhythm (standard deviation of interval duration between sinusoidal contraction (SDNN), standard deviation of average values RR-intervals (SDANN), indicators of the autonomous regulation contour (RMSSD, pNN50), triangulation index, power values in different frequency ranges, low-high frequency spectral components, their ratio ((ULF, VLF, LF, HF, LF/HF) etc.) These indicators are now used in clinical practice. However, the interest of investigators is attracted by non-linear mathematical methods, using, for example, postulates from the theory of determinated chaos. So, in [2] the investigation was into the supposition that a non-linear component HRV might show periodical structure in a 24 hour period, which was partially proved. There are contradictory data of the influence on non-linear components of breathing. The authors in [4] have not discovered reliable differences in forced and free breathing in the non-linear component HRV. Just the opposite is stated in [3] concerning the expressed non-linear component HRV in forced breathing. In [7] it is shown that

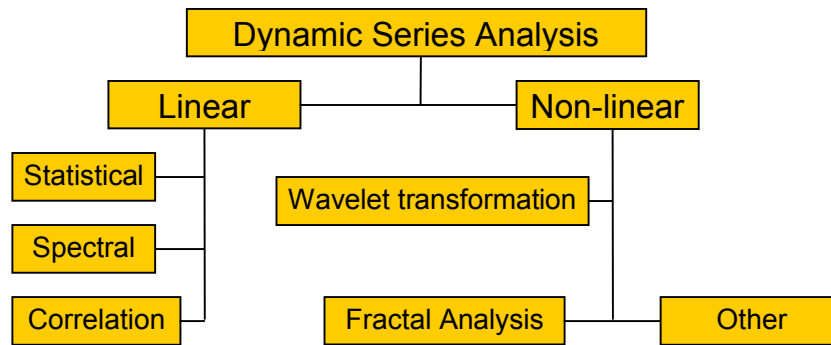


Fig. 1. Modern methods of investigation and analysis of processing methods based on the analyses of non-linear dynamics HRV can better discover patients with the risk of sudden death. In [6] the HRV changes are investigated in 92 episodes of the paroxysmal fibrillation of the auricle. The non-linear methods include such indicators as entropy approximation (ApEn). The authors conclude that the reduction of non-linear criteria reflects the changes of the sympatho-vagus regulation before the paroxysmal fibrillation of the auricle. In [5] it is also noted that methods of HRV evaluation based on non-linear analysis are better than standard methods in discovering changes in patients before the beginning of the ventricle fibrillation [13].

However, non-linear HRV analysis demands the prolonged formation of a data base for building a restored attractor, the dimension trend evaluation of which might last for several hours, which is not acceptable in conditions of urgent cardiology, and demands the transition from RR-intervals to complete ECG. This transition certainly makes the task more complicated, but at the same time enhances the reliability of entropy evaluation [8]. In [9] and [16] it is shown that there are currently no indicators satisfactorily describing the reactions of the cardio-vessel system to different external influences (physical uploads, stress, etc). In [10], based on the complete ECG it is proved that the functioning of the heart of a healthy person is not regular.

2 The method of fractal analysis

The method of fractal analysis consists of the transition from the signal to the restored attractor for the numeric characteristics of which probable (fractal) dimensions are used, expressed by the equation dimensions of Renyi:

$$D_q = \lim_{\varepsilon \rightarrow 0} \lim_{\tau \rightarrow 0} \lim_{m \rightarrow \infty} \left[\frac{\ln I_q(\varepsilon)}{\ln(1/\varepsilon)} \right], I_q = \frac{\sum_{i=1}^{M(\varepsilon)} p_i^q}{1-q}$$

at $q=0$ this is a well known dimension of Kolmogorov-Hausdorff:

$$D_F = \lim_{\varepsilon \rightarrow 0} \frac{\ln M(\varepsilon)}{\ln(1/\varepsilon)}$$

However, to characterize the attractor not only metric qualities are necessary, but also the probability of finding a point on the attractor. Usually for this purpose informational dimension and related informational entropy is used, as well as correlation dimension and correlation entropy:

$$D_C = \lim_{\varepsilon \rightarrow 0} \frac{\ln(\sum_{i=1}^{M(\varepsilon)} p_i^2)}{\ln(\varepsilon)} = \lim_{\varepsilon \rightarrow 0} \frac{\ln(C(\varepsilon))}{\ln(\varepsilon)}, I_C = \ln \frac{C(r, N)}{C(r, N+1)}$$

$$C(\varepsilon) = \lim_{m \rightarrow \infty} \frac{1}{m^2} \sum_{i,j=1}^m \theta(\varepsilon - \rho(x_i, x_j)), C(r) = \sum_{i=0}^{m-2} \sum_{j=i+1}^{m-1} \frac{\theta(\varepsilon - \rho(x_i, x_j))}{m(m-1)/2}$$

$$\theta(\alpha) = \begin{cases} 1, & \alpha \geq 0 \\ 0, & \alpha < 0 \end{cases}$$

For finding the characteristics of the attractor we need a definite number of points, that could be evaluated with the well-known equations of Eckmann or Nerenberg:

$$D_{\max} = \frac{2 \ln M}{\ln(1/r)}, r = \frac{\varepsilon}{\varepsilon_{\max}};$$

$$M \geq M_{\min} = 10^{2+0.4D}$$

For giving the phase space, the method of progressive differentiation is usually used or the method of Takens delay:

$$\vec{x}(t) = (a(t), \frac{da(t)}{dt}, \dots, \frac{d^{n-1}a(t)}{dt^{n-1}});$$

$$\vec{x}(t) = (a(t), a(t + \tau\Delta t), \dots, a(t + \tau(N-1)\Delta t))$$

The delay parameter in the last case is usually calculated as the first zero of the autocorrelation function, or as the first minimum of the function of mutual information:

$$B(\tau) = \frac{1}{m} \sum_{k=0}^{m-1} (a_k - \bar{a})(a_{k+\tau} - \bar{a}), m = M - (N-1)\tau;$$

$$I(\tau) = \sum_{a_k} P(a_k, a_{k+\tau}) \ln \left(\frac{P(a_k, a_{k+\tau})}{P(a_k)P(a_{k+\tau})} \right)$$

The methods of calculation of the correlation dimensions and correlation entropy are presented here:

$$C(r) \propto r^{D_2}$$

$$\ln C(r) \propto D_2 \ln r$$

$$C(r, N) \propto r^{D_2} \exp(-N \cdot I_2)$$

$$I_2 = \ln \frac{C(r, N)}{C(r, N+1)}$$

According to the well-known Takens theory the dimension of the phase space should be evaluated like this:

$$N \leq 2D_2 + 1$$

3 Firmware complex

Unfortunately, the Holter monitor is a three-channel static device, allowing the processing of the signal only after the device has been removed. But our practical interest lies in predicting the changes of the fractal characteristics. That is why our current software which is presently being developed, though working with the static records, still calculates the characteristics on-line, progressively shifting the window width on the required number of points.

So currently the complex calculates on-line:

- the histogram of variability
- low and high frequency spectral components ULF, VLF, LF, HF
- autocorrelation function
- correlation dimensions
- correlation entropy

and also builds graphs of a two / three dimensional attractor with their successive updating. The interface of the complex is shown in fig. 2

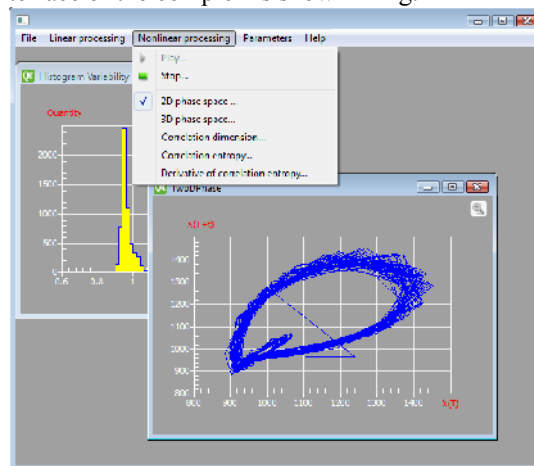


Fig. 2. Interface of the firmware complex

4 Results

According to the above-described method with the specially elaborated software, the correlation dimension is evaluated every second for the whole period of the cardiogram measurement. The adjustments of the program parameters allow the playback of the initial mass with any given speed. On the basis of the calculated data the dynamic trend is built.

The results of the program work are shown here for patients with different diseases, such as patients recovering from stroke (fig .3), vegetative conditions (fig. 4), pneumonia (fig. 5) and the most interesting - life-threatening sciatical risk (fig .6)

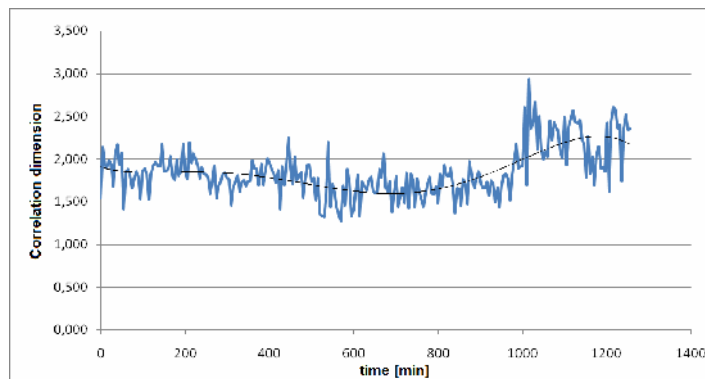


Fig. 3. Recovering after stroke

In this graph the significant change of the correlation dimension (more than 1) is clearly seen.

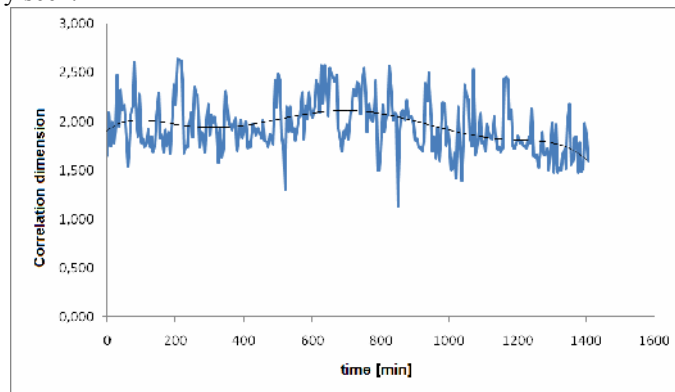


Fig. 4. Vegetative condition

In the vegetative condition the changes are much smaller and predictable (approximately 0.5)

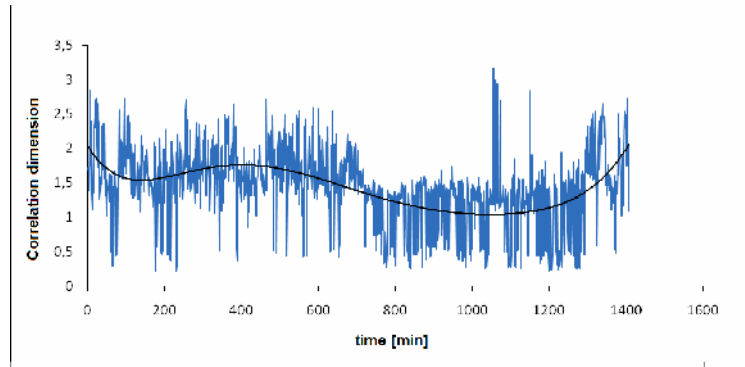


Fig. 5. Pneumonia

In the severe pneumonia condition the trend changes of the correlation dimension reach approximately 2 during the day. Finally, in the near-death state (fibrillation of ventricles), for a period of time the trend stays permanent (fig .6). However,

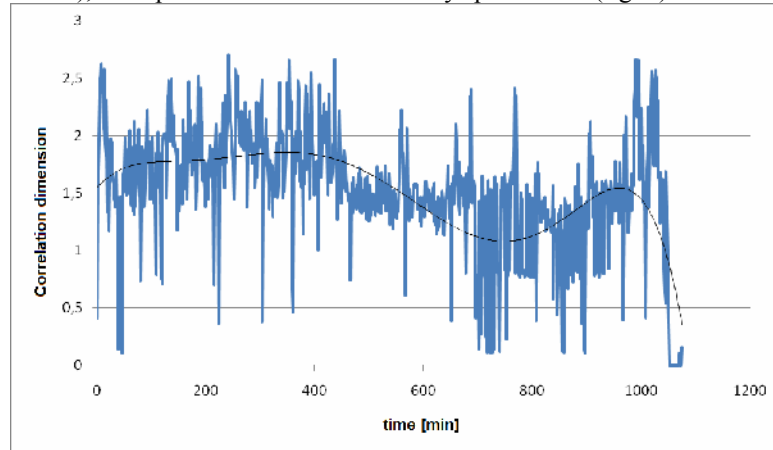


Fig. 6. Changing of cardio-rhythm with the risk of death.

further on, sharp fluctuations start, followed by a rapid dropping down to zero (case of death). It is noted that this dropping down is observed for several minutes. However, it is hoped that prediction can be made of the dropping down of the trend due to the sharp increase after a long period of calm-condition of the system. In this case an attempt will be made to reconstruct such a signal with the help of the non-linear system of differential equations with right sides as polynomials:

$$\begin{cases} \dot{x}_1 = f_1(x_1, x_2 \dots x_N) \\ \dot{x}_2 = f_2(x_1, x_2 \dots x_N) \\ \dots \\ \dot{x}_N = f_N(x_1, x_2 \dots x_N) \end{cases} \quad f_j = \sum_{l_1, l_2, \dots, l_N=0}^{\nu} C_{j, l_1, l_2, \dots, l_N} \prod_{k=1}^N x_k^{l_k}, \sum_{k=1}^N l_k \leq \nu$$

And also finding the unknown coefficients, for example, with the method of least squares.

5 Conclusion

Unfortunately, nowadays for the purpose of functional diagnosis of the body condition, the linear indicators used are taken from a patient's biomedical signals. The latest work in different aspects of cardio-rhythm studies in normal condition and in pathology shows that, apart from the classical methods of analysis in the time and frequency field, there is a recurring tendency to explore the cardio-rhythm from the point of view of non-linear analysis. Various influences, including the neurohumoral mechanisms of higher vegetative centres, cause the non-linear character of the cardio-rhythm changes, for the description of which special methods are necessary (graphs of the attractor, correlation dimensions, entropy etc). All these methods are of great interest for researchers; however, the practical application is not clear and as a result not limited.

However, it is necessary to emphasise the qualitative character of the changes in such indicators. The software currently elaborated here will significantly improve the efficiency of investigations made into the topic.

This work was done with the support of the RFBR (grant 09-08-01135-a)

References

1. Antonov V., Fedulin A., Nosyrev S., Kovalenko A. Critical Condition in Human. The Entropy Based Technology of Definition - International Journal Communications in Dependability and Quality Management (CDQM – Journal) Vol. 10. #1 (2007)
2. Curione M., Bernardini F., Cedrone L. et al. The chaotic component of human heart rate variability shows a circadian periodicity as documented by the correlation dimension of the time-qualified sinus R-R intervals. Clin Ter (1998)
3. Fortrat J.O. Yamamoto Y., Hughson R.L. Respiratory influences on non-linear dynamics of heart rate variability in humans. Biol Cybern (1997)
4. Kanters J.K., Hojgaard M.V., Agner E et al. Influence of forced respiration on nonlinear dynamics in heart rate variability. Am J Physiol (1997)
5. Makikallio T.H., Koistinen J., Jordaens L. et al. Heart rate dynamics before spontaneous onset of ventricular fibrillation in patients with healed myocardial infarcts. Am-J-Cardiol. (1999)
6. Vikman S., Yli-Mayry S., Makikallio T. H. et al. Differences in heart rate dynamics before the spontaneous onset of long and short episodes of paroxysmal atrial fibrillation. Ann Noninvasive Electrocardio (2001)
7. Voss A., Kurths J., Klein H.J. et al. The application of methods of nonlinear dynamics for the improved and predictive recognition of patients threatened by sudden cardiac death. Cardivasc.Res (1996)

8. Анищенко В. С., Астахов В. В., Вадивасова Т. Е., Нейман А. Б., Стрелкова Г. И., Шиманский-Гайер Л. Нелинейные эффекты в хаотических и стохастических системах, Институт компьютерных исследований Москва-Ижевск (2003)
9. Анищенко В. С., Сапарин П. И. Нормированная энтропия как диагностический признак реакции сердечно-сосудистой системы человека на внешнее воздействие, Изв.вузов «ПНД», т.1, № 3, 4 (1993)
10. Анищенко В. С., Янсон Н. Б., Павлов А. Н. Может ли режим работы сердца здорового человека быть регулярным? Радиотехника и электроника, т. 48, №8 (1997)
11. Антонов В. И., Загайнов А. И., Коваленко А. Н., Динамический тренд корреляционной размерности как характеристический показатель жизнедеятельности организма, Научно-технические ведомости СПбГПУ, издательство СПбГПУ (2009)
12. Вариабельность сердечного ритма (Рабочая группа Европейского Кардиологического общества и Северо-Американского общества стимуляции и электрофизиологии). Вестник аритмологии. №11 (1999)
13. Колюцкий А.К., Иванов Г.Г., Дворников В.Е., Грибанов А.Н., Юзеф Х., Рехвиашвили М.В., Котлярова Л.В., Тюрин А.В., К.М. Шумилова. Исследование вариабельности сердечного ритма при анализе аритмий Вестник Российского университета дружбы народов. Серия "Медицина". №2 (2001)
14. Павлов А. Н., Янсон Н. Б., Анищенко В. С., Гриднев В. И., Довгалевский П. Я. Диагностика сердечно-сосудистой патологии методом вычисления старшего показателя Ляпунова по последовательности RR – интервалов, Изв.вузов «ПНД», т.6, №2 (1998)
15. Рябыкина Г.В., Соболев А.В. Вариабельность ритма сердца. Монография. Москва (1998)
16. Янсон Н. Б., Анищенко В. С. Моделирование динамических систем по экспериментальным данным, Изв.вузов «ПНД», т.3, №3 (1995)

New technology in shopping: Forecasting electronic shopping with the use of a Neuro-Fuzzy System

ATSALAKIS GEORGE

*Technical University of Crete, Department of Production Engineering and Management, Crete, Greece,
e-mail: atsalak@otenet.gr*

Abstract: This paper presents the application of neuro-fuzzy techniques in forecasting a new technology in shopping. Neural networks have been used successfully to forecast time series due to the significant properties of treating non linear data with self learning capability. However, neural networks suffer from the difficulty of dealing with qualitative information and the “black box” syndrome that more or less limits their applications in practice. To overcome the drawbacks of neural networks, in this study we proposed a fuzzy neural network that is a class of adaptive networks and which is functionally equivalent to a fuzzy inference system. The results derived from the experiment based on the electronic sales indicate that the suggested fuzzy neural network could be an efficient system to forecast a new technology in shopping. Experimental results also show that the neuro-fuzzy approach outperforms the other two conventional models (AR and ARMA).

Keywords: new technology forecasting, electronic shopping forecasting, neuro-fuzzy forecasting, ANFIS,

1. Introduction

Sales time series are very complex for identification and forecasting because of their volatile behavior. If we consider that the use of the new technology to predict shopping method time series only have an interior relation, the future prices can be forecasted by using the following formula:

$$y_{t+1} = f(y_{t-k}, \dots, y_t) \quad (1)$$

where y_{t+1} is the rate to be forecasted and y_{t-k} is the influence factor. Traditional models that have been used to forecast sales time series are all based on the probability theory and statistical analysis with a certain number of distributions assumed in advance. In most cases these assumptions are unreasonable and non-realistic. Moreover the linear structure of these models doesn't guarantee the accuracy of forecasting.

Recent studies have addressed the problem of sales time series forecasting by using different methods including artificial neural network and model based approaches due to the significant properties of handling non-linear data with self learning capabilities (Hornik, 1991; Jain, 1997; Skapura, 1996). Neural networks have been accused by researches of being 'black boxes' whose degree of input influence on the output of the model can not be known (Shapiro 2002, Pao, 1989). Fuzzy logic is an effective rule-based modeling in soft computing, that not only tolerates imprecise information, but also forms a framework of approximate reasoning. The disadvantage of fuzzy logic is the lack of self learning capability. The combination of

fuzzy logic and neural network can overcome the disadvantages of the above approaches. This study, is proposes the use of a hybrid intelligent system called ANFIS (the Adaptive Neuro Fuzzy Inference System) for forecasting a new shopping technology, called e-shopping turnover. ANFIS, combines both the learning capabilities of a neural network and reasoning capabilities of fuzzy logic in order to provide enhanced forecasting capabilities, as compared to using a single methodology alone. ANFIS has been used by many researchers to forecast various time series, (Jang et al., 1997, Atsalakis, 2009, Atsalakis et al., 2007, Atsalakis & Minoudaki, 2007, Atsalakis & Ucenic, 2006, Atsalakis, 2005, Ucenic & Atsalakis, 2006).

2. Model structure

2.1 ANFIS architecture

This paper considers the development of an e-shopping forecasting system based on the innovative neuro-fuzzy methodology of Jang (Jang, 1993), known as the Adaptive-Network-based Fuzzy Inference System (ANFIS), which was successfully employed to produce a control strategy for the classical inverted pendulum problem. With the ANFIS approach, implementation of the model design differs in form from the more traditional ANN in that it is not fully connected, and in that not all the weights or nodal parameters are modifiable. Essentially, the fuzzy rule base is encoded in a parallel fashion so that all the rules are activated simultaneously, so as to allow network training algorithms to be applied. As in Jang's original work, here a backpropagation algorithm is used to optimize the fuzzy sets of the premises in the ANFIS architecture, and a least squares procedure is applied to the linear coefficients in the consequent terms.

Let X be a space of objects and x be a generic element of X . A classical set $A \subseteq X$ is defined as a collection of elements or objects $x \in X$ such that each x can either belong or not belong to the set A . By defining a characteristic function for each element x in X , we can represent a classical set A by a set of ordered pairs $(x, 0)$ or $(x, 1)$ which indicates $x \in A$ or $x \notin A$, respectively. On the other hand, a fuzzy set expresses the degree to which an element belongs to a set. Hence the characteristic function of a fuzzy set is allowed to have values between 0 and 1, which denotes the degree of membership of an element in a given set. Thus, a fuzzy set A in X is defined as a set of ordered pairs:

$$A = \{(x, \mu_A(x)) \mid x \in X\} \quad (2)$$

where $\mu_A(x)$ denotes the membership function (MF) for the fuzzy set A .

The MF maps each element of X to a membership grade (or a value) between 0 and 1. Usually X is referred to as the universe of discourse or simply the universe. The most widely used MF is the generalized bell MF (or the bell MF), which is specified by three parameters $\{a_i, b_i, c_i\}$ and defined as follows (Loukas, 2001, Jang and Chuen-Tsai, 1995):

$$\mu_{A_i}(x) = \frac{1}{1 + \left[\left(\frac{x - c_i}{a_i} \right)^2 \right]^{b_i}} \quad (3)$$

Parameter b is usually positive. A desired bell MF can be obtained by a proper selection of the parameter set $\{a_i, b_i, c_i\}$. During the learning phase of ANFIS, these parameters are changing continuously in order to minimize the error function between the target output values and the calculated ones (Lee 1990a, 1990b).

The proposed neuro fuzzy model of ANFIS is a multilayer neural network-based fuzzy system. Its topology is depicted in Figure 1, and the system has a total of five layers. In this connected structure, the input and output nodes represent the training values and the predicted values, respectively, and in the hidden layers, there are nodes functioning as membership functions (MFs) and rules. This architecture has the benefit that it eliminates the disadvantage of a normal feed forward multilayer network, whereby it is difficult for an observer to understand or modify the network.

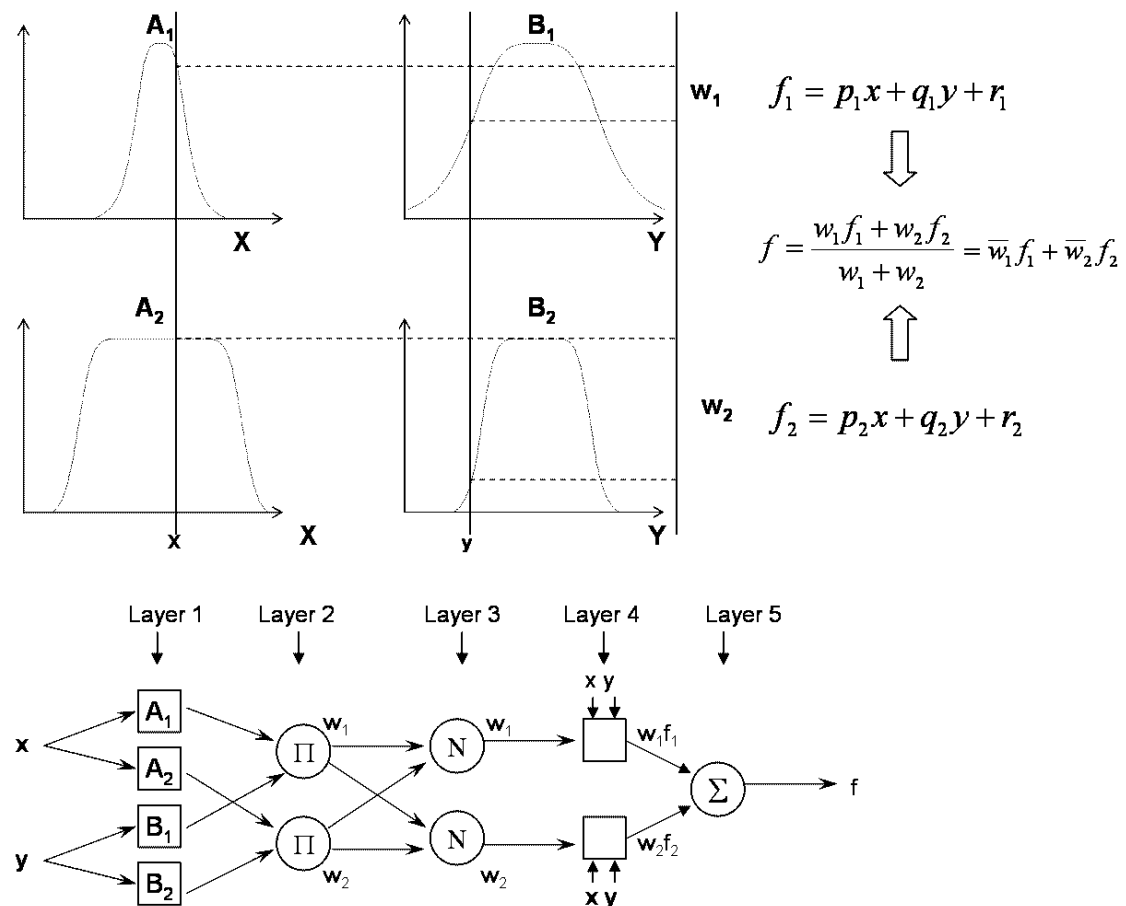


Figure 1: An illustration of the reasoning mechanism for a Sugeno-type model and the corresponding ANFIS architecture (Jang 1997)

For simplicity, it is assumed that the examined fuzzy inference system has two inputs, x and y , and one output. For a first-order Sugeno fuzzy model (Jang, 1997), a common rule set with two fuzzy if-then rules is defined as:

$$\text{Rule1: If } x \text{ is } A_1 \text{ and } y \text{ is } B_1 \text{ then } f_1 = p_1 \cdot x + q_1 \cdot y + r_1 \quad (4)$$

$$\text{Rule2: If } x \text{ is } A_2 \text{ and } y \text{ is } B_2 \text{ then } f_2 = p_2 \cdot x + q_2 \cdot y + r_2 \quad (5)$$

As seen from Figure1, different layers of ANFIS have different nodes. Each node in a layer is either fixed or adaptive (Jang 1993). Different layers with their associated nodes are described below:

Layer 1: Every node i in this layer is a square node with a node function.

$$O_{1,i} = \mu_{A_i}(x) \text{ for } i = 1, 2, \text{ or}$$

$$O_{1,i} = \mu_{B_{i-2}}(y) \text{ for } i = 3, 4, \quad (6)$$

where x - is the input to node i and A_i - is the linguistic label (small, large, etc.) associated with this node. In other words, $O_{1,i}$ is the membership function of a fuzzy set A_i and it specifies the degree to which the given input x satisfies the quantifier A_i . Usually $\mu_{A_i}(x)$ is designated as being bell-shaped with a maximum equal to 1 and minimum equal to 0, such as the generalized bell function depicted below:

$$\mu_{A_i}(x) = \frac{1}{1 + \left[\left(\frac{x - c_i}{a_i} \right)^2 \right]^{b_i}} \quad (7)$$

where a_i, b_i, c_i is the parameter set. As the values of these parameters change, the bell-shaped functions vary accordingly, thus exhibiting various forms of membership function on linguistic label A_i . Parameters in this layer are referred to as premise parameters.

Layer 2: Every node in this layer is a circle node labelled Π , which multiplies the incoming signal and sends the product out.

$$O_{2,i} = w_i = \mu_{A_i}(x) * \mu_{B_i}(y), \quad i = 1, 2. \quad (8)$$

Layer 3: Every node in this layer is a circle-fixed node labelled N. The i -th node calculates the ratio of the i -th rule's firing strength to the sum of all rules' firing strengths:

$$O_{3,i} = \bar{w}_i = \frac{w_i}{w_1 + w_2}, \quad i = 1, 2. \quad (9)$$

For convenience, outputs of this layer are called normalized firing strengths.

Layer 4: Every node i in this layer is an adaptive square node with a node function

$$O_{4,i} = \bar{w}_i \cdot f_i = \bar{w}_i(p_1 \cdot x + q_i \cdot y + r_i) \quad (10)$$

where: \bar{w}_i is a normalized firing strength from layer 3 and $\{p_i, q_i, r_i\}$ is the parameter set in this layer. Parameters in this layer are referred to as consequent parameters.

Layer 5: The single node in this layer is a circle fixed node labelled Σ , that computes the overall output as the summation of all incoming signals:

$$\text{overall output} = O_{5,i} = \sum_i \bar{w}_i \cdot f_i = \frac{\sum_i w_i \cdot f_i}{\sum_i w_i} \quad (11)$$

This architecture develops an adaptive network that is functionally equivalent to a two inputs first-order Sugeno fuzzy model with four rules, where each input has two membership functions. The main advantage of this model is its transparency and efficiency.

2.2 Learning Algorithm of ANFIS

The learning algorithm for ANFIS is a hybrid algorithm, which is a combination of gradient descent and the least-squares method. More specifically, in the forward pass of the hybrid learning algorithm, node outputs go forward until layer 4 and the consequent parameters are identified by the least-squares method (Jang, 1993). In the backward pass, the error signals propagate backwards and the premise parameters are updated by gradient descent. Table 1 summarizes the activities in each pass.

Table 1: Errors for one step ahead forecasting results

	Forward pass	Backward pass
Premise parameters	Fixed	Gradient descent
Consequent parameters	Least-squares estimator	Fixed
Signals	Node outputs	Error signals

The consequent parameters are optimized under the condition that the premise parameters are fixed. The main benefit of the hybrid approach is that it converges much faster since it reduces the search space dimensions of the original pure backpropagation method used in neural networks. The overall output can be expressed as a linear combination of the consequent parameters. The error measure to train the above-mentioned ANFIS is defined as follows (Jang, 1997):

$$E = \sum_{k=1}^n (y_k - \hat{y}_k)^2 \quad (12)$$

where y_k and \hat{y}_k are the kth desired and estimated output, respectively, and n is the total number of pairs (inputs-outputs) of data in the training set.

3. Experimental data used for training and testing the Neuro-fuzzy System

The experimental data consisted of a monthly time series of electronic sales that took place in the USA from January 1992 until December 2009 (216 samples). Figure 2 depicts the first 172 samples used for training the model and the remaining 42 that were used to test the performance of the resulting model. The structure of ANFIS consists of two inputs and one output which means that the forecasting system is used to forecast the subsequent month's electronic sales based on the values of one month ago and two months ago. Each input has two generalized bell MFs. Figure 3 depicts the initial forms of the MFs before the training and the final MFs after the training (fine-tuning).

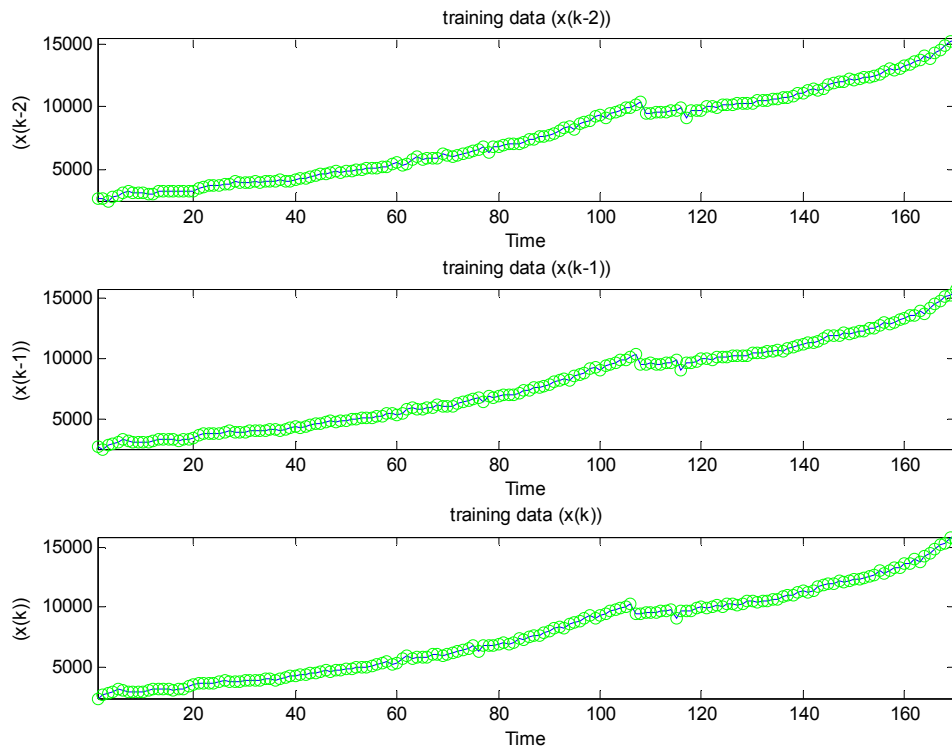


Figure 2: Graphical representation of the electronically sales.

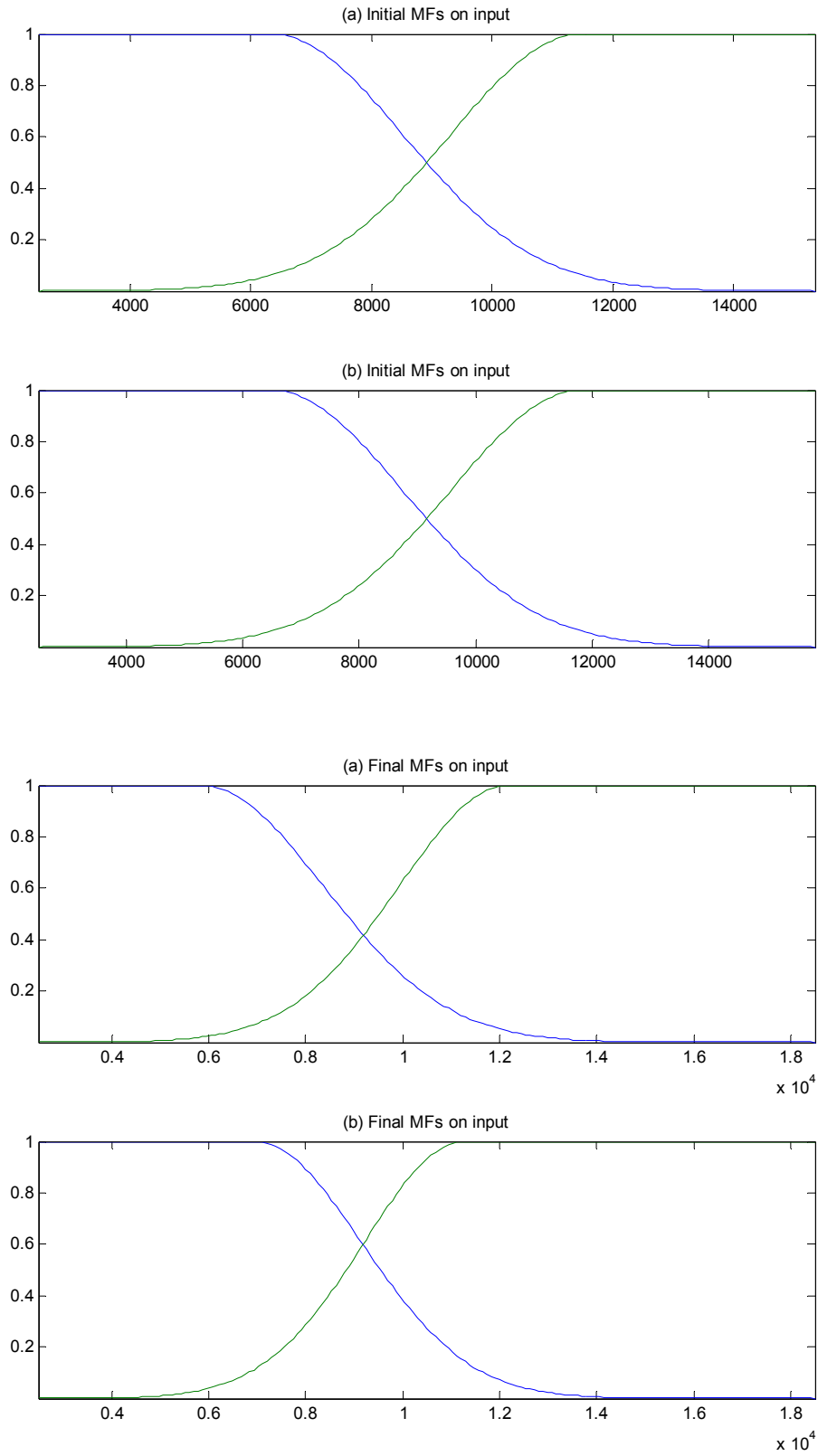


Figure 3: Illustration of MFs before and after the training.

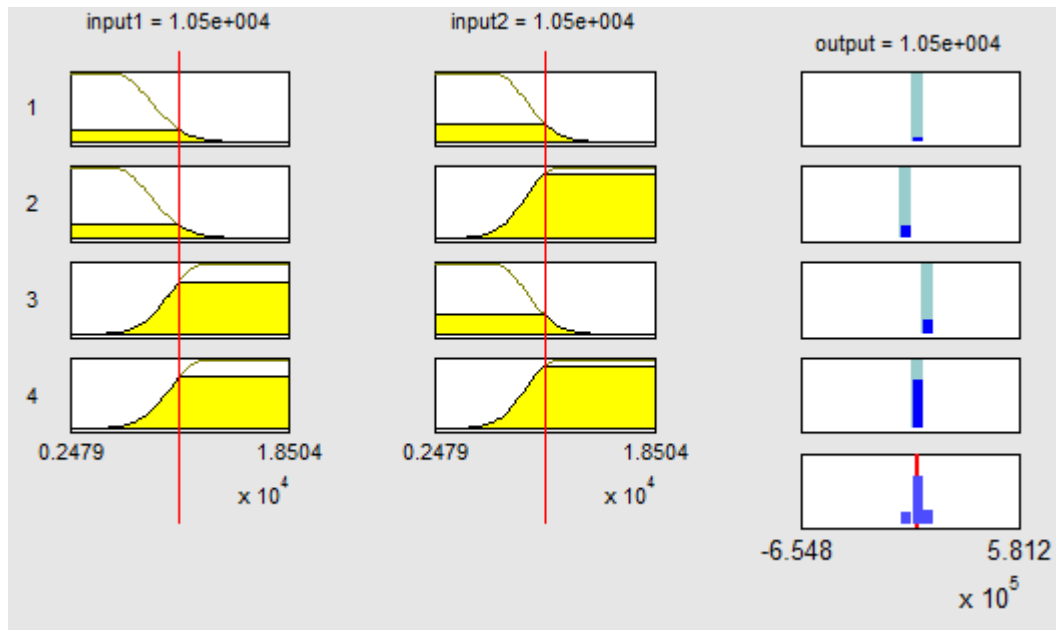


Figure 4: A view of the rules

The network used 4 rules and worked 800 epochs to converge with the optimal fuzzy inference system. Figure 4 depicts the function of the rules. Table 2 describes the type and the values of the ANFIS parameters.

Table 2: ANFIS parameter types and their values used for training

ANFIS parameter type	Value
MF type	Bell function
Number of MFs	2
Output MF	Linear
Number of Nodes	21
Number of linear parameters	12
Number of nonlinear parameters	16
Total number of parameters	28
Number of training data pairs	170
Number of evaluating data pairs	42
Number of fuzzy rules	4

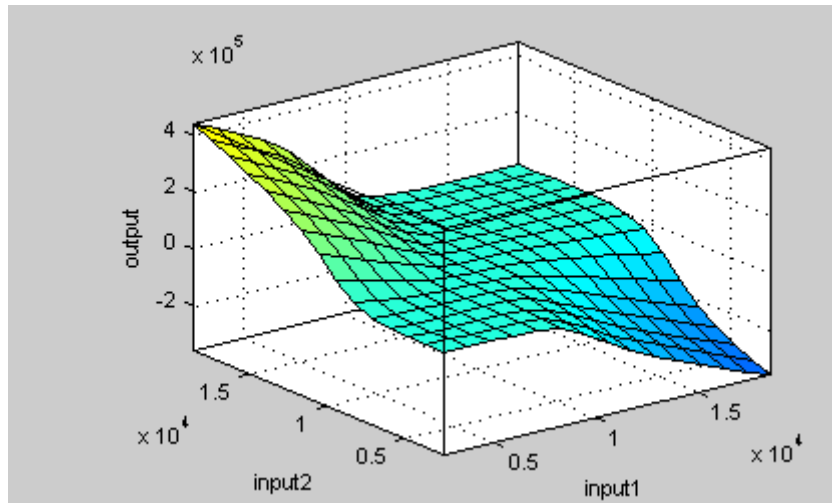


Figure 5: The control surface of the ANFIS e-shopping forecasting model

Figure 5 illustrates a 3D representation of the control surface of the two inputs in relation to the output of the model. The smooth distribution of the surface, reconfirm the satisfactory performance results of the model.

4. Performance of the model

The size of the sample used for the evaluation phase for the period of June 2006 until December 2009 was 42. Figure 5 illustrates the results comparing the actual data with the forecasted values. The same data have been used to run an Autoregressive (AR) and Autoregressive Moving Average (ARMA) forecasting model.

Table 3 depicts the error analysis according to some well known statistical errors: Mean square error (MSE), Root mean square error (RMSE), Mean absolute error (MAE) and Mean absolute percentage error (MAPE) (Makridakis, et al., 1983). ANFIS is superior in performance in comparison with the AR and ARMA models, based on the four errors (figures in bold) depicted below:

Table 3: Errors for one month ahead forecasting results

	ANFIS	AR	ARMA
MSE	2.2267	4.1221	4.1450
RMSE	149.22	203.02	203.59
MAE	101.59	133.84	132.66
MAPE	1.1140	1.5524	1.5301

The forecasting performance of ANFIS is satisfactory in research and acceptable in practice as can be seen in the Figure 6. The square signs on the blue line depict the actual e-shopping monthly sales and the asterisks in the red line depict the forecasting e-shopping monthly sales.

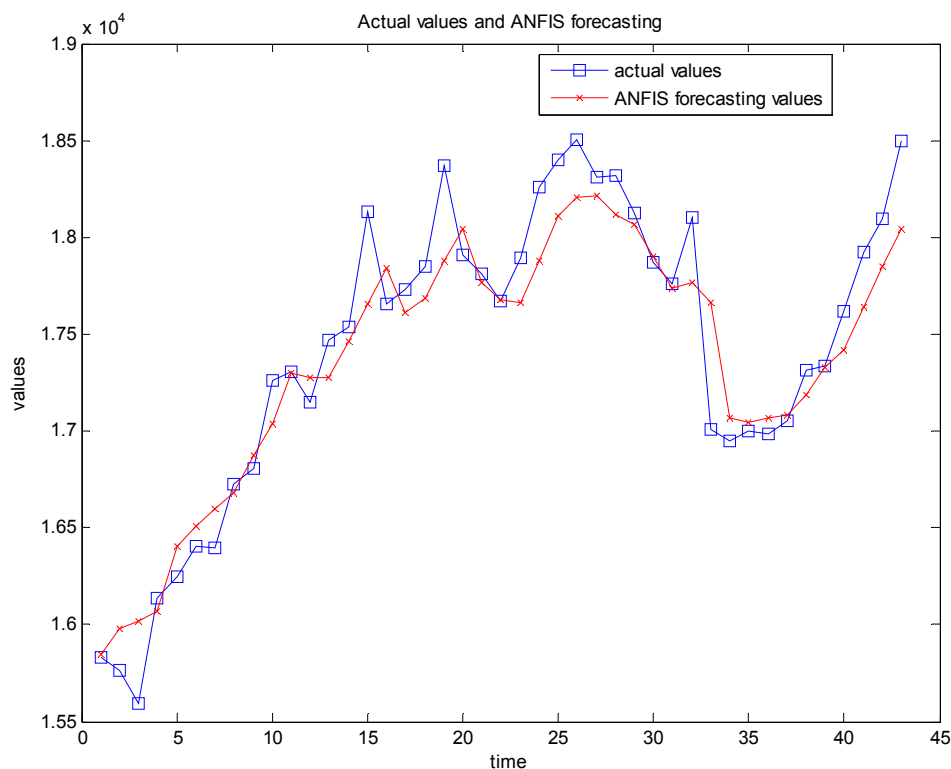


Figure 6: Out of sample actual and ANFIS forecasted e-shopping sales

5. Conclusion

This paper investigated the modeling and forecasting method of a neuro-fuzzy network (ANFIS) to forecast monthly electronic sales. Based on the above results, the suggested neuro-fuzzy model could be an efficient system of forecasting new technology shopping methods such as electronic shopping. The following benefits arose from the use of ANFIS for forecasting electronic shopping:

- a) It is a general framework that combines the technologies of neural networks and fuzzy systems.
- b) Both numerical and linguistic knowledge can be combined into a fuzzy rule base.
- c) The fuzzy rule base represents the knowledge of the network structure so that structure learning techniques can easily be accomplished.
- d) Fuzzy membership functions can be tuned optimally by using learning methods.
- e) The architecture requirements are fewer and simpler compared to neural networks, which require extensive trials and errors for optimization of their architecture.
- f) ANFIS does not require extensive initializations through several random starts before training, as always occurs in neural networks.

Other advantages of the two-phase neuro fuzzy hybrid technique in the ANFIS model also include its nonlinear ability, its capacity for fast learning from numerical and linguistic knowledge, and its adaptation capability.

6. References

Atsalakis, G., (2005), Exchange rate forecasting by neuro-fuzzy techniques, *Journal of Financial Decision Making*, Vol. I (2), pp. 15-26.

Atsalakis, G., Skiadas, C. and Braimis, I., (2007), Probability of trend prediction of exchange rate by neuro-fuzzy techniques. *Recent Advances in Stochastic Modeling and Data Analysis*. London, World Scientific Publishing Co. Pte. Ltd, pp. 414-422.

Atsalakis, G., Minudaki C. (2007), Prediction of daily irrigation water demand using Adaptive Neuro-fuzzy inference system (ANFIS), *International conference on energy, environment, ecosystems and sustainable development*. Greece Water Economics, Statistics and Finance, pp. 368-373, Ag. Nikolaos, Greece.

Atsalakis G., Ucenic C. (2006), Forecasting the production level for wind energy using a neuro- fuzzy model, *Journal of WSEAS Transactions on Environment and Development*, Vol. 2(6), pp. 823-828.

Atsalakis G. (2009). Wind energy production forecasting. In Mastorakis N., Mladenov, V., Vasiliki, T. (Eds.) *Lecture Notes in Electrical Engineering* (vol. 2, pp. 1-13). New York: Springer

Hornik K., (1991), Approximation capabilities of multi-layer feed- forward networks, *Neural Networks* 4, pp. 251-257.

Jain B.A. and Nag B.N.,(1997), Performance evaluation of neural network decision models, *Management Information Systems* 14, pp. 201-216.

Jang J.S.R., (1993), ANFIS: Adaptive network-based fuzzy inference system. *IEEE Trans Systems, Man Cybern* 23(3), pp. 665-685.

Jang J. S. R., and Chuen-Tsai S., (1995), Neuro-fuzzy modeling and control *Proc. IEEE* (83) 378-406.

Jang, J-S.R., Sun, C-T.E, and Mizutani, E., (1997), *Neuro-fuzzy and soft computing: a computational approach to learning and machine intelligence*, Prentice Hall.

Lee C. C., (1990a), Fuzzy logic in control systems: fuzzy logic controller. I *IEEE Trans. on Syst. Man Cybern*, (20) pp. 404-18.

Lee C. C., (1990b), Fuzzy logic in control systems: fuzzy logic controller. II *IEEE Trans. on Syst. Man Cybern*. (20) pp. 419-35.

Loukas Y. L., (2001), Adaptive neuro-fuzzy inference system: an instant and architecture-free predictor for improved QSAR studies *J. Med. Chem.*(44) pp. 2772-83.

Makridakis, S., Wheelwright SC, and McGee VE., (1983), *Forecasting: methods and applications*, 2nd edition. Wiley, New York.

Pao Y.H., (1989), *Adaptive pattern recognition and neural networks*, Addison Wesley, New York

Shapiro A.F., (2002), The merging of neural networks, fuzzy logic, and genetic algorithms, *Insurance: Mathematics and Economics* 31, pp. 115-131.

Skapura D., (1996), *Building Neural Networks*, Addison Wesley, New York (1).

Ucencic C., Atsalakis G. (2006), Forecasting electricity demand using a neuro- fuzzy approach versus traditional methods, *Journal of WSEAS Transactions on Business and Economics*, Issue 1, Volume 3, pp. 9-17.

Clustering Complex Heterogeneous Data Using a Probabilistic Approach

Helena Bacelar-Nicolau, Fernando Nicolau,
Áurea Sousa and Leonor Bacelar-Nicolau

University of Lisbon, Faculty of Psychology, Lab. of Statistics and Data Analysis, Portugal

Email: hbacelar@fp.ul.pt

New University of Lisbon, FCT, Department of Mathematics, Portugal

Email: fnicolau@gmail.com

University of Azores, Department of Mathematics, Portugal

Email: aurea@uac.pt

University of Lisbon, Faculty of Medicine, Lab. of Biomathematics & Institute of
Preventive Medicine, Portugal

Email: lnicolau@fm.ul.pt

Abstract: In cluster analysis regarding complex data bases, very often the question arises of how we should measure the similarity between statistical data units in a coherent way, if different types of variables are involved. In this paper we analyze and give a solution to the problem when interval and binary variables come together. We use a global generalized (three-way) affinity coefficient and compare a hierarchical clustering probabilistic approach to the empirical one. Application on an example issued from the literature of symbolic data analysis briefly illustrates how both coefficients work.

Keywords: similarity coefficient, interval variables, binary variables, hierarchical clustering model, probability distribution function, three-way / symbolic data.

1 Introduction

In complex data bases, we are very often working with matrices where data units are described by a heterogeneous set of variables. Therefore the question arises of how we should measure the similarity between statistical data units in a coherent way, if different types of variables are involved. Usually partial similarity coefficients for each type of variables are computed, and then a convex linear combination of those similarities gives a global similarity between data units. Such procedure should be performed in a consistent way, combining comparable similarity coefficients in a valid / robust global similarity index. So far we have been using the so-called affinity coefficient - proposed by Matusita (1951), extended to cluster analysis framework e.g. in Bacelar-Nicolau (1988) - and generalized affinity coefficients for that purpose, respectively in two-way and in three-way or *symbolic* clustering contexts, by Bacelar-Nicolau e.g. in Bock and Diday (2000), pp160-165.

Here we apply the above procedure in the case where heterogeneous variables of two pertinent types, such as interval and binary variables, are simultaneously present. We use a global standardized generalized affinity coefficient and compare

this probabilistic approach – e.g. proposed in Lerman (1972, 1981) and extended in Bacelar-Nicolau (1987, 1988) - to the empirical one. Application on an example issued from the literature of symbolic data analysis briefly illustrates how both coefficients work.

2 Three-way Affinity Coefficient

Let D be a set of statistical data units and let V be a set of p variables, as depicted in the previous section. The weighted generalized affinity coefficient $a(k, k')$ between a pair of data units $k, k' \in D$ ($k, k' = 1, \dots, n$), may be defined in a three-way context, as the weighted mean of local affinities between k and k' over the j -th variable ($j = 1, \dots, p$), as follows:

$$a(k, k') = \sum_{j=1}^p \pi_j \cdot \text{aff}(k, k'; j) = \sum_{j=1}^p \pi_j \cdot \sum_{\ell=1}^{m_j} \sqrt{\frac{x_{kj\ell} \cdot x_{k'j\ell}}{x_{kj} \cdot x_{k'j}}}, \quad (1)$$

where: $\text{aff}(k, k'; j)$ is the local affinity over the j -th variable, m_j represents the number of modalities of j -th variable; $x_{kj\ell}$ is a positive real value (negative values may be treated with a convenient version of the affinity coefficient) whose meaning depends on the type of j -th variable or equivalently on the nature of j -th corresponding sub-table on the whole data matrix; and weights π_j verify $0 \leq \pi_j \leq 1$, $\sum \pi_j = 1$.

Either the local affinities or the whole weighted generalized affinity coefficient, take values in the interval $[0, 1]$ and satisfy a set of proprieties which characterize affinity measurement as a robust similarity coefficient (e.g. Bacelar-Nicolau (2002) and Bacelar-Nicolau et al (2009)).

3 Three-way Affinity Coefficient with Heterogeneous and Complex Variables

Let V be a set of p heterogeneous variables, namely of binary and interval types. Let $Y_{j'}$ represent a $m_{j'}$ – dimensional binary vector and $Y_{j''}$ represent an interval variable, where j' and j'' belong to $\{1, \dots, p\}$.

Thus the corresponding generalized columns or sub-tables into the whole data matrix have n rows, and the k -th row ($k = 1, \dots, n$) encloses: for $Y_{j'}$, an element $\{0, 1\}_k^{m_{j'}}$ of the power set $\{0, 1\}^{m_{j'}}$, the whole binary sub-table being an element of $\{0, 1\}^{n \times m_{j'}}$; for $Y_{j''}$, an interval $I_{kj''}$ of the real axis.

The generalized global and local affinity coefficients in (1) still apply, the meaning of real values $x_{kj\ell}$ depending on each type of variable (e.g. Nicolau et al (2007), and Bacelar-Nicolau et al (2009)):

- For an $m_{j'}$ - dimensional binary vector $Y_{j'}$ the local affinity $aff(k, k'; j')$ may be computed from the 2×2 contingency table associated to the pair (k, k') of rows over the binary vector $Y_{j'}$. Let $s_{j'}$, $t_{j'}$, $u_{j'}$ and $v_{j'}$ represent the cardinals of positive agreements ($x_{kj'\ell} = x_{k'j'\ell} = 1$), negative agreements ($x_{kj'\ell} = x_{k'j'\ell} = 0$), and disagreements (respectively $x_{kj'\ell} = 1, x_{k'j'\ell} = 0$ and $x_{kj'\ell} = 0, x_{k'j'\ell} = 1$), respectively.

Then we have: $s_{j'} = \sum_{\ell=1}^{m_{j'}} x_{kj'\ell} x_{k'j'\ell}$, $t_{j'} = \sum_{\ell=1}^{m_{j'}} (1 - x_{kj'\ell})(1 - x_{k'j'\ell})$, $u_{j'} = \sum_{\ell=1}^{m_{j'}} x_{kj'\ell}(1 - x_{k'j'\ell})$ and $v_{j'} = \sum_{\ell=1}^{m_{j'}} (1 - x_{kj'\ell})x_{k'j'\ell}$. Thus the local affinity becomes: $aff(k, k'; j') = \frac{s_{j'}}{\sqrt{m_{kj'} m_{k'j'}}$, where $s_{j'} + v_{j'} = m_{k'j'}$ and

$s_{j'} + u_{j'} = m_{kj'}$, that is the well known Ochiai coefficient for binary data.

- For an interval variable $Y_{j''}$, associated to a generalized column j'' where each cell (k, j'') contains an interval $I_{kj''}$, ($k = 1, \dots, n$), a similar reasoning allows us to a local affinity which is a generalized Ochiai coefficient: instead of cardinal numbers we obtain convenient interval ranges. In fact, let $I_{j''}$ be the union of the intervals $I_{kj''} : I_{j''} = \cup I_{kj''}$ ($k = 1, \dots, n$) and let $\{I_{j''\ell} : \ell = 1, \dots, m_{j''}\}$ be a set of $m_{j''}$ elementary intervals, such that, for $\ell, \ell' = 1, \dots, m_{j''}$, $\ell \neq \ell'$; $k = 1, \dots, n$:

$$I_{j''} = \cup I_{j''\ell}; |I_{j''\ell} \cap I_{j''\ell'}| = 0; |I_{kj''} \cap I_{j''\ell}| = |I_{j''\ell}|, \text{ if } |I_{kj''} \cap I_{j''\ell}| \neq 0, \\ |I_{kj''} \cap I_{j''\ell}| = 0, \text{ otherwise, where } || \text{ symbolizes the interval range.}$$

Then, if we represent by $x_{kj''\ell}$ the interval range $x_{kj''\ell} = |I_{kj''} \cap I_{j''\ell}|$, we will have: $x_{kj''\ell} = |I_{j''\ell}|$ if $I_{kj''} \cap I_{j''\ell} = I_{j''\ell}$, $x_{kj''\ell} = 0$, otherwise; therefore

$$x_{kj''\bullet} = |I_{kj''}|, \quad x_{k'j''\bullet} = |I_{k'j''}| \quad \text{and} \quad \sum_{\ell=1}^{m_{j''}} \sqrt{x_{kj''\ell} x_{k'j''\ell}} = |I_{kj''} \cap I_{k'j''}|.$$

Hence the local affinity between two intervals $aff(I_{kj''}, I_{k'j''}) = aff(k, k', j'')$ is also defined as in formula (1) above, after a suitable transformation of the original data matrix. Besides $aff(I_{kj''}, I_{k'j''}) = \frac{|I_{kj''} \cap I_{k'j''}|}{\sqrt{|I_{kj''}| \cdot |I_{k'j''}|}}$, for $k, k' = 1, \dots, n$, which is the generalized Ochiai coefficient for interval variables.

4 Asymptotic Standardized Three-way Affinity Coefficient

Prior knowledge on the data base may often be taken in account as statistical reference hypothesis R allowing us to compute standardized affinity values and/or the corresponding cumulative distribution function values. New similarity coefficients arise and as a result new semiprobabilistic or probabilistic clustering models, instead of empirical clustering models may be selected.

In a three-way clustering probabilistic analysis, a permutational reference hypothesis R based on a well known limit theorem of Wald and Wolfowitz (other reference hypothesis have been used based, for instance, on the limit theorem of delta-method), very often holds. Then the random variable associated to $aff(k, k'; j)$ has asymptotic normal distribution (e.g. Bacelar-Nicolau (1988) and Bacelar-Nicolau et al (2009), whose asymptotic mean value and variance are as follows:

$$\mu_{WW}^*(k, k'; j) = \frac{I}{m_j} \sum_{\ell=1}^{m_j} \sqrt{\frac{x_{kj\ell}}{x_{kj\bullet}}} - \frac{m_j}{\sum_{\ell'=1}^{m_j} \sqrt{\frac{x_{k'j\ell'}}{x_{k'j\bullet}}}}$$

$$\sigma_{WW}^{*2}(k, k'; j) = \frac{I}{m_j - I} \sum_{\ell=1}^{m_j} \left(\sqrt{\frac{x_{kj\ell}}{x_{kj\bullet}}} - \frac{I}{m_j} \sum_{\ell'=1}^{m_j} \sqrt{\frac{x_{kj\ell'}}{x_{kj\bullet}}} \right)^2 \times \sum_{\ell=1}^{m_j} \left(\sqrt{\frac{x_{k'j\ell}}{x_{k'j\bullet}}} - \frac{I}{m_j} \sum_{\ell'=1}^{m_j} \sqrt{\frac{x_{k'j\ell'}}{x_{k'j\bullet}}} \right)^2$$

This leads us to a local asymptotic normal affinity coefficient whose realization $aff_{WW}(k, k'; j)$ also satisfies the main properties of a similarity coefficient. Thus instead of using the basic generalized affinity coefficient $a(k, k')$ between data units $k, k' \in D$ ($k, k' = 1, \dots, n$), we may use:

$$a_{WW}(k, k') = a^*(k, k') = \sum_{j=1}^p \pi_j \cdot aff_{WW}^*(k, k'; j)$$

where $aff_{WW}^*(k, k'; j) = (aff(k, k'; j) - \mu_{WW}^*(k, k'; j)) / \sigma_{WW}^*(k, k'; j)$.

If reference hypothesis $R \equiv WW$ holds, using $a_{WW}(k, k')$ instead of $a(k, k')$ allows us to deal with comparable similarity values issued from random variables with the same (asymptotic standard normal) distribution. The statistical procedure shows to be quite robust even in case of small samples. This approach also brings us to a third coefficient related to affinity measurement that is a probabilistic coefficient which may evaluate the significance of each affinity value – e.g. in Lerman (1972, 1981) and in Bacelar-Nicolau (1987, 1988) -. In the present work we will not use this probabilistic coefficient yet.

5 Example/Case Study

The methods have been applied to data bases related to health sciences, education and management areas, for instance in Nicolau et al (2007), Bacelar-Nicolau et al (2008), Bacelar-Nicolau (2002), Sousa (2005).

Here a small example issued from the literature of three-way and symbolic data analysis, found in Ichino and Yaguchi (1994) and Bock and Diday (2000) briefly illustrates how both three-way affinity coefficients work.

The data set consists of 8 oils and fats (*1-Linseed oil (LS)*, *2-Perilla oil (P)*, *3-Cotton seed (CS)*, *4-Sesame oil (S)*, *5- Camellia (C)*, *6-Olive oil (O)*, *7-Beef Tallow (T)*, *8-Lard (L)*) described by four interval variables and one nominal qualitative feature. The following table shows the original data base.

Table 1. Data Matrix (Fats and Oils)

Sample name	Specific gravity (g/cm ³)	Freezing point (°C)	Iodine value	Saponification value	Major Fatty Acids
<i>LS</i>	[0.930, 0.935]	[-27, -8]	[170, 204]	[118, 196]	L, Ln, O, P, M
<i>P</i>	[0.930, 0.937]	[-5, -4]	[192, 208]	[188, 197]	L, Ln, O, P, S
<i>CS</i>	[0.916, 0.918]	[-6, -1]	[99, 113]	[189, 198]	L, O, P, M, S
<i>S</i>	[0.920, 0.926]	[-6, -4]	[104, 116]	[187, 193]	L, O, P, S, A
<i>C</i>	[0.916, 0.917]	[-21, -15]	[80, 82]	[189, 193]	L, O
<i>O</i>	[0.914, 0.919]	[0, 6]	[79, 90]	[187, 196]	L, O, P, S
<i>T</i>	[0.860, 0.870]	[30, 38]	[40, 48]	[190, 199]	O, P, M, S, C
<i>L</i>	[0.858, 0.864]	[22, 32]	[53, 77]	[190, 202]	L, O, P, M, S, Lu

L: Linoleic acid *Ln*: Linolenic acid *O*: Oleic acid *P*: Palmitic acid *M*: Myristic acid
S: Searic acid *A*: Arachic acid *C*: Capric acid *Lu*: Lauric acid

In order to apply either the empirical three-way affinity coefficient or the asymptotic standardized one, a transformed data matrix was computed. Each interval variable (generalized column) gave place to a sub-table with a suitable number of columns corresponding to a set of elementary intervals. For instance in case of the first interval variable, *Specific gravity (g/cm³)*, each of the 13 columns of such sub-table contains the ranges of the intersection intervals between each of the 13 elementary intervals and each of the 8 intervals in the first generalized column of Table 1. Similarly each of the other three interval variables gave three sub-tables of 13, 15 and 10 elementary intervals, respectively. The last generalized column of Table 1, describing the *Major Fatty Acids*, gave place to a binary sub-table of 9 columns. Several hierarchical agglomerative clustering models were used, based either on the empirical three-way affinity coefficient or on the asymptotic standardized one, with equal weights. The main clustering results were very similar for both coefficients although the levels the main clusters merge together are different in the two groups of dendrograms. Tables 2 and 3 represent the similarity matrices and Figures 1 and 2 show the dendrograms associated to each coefficient and to the Complete Linkage aggregation criterion.

Table 2. Similarity Matrix (Fats and Oils): three-way affinity coefficient

	LS	P	CS	S	C	O	T	L
LS	1.000000							
P	0.492318	1.000000						
CS	0.212840	0.427221	1.000000					
S	0.175470	0.437504	0.534230	1.000000				
C	0.284173	0.259825	0.401246	0.289791	1.000000			
O	0.202101	0.356663	0.460931	0.342185	0.449477	1.000000		
T	0.165291	0.275556	0.337778	0.201650	0.163246	0.267497	1.000000	
L	0.185283	0.280774	0.336534	0.216770	0.202073	0.278769	0.467265	1.000000

Table 3. Similarity Matrix (Fats and Oils): Standardized three-way affinity coefficient

	LS	P	CS	S	C	O	T	L
LS	1.000000							
P	1.054071	1.000000						
CS	-0.177319	0.814400	1.000000					
S	-0.312900	0.864528	1.227810	1.000000				
C	0.486189	0.392913	0.895965	0.516401	1.000000			
O	-0.191838	0.556516	0.945541	0.524721	1.145654	1.000000		
T	-0.390200	0.128798	0.435851	-0.232820	-0.066975	0.061236	1.000000	
L	-0.347061	0.105382	0.422068	-0.217022	0.106450	0.081614	0.930447	1.000000

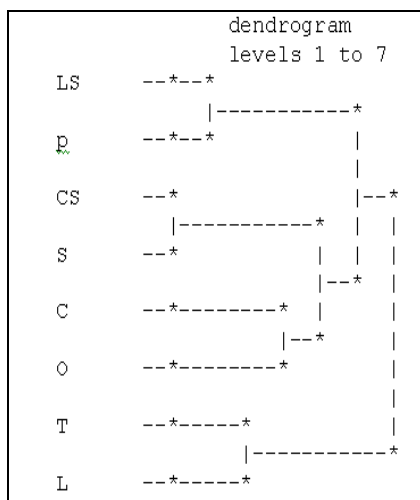


Fig. 1. Three-way affinity coefficient; Complete Linkage aggregation criterion

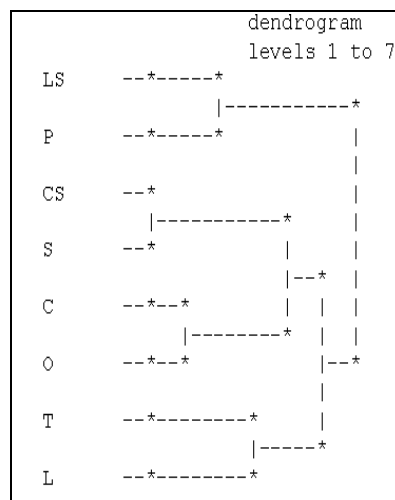


Fig. 2. Standardized three-way affinity coefficient; Complete Linkage aggregation criterion

The dendrograms give a good illustration for chemical properties of the fats and oils: it is known that both elements of each one of the sample pairs (LS, P), (CS, S), (C, O) have similar properties, given that LS and P are used for painting, CS and S for food, C and O for cosmetics and the pair (T, L) has animal origin. In addition cluster {CS, S, C, O} has been found in other statistical approaches as well, particularly in Ichino and Yaguchi (1994) and validity coefficients, not presented here, provide a helpful complement to the cluster analysis.

6 Conclusions. Future Developments

Both the empirical and the asymptotic standardized three-way (weighted generalized) affinity coefficients $a(k, k')$ and $a_{ww}(k, k')$ support in a consistent way hierarchical cluster analysis models for statistical data units, when mixed and complex variable types are present in a database. Besides, $a_{ww}(k, k')$ is often applied instead of $a(k, k')$. Indeed, if V is a set of p independent heterogeneous variables, using $a_{ww}(k, k')$ instead of $a(k, k')$ means doing local standardization accordingly to the different variable types, which in this way all

become asymptotic standard normal variables as well as their convex linear combination. Future developments concern three-way cluster analysis based on a probabilistic coefficient as well as on empirical and semi-probabilistic clustering models.

Acknowledgments: This research was partially supported by FCT/POCTI/ and POCTI/FEDER, in the scope of CEaul Research Project on Applied Multivariate Data Analysis and Modelling.

References

1. Bacelar-Nicolau, H., On the distribution equivalence in cluster analysis. *Proceedings of the NATO ASI on Pattern Recognition Theory and Applications*. Springer-Verlag, 73-79 (1987).
2. Bacelar-Nicolau H., Two probabilistic models for classification of variables in frequency tables, in *Classification and Related Methods of Data Analysis* (H. H. Bock, ed.), North Holland, 181-186 (1988).
3. Bacelar-Nicolau H., On the Generalized Affinity Coefficient for Complex Data, *Biocybernetics and Biomedical Engineering*, **22**, 1, 31-42 (2002).
4. Bacelar-Nicolau H., Nicolau, F. C., Sousa, A. and Bacelar-Nicolau, L., Measuring similarity of complex and heterogeneous data in clustering of large data sets, *Biocybernetics and Biomedical Engineering, PWN-Polish Scientific Publishers Warszawa*, **29**, 2, 9-18 (2009).
5. Bacelar-Nicolau, L., *Caracterização dos Sistemas de Informação das Organizações com base no modelo de Nolan. Aplicação de modelos de classificação hierárquica aos organismos da Administração Pública*. Master Thesis, Univ. Nova de Lisboa (2002).
6. Bock H.H. and Diday E. [eds.], *Analysis of Symbolic Data Exploratory Methods for Extracting Statistical Information from Complex Data*, Springer (2000).
7. Ichino, M. and Yaguchi, H., Generalized Minkowski Metrics for Mixed Feature Type Data Analysis. *IEEE Transactions on Systems, Man and Cybernetics*, **24**, 4, 698-708 (1994).
8. Lerman, I. C., Étude Distributionelle de Statistiques de Proximité entre Structures Algébriques Finies du Même Type; Application à la Classification Automatique. *Cahiers du B.U.R.O.*, 19, Paris (1972).
9. Lerman I. C., *Classification et Analyse Ordinale des Données*, Dunod (1981).
10. Matusita K., On the theory of statistical decision functions. *Ann. Instit. Stat. Math.*, **III**, 1-30 (1951).

SMTDA 2010: Stochastic Modeling Techniques and Data Analysis
International Conference, Chania, Crete, Greece, 8 - 11 June 2010

11. Nicolau, F. C., Bacelar-Nicolau, H., Sousa, A., Bacelar-Nicolau, L., Silva, O. and Magalhães, B., Probabilistic Models in Three Way Cluster Analysis. *Proceedings of the 56th Session of the International Statistical Institute, Lisbon, 2007*, published on the ISI 2007 CD Proceedings (2007).
12. Nicolau F. C. and Bacelar-Nicolau, H., Some Trends in the Classification of Variables, in *Data Science, Classification and Related Methods* (Hayashi et al, eds.), Springer, 89-98 (1998).
13. Sousa, A., *Contribuições à Metodologia VL e índices de validação para Dados de Natureza Complexa*. PhD Thesis, Univ. Azores (2005).

Impulse control problem of partially observed diffusion processes

Baghery-Kabbaj F. and Massa-Turpin I.

Laboratoire de Mathematiques de Valenciennes
Universite de Valenciennes et du Hainaut Cambresis, 59313 Valenciennes Cedex
09, France
(e-mail: fbaghery@univ-valenciennes.fr)

Abstract. We investigate the problem of impulse control of a partially observed diffusion process. We study the impulse control of Zakai type equations. The associated value function is characterized as the only viscosity solution of the corresponding quasi-variational inequality. We show the optimal cost function for the problem with incomplete information can be approximated by a sequence of value functions of the previous type.

Keywords: impulse control, partially observed diffusion process, nonlinear filtering, diffusion process, Hamilton Jacobi Bellman quasi-variational inequality, viscosity solutions.

1 Introduction

The impulse control is double sequences

$$v = (\theta_1, \theta_2, \dots, \theta_j, \dots; \zeta_1, \zeta_2, \dots, \zeta_j, \dots; j \in \mathbb{N}^*)$$

where the θ'_n s represent the successive instants of impulse, and the ζ'_n s are the corresponding impulsions assumed to take their values in a compact set. The applications are numerous, for instance in management (in a large sense: firms, natural resource, informatic, production, stock...), economics, finance, medicine... . From an analytic point of view, the study of such problems leads to quasi-variational inequalities: we search a function v ($v = v(x)$ or $v(x, t)$), such that

$$\begin{cases} Av - f \leq 0, v - Mv \leq 0, \\ (Av - f)(v - Mv) = 0 \text{ in } O \text{ (or } Q) \end{cases} \quad (1)$$

where A is a second order elliptic or parabolic differential operator, O is an open of \mathbb{R}^d and $Q = O \times]0, T[$. In the case of partial observations, the proper strategies, called admissible controls, must depend on the observation process in a nonanticipative way. The main known results establish the existence of optimal strategies ([1], [2] for Markov Chains; [7] for Feller-Markov processes). Here our purpose is to characterize the value function associated to the impulse control problem. The initial problem is approximated

by a sequence of optimal stopping-time problems. For such problems we prove that the corresponding value functions are unique viscosity solution of corresponding variational inequalities.

2 Impulse and continuous controls of a diffusion process

2.1 Set-up

On a standard probability space $(\Omega, F, \hat{P}, F_s)$, are defined two independant Brownian Motion W and Y respectively n and m dimensional. The impulse controls v are the sets $\{\theta_1, \theta_2, \dots; \zeta_1, \zeta_2, \dots\}$ where $(\theta_i)_{i \in \mathbb{N}^*}$ is a nondecreasing sequence of stopping times with respect to $(F_s^Y = \sigma(Y_r; t \leq r \leq s))$, $(\theta_i)_{i \in \mathbb{N}^*}$ converges to $+\infty$ and $(\zeta_i)_{i \in \mathbb{N}^*}$ is a sequence of random vectors valued in a compact subset of $(\mathbb{R}^+)^d$, adapted to $F_{\theta_i}^Y$.

ξ_0 is a given d -dimensional random vector and for each strategy (α, v) , we inductively define a sequence of processes with jumps:

$$\begin{cases} dX^0(s) = [b(X^0(s), \alpha_s) - h(X^0(s))\gamma(X^0(s), \alpha_s)] ds + \sigma(X^0(s), \alpha_s)dW_s + \gamma(X^0(s), \alpha_s)dY_s, s > t \\ X_0(t) = \xi_0 \end{cases} \quad (2)$$

par

$$\begin{cases} dX_s^n = [b(X_s^n, \alpha_s) - h(X_s^n)\gamma(X_s^n, \alpha_s)] ds + \sigma(X_s^n, \alpha_s)dW_s + \gamma(X_s^n, \alpha_s)dY_s, \theta_n < s \leq T \\ X^n(\theta_n) = X^{n-1}(\theta_n) + \zeta_n \\ X^n(s) = X^{n-1}(s), t \leq s < \theta_n \end{cases} \quad (3)$$

We set :

$$X^{t, \alpha, v}(s) = \lim_{n \rightarrow +\infty} X^n(s), s \geq t, \hat{P} a.s.$$

Then the process $(X_s)_{s \geq t}$ which is right continuous and has left limits, satisfies the following stochastic differential equation:

$$\begin{cases} dX(s) = [b(X(s), \alpha(s)) - h(X(s))\gamma(X(s), \alpha(s))] ds + \sigma(X(s), \alpha(s))dW_s, t < s \leq T \\ \quad + \gamma(X(s), \alpha(s))dY_s + \sum_{i=1}^{+\infty} \zeta_i \delta(s - \theta_i) ds \\ X(t) = \xi_0 \end{cases} \quad (4)$$

where $\delta(t)$ is the Dirac measure. $(X_s)_{s \geq t}$ is our state process observed through the process (Y_s) . Introducing the following martingale process,

$$\lambda_s = \exp\left[\int_t^s h(X_r) dY_r - \frac{1}{2} \int_t^s |h(X_r)|^2 dr\right]$$

we define a new probability measure by

$$dP^{\alpha, v} |_{F_s} := \lambda_s d\hat{P} |_{F_s} .$$

Then the observation process (Y_s) satisfies:

$$\begin{cases} dY_s = h(X_s)ds + dB_s \\ Y_t = 0 \end{cases}.$$

Let also suppose:

(A1) ξ_0 has a law of distribution μ , that admits a density $x_0 \in H_\rho^0 \cap (L^1(\mathbb{R}^d))^+$.

We note that if $\beta > \frac{d}{2}$ then $H_\rho^0 \subset L^1(\mathbb{R}^d)$.

(A2) $l : \mathbb{R}^d \times U \rightarrow \mathbb{R}$, $g : \mathbb{R}^d \rightarrow \mathbb{R}$ and $k : X \rightarrow \mathbb{R}$ are positive measurable functions such that

$$\begin{cases} \frac{l(\alpha)}{\rho} \in L^2(\mathbb{R}^d) \text{ uniformly with respect to } \alpha \text{ and } \frac{g}{\rho} \in L^2(\mathbb{R}^d) \\ k(\zeta) \equiv k_1 > 0 \end{cases}$$

We associate to the problem a cost defined on $[0, T] \times H_\rho^{0+} \times \mathcal{A}_{t,T} \times \mathcal{V}_{t,T}$ by

$$J(t, x_0, \alpha, v) = E^{\alpha, v} \left[\int_t^T l(X_s, \alpha_s) q(s) ds + g(X_T) q_T + \sum_{i=1}^{+\infty} k(\zeta_i) q(\theta_i) \chi_{\{\theta_i < T\}} \right]. \quad (5)$$

with

$$q(s) := \exp(-\lambda(s-t)), \quad \forall s \in [t, T]. \quad (6)$$

2.2 Notations

Let the terminal time $T > 0$ be fixed and let give us $t \in [0, T]$. On the standard probability space $(\Omega, \mathcal{F}, (\mathcal{F}_s)_{s \geq t}, P)$ are defined

- $\alpha = (\alpha_s)_{t \leq s \leq T}$, the admissible control processes i.e (\mathcal{F}_s^Y) -adapted processes valued in U , compact subset of \mathbb{R}^l . The set of admissible control processes is denoted by $\mathcal{A}_{t,T}$

- $\mathcal{V}_{t,T}$ denotes the set of impulse controls v .

- $\mathcal{W}_{t,T} := \mathcal{A}_{t,T} \times \mathcal{V}_{t,T}$, the set of admissible strategies.

- $M_{d \times n}$ the space of $(d \times n)$ -matrix.

We introduce weighted Sobolev spaces.

(A0) $\rho : \mathbb{R}^d \rightarrow \mathbb{R}$ is a positive real-valued function such that $\rho \in C^2(\mathbb{R}^d)$.

For instance we can choose weight functions ρ of the form:

$$\rho_\beta(\xi) = (1 + |\xi|_{\mathbb{R}^d}^2)^{\beta/2}, \quad \beta > 0. \quad (7)$$

We define the weighted Sobolev space $H_\rho^k(\mathbb{R}^d)$ as the completion of $C_c^\infty(\mathbb{R}^d)$ with respect to the weighted norm

$$x \mapsto \|x\|_{H_\rho^k} := \sum_{|\alpha| \leq k} \left(\int_{\mathbb{R}^d} |\partial_\alpha [\rho(\xi)x(\xi)]|^2 d\xi \right)^{1/2}.$$

2.3 Differential operators

We define the differential operators A_α and $S_\alpha = (S_\alpha^1, \dots, S_\alpha^m)$ by

$$A_\alpha x(\xi) = \sum_{i,j=1}^d a_{ij}(\xi, \alpha) \partial_{ij} x(\xi) + \sum_{i=1}^d b_i(\xi, \alpha) \partial_i x(\xi) \quad \text{for } \xi \in \mathbb{R}^d \text{ and } \alpha \in U, \quad (8)$$

$$S_\alpha^k x(\xi) = \sum_{i=1}^d d_{ik}(\xi, \alpha) \partial_i x(\xi) + e_k(\xi, \alpha) x(\xi) \quad \text{for } \xi \in \mathbb{R}^d, \alpha \in U, \text{ and } k \in \{1, \dots, m\}. \quad (9)$$

with $a_{ij} = \frac{1}{2}((\sigma\sigma')_{ij} + (\gamma\gamma')_{ij})$, $d_{ik} = -\gamma_{ik}$ and $e_k = h_k + \sum_{i=1}^d \partial_i \gamma_{ik}$. We can associate a formal adjoint process to it:

$$A_\alpha^* x(\xi) = \sum_{i,j=1}^d \partial_i (a_{ij}(\xi, \alpha) \partial_j x(\xi)) + \sum_{i=1}^d \partial_i (c_i(\xi, \alpha) x(\xi)), \quad \text{for } \xi \in \mathbb{R}^d \text{ and } \alpha \in U \quad (10)$$

with $c_i := -b_i + \sum_{j=1}^d \partial_j a_{ij}$.

When concerning with optimal control problems of partially observed diffusion processes, the separated problem is introduced to retranscribe the problem into a totally observable one. We then treat a SPDE called Zakai equation. Here we study the last type equations in order to rely them after to the original problem and characterize the value function associated to impulse control problems of partially observable diffusions.

2.4 Filter

We introduce the normalized and unnormalized filters:

$$\begin{cases} A_s^{\alpha,v}(f) = \hat{E}[f(X^{\alpha,v}(s)) \lambda_s / F_s^Y] \\ \Pi_s^{\alpha,v}(f) = E^{\alpha,v}[f(X^{\alpha,v}(s)) / F_s^Y] \end{cases}.$$

We consider for every α and v given, the following one to one applications

$$\begin{aligned} \phi_n : \mathbb{R}^d &\rightarrow \mathbb{R}^d \text{ and } \phi_n^{-1} : \mathbb{R}^d \rightarrow \mathbb{R}^d \\ \xi &\mapsto \xi + \zeta_n & \eta &\mapsto \eta - \zeta_n \end{aligned}$$

and we define recursively the processes

$$\begin{cases} dp_0(s) = A_{\alpha_s}^* p_0(s) ds + \sum_{k=1}^m S_{\alpha_s}^k p_0(s) dY_s, \quad t < s \leq T \\ p_0(t) = x_0 \end{cases}$$

$$\begin{cases} dp_n(s) = A_{\alpha_s}^* p_n(s) ds + \sum_{k=1}^m S_{\alpha_s}^k p_n(s) dY_s, \quad \theta_n < s \leq T \\ p_n(\theta_n) = p_{n-1}(\theta_n) \circ \phi_n^{-1} \\ p_n(s) = p_{n-1}(s), \quad t \leq s < \theta_n \end{cases}.$$

We then set

$$p^{\alpha,v}(s) = \lim_{n \rightarrow +\infty} p_n^{\alpha,v}(s), s \geq t \hat{P} p.s. \text{ dans } L^2.$$

Thus

Proposition 1 *The process $(p(s))$ is right continuous and verifies*

$$p(s) \in L^2(\Omega; C[(\theta_n, \theta_{n+1}); H_\rho^0]), \forall n \in \mathbb{N} \text{ with } \theta_0 = t,$$

$$p(s) \in L_Y^2(t, T; H_\rho^1) \text{ ie } \hat{E} \int_t^T \|p(s)\|_{X_1}^2 ds < +\infty,$$

$$\text{and } A_s^{\alpha,v}(f) = \hat{E}[f(X^{\alpha,v}(s))\lambda_s/F_s^Y] = \int_{\mathbb{R}^d} f(\xi) p_s^{\alpha,v}(\xi) d\xi.$$

The cost can be reformulated as a function of the density process:

$$\begin{aligned} J(t, x_0, \alpha, v) &= \hat{E} \left[\int_t^T (l(\alpha_s), p(s)) q(s) ds + (g, p(T)) q_T + \sum_{i=1}^{+\infty} k_1(1, p(\theta_i)) q(\theta_i) \chi_{\{\theta_i < T\}} \right] \\ &:= \hat{E} \left[\int_t^T L_1(\alpha_s, p(s)) q(s) ds + G_1(p(T)) q_T + \sum_{i=1}^{+\infty} K_1(\zeta_i, p(\theta_i)) q(\theta_i) \chi_{\{\theta_i < T\}} \right] \end{aligned}$$

with

$$\begin{cases} L_1(\alpha, x) = (l(\alpha), x)_H = \left(\frac{l(\alpha)}{\rho^2}, x\right)_{H_\rho^0} \\ G_1(x) = (g, x)_H = \left(\frac{g}{\rho^2}, x\right)_{H_\rho^0} \\ K_1(\zeta, x) = k_1(1, x) \end{cases}, \forall x \in H_\rho^{0,+}, \forall \alpha \in U, \forall \zeta \in X,$$

where (\cdot, \cdot) denotes scalar product in corresponding spaces.

Our objective is then to characterize the minimal cost function (or value function) defined as follows:

$$V_1(t, x) = \inf_{(\alpha, v) \in W_{t,T}} J(t, x, \alpha, v).$$

In fact, in the separable problem the impulse cost function doesn't satisfy anymore the classical condition to be strictly positive that leads difficulties for traiting directly the problem. To approximate the value function V_1 we then introduce a sequence of problems with impulse costs $K^\varepsilon > k_1\varepsilon$.

3 Impulse control of Zakai equations

3.1 Approximation

Let $\varepsilon > 0$ and $(\alpha, x, \zeta) \in U \times H_\rho^0 \times H$ be given, we introduce

$$\begin{cases} K^\varepsilon(\zeta, x) := \begin{cases} k_1(1, x) & \text{if } (1, x)_H > \varepsilon \\ k_1\varepsilon & \text{if not} \end{cases}, k_1 > 0 \\ L(\alpha, x) = (l(\alpha), x^+) \\ G(x) = (g, x^+) \end{cases}$$

If we consider the cost function

$$J^\varepsilon(t, x, \alpha, v) = \hat{E} \left[\int_t^T L(\alpha_s, p(s)) q(s) ds + G(p(T)) q_T + \sum_{i=1}^{+\infty} K^\varepsilon(\zeta_i, p(\theta_i)) q(\theta_i) \chi_{\{\theta_i < T\}} \right]$$

then it corresponds on H_ρ^{0+} to

$$\hat{E} \left[\int_t^T L_1(\alpha_s, p(s)) q(s) ds + G_1(p(T)) q_T + k_1 \sum_{i=1}^{+\infty} (1, p(\theta_i)) q(\theta_i) \chi_{\{\theta_i < T\}} \chi_{\{(1, p(\theta_i)) > \varepsilon\}} \right].$$

Theorem 2 *We have*

$$V^\varepsilon(t, x) \rightarrow_{\varepsilon \searrow 0} V_1(t, x) \text{ on } H_\rho^{0+}.$$

V^ε is characterized as the only viscosity solution of the following Hamilton Jacobi Bellman quasi variational inequality. Indeed the Dynamic Programming Principle leads formally to the Hamilton Jacobi Bellman Quasi Variational Inequality whose V_ε should be solution:

$$\forall (t, x) \in [0, T] \times H_\rho^0$$

$$\max \left[-\frac{\partial V}{\partial t}(t, x) - \inf_{\alpha \in U} \{B^\alpha V(t, x) + L(\alpha, x) - \lambda V(t, x)\}; (V - MV)(t, x) \right] = 0, \\ V(T, x) = G(x), \quad (11)$$

where the operators B^α and M are respectively defined by

$$B^\alpha V(t, x) = \frac{1}{2} \sum_{k=1}^m \langle D^2 V(t, x) S_\alpha^k x, S_\alpha^k x \rangle_0 + \langle A_\alpha^* x, DV(t, x) \rangle_{\langle H_\rho^{-1}, H_\rho^1 \rangle},$$

and

$$MV(t, x) = \inf_{\zeta \in X} \{K_\varepsilon(\zeta, x) + V(t, \Gamma(\zeta, x))\}. \quad (12)$$

3.2 Viscosity solutions

Definition 3 *A function $V \in C([0, T] \times H_\rho^0; \mathbb{R})$ is called viscosity sub-solution (respectively super-solution) of the problem (11) if:*

- 1) $V(T) \leq G$ on H_ρ^0 (resp. $V(T) \geq G$) and
- 2) for every $\varphi \in C^{1,2}((0, T) \times H_\rho^{-1})$, for all $\delta \in C^1(0, T)$ such that $\delta > 0$ on $[0, T]$, then at every global maximal point $(t, x) \in (0, T) \times H_\rho^0$ of $V - \left(\varphi + \frac{\delta}{2} \|x\|_0^2\right)$ (resp. at every global minimal point of $V - \left(\varphi - \frac{\delta}{2} \|x\|_0^2\right)$), we have:

$$x \in H_\rho^1$$

and

$$\max \left[-\frac{\partial \varphi}{\partial t}(t, x) - \frac{\delta'(t)}{2} \|x\|_0^2 - \inf_{\alpha \in U} \left\{ B_\alpha \left(\varphi + \frac{\delta}{2} \|\cdot\|_0^2 \right) (t, x) + L(\alpha, x) - \lambda V(t, x) \right\}; (V - MV)(t, x) \right] \leq 0 \quad (13)$$

(resp.

$$\max \left[-\frac{\partial \varphi}{\partial t}(t, x) + \frac{\delta'(t)}{2} \|x\|_o^2 - \inf_{\alpha \in U} \left\{ B_\alpha(\varphi - \frac{\delta}{2} \|\cdot\|_o^2)(t, x) + L(\alpha, x) - \lambda V(t, x) \right\}; (V - MV)(t, x) \right] \geq 0. \quad (14)$$

It is a viscosity solution of (11) if it is both a sub- and super-solution.

Remark 4 In the rest of the paper this problem is reduced to a sequence of iterated stopping problems, that is useful for numerical applications.

References

1. Anderson R. F. and Friedman A. *Optimal inspection in a stochastic control problem with costly observations II*. Math Oper Res **3**, 67-81(1978).
2. Anderson R.F and Friedman A. *Multi-dimensional quality control problems and quasi variational inequalities*. Trans Am Math Soc **246**, 31-76 (1978).
3. Baghery-Kabbaj F. *Sur les inéquations quasi variationnelles et le contrôle optimal des systèmes stochastiques multi-niveaux de production/stockage: approche théorique et numérique*. Thèse de doctorat, Université Paris 6 (1989).
4. Gozzi F. and Swiech A. *HJB equation for the optimal control of the Duncan-Mortensen-Zakai equation*. J Func Anal . **172** (2), 466-510 (2000).
5. Hanouzet B. and Joly J.L. *Convergence uniforme des itérations définissant la solution faible d'une inéquation quasi-variationnelle*. C.R.A.S t. **286**, 735-738 (1978).
6. Ishii H. *Viscosity Solutions of Nonlinear Second Order Elliptic PDEs Associated with Impulse Control Problems II*. Funkcialaj Ekvacioj, 38, 297-328 (1995).
7. Maziotto G., Stettner L., Szpirglas J. and Zabczyk J. *On impulse control with partial observation*. SIAM J Cont Opt **26** n4, 964-984 (1988).

Adaptive bandwidth selection in hazard rate estimation

Dimitrios Bagkavos¹ and Aglaia Kalamatianou²

¹ Information Resources International, Athens
Greece, 47 Ifigenias Str.
(e-mail: dimitris.bagkavos@infores.com)

² Panteion University
Dept. of Sociology
L. Syggrou 136
17671, Athens, Greece

Abstract. We consider the issue of bandwidth selection in adaptive kernel based hazard rate estimation under the local linear framework when the data are randomly right censored. Specifically, the Akaike Information Criterion method is extended from the density setting and evaluated numerically as a potential bandwidth selector when a kernel hazard rate estimate uses a variable, according to each data point, smoothing scheme. We conclude with Monte carlo simulations on distributional datasets.

Keywords: Stochastic simulation, variable bandwidth, kernel, hazard rate, bandwidth selection, local linear.

1 Introduction

This paper considers kernel based nonparametric estimation in presence of random right censoring, of the hazard rate function which is formally defined as

$$\lambda(x) = \lim_{dx \rightarrow 0+} \frac{P(x \leq X < x + dx | x \leq X)}{dx} \quad (1)$$

and expresses the probability that an item with continuous lifetime $X > 0$ will experience an event which is the primary interest of the study, in the interval $(x, x + dx)$ given that no such event occurred up to time x .

A summary of early studies on this topic, based on conventional kernel methods, can be found in [7]. One of their main characteristics is that the amount of smoothing applied to the estimate, controlled by a parameter usually referred to as the bandwidth, remains constant across x . However, when the distribution of the underlying data varies considerably within the region of estimation it is desirable that bandwidth also changes appropriately. An intuitive smoothing scheme, introduced first by [1] in the density setting is to vary bandwidth inversely proportionally with the underlying curve since in this case, less smoothing is applied when more structure is present and vice versa. [1] and [10] established that optimal theoretical results are achieved

when bandwidth is inversely proportional to the square root of the density. In [5] and [14] it was shown that the method carries over its excellent theoretical properties to the hazard setting. Moreover, in [5] it was shown that the finite sample behavior of a variable bandwidth estimate parallels the simulation results of [9] in density context which justified its use in case of complex structures such as multimodal curves.

However, proper implementation of such a method involves a bandwidth selector that estimates the correct amount of smoothing to be applied by taking into account its variable form. The purpose of the present article is to develop an automatic, data based bandwidth selector for an estimate which combines the local linear and the square root law techniques under random right censoring.

The rest of the article is organized as follows: In section 2 we formulate the proposed estimate while in section 3 we propose a bandwidth selector for the estimate in question and finally in section 4 we use distributional data to examine the estimates performance in comparison with other estimates with similar asymptotic properties. All proofs are deferred for the last section.

2 Local linear variable bandwidth hazard rate

Let T_1, T_2, \dots, T_N be a sample of i.i.d. survival times censored on the right by i.i.d. random variables U_1, U_2, \dots, U_N , which are independent from the T_i 's. Let f_T be the common probability density and F_T the distribution function of the T_i 's. Denote by H the distribution function of the U_i 's. Typically the randomly right censored observed data are denoted by the pairs (X_i, δ_i) , $i = 1, 2, \dots, N$ with $X_i = \min\{T_i, U_i\}$ and $\delta_i = 1_{\{T_i \leq U_i\}}$ where $1_{\{\cdot\}}$ is the indicator random variable of the event $\{\cdot\}$. The distribution function of X_i 's is $1 - F = (1 - F_T)(1 - H)$. By the definition of conditional probability the hazard rate function (1) can be written as

$$\lambda(x) = \frac{f_T(x)}{1 - F_T(x)}, \quad F_T(x) < 1,$$

on an interval $[0, T]$ of the real line, with $T = \sup\{x : F_T(x) < 1 - \varepsilon\}$ for a small $\varepsilon > 0$. Partition the interval into n disjoint subintervals $\{I_j, j = 1 \dots n\}$ of equal length $\Delta = T/n$ and denote with $x_j = (j - \frac{1}{2})\Delta$, $j = 1 \dots n$, the center of the interval I_j . A natural estimate of the hazard rate is

$$c_j = \frac{d_j}{\Delta n_j}, \quad j = 1, 2, \dots, n$$

with

$$d_j = \sum_{i=1}^N 1_{\{X_i \in I_j, \delta_i=1\}}, \quad n_j = \sum_{i=1}^N 1_{\{X_i > \Delta(j-1)\}}$$

because c_j is an empirical estimate of $P(X \in (x_j, x_j + \Delta) | X > x_j)$, $j = 1, 2, \dots, n$ which if Δ is small should be close to $\lambda(x_j)$. The essence of the local linear fitting approach is to model the scatterplot data (x_j, c_j) locally by a weighted least squares simple linear regression model. See [3] for precise formulation and justification. Using the square root law to control the size of the local neighborhood, the local linear hazard rate estimate $\hat{\lambda}(x|h)$ is defined as the estimated intercept $\hat{\beta}_0$ of the fitted line, obtained by solving

$$\min_{\beta_0, \beta_1} \sum_{j=1}^n \{c_j - \beta_0 - \beta_1(x_j - x)\}^2 \frac{\lambda^{1/2}(x_j)}{h} K\left(\frac{x_j - x}{h} \lambda^{1/2}(x_j)\right).$$

Here, K is a kernel function, used to assign weight to each point. Straight-forward calculations give

$$\hat{\lambda}(x|h) = h^{-1} \sum_{j=1}^n \frac{S_{n,1}(x)(x_j - x) - S_{n,2}(x)}{S_{n,1}^2(x) - S_{n,0}(x)S_{n,2}(x)} \lambda^{1/2}(x_j) K\left(\frac{x_j - x}{h \lambda^{1/2}(x_j)}\right) c_j \quad (2)$$

with

$$S_{n,l}(x) = \sum_{j=1}^n \lambda^{1/2}(x_j) K\left(\frac{x_j - x}{h} \lambda^{1/2}(x_j)\right) (x_j - x)^l, \quad l = 0, 1, 2.$$

Estimator $\hat{\lambda}(x|h)$, is typically called the *ideal* estimate and cannot be used directly in practice as it depends on the true hazard rate function. Replacing $\lambda(x_j)$ in (2) with another kernel estimate, usually referred to as the *pilot*, leads to the practically useful *adaptive* version of $\hat{\lambda}(x|h)$, denoted by $\hat{\lambda}(x|h_1, h_2)$ and defined by

$$\begin{aligned} \hat{\lambda}(x|h_1, h_2) &= h_2^{-1} \sum_{j=1}^n \frac{S_{n,1}(x)(x_j - x) - S_{n,2}(x)}{S_{n,1}^2(x) - S_{n,0}(x)S_{n,2}(x)} \\ &\quad \times \tilde{\lambda}^{1/2}(x_j|h_1) K\left(\frac{x_j - x}{h_2} \tilde{\lambda}^{1/2}(x_j|h_1)\right) c_j \end{aligned}$$

where $\tilde{\lambda}(x|h)$ has been studied in [3] and is given by

$$\tilde{\lambda}(x|h) = \frac{T_{n,1}^*(x)S_{n,1}^*(x) - T_{n,0}^*(x)S_{n,2}^*(x)}{S_{n,1}^*(x)S_{n,1}^*(x) - S_{n,0}^*(x)S_{n,2}^*(x)}$$

where

$$\begin{aligned} T_{n,l}^*(x) &= \sum_{j=1}^n c_j K\left(\frac{x_j - x}{h}\right) (x_j - x)^l, \quad l = 0, 1 \\ S_{n,l}^*(x) &= \sum_{j=1}^n K\left(\frac{x_j - x}{h}\right) (x_j - x)^l, \quad l = 0, 1, 2. \end{aligned}$$

3 Bandwidth selection

In implementing estimator $\hat{\lambda}(x|h_1, h_2)$ one needs bandwidth selection rules for h_1 and h_2 . Selection of the pilot bandwidth h_1 has been studied in detail in [3]. For this reason we focus here on selection of h_2 . The Akaike's Information Criterion (AIC) bandwidth selection method was introduced in [12] and was also discussed for $\tilde{\lambda}(x|h)$ in [3]. Working similarly and in analogy with calculations yielding (2.5) in [12] and taking into account the binning approximations of [20] yields

$$\text{AIC}(h_2) = \log \{\text{RSS}\} + \frac{n + \text{tr}(S)}{n - [\text{tr}(S) + 2]} \quad (3)$$

with

$$\text{RSS} = \sum_{i=1}^n \left(c_i - \hat{\lambda}(x_i|h_1, h_2) \right)^2$$

and

$$\text{tr}(S) = K(0) \sum_{i=1}^n \frac{S_{n,2}(x_i)}{S_{n,2}(x_i)S_{n,0}(x_i) - S_{n,1}^2(x_i)}.$$

Minimization of (3) over h_2 , yields the suggested bandwidth to use in $\hat{\lambda}(x|h_1, h_2)$. Minimization is done in the interval $(0, X_{(N)})$, where $X_{(N)}$ denotes the largest sample observation. As the optimization technique, one may use a nonlinear minimization function subject to Box constrains. In the next section this is implemented by using the function `nlinmb` of S-plus. As pointed out in [12] such an approach may not always return the true minimum, and for this reason one may try to run the minimization function several times changing the starting values. However this did not seem to be a problem in producing the simulation results of section 4.

As analytical evaluation of the AIC bandwidth selector is not feasible, an alternative way is to use another bandwidth selector as benchmark. Since our assessment in the next section is based on the MISE criterion, use of a plug-in rule is well suited as by definition such a selector is based on MISE minimization. Provided that as $N \rightarrow +\infty$, $Nh \rightarrow 0$, the MISE can be well approximated by the AMISE which is defined as

$$\text{AMISE} \left\{ \hat{\lambda}(x|h) \right\} = h^8 \mu_4^2(u) R(g) + (Nh)^{-1} R(K) \int \frac{\lambda^{\frac{3}{2}}(x)}{1 - F(x)} dx$$

which is minimized by

$$h = \left(\frac{1}{8N} \frac{R(K)}{\mu_4^2(u)} \frac{\int \frac{\lambda^{\frac{3}{2}}(x)}{1 - F(x)} dx}{R(g)} \right)^{-\frac{1}{9}}. \quad (4)$$

Now, (4) cannot be used in practice as it contains unknown quantities. Moreover, using kernel based estimates for $R(g)$ is not advisable and the primary reason at least for small to medium sized samples is that due to the many derivatives involved in $R(g)$ the resulting estimate will be highly unstable. For this reason, potential use of (4) should be limited only when there is strong confidence on a parametric model.

4 Numerical examples

In this section we use distributional data to assess the proposed bandwidth selector and to exhibit the practical performance of the variable bandwidth estimator.

This is achieved via MISE comparisons for five known distributions with different hazard rate shapes over four different sample sizes and four different levels of censoring. The distributions we consider and the intervals over which the hazard rate is estimated are the standard Lognormal, $(LN(0, 1), [0.01, 4])$, the Weibull with shape parameter 0.5 and scale parameter 0.8 ($W(0.5, 0.8), [0.01, 4]$), the χ_{12}^2 with 12 degrees of freedom estimated at $[0.01, 20]$ and the truncated to $(0, +\infty)$ normal mixtures $\frac{2}{3}N(4, 0.4) + \frac{1}{3}N(3, 0.2)$ and $0.6N(-3, 9) + 0.4N(10, 9)$ estimated at $[2.4, 3.8]$ and $[0.01, 12]$ respectively. The sample sizes are 100, 200, 400 and 1000 observations and the amounts of censoring are 0% (no censoring), 10%, 20% and 30%. Denote with $\hat{\lambda}^*$ the estimate for which we evaluate the MISE and with λ the true hazard rate function. Then, in all cases the MISE is approximated by averaging over 1000 iterations the difference $(\hat{\lambda}^* - \lambda)^2$, calculated across 100 equispaced grid points covering the whole region of estimation. Simpson's extended numerical integration method is used to integrate the approximate mean square error. In all cases, implementation of censoring and selection of Δ is done as in section 4 of [3].

In assessing the proposed bandwidth selector and since the objective is to study behavior of h as obtained by minimization of (3) we use the 'ideal' variable bandwidth estimate $\hat{\lambda}(x|h)$. As a benchmark we also use bandwidth obtained by (4) with the unknown functionals calculated by use of the true distribution. While this approach is not available in practice since it depends on the true curve, it is still useful as it provides a lower bound on the error and hence the maximum potential that can be achieved by the estimate and the bandwidth rule proposed.

In tables 1 and 2 we present the results of this simulation study. An overall conclusion, drawn by averaging the percentage differences of MISE's on both tables is that the AIC method is fairly close to the benchmark plug-in method with the latter being approximately 30% more precise. We feel that this difference is rather small given that the plug-in rule figures actually represent a lower bound in MISE. Moreover, we feel that the MISE figures produced by use of the AIC bandwidth are acceptable for hazard rate estimates given the sample sizes and amounts of censoring considered. These two facts suggest

Table 1. Approximate MISE's of $\hat{\lambda}(x|h)$ using the plug in (h_{PI}) and AIC (h_{AIC}) bandwidth selectors, estimating the hazard rate from the χ_{12}^2 , W(0.5,0.8) and LN(0,1) distributions for various sample sizes (N) and amounts of censoring.

Cens	N	χ_{12}^2		W(0.5,0.8)		LN(0,1)	
		h_{PI}	h_{AIC}	h_{PI}	h_{AIC}	h_{PI}	h_{AIC}
0%	100	1.2832	1.896	0.9143	1.351	0.6514	0.9625
	200	0.9394	1.388	0.758	1.12	0.3385	0.5002
	400	0.5929	0.876	0.6017	0.889	0.0257	0.0379
	1000	0.3059	0.452	0.4534	0.67	0.0171	0.0253
10%	100	1.3942	2.06	1.0011	1.4792	0.7132	1.0538
	200	1.0206	1.508	0.8299	1.2263	0.3707	0.5477
	400	0.6443	0.952	0.6587	0.9733	0.0281	0.0415
	1000	0.3303	0.488	0.4965	0.7336	0.0187	0.0277
20%	100	1.5052	2.224	1.0961	1.6195	0.7808	1.1537
	200	1.1018	1.628	0.9087	1.3426	0.4058	0.5996
	400	0.6957	1.028	0.7212	1.0657	0.0307	0.0454
	1000	0.3573	0.528	0.5436	0.8032	0.0205	0.0303
30%	100	1.6156	2.3872	1.2	1.7731	0.8549	1.2632
	200	1.4756	2.1804	0.9948	1.4699	0.4443	0.6565
	400	0.7452	1.1012	0.7896	1.1667	0.0336	0.0497
	1000	0.3836	0.5668	0.5952	0.8794	0.0225	0.0332

appropriateness of the AIC method for bandwidth selection at least for the distributions considered here.

References

1. Abramson, I. (1982). On bandwidth variation in kernel estimates - a square root law, *Annals of Statistics*, **10**, 1217–1223.
2. Bagkavos, D. (2003). Bias reduction in nonparametric hazard rate estimation. PhD thesis, The University of Birmingham, UK.
3. Bagkavos, D., 2010. Local Linear Hazard Rate Estimation And Bandwidth Selection. *To appear in Annals of the Institute of Statistical Mathematics*.
4. Bagkavos, D. and Patil, P.N., 2008. Local Polynomial Fitting in Failure Rate Estimation. *IEEE Transactions on Reliability*, **56**, 126–163.
5. Bagkavos, D. and Patil, P.N., 2009. Variable Bandwidths For Nonparametric Hazard Rate Estimation *Communications in Statistics, theory and methods*, **38**, 1055-1078.
6. Cai, Z. and Tiwari, R., 2000. Application of a local linear autoregressive model to BOD time series. *Environmetrics*, **11**, 341–350.
7. Gefeller, O. and Michels, M., 1992. A review on smoothing methods for the estimation of the hazard rate based on kernel functions. In: Dodge, Y., Whittaker, J. (Eds.), *Computational Statistics*. Physica-Verlag, Switzerland, pp. 459-464.

Table 2. Approximate MISE's of $\hat{\lambda}(x|h)$ using the plug in (h_{PI}) and AIC (h_{AIC}) bandwidth selectors, estimating the hazard rate from the $\frac{2}{3}N(3, 1) + \frac{1}{3}N(2, 0.2^2)$ and $0.6N(-3, 9) + 0.4N(10, 9)$ distributions for various sample sizes (N) and amounts of censoring.

Cens	N	$\frac{2}{3}N(3, 1) + \frac{1}{3}N(2, 0.2^2)$		$0.6N(-3, 9) + 0.4N(10, 9)$	
		h_{PI}	h_{AIC}	h_{PI}	h_{AIC}
0%	100	0.4364	0.5567	0.6043	0.7708
	200	0.2743	0.3499	0.3797	0.4844
	400	0.1121	0.143	0.1552	0.198
	1000	0.0612	0.0781	0.0848	0.1082
10%	100	0.473	0.6034	0.655	0.8355
	200	0.2973	0.3792	0.4117	0.5251
	400	0.1215	0.155	0.1682	0.2146
	1000	0.0664	0.0847	0.0919	0.1172
20%	100	0.5128	0.6541	0.7099	0.9056
	200	0.3223	0.4111	0.4461	0.5691
	400	0.1317	0.168	0.1823	0.2326
	1000	0.072	0.0918	0.0996	0.1271
30%	100	0.5558	0.709	0.7696	0.9817
	200	0.3493	0.4456	0.4837	0.617
	400	0.1428	0.1821	0.1977	0.2522
	1000	0.078	0.0995	0.108	0.1378

8. Jones, M.C. (1993). Simple boundary correction for density estimation. *Statistics and Computing*, **3**, 135–146.
9. Jones, M.C., and Signorini, D.F. (1997). A comparison of higher order bias kernel density estimators., *Journal of the American Statistical Association*, **91**, 401–407.
10. Hall, P. and Marron, J.S. (1988). Variable window width kernel estimates of probability densities, *Probability Theory and Related Fields*, **80**, 37–49.
11. Hurvich, C. and Tsai, C., 1989. Regression and Time series model selection in small samples. *Biometrika*, **76**, 297–307.
12. Hurvich, C., Simonoff, J. and Tsai, C., 1997. Smoothing parameter selection in nonparametric regression using an improved Akaike information criterion *Journal of the Royal Statistical Society Ser. B*, **60**, 271–293.
13. Müller, H-G. and Wang J.L. (1994). Hazard rate estimation under random censoring with varying kernels and bandwidths., *Biometrics*, **50**, 61–76.
14. Nielsen, J.P., 2003. Variable bandwidth kernel hazard estimators. *Nonparametric Statistics*, **15**, 355–376.
15. Nielsen, J.P., 1998. Multiplicative bias correction in kernel hazard estimation. *Scandinavian Journal of Statistics*, **25**, 541–553.
16. Simonoff, J. (1996). *Smoothing methods in statistics*, Springer, New York.
17. Sorbye, S. and Godtlielsen, F. (2002). Finite sample properties of an adaptive density estimator, *Nonparametric Statistics*, **14** 383–398.
18. Tanner, M. and Wong, W., 1983. The estimation of the hazard function from randomly censored data by the kernel method. *Annals of Statistics*, **11**, 989–993.

19. Wand, M.P., 1997. Data-based choice of histogram bin width. *American Statistician*, **51**, 59–64.
20. Turlach, B. A. and Wand, M. P. (1996). Fast computation of auxiliary quantities in local polynomial regression. *Journal of Computational and Graphical Statistics*, **5**, 337–350.
21. Wang, J.L., Müller, H.-G. and Capra, W.B., 1998. Analysis of Oldest-Old Mortality: Lifetables Revisited. *Annals of Statistics*, **28**, 126–163.

A fixed-laged smoothing algorithm for Jump-Markov State-Space Systems

Noémie Bardel¹ and François Desbouvries¹

CITI Department and CNRS UMR 5157
TELECOM SudParis
91011 Evry, France
(e-mail: {noemie.bardel, francois.desbouvries}@it-sudparis.eu)

Abstract. Let us consider the classical conditionally linear Gaussian model, also called Jump-Markov State-Space (JMSS) model, described by the equations :

$$x_{n+1} = F_{n+1}(r_{n+1})x_n + v_n, \quad (1)$$

$$y_n = H_n(r_n)x_n + w_n, \quad (2)$$

in which $\{r_n\}$ denote a discrete Markov Chain with known transition probabilities, $\{v_n\}$, $\{w_n\}$, x_0 are Gaussian vectors independent, mutually independent and independent of r_1, \dots, r_N .

The Bayesian fixed-lag smoothing problem we address here consists in computing efficiently fixed-lag state estimates $E[x_n|y_{1:n+T}]$ and $E[r_n|y_{1:n+T}]$, where T is a fixed positive integer. Let us start from the following factorization :

$$E[x_n|y_{1:n+T}] = \sum_{r_n} E[x_n|r_n, y_{1:n+T}]p(r_n|y_{1:n+T}) \quad (3)$$

The first term in the sum can be computed by a Kalman smoother, however the exact computation of the second term requires an exponential computational cost, and one needs to use suboptimal solutions. In Doucet *et al.* (*IEEE Trans. On Signal Processing*, 2001), a particle smoother gives an approximation $\hat{p}(r_n|y_{1:n+T}) = \sum_{i=1}^N w_n^i \delta_{r_n^i}(r_n)$. However, to maintain a diversity in the particles and avoid the problem of sample depletion, one has to include at each time a Monte Carlo Markov Chain (MCMC) step, which is computationally intensive.

In this paper we propose an alternative fixed-lag smoothing algorithm based on a different way to approximate $p(r_n|y_{1:n+T})$. More precisely, let us assume that $(r_{1:N}, y_{1:N})$ is a Partially Pairwise Markov Chain (PPMC), whose joint distribution satisfies :

$$p(r_{1:N}, y_{1:N}) = p(r_1, y_1) \prod_{n=1}^{N-1} p(r_{n+1}, y_{n+1}|r_n, y_{1:n}) \quad (4)$$

The interests of this assumption are multiple. First it takes into accounts long memory observations; next it allows the exact computation of the densities $p(r_n|y_{1:n+T})$ by a forward-backward procedure. Finally the parameters of the PPMC which is the closest to the true model $(r_{1:N}, y_{1:N})$ are estimated by an Iterative Conditional Estimation (ICE) method.

To sum up, rather than using a Particle Smoother for approximating $p(r_n|y_{1:n+T})$, we approximate the stochastic model which describes the relation between $r_{1:N}$ and $y_{1:N}$, but we compute $p(r_n|y_{1:n+T})$ exactly.

Financial Forecasting using Neural Networks

Dagmar Blatná, Jiří Trešl

University of Economics, Prague
Prague, Czech Republic
Email: blatna@vse.cz, tresl@vse.cz

Abstract: The possibility of application of neural networks for the prediction of both stock and exchange rate returns was investigated. First, the capability of neural networks to reveal specific underlying process was studied using different simulated time series. Second, actual weekly returns from Czech financial markets were analyzed and predicted. Particularly, the problems connected with capturing of outliers and structural breaks were discussed. The predictive power of neural networks was investigated both as a function of network architecture and the length of training set.

Keywords: Neural networks, Financial time series, Predictive power

1 Introductory Remarks to Neural Networks

Artificial neural networks (ANN) are now frequently used in many modelling and forecasting problems, mainly thanks to the possibility of the use of computer intensive methods. Recently, they have been increasingly applied in financial time series analysis as well, see e.g. Franses and van Dijk (2000), McNelis (2005). The main advantage of this tool is the ability to approximate almost any nonlinear function arbitrarily close. Particularly in financial time series with complex nonlinear dynamical relationships, the ANN can provide a better fit compared with parametric nonlinear models. On the other hand, usually it is difficult to interpret the meaning of parameters and ANN are often treated as “black box” models constructed for the pattern recognition and prediction. Further, excellent in-sample fit does not guarantee satisfactory out-of-sample forecasting.

Generally, the ANN is supposed to consist of several layers. The *input layer* is formed by individual inputs (explanatory variables). These inputs are multiplied by *connection strengths* called *weights* in statistical terminology. Further, there is one or more *hidden layers*, each consisting of certain number of *neurons*. In the hidden layer, the linear combinations of inputs are created and transformed by the *activation functions*. Finally, the *output* is obtained as a weighted mean of these transformed values. Usually, this kind of ANN is referred to as *multilayered feed forward network* and we restrict ourselves to the models with one or two hidden layers. It is useful to realize, information flows only in one direction here, from inputs to output. In time series problems, variables are measured over a time interval and we suppose to exist relationships among variables at successive times. In this case, our objective is to predict future values of a variable at a given time either from the same or other variables at earlier times. We restrict here to the case,

when single numeric variable is observed and its next values are predicted using number of lagged values.

The mathematical representation of the feedforward network with one hidden layer and logsigmoid activation function is given in McNellis (2005):

$$n_{k,t} = w_{k,0} + \sum_{i=1}^I w_{k,i} x_{i,t}, \quad N_{k,t} = 1 / [1 + \exp(-n_{k,t})], \quad Y_t = \gamma_0 + \sum_{k=1}^K \gamma_k N_{k,t} + \sum_{i=1}^I \beta_i x_{i,t}$$

The first equation describes the creation of linear combination of input variables, whereas the second one expresses the transform by logsigmoid activation function. The third equation explains that output value can be obtained either from neurons or from inputs directly. Clearly, having no hidden layer, the model reduces to purely linear one.

2 Predictions with Simulated Data

First, the various ANN types were trained and applied to three kinds of simulated time series. The main aim was to investigate prediction ability with respect to the length of time series (250 or 500), the number of lagged explanatory values (10 or 20) and the number of hidden layers (one or two). In each case, 10 last values were used for prediction, so either 240 or 490 values were left as training data. To quantify the prediction power, the following goodness-of-fit measures were computed: *Mean Prediction Error* (MPE), *Mean Deviation of Prediction Error* (MDPE) and *Mean Absolute Prediction Error* (MAPE):

$$MPE = \frac{1}{h} \sum_{j=1}^h (y_{n+j} - Y_{n+j}) = \frac{1}{h} \sum_{j=1}^h e_{n+j}, \quad MDPE = \frac{1}{h} \sum_{j=1}^h |e_{n+j} - \bar{e}|, \quad MAPE = \frac{1}{h} \sum_{j=1}^h |e_{n+j}|$$

In all formulas, n denotes the number of training data and h the prediction length. Further, the following structural notation will be used: *time series length – number of lagged values – number of neurons in the first hidden layer – number of neurons in the second hidden layer*. For example, the notation 250-10-03-01 specifies 250 data in time series, 10 lagged explanatory values and three (resp. one) neurons in the first (resp. second) hidden layer. All computations were performed with the use of *STATISTICA* software, version 7.

Simulation 1: Deterministic Chaos. Even simple nonlinear *deterministic* systems can under certain conditions pass to chaotic states due to extremely sensitivity both to initial conditions and control parameters (see e.g. Hilborn (2001)). As an example, consider discrete time system described by *logistic difference equation*

$$y_{t+1} = 4y_t(1 - y_t).$$

Clearly, the values from the interval $<0,1>$ will be mapped again into this interval. As for modelling, it is obvious from the following table, longer time series provided better results. On the other hand, the number of lagged values and hidden layers were of minor importance here.

Network Type	MPE	MDPE	MAPE
500-20-07-00	-0.048	0.100	0.080
500-20-10-08	-0.013	0.220	0.217
500-10-02-00	-0.139	0.203	0.188
500-10-02-02	-0.079	0.121	0.111
250-20-04-00	-0.042	0.325	0.325
250-20-10-10	+0.065	0.252	0.251
250-10-05-00	-0.066	0.295	0.305
250-10-05-04	-0.082	0.234	0.246

Tab.1. Results of ANN Modelling: Deterministic Chaos

Simulation 2: Bilinear Process. The simplest diagonal form of this process can be, according to Tsay (2002), written as:

$$y_t = \alpha y_{t-1} u_{t-1} + u_t, \quad u_t \approx N(0, \sigma^2), \quad |\lambda| = |\alpha\sigma| < 1$$

On contrary to the previous case, there is no preferred model.

Network Type	MPE	MDPE	MAPE
500-20-01-00	0.740	1.326	1.431
500-20-02-01	0.428	1.282	1.337
500-10-04-00	0.716	1.257	1.328
500-10-07-02	0.619	1.291	1.346
250-20-01-00	0.746	1.324	1.479
250-20-01-01	0.501	1.348	1.457
250-10-04-00	0.456	1.265	1.320
250-10-05-05	0.409	1.273	1.277

Tab.2. Results of ANN Modelling: Bilinear Process

Simulation 3: Kesten Process. This process is a natural generalization of classical AR(1) process discussed in Sornette (2000):

$$y_t = \alpha y_{t-1} + u_t, \quad u_t \approx N(0, \sigma^2), \quad \alpha \approx R(a, b),$$

where R denotes regular distribution. Again, MDPE and MAPE exhibit relatively slow variations and the best results are achieved with 250-10-03-00 model.

Type	MPE	MDPE	MAPE
500-20-03-00	0.511	1.211	1.144
500-20-06-05	0.551	1.279	1.205
500-10-02-00	0.441	1.062	1.022
500-10-03-02	0.363	1.077	1.005
250-20-01-00	0.314	1.243	1.191
250-20-04-03	0.728	1.402	1.337
250-10-03-00	0.215	0.937	0.887
250-10-01-01	0.595	1.131	1.131

Tab.3. Results of ANN Modelling: Kesten Process

3 Predictions with Financial Data

The main aim was the testing of ANN predictive power in financial applications. We employed weekly logarithmic stock returns (companies CEZ, KB, TEL, UNIP) and weekly exchange rate returns (CZK/EUR, CZK/GBP, CZK/CHF, CZK/USD) during 2005-2008, i.e. 200 weekly values for each time series. In all cases, 25 preceding values were used and 12 values were left for prediction testing. Further, both linear models and neural networks with one and two hidden layers were applied. Graphical presentation of results achieved is on the following figures:

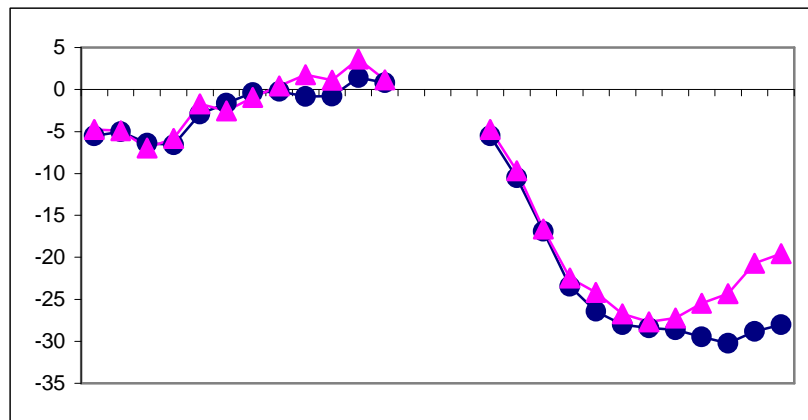


Fig.1. CEZ returns: actual values (circles) versus predictions (triangles).
Left: original values Right: Cumulative values Model: 200-25-05-00

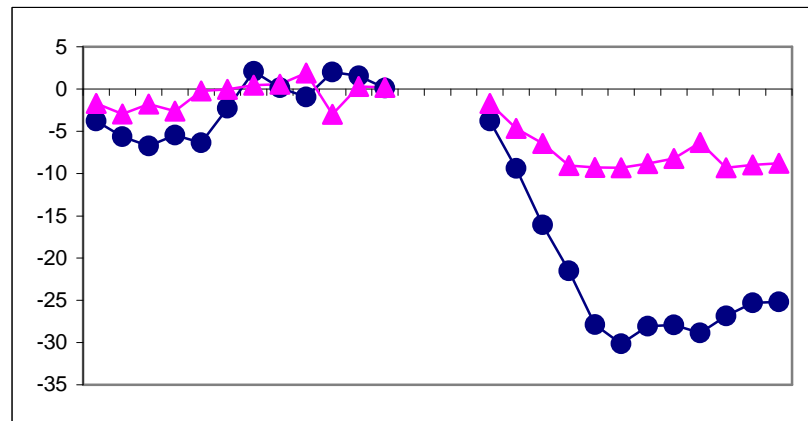


Fig.2. KB returns: actual values (circles) versus predictions (triangles).
Left: original values Right: Cumulative values Model: 200-25-12-10

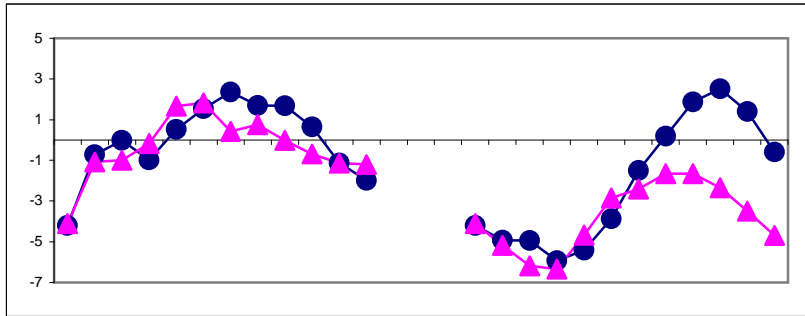


Fig.3. TEL returns: actual values (circles) versus predictions (triangles).
 Left: original values Right: Cumulative values Model: 200-25-12-06

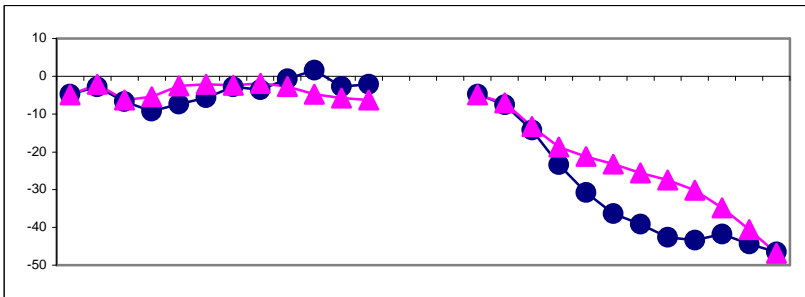


Fig.4. UNIP returns: actual values (circles) versus predictions (triangles).
 Left: original values Right: Cumulative values Model: 200-25-03-04

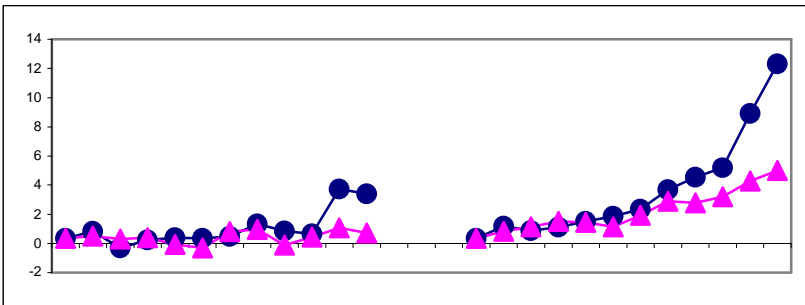


Fig.5. CZK/EUR returns: actual values (circles) versus predictions (triangles).
 Left: original values Right: Cumulative values Model: 200-25-06-00

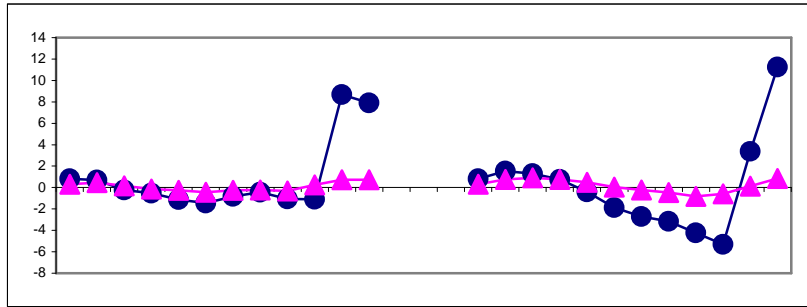


Fig.6. CZK/GBP returns: actual values (circles) versus predictions (triangles).
 Left: original values Right: Cumulative values Model: 200-25-06-00

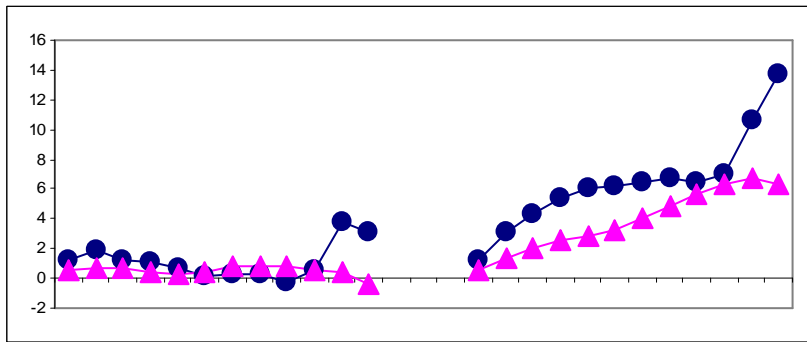


Fig.7. CZK/CHF returns: actual values (circles) versus predictions (triangles).
 Left: original values Right: Cumulative values Model: 200-25-12-06

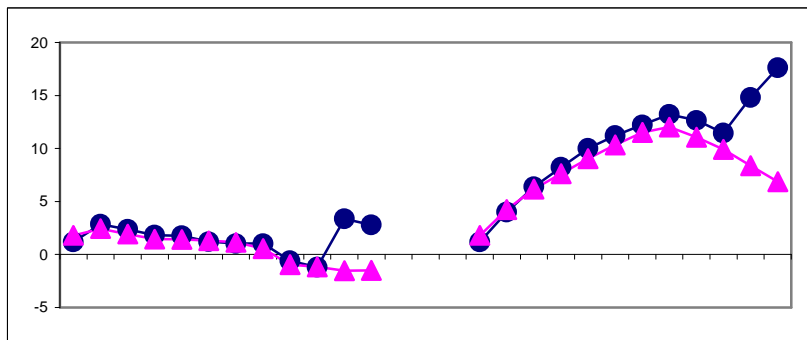


Fig.8. CZK/USD returns: actual values (circles) versus predictions (triangles).
 Left: original values Right: Cumulative values Model: 200-25-05-00

Stock	Model	Type	MPE	MDPE	MAPE
CEZ	Linear		-1.550	1.227	1.910
	One Layer	200-25-05-00	-0.704	0.869	1.054
	Two Layers	200-25-06-02	-1.565	1.281	2.075
KB	Linear		-2.197	3.211	3.460
	One Layer	200-25-04-00	-1.833	2.964	3.138
	Two Layers	200-25-12-10	-1.368	2.356	2.672
TEL	Linear		+0.906	1.322	1.296
	One Layer	200-25-01-00	+0.527	1.572	1.538
	Two Layers	200-25-12-06	+0.342	0.865	0.868
UNIP	Linear		-2.611	1.892	3.044
	One Layer	200-25-02-00	-0.153	2.897	2.943
	Two Layers	200-25-03-04	+0.028	2.597	2.592

Tab.4. Results of ANN Modelling: Stock Returns

Stock	Model	Type	MPE	MDPE	MAPE
CZK/EUR	Linear		+1.087	0.823	1.121
	One Layer	200-25-06-00	+0.610	0.753	0.786
	Two Layers	200-25-02-01	+1.273	0.830	1.290
CZK/GBP	Linear		+0.730	2.389	2.059
	One Layer	200-25-06-00	+0.870	2.237	1.787
	Two Layers	200-25-04-02	+1.090	2.343	1.801
CZK/CHF	Linear		+1.537	0.959	1.537
	One Layer	200-25-08-00	+0.152	1.293	1.247
	Two Layers	200-25-12-06	+0.623	1.021	1.048
CZK/USD	Linear		+0.913	1.104	1.519
	One Layer	200-25-05-00	+0.896	1.236	1.044
	Two Layers	200-25-03-04	-0.642	1.253	1.395

Tab.5. Results of ANN Modelling: Exchange Rate Returns

4 Conclusions

The first group of findings is related to artificial data. The best results were obtained for deterministic chaotic process, because there is relatively simple relation between neighbouring values. Second, the process itself is bounded between zero and one and the notion of outliers is meaningless here. On the other hand, the results for both bilinear and Kesten processes are markedly worse due to ability to create sudden random excursions. Further, the results seem to be similar for the lengths of time series used (500 and 250), number of lagged values (20 and 10) and number of hidden layers (two and one).

As for stock returns, different kinds of individual behaviour were revealed. Both for CEZ and TEL, there has been good agreement between real data and predictions till 7th week and some deviations occurred after this time. On the other hand, predictions of UNIP returns balanced out with respect to their sign, so that corresponding mean predicted error was very small. The worst results were observed in the case of KB returns, where both actual values and predictions exhibited negative signs up to 6th week, but absolute values of predictions were systematically lower. In most cases, neural networks with two hidden layers turned out to be the best alternative.

Exchange rate returns exhibited similar behaviour, but there were strongly manifested outliers. In all cases, 11th and 12th actual values were strong positive outliers with markedly worse predictions. Thus, the corresponding deviations occurred, but the general agreement between actual values and predictions has been observed till 10th week for CZK/USD and CZK/EUR returns, whereas CZK/CHF ones exhibit some kind of sign compensation. Further, the signs of actual values and predictions in 11th and 12th weeks were the same for CZK/EUR and CZK/GBP returns and opposite for CZK/USD ones. In most cases, neural networks with one hidden layer proved to be sufficient.

References

1. McNelis, P.D. (2005). *Neural Networks in Finance*. Elsevier Academic Press.
2. Franses, P.H. and van Dijk, D. (2000). *Non-Linear Time Series Models in Empirical Finance*. Cambridge University Press.
3. Hilborn, R. (2001). *Chaos and Nonlinear Dynamics*. Oxford University Press.
4. Tsay, R.S. (2002). *Analysis of Financial Time Series*. Wiley.
5. Sornette, D. (2000). *Critical Phenomena in Natural Sciences*. Springer.

Non-normality on the power of randomization tests: a simulation study using R

by

Fernando Branco¹, Amílcar Oliveira^{2,3} and Teresa Oliveira^{2,3}

Universidade Lusófona, Lisboa¹

DCeT² - Universidade Aberta, Lisboa

CEAUL³-Center of Statistics and Applications, University of Lisbon

Abstract

The aim of the present research is to evaluate the impact of non-normality on the power of the randomization test for difference between the means of two independent groups. In literature, many studies such as we can see in Micceri, 1989; Mosteller & Tukey, 1968; Stigler, 1977; Wilcox, 1995a, 1995b; suggest that non-normality is common in research data sets. To manipulate non-normality, we used the set of 15 distributions used in Marron and Wand (1992)'s simulation study. These distributions, which have been used in quite a few subsequent studies, can all be written as mixtures of Gaussian distributions. They include distributions that are essentially normal with heavy tails and some outliers ('mild non-normality') and others with a more extreme non-normality, namely multi-modal distributions ('extreme non-normality'). We evaluated the power of the randomization test, and also the power of the Student-t test, as a comparison standard, with data simulated from the 15 Marron-Wand distributions for seven values of effect size and three sample sizes ($n_1 = n_2 = 8$, $n_1 = n_2 = 16$, $n_1 = n_2 = 32$). For each condition, we generated 20 000 samples, and for each one the power of randomization tests was estimated using 1 000 permutations. We set the value of Type I error probability at 0.05. The results show that, in terms of power, the two tests are similar, with a slight advantage for the randomization test over the Student-t test. When we compare the non-normal distributions with the Gaussian, we observe some gains in power in the case of 'mild non-normality' distributions and decreases in power in the case of 'extreme non-normality' distributions. These differences in power are inversely related with sample size.

1. Introduction

Randomization tests are significance tests based on the random assignment of experimental units to treatments in order to test hypotheses about treatment effects. Thus the validity of these tests is based on a random-assignment model, while the validity of classical tests, e.g. Student-t test, is based on a random-sampling model.

In experimental research, hardly ever do we have random samples, so randomization tests allow us to drop the assumption of random sampling from a specified population, the most implausible assumption of typical experimental research.

The randomization idea appears with Fisher (1935), but it was Pitman (1937a, 1937b, 1938) who first presents a type of significance tests, “which may be applied to samples from any population”, based on random assignment alone. These tests were further developed by Kempthorne (1952, 1955), Hinkelmann and Kempthorne (1994), Edgington (1964, 1966, 1969a, 1969b, 1995) and Edgington and Onghena (2007).

With advent of computers and the increase in the speed of computations, the interest in these tests has shifted from theoretical considerations - the validation of classical methods - to practical applicability. Even with moderate sample sizes, there may be so many data permutations that it would not be feasible to generate them all. Contributions from Dwass (1957) and Chung and Fraser (1958) provided the possibility to use only a subset of all possible data permutations, thus rendering practical this computer intensive technique. Manly (1997) and Edgington and Onghena (2007) present some research applications illustrating the use of this technique.

When analysing data from an experiment, where the experimental units are randomly assigned to treatments, if we use a test statistic, like t or F , the distinction between a randomization and a classical test is the way to calculate the significance. In the case of a randomization test, the significance is calculated by a procedure in which the data are repeatedly permuted, and the significance thus obtained is exact, conditional on the data. With this procedure, the researcher can calculate the significance of any statistical test, even of one whose sampling distribution has not yet been analytically derived. Thus, to analyse the data, the researcher is free to choose the test that is most likely to be sensitive to the type of treatment effect that is expected, Branco et al (2010).

When the assumptions for using classical tests are met, the classical and randomization tests are equivalent in terms of statistical power.

The concept of statistical power was developed by Neyman and Pearson. In a series of papers (Neyman & Pearson, 1928a, 1928b, 1933), these authors stated that the choice of a test must take in consideration not only the hypothesis but also the alternatives against which it is being tested. They introduced the distinction between errors of the first and second kind. Power, the complement of an error of the second kind, is the probability of rejecting a false null hypothesis.

Although the Neyman-Pearson theory of statistical inference is mainstream in the social and behavioural sciences (see, e.g., Hays, 1994; Marascuilo & Serlin, 1988; Winer, Brown, & Michels, 1991), power analyses were neglected and we must credit Cohen (1962) for introducing the notion of statistical power to behavioural scientists. In his handbook on power, Cohen (1969, updated in 1988), the author allowed researchers, when planning an experiment, to determine the sample size needed to detect a given population effect size, taking in account the two types of errors.

As stated above, the classical and randomization tests are equivalent in terms of power, when the assumptions for using classical tests are met. But, in empirical research, it is well known that seldom the data are well behaved, and frequently present a non-normal shape.

Indeed, Micceri (1989) and Stigler (1977) have shown that many data sets collected in empirical research usually have non-normality. Mosteller and Tukey (1968), Bradley (1977) and Wilcox (1995a, 1995b) reached similar conclusions. However the data analyzed by Stigler and by Micceri suggest different types of non-normality: while Stigler's data are approximately normal, with heavy tails and some outliers, the data described by Micceri present a more extreme non-normality with distributions not only asymmetric but multimodal.

The data collected in empirical research can come from many different distributions and we can not cover all possibilities. In this study we used the set of 15 distributions used by Marron and Wand (1992) in their simulation study, which were later used in many others, which are mixtures of normal. These 15 distributions include some distributions of the type described by Stigler, but most of them have extreme non-normality, as the ones analyzed by Micceri.

In Table 1 we list the 15 Marron-Wand distributions that can be written as mixtures of Gaussians. For each distribution, we show the parameters of the Gaussian distributions that constitute them, together with their weighting.

Table 1 The 15 Marron-Wand distributions

Distribution	Mean	Variance	Weighting
1. Gaussian	0	1	1
2. Skewed	-0.3	1.4400000	0.2

Distribution	Mean	Variance	Weighting
	0.3	0.6400000	0.2
	1.0	0.4444444	0.6
3. Strong Skewed	0.000000	1.000000000	0.125
	-1.000000	0.444444444	0.125
	-1.666667	0.197530864	0.125
	-2.111111	0.087791495	0.125
	-2.407407	0.039018442	0.125
	-2.604938	0.017341530	0.125
	-2.736626	0.007707347	0.125
	-2.824417	0.003425487	0.125
4. Kurtotic	0	1.00	0.6666667
	0	0.01	0.3333333
5. Outlier	0	1.00	0.1
	0	0.01	0.9
6. Bimodal	-1	0.4444444	0.5
	1	0.4444444	0.5
7. Separated Bimodal	-1.5	0.25	0.5
	1.5	0.25	0.5
8. Asymmetric Bimodal	0.0	1.0000000	0.75
	1.5	0.1111111	0.25
9. Trimodal	-1.2	0.3600	0.45
	1.2	0.3600	0.45
	0.0	0.0625	0.10
10. Claw	0.0	1.00	0.5
	-1.0	0.01	0.1
	-0.5	0.01	0.1
	0.0	0.01	0.1
	0.5	0.01	0.1
	1.0	0.01	0.1
11. Double Claw	-1.0	0.4444444	0.490000000
	1.0	0.4444444	0.490000000
	-1.5	0.0001000	0.002857143
	-1.0	0.0001000	0.002857143
	-0.5	0.0001000	0.002857143
	0.0	0.0001000	0.002857143
	0.5	0.0001000	0.002857143
	1.0	0.0001000	0.002857143
	1.5	0.0001000	0.002857143
12. Asymmetric Claw	0.0	1.000000	0.50000000
	-1.5	0.160000	0.25806452
	-0.5	0.040000	0.12903226
	0.5	0.010000	0.06451613
	1.5	0.002500	0.03225806
	2.5	0.000625	0.01612903
13. Asymmetric Double Claw	-1.0	0.4444444	0.460000000
	1.0	0.4444444	0.460000000
	-1.5	0.0001000	0.003333333
	-1.0	0.0001000	0.003333333
	-0.5	0.0001000	0.003333333
	0.5	0.0049000	0.023333333
	1.0	0.0049000	0.023333333
	1.5	0.0049000	0.023333333
14. Smooth Comb	-1.4761905	0.2579994961	0.50793651
	0.8095238	0.0644998740	0.25396825
	1.9523810	0.0161249685	0.12698413
	2.5238095	0.0040312421	0.06349206
	2.8095238	0.0010078105	0.03174603
	2.9523810	0.0002519526	0.01587302

Distribution	Mean	Variance	Weighting
15. Discrete Comb	-2.1428571	0.081632653	0.28571429
	-0.4285714	0.081632653	0.28571429
	1.2857143	0.081632653	0.28571429
	2.2857143	0.002267574	0.04761905
	2.5714286	0.002267574	0.04761905
	2.8571429	0.002267574	0.04761905

In order to illustrate the shape of these distributions, we present in Figure 1 graphics of the respective densities.

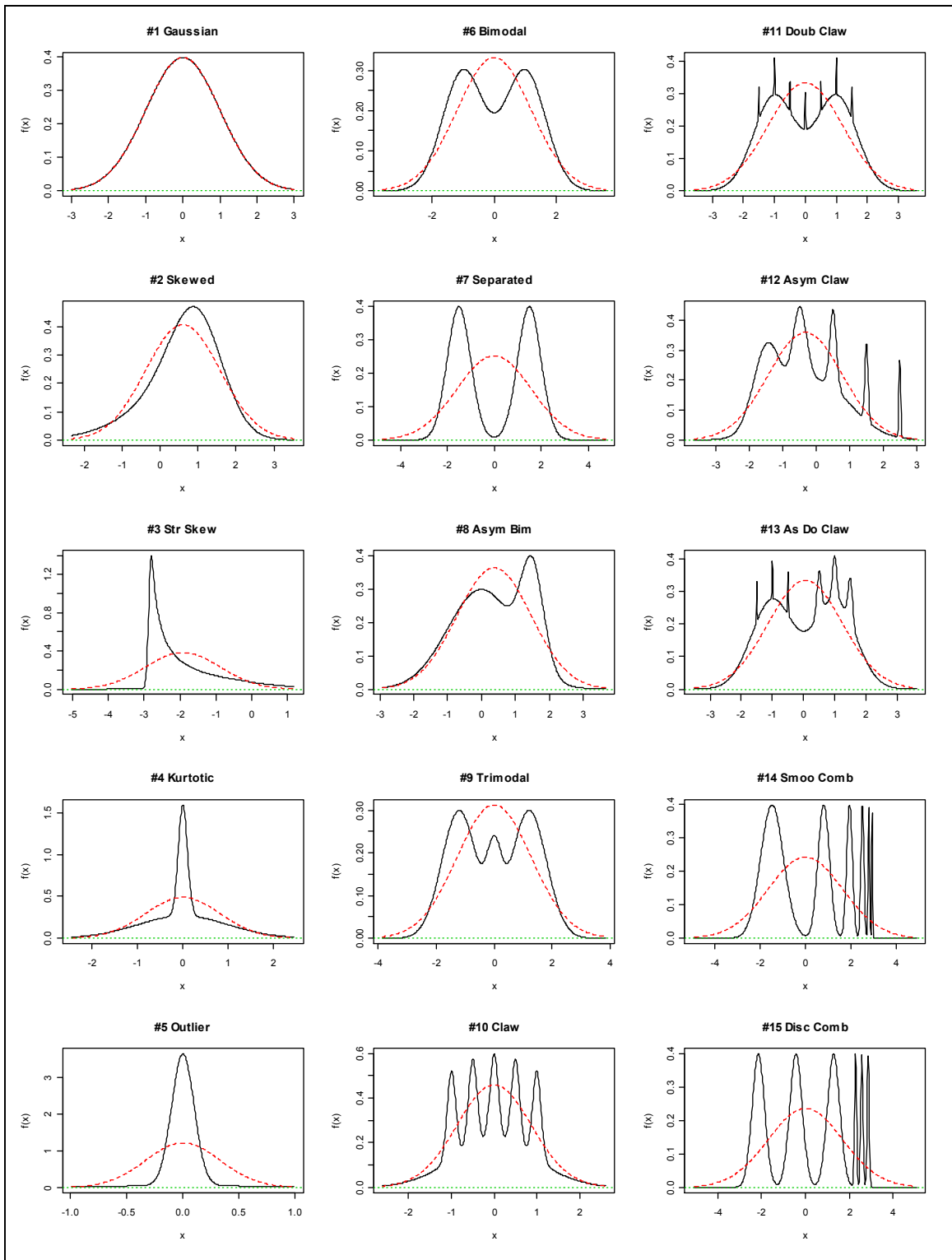


Figure 1 The 15 Marron-Wand densities

The aim of the present research is to evaluate the impact of nonnormality on the power of the randomization test for difference between the means of two independent groups.

2. Method

We evaluated the power of randomization tests and the Student t test when comparing two independent balanced groups by manipulating the following three variables:

- Sample sizes, with three levels: $n_1 = n_2 = 8$, $n_1 = n_2 = 16$ and $n_1 = n_2 = 32$;
- Effect size, with 7: -0.8, -0.5, -0.2, 0.0, 0.2, 0.5, 0.8;
- Population distribution, with 15 levels: the Marron-Wand distributions, mixtures of normal, as described in Table 1.

Regarding the size of groups, we use groups of 8, 16 and 32 elements since these values correspond respectively to samples as small, medium and large in experimental studies in social and behavioural sciences.

The values of effect size were chosen taking into account Cohen's guidelines (1962, 1988). This author stated that values of 0.2, 0.5 and 0.8 correspond to "small", "medium" and "large" effects in the social sciences research, particularly in psychology. These conventional values received empirical support by Lipsey (1990) in a study incorporating the results of 102 meta-analysis summarizing the results of 6700 individual studies in the field of behavioural sciences.

To simulate data from these distributions, we write programs in R (R Development Core Team, 2008), using the package 'norlmix' (Mächler, 2007). For each distribution we simulated 20 000 samples and for each of these samples, we generated 999 random combinations to estimate the significance of the randomization tests.

Values for the number of samples and the number of resamples have been chosen taking into account the recommendations of Oden (1991), Westfall & Young (1993) and Zhang & Boos (2000). Power was evaluated for two-tailed tests for $\alpha = 0.05$. We calculated the power of a test as the proportion of samples in which the probability value associated with the test statistic was equal to or less than the value of α .

In what regards randomization tests, with sample sizes $n_1 = n_2 = 8$, the total number of combinations is 12 870; this number rises to 601 080 390 in the case of sample sizes $n_1 = n_2 = 16$, and 1.83262×10^{18} , when sample sizes are $n_1 = n_2 = 32$. Since we used, to estimate the significance of the randomization test, a reference set of 1000 combinations (one observed, plus 999 randomly generated), we have construct 99% confidence intervals for each power value. When comparing the power of randomization tests with the power of Student t test, we use the information provided by these confidence intervals.

3. Results

First we present the power of randomization tests for the Gaussian distribution, then we compare their power in the case of the Marron-Wand 02-14 distributions with their power in the case of Gaussian distribution and, finally, we compare the power of randomization tests with the power of Student t test.

3.1. Power of randomization tests (Gaussian distribution)

The power of randomization in the case of Gaussian distribution is presented in Table 2. As expected, the power increases with sample size, but is generally low, only exceeding the value 0.80 in the case of samples with 32 elements per group and a “large” effect size.

Table 2 Gaussian distribution: Power of the randomization tests

Effect Size	$n_1 = n_2 = 8$	$n_1 = n_2 = 16$	$n_1 = n_2 = 32$
-0.80	0.315	0.590	0.880
-0.50	0.153	0.275	0.501
-0.20	0.065	0.087	0.128
0.00	0.049	0.050	0.049
0.20	0.065	0.083	0.121
0.50	0.153	0.277	0.506
0.80	0.325	0.587	0.880

3.2. Influence of non-normality on the power of randomization tests

To present the results, we will distinguish two groups of Marron-Wand distributions: The first group includes the 02-05 distributions, similar to those analyzed by Stigler ('mild' non-normality), the second group comprises the 06-15 distributions, analogous of those described by Micceri ('extreme' non-normality).

3.2.1. 'Mild non-normality'

In Table 3 we present the difference between the power of randomization tests for the first group of Marron-Wand distributions (MW02-05) and its power for the Gaussian distribution. These four distributions are all unimodal, unlike the other distributions that have two or more modes.

Table 3 Difference in power between the 'mild' non-normal distributions and the Gaussian

Sample size	Effect Size	MW02	MW03	MW04	MW05
$n_1 = n_2 = 8$	-0.80	0.029	0.051	0.034	0.326
	-0.50	0.012	0.035	0.023	0.341
	-0.20	0.002	0.010	0.007	0.098
	0.00	0.003	0.000	0.003	0.001
	0.20	0.005	0.009	0.005	0.093
	0.50	0.013	0.039	0.023	0.339
	0.80	0.021	0.045	0.034	0.319
$n_1 = n_2 = 16$	-0.80	0.010	0.013	0.008	0.120
	-0.50	0.015	0.018	0.016	0.217
	-0.20	0.000	0.001	0.003	0.105
	0.00	0.001	0.000	0.000	-0.001
	0.20	0.004	0.010	0.003	0.106
	0.50	0.015	0.025	0.020	0.218
	0.80	0.019	0.022	0.016	0.114
$n_1 = n_2 = 32$	-0.80	0.001	-0.004	-0.001	-0.013
	-0.50	0.006	0.010	0.004	0.099
	-0.20	0.002	-0.004	0.000	0.074
	0.00	0.001	-0.001	0.001	0.001
	0.20	0.004	0.005	0.003	0.079
	0.50	0.006	0.009	0.004	0.097
	0.80	0.001	-0.001	-0.002	-0.011

We can see that for these distributions, the differences are generally positive, indicating gains in power. Excluding the MW05 distribution, the differences vary between -0.004 and 0.051. But in the case of the MW05 distribution, strongly kurtotic, there are appreciable gains in power (with a maximum of 0.341). We also note that, for all these distributions, gains in power are inversely related to samples size.

3.2.1. 'Extreme non-normality'

We present in Table 4 the difference between the power of randomization tests for the second group of Marron-Wand distributions (MW06-15) and its power for the normal distribution. These ten distributions are all multimodal and have a more extreme non-normality.

Table 4 Difference in power between the ‘extreme’ non-normal distributions and the Gaussian

Sample size	Effect Size	MW06	MW07	MW08	MW09	MW10	MW11	MW12	MW13	MW14	MW15
$n_1 = n_2 = 8$	-0.80	-0.016	-0.033	-0.010	-0.024	0.000	-0.018	-0.005	-0.021	-0.029	-0.029
	-0.50	-0.012	-0.016	-0.006	-0.011	0.003	-0.008	-0.004	-0.012	-0.013	-0.011
	-0.20	-0.002	0.000	0.000	0.000	-0.002	0.001	0.000	-0.002	0.000	-0.002
	0.00	0.001	0.002	0.002	0.000	0.004	0.002	-0.004	0.000	0.001	0.001
	0.20	-0.003	-0.001	0.001	-0.003	-0.001	0.000	0.000	-0.003	-0.003	-0.002
	0.50	-0.008	-0.015	-0.007	-0.015	-0.002	-0.005	-0.003	-0.012	-0.013	-0.013
	0.80	-0.029	-0.046	-0.011	-0.029	-0.008	-0.024	-0.008	-0.027	-0.031	-0.037
$n_1 = n_2 = 16$	-0.80	-0.017	-0.018	-0.009	-0.009	0.001	-0.004	0.002	-0.009	-0.005	-0.016
	-0.50	-0.007	-0.014	0.001	-0.010	-0.001	-0.011	-0.005	-0.008	-0.009	-0.009
	-0.20	-0.004	-0.005	0.000	-0.003	-0.002	-0.006	-0.002	-0.003	-0.002	-0.005
	0.00	0.000	0.000	0.001	0.004	-0.001	0.000	0.002	0.002	0.001	-0.001
	0.20	0.002	0.001	0.001	0.003	0.006	-0.001	0.001	-0.003	0.001	0.001
	0.50	-0.011	-0.018	-0.002	-0.010	0.004	-0.012	-0.005	-0.008	-0.014	-0.010
	0.80	-0.004	-0.010	-0.007	-0.008	0.001	-0.004	-0.001	-0.003	-0.011	0.000
$n_1 = n_2 = 32$	-0.80	0.002	0.004	0.000	0.005	0.002	0.004	0.002	0.002	0.000	0.001
	-0.50	-0.004	-0.009	-0.007	-0.014	0.000	-0.006	-0.008	-0.001	-0.009	-0.007
	-0.20	-0.008	-0.009	0.000	-0.007	-0.007	-0.005	-0.006	-0.010	-0.008	-0.005
	0.00	0.000	0.000	0.003	0.003	0.000	0.000	-0.002	0.003	0.000	0.001
	0.20	0.002	0.000	0.001	-0.002	0.002	0.001	0.002	0.001	-0.002	-0.002
	0.50	-0.010	-0.012	-0.003	-0.002	-0.003	-0.011	-0.003	-0.011	-0.006	-0.008
	0.80	0.001	0.003	0.002	0.003	0.001	0.006	0.004	0.003	0.001	0.008

Here, the differences are generally negative, implying loss of power. But the biggest loss does not exceed 0.046 and there is an inverse relationship between losses and samples size: for samples with 16 elements, the maximum loss is 0.018, and it is 0.014 for samples with 32 elements.

3.3. Comparison of the power of randomization tests and Student t

The randomization and Student t tests showed, in general, similar power, with a slight advantage for the former. The differences are, on the whole, very small and tend to decline with increasing sample sizes. If we do not consider the MW05 distribution, differences in power vary between -0.009 and 0.013. However, in the case of the MW05 distribution, the differences are all

positive and, as shown in Table 5, for $n_1 = n_2 = 8$ they are all statistically significant and for $n_1 = n_2 = 16$ they are significant in the interval -0.02 to 0.02.

Table 5 Difference between the power of randomization tests and t de Student to Marron-Wand 05 ('Outlier') distribution.

Effect Size	$n_1 = n_2 = 8$	$n_1 = n_2 = 16$	$n_1 = n_2 = 32$
-0.80	0.050	0.025	0.009
-0.50	0.098	0.040	0.021
-0.20	0.065	0.056	0.022
0.00	0.028	0.023	0.013
0.20	0.061	0.057	0.024
0.50	0.102	0.036	0.020
0.80	0.053	0.025	0.010

Note: Significant differences are represented in bold.

We can observe that for this distribution, Marron-Wand 05 ('Outlier'), the Student t test is too conservative, since for an 0.00 effect size the power achieved, respectively for samples with 8, 16 and 32 elements per group, is 0.021, 0.027 and 0.037, whereas the corresponding values for the randomization test are 0.049, 0.049 and 0.050.

4. Conclusions

In this study we evaluated the power of randomization tests for comparing two independent balanced samples for non-normal distributions. The effect on the power of these tests is different for the two types of non-normality we have considered: mild and extreme non-normality.

For the Marron-Wand 02-05 distributions, similar to those described by Stigler (normal with heavy tails and some outliers), all unimodal, there is an increase in power relative to the Gaussian distribution. In the case of one of these distributions (MW05), the increase is rather large.

Regarding the Marron-Wand 06-15 distributions, similar to those analyzed by Micceri, with extreme non-normality, with multiple modes, there is a decrease in power, although generally a small one.

These differences in power are inversely related to samples size.

Concerning the comparison of the randomization test with the Student's t test, it was found that, in general, they have similar power, with some advantage to the former. This advantage is only significant in the case of one of the simulated distributions, MW05, strongly kurtotic, with outliers, and reduces with increasing sample size.

These results suggest that if an investigator, when planning an experiment, chooses his samples size in function of a given population effect size and a given power, assuming a normal distribution, the power of his randomization test will not be diminished by more than 0.05, if his data come from a non-normal distribution.

However, it is important to note that our results were obtained with balanced groups and with the same distribution. They can not therefore be generalized to situations where the groups are not balanced or have different distributions or are heteroscedastic.

References

- Boos, D. D., & Zhang, J. (2000). Monte Carlo evaluation of resampling-based hypothesis tests. *Journal of the American Statistical Association*, 95, 486-492.
- Bradley, J. V. (1977). A common situation conducive to bizarre distribution shapes. *The American Statistician*, 31, 147-150.
- Branco, F., Oliveira, A. & Oliveira, T.A.(2010). Biometrical Letters, Vol.47. In Press.
- Chung, J. H. & Fraser, D. A. S. (1958). Randomization tests for a multivariate two sample problem. *Journal of the American Statistical Association*, 53, 729-735.
- Cohen, J. (1962). The statistical power of abnormal-social psychological research: A review. *Journal of Abnormal and Social Psychology*, 65, 145-153.
- Cohen, J. (1969). *Statistical power analysis for the behavioral sciences*. New York: Academic Press.
- Cohen, J. (1988). *Statistical power analysis for the behavioral sciences* (2nd ed.). Hillsdale, NJ: Lawrence Erlbaum.
- Dwass, M. (1957). Modified randomization tests for nonparametric hypotheses. *Annals of Mathematical Statistics*, 28, 181-187.
- Edgington, E. S. (1964). Randomization tests. *Journal of Psychology*, 57, 445-449.
- Edgington, E. S. (1966). Statistical inference and nonrandom samples. *Psychological Bulletin*, 66, 485-487.
- Edgington, E. S. (1969a). Approximate randomization tests. *Journal of Psychology*, 72, 143-149.

- Edgington, E. S. (1969b). *Statistical inference: The distribution-free approach*. New York: McGraw-Hill.
- Edgington, E. S. (1995). *Randomization tests* (3rd ed.). New York: Marcel Dekker.
- Edgington, E. S. & Onghena, P. (2007). *Randomization tests* (4th ed.). Boca Raton, FL: Chapman & Hall/CRC.
- Fisher, R. A. (1966). *The design of experiments* (8th ed.). Edinburgh: Oliver & Boyd. [First edition: 1935]
- Hays, W. L. (1994). *Statistics* (5th ed.). Belmont, CA: Wadsworth.
- Hinkelmann, K. & Kempthorne, O. (1994). *Design and analysis of experiments, Volume I: Introduction to experimental design*. New York: Wiley.
- Kempthorne, O. (1952). *The design and analysis of experiments*. New York: Wiley.
- Kempthorne, O. (1955). The randomization theory of experimental inference. *Journal of the American Statistical Association*, 50, 964-967.
- Lipsey, M. W. (1990). *Design sensitivity: Statistical power for experimental research*. Newbury Park, CA: Sage.
- Mächler, M. (2007). *nor1mix: Normal (1-d) Mixture Models (S3 Classes and Methods)*. R package, version 1.0-7.
- Manly, B. F. J. (2007). *Randomization, bootstrap and Monte Carlo methods in Biology* (3rd ed.). Boca Raton, FL: Chapman & Hall/CRC.
- Marascuilo, L. A. & Serlin, R. C. (1988). *Statistical methods for the social and behavioral sciences*. New York: Freeman.
- Marron, J. S., & Wand, M. P. (1992). Exact mean integrated squared error. *Annals of Statistics*, 20, 712-736.
- Micceri, T. (1989). The unicorn, the normal curve, and other improbable creatures. *Psychological Bulletin*, 105, 156-166.
- Mosteller, F., & Tukey, J.W. (1968). Data analysis, including statistics. In G. Lindzey & E. Aronson (Eds.), *The handbook of Social Psychology: Research methods* (pp. 80-203). Reading, MA: Addison-Wesley.
- Neyman, J., & Pearson, E. (1928a). On the use and interpretation of certain test criteria for purposes of statistical inference: Part I. *Biometrika*, 20A, 175-240.
- Neyman, J., & Pearson, E. (1928b). On the use and interpretation of certain test criteria for purposes of statistical inference: Part II. *Biometrika*, 20A, 263-294.

- Neyman, J., & Pearson, E. (1933). On the problem of the most efficient tests of statistical hypothesis. *Philosophical Transactions of the Royal Society of London, Series A*, 231, 289-337.
- Oden, N. L. (1991). Allocations of effort in Monte Carlo simulation for power of permutations tests. *Journal of the American Statistical Association*, 86, 1074-1076.
- Pitman, E. J. G. (1937a). Significance tests which may be applied to samples from any population. *Journal of the Royal Statistical Society, B*, 4, 119-130.
- Pitman, E. J. G. (1937b). Significance tests which may be applied to samples from any population. II. The correlation coefficient. *Journal of the Royal Statistical Society, B*, 4, 225-232.
- Pitman, E. J. G. (1938). Significance tests which may be applied to samples from any population. III. The analysis of variance test. *Biometrika*, 29, 322-335.
- R Development Core Team (2008). R: A language and environment for statistical computing. R Foundation for Statistical Computing, Vienna, Austria. ISBN 3-900051-07-0, URL <http://www.R-project.org>.
- Stigler, S. M. (1977). Do robust estimators work with real data? *The Annals of Statistics*, 5, 1055-1098.
- Westfall, P. H., & Young, S. S. (1993). *Resampling-based multiple testing*. New York: Wiley.
- Wilcox, R. R. (1995a). ANOVA: A paradigm for low power and misleading measures of effect size? *Review of Educational Research*, 65, 51-77.
- Wilcox, R. R. (1995b). ANOVA: The practical importance of heteroscedastic methods, using trimmed means versus means, and designing simulation studies. *British Journal of Mathematical and Statistical Psychology*, 48, 99-114.
- Winer, B. J., Brown, D. R., & Michels, K. M. (1991). *Statistical principles in experimental design* (3rd ed.). New York: McGraw-Hill.

Forecasting the Incidence of Cancer in Regional Victoria, Australia

Nicholas Brown, Philippa Hartney,
Rachael Hamilton-Keene and Terry Mills

Loddon Mallee Integrated Cancer Service
Bendigo, Victoria, Australia
Email: tmills@bendigohealth.org.au

Abstract: Loddon Mallee Integrated Cancer Service (LMICS) is responsible for planning the delivery of cancer services in the Loddon Mallee Region of Victoria, Australia. Forecasting the incidence of cancer in the region plays a key role in strategic planning for these services. In this paper, we describe the context of our work, present a review of the literature on forecasting the incidence of cancer, discuss contemporary approaches to the problem especially functional data analysis, describe our experience with the models at LMICS, and list special issues associated with applying these models in regional Australia. The extensive bibliography illustrates the world-wide interest in this forecasting problem.

Keywords: Stochastic models, Functional data analysis, Poisson regression, Strategic planning, Health care

1 Introduction

Cancer is a major cause of death in Australia. Governments need to predict the resources required to deal with the disease, and to evaluate anti-cancer programs. For this reason, “[c]ancer, except for basal cell and squamous cell carcinoma of the skin, is a notifiable disease in all states and territories of Australia” (AIHW (2008a), p. 1). Thus, forecasting plays a key role in the fight against cancer.

We will need to define some terms and concepts.

In any year, the *incidence* of cancer is the number of new cases that have been diagnosed in that year. In any year, and for any specific age-group, the *age-specific incidence* is the number of new cases that have been diagnosed in that year for that particular age group.

The *incidence rate* is the incidence per 100,000 head of population. The *age-specific incidence rate* is the age-specific incidence per 100,000 head of population in the associated age group.

The *prevalence* of cancer may be defined as the number of people living in the region who have been diagnosed with cancer during the last 5 years. One might also call this *5-year prevalence* (AIHW (2008b)).

The state of Victoria in Australia has developed a plan to guide the prevention of cancer and care for cancer patients in the state. One of the key principles of the plan is that “patients should be treated as close to home as possible whilst maintaining quality and safety of care” (DHS (2009), p. 13).

Loddon Mallee Integrated Cancer Service plays an important role in implementing the state-wide plan in the Loddon Mallee Region (LMR) in Victoria. LMR covers an area of 56,956 sq. km., which is about 25% of the state of Victoria, and has a population of a little more than 300,000, which is about 6% of the state’s population. The region is large in area and sparsely populated. These factors underpin the challenges associated with treating patients close to home in LMR.

The following two examples illustrate that forecasting the incidence of cancer is an essential part of strategic planning for the delivery of cancer services in LMR.

Positron emission tomography (PET) is an imaging technique that is useful in estimating the stage to which cancer has developed in a patient. PET scanners are expensive and, at present, there is no PET scanner in the region. To develop a business case for a PET scanner, it is necessary to estimate the demand for PET scans which involves forecasting the incidence of cancer in the region. These estimates can be included in applications for funding for the scanner.

The cancer journey can span many years. Providing service for cancer patients and their carers is not limited to providing care for patients who have been diagnosed with cancer during the current year (those counted in the incidence data). In planning services for supportive care, one needs to estimate the prevalence of cancer by using the incidence of cancer and the probability of survival for a given number of years (Pisani (2002)). Thus, forecasting the incidence of cancer is part of forecasting the prevalence of cancer and, hence, contributes to strategic planning for supportive care in the region.

This paper deals with forecasting the incidence of cancer in LMR. We assess the research literature on the subject in light of our experience in dealing with practical problems. We emphasise concepts and issues rather than numerical results.

2 Review of the Literature

Governments around the world are interested in forecasting the incidence (or incidence rates) of cancer so that they can plan accordingly. This has led to the publication of case studies from many countries such as Australia (AIHW 2005), Bulgaria (Hristova et al. (1997)), China (Yang et al. (2005)), Japan (Fujimoto et al. (1988)), New Zealand (New Zealand Ministry of Health (2002)), Finland and other Nordic countries (Dyba (2000), Møller et al. (2002, 2003), Teppo et al. (1974)), Scotland (Scottish Executive Health Department (2004)), USA (Tiwari et al. (2004), Pickle et al. (2007)), Wales (White et al. (2006)). The collection of papers in Magnus (1982) further illustrates this level of international interest.

An important general lesson one may draw from this international literature is that the appropriate model for forecasting the incidence of cancer may vary with geographic location, and the site of the cancer. For example, Møller et al. (2002) found that the appropriate model for Iceland was different from the models used in other Nordic countries. Fujimoto et al. (1988) used different models for different types of cancer in the same geographic location. We cannot assume that a model that works for Australia will also work for LMR, or that a model that works for breast cancer will work for lung cancer.

Which explanatory variables should be used in a model? Unfortunately, the aetiology of many cancers is not well enough understood to form part of a model. Even when causes may be known (eg smoking and lung cancer), to forecast the incidence of cancer using this link brings new complications into the model. However, it has been noted often (eg Barber et al. (2009)) that the age-distribution of the population is a very important factor in describing the incidence of cancer, even though age does not cause cancer. Because the demographic profile is reasonably predictable, researchers have tended not to look further for explanatory variables beyond time and the demographic profile of the region.

Frost (1939) is an early paper that discusses “the cohort effect” in the variation of vital rates. He explains his ideas with graphical methods applied to data on deaths from tuberculosis in Massachusetts between 1870 and 1930. The same general idea has been applied to modelling incidence and mortality rates for cancer (Clayton and Schifflers (1987a, 1987b). Day and Charnay (1982) present an overview of this approach in the context of cancer.

3 Contemporary Approaches

Since incidence data are count data, it is not surprising that Poisson regression models have played a role in forecasting the incidence of cancer (Hakulinen and Dyba (1994), Dyba (2000)).

Functional data analysis (FDA) has its mathematical roots in the study of random functions, and is now applied in a wide range of areas (Ramsay and Silverman (2002, 2005)). Erbas et al. (2007) have applied FDA to forecasting mortality rates of breast cancer in Australia; the same principles apply to forecasting incidence rates; see also Hyndman and Ullah (2005). FDA methods are facilitated by recent developments in R (R Development Core Team (2008), Ramsay et al. (2009)). The Australian Institute of Health and Welfare used FDA in a recent report on forecasting the incidence of cancer; the report also contains a brief overview of statistical methods for projecting the incidence of cancer (AIHW (2005)).

Any forecasting exercise should have a clear aim that stems from the context of the problem. This will assist in defining the response variable, identifying explanatory variables, choosing the model and its assumptions, and assessing the accuracy required. This can be illustrated by the PET scanner issue.

To assess the need for a PET scanner in the region, we aim to forecast the incidence rather than the incidence rate. Because we are not comparing our region to other regions, we do not need to forecast the standardised incidence rate (Estève et al. (1994, Chapter 2)). Since a PET scan is used soon after the patient is diagnosed with cancer, one would be interested in forecasting incidence rather than prevalence.

Thus, in this example, the response variable is the incidence of all cancers in a year (X), the explanatory variable is time (t , year), the model used is simple linear regression ($X = a + bt + \varepsilon$). The model fits well ($R^2=0.93$, $p = 2.3e-15$) and leads to useful forecasts with prediction intervals of a reasonable size. See Figure 1. Residual analysis shows that there is some structure left in the residuals that warrants further investigation.

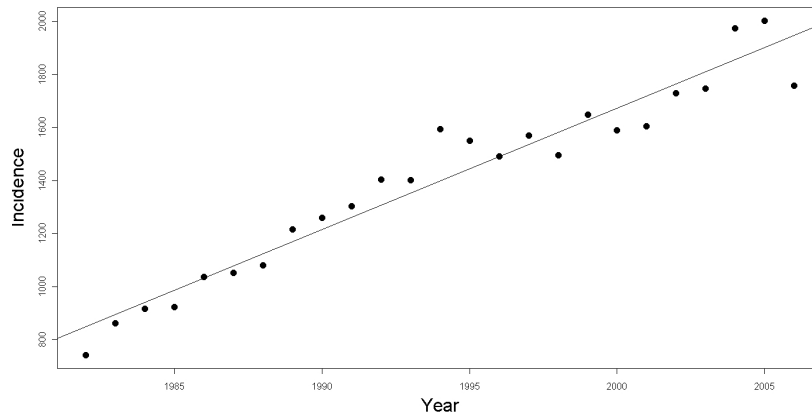


Figure 1: Incidence of all cancers in LMR, 1982-2006

Several brave authors have written articles on whether predictions of the incidence of cancer really work (Hakulinen et al. (1986), Dyba and Hakulinen (2008)). It is too early for us to judge the accuracy of our own forecasts using this simple model.

If the aim is to assess the demand for a PET scanner in the region, then the width of the prediction interval must be appropriate for that purpose. Yet again we see that a clear purpose is essential to the modelling.

4 Regional Issues

There are issues concerning the data, some of which arise from the regional context. First, for privacy reasons, if the incidence is less than 5 then LMICS is not provided with the incidence data. This will occur in a region such as LMR for specific cancers, or for specific sub-regions of LMR. Second, when the incidence is small, the incidence series can be quite volatile thus limiting the value of forecasts. Third, the most recent data available may be two or more years old; this is the cost of striving to produce incidence data that are very accurate. Fourth, LMICS has available data on age-specific incidence rates for only 11 years. This makes it difficult to use age-period-cohort models. Finally, to obtain better estimates of the prevalence of cancer, it would be very helpful for LMICS to have more local data on survival rates in addition to the statewide data reported in English et al. (2007).

5 Conclusions and further work

The main conclusion is that stochastic models and data analysis are essential tools in planning for services for cancer patients and their carers. This is a contribution of mathematics and statistics to an important problem in public health.

The research literature comes from the experience of researchers in many different countries. The most appropriate model may depend on the geographic location of the region, and the type of cancer being studied.

Our experience illustrates that one must have a clear view of the purpose of the forecasting problem in order to build the model. Data at a regional level may not be as extensive as that at a national level; the challenge is to make the best use of available data. And simple models can work well.

There are many questions for us to resolve in this area.

The continuing problem facing us is to decide which models work best for forecasting the incidence of cancer in LMR. Comparisons of competing methods have been made by Dyba and Hakulinen (2000).

“The prediction should always be accompanied by a prediction interval, a measure of its precision, in order to be properly used in the decisive process” Dyba (2000). Usually researchers use 95% or 90% prediction intervals, Erbas et al. (2007) use 80% prediction intervals. Landon and Singpurwalla (2008) present a method for choosing the coverage probability for prediction intervals based on decision theory. Can the ideas of Landon and Singpurwalla be used in the context of forecasting the incidence of cancer?

It is always precarious to make long term predictions in health or technology. Predicting the incidence of cancer falls in both areas.

Acknowledgements

We acknowledge continued support for our work at LMICS from Department of Health, Victoria. We thank the Cancer Council of Victoria for providing data on the incidence of cancer.

References

1. AIHW, *Cancer incidence projections, Australia 2002 to 2011*. Cancer Series. Canberra, Australian Institute of Health and Welfare, 152pp. (2005).

2. AIHW, *Cancer in Australia: an overview, 2008*. Cancer Series. Canberra, Australian Institute of Health and Welfare. **25**, 153pp. (2008a).
3. AIHW, *Cancer survival and prevalence in Australia: Cancers diagnosed from 1982 to 2004*. Cancer Series. Canberra, Australian Institute of Health and Welfare. **42**, 88pp. (2008b).
4. Barber, T., Brown, N., Hamilton-Keene, R., Hartney, P., and Mills T., Forecasting for cancer services, *Nosokinetics News*, **6**(2), 2–3 (2009).
5. Clayton, D. and Schifflers, E., Models for temporal variation in cancer rates I: Age-period and age-cohort models, *Statistics in Medicine*, **6**(4), 449–467 (1987a).
6. Clayton, D. and Schifflers, E., Models for temporal variation in cancer rates II: Age-period-cohort models, *Statistics in Medicine*, **6**(4), 469–481 (1987b).
7. Day, N. E. and Charnay, B., (1982) Time trends, cohort effects, and aging as influence on cancer incidence, in *Trends in Cancer Incidence: Causes and Practical Implications*. (K. Magnus, ed.). Washington: Hemisphere Publishing, 51–65 (1982).
8. DHS, *Victoria's cancer action plan 2008-2011*. Melbourne: Department of Human Services. <http://www.health.vic.gov.au/cancer/vcap.htm> (2009).
9. Dyba, T., (2000) Precision of cancer incidence predictions based on Poisson distributed observations. Doctoral thesis, Faculty of Social Science, Helsinki, University of Helsinki (2000).
10. Dyba, T. and Hakulinen, T., Comparison of different approaches to incidence prediction based on simple interpolation techniques, *Statistics in Medicine*, **19**(13), 1741–1752 (2000).
11. Dyba, T. and Hakulinen, T., Do cancer predictions work? *European Journal of Cancer*, **44**(3), 448–453 (2008).
12. Dyba, T., Hakulinen, T., and Paivarinta, L., A simple non-linear model in incidence prediction, *Statistics in Medicine*, **16**(20), 2297–2309 (1997).
13. Elkum, N. B., Predicting confidence intervals for the age-period-cohort model, *Journal of Data Sciences*, **3**(4), 403–414 (2005).
14. English, D., Farrugia, H., Thursfield, V., Chang, P. and Giles, G., *Cancer survival Victoria 2007*. Melbourne: Cancer Council of Victoria, 2007.
15. Erbas, B., Hyndman R.J., and Gertig, D., Forecasting age-specific breast cancer mortality using functional data models, *Statistics in Medicine*, **26**(2), 458–470 (2007).
16. Estève, J., Benhamou, E., and Raymond, L., *Statistical Methods in Cancer Research. Vol. IV: Descriptive Epidemiology*. Lyon, International Agency for Research on Cancer (1994).

17. Frost, W., The age selection of mortality from tuberculosis in successive decades, *American Journal of Epidemiology*, **30**(Section A), 91–96 (1939).
18. Fujimoto, I., Hanai, A., Tominaga, S. and Kuroishi, T., Predictions of the incidence of cancer in Japan in the year 2000 [in Japanese], *Gan No Rinsho*, **34**(14), 1911–1916 (1988).
19. Hakulinen, T. and Dyba, T., Precision of incidence predictions based on Poisson distributed observations, *Statistics in Medicine*, **13**(15), 1513–1523 (1994).
20. Hakulinen, T., Teppo, L. and Saxén, E., Do the predictions for cancer incidence come true? Experience from Finland, *Cancer*, **57**(12), 2454–2458 (1986).
21. Hristova, L., Dimova, I., and Iltcheva, M., Projected cancer incidence rates in Bulgaria, 1968–2017, *International Journal of Epidemiology*, **26**(3), 469–475 (1997).
22. Hyndman, R. J. and Ullah, S., Robust forecasting of mortality and fertility rates: a functional data approach. *Department of Econometrics and Business Statistics, Working Papers*. Melbourne, Monash University, 24pp. (2005).
23. Kupper, L.L., Janis, J.M., Karmons, A. and Greenberg, B.G., Statistical age-period-cohort analysis: A review and critique, *Journal of Chronic Diseases*, **38**(10), 811–830 (1985).
24. Kupper, L.L., Janis, J.M., Karmons, A. and Greenberg, B.G., Authors' reply. *Journal of Chronic Diseases*, **38**(10), 837–840 (1985).
25. Landon, J. and Singpurwalla, N.D., Choosing a coverage probability for prediction intervals. *The American Statistician*, **62**(2), 120–124 (2008).
26. Magnus, K. (Editor), *Trends in Cancer Incidence. Causes and Practical Implications*, Washington, Hemisphere Publishing Corp. (1982).
27. Møller, B., Fekjær, H., Hakulinen, T., Sigvaldson, H., Storm, H., Talbäck, M. and Haldorsen, T., Prediction of cancer incidence in the Nordic countries: empirical comparison of different approaches, *Statistics in Medicine*, **22**(17), 2751–2766 (2003).
28. Møller, B., Fekjær, H., Hakulinen, T., Tryggvadóttir, L., Storm, H., Talbäck, M., and Haldorsen, T., Prediction of cancer incidence in the Nordic countries up to the year 2020, *European Journal of Cancer Prevention*, **11**(Supplement 1), S1–S96 (2002).
29. New Zealand Ministry of Health., *Cancer in New Zealand: Trends and projections*, <http://www.moh.govt.nz/moh.nsf/pagesmh/1780> (2002).
30. Osmond, C. and Gardner, M.J., Age, period and cohort models applied to cancer mortality rates, *Statistics in Medicine*, **1**(3), 245–259 (1982).

31. Pickle, L.W., Hao, Y., Jemal, A., Zou, Z., Tiwari, R.C., Ward, E., Hachey, M., Howe, H.L. and Feuer, E.J., A new method for estimating United States and state-level cancer incidence counts for the current calendar year, *CA: A Cancer Journal for Clinicians*, **57**(1), 30–42 (2007).
32. Pisani, P., Bray, F., and Parkin, D.M., Estimates of world-wide prevalence of cancer for 25 sites in the adult population. *Int. J. Cancer*. 97, 72–81 (2002).
33. R Development Core Team, R: A language and environment for statistical computing. R Foundation for Statistical Computing. Vienna, Austria, <http://www.R-project.org> (2008).
34. Ramsay, J.O. and Silverman, B.W., *Applied Functional Data Analysis*. New York, Springer-Verlag (2002).
35. Ramsay, J.O. and Silverman, B.W., *Functional Data Analysis*. Second ed., New York, Springer-Verlag (2005).
36. Ramsay, J.O., Hooker, G., and Graves, S., *Functional Data Analysis with R and MATLAB*, Dordrecht, Springer (2009).
37. Scottish Executive Health Department, *Cancer in Scotland: Sustaining change. Cancer incidence projections for Scotland (2001-2020). An aid to planning cancer services*. Edinburgh, Scottish Executive, <http://www.scotland.gov.uk/Publications/2004/12/20257/46696> (2004).
38. Teppo, L., Hakulinen, T., and Saxén, E., The prediction of cancer incidence in Finland for the year 1980 by means of cancer registry material, *Annals of Clinical Research*, **6**(2), 122–125 (1974).
39. Tiwari, R.C., Ghosh, K., Jemal, A., Hachey, M., Ward, E., Thun, M.J., and Feuer, E.J., A new method for predicting US and state-level cancer mortality counts for the current calendar year, *CA: A Cancer Journal for Clinicians*, **54**(1), 30–40 (2004).
40. White, C., Wade, R., Howe, J., and Steward, J., Projection of incidence and mortality for cancer of the large bowel to 2015. *WCISU Occasional Report*, Welsh Cancer Intelligence & Surveillance Unit. 11pp. http://www.wales.nhs.uk/sites3/Documents/242/OR_S0601_050106b.pdf (2006).
41. Yang, L., Parkin, D., Ferlay, J. Li, L. and Chen, Y., Estimates of cancer incidence in China for 2000 and projections for 2005, *Cancer Epidemiology, Biomarkers & Prevention*, **14**(1), 243–250 (2005).

New Approach to Dynamic XL Reinsurance

Ekaterina V. Bulinskaya and Alexander N. Gromov

¹ Department of Mechanics and Mathematics
Lomonosov Moscow State University
Moscow, Russia
(e-mail: ebulinsk@mech.math.msu.su)

² Department of Mechanics and Mathematics
Lomonosov Moscow State University
Moscow, Russia
(e-mail: gromovaleksandr@gmail.com)

Abstract. Dynamic programming technique is applied to find optimal strategy for dynamical XL reinsurance. More precisely, we consider a risk process modelled by compound Poisson process and excess of loss reinsurance, defined by retention level and limit. We find optimal survival probability as a solution of corresponding Hamilton-Jacobi-Bellman (HJB) equation and show the existence of optimal reinsurance strategy. Numerical examples in case of exponentially, log-normally and Pareto distributed claims are provided.

Keywords: Survival probability, Excess of loss reinsurance, Hamilton-Jacobi-Bellman equation, Dynamic programming.

1 Introduction

We consider an insurance company that has a possibility to choose and buy dynamically an excess of loss reinsurance. In this situation our goal is to derive the optimal reinsurance strategy that maximizes the survival probability of the cedent. The corresponding problem for XL contract without limiting level has been solved by Hipp and Vogt, 2003 [3].

We model risk process R_t of the cedent by a Lundberg process with claim arrival intensity λ and absolutely continuous claim size distribution F . Let T_i be the occurrence time of the i -th claim, N_t the number of claims in time interval $(0, t]$ and W_i the amount of the i -th claim. Assume that c is the premium intensity of the insurer which contains positive safety loading, i.e. $c > \lambda E[W_i]$. The reinsurer uses the expected value principle with safety loading $\theta > 0$ for premium calculation. We also assume that $(1 + \theta)\lambda E[W_i] > c$, because otherwise the cedent could reinsure his total portfolio and at the same time collect positive premium.

According to XL contract claim W is divided into the cedent's payment $\min\{b, W\} + \max\{0, W - M - b\}$ and the reinsurer's payment $\min\{M, \max\{0, W - b\}\}$. In this paper parameters of excess of loss reinsurance contract, i.e. the retention level b and the limiting level $b + M$ are supposed to be chosen dynamically. Thus we consider predictable strategies $Z_t = (b_t, M_t)$

and the insurer adjusts retention b_t and limit $b_t + M_t$ at any time $t \geq 0$ using claim history available before t . We will show that optimal strategy exists and its components are given as $b_t = b(R_{t-}^Z)$, $M_t = M(R_{t-}^Z)$, where $b(s)$ and $M(s)$ are measurable functions and R_t^Z is the risk process under strategy Z_t . Let $\rho = \lambda(1 + \theta)$, then

$$R_t^Z = s + ct - \rho \int_0^t E \min\{M_x, \max(0, W - b_x)\} dx - \sum_{i=1}^{N_t} (\min\{W_i, b_{T_i}\} + \max\{0, W_i - b_{T_i} - M_{T_i}\}), \quad (1)$$

where s is the initial surplus.

Our goal is to maximize survival probability. Assume that τ_Z is the ruin time of the cedent using strategy Z_t , it is given by

$$\tau_Z := \inf\{t \geq 0 : R_t^Z < 0\}.$$

Then the survival probability of the insurer using strategy Z_t with initial surplus s is

$$\delta_Z(s) = P\{\tau_Z = \infty | R_0 = s\} \quad (2)$$

and we will calculate the function $\delta(s) = \sup_Z \{\delta_Z(s)\}$ to find an optimal strategy Z^* where supremum is attained.

2 Hamilton-Jacobi-Bellman equation

From the definition of $\delta(s)$ we conclude that for arbitrary $\varepsilon > 0$ there exists a strategy \tilde{Z}_t with $\delta_{\tilde{Z}}(s) > \delta(s) - \varepsilon$. Next, for some small $h > 0$, we consider a strategy

$$Z_t^h = (b_t^h, M_t^h) = \begin{cases} (b, M), & t \in [0, h \wedge T_1], \\ \tilde{Z}_{t-h \wedge T_1}(R_{h \wedge T_1}), & t > h \wedge T_1. \end{cases}$$

Then using the formula of total probability and given above inequality for $\delta_{\tilde{Z}}(s)$ we obtain that

$$\delta(s) \geq \delta_{\tilde{Z}}(s) = P\{\tau_{\tilde{Z}} = \infty | T_1 > h\} P\{T_1 > h\} + P\{\tau_{\tilde{Z}} = \infty | T_1 \leq h\} P\{T_1 \leq h\}$$

which is bounded from below by

$$\delta(s + K_Z h) e^{-\lambda h} + \int_0^h E[\delta(s + K_Z t - \min\{W, M\} - \max\{0, W - b - M\})] \lambda e^{-\lambda t} dt - \varepsilon,$$

where $K_Z = c - \rho E \min\{M, \max\{0, W - b\}\}$. Then, assuming that $\delta(s)$ is differentiable, as in [3] or [6] we obtain HJB equation for optimal survival probability $\delta(s)$:

$$\sup_{b, M} \{K_Z \delta'(s) - \lambda \delta(s) + \lambda E[\delta(s - \min\{W, b\} - \max\{0, W - b - M\})]\} = 0,$$

where supremum is taken over all $b > 0$ and $M \geq 0$ for which the following inequality holds

$$c > \rho E \min\{M, \max(0, W - b)\}, \quad (3)$$

because otherwise the insurer has a negative net premium income. Moreover, since we are looking for a nondecreasing solution $\delta(s)$ we can rewrite the above equation as

$$\delta'(s) = \inf_{b, M} \lambda \frac{\delta(s) - E[\delta(s - \min\{W, b\} - \max\{0, W - b - M\})]}{c - \rho E \min\{M, \max\{0, W - b\}\}}. \quad (4)$$

3 Existence of the solution

In this section we prove the existence of the solution of (4). Moreover, we obtain equations for optimal (b, M) , i.e. points at which infimum in (4) is attained.

Theorem 1. *There exists an increasing solution $V(s)$ of equation (4), which is continuous on $[0, +\infty)$ and continuously differentiable on $(0, +\infty)$; moreover, $V(s) = 0$ for $s < 0$ and $V(s) \rightarrow 1$ as $s \rightarrow \infty$.*

Proof. We obtain the solution $V(s)$ using successive approximations. We define a sequence of functions $V_n(s)$ as $V_0(s) = \delta_0(s)$ (i.e. the survival probability without reinsurance) and

$$V'_{n+1}(s) = \inf_{(b, M)} \left\{ \lambda \frac{V_n(s) - E[V_n(s - \min\{W, b\} - \max\{0, W - b - M\})]}{c - \rho E \min\{M, \max(0, W - b)\}} \right\} \quad (5)$$

for $n = 0, 1, 2, \dots$.

Using induction, we show that $V'_{n+1}(s) \leq V'_n(s)$. (The similar approach is utilized in [3]). Then applying induction it is also easy to prove that $V_n(s) = 0$ for $s < 0$.

We demonstrate now that for $s > 0$ infimum in (5) is positive. Firstly, assume that function $U(s)$ is continuous for $s \geq 0$, continuously differentiable for $s > 0$ and $U(s) = 0$ for $s < 0$. Next define function $H(b, M)$ via

$$H(b, M) = \lambda \frac{U(s) - E[U(s - \min\{W, b\} - \max\{0, W - b - M\})]}{c - \rho E \min\{M, \max(0, W - b)\}}$$

Using Lagrange approach we prove the following

Lemma 1. *Infimum of the function $H(b, M)$ over all $b > 0, M \geq 0$, that satisfy (3), is attained at one of the following points (b, M)*

(i) *at point $b = \infty, M = 0$, and equals*

$$\frac{\lambda}{c}(U(s) - E[U(s - W)]);$$

(ii) *at $b = 0, M = M^*$, where M^* is solution of the following equation:*

$$H(0, M) = \lambda \frac{E[U'(s + M - W)] - \int_0^M U'(s + M - x)dF(x)}{\rho(1 - F(M))}$$

and equals $H(0, M^)$;*

(iii) *at $b = b^* \leq s, M = M^*$, where (b^*, M^*) satisfies the following system*

$$\begin{cases} H(b, M) = \lambda \rho^{-1} U'(s - b) \\ H(b, M) = \lambda \rho^{-1} \frac{E[U'(s + M - W)] - \int_0^{b+M} U'(s + M - x)dF(x)}{(1 - F(b + M))} \end{cases}$$

and equals $H(b^, M^*) = \lambda \rho^{-1} U'(s - b^*)$.*

Now, applying Lemma 1 to function $U(s) = V_n(s)$ one could obtain by induction that $V'_n(s) > 0$ for $s > 0$. So, $V'_n(s)$ is a decreasing sequence of continuous functions, and since $V'_n(s) > 0$ the sequence $V'_n(s)$ converges to a function $v(s)$. Using approach similar to that in [3] or [6] we prove the continuity of $v(s)$. Finally, defining $V(s) = 1 - \int_s^\infty v(u)du$, we have $V(s)$ satisfying the following equation

$$V'(s) = \inf_{b, M} \lambda \frac{V(s) - E[V(s - \min\{W, b\} - \max\{0, W - b - M\})]}{c - \rho E \min\{M, \max\{0, W - b\}\}}$$

4 Existence of the optimal strategy

In previous section we have proved existence of the solution of (4). In this section we show that the strategy $Z_t^* = (b_t^*, M_t^*)$ derived from the minimizer $(b^*(s), M^*(s))$ in (4) maximizes the survival probability. More precisely, we prove the following result

Theorem 2. *There exists a measurable function $Z^*(s) = (b^*(s), M^*(s))$ such that the infimum in the Hamilton-Jacobi-Bellman equation (4) is attained at $(b, M) = Z^*(s)$ for $s \geq 0$. This function defines an optimal reinsurance strategy Z_t^* , i.e. $\delta_{Z^*}(s) \geq \delta_Z(s)$ for any other predictable strategy Z_t .*

Proof. The existence of the function $Z^*(s)$ is implied by general results for Bellman's equations (see, e.g., [7]).

Let $V^*(s)$ be the increasing solution of (4) constructed in the previous section; then from Theorem 1 we have $0 \leq V^*(s) \leq 1$, $V^*(s) = 0$ for $s < 0$ and $\lim_{s \rightarrow \infty} V^*(s) = 1$. Put by definition $\delta^*(s) = V^*(s)$.

We have to establish that the strategy $Z_t^* = (b_t^*, M_t^*) = Z^*(R_{t-}) = (b^*(R_{t-}), M^*(R_{t-}))$ defined by measurable function $Z^*(s) = (b^*(s), M^*(s))$ is such that $\delta^*(s) = \delta_{Z^*}(s)$ and for any predictable strategy Z_t we have $\delta_{Z^*}(s) \geq \delta_Z(s)$. We define $R^*(t)$ and $R(t)$ as the risk processes of the insurance company with reinsurance strategies Z_t^* and Z_t respectively. Let τ^* and τ be the corresponding ruin times. Let $X^*(t)$ and $X(t)$ be the corresponding stopped processes. Define $W^*(t)$ and $W(t)$ via

$$W^*(t) = \delta^*(X^*(t)) = \delta^*(R_{t \wedge \tau^*}), \quad W(t) = \delta^*(X(t)) = \delta^*(R_{t \wedge \tau}).$$

Then, as in [5], we obtain the following formula for $E[W_t]$ (and the similar formula for $E[W^*(t)]$)

$$\begin{aligned} E[W_t] &= V(s) + E \left[\int_0^t V'(X_y) (c - \rho E \min\{M, \max(0, W - b_y)\}) dy \right] \\ &+ \lambda E \int_0^t [V(X_y - \min\{W, b_y\}) - \max\{0, W - b_y - M_y\}) - V(X_y)] dy \quad (6) \end{aligned}$$

From the HJB equation (4) we conclude that under any strategy $Z_t = (b_t, M_t)$

$$\begin{aligned} &\delta^{*'}(X_Z(s))(c - \rho E \min\{M_s, \max\{0, W - b_s\}\}) - \lambda \delta^*(X_Z(s)) \\ &+ \lambda E[\delta^*(X_Z(s) - \min\{W, b_s\}) - \max\{0, W - b_s - M_s\}] \leq 0 \end{aligned}$$

with equality under the strategy Z_t^* . Using this inequality we obtain from (6) that $E[\delta_Z(X_Z(t))] \leq \delta^*(s)$ with equality for Z_t^* . Finally, letting $t \rightarrow 0$ we have $\delta^*(s) = \delta_{Z^*}(s)$ and $\delta_{Z^*}(s) \geq \delta_Z(s)$ for any strategy Z_t .

5 Numerical examples

5.1 Exponentially distributed claims

At first, we assume that claims have exponential distribution with mean m . Even in this simple case one has to compute solution of the HJB equation (4) using approximation method and calculate functions $V_n(s)$, as defined in Theorem 1. For the first step (i.e. for $V_0(s) = \delta_0(s)$ the survival probability without reinsurance) we have the following formula (see [4]):

$$\delta_0(s) = 1 - \frac{\lambda m}{c} \exp \left\{ - \left(m - \frac{\lambda}{c} \right) s \right\}.$$

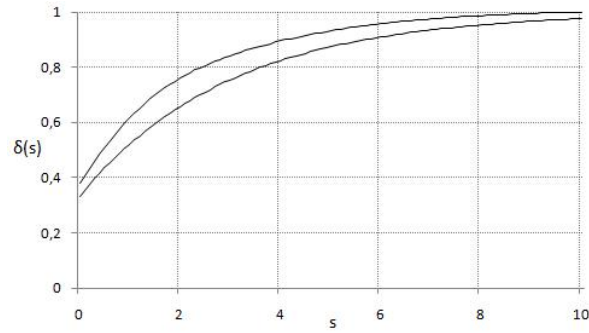


Fig. 1. The survival probabilities

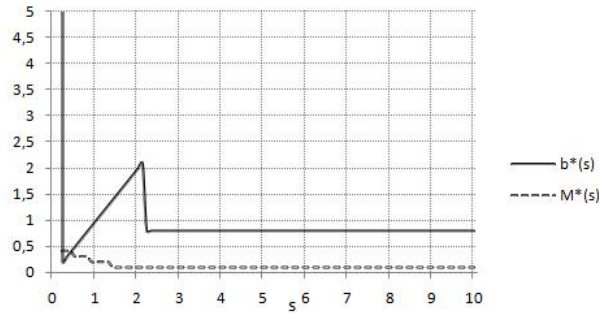


Fig. 2. Optimal strategy for exponential distribution

We use the following values of parameters: $c = 1.5$, $\rho = 1.6$, $\lambda = 1$ and $m = 1$. We start with $V(0) = \delta_0(0)$ and then norm $V(s)$ dividing it by $V(s_0)$, where s_0 is considerably high. Figure 1 shows that survival probability of a company using optimal XL strategy (i.e. the solution $V(s)$ of equation (4)) is considerably larger than survival probability without reinsurance (lower graph). Figure 2 provides the optimal strategy $Z^*(s) = (b^*(s), M^*(s))$ for values $s \in [0, 10]$. For small s the optimal strategy is $(\infty, 0)$, i.e. the insurer keeps the whole risk. From $s \approx 0.3$ to $s \approx 2.2$ we have $b^*(s) \approx s$ and at the same time the width of reinsured layer decreases. Then for $s > 2.2$ the optimal reinsurance parameters are nearly constant $b \approx 0.9$ and $M \approx 0.1$.

5.2 Log-Normally distributed claims

Now consider claims having log-normal distribution with density

$$f(x) = \frac{1}{\sqrt{2\pi\sigma^2x}} \exp\left(-\frac{(\ln x - \mu)^2}{2\sigma^2}\right).$$

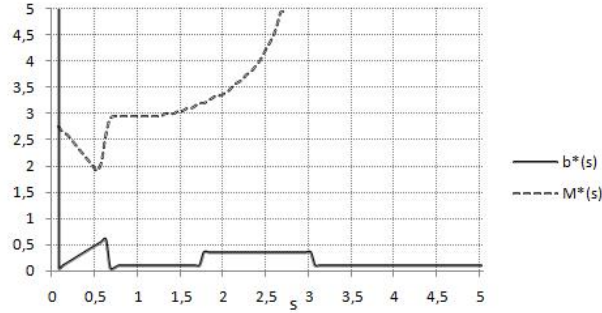


Fig. 3. Optimal strategy for log-normal distribution

To compute optimal strategy in this case we choose $\lambda = 1$, $c = 4$, $\rho = 4.5$ and distribution parameters $\mu = 1$, $\sigma = 0.5$. In case of log-normally distributed claim severities we have $\delta_0(0) = 1 - c^{-1} \exp(\mu + \sigma^2/2)$. Figure 3 depicts the optimal retention level $b^*(s)$ and layer width $M^*(s)$ for $s \in [0, 5]$. One could see that in this case $M^*(s)$ is not constant and grows from $s \approx 0.51$. Also, minimal value of M , i.e. minimal reinsured layer, is attained at $s \approx 0.6$.

5.3 Pareto distributed claims

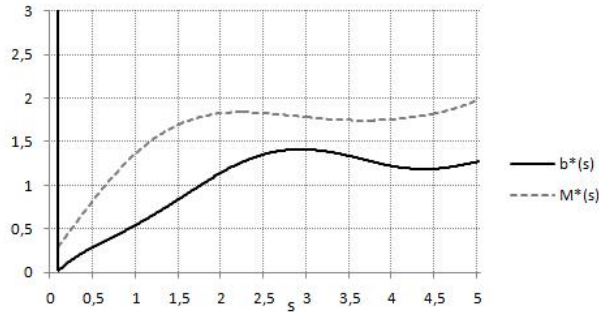


Fig. 4. Optimal strategy for Pareto distribution

Finally, we consider Pareto distributed claims, i.e. claims with probability density function

$$f(x) = \frac{\alpha\theta^\alpha}{(x + \theta)^{\alpha+1}}, \quad x > 0.$$

In this example we use distribution parameters $\theta = 1$ and $\alpha = 2$. As in case of exponentially distributed claims we choose $\lambda = 1$, $c = 1.5$ and $\rho = 1.7$. For Pareto distributed claims we have $\delta_0(0) = 1 - c^{-1}(\alpha - 1)^{-1}$. Figure 4 shows the optimal strategy $(b^*(s), M^*(s))$ in the described case. Contrary to the first example, in this case there is no s for which $b^*(s) = s$, i.e. we always have to choose $b^*(s) < s$. Also, the optimal retention $b^*(s)$ and layer width $M^*(s)$ do not tend to be constants, but increase and decrease approximately in the same intervals.

6 Conclusion

In this paper we discussed the problem of optimal XL reinsurance in a dynamic setting. We not only proved the existence of the optimal strategy, maximizing the survival probability, but we provided equations for optimal parameters b and M (see Lemma 1). Also we computed optimal strategy for different claim types.

Acknowledgement. The research is partially supported by RFBR grant 10-01-00266a.

References

1. Bremaud, P. *Point Processes and Queues: Martingale Dynamics*, Springer-Verlag, Berlin (1981).
2. Grandell, J. *Aspects of Risk Theory*, Springer (1991).
3. Hipp C., and Vogt M. "Optimal dynamic XL reinsurance", *ASTIN Bulletin* 33, 193–207 (2003).
4. Rolski, T., Schmidli, H., Schmidt, V., and Teugels, J. *Stochastic Processes for Insurance and Finance*, Wiley Series in Probability and Statistics (1998).
5. Schäl M. "On piecewise deterministic Markov control processes: Control of jumps and of risk processes in insurance", *Insurance: Mathematics and Economics* 22, 75–91 (1998).
6. Schmidli, H. "Optimal Proportional Reinsurance Policies in a Dynamic Setting", *Research Report* 403, Dept. Theor. Statis, Aarhus University (2000).
7. Yushkevich, A.A. "Bellman inequalities in Markov decision deterministic drift processes", *Stochastics* 23, 25–77(1987).

Discrete Time Models with Dividends and Reinsurance

Ekaterina V. Bulinskaya¹ and Daria A. Yartseva²

¹ Department of Mathematics and Mechanics
Moscow State University, Russia
(e-mail: ebulinsk@mech.math.msu.su)

² Department of Mathematics and Mechanics
Moscow State University, Russia
(e-mail: yartseva@gmail.com)

Abstract. We consider two discrete time models of insurance company capital. In the first one it is supposed that the company uses the barrier strategy of dividend payment and quota share reinsurance. Equations describing average costs and average time until ruin are established. The properties of these equations solutions are studied. The method of finding upper and lower bounds is proposed. The second model deals with non-proportional reinsurance. We find the strategy minimizing average payment for bank loan taken if the company cannot pay indemnity.

Keywords: Upper and lower bounds, Continuous claims distribution, Optimal reinsurance.

1 Introduction

The optimal reinsurance and optimal dividends problems were considered by many authors. The study of optimal dividends problem goes back to de Finetti [1]. The case of compound Poisson claims process was investigated by Dickson and Waters [2], Gerber *et al.* [3]. Beveridge *et al.* [4] suggested that reinsurance may increase net income of shareholders and studied this problem numerically. For classical risk model with possibility of reinsurance Schmidli [5] proved that there exists an optimal reinsurance strategy minimizing the ruin probability. Pechlivanides [6] considered a discrete-time model and found optimal reinsurance and dividend strategies in some special cases. Below we tackle two discrete-time models incorporating reinsurance with or without dividend payment.

2 The first model

Consider the following model. Let p be premiums collected during one year and x the initial capital of insurance company. By ξ_i denote the claims amount paid to policy holders during the i th year, $i \geq 1$. Assume ξ_i to be i.i.d. positive random variables with probability density function p_ξ . Let d denote the dividend barrier.

The company uses the quota share reinsurance with quota equal to $t_q(x)$, $0 \leq t_q(x) \leq 1 - \varepsilon$. Reinsurance safety loading is θ ($0 \leq \theta \leq 1$), the commission rate is t_c ($0 \leq t_c \leq 1$), the discount rate is β .

Let S_i be the capital of the company at the end of the i th year, $i \geq 0$, $S_0 = x$. The following formula determines S_i for $i \geq 1$:

$$S_i = \min[S_{i-1} + p(1 - t_q(S_{i-1})) + pt_q(S_{i-1})(t_c - \theta) - \xi_i(1 - t_q(S_{i-1})), d].$$

The ruin time is $\tau_x = \min\{n : S_n < 0\}$. The discounted costs are $\beta^{\tau_x} |S_{\tau_x}|$, average discounted costs are $l(x) = E\beta^{\tau_x} |S_{\tau_x}|$, average time until ruin is $T(x) = E\tau_x$.

We assume that $p_\xi(x) \in C[0, \infty)$, $t_q(x) \in C[0, d]$.

2.1 Main equations

By using the law of total probability we get the following equations for $l(x)$.

If $d \geq x \geq d - p(1 - t_q(x)) - pt_q(x)(t_c - \theta)$, then

$$\begin{aligned} l(x) &= \beta l(d) \int_0^{f_1(x)} p_\xi(y) dy \\ &+ \beta \int_{f_1(x)}^{f_2(x)} l(x + p(1 - t_q(x)) + pt_q(x)(t_c - \theta) - y(1 - t_q(x))) p_\xi(y) dy \\ &+ \beta \int_{f_2(x)}^{+\infty} (y(1 - t_q(x)) - (x + p(1 - t_q(x)) + pt_q(x)(t_c - \theta))) p_\xi(y) dy. \end{aligned}$$

If $d - p(1 - t_q(x)) - pt_q(x)(t_c - \theta) \geq x \geq 0$, then

$$\begin{aligned} l(x) &= \beta \int_0^{f_2(x)} l(x + p(1 - t_q(x))(1 - t_c + \theta) - y(1 - t_q(x))) p_\xi(y) dy \\ &+ \beta \int_{f_2(x)}^{+\infty} (y(1 - t_q(x)) - (x + p(1 - t_q(x)) + pt_q(x)(t_c - \theta))) p_\xi(y) dy, \end{aligned}$$

where

$$f_1(x) = \frac{x + p(1 - t_q(x)) + pt_q(x)(t_c - \theta) - d}{1 - t_q(x)}, \quad (1)$$

$$f_2(x) = \frac{x + p(1 - t_q(x)) + pt_q(x)(t_c - \theta)}{1 - t_q(x)}. \quad (2)$$

2.2 Existence of solution

Average costs satisfy the equation $l(x) = Al(x)$ with the mapping $A : C[0, d] \rightarrow C[0, d]$ given by

$$Ag(x) = \beta g(d) \int_0^{f_1(x)} p_\xi(y) dy + \beta \int_{f_1(x)}^{f_2(x)} g(h(x, y)) p_\xi(y) dy + f_3(x),$$

here $f_1(x), f_2(x), f_3(x)$ are continuous functions, and $h(x, y)$ decreases from d to 0 while y increases from $f_1(x)$ to $f_2(x)$.

Consider the space $C[0, d]$ with metrics

$$\rho(g_1(x), g_2(x)) = \max_{0 \leq y \leq d} |g_1(y) - g_2(y)|.$$

Theorem 1. *A is a contracting mapping.*

Proof. We prove that $\rho(Ag_1(x), Ag_2(x)) \leq \beta \rho(g_1(x), g_2(x))$ for any functions $g_1(x), g_2(x) \in C[0, d]$ using the following relations

$$\begin{aligned} \rho(Ag_1(x), Ag_2(x)) &= \max_{0 \leq z \leq d} |(g_1(d) - g_2(d))\beta \int_0^{f_1(z)} p_\xi(y) dy \\ &\quad + \beta \int_{f_1(z)}^{f_2(z)} (g_1(h(z, y)) - g_2(h(z, y))) p_\xi(y) dy| \\ &\leq \max_{0 \leq z \leq d} |g_1(z) - g_2(z)| |\beta \int_0^{f_1(z)} p_\xi(y) dy + \beta \int_{f_1(z)}^{f_2(z)} p_\xi(y) dy| \\ &\leq \beta \max_{0 \leq z \leq d} |g_1(z) - g_2(z)| = \beta \rho(g_1(x), g_2(x)). \end{aligned}$$

Thus we get that the equation for $l(x)$ has a unique solution.

Theorem 2. *Let A be a contracting mapping $C[0, d] \rightarrow C[0, d]$ and $\rho(Ag_1(x), Ag_2(x)) \leq \beta \rho(g_1(x), g_2(x))$, where $0 < \beta < 1$. A has the form $Ag(x) = \int_0^d K(x, y)g(y)dy$, where $K(x, y) \geq 0$ for any x and y .*

If a function $\phi(x) \in C[0, d]$ satisfies inequality $\phi(x) \geq A\phi(x)$, $x \in [0, d]$, then $\phi(x) \geq 0$, $x \in [0, d]$.

Proof. Suppose the statement: $\phi(x) \geq 0$ for any $x \in [0, d]$, is false. Let I be a set such that $\phi(x) < 0, x \in I$, and $\phi(c) = \min_{0 \leq x \leq d} \phi(x), \phi(c) < 0$.

According to our assumptions $\phi(c) \geq A\phi(c) = \int_0^d K(c, y)\phi(y)dy$. Thus,

- 1) $\int_0^d K(c, y)\phi(y)dy = \int_{[0, d] \setminus I} K(c, y)\phi(y)dy + \int_I K(c, y)\phi(y)dy \geq \int_I K(c, y)\phi(y)dy$, since $\int_{[0, d] \setminus I} K(c, y)\phi(y)dy \geq 0$.
- 2) $\int_I K(c, y)\phi(y)dy = -\int_I K(c, y)|\phi(y)|dy$, since $\phi(y) < 0$ for $y \in I$.
- 3) $\int_I K(c, y)|\phi(y)|dy \leq |\phi(c)| \int_I K(c, y)dy$ we get from definition of $\phi(c)$.

4) Put $g_i(x) = i$, $i = 1, 2$, then $Ag_i(x) = i \int_0^d K(x, y)dy$. As A is a contracting mapping $\rho(Ag_1(x), Ag_2(x)) \leq \beta\rho(g_1(x), g_2(x)) = \beta$ and $\max_{0 \leq x \leq d} \int_0^d K(x, y)dy \leq \beta$. It follows immediately that $\int_I K(c, y)dy \leq \int_0^d K(c, y)dy \leq \beta$.

Combining 1), 2), 3) and 4) we obtain $\phi(c) \geq \beta\phi(c)$, hence $\phi(c) \geq 0$. This contradiction ends the proof.

Theorem 3. *Let assumptions of Theorem 2 be fulfilled. If $l(x)$ is a solution of equation $l(x) = Al(x) + h(x)$ and $\psi(x)$ satisfies inequality $\psi(x) \geq A\psi(x) + h(x)$, then $\psi(x) \geq l(x)$.*

Proof. It is obvious that $\psi(x) - l(x) \geq A(\psi(x) - l(x))$. Using Theorem 2 we get that $\psi(x) - l(x) \geq 0$.

2.3 Lower bounds for solution

Suppose that $g(x)$ satisfies the equation $g(x) = Bg(x) + f_3(x)$, where

$$Bg(x) = \beta g(d) \int_0^{f_1(x)} p_\xi(y)dy + \beta \int_{f_1(x)}^{f_2(x)} g(h(x, y))p_\xi(y)dy, \quad 0 \leq x \leq d,$$

with $f_3(x)$ not identically zero, $f_1(x)$ and $f_2(x)$ having the form (1) and (2) respectively.

Then there exists a non-negative $\phi(x) \not\equiv 0$ such that $\phi(x) \leq B\phi(x) + f_3(x)$.

In fact, put

$$\phi(d) = c_1 = \frac{f_3(d)}{1 - \beta \int_0^{f_1(d)} p_\xi(y)dy} \quad (3)$$

and

$$\phi(x) = \beta c_1 \int_0^{f_1(x)} p_\xi(y)dy + f_3(x), \quad 0 \leq x < d. \quad (4)$$

It can be easily shown that $\phi(x) \leq B\phi(x) + f_3(x)$ for $x \in [0, d]$, $\phi(x) \in C[0, d]$ and $\phi(x) \not\equiv 0$. It follows from Theorem 3 that $\phi(x) \leq g(x)$. Thus we get a lower bound for $l(x)$.

$$l(x) \geq \beta \frac{f_3(d)}{1 - \beta \int_0^{f_1(d)} p_\xi(y)dy} \int_0^{f_1(x)} p_\xi(y)dy + f_3(x),$$

where

$$f_3(x) = \int_{f_2(x)}^\infty (y(1 - t_q(x)) - (x + p(1 - t_q(x) + pt_q(x)(t_c - \theta)))p_\xi(y)dy.$$

2.4 Average time until ruin

Average time until ruin $T(x)$ satisfies the following equations.

If $d \geq x \geq d - p(1 - t_q(x)) - pt_q(x)(t_c - \theta)$, then

$$T(x) = 1 + T(d) \int_0^{f_1(x)} p_\xi(y) dy + \int_{f_1(x)}^{f_2(x)} T(x + p(1 - t_q(x)) + pt_q(x)(t_c - \theta) - y(1 - t_q(x))) p_\xi(y) dy.$$

If $d - p(1 - t_q(x)) - pt_q(x)(t_c - \theta) \geq x \geq 0$, then

$$T(x) = 1 + \int_0^{f_2(x)} T(x + p(1 - t_q(x)(1 - t_c + \theta)) - y(1 - t_q(x))) p_\xi(y) dy.$$

Similar to Theorem 1, it can be proved that these equations have a unique solution if $\int_0^{d + p + p(t_c - \theta)\frac{1 - \varepsilon}{\varepsilon}} p_\xi(y) dy < 1$.

We obtain lower bounds of $T(x)$ by substituting $\beta = 1$ and $f_3(x) \equiv 1$ into (3) and (4). The result is the inequality

$$T(x) \geq \frac{1}{1 - \int_0^{f_1(d)} p_\xi(y) dy},$$

where $f_1(x)$ has the form (1).

Using the results of Theorem 2 we get upper and lower bounds for $T(x)$.

Theorem 4. *Suppose $t_q(x) \equiv t_q$. Average time until ruin satisfies the following inequalities*

$$T(x) \geq \left(1 - F_\xi \left(\frac{p(1 - t_q) + pt_q(t_c - \theta)}{1 - t_q} \right) \right)^{-1}$$

and

$$T(x) \leq \left(1 - F_\xi \left(\frac{d + p(1 - t_q) + pt_q(t_c - \theta)}{1 - t_q} \right) \right)^{-1}.$$

In some cases it is possible to find the explicit form of $T(x)$ and establish the optimal reinsurance strategy maximizing the average time until ruin.

Theorem 5. *Let ξ_i be uniformly distributed on $[0, c]$ and parameters satisfy $d - p(t_c - \theta) \leq 0$ and $c > d\varepsilon^{-1} + p + p(t_c - \theta)(1 - \varepsilon)\varepsilon^{-1}$. If $t_q(x) \equiv t_q$ then*

$$T(d) = \left(1 - \frac{1}{c(1 - t_q)} (p(1 - t_q) + pt_q(t_c - \theta) + \frac{d^2}{2} + d - \frac{d^2}{c(1 - t_q)^2}) \right)^{-1}$$

and

$$T(x) = T(d) \left(1 - \frac{d-x}{c(1-t_q)} \right).$$

Optimal reinsurance strategy $t_q^* = 1 - \varepsilon$.

3 The second model

Suppose the insurance company uses non-proportional reinsurance. Let x be the initial capital of the insurance company and p premiums collected during one year. Assume b to be the retention level and ρ the load factor of the reinsurance company. Let ξ_i be the claims paid to policy holders during the i th year, $i \geq 1$. Assume ξ_i to have probability density function $p_\xi(x)$ and $\bar{F}_\xi(x) = \int_x^\infty p_\xi(y)dy$.

By $a(x, b)$ denote the capital of the company before the claims arrival, then

$$a(x, b) = x + p - \rho E(\xi - b)^+,$$

where $f(x)^+ = \max(0, f(x))$.

The company pays $\eta = \min(\xi, b)$ to policy holders. If the capital is not enough to satisfy the claims, a bank loan is taken with interest rate r . Let $g_n(x, b)$ be the average total payment for the bank loan during n years. We want to minimize $g_n(x, b)$ thus finding the optimal b . By definition put

$$u_n(x) = \min_{b>0} g_n(x, b),$$

$$g_1(x, b) = rE(\eta - a(x, b))^+,$$

and

$$\begin{aligned} g_n(x, b) &= g_1(x, b) + h_{n-1}(x, b) \\ &= g_1(x, b) + \int_0^b u_{n-1}(a(x, b) - y)p_\xi(y)dy + u_{n-1}(a(x, b) - b)\bar{F}_\xi(b). \end{aligned}$$

3.1 One step

We start with finding $u_1(x)$.

Firstly, if $a(x, b) \geq b$, then $g_1(x, b) = 0$. Put $m(b) = b + \rho \int_b^\infty \bar{F}_\xi(y)dy$, then $a(x, b) - b = x + p - m(b)$. The derivative of $m(b)$ is $m'(b) = 1 - \rho \bar{F}_\xi(b)$, and the plot of $m(b)$ is depicted in Figure 1, where $\bar{F}_\xi(b^*) = \rho^{-1}$.

It can be seen that if $x \geq x^* = m(b^*) - p$, then $g_1(x, b) = 0$, for $b \in [b_1(x), b_2(x)]$, $m(b_i(x)) = x + p$, $i = 1, 2$. Hence $u_1(x) = 0$, if $x \geq x^*$.

Secondly, if $x < x^*$, then the partial derivative of $g_1(x, b)$ with respect to b has the form

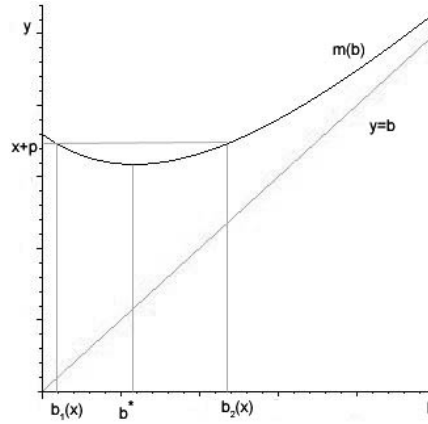


Fig. 1. Plot of $m(b)$

$$\frac{\partial g_1}{\partial b} = r\bar{F}_\xi(b) - r\bar{F}_\xi(a(x, b)) \frac{\partial a}{\partial b} = r\bar{F}_\xi(b)(1 - \rho\bar{F}_\xi(a(x, b))) = r\bar{F}_\xi(b)G_1(x, b).$$

The function $G_1(x, b)$ is less than zero, if $a(x, b) < b^*$, and greater than zero if $a(x, b) > b^*$. So, if $x \geq \hat{x} = b^* - p$, then $b^1(x)$ given by $a(x, b^1(x)) = b^*$ provides the minimum of $g_1(x, b)$. If $x < \hat{x}$, then $b = \infty$ is optimal.

Combining all the results, we get the following

Theorem 6. *Optimal reinsurance strategy $\hat{b}(x)$ and minimum average payment to the bank are*

If $x \geq x^$, then $\hat{b}(x) = b^*$ and $u_1(x) = 0$.*

If $x^ > x \geq \hat{x}$, then $\hat{b}(x) = b^1(x)$ and $u_1(x) = r \int_{b^*}^{b^1(x)} \bar{F}_\xi(y) dy$.*

If $\hat{x} \geq x \geq -p$, then $\hat{b}(x) = \infty$ and $u_1(x) = r \int_{x+p}^{\infty} \bar{F}_\xi(y) dy$.

If $-p > x$, then $\hat{b}(x) = \infty$ and $u_1(x) = r(E\xi - x - p)$.

The plot of $\hat{b}(x)$ is depicted in Figure 2.

3.2 Some comments on the case $n \geq 2$

It can be shown that optimal reinsurance strategy satisfies equation

$$rG_1(x, b) + H_{n-1}(x, b) = 0, \tag{5}$$

where

$$H_{n-1}(x, b) = \rho \int_0^b u'_{n-1}(a(x, b) - y) p_\xi(y) dy + (\rho\bar{F}_\xi(b) - 1)u'_{n-1}(a(x, b) - b).$$

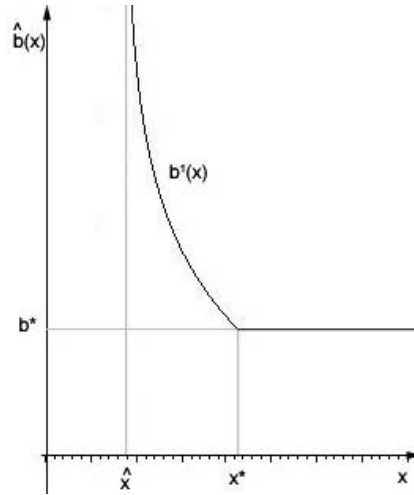


Fig. 2. Plot of $\hat{b}(x)$

For $n = 2$ it can be proved that $r \frac{\partial G_1(x,b)}{\partial b} + \frac{\partial H_1(x,b)}{\partial b} \geq 0$, hence equation (5) has a solution. Moreover, this solution is unique and greater than b^* for some x . If it is not unique, it could be chosen to be equal to b^* .

For any $n \geq 2$ it easily follows by induction that optimal b is equal to b^* for $x \geq nx^*$.

Acknowledgement. The research was partially supported by RFBR grant 10-01-00266a.

References

1. De Finetti, B., “Su un’impostazione alternativa della teoria collettiva del rischio”, *Transactions of the 15th Int. Congress of Actuaries*, 2, 433–443 (1957).
2. Dickson D.C.M., Waters H.R., “Some Optimal Dividends Problems”, *ASTIN Bulletin*, 34(1), 49–74 (2004).
3. Gerber H.U., Shiu E.S.W., Smith N., “Maximizing Dividends without Bankruptcy”, *ASTIN Bulletin* 36(1), 5–23 (2006).
4. Beveridge, C., Dickson, D., Wu, X., “Optimal dividends under reinsurance”, *Bulletin of the Swiss Association of Actuaries*, 1(1), 149–166 (2008).
5. Schmidli, H., “On Cramer-Lundberg approximations for ruin probabilities under optimal excess of loss reinsurance”, *Journal of Numerical and Applied Mathematics*, 96, 198–205 (2008).
6. Pechlivanides, P.M., “Optimal Reinsurance and Dividend Payment Strategies”, *ASTIN Bulletin*, 10(1), 34–46 (1978).

Complex modelling and hierarchical control of hydraulic systems

Enrico Canuto¹, Wilber Acuña-Bravo¹ and Manolis Christodoulou²

¹ Politecnico di Torino, Dipartimento di Automatica e Informatica, Corso Duca degli Abruzzi 24, 10129 Torino, Italy

E-mail: enrico.canuto@polito.it, wilber.acunabravo@polito.it

² Technical University of Crete, 73100 Chania, Greece, and Politecnico di Torino, Dipartimento di Automatica e Informatica, Corso Duca degli Abruzzi 24, 10129 Torino, Italy.

E-mail: manolis@polito.it

Abstract: The paper outlines the general control problem of a complex hydraulic circuit, either fixed or mobile, where a variable flow pump must meet the demand of a finite number of hydraulic variable loads. They may comprise hydraulic cylinders (motors) moving a load along a reference trajectory, primary lubricating (steady) flows, secondary flows. The pump flow is distributed to motor volumes through solenoid-driven proportional valves. Cylinder reference flow must meet motor load reference rate, whereas load resistance and inertial forces impose cylinder pressure. Proportional valves ensure flow to cylinders by regulating their apertures, thus performing a low-level (local) control task. Higher level task must ensure a sufficient pressure drop from pump output volume and supply line to cylinder volumes, in presence of variable cylinder pressure range and rate. Pressure rates may be rather high because of sudden load resistance. Moreover, cylinders and secondary flows must be ranked within the maximum available pump flow. Pressure range is limited by relief valves, not treated here. Essential dynamics of the main hydraulic elements common to cylinders and variable flow pumps are recalled, first; they are simplified through smooth singular perturbation in view of the control embedded model. Then hierarchical control problem is formulated and solved within the Embedded Model Control architecture. Simulated results refer to the higher-level task.

Keywords: Hydraulics, hierarchical control, modeling, variable-flow pumps, proportional valves

1 Introduction

The paper outlines the general control problem of hydraulic circuits, either fixed or mobile, where a variable-flow pump must meet the demand of a finite number of hydraulic variable loads (Jelali and Kroll, 2003, Manring, 2005). They may comprise hydraulic cylinders (motors) moving a load along a reference trajectory, primary lubricating (quasi-steady) flows, secondary arbitrary flows imposed by operators. The pump flow is distributed to motor volumes through solenoid-driven, proportional valves. Cylinder reference flow must meet load reference rate, whereas load resistance and inertial forces impose cylinder pressure. Proportional valves ensure flow to cylinders by regulating their apertures: the latter must be meant as a lower-level (local) control task. A similar regulation occurs in axial-piston pumps (Kugi, 2001, Manring, 2005), where an actuating cylinder regulates

the tilt of a disk and the volume of the rotating cylinders carrying fluid from tank to line. The actuating cylinder, either single or in pair, has a single volume where input and output flows are regulated by a solenoid-driven valve. Besides local flow regulation, a higher-level control must be implemented to ensure a sufficient pressure drop from the the pump output volume to cylinder volumes, in presence of a variable cylinder pressure range (typically 25 MPa) and rate. Pressure rates may be rather high, around 100 MPa/s in mobile circuits, because of sudden load resistance. Moreover, cylinders and secondary flows must be ranked within the maximum available pump flow. Pressure control becomes essential in mobile hydraulics to reduce power losses to a minimum (Kim and Cho, 1991, Erkkila, 1999), which is obtained by forcing pump output pressure to track the largest pressure as demanded by loads (load-sensing control).

This paper aims to provide a unified lumped-parameter model of the whole circuit in terms of state equations. A model of this kind, called *fine*, may be used for simulation. Then in view of the control design, a simplified model is obtained through ‘smooth singular perturbations’, which departs from the traditional method of Kokotovic, Khalil and O’Reilly (1986) by making explicit the control time unit. The simplified model according to the Embedded Model Control (EMC) architecture in Canuto (2007) is implemented as the core of the control unit, and must be written in discrete-time. Here continuous-time is adopted for simplicity’s sake. Control design starts by constructing the state and command reference (reference generator in the EMC), which enlightens the hierarchical nature of the hydraulic circuit control, where flow control is lower-level and local (each cylinder, the pump), whereas the pressure control is higher-level and global (load-sensing in the literature). Because of a single pump command, it shown that pump flow and pressure control can be designed as a single control algorithm, taking advantage of the embedded model. Control law and noise estimator (Canuto 2007, 2008 and 2010) are restricted to pump flow regulation and pressure control, assuming some cylinder flow control exists and provides the necessary measurements to higher-level control. Interesting to say, pump flow and pressure control may be designed as a single control unit because of the single pump command channel (the valve solenoid driving the actuating cylinder). The paper terminates with simulated results from a fine simulator of the load-sensing pressure control: the adopted axial-piston pump already includes a mechanical feedback ensuring flow regulation. Analytical results and design are given without proof. What is left outside the paper is the stability proof in presence of parametric uncertainty and neglected dynamics (Canuto, 2007 and 2008). Simulated results are provided in presence of uncertainty.

2 Hydraulic elements and dynamics

Hydraulic circuits are essentially made of a single hydraulic pump, a line distributing the pressurized fluid, a parallel of hydraulic loads which may be either passive (lubrication) or active, like hydraulic motors (cylinders) (see Fig. 1). Here axial-piston pumps and cylinders are considered, made of two variables volumes

(Jelali and Kroll, 2001, Manning, 2005). For the cylinders, they are here referred to as positive and negative, depending on the common sign of the piston rate and valve stroke when they receive fluid flow. In pumps, a single (negative) actuating cylinder is assumed, whereas the output volume is added to the supply line. From pump to load volumes, pressure should decrease to allow fluid flow. Flow to load volumes must be regulated to meet load requirements. Pump, line and loads are protected against overpressure by relief valves. Overpressure is caused by sudden volume restrictions to be avoided by flow and pressure regulation.

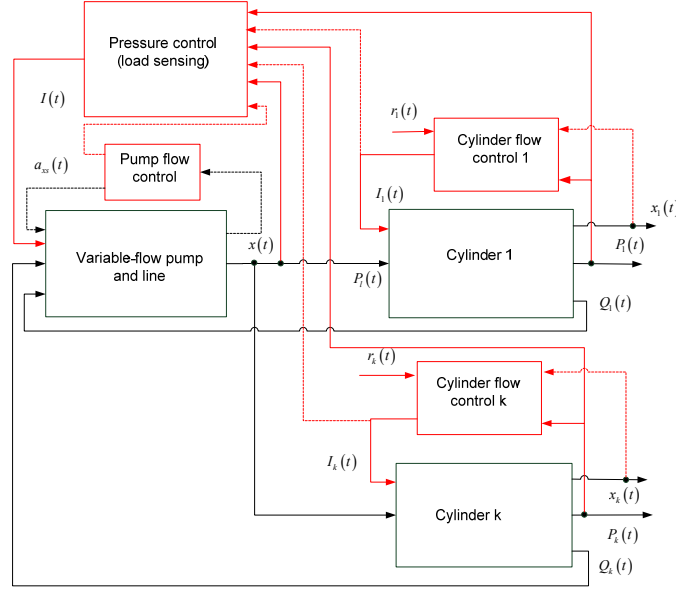


Fig. 1. Higher-level block-diagram of a hierarchical hydraulic control system.

2.1 Cylinder and pump dynamics

The essential storage element in pumps and cylinders is a fluid volume at pressure $P_p \geq 0$ [MPa] (with respect to the tank pressure set to zero) having fixed section area A_p , mean length L_0 and variable displacement x . The volume state equation, in terms of acceleration $a_p = A_p P_p(t) / m$ and neglecting temperature effects, follows from the continuity equation (Jelali and Kroll, 2001, Manning, 2005)

$$\begin{aligned} \dot{a}_p(t) &= \Omega_p^2(t, x) (Q_p(t) - \dot{x} A_p - Q_L(P_p, P_n, t)) / A_p, \quad a_p(0) = a_{p0} \\ L_p &= L_0 + x, \quad \Omega_p^2(t, x) = A_p \beta(t) / (m L_p(x)), \quad |x| \leq x_{\max} \end{aligned} \quad (1)$$

where Q_p is the commanded flow positive if entering the volume, Q_L is the leakage flow, $P_n \geq 0$ is the pressure of the negative volume, and $\Omega_p^2(x)$ is the angular acceleration defined by geometry, fluid properties and load mass m . Subscripts p and n refer to positive and negative \dot{x} . A similar equation holds for the negative volume, upon definition of the acceleration $a_n = A_n P_n(t) / m$, of the flow Q_n which is now positive when discharging, and sign changes in x and \dot{x} ,

as shown in Fig. 2, where subscript k denotes a specific cylinder. Equation (1) must be completed with the load dynamics

$$\dot{x}(t) = v(t), \quad x(0) = x_0$$

$$\dot{v}(t) = -\Omega^2(P_p, P_n)x(t) - f(t, P_p, P_n)v(t) + a_i(t) - a_d(t) + a_u(t), \quad v(0) = v_0, \quad (2)$$

where $\Omega^2 = K/m$ [rad/s²] is the angular acceleration imposed by elastic (spring, fluid) reactions, f [rad/s] accounts for (viscous) friction, a_u account for load accelerations [m/s²], and in axial-piston pumps for a bias. End-stroke dynamics is neglected. In axial-piston pumps a centrifugal acceleration $(k_\omega \omega^2/m)x$ adds (Manring, 2005, Kugi, 2001), which depends on the pump rate ω , and is such to reduce Ω^2 until sign changes at higher rates. Here $\Omega^2 - k_\omega \omega^2/m > 0$ is assumed in the range $0 \leq \omega \leq \omega_{\max}$. The commanded flows Q_p is regulated through a proportional valve, leading to

$$Q_p = \mu(s, \rho) \sqrt{\Delta P_p(s)}, \quad \Delta P_p \geq 0$$

$$\Delta P_p(s \geq 0) = P_i - P_p, \quad \Delta P_p(s < 0) = P_p, \quad (3)$$

where $\mu(s, \rho)$ is monotonic in the valve stroke s , depends on fluid density ρ , and $\mu(0, \rho) = 0$. P_i is the line pressure to be defined below. Changing the sign of s and μ in (3), and subscripts from p to n , yields Q_n . Generic intake flow $Q \geq 0$, intake pressure P and section area A are defined by

$$Q(s \geq 0) = Q_p(s \geq 0), \quad Q(s < 0) = -Q_n(s < 0)$$

$$P(s \geq 0) = P_p(s \geq 0), \quad P(s < 0) = P_n(s < 0) \quad . \quad (4)$$

$$A(s \geq 0) = A_p, \quad A(s < 0) = A_n$$

Knowing $\text{sgn}(s)$, equation (3) may be inverted for the valve stroke s .

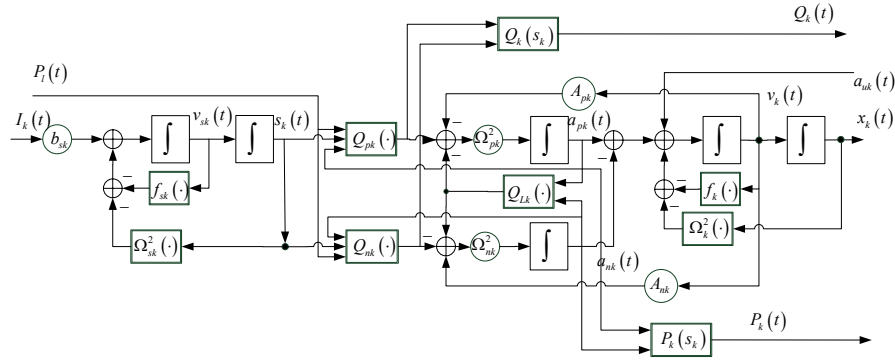


Fig. 2. Block-diagram of the k -th cylinder dynamics.

Valve dynamics, neglecting solenoid dynamics, is 2nd order and holds

$$\dot{s}(t) = v_s(t), \quad s(0) = s_0$$

$$\dot{v}_s(t) = -\Omega_s^2(P)s(t) - a_c(t) - f_s(t, P)v_s(t) + b_s I(t - \delta_s), \quad v_s(0) = v_{s0}, \quad (5)$$

where Ω_s^2 and f_s have the same meaning as Ω^2 and f in (2), $b_s = \phi_s/m_s$ depends on the solenoid force constant ϕ_s , and on the spool mass m_s , whereas the

(lower-level) at the right pressure P_l (higher-level). How they are interconnected (see Fig. 1) is better appreciated pursuing model simplification.

3 Model simplification and control hierarchy

3.1 Model simplification

Simplification is afforded through singular perturbation method of Kokotovic, Khalil and O'Reilly (1986), but modified to account for control unit time T (smooth singular perturbation, Acuña-Bravo et al., 2009) and assuming dynamics is averaged during this time. Briefly, the T -average equation of a 1st order dynamics with time constant τ , writes

$$\begin{aligned}\varepsilon \Delta x(t) &= -\underline{x}(t) + b\underline{u}(t) \cong 0 \\ \Delta x(t) &= x(t+T/2) - x(t-T/2), \\ \underline{x}(t) &= \int_{t-T/2}^{t+T/2} x(\tau) d\tau / T\end{aligned}\quad (8)$$

having denoted the singular perturbation with $\varepsilon = \tau / T < 1$, and assuming $|\Delta x|$ is bounded. Then, neglecting $\varepsilon |\Delta x|$, (8) may be solved for \underline{x} . The following result follows.

Result 1. Considering (1), (2), (5) and (6), and defining the singular perturbations

$$\begin{aligned}T\varepsilon_p &= \Omega_p^{-1}, T\varepsilon_n = \Omega_n^{-1}, T\varepsilon = |\Omega|^{-1}, T\varepsilon_s = \Omega_s^{-1} \\ T\varepsilon_l &= \tau_l = V_l \underline{P}_l / (\beta \underline{Q}_l)\end{aligned}, \quad (9)$$

the following 1st order simplified dynamics applies to each cylinder k

$$\begin{aligned}\dot{x}_k(t) &= (Q_k(s_k, \Delta P_k) - Q_{Lk}(t)) / A_k(s_k) \\ s_k(t) &= b_{sk} I_k(t) / \Omega_{sk}^2(P_k) \\ \Delta P_k(t) &= P_l / 2 - m_k (\Omega_k^2(P_k) x_k(t) + a_{ik}(t)) / (2A_k(s_k))\end{aligned}, \quad (10)$$

where underlying as in (8) has been dropped. The physical meaning of the first four singular perturbations in (9) corresponds to fluid incompressibility and to high stiffness of elastic connection if coupled with small masses. The fifth perturbation is more complex and requires the definition of a reference flow \underline{Q}_l and pressure \underline{P}_l , to be done below, as they provide the time constant τ_l . Equation (6) and (7) lead to the flow balance

$$K_l(\omega)x = \sum_{k=1}^n Q_k(s_k, \Delta P_k) + Q_0(t, P_l) + l(s)Q_a(s, \Delta P_a). \quad (11)$$

Finally applying (10) to pump yields

$$\begin{aligned}\dot{x}(t) &= (Q_a(s, \Delta P_a) - Q_L(t)) / A_a \\ s(t) &= b_s I(t) / \Omega_s^2 \\ \Delta P_a(t) &= \gamma_l P_l + (m a_u - (m \Omega^2 - k_\omega \omega^2) x(t)) / A_a, s \geq 0 \\ \Delta P_a(t) &= (1 - \gamma_l) P_l - (m a_u - (m \Omega^2 - k_\omega \omega^2) x(t)) / A_a, s < 0\end{aligned}, \quad (12)$$

where $|\gamma_l| < 1$.

As Fig. 1 and Fig. 4 shows, equations (10) and (12) define $n+1$ parallel 1st order dynamics, which are driven by solenoid currents I_k and I , leakages Q_L and Q_{Lk} , and load accelerations a_{uk} . Flows, which are intermediate variables in (10) and (12), are related through (11). Since the latter is parameterized by P_l , the latter may be solved from (11). Actually, two alternative treatments may be pursued.

- 1) Reference control employs (11) to derive the reference pump flow and stroke, given a reference \underline{P}_l .
- 2) Control law renounces to approximation (11), thus treating P_l as the line volume state variable (see dashed blocks in Fig. 4) which must be forced to track the reference \underline{P}_l .

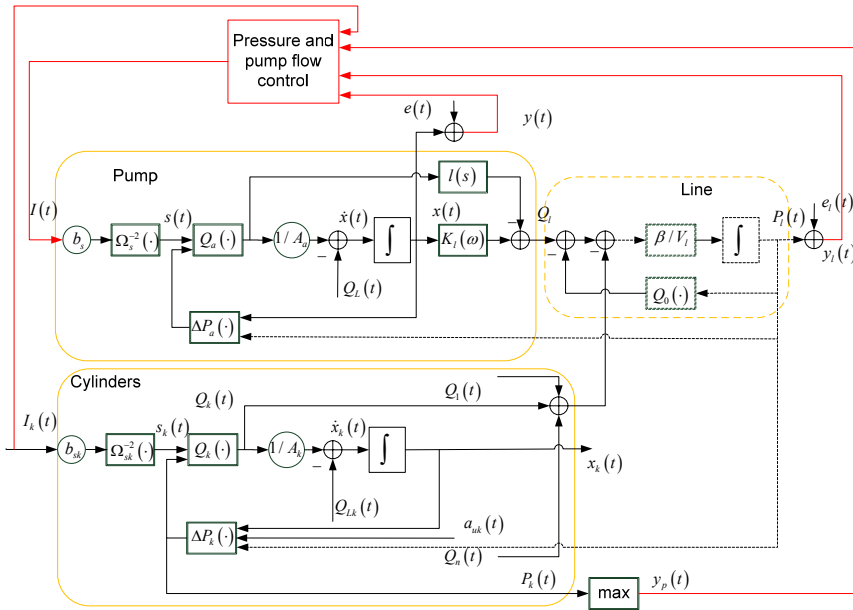


Fig. 4. Block-diagram of the simplified model with pump/line control..

Pressure drops in the flow equations add a nonlinear feedback to each 1st order dynamics.

3.2 Reference generator and hierarchy

It is now possible to solve the simplified model (10), (11) and (12) for the lower-level control objective, i.e. cylinder and pump flow, in the form of a reference generator, neglecting unknown disturbance like leakage Q_L and unknown components of a_{uk} and Q_0 , as well as parameter uncertainty. The latter accommodation is a task of the control law. Reference variables are underlined.

Result 2. Reference cylinder stroke \underline{r}_k is tracked by $n+1$ 1st order nonlinear feedback laws which satisfy valve and pump flow constraints, and are parameterized by pressure drops $\underline{\Delta P}_a$ and $\underline{\Delta P}_k$, as follows

$$\begin{aligned}
\dot{\underline{x}}_k(t) &= h_k(r_k - \underline{x}_k), \quad \underline{x}_k(0) = \underline{x}_{k0} \\
\underline{Q}_k(t, \underline{s}_k, \underline{\Delta P}_k) &= A_k(\underline{s}_k) h_k(r_k - \underline{x}_k), \quad k = 1, \dots, n \\
r &= \left(\sum_{k=1}^n \underline{Q}_k + \underline{Q}_0 + l(\underline{s}) \underline{Q}_a(t, \underline{s}, \underline{\Delta P}_a) \right) / K_l(\underline{\omega}), \quad r \leq r_{\max}, \\
\dot{\underline{x}}(t) &= h(r - \underline{x}), \quad \underline{x}(0) = \underline{x}_0 \\
\underline{Q}_a(t, \underline{s}, \underline{\Delta P}_a) &= A_a h(r - \underline{x})
\end{aligned} \tag{13}$$

where $h_k > 0$, $h > 0$ are stabilizing tracking gains.

Equation (13) provides valve stroke and currents (Kemmetmuller, Fuchshumer and Kugi, 2010), as follows

$$\begin{aligned}
\underline{s}_k(t) &= \frac{\underline{Q}_k(t)}{\mu_k \sqrt{\underline{\Delta P}_k(\underline{s}_k)}}, \quad \underline{s}(t) = \frac{\underline{Q}_a(t)}{\mu \sqrt{\underline{\Delta P}_a(\underline{s})}} \\
\underline{I}_k(t) &= \Omega_{sk}^2 \underline{s}_k(t) / b_{sk}, \quad |\underline{I}_k(t)| \leq I_{k,\max}, \\
\underline{I}(t) &= \Omega_s^2 \underline{s}(t) / b_s, \quad 0 \leq \underline{I}(t) \leq I_{\max}
\end{aligned} \tag{14}$$

where pressure drops derive from (10) and (12). Pump stroke \underline{x} derives from (11). The bound to the reference pump stroke r in (13) may require iteration to reallocate cylinder rates according to

$$\sum_{k=1}^n |\dot{\underline{x}}_k| A_k(\underline{s}_k) + \underline{Q}_0 + l(\underline{s}) |\dot{\underline{x}}| A_a \leq r_{\max} K_l(\underline{\omega}), \tag{15}$$

and to the current bounds in (14).

Equation (14) may be solved for valve strokes, only if the line pressure \underline{P}_l ensures feasible (positive) pressure drop in (10) and (12), i.e.

$$\underline{P}_l > \max(\max_k(\underline{P}_k), \underline{P}_a), \tag{16}$$

which is the higher-level control objective. Bias (spring) force $ma_u > 0$ ensures $\underline{\Delta P}_a > 0$ in (12) as $s \geq 0$. The higher-level objective imposes \underline{P}_l to track the reference

$$\underline{P}_l = \max(\max_k(\underline{P}_k), \underline{P}_a) + \underline{\Delta P}, \tag{17}$$

where $\underline{\Delta P}$ is a pressure drop to be designed. Design follows from line dynamics (6) –singular perturbation ε_l in (9) is now abandoned- fixing the slew rates of the pump and load flows, namely $\dot{Q}_{l,\max}$ and \dot{Q}_{\max} , where

$$\dot{Q}_{l,\max} = K(\omega) \dot{x}_{\max} = \frac{K(\omega) Q_{a,\max} b_s}{\Omega_s^2 A_a} I_{\max}. \tag{18}$$

Alternative to $\underline{\Delta P}$, the pressure control BW f_{AP} may be designed, by giving pressure and flows in (6) an harmonic profile with $\omega = 2\pi f$: it results

$$\underline{\Delta P} \geq \frac{\beta}{V_{l,\min} (2\pi f_{AP})^2} |\dot{Q}_{a,\max} - \dot{Q}_{\max}|. \tag{19}$$

Assuming, as a worst-case, zero pump flow and

$$\dot{Q}_{l,\max} = 0, \quad \dot{Q}_{\max} = 0.002 \text{ m}^3/\text{s}^2, \quad V_{l,\min} = 0.001 \text{ m}^3, \quad \underline{\Delta P} \leq 4 \text{ MPa}, \tag{20}$$

a minimum BW $f_{AP} \geq 3 \text{ Hz}$ results, together with $T \ll (2\pi f)^{-1} \cong 20 \text{ ms}$.

4 Hierarchical control through a single pump/line control law

Here we shall restrict to pump flow (lower-level) and line pressure (higher-level) control, assuming to know solenoid currents I_{sk} and the load-sensing pressure

$$y_p(t) = \max(P_k(t)) + v_p(t), \quad (21)$$

from cylinder control. In (21) v_p denotes the measurement error. Load-sensing pressure has been used in the reference generator to build the line pressure reference (17). Further measures provide pump stroke and line pressure as follows

$$\begin{aligned} y_l(t) &= P_l(t) + e_l(t) \\ y(t) &= x(t) + e(t) \end{aligned} \quad (22)$$

They are corrupted by the model errors e_l and e , which include measurement errors and the effects of the dynamics (valve, load) that has been neglected during simplification.

Singular perturbations in (9) apply to valve and actuating volume dynamics, i.e.

$$T\varepsilon_s = \Omega_s^{-1} \leq 2 \text{ ms}, \quad T\varepsilon_a = \Omega_a^{-1} \leq 0.5 \text{ ms}. \quad (23)$$

The latter inequalities together with (19) constrain T to stay within

$$2 \text{ ms} < T < 20 \text{ ms}. \quad (24)$$

Pump hierarchical control (flow and pressure) is driven by two measures and a single command; it can be solved as a single control law as flow and pressure are state variables with their own reference. According to EMC, equations (12) and (6) are rewritten separating known and unknown disturbance, as follows

$$\begin{aligned} \dot{x}(t) &= b_a I(t) + d(t) + w(t) \\ \dot{P}_l(t) &= b_l x(t) - \underline{d}_l(t) + d_l(t) + w_l(t) \\ b_a &= b_s \mu(s, \rho) \sqrt{\Delta P_a(s)} / (\underline{A}_a \underline{\Omega}_s^2) \\ b_l &= \underline{K}(\underline{\omega}) \underline{\beta}(t) / \underline{V}_l(t) \\ \underline{d}_l(t) &= \underline{\beta}(t) \left(\sum_{k=1}^n \underline{Q}_k + \underline{Q}_0 + \underline{A}_a b_a \sqrt{\Delta P_a(s)} I(t) \right) / \underline{V}_l(t) \end{aligned} \quad (25)$$

where underline means either reference or nominal values. Unknown disturbance is the sum of a state d and of a wide-band noise w (discrete-time white noise), arbitrary and unpredictable. The latter are the only channels wherethrough updating the embedded model as in Canuto, Massotti and Molano (2010). The state components are such to load itself with parametric uncertainty within the BW of the noise estimator, thus avoiding, with some limitations, adaptive control complexity and delays (Canuto, 2008). As such, they must satisfy stochastic equations as follows

$$\begin{aligned} \dot{d}_l(t) &= w_{dl}(t) \\ \dot{d}(t) &= w_d(t) \end{aligned} \quad (26)$$

where w_{dl} , w_l are further ‘white noises’. The ensemble (25) and (26) is the embedded model, which is actually implemented as a discrete-time equation and is observable from the measurements (22).

Control law follows by forcing the controllable state variables x (proportional to pump flow) and P_l (the line pressure) to track references in (13) and (14), and by adding disturbance rejection. The latter is not immediate here as known and unknown flows in (25) are not co-located with the current command (see Canuto, 2007). Applying Davison-Francis matrix equation (see Canuto, 2007) to (25) and (26), the control law results

$$I(t) = \underline{I}(t) + (k_x(\underline{x} - x + \underline{d}_l - d_l) / b_l - k_l(\underline{P}_l - P_l) - d(t)) / b_a. \quad (27)$$

Feedback gains ensuring stable tracking are k_x and k_l , and are fixed by stable closed-loop eigenvalue $A_c = \{-p_{c0}, -p_{c1}\}$ through

$$k_l = p_{c1} + p_{c0}, \quad k_x = p_{c1} p_{c0}. \quad (28)$$

At the limit $f_c \cong 3$ Hz imposed by f_{AP} , $k_l \cong 40$ rad/s, $k_x \cong 400$ rad/s². Note all other gains in (27) are model-based. Control law (27) and gains (28) ensure model-based stability.

When as in Acuña-Bravo et al. (2009), pump is endowed with a mechanical feedback, from pump stroke to valve as in Fig. 3 (dashed lines), in (22) only pressure measurement is available. Thus, only pressure control is implemented but keeping the same embedded model as in (25) and (26). The only difference regards pump dynamics in (25) that must have a nonzero pole imposed by mechanical link.

5 Pump and line noise estimator

State variables in (27) are provided by the embedded model, which must be driven by the same command to the plant and by noise realization. Noise realization must be kept as the control unit cornerstone as it allows the embedded model to causally include model uncertainty, both disturbance and parametric discrepancies. The key instrument is the noise estimator, based on Kalman filter innovation, but extended to any noise layout (Canuto, Massotti and Molano, 2010), not necessarily forcing all the state variables of the embedded model. Here the noise layout strictly follows the Kalman scheme, directly forcing all state variables, but disturbance dynamics (26) and noise estimator need to be modified according to measurement size and location.

Consider first measurements as in (22) and Fig. 4: in that case the embedded model is observable and the noise estimator is multivariate. Following Canuto, Massotti and Molano (2010), each model error must feed the least number of noise components (decoupling), and specifically the closest ones, as follows

$$\begin{aligned} \begin{bmatrix} w_l \\ w_{dl} \end{bmatrix} (t) &= \begin{bmatrix} m_l \\ m_{dl} \end{bmatrix} e_l(t) = \begin{bmatrix} m_l \\ m_{dl} \end{bmatrix} (y_l(t) - P_l(t)) \\ \begin{bmatrix} w \\ w_d \end{bmatrix} (t) &= \begin{bmatrix} m \\ m_d \end{bmatrix} e(t) = \begin{bmatrix} m \\ m_d \end{bmatrix} (y(t) - x(t)) \end{aligned} \quad (29)$$

As a consequence, gain equations decompose into a pair of 2nd order polynomials with their coefficients being fixed by the closed-loop eigenvalues.

When in (22) only the line pressure is available, the disturbance states in (26) become unobservable. Recovery is pursued by changing dynamics as follows

$$\begin{aligned} \dot{d}_l(t) &= -p_l d(t) + w_{dl}(t) \\ \dot{d}(t) &= w_d(t) \end{aligned} \quad (30)$$

with a caveat that observability now depends on $p_l \neq 0$. Noise estimator is driven by the sole pressure model error:

$$\begin{aligned} \begin{bmatrix} w_l \\ w_{dl} \end{bmatrix}(t) &= \begin{bmatrix} m_l \\ m_{dl} \end{bmatrix} e_l(t) = \begin{bmatrix} m_l \\ m_{dl} \end{bmatrix} (y_l(t) - P_l(t)) \\ \begin{bmatrix} w \\ w_d \end{bmatrix}(t) &= \begin{bmatrix} m \\ m_d \end{bmatrix} e_l(t) = \begin{bmatrix} m \\ m_d \end{bmatrix} (y_l(t) - P_l(t)) \end{aligned} \quad (31)$$

Gains derive from the coefficients c_{mk} , $k=0, \dots, 3$ of the 4th order polynomial imposed by the four closed-loop eigenvalues $\Lambda_m = \{-p_{m0}, \dots, -p_{m3}\}$.

Closed-loop eigenvalues are designed to guarantee closed-loop stability versus parametric uncertainty and neglected dynamics, a subject left outside of the paper (see Canuto 2007, Ospina and Canuto 2008). It results into the BW f_m reported in Table 1.

6 Simulated results

The following results derive from simulated runs, based on a fine plant model and plant-estimated parameters. A single cylinder is simulated and the valve pressure drop ΔP_k is assumed to be kept constant by a local compensator (Erkkila, 1999). A variable lubricating flow Q_0 around a mean value is added, together with an arbitrary flow imposed by operators. Pump stroke is assumed to be regulated by a mechanical link. The main data are listed in Table 1.

No.	Type	Symbol	Unit	Value	Comments
0	Line volume	V_l	dm ³	0.25	±10%
1	Load pressure slew rate	\dot{P}_{\max}	MPa/s	130	
2	Load flow slew rate	\dot{Q}_{\max}	dm ³ /s ²	2	±10% uncertain
3	Cylinder control delay	δ_{\max}	ms	50	
4	Line pressure drop	$\underline{\Delta P}$	MPa	2	Adds to valve pressure drop
5	Lubricating flow	Q_0	dm ³ /s	0.13	±10%
6	Peak pump flow	$Q_{l,\max}$	dm ³ /s	2	@ $\omega \cong 200$ rad/s
7	Pump current range	I	A	0.4 ÷ 1.2	useful range
8	Current delay	$\delta_{s,\max}$	ms	5	
9	Pump flow slew rate	$\dot{Q}_{l,\max}$	dm ³ /s ²	5	±10% uncertain
10	Control time unit	T	ms	5	see (24)
11	Control law BW	f_c	Hz	2	see below (28)
12	Noise estimator BW	f_m	Hz	10	see below (31)

Control law BW in Table 1 has been fixed at 2 Hz, as dictated by the pump pole of the mechanical feedback which is around 10 rad/s (Acuña-Bravo et al., 2009). The

pump flow BW is not enlarged, but pump flow dynamics is exploited beyond 2 Hz to track quick, but small demands.

Worst-case simulated results are shown in Fig. 5, Fig. 6, Fig. 7 and Fig. 8. Fig. 5 shows the pump solenoid current I , in digital units (10 bit range). The low constant profile at the extremes is the lubricating flow (< 100 bits); at 5 s the pump starts supplying a cylinder flow (500 bits), and at 9 s an arbitrary flow demand (300 bits) occurs. Small oscillations close to 7 s and 17 s correspond to a sudden raise and decrease of the reference pressure as in Fig. 7.

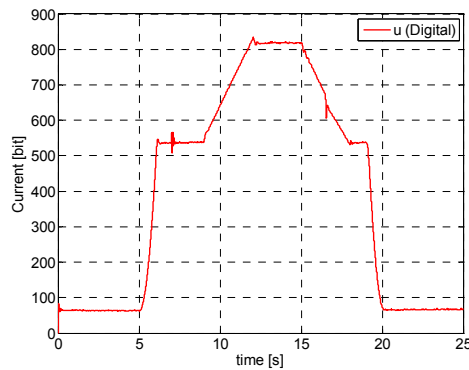


Fig. 5. Pump solenoid current.

Fig. 6 shows the pressure error $P_l - P_i$ between line pressure reference and measurement. Due to a rather small line volume (0.25 dm^3), the error overshoots the 2 MPa target when either the cylinder flows settles (because of cylinder flow uncertainty and delay) or the load pressure suddenly raise or decrease. Overshoots are acceptable as far as the pressure remains below the relief limit of 25 MPa. Undershoots force one-way valves to impede flow reversal, thus saturating dynamics and degrading performance.

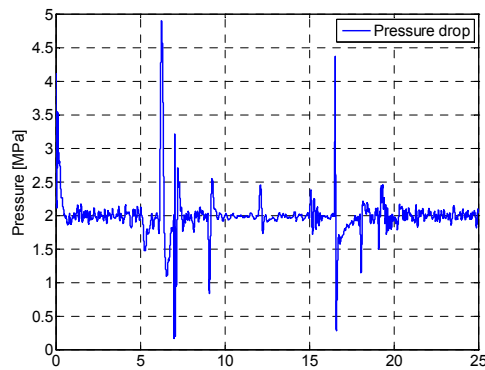


Fig. 6. Pressure drop corresponding to Fig. 7.

Fig. 7 shows reference (dashed) and measured line pressures, in absence of the arbitrary flow occurring in Fig. 5 from 9 to 17 s. Only neglected dynamics has been simulated, i.e. pump dynamics and solenoid delay. The same sharp pressure errors occur under the same circumstances; they may be weakened either by increasing the reference pressure above 2 MPa or by enlarging the line volume. Control law BW f_c fixed at 2 Hz cannot be widened, as it is bounded, in the present case, by pump flow mechanical loop.

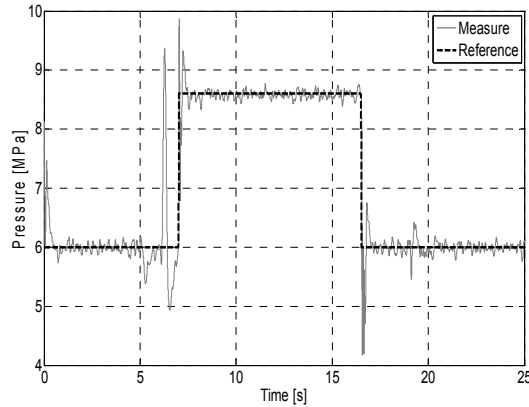


Fig. 7. Reference and measured line pressure.

Fig. 8 shows control robustness with respect to neglected dynamics and parametric uncertainty (robustness proof is provided in the paper). Uncertainty has been simulated through parameter discrepancy as listed in Table 1. Oscillations occurring when the cylinder flow demand ends are mainly due to line volume uncertainty. They are attenuated by further narrowing control law BW $f_c < 2$ Hz as shown in the same Fig. 8.

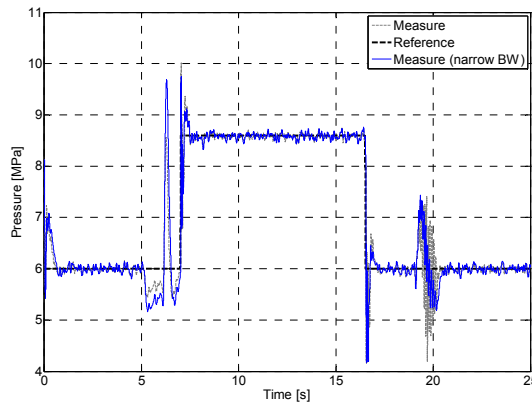


Fig. 8. Reference and measured line pressure under worst-case conditions.

Conclusions and acknowledgments

A state equation model has been developed for a generic hydraulic circuit including variable-flow pump, line and loads. The model is then simplified through smooth singular perturbations so as to provide the embedded model for control design and implementation. The latter is augmented with unknown disturbance dynamics to recover parametric uncertainty and neglected disturbance. Control law is not adaptive. Embedded model allows to derive reference generator, control law and noise estimator, the essential parts of the Embedded Model Control. Control hierarchy is discussed and it is shown that it reduces to a single control unit driving the pump solenoid current, and sensible to load pressure. Simulated results give a posteriori demonstration of control robustness, not proven in the paper. Study and simulated results were in part supported by Centro Ricerche FIAT, Turin, Italy.

References

1. Acuña-Bravo, W., Canuto, E., Malan, S., Colombo, D., Forestello, M. and Morselli, R. (2009) Fine and simplified dynamic modelling of complex hydraulic systems, in *Proc. of the American Control Conference*, pp. 5480-5485.
2. Canuto, E. (2007) Embedded Model Control: outline of the theory. *ISA Trans.* **46** (3), 363-377.
3. Canuto, E (2008) Drag-free and attitude control for the GOCE satellite. *Automatica*, **44**, 1766-1780.
4. Canuto, E, Molano, A. and Massotti, L. (2010) Drag-free control of the GOCE satellite: noise and observer design. *IEEE Trans. on Control System Technology*, **18**, 501-509.
5. Erkkila, M. (1999) Practical modeling of load sensing systems, in *Proc. 6th Scandinavian Int. Conf. on Fluid Power*, Tampere, Finland, 445-458.
6. Jelali, M. and Kroll, A. (2003) *Hydraulic servo-systems: modelling, identification and control*, Springer, London.
7. Kemmetmuller, W., Fuchshumer, F. and Kugi, A. (2010) Nonlinear pressure control of self-supplied variable displacement axial piston pumps, *Control Engineering Practice*, **18**, 84-93.
8. Kim, S. D. and Cho, H.S. (1991) A suboptimal controller design method for the energy of load-sensing hydraulic servo system, *J. of Dynamic Systems, Measurement and Control*, **113**, 487-493.
9. Kokotovic, P. V., Khalil, H. K. and O'Reilly, J. (1986) *Singular perturbation methods in control: analysis and design*, Academic Press, London.
10. Kugi, A. (2001) *Nonlinear control based on physical models: electrical, mechanical and hydraulic systems*, Lecture Notes in Control and Information Sciences, 260, Springer, London.
11. Manring, N.D. (2005) *Hydraulic control systems*, John Wiley & Sons, Hoboken (NJ).
12. Ospina, J. and Canuto, E. (2008) Embedded Model Control and the error loop, in *Proc. 8th International FLINS Conference*, World Scientific Pu. (Singapore), September 22-24, 2008, 975-980.

Application of the computer simulation technique for investigating problems of parametric AFT-model construction

Ekaterina V. Chimitova and Natalia S. Galanova

Department of Applied Mathematics, Novosibirsk State Technical University
Novosibirsk, Russia
Email: chim@mail.ru, Natalia-Galanova@yandex.ru

Abstract: This paper is devoted to the investigation of the problems of selecting distribution law for time-to-event data obtained by accelerated life testing. The problems of parametric model verification based on testing goodness-of-fit to a specified distribution law by samples of residuals have been considered. By means of computer simulation methods the statistical properties of model parameters estimators have been investigated depending on sample size, censoring degree and plan of experiment. The statistic distributions and the power of nonparametric goodness-of-fit tests have been studied. The Kolmogorov-Smirnov, Anderson-Darling and Cramer-von Mises-Smirnov goodness-of-fit tests have been considered.

Keywords: Monte-Carlo method; parametric AFT-model; censored samples; maximum likelihood estimation; the Kolmogorov-Smirnov, the Anderson-Darling, the Cramer-von Mises-Smirnov goodness-on-fit tests.

1 Introduction

There are many problems of longevity and aging data in different areas such as medicine, survival analysis, reliability studies, econometrics, etc. This is so-called time-to-event data. In medicine this event may be time of death, time of changes in some bio-chemical indices or time of remission after some treatment. In engineering this event may be time of failure for some interesting device or technical system.

Let the nonnegative random variable T denote the time-to-event or failure time of an individual. The probability of an item surviving up to time τ is given by the survival function:

$$S(\tau) = \Pr(T > \tau) = 1 - F(\tau), \quad (1)$$

where $F(\tau)$ is cumulative distribution function of random variable T .

In survival analysis an individual's survival depends on some characteristics or conditions of the experiment. Usually these characteristics are coded as the so-called covariates, which could be time-dependent.

It is often necessary to obtain reliability results from experiment more quickly than it possible with data obtained under normal conditions. In these cases experimenter may use Accelerated Failure Time Models. In AFT-models time-to-event data are obtained under some accelerated stress conditions, which shorten the life of test items. For example, covariate $x(\cdot)$ is accelerated with respect to a covariate $y(\cdot)$, if:

$$S_{x(\cdot)}(t) \leq S_{y(\cdot)}(t), \text{ for } t \geq 0. \quad (2)$$

The aim of such testing is to estimate survival function of an individual in normal conditions basing on data obtained in Accelerated Life Testing.

2 AFT-model

Consider two plans of experiment [1]:

1. Individuals are divided into k groups and tested under accelerated constant over time stresses $\bar{x}_1, \dots, \bar{x}_k$. Therefore n_i items are tested under \bar{x}_i stress condition, where $i = 1, \dots, k$.

2. Individuals are tested under step stress condition $x(t)$:

$$x(t) = \begin{cases} \bar{x}_1, & t_0 < t \leq t_1 \\ \bar{x}_2, & t_1 < t \leq t_2 \\ \dots \\ \bar{x}_k, & t_{k-1} < t \leq t_k \end{cases}. \quad (3)$$

In addition plan of experiment may be the combination of these two plans.

Under the AFT-model survival function $S_{x(\cdot)}(t)$ is determined by baseline survival function $S_0(t, \theta)$ and positive function $r[\cdot]$:

$$S_{x(\cdot)}(t) = S_0 \left(\int_0^t \frac{ds}{r[x(s)]}, \theta \right). \quad (4)$$

Stress function $r[\cdot]$ is usually parameterized in one of following ways:

1. Log-linear model: $r(x) = e^{\beta_0 + \beta_1 x}$;
2. Power rule model: $r(x) = e^{\beta_0 + \beta_1 \ln(x)}$;
3. Arrhenius model: $r(x) = e^{\beta_0 + \beta_1/x}$;
4. Model for vector stress: $r(x) = e^{\beta_0 + \beta_1 x_1 + \dots + \beta_m x_m}$.

For parametric AFT-models it is supposed that baseline survival function $S_0(t, \theta)$ belongs to some parametric family of distributions. For example: exponential model, Weibull model, Gamma model, power generalized Weibull model, inverse Gaussian model and so forth.

In survival analysis and reliability studies, time-to-event data are usually right censored. That means a time-to-event T is observed only if $T \leq T_C$, where T_C is a censoring time.

There are various types of right censoring schemes [3]:

1. Type I censoring: all items are tested until a pre-specified censoring time T_C ;
2. Type II censoring: only $k < n$ first failure times are observed, and for remained subjects censoring time is $T_C = T_k$, where T_k is failure time of k -th item;
3. Type III censoring (random censoring): there are failure times T_1, \dots, T_n and the censoring times C_1, \dots, C_n are independent positive random variables.

Let denote T_i and C_i the failure and censoring times of i -th item respectively. Set

$$X_i = \min(T_i, C_i). \quad (5)$$

Usually right censored data are presented as:

$$(X_1, \delta_1), \dots, (X_n, \delta_n), \quad (6)$$

where $\delta_i = 1_{\{T_i \leq C_i\}}$, $i = 1, \dots, n$ is an indicator of the event.

Estimates of parameters of AFT-models are found with maximum likelihood method, where likelihood function is:

$$L(T_n) = \prod_{i=1}^n f^{\delta_i}(X_i) \cdot S^{1-\delta_i}(X_i), \quad i = 1, \dots, n. \quad (7)$$

If plan of experiment is determined by (3) than survival function of item which failed under x^j stress is [1]:

$$S_{x^j}(t) = S_0 \left(\frac{t - t_i}{r(x^j, \beta)} + \sum_{j=1}^i \frac{t_j - t_{j-1}}{r(x^j, \beta)} \right). \quad (8)$$

It is often difficult to choose the distribution law for baseline survival function $S_0(t, \theta)$ because usually there is no prior information about lifetime distribution. After estimation of model parameters one should test goodness-of-fit of obtained model to the sample of observations. So, testing goodness-of-fit is an essential part of statistical analysis. One approach to testing goodness-of-fit with parametric AFT-model is based on residuals which in case of fixed covariates can be calculated as following:

$$z_i = \frac{t_i}{r[x^i(\cdot), \hat{\beta}]}. \quad (9)$$

If the model (4) is appropriate the sample of residuals z_1, \dots, z_n belongs to the distribution $F_0(t, \hat{\theta})$, which is standardized by the scale parameter. The hypothesis about goodness-of-fit of the sample of residuals to $F_0(t, \hat{\theta})$ can be tested with the

classical Kolmogorov-Smirnov, Cramer-von Mises-Smirnov, Anderson-Darling tests. The Kolmogorov test statistic

$$D_n = \sup_{t < \infty} |F_n(t) - F_0(t, \hat{\theta})|, \quad (10)$$

the Cramer-von Mises-Smirnov test statistic

$$W_n^2 = n \int_{-\infty}^{\infty} (\hat{F}_n(t) - F_0(t, \hat{\theta}))^2 dF_0(t, \hat{\theta}) \quad (11)$$

and the Anderson –Darling test statistic

$$A_n^2 = n \int_{-\infty}^{\infty} (\hat{F}_n(t) - F_0(t, \hat{\theta}))^2 \frac{dF_0(t, \hat{\theta})}{F_0(t, \hat{\theta})(1 - F_0(t, \hat{\theta}))}. \quad (12)$$

It should be noted that we have a composite hypothesis, for which test statistic distributions $G(S|H_0)$ are affected by a number of factors: the form of assuming lifetime distribution $F_0(t, \theta)$, the type and the number of estimated parameters, the method of parameter estimation and other factors.

In [5], [6] the approximations of statistic distribution models and the tables of percentage points were obtained for testing composite hypotheses by the Kolmogorov-Smirnov, Cramer-von Mises-Smirnov, Anderson-Darling tests using the maximum likelihood estimates of unknown parameters. The set of distribution families relative to which one can test composite goodness-of-fit hypotheses using the constructed approximations contains 21 distribution laws including the exponential, Rayleigh, Maxwell, Weibull, log-normal distributions and others. In this paper we have investigated statistic distributions in testing goodness-of-fit of samples of residuals (9) to the distribution $F_0(t, \hat{\theta})$.

It has been shown that test statistic distributions $G(S|H_0)$ don't depend on the stress function $r[\cdot]$ in case of uncensored time-to-event data. So for testing goodness-of-fit with parametric AFT-model by residuals (9) one can use approximations of $G(S|H_0)$ obtained in [5], [6]. Or approximate p -values can be obtained by simulation.

In case of censored data approximate p -values in testing goodness-of-fit can be obtained by simulation only if there is sufficient knowledge of the censoring process. It is quite possible if we have type I or type II censored data, but in case of random censoring process which often occurs in survival analysis there is a problem of ambiguity in simulating censored observations because the distribution of censoring times is unknown. In case of independent random censoring we can neglect censored observations if the censoring degree is not large.

3 Example: Veteran's Administration Lung Cancer Trial

Let consider lung cancer survival data for patients (data were given in [7]) assigned to one of two chemotherapy treatments (Standard and Test). The data include observations of 137 patients and 9 observations from the sample are censored. In addition to treatment (trt) several factors are given: (PS) – Performance status (Karnofsky score); (Age) – Age of patient; (Diag) – the number of months from diagnosis of cancer to entry into the study; Cell-type of the tumor: squamous, small, adeno and large.

The stress function is determined as:

$$r(x, \beta) = \exp\{\beta_0 + \beta_1(PS) + \beta_2(age) + \beta_3(diag) + \beta_4 I(\text{cell-type} = \text{squamous}) + \beta_5 I(\text{cell-type} = \text{small}) + \beta_6 I(\text{cell-type} = \text{adeno}) + \beta_7 I(\text{trt} = \text{Test})\} \quad (13)$$

These data were widely discussed in [2], [4], but there only the Weibull parameterization of $S_0(t, \theta)$ was taken. Let consider the problem of choosing distribution law for baseline survival function $S_0(t, \theta)$ for lung cancer data. For this purpose we have developed the software system which enables

- to compute MLEs for parameters of AFT-model for a wide range of lifetime distribution laws,
- to obtain samples of residuals for AFT-model,
- to test goodness-of-fit by Kolmogorov-Smirnov, Cramer-von Mises-Smirnov and Anderson-Darling tests,
- to simulate distributions of MLEs for model parameters and test statistic distributions,
- to estimate precise confidence intervals for parameters and survival functions.

In table 1 the distribution laws considered as possible parameterization of $S_0(t, \theta)$ are presented.

Table 1 – Lifetime distributions

Exponential	$S_0(t) = \exp\left\{-\frac{t}{r(x, \beta)}\right\}$
Weibull	$S_0(t, \theta) = \exp\left\{-\left(\frac{t}{r(x, \beta)}\right)^\theta\right\}$
Power Generalized Weibull	$S_0(t, \theta) = \exp\left\{1 - \left[1 + \left(\frac{t}{r(x, \beta)}\right)^{\theta_0}\right]^{1/\theta_1}\right\}$
Gamma	$S_0(t, \theta) = 1 - \frac{1}{\theta} \Gamma\left(\frac{t}{r(x, \beta)}, \theta + 1\right)$

Inverse Gaussian	$S_0(t, \theta) = 1 - \Phi\left(\sqrt{\frac{\theta}{t}}\left(\frac{t}{r(x, \beta)} - 1\right)\right) - \exp\left\{\frac{2\theta}{r(x, \beta)}\right\} \Phi\left(-\sqrt{\frac{\theta}{t}}\left(\frac{t}{r(x, \beta)} + 1\right)\right)$
------------------	--

In table 2 statistic values and achieved significance levels (p -values) in goodness-of-fit testing by samples of residuals are given. When testing goodness-of-fit with the exponential and Weibull distribution laws we have used the approximations of statistic distributions obtained in [5], [6]. As to the Gamma, PGW and Inverse Gaussian distributions p -values have been obtained by simulations. Analysis of residuals has been considered for the sample of 128 complete observations without 9 censored observations.

As it is seen from the table 2 the Power Generalized Weibull AFT-model fits to data better than other considered distribution laws.

Table 2. Statistic values and significance levels for goodness-of-fit tests

$F_0(t, \theta)$	Kolmogorov test		Cramer-von Mises-Smirnov test		Anderson-Darling test	
	S_n	$P\{S > S_n\}$	S_n	$P\{S > S_n\}$	S_n	$P\{S > S_n\}$
Exponential	0.887	0.197	0.169	0.108	1.149	0.079
Weibull	0.685	0.315	0.109	0.077	0.729	0.059
PGWD	0.632	0.304	0.056	0.259	0.330	0.325
Gamma	0.679	0.379	0.092	0.167	0.584	0.146
IGD	1.137	0.019	0.262	0.009	1.334	0.010

The empirical distribution function of residuals for Generalized Weibull AFT-model and corresponding standardized by the scale PGW cumulative distribution function are presented in figure 1.

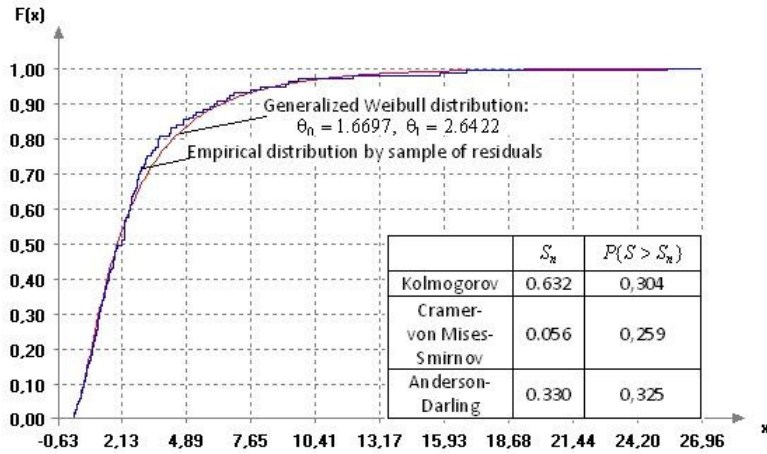


Figure 1. The empirical distribution by sample of residuals for PGW-model

In table 3 there are MLEs of Generalized Weibull AFT-model parameters obtained by the sample of 137 observations including 9 censored observations.

Table 3. MLEs for Power Generalized Weibull AFT-model

Parameter	MLE	Parameter	MLE
β_0	1.4061	β_5 (Small)	-0.6108
β_1 (PS)	0.0348	β_6 (Adeno)	-0.7555
β_2 (Age)	0.0081	β_7 (Trt)	-0.1318
β_3 (Diag)	-0.0019	θ_0	1.7090
β_4 (Squamous)	0.0942	θ_1	2.8298

Consider reduced model with only PS covariate included. Let compare Weibull and Power Generalized Weibull AFT-models for lung cancer survival data. In table 4 the results of parameter estimation and testing goodness-of-fit with these two models are given. And figure 2 illustrates the difference between these two models for values of Performance Status equal to 20, 50 and 80.

Table 4. Comparison of Weibull and PGW reduced models for lung cancer data.

	Weibull	PGW	Test	Weibull		PGW	
				S_n	$P\{S > S_n\}$	S_n	$P\{S > S_n\}$
β_0	2.556	1.076	Kolmogorov	1.238	0.001	0.722	0.207
β_1	0.036	0.039	Cramer-von Mises-	0.321	0.0	0.096	0.053

			Smirnov				
θ_0	0.976	1.697,	Anderson-	1.741	0.0	0.506	0.351
θ_1		3.142	Darling				

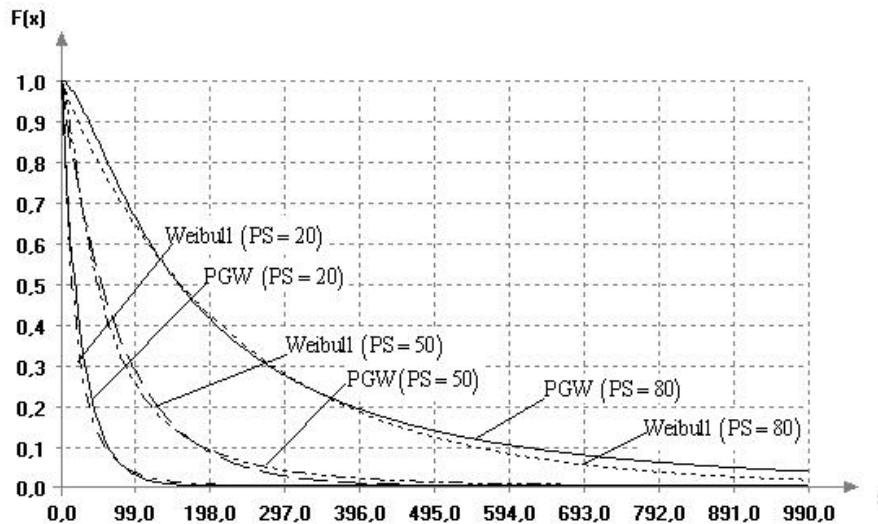


Figure 2. Survival functions for various PS values

As it is seen from the table 4 the Generalized Weibull AFT-model fits to the reduced data much better than the Weibull AFT-model, and one can see the difference between these two models from the figure 2.

3 Conclusions

We have briefly discussed the problem of the choice of parametric AFT-model. By means of computer simulation technique and developed software system we have investigated omnibus statistics distributions for testing goodness-of-fit with AFT-model basing on residuals. It has been shown that in case of complete samples it is possible to use the approximations of statistic distributions given in [5], [6] or to obtain p -values by simulation for data without covariates. In case of random censored samples which often occur in survival analysis there is a problem of ambiguity in simulating censored observations because the distribution of censoring times is unknown.

In this paper we considered the example of Veteran's Administration Lung Cancer Trial which include 128 complete lifetimes and 9 random censored observations. Various parameterizations of the baseline survival function for the AFT-model

have been compared for these data. Goodness-of-fit testing has been carried out by sample of only complete observations. It is reasoned with the problem of estimating distribution law for censored observations which are related with covariate values. Further investigations of this area would be useful.

4 Acknowledgements

These researches have been partially supported by the Russian Foundation for Basic Research (Grant No. 09-01-00056-a) and the Federal targeted program of the Ministry of Education and Science of the Russian Federation "Scientific and scientific-educational personnel of innovative Russia"

References

1. Huber C., Limnius N., Nikulin M. (2008). *Mathematical Methods in Survival Analysis, Reliability and Quality of Life*. Wiley-ISTE, New Jersey.
2. Kalbeisch J.D., Prentice R.L. (1980). *The statistical analysis of failure time data*. John Wiley and Sons, Inc., New York.
3. Klein J.P., Moeschberger M.L. (2003). *Survival analysis: techniques for censored and truncated data*. Springer, New York.
4. Lawless J.F. (2003). *Statistical models and methods for lifetime data*. John Wiley and Sons, Inc., Hoboken, New Jersey.
5. Lemeshko B.Yu., Lemeshko S.B. (2009). Distribution models for nonparametric tests for fit in verifying complicated hypotheses and maximum-likelihood estimators. Part 1. *Measurement Techniques*. Vol. 52, No. 6. pp. 555-565.
6. Lemeshko B.Yu., Lemeshko S.B. (2009). Models for statistical distributions in nonparametric fitting tests on composite hypotheses based on maximum-likelihood estimators. Part II. *Measurement Techniques*. Vol. 52, No. 8. pp. 799-812.
7. Prentice (1973). Exponential survivals with censoring and explanatory variables. *Biometrika*, 60, pp. 279-288.

Strategies for Energy Management in Home Automation Systems

G. Conte, A. Perdon, D. Scaradozzi, M. Rosettani, G. Morganti, F. Dezi

Dipartimento di Ingegneria Informatica, Gestionale e dell'Automazione
Università Politecnica delle Marche – Ancona, Italy
Email: gconte@univpm.it, perdon@univpm.it, d.scaradozzi@univpm.it,
morganti@diiga.univpm.it, rosettani@diiga.univpm.it.

Abstract: This paper deals with the problem of resource management and allocation in home automation systems. In many situations, the global, concurrent demand of resources, like electricity and gas, by home appliances may exceed actual availability and this originate conflicts, whose solution requires the use of suitable control strategies. Here, we summarize and discuss different control strategies, which have been proposed by the authors in recent papers. Performances are compared with respect to generic scenarios and advantages and drawbacks of each one are briefly discussed.

Keywords: Home automation, Resource management, Optimization

1 Introduction

A home automation or domotic system consists of a set of appliances and devices for home management which can be viewed as individual agents acting in a common environment and sharing common resources (see [3, 14] and the references therein). In home installation, resources availability is limited and concurrent use may cause conflicts that degrade the performances of single appliances with respect to the user expectations and that increase costs or time for accomplishing individual tasks.

The general strategy to solve this conflict consists in determining an order of priority of each agent with respect the others in accessing a given resource when the available amount cannot satisfy the global actual demand. A collateral effect of this solution is a loss of efficiency in terms of delays in executing the assigned task, occurring when an agent must yield and wait until the resource is free. The resulting situation is handled by considering also time as a system's resource that, although not limited in principle, has to be saved ([5]).

From a general point of view, this give rise to an optimization problem that, roughly, consists in allocating resources, respecting constraints and limitations, while minimizing the time required for completing all the tasks in a generic scenario. A paradigmatic framework in which the above problem can be formally stated and analyzed has been developed in a previous series of papers [3, 4, 7], using the theoretic approach of Multi Agent System Theory (see e.g. [9, 10, 17] for general aspects). Multi Agent System theory has been applied to the study and characterization of domotic environments by several authors. Examples are provided in [8, 12, 16].

In the Multi Agent approach we consider, appliances are described by suitable agents, which act in an abstract environment, and their behavior is modeled as a

sequence of transitions from state to state, which occur according to specific rules only if a specific amount of a given resource (to be consumed in the new state) is available. Availability of resources is therefore influenced by the agents' behavior and, in turn, it determines the possibility of state transitions which evolve towards the completion of the tasks. Resource management on the basis of priority indices can be implemented, essentially, by means of two different kinds of control architectures: a centralized one, in which a single controller monitors availability of resources and allocates them, or a distributed one, in which each agent regulates its own behavior (see [1, 15]). The basic information that is needed in both cases is a measure of the actual electric load that, in real domestic installations, can be evaluated by dedicated devices.

Performances of the system in terms of execution time and other indices for a given scenario can be described by suitable objective functions and the resulting optimization problem can be dealt with by different methods, according to the chosen control architecture.

In this paper, we recall and discuss the basic aspects of three of different control strategies (two of which have already been presented in a previous series of papers [3-7, 15, 18]) that solve the resource management and allocation problem. The first and the second ones refer to the case of centralized control architecture and they are based, respectively, on linear programming and on game theoretic methods ([2, 11]). The third one (see [15]) refers to the case of distributed control architecture and it makes use of off-line optimization by means of genetic algorithms. The three control strategies exhibit very different characteristics and their comparison, together with the evaluation of performances in similar conditions, is useful for understanding the potential of one choice with respect to the other.

2 The Electricity Management Problem

Typically, one of the resources whose management in home automation systems is more critical is electricity. This is due to the fact that, in general, electricity is the most expensive resource appliances can use and, because of the problems connected to its large scale production, providers adopt policies that contrast excessive consumption. A policy of that kind specifies a (set of) threshold(s) for the consumption. When consumption surpasses a threshold, the system enters a condition called overload and persistence of the overload for a time longer than a fixed duration causes the cost of the resource to increase largely or the resource to be cut off. The last situation is particularly penalizing, since it originates a black-out of the system and manual intervention is required to restore the supply.

In typical Italian home installation, the overall threshold, generally at 3kW, defines an overload that can persist for a short Limit Time T_{lim} (between¹ 120s and 240s) before the cost of the resource increases largely and, after some time, it is finally cut off.

¹ These values may change slightly, depending on the provider and on the model of the meter. The interval we consider refers to the GEM employed by the provider ENEL in the majority of its installations.

Implementing a control strategy to avoid or reduce overloads, performances of the controlled system can be evaluated in terms of occurrence of overloads and of delay in accomplishing tasks. This must be done with respect to a given scenario S , which specifies the number, kind and scheduling, over a period of time, of the tasks that the user asks the system to perform. For example, a one-day scenario S may include activation of the dishwasher, of the electric oven, of the washing machine, and so on, at given times and for given specific tasks.

Concerning the role of delays in defining performance indices, we consider, for each task the system can accomplish, a Nominal Time T_{nom} , equal to the duration of the task in case the required resources are available, and we compare it with the time actually occurred in given scenario, which will be denoted by T_{ex} , when control is active. The relative delay referred to each scheduled task i , $i=1, \dots, n$, in the scenario S is defined by

$$\Delta_i = \frac{T_{ex} - T_{nom}}{T_{nom}} \quad (1)$$

and the average, overall relative delay, denoted by Δ_S , is defined as the averaged, weighted sum of the relative delays concerning each task in S , namely

$$\Delta_S = \frac{\sum_i \gamma_i \Delta_i}{n} \quad (2)$$

The weights γ_i 's in the above formula describe the importance the user assigns to each task and their choice forces the performance index to fit the user's preferences. Other indices can be defined in similar way and they can be straightforwardly included in our approach. A second important performance index is the number of overloads OL_S which occur in executing the tasks scheduled in a given scenario S . Overloads need to be taken into account, because in general they stress the system and may cause the cost of the resource to increase. Overall performance indices can be defined by combining the two defined above as we will do in Section 4.

3 Centralized Control Architecture

In the case of centralized control architecture, we consider two possible control strategies to allocate resources. We assume that the home automation system includes an agent which plays the role of supervisor and allocates the resource. The supervisor monitors each plug by measuring the consumption of electricity at each one of them and it has computational capabilities that will be indirectly specified in the following. As soon as agent A_i , $i = 1, \dots, N$, is turned on, load at the dedicated plug takes a positive value P_i and this, together with the switching time T_i , is assumed to represent, for the supervisor, the current demand, indicated by (P_i, T_i) of the agent A_i . The supervisor knows the value of the threshold and, to allocate the resource when the global demand exceeds the availability, it can disconnect any one of the plugs. In case of disconnection, the supervisor is able to measure the duration D_i of the time interval in which the plug and, therefore, the associated agent A_i remained disconnected.

When agents turn on, the supervisor evaluates the global electric load and, if it

does not exceed the threshold, it remains inactive. Alternatively, before the Limit Time T_{lim} expires and black out occurs, the supervisor decides how to allocate the resource and it acts by disconnecting some of the plugs to lower the load. The first strategy we consider is based on game theoretic methods and it has been described in [18]. Conceptually, it uses the solution of a cooperative game in a Cournot Oligopoly ([2]).

Let us denote by P the available amount of resource, corresponding to the threshold, and by P_i ($P_i > 0$) the resource required by agent A_i , $i = 1, \dots, N$, starting from time T_i , $i = 1, \dots, N$. Assuming that an overload occur at some time T_o , the supervisor computes the values (X_1^*, \dots, X_N^*) that maximize the payoff functions $\pi_i = X_i(P - \sum_j X_j - C_i)$, $i = 1, \dots, N$, where C_i denotes a weigh associated to the current demand (P_i, T_i) of the agent A_i . (X_1^*, \dots, X_N^*) , is a Nash-Cournot equilibrium point that determines the best allocation, with respect to the payoff functions, of the available resource among all agents. Since such allocation will not be directly applicable (because, first of all, the supervisor is only capable of a discrete on-off action on each plug, not of exerting a continuous regulation, and, moreover, because it would be useless, also if it was possible, to supply to an agent less or more power than required), the supervisor finds one which is close to it, in a suitable sense, by determining a subset J of indices in $\{1, 2, \dots, N\}$ in such a way that the characteristic function

$$v(J) = \frac{\sum_{i \in J} P_i}{\left(\sum_{i \in J} (X_i^* - P_i)^2 \right)^{1/2} \left(\frac{P - \sum_{i \in J} P_i}{\text{card}(J)} \right)} \quad (3)$$

is maximized. Then, it cuts off power to the agents A_i for which $i \notin J$, closing the first phase of the decisional process.

The weights C_i used in the evaluation of the payoff functions depend, in particular, on the time elapsed from the switching instant T_i and the present time T , that is $(T - T_i)$, and on the duration D_i of the time interval in which, possibly, the agent A_i remained disconnected, starting from T_i . More precisely, C_i is defined by the following expression:

$$C_i = \frac{P}{N} \left(1 - \frac{D_i}{(T - T_i)} \right) \quad (4)$$

The agents A_i , $i \in J$, chosen in the first phase of the decisional process form a winning coalition that hold temporary. After a fixed waiting time, which is a parameter of the control action, in a second phase, the supervisor evaluates again the payoff functions, using updated values of the weights C_i , and, depending on the results, it computes a new winning coalition, that may coincide with the previous one or not.

In the above scheme, the supervisor works in real time, optimizing the allocation of the available resource on the basis of the information it has at each instant. It is possible to structure the system in such a way that the supervisor is not given the possibility to disconnect specific plugs, that is specific agents (e.g. for safety reasons or simply for user's convenience). When the supervisor detects a demand

from one of such agents, it simply reduces the threshold, in its computation, by a corresponding value.

The second control strategy we consider is a simpler one that formalizes the resource allocation problem as a Knapsack Problem and uses linear programming to solve it (see e.g. [11]). As done before, let us denote by P the available amount of resource, corresponding to the threshold, and by P_i ($P_i > 0$) the resource currently required by agent A_i , $i = 1, \dots, N$. Moreover, for each agent A_i , let C_i denote a weight associated to the current demand P_i . Assuming that an overload occur at some time T_o , the supervisor solves the problem described by

$$\text{maximize } \sum_{i=1}^N X_i C_i \text{ subject to } \sum_{i=1}^N X_i P_i \leq P, \text{ with either } X_i = 0 \text{ or } X_i = 1.$$

After finding the solution (X_1^*, \dots, X_N^*) , the supervisor disconnect the agents A_i for which $X_i = 0$. The problem is NP-hard, but, given the limited number of agents in realistic situations, it has a feasible size and it can be solved in relatively short time by branch and bound. The weights C_i can be assigned in two ways: either as a function of the current state of the agent and of the preferences of the end user (dynamic weights), or by choosing constant values (static weights). In the second case, taking equal weights, the strategy maximize the number of agents which share the resource, cutting off those which have greater demand. To make possible the use of dynamic weights, we must assume the possibility for the supervisor to know the individual status of each agent, by exchanging information on a communication network.

It is clear that both the above described strategies avoid black outs by limiting the time during which the system is in an overload condition. On the other hand, by denying resource to some of the agents, they cause the performance index Δ_S to take a positive value. Minimization of such value and, consequently, improvement of performances depend, in the case of the second strategy, on the choice of the weights C_i . Similarly, in the case of the first strategy, one can influence Δ_S by modifying the characteristic function $v(J)$ in (3) or the way in which the C_i are defined in (4).

4 Distributed Control Architecture

We assume, in the case of distributed control architecture, that the home automation system does not include any supervisor, but only a device, called meter, that is able to dispatch the measure of the global electric load.

A distributed control strategy for managing electricity can be designed following the lines of the Power Levelling Strategy introduced and discussed in [4]. When an overload occurs, each domestic agent enters in an overload status, in which it waits for a given time before yielding and going to a standby status, from which it tries to resumes its operation, making a new demand, after a given time has elapsed. The time each agent A_i waits before yielding is called Overload Time and it is denoted by τ_{oi} . The time each agent A_i waits before trying to resume operation is called Suspension Time and it is denoted by τ_{si} (see [4, 5] for a detailed discussion and description of the power levelling strategy).

The Overload Time τ_{oi} and the Suspension Time τ_{si} are the parameters of the

individual control action that each domotic agent A_i employs to regulate its own behavior. Their choice affects the performances of the system in each scenario S in terms of number of overloads OL_s , which one would limit, and in terms of average relative delay Δ_s , which one would limit too. The two objectives are mutually in contrast and the choice of the above control parameters has to be performed by solving an optimization problem. In the multi agent framework developed in [4, 5, 6], the optimization problem concerning the choice of τ_{oi} and τ_{si} for each domotic agent A_i in a given scenario has been formally stated by defining the objective function to be minimized as

$$f_s(\tau_{o1}, \tau_{s1}, \dots, \tau_{oN}, \tau_{sN}) = \alpha OL_s + \beta \Delta_s \quad (5)$$

where S denote the scenario. Since an analytic expression of f_s cannot be easily found, a suitable simulation/optimization method has been used to find the best set of parameters. Metaheuristic methods based on Tabu Search and on Genetic Algorithms have been implemented, in a LabVIEW environment, using the HAS-SIM simulator described in [4, 5, 6]. Comparison in [13] has shown that Genetic Algorithms, although computationally more expensive than Tabu Search, produce better solutions.

The control strategy briefly recalled above guarantees that blackout do not occur, since the system remains in overload conditions for a time smaller than the Limit Time T_{lim} , but, contrary to what happens in the case of centralized control architectures, overloads may occur frequently.

5 Simulation and Comparative Tests

To compare at various levels the performances of strategies of the above described kinds, the behavior of a home automation system that includes two domotic agents and one domotic object (that is two agents that can be disconnected or put in a standby status and one which cannot) has been simulated in different scenarios using the HAS-SIM simulator. The load profiles of the two domotic agents, representing respectively a washing machine and a dishwasher, are illustrated in Figure 1 and 2. The domotic object is characterized by a fixed load of 2.5kW and it represents appliances and devices that cannot be disconnected or put in a standby status. Threshold is fixed at 3kW and the scenario's schedule is a simple one: the third agent is always on and the other two turn on at the same time T_0 .

In the case of distributed control architecture, the simulator has been first used to optimize off-line, using genetic algorithms, the control parameters, namely the Overload Time and the Suspension Time for the dishwasher and for the washing machine. Performances are therefore those corresponding to the best choice of parameters. Five different tests have been performed using different weights γ_i to compute by (2) the performance index Δ_s as described in Table I and Table II.

The electricity consumption profiles corresponding to the best performances, respectively when the weights are (1, 1) in the distributed case and (3, 1) in the centralized one (the two centralized strategies present similar results), are illustrated in Figure 3 and Figure 4.

We can see that the system behavior is quite similar in the two configurations. In particular, the time globally required for performing all the scheduled tasks is more

or less the same. In the case of the distributed control architecture, we observe one overload more than in the other case. The centralized control architecture, in addition, allocates the resource to the standby agent as soon as it is made available. The reaction of the distributed system when the resource becomes available is slower, since the agent whose demand is pending waits, in any case, until its Suspension Time has elapsed.

6 Conclusion

Centralized control architectures and distributed ones represent two possible choices for realizing home automation systems endowed with efficient control strategies. Both choices appear to be practicable from a technological point of view, using well established signal acquisition and processing techniques and, regarding the hardware, devices like low cost microcontrollers. Transmission of information presents unsolved problems, related to the choice of the technology (wireless, dedicated bus, power line) and to that of the protocol (LonTalk, KONNEX, others) to be used. Centralized control architectures are simpler to realize, but they present the additional cost of the supervisor that users may not be willing to pay.

References

1. Abras S., S. Ploix, S. Pesty and M. Jacomino, "A multi-agent home automation system for power management" in Proceedings of the Third International Conference in Control, Automation and Robotics, ICINCO 2006.
2. Branzei R., Dimitrov D., Tijs S., "Models in Cooperative Game Theory", Springer, 2008
3. Conte G. and D. Scaradozzi, "Viewing home automation systems as multiple agents systems" in Multi-agent system for industrial and service robotics applications, RoboCUP2003, 2003.
4. Conte G., D. Scaradozzi, "An Approach to Home Automation by means of MAS Theory", CRC Press, ISBN: 0849379857, U.S.A, 2007
5. Conte G., D. Scaradozzi, A. Perdon, M. Cesaretti and G. Morganti, "A Simulation Environment for the Analysis of Home Automation Systems", in MED07, Greece, 2007.
6. Conte G., D. Scaradozzi, A. Perdon, M. Cesaretti and G. Morganti, "Tuning and Optimizing Control Laws in Distributed Home Automation Systems", Workshop on Networked Distributed Systems for Intelligent Sensing and Control, Greece, 2007.
7. Conte G., G. Morganti, A. Perdon and D. Scaradozzi, "Multi-Agent System Theory for Resource Management in Home Automation Systems", Journal of Physical Agents, Vol. 3, 2/2009.
8. De Carolis B., G. Cozzolongo, S. Pizzutilo, and V. L. Plantamura, "Agent-based home simulation and control" in ISMIS, 2005, pp. 404–412.
9. Ferber J., "Multi-Agent Systems: An Introduction to Distributed Artificial Intelligence". Boston, MA, USA: Addison-Wesley Longman Publishing Co., Inc., 1999.
10. Flores-Mendez R. A., "Towards a standardization of multi-agent system framework," Crossroads, vol. 5, no. 4, pp. 18–24, 1999.
11. R. J. Vanderbei, "Linear Programming Foundations and Extensions", Springer, 2001.
12. Lesser V., M. Atighetchi, B. Benyo, B. Horling, A. Raja, R. Vincent, T. Wagner, X.

Ping, and S. X. Zhang, "The intelligent home testbed," in Proceedings of the Autonomy Control Software Workshop, 1999.

13. Morganti G., A. Perdon, Conte G., D. Scaradozzi, and A. Brintrup, "Optimising home automation systems: a comparative study on tabu search and an evolutionary multi-objective algorithm," in MED 2009, Greece, 2009.
14. Nugent C. D.; Finlay, D. D.; Fiorini, P.; Tsumaki, Y.; Prassler, E., "Editorial Home Automation as a Means of Independent Living," Automation Science and Engineering, IEEE Transactions on , vol.5, no.1, pp.1-9, Jan. 2008
15. Qinglong W., Fei-Yue W., Yuetong L., "A mobile-agent based distributed intelligent control system architecture for home automation", in 2001 IEEE International Conference on Systems, Man, and Cybernetics, Tucson, AZ, USA, 2001.
16. Rao S. P., D. J. Cook, "Predicting inhabitant actions using action and task models with application to smart homes" International Journal of Artificial Intelligence Tools, 2004.
17. Sycara K., "Multiagent systems," AI Magazine, vol. 10, no. 2, pp. 79–93, 1998.
18. Giuseppe Conte, Anna Maria Perdon, David Scaradozzi, Gianluca Morganti, Matteo Rosettani, "Resource Management in Home Automation Systems", MED 10, 2010

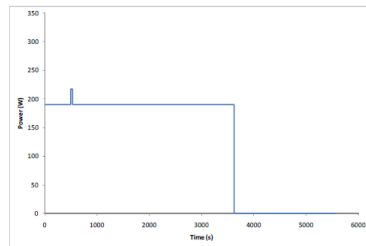


Fig. 1. Dishwasher's load profile.

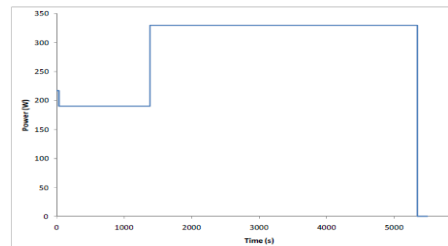


Fig. 2. Washing machine's load profile.

TABLE I
DECENTRALIZED CONTROL ARCHITECTURE - SIMULATION RESULTS

WM	Weights		Δ_S	OL_S	$f(S)$
	DW				
1	1		0.192	2	39.2
2	1		0.456	2	65.6
3	1		0.630	2	83.0
1	2		0.191	2	39.1
1	3		0.191	2	39.1

TABLE II
CENTRALIZED CONTROL ARCHITECTURE - SIMULATION RESULTS

WM	Weights		Δ_S	OL_S	$f(S)$
	DW				
1	1		0.591	1	69.2
2	1		0.722	1	82.2
3	1		0.526	1	62.6
1	2		0.402	1	50.3
1	3		0.195	1	29.6

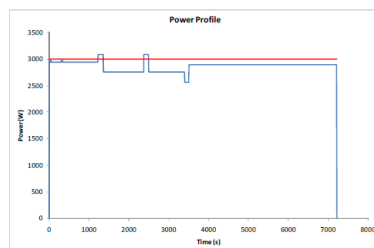


Fig. 3. Consumption profile with distributed control architecture; weights (1,1).

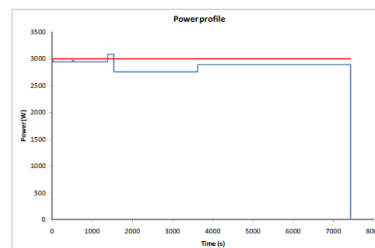


Fig. 4. Consumption profile with centralized control architecture: weights (3,1).

Semi-Markov Disability Insurance Models

Guglielmo D'Amico, Montserrat Guillen and Raimondo Manca

Dipartimento di Scienze del Farmaco,
Università "G. D'Annunzio" of Chieti-Pescara, Chieti, Italy
Email: g.damico@unich.it

Departament d'Econometria, Estadística I Economia Espanyola, RFA-IREA,
Universitat de Barcelona, Spain
Email: mguillen@ub.edu

Dipartimento di Matematica per le decisioni economiche, finanziarie e assicurative,
Università "La Sapienza" di Roma, Roma, Italy
Email: raimondo.manca@uniroma1.it

Abstract: In this paper, we present a stochastic model for disability insurance contracts. The model is based on a discrete time non-homogeneous semi-Markov process to which the backward recurrence time process is joined. This permits to study in a more complete way the disability evolution and to face in a more effective way the duration problem. The use of semi-Markov reward processes gives the possibility of deriving equations of the prospective and retrospective reserves. The model is applied to a sample of contracts drawn at random from a mutual insurance company.

1 Introduction

Non-homogeneous semi-Markov processes (NHSMP) were defined independently by Hoem (1972) and Iosifescu Manu (1972). The approach of Iosifescu Manu was further generalized in Janssen and De Dominicis (1984).

The development of the theory of semi-Markov processes quickly found applications in finance and insurance problems. The reader can find examples in Janssen (1966), Hoem (1972), CMIR (1991), Carravetta et al (1981), Balcer and Sahin (1979, 1986) Janssen and Manca (1997) and, more recently, in the book by Janssen and Manca (2007).

A generalization of the NHSMP transition probabilities is obtained by introducing the initial and final backward times, see D'Amico et al. (2009). The backward time gives the possibility to consider the dependence of the transition probabilities on the time of entrance into a given state.

A detailed description of continuous time homogeneous semi-Markov processes with backward is reported in Limnios and Oprüşan (2001) and in Janssen and Manca (2006). The discrete time non-homogeneous semi-Markov reward process with backward is presented in Stenberg et al (2007).

In this paper we generalize the results obtained by D'Amico et al. (2009) introducing the reward structure. The reward structure gives the possibility to determine equations for the prospective and retrospective mathematical reserves

and a discrete version of the Thiele differential equation in a semi-Markov environment.

To the best of the authors' knowledge, it is the first time that the general formulae of a discrete time NHSMP with rewards and initial and final backward processes are presented together with the corresponding mathematical reserves.

The paper is organized in the following way. Next section presents a short introduction to NHSMP considering initial and final backward recurrence times. Section 3 analyzes semi-Markov reward processes with initial and final backward times. Successively, prospective and retrospective reserves are determined. Section 4 describes the disability data from a mutual insurance company from Catalunya and gives the results obtained by the model with these data.

2 Semi-Markov processes

We follow the notation given in Janssen and Manca (2006). In a semi-Markov process (SMP) environment, two random variables (r.v.) run together. $J_n, n \in \mathbb{N}$, with state space $I = \{1, 2, \dots, m\}$, represents the state at the n -th transition. $T_n, n \in \mathbb{N}$, with state space equal to \mathbb{R}^+ , represents the time of the n -th transition,

$$J_n : \Omega \rightarrow I, \quad T_n : \Omega \rightarrow \mathbb{R}^+.$$

We suppose that the process (J_n, T_n) is a non-homogeneous Markov renewal process and by $\{T_n\}$ we denote the inter-arrival time process. The kernel $\mathbf{Q} = [Q_{ij}(s,t)]$ associated to the Markov renewal process is defined in the following way:

$$Q_{ij}(s,t) = P[J_{n+1} = j, T_{n+1} \leq t \mid J_n = i, T_n = s]$$

and so:

$$p_{ij}(s) = P[J_{n+1} = j \mid J_n = i, T_n = s] = \lim_{t \rightarrow \infty} Q_{ij}(s,t); \quad i, j \in I, \quad s, t \in \mathbb{R}^+, \quad s \leq t.$$

$\mathbf{P}(s) = [p_{ij}(s)]$ is the transition matrix of the embedded non-homogeneous Markov chain.

Furthermore, it is necessary to introduce the probability that the process will leave state i from time s within time t :

$$H_i(s,t) = P[T_{n+1} \leq t \mid J_n = i, T_n = s].$$

Obviously it follows that:

$$H_i(s,t) = \sum_{j=1}^m Q_{ij}(s,t).$$

Now it is possible to define the distribution function of the waiting time in each state i , given that the state successively occupied is known:

$$F_{ij}(s,t) = P[T_{n+1} \leq t | J_n = i, J_{n+1} = j, T_n = s].$$

The related probabilities can be obtained by means of the following formula:

$$F_{ij}(s,t) = \begin{cases} Q_{ij}(s,t) / p_{ij}(s) & \text{if } p_{ij}(s) \neq 0 \\ 1 & \text{if } p_{ij}(s) = 0 \end{cases}.$$

The main difference between a discrete time non-homogeneous Markov process and a DTNHSMP is in the distribution functions $F_{ij}(s,t)$. In a Markov environment, this function has to be a geometric distribution function. Instead, in the semi-Markov case the distribution functions $F_{ij}(s,t)$ may be of any type.

By means of the $F_{ij}(s,t)$ we can take into account the problem given by the duration inside the states. In the disability context, we know that the transition probabilities depend on the time an individual has remained in a certain state level.

Now, let $N(t) = \sup\{n \in \mathbb{N} | T_n \leq t\}$, then the NHSMP $Z(t)$ can be defined as $N(t) = \sup\{n \in \mathbb{N} | T_n \leq t\}$, denoting the state occupied by the process at each time.

The transition probabilities are defined in the following way:

$$\phi_{ij}(s,t) = P[Z(t) = j | Z(s) = i, T_{N(s)} = s].$$

They are obtained by solving the following evolution equations:

$$\phi_{ij}(s,t) = d_{ij}(s,t) + \sum_{\beta=1}^m \sum_{\vartheta=s+1}^t b_{i\beta}(s,\vartheta) \phi_{\beta j}(\vartheta,t) \quad (2.1)$$

where

$$b_{ij}(s,t) = P[J_{n+1} = j, T_{n+1} = t | J_n = i, T_n = s] = \begin{cases} Q_{ij}(s,t) - Q_{ij}(s,t-1) & \text{if } t > s \\ 0 & \text{if } t = s \end{cases}$$

and

$$d_{ij}(s,t) = \begin{cases} 1 - H_i(s,t) & \text{if } i = j \\ 0 & \text{if } i \neq j. \end{cases}$$

The first part of formula (2.1) gives the probability that the system does not have transitions up to the time t given that it entered in the state i at time s . $d_{ij}(s,t)$, in a

disability insurance model represents the probability that the policyholder does not have any new evaluation from the time s up to the time t . This part makes sense if and only if $i=j$.

In the second part of (2.1), $b_{i\beta}(s, \mathcal{G})$ represents the probability that the system enters state β just at time \mathcal{G} given that it entered in the state i at time s . After the transition, the system will go to state j following one of the possible trajectories that go from state β at the time \mathcal{G} and bring the system to be in state j at time t .

There are well known algorithms making possible the solution of equation (2.1), see for example Janssen and Manca (2007).

Definition 1: Let $B(t) = t - T_{N(t)}$ be the backward recurrence time process (see Limnios and Oprisan (2001), Janssen and Manca (2006)).

The backward recurrence time process denotes the time since the occurrence of last transition.

In D'Amico, Guillen and Manca (2009) the following probabilities were defined:

$$\begin{aligned} {}^b\phi_{ij}(l, s; t) &= \mathbb{P}[Z(t) = j | Z(s) = i, B(s) = s - l] \\ &= \mathbb{P}[J_{N(t)} = j | J_{N(s)} = i, T_{N(s)} = l, T_{N(s)+1} > s] \end{aligned} \quad (2.2)$$

$$\begin{aligned} \phi_{ij}^b(s; l', t) &= \mathbb{P}[Z(t) = j, B(t) = t - l' | Z(s) = i] \\ &= \mathbb{P}[J_{N(t)} = j, T_{N(t)} = l', T_{N(t)+1} > t | J_{N(s)} = i, T_{N(s)} = s] \end{aligned} \quad (2.3)$$

Formulae (2.2) and (2.3) represent the semi-Markov transition probabilities with initial and final backward recurrence time respectively.

In (2.2) we know that at time s the system is in the state i . We know also that it entered in this state at time l and $s-l$ represents the initial backward time. Then we are looking for the probability to be in the state j at time t .

In (2.3) we know that the system entered in the state i at time s . In this case we are interested in the probability to be in the state j at time t with the entrance in this state at time l' . The final backward time is $t-l'$.

Putting the two cases together we obtain the transition probabilities with initial and final backward times:

$$\begin{aligned} {}^b\phi_{ij}^b(l, s; l', t) &= \mathbb{P}[Z(t) = j, B(t) = t - l' | Z(s) = i, B(s) = s - l] = \\ &= \mathbb{P}[J_{N(t)} = j, T_{N(t)} = l', T_{N(t)+1} > t | J_{N(s)} = i, T_{N(s)} = l, T_{N(s)+1} > s] \end{aligned} \quad (2.4)$$

In Figure 1 a trajectory of an NHSMP with initial and final backward times is reported. In this figure we have that $N(s) = n$, $N(t) = h - 1$, the starting backward $B(s) = s - T_n = s - l$ and the final backward $B(t) = t - T_{h-1} = t - l'$.

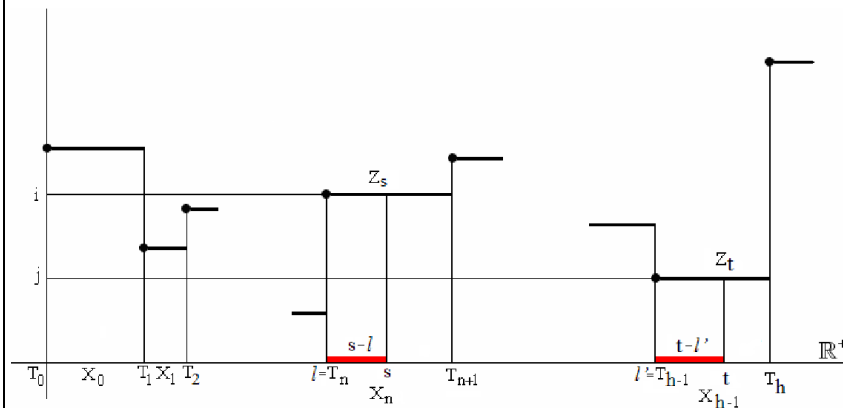


Figure 1: Initial and final backward trajectory

To present the evolution equations of probabilities (2.2), (2.3) and (2.4) we introduce the following notation:

$$d_{ij}(l, s; t) = \begin{cases} \frac{1 - H_i(l, t)}{1 - H_i(l, s)} & \text{if } i = j \\ 0 & \text{if } i \neq j \end{cases}$$

which represents the probability to have no transition from state i between times l and t given that no transition occurred from state i between times l and s .

Moreover by

$$b_{ij}(l, s; t) = \frac{b_{ij}(l, t)}{1 - H_i(l, s)}$$

we denote the probability to make next transition from state i to state j from time l to time t given that the system does not make transitions from state i between times l and s .

The relations (2.5), (2.6) and (2.7) represent the evolution equations of (2.2), (2.3) and (2.4) respectively:

$${}^b\phi_{ij}(l, s; t) = d_{ij}(l, s; t) + \sum_{\beta=1}^m \sum_{\vartheta=s+1}^t b_{i\beta}(l, s; \vartheta) \phi_{\beta j}(\vartheta, t), \quad (2.5)$$

$$\phi_{ij}^b(s; l', t) = d_{ij}(s, t) \mathbf{1}_{\{l'=s\}} + \sum_{\beta=1}^m \sum_{\vartheta=s+1}^{l'} b_{i\beta}(s, \vartheta) \phi_{\beta j}^b(\vartheta; l', t), \quad (2.6)$$

where $\mathbf{1}_{\{l'=s\}} = 1$ if and only if $l' = s$.

$${}^b\phi_{ij}^b(l, s; l', t) = d_{ij}(l, s; t) \mathbf{1}_{\{l'=l\}} + \sum_{\beta=1}^m \sum_{\vartheta=s+1}^{l'} b_{i\beta}(l, s; \vartheta) \phi_{\beta j}^b(\vartheta; l', t). \quad (2.7)$$

Expression (2.5) provides the probability that the system is in the state j at time t given that it was in the state i at time s and entered in this state at time l . If in (2.5) $l = s$ then we recover the equation (2.1).

Expression (2.6) gives the probability that the system will arrive in the state j just at time l' and will remain in this state, without any other transition, up to time t given that it entered at time s in state i . The part $d_{ij}(s; t) \mathbf{1}_{\{l'=s\}}$ of (2.6) represents the probability not to have a transition from time s to time t . Consequently the final backward time $t - l'$ must be exactly equal to $t - s$ and it has sense only if $i = j$. The second part of (2.6) means that the system does not move from time s to time ϑ and that, just at this time, it jumps to state β . Afterwards, following one of the possible trajectories, the system arrives in state j just at time l' and does not move from this state at least up to time t .

Remark 1. It should be noted that considering all the possible final backward process values we recover the transition probabilities (2.1) that is:

$$\phi_{ij}(s, t) = \sum_{l'=s}^t \phi_{ij}^b(s; l', t).$$

Expression (2.7) gives the probability that the system entered in the state j at time l' and remained inside this state without any other transition up to the time t given that it entered in the state i at time l and it did not move up to s . The term $d_{ij}(l, s; t) \mathbf{1}_{\{l'=l\}}$ gives the probability not to have transitions from l to t outside state i given that no transition occurred from l to s . This probability contributes only if $i = j$ and $l' = l$. The second part of (2.7) represents the probability to make next transition from i at time l to whatever state β at whatever time ϑ and then to

move following whatever trajectory which make provision for the entrance in j at time l' with no transition up to time t . This probability is conditioned on the permanence of the system in i from time l up to time s .

Remark 2. Relation (2.7) is a mixture of (2.5) and (2.6). This last evolution equation is the one used to construct the model for the disability insurance. This kind of model was suggested by Haberman and Pitacco (1999) but there were no formulae to the problem, or they were not presented.

3 Semi-Markov reward processes with backward times

Now we introduce the reward structure. A permanence reward $\psi_i(s, t)$ is paid when the process visits state i at time t for a contracts starting at time s . An impulse reward $\gamma_{ij}(s, t)$ is paid due to the transition from state i to state j at time t for a contracts starting at time s . We assume that permanence and impulse rewards are amount of money. They have to be discounted using a discrete time non-homogeneous discount factor $v(s, t)$.

Following the line of research in Stenberg et al. (2007) we define the accumulated reward process with initial and final backward times by means of the following relation:

Definition 2. Let $\xi_{ij}(l, s; l', t)$ be the discounted accumulated semi-Markov reward process with initial and final backward times, defined by

$$\begin{aligned} \xi_{ij}(l, s; l', t) = & \chi(T_{N(s)+1} > t | J_{N(s)} = i, T_{N(s)} = l, T_{N(s)+1} > s) \delta_{ij} \chi(l' = l) \left[\sum_{\tau=s+1}^t \psi_i(s, \tau) v(s, \tau) \right] \\ & + \sum_{k \in I} \sum_{\theta=s+1}^{l'} \chi(J_{N(s)+1} = k, T_{N(s)+1} = \theta | J_{N(s)} = i, T_{N(s)} = l, T_{N(s)+1} > s) \cdot \\ & \left[\sum_{\tau=s+1}^{T_{N(s)+1}} \psi_i(s, \tau) v(s, \tau) + v(s, T_{N(s)+1}) \left(\gamma_{i, J_{N(s)+1}}(s, T_{N(s)+1}) + \xi_{J_{N(s)+1}, j}(T_{N(s)+1}, T_{N(s)+1}; l', t) \right) \right]. \end{aligned} \quad (3.1)$$

The process $\xi_{ij}(l, s; l', t)$ describes the discounted total amount of money accumulated from time s up to time t considering that the semi-Markov process will be in state j at time t with entrance in this state at time l' (final backward equal to $t-l'$) given that at time s it was in state i with entrance in this state at time l (initial backward equal to $s-l$).

Let us denote by ${}^bV_{ij}^b(l, s; l', t) = E[\xi_{ij}^b(l, s; l', t)]$. To compute the expectation of (3.1) we have to consider that:

- i)
$$E\left[\chi\left(T_{N(s)+1} > t \mid J_{N(s)} = i, T_{N(s)} = l, T_{N(s)+1} > s\right)\right] =$$
- ii)
$$P\left(\chi\left(T_{N(s)+1} > t \mid J_{N(s)} = i, T_{N(s)} = l, T_{N(s)+1} > s\right)\right) = \left(\frac{1-H_i(l, t)}{1-H_i(l, s)}\right);$$
- iii)
$$\chi\left(J_{N(s)+1} = k, T_{N(s)+1} = \theta \mid J_{N(s)} = i, T_{N(s)} = l, T_{N(s)+1} > s\right)$$
 and $\xi_{J_{N(s)+1}, j}\left(T_{N(s)+1}, T_{N(s)+1}; l', t\right)$ are independent random variables ;
- iii)
$$E\left[\chi\left(J_{N(s)+1} = k, T_{N(s)+1} = \theta \mid J_{N(s)} = i, T_{N(s)} = l, T_{N(s)+1} > s\right)\right] = \frac{b_{ik}(s-l, \theta)}{1-H_i(s-l, s)}$$

by taking expectation in (3.1) we get the following equation:

$${}^bV_{ij}^b(l, s; l', t) = \chi(l' = l) d_{ij}(l, s; t) \left[\sum_{\tau=s+1}^t \psi_i(s, \tau) v(s, \tau) \right] + \sum_{k \in I} \sum_{\theta=s+1}^{l'} b_{ik}(l, s; \theta) \left[\sum_{\tau=s+1}^{\theta} \psi_i(s, \tau) v(s, \tau) + \gamma_{i,k}(s, \theta) v(s, \theta) + {}^bV_{kj}^b(\theta, \theta; l', t) v(s, \theta) \right].$$

(3.2)

Equation (3.2) is the evolution equation representing the actuarial value of the total rewards accumulated in the interval $[s, t]$.

Following the approach of Stemberg et al (2007) it is possible to derive recursive equations for the higher order moments of the reward process $\xi_{ij}^b(l, s; l', t)$.

It should be noted that equation (3.2) makes provision in a complete way of the duration dependence by using the backward process at initial and final times simultaneously. Moreover the process considers also the final state j and this would be also an advantage in defining the retrospective reserve (see subsection below).

There are some interesting particular cases of equation (3.2). First of all we can ignore the duration effects on the starting state by not considering the initial backward value. In this case, by putting $B(s) = 0$ we obtain the following definition:

Definition 3. Let $\xi_{ij}(s; l', t)$ be the discounted accumulated semi-Markov reward process with final backward time, defined by

$$\begin{aligned} & \xi_{ij}(s; l', t) \\ &= \chi(T_{N(s)+1} > t \mid J_{N(s)} = i, T_{N(s)} = s, T_{N(s)+1} > s) \delta_{ij} \chi(l' = s) \left[\sum_{\tau=s+1}^t \psi_i(s, \tau) v(s, \tau) \right] \\ &+ \sum_{k \in I} \sum_{\theta=s+1}^{l'} \chi(J_{N(s)+1} = k, T_{N(s)+1} = \theta \mid J_{N(s)} = i, T_{N(s)} = s, T_{N(s)+1} > s) \cdot \\ &\left[\sum_{\tau=s+1}^{T_{N(s)+1}} \psi_i(s, \tau) v(s, \tau) + v(s, T_{N(s)+1}) \left(\gamma_{i, J_{N(s)+1}}(s, T_{N(s)+1}) + \xi_{J_{N(s)+1}, j}(T_{N(s)+1}; l', t) \right) \right]. \end{aligned} \quad (3.3)$$

If we denote by $V_{ij}^b(s; l', t) = E[\xi_{ij}(s; l', t)]$, by taking the expectation of (3.3) we have:

$$\begin{aligned} V_{ij}^b(s; l', t) &= \delta_{ij} \chi(l' = s) (1 - H_i(s, t)) \left[\sum_{\tau=s+1}^t \psi_i(s, \tau) v(s, \tau) \right] \\ &+ \sum_{k \in I} \sum_{\theta=s+1}^{l'} b_{ik}(s, \theta) \left[\sum_{\tau=s+1}^{\theta} \psi_i(s, \tau) v(s, \tau) + \gamma_{i,k}(s, \theta) v(s, \theta) + \xi_{k,j}(\theta; l', t) v(s, \theta) \right]. \end{aligned} \quad (3.4)$$

If we ignore the duration effects on the arriving state by not considering the final backward value and we do not take care for the arriving state j we have the process $\xi_i(l, s; t)$. It represents the discounted accumulated semi-Markov reward process with initial backward time. This process has been defined and analyzed by Stenberg et al (2007).

3.1 Prospective reserves

^{3.2} Let us assume that the policy is issued at time s in state $Z(s)=i$ of the semi-Markov chain with backward value $B(s)=s-l$. Premiums and benefits for the policy are paid by the insured and by the insurer depending on the state of the disability degree.

The permanence reward $\psi_i(s, t)$ considers the payment of a premium or a benefit due to the occupancy of state i at time t for a contract starting at time s .

The impulse reward $\gamma_{ij}(s, t)$ can be used to consider an insurance benefit or lump sum.

In general the prospective premium reserve is defined as the expected value of the loss function, see Wolthuis (2003). In our case the random process $\xi_{ij}(l, s; l', t)$

represents the discounted accumulated rewards process with initial and final backward values and expresses the difference between future benefits and premium payments with constraints on the duration in the starting and arriving states. Consequently $\xi_{ij}(l, s; l', t)$ is a constrained loss function and its expectation represents the prospective reserve with full backward information. A particular case of ${}^bV_{ij}^b(l, s; l', t)$ is ${}^bV_{ij}(l, s; t)$ which is the prospective reserve with initial backward.

In life insurance generally the policy terminates with the death of the policyholder. The death occurs at a random time, for this reason the prospective reserves is considered for $t \rightarrow \infty$, see for example Wolthuis (2003).

Let denote by $\xi_i(l, s) = \xi_i(l, s; \infty)$. By conditioning on the state at time $s+l$ we have:

$$\begin{aligned} \xi_i^*(l, s) &= \chi(T_{N(s)+1} > s+1 | J_{N(s)} = i, T_{N(s)} = l, T_{N(s)+1} > s) [\psi_i(s, s+1)v(s, s+1) + \xi_i^*(l, s+1)] \\ &+ \sum_{k \neq l} \chi(J_{N(s)+1} = k, T_{N(s)+1} = s+1 | J_{N(s)} = i, T_{N(s)} = l, T_{N(s)+1} > s) \cdot \\ &[\psi_{J_{N(s)+1}}(s, T_{N(s)+1})v(s, T_{N(s)+1}) + \gamma_{i, J_{N(s)+1}}(s, T_{N(s)+1})v(s, T_{N(s)+1}) + \xi_{J_{N(s)+1}}^*(T_{N(s)+1}, T_{N(s)+1})v(s, T_{N(s)+1})]. \end{aligned} \quad (3.5)$$

If we denote by $W_i(l, s) = E[\xi_i(l, s)]$, by taking the expectation of (3.5), by applying similar arguments to i), ii) and iii) we obtain

$$\begin{aligned} W_i(l, s) &= \left(\frac{1 - H_i(s-l, s+1)}{1 - H_i(s-l, s)} \right) [\psi_i(s, s+1) + W_i(l, s+1)]v(s, s+1) \\ &+ \sum_{k \neq l} \left(\frac{b_{ik}(s-l, s+1)}{1 - H_i(s-l, s)} \right) [\psi_k(s, s+1) + \gamma_{i,k}(s, s+1) + W_k(s+1, s+1)]v(s, s+1) \end{aligned} \quad (3.6)$$

Equation (3.6) expresses the change of the prospective reserve for state i at time s with duration $s-l$ from time s to time $s+l$. Therefore it can be seen as a generalization of the Thiele differential equation for a disability insurance contract described by a non-homogeneous semi-Markov chain.

3.2 Retrospective reserves

In general retrospective reserves are defined as the expected discounted value of past premiums minus past benefits.

There are different definitions of retrospective reserves. Here we consider the conditional retrospective reserve defined by Norberg (1990) and we adapt it to our general framework.

For the retrospective reserve notation see Janssen, Manca and Volpe di Prignano (2009).

Let us denote the conditional retrospective premium reserve relative to the period $[s, t]$ with initial and final backward values by ${}^bM_{ij}^b(l, s; l', t)$.

We assume that the function ${}^bM_{ij}^b(l, s; l', t)$ satisfy for all states i, j and times $l \leq s \leq l' \leq t$ the following relation:

$$v(s, t) {}^b\phi_{ij}^b(l, s; l', t) {}^bM_{ij}^b(l, s; l', t) = -{}^bV_{ij}^b(l, s; l', t) \quad (3.7)$$

from which we get

$${}^bM_{ij}^b(l, s; l', t) = -{}^bV_{ij}^b(l, s; l', t) \frac{1}{v(s, t) {}^b\phi_{ij}^b(l, s; l', t)} \quad (3.8)$$

If ${}^b\phi_{ij}^b(l, s; l', t) = 0$ we set ${}^bM_{ij}^b(l, s; l', t) = 0$.

Notice that it is possible to derive recursive equation for the retrospective reserves by using relation (3.2) and (3.6) for the prospective reserves.

4 Real data numerical example

The model has the following four states:

W – active; 2) P – pensioner; 3) Di – disabled; 4) De – dead

interrelated as indicated In Figure 2.

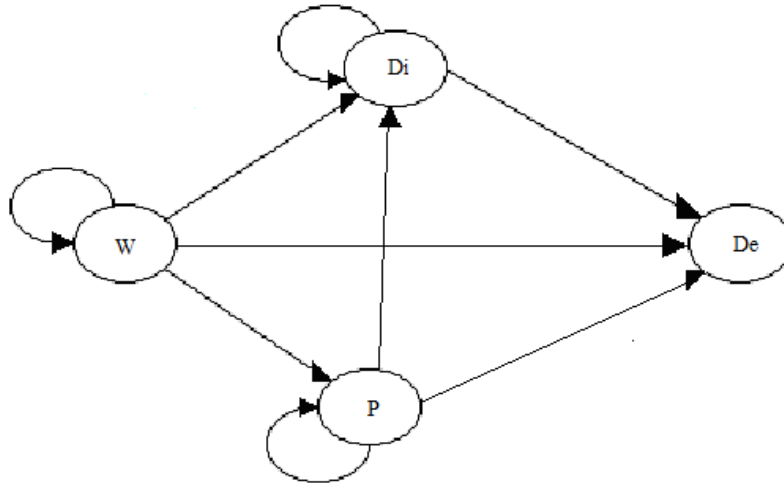


Figure 2: Graph of the disability model

It is well known that transition probabilities from the disabled state are function of the duration in the current state (see Haberman and Pitacco (1999)). In the SMP environment this aspect is considered but the (2.1) solution is not sensitive to the duration aspect. The introduction of the backward process as in (2.7) permits to manage transition probabilities that depend on the initial and final durations.

The data analyzed come from a sample of contracts drawn at random from a mutual insurance company from Catalunya. 150,000 insurance contracts are analysed and 2,800 LTC spells are observed for a large period from 1975 to 2005. In order to simplify the model, we chose to work with a five year interval.

Owing to lack of space, we do not show the kernel estimates and other results, but we can make them available upon request. We would only to point that, as it is possible to see in Figure 3, the transition probability values change in function of both the initial and final backward times, so the model results to be sensitive to both backward times.

In all histograms W is the starting state. The blue colour reports the results in absence of initial backward ($IBk=0$), the red colour the case with 1 year of initial backward recurrence time ($IBk=1$). The first observation is that the probability distribution is spread among the final backward recurrence times (for example in the south west histogram $FBk=0, 1, 2$ and 3) and the arriving states. Indeed, in the north-west part there are eight possible events with arriving time equal to starting time plus one ($AT=ST+1$), four in the case of final backward time equal to 1 and

four with final backward time equal to 0. In the north-east, with arriving time equal to starting time plus two ($AT=ST+2$), there are twelve possible cases, four for each different final backward time and so on. The first blue and red bars of each histogram represent the probability to stay in the starting state; it decreases in function of the arriving time. It is also interesting to observe that the shape of the histograms changes in function of both the initial and final backward times, so the model results to be sensitive to both backward times.

To help the Figure 3 understanding the first two bars of the first histogram represent respectively the probabilities $b_{11}^b(0,0;0,1)$, $b_{11}^b(0,1;1,2)$

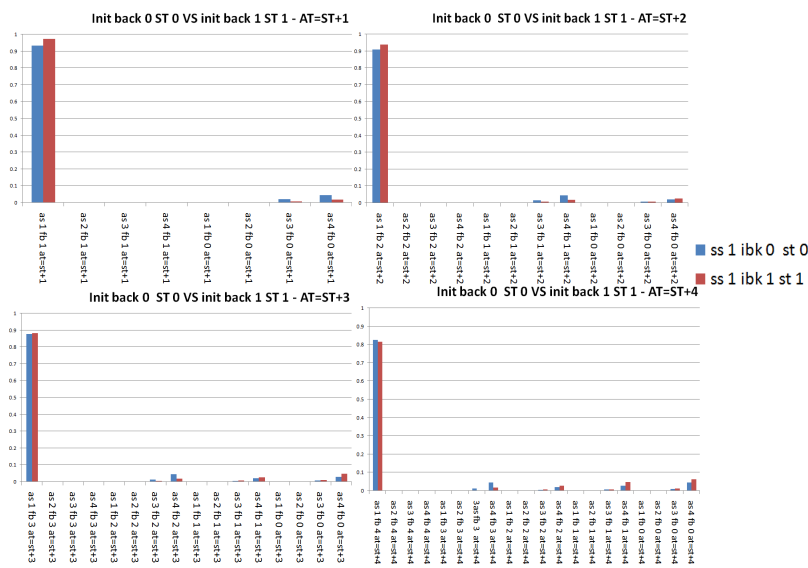


Figure 3: comparison between initial and final recurrence backward times

The same behaviour is translated to the accumulated reward process. We assumed the following reward structure:

$$\psi_W(s,t) = -5000, \psi_P(s,t) = 15000, \psi_{Di}(s,t) = 30000, \gamma_{W,Di}(s,t) = \gamma_{P,Di}(s,t) = 2000$$

Final backward	$V_1(0,3;l^*,10)$	$V_1(1,3;l^*,10)$	$V_1(2,3;l^*,10)$	$V_1(3,3;l^*,10)$
$l^*=3$	-4622.85	-8392.82	-11732.10	-13395.30
$l^*=4$	-420821.00	-424019.00	-426845.00	211.25
$l^*=5$	-415040.00	-417212.00	-419330.00	-1537.27
$l^*=6$	-401852.00	-402520.00	-403586.00	-8536.55
$l^*=7$	-371546.00	-370686.00	-369788.00	-20629.00
$l^*=8$	-291318.00	-285725.00	-279689.00	-23346.60

$l^*=9$	-131829.00	-125292.00	-115690.00	-20180.90
$l^*=10$	-3209.33	-11431.30	-15806.30	-17031.90

Table 1: expected accumulated reward values

Table 1 shows the dependence of the accumulated reward process in function of the initial and final backward. In fact, by comparing two columns we see different expected reward values due to different initial backward values. By comparing two rows we see the effects due to different final backward values.

References

- 1 Balcer, Y., Sahin, I., 1979. Stochastic models for a pensionable service. *Operations Research*, 27, 888-903.
- 2 Balcer, Y, Sahin, I., 1986. Pension accumulation as a semi-Markov reward process, with applications to pension reform. In Janssen J. (Ed). *Semi-Markov models*, Plenum N.Y.
- 3 Carravetta M., De Dominicis R., Manca R., 1981. Semi-Markov stochastic processes in social security problems. *Cahiers du C.E.R.O.*, 23, 333-339.
- 4 CMIR12, 1991 (Continuous Mortality Investigation Report, number 12). The analysis of permanent health insurance data. The Institute of Actuaries and the Faculty of Actuaries.
- 5 D'Amico, G., Guillen, M. and Manca, R. (2009). Full backward non-homogeneous semi-Markov processes for disability insurance models: a Catalunya real data application. *Insurance: Mathematics and Economics*, 45, 173-179.
- 6 Haberman S., Pitacco E. (1999). *Actuarial models for disability insurance*. Chapman & Hall.
- 7 Hoem, J.M., 1972. Inhomogeneous semi-Markov processes, select actuarial tables, and duration-dependence in demography, in T.N.E. Greville, *Population, Dynamics*, Academic Press, 251-296.
- 8 Iosifescu Manu A., 1972. Non homogeneous semi-Markov processes, *Stud. Lere. Mat.* 24, 529-533.
- 9 Janssen, J., 1966. Application des processus semi-markoviens à un problème d'invalidité, *Bulletin de l'Association Royale des Actuaries Belges*, 63, 35-52.
- 10 Janssen, J., De Dominicis R., 1984. Finite non-homogeneous semi-Markov processes. *Insurance: Mathematics and Economics*, 3, 157-165.
- 11 Janssen J., Manca R., 1997. A realistic non-homogeneous stochastic pension funds model on scenario basis. *Scandinavian Actuarial Journal* 113-137.

- 12 Janssen J., Manca R., 2006. Applied semi-Markov processes. Springer.
- 13 Janssen J., Manca R., 2007. Semi-Markov Risk Models for Finance, Insurance and Reliability. Springer.
- 14 Janssen J., Manca R., Volpe di Prignano, E., 2009. Mathematical Finance. ISTE Wiley.
- 15 Limnios, N., Oprişan, G., 2001. Semi-Markov Processes and Reliability. Birkhauser, Boston.
- 16 Norberg, R., 1990. Payment measures, interest and discounting an axiomatic approach with application to insurance. Scandinavian Actuarial Journal, 1-22.
- 17 Stenberg F., Manca R., Silvestrov D., 2007. An algorithmic approach to discrete time non-homogeneous backward semi-Markov reward processes with an application to disability insurance. Methodology and Computing in Applied Probability, 9, 497-519.
- 18 Wolthuis, H., 2003. Life Insurance Mathematics (The Markovian Model), second edition, Instituut voor Actuarie en Econometrie, Amsterdam.

Some Dimension Reduction Methods in non-parametric spatial modelling

Sophie Dabo-Niang¹ Jean-Michel Loubes² and Anne-Françoise Yao³

¹ Laboratoire EQUIPPE, University Lille 3
Domaine du pont de bois, BP 60149,
59653 Villeneuve d'ascq cedex, France.
(e-mail: sophie.dabo@univ-lille3.fr)

² University Toulouse 3, Institut de Mathématiques de Toulouse
Equipe de Statistique et Probabilités
route de Narbonne, 31062 Toulouse.
(e-mail: loubes@math.univ-toulouse.fr)

³ Laboratoire LMGEM, University Aix-Marseille 2
Campus de Luminy, case 901, 13288Marseille cedex 09.
(e-mail: anne-francoise.yao@univmed.fr)

Abstract. Let $Z_{\mathbf{i}} = (X_{\mathbf{i}}, Y_{\mathbf{i}})$, $\mathbf{i} \in \mathbb{N}^N$ ($N \geq 1$) a spatial random field. In this work, we deal with the problem of estimation of the *regression* of the $Y_{\mathbf{i}}$'s given respectively the $X_{\mathbf{i}}$ in dimension reduction setting. We suppose that the $Z_{\mathbf{i}}$'s have the same distribution as a variable $Z = (X, Y)$, where Y is a real-valued and integrable variable and X valued in a separable space \mathcal{E} (of eventually infinite dimension).

Keywords: Random fields, Spatial statistic, Functional data analysis, Dimension reduction.

1 Introduction

In many areas: geology, oceanography, econometrics, soil science, epidemiology, physics, environment, risk management, image processing, the data are spatially dependent (see e.g. [12], [4] or [6]). Then their treatment requires specific tools provided by spatial statistic.

In this setting, unlike the parametric case, nonparametric spatial regression is only tackled in a few papers, among them see for instance [10], [3], or [5]. Their results show that, as in the *i.i.d.* case, the spatial nonparametric estimator of the regression function is penalized by the dimension of the regressor. Then, we propose the estimation of the regression function $m(x) = \mathbf{E}(Y|X = x)$ using some dimension reduction methods. Under the assumption: that there exist Φ a mapping from \mathcal{E} to \mathbb{R}^D , with D as *small* as possible, and a function $g : \mathbb{R}^D \rightarrow \mathbb{R}$, an unknown function such that the function $m(\cdot)$ can be written as

$$m(x) = g(\Phi .x). \quad (1)$$

Actually, Model (1) conveys the idea that “less information on X ”, $\Phi .X$, gives as much information on $m(\cdot)$ as X . The function g thus becomes the

regression function of Y given the D dimensional vector $\Phi.X$. Estimating the matrix Φ and then the function g (by nonparametric methods) provides an estimator which converges faster than the estimator of the direct nonparametric estimator of m .

In this paper we propose two methods of estimation of Model (1) when X is a finite dimensional space in Section 2 and secondly when X is a high-dimensional random variable (such as a curve).

The next section is devoted to general setting and notations.

2 General setting and notations

We are dealing with a measurable strictly stationary spatial process $Z_{\mathbf{i}} = (X_{\mathbf{i}}, Y_{\mathbf{i}})$, $\mathbf{i} \in \mathbb{N}^N$ ($N \geq 1$), defined on a probability space $(\Omega, \mathcal{A}, \mathbf{P})$ which is such that: the $Z_{\mathbf{i}}$'s have the same distribution as a variable $Z = (X, Y)$, where Y is a real-valued and integrable variable and X valued in \mathbb{R}^d . In what follows, we will denote by μ the probability distribution of X , by $\nu_{\mathbf{i}, \mathbf{j}}$ the joint probability distribution of $(X_{\mathbf{i}}, X_{\mathbf{j}})$ ($\forall \mathbf{i}, \mathbf{j}$). The letter in bold $\mathbf{i} = (i_1, \dots, i_N) \in \mathbb{Z}^N$ is referred as a site, $\|\cdot\|$ will denote any norm over \mathbb{Z}^N , C an arbitrary constant. We will write $\mathbf{n} \rightarrow +\infty$ if $\min_{k=1, \dots, N} n_k \rightarrow +\infty$ and we set $\hat{\mathbf{n}} = n_1 \times \dots \times n_N$.

We aim to estimate Model (1) from observations of process $Z_{\mathbf{i}} = (X_{\mathbf{i}}, Y_{\mathbf{i}})$, on a lattice of \mathbb{R}^N . Without the lost of generality, we assume this latter lattice is a rectangular set $\mathcal{I}_{\mathbf{n}} = \{\mathbf{i} = (i_1, \dots, i_N) \in \mathbb{N}^N, 1 \leq i_k \leq n_k, k = 1, \dots, N\}$, $\mathbf{n} \in (\mathbb{N}^*)^N$. We measure the spatial dependency using an α -mixing condition. For $\mathcal{B}(S)$ (*resp.* $\mathcal{B}(S')$) denotes the Borel σ -fields generated by $(Z_{\mathbf{i}}, \mathbf{i} \in S)$ (*resp.* $(Z_{\mathbf{i}}, \mathbf{i} \in S')$), let $\alpha(\mathcal{B}(S), \mathcal{B}(S')) = \sup_{A \in \mathcal{B}(S), B \in \mathcal{B}(S')} |P(B \cap A) - P(B)P(A)|$. Then a field $(Z_{\mathbf{i}})$ is said to satisfy a *mixing condition* if there exists a function $\mathcal{X} : \mathbb{R}^+ \rightarrow \mathbb{R}^+$ with $\mathcal{X}(t) \downarrow 0$ as $t \rightarrow \infty$, such that for all $S, S' \subset (\mathbb{N}^*)^N$,

$$\alpha(\mathcal{B}(S), \mathcal{B}(S')) \leq \psi(\text{Card}S, \text{Card}S') \mathcal{X}(d(S, S')) \quad (2)$$

where $\text{Card}S$ (*resp.* $\text{Card}S'$) is the cardinality of S (*resp.* S'), $d(S, S')$ the Euclidean distance between S and S' , and $\psi : \mathbb{N}^2 \rightarrow \mathbb{R}^+$ is a symmetric positive function nondecreasing in each variable. In this paper we will deal with the strong mixing case, defined as $\psi \equiv 1$ and consider two main cases, the polynomial case where $\forall u \in \mathbb{R}^+, \chi(u) \leq Cu^{-\theta}$, for some $\theta > 0$, and also the geometrically strong mixing case (GSM) characterized by $\chi(u) \leq C\rho^u$, for some $\rho \in (0, 1)$.

3 An inverse regression model in spatial setting

In this Section, we deal with the case where $\mathcal{E} = \mathbb{R}^d$. An estimation of Φ is done through an estimation of his range $\text{Im}(\Phi^T)$ (where Φ^T is the transpose of Φ) called *Effective Dimensional Reduction space* (EDR).

Various methods for dimension reduction exist in the literature for *i.i.d* observations, see for instance the additive models [8]). Here, we aim at generalizing the *inverse regression* method, proposed in [9] to spatial models. Roughly speaking, its work relies on an estimate of the variance of the inverse regression, $\Sigma_e := \mathbf{var}(\mathbf{E}(X|Y))$ which warrants a good estimation of the EDR space. In his initial version, Li suggested an estimator based on the regressogram estimate of $\mathbf{E}(X|Y)$ but the drawbacks of this estimator led other authors to suggest alternatives based on the nonparametric estimation of $\mathbf{E}(X|Y)$ to recover the optimal rate of convergence in \sqrt{n} . Here, we propose a spatial counterpart under strong mixing conditions of the estimating method of [13] which uses a kernel estimation of $\mathbf{E}(X|Y)$.

3.1 Estimation of the covariance of Inverse Regression Estimator

We solve the problem of estimation in three main step:

1. Estimation of $\mathbf{E}(X|Y)$
2. Estimation of $\Sigma_e = \mathbf{var} \mathbf{E}(X|Y)$ and $\Sigma = \mathbf{var} X$ (we assume the existence of both matrix).
3. Computing Principal Component Analysis of the estimation $\Sigma^{-1} \Sigma_e$

In the following, without the lost of generality, we will assume that X is centred.

Step 1 is based on spatial kernel regression estimation:

$$r_{\mathbf{n}}(y) = \begin{cases} \frac{\varphi_{\mathbf{n}}(y)}{\hat{f}_{\mathbf{n}}(y)} & \text{if } f_{\mathbf{n}}(y) \neq 0, \\ \frac{1}{\hat{\mathbf{n}}} \sum_{i \in \mathcal{I}_{\mathbf{n}}} Y_i & \text{if } f_{\mathbf{n}}(y) = 0, \end{cases}$$

with for all $y \in \mathbb{R}$,

$$f_{\mathbf{n}}(y) = \frac{1}{\hat{\mathbf{n}} h_{\mathbf{n}}} \sum_{i \in \mathcal{I}_{\mathbf{n}}} K\left(\frac{y - Y_i}{h_{\mathbf{n}}}\right)$$

$$\varphi_{\mathbf{n}}(y) = \frac{1}{\hat{\mathbf{n}} h_{\mathbf{n}}} \sum_{i \in \mathcal{I}_{\mathbf{n}}} X_i K\left(\frac{y - Y_i}{h_{\mathbf{n}}}\right),$$

where $f_{\mathbf{n}}$ is a kernel estimator of the density, $K : \mathbb{R}^d \rightarrow \mathbb{R}$ is a bounded integrable kernel such that $\int K(x) dx = 1$ with bandwidth $h_{\mathbf{n}} \geq 0$ is such that $\lim_{n \rightarrow +\infty} h_{\mathbf{n}} = 0$.

We can now define the kernel-type estimator of Σ_e

$$\Sigma_{e,\mathbf{n}} = \frac{1}{\hat{\mathbf{n}}} \sum r_{\mathbf{n}}(Y_i) r_{\mathbf{n}}(Y_i)^T - \bar{X} \bar{X}^T. \quad (3)$$

where $\bar{X} = \frac{1}{\hat{\mathbf{n}}} \sum_{i \in \mathcal{I}_{\mathbf{n}}} X_i$.

In the following, we will provide the asymptotic behaviour of this estimate.

Once the variance of the inverse regression is estimated, the methodology described in [9] can be used to estimate the EDR space. More precisely, if

X is such that for all vector b in \mathbb{R}^d , there exists a vector B of \mathbb{R}^D such that $\mathbf{E}(b^T X | \Phi.X) = B^T(\Phi.X)$ (this latter condition is satisfied as soon as X is elliptically distributed), then, if Σ denotes the variance of X , the space $\text{Im}(\Sigma^{-1} \mathbf{var}(\mathbf{E}(X|Y)))$ is included into the *EDR space*. Moreover, the two spaces coincide if the matrix $\Sigma^{-1} \mathbf{var}(\mathbf{E}(X|Y))$ is of full rank. Hence, the estimation of the *EDR space* is essentially based on the estimation of the covariance matrix of the *inverse regression* $\mathbf{E}(X|Y)$ and Σ which is estimated by using a classical empirical estimator.

3.2 Weak consistency

In this section, we will make the following technical assumptions

$$\left\| \frac{r(Y)}{f(Y)} \right\|_{4+\delta_1} < \infty, \text{ for some } \delta_1 > 0 \quad (4)$$

and

$$\left\| \frac{r(Y)}{f(Y)} \mathbf{1}_{\{f(Y) \leq e_n\}} \right\|_2 = \mathcal{O} \left(\frac{1}{\hat{\mathbf{n}}^{\frac{1+\delta}{2}}} \right). \text{ for some } 1 > \delta > 0. \quad (5)$$

We also assume some regularity conditions on the functions: $K(\cdot)$, $f(\cdot)$ and $r(\cdot)$:

- The kernel function $K(\cdot) : \mathbb{R} \rightarrow \mathbb{R}^+$ is a k -order kernel with compact support and satisfying a Lipschitz condition $|K(x) - K(y)| \leq C|x - y|$
- $f(\cdot)$ and $r(\cdot)$ are functions of $C^k(\mathbb{R})$ ($k \geq 2$) such that $\sup_y |f^{(k)}(y)| < C_1$ and $\sup_y \|\varphi^{(k)}(y)\| < C_2$ for some constants C_1 and C_2 .

Set $\Psi_n = h_n^k + \frac{\sqrt{\log \hat{\mathbf{n}}}}{\sqrt{\hat{\mathbf{n}} h_n}}$.

Theorem 1. Assume that we have: $\alpha(t) \leq Ct^{-\theta}$, $t > 0$, $\theta > 2N$ and $C > 0$. If $\psi : v \mapsto \mathbf{E}(\|X\|^2 | Y = v)$ is continuous. Then for a choice of h_n such that $\hat{\mathbf{n}} h_n^3 (\log \hat{\mathbf{n}})^{-1} \rightarrow 0$ and $\hat{\mathbf{n}} h_n^{\theta_1} (\log \hat{\mathbf{n}})^{-1} \rightarrow \infty$ with $\theta_1 = \frac{4N+\theta}{\theta-2N}$, we get

$$\Sigma_{e,n} - \Sigma_e = \mathcal{O}_p \left(h_n^k + \frac{\Psi_n^2}{e_n^2} \right).$$

Corollary 1. Choosing $h \simeq n^{-c_1}$, $e_n \simeq n^{-c_2}$ for some positive constants c_1 and c_2 such that $\frac{c_2}{k} + \frac{1}{4k} < c_1 < \frac{1}{2} - 2c_2$, leads to

$$\Sigma_{e,n} - \Sigma_e = o_p \left(\frac{1}{\sqrt{\hat{\mathbf{n}}}} \right). \quad (6)$$

3.3 Applications

Using the spatial dependency in practice

Thanks to the stationarity of the process, it suffices to compute the estimators at given points y_j (observed at the site \mathbf{j}). Thus the inverse regression at y_j is defined by :

$$r_{e,n}(y_j) = \frac{\varphi_n(y_j)}{f_{e,n}(y_j)} \quad \text{with}$$

$$f_n(y_j) = \frac{1}{\hat{n}h_n} \sum_{\mathbf{i} \in \mathcal{I}_n} K\left(\frac{y_j - Y_i}{h_n}\right) \mathbf{I}_{V_j}(\mathbf{i}), \varphi_n(y_j) = \frac{1}{\hat{n}h_n} \sum_{\mathbf{i} \in \mathcal{I}_n} X_i K\left(\frac{y_j - Y_i}{h_n}\right) \mathbf{I}_{V_j}(\mathbf{i})$$

and $f_{e,n}(y_j) = \max(e_n, f_n(y_j))$ where the set $V_j = \{\mathbf{i}, \varphi(\|\mathbf{i} - \mathbf{j}\|) > C \|\mathbf{i} - \mathbf{j}\|^{-\theta}\}$ (in the polynomial case) or $V_j = \{\mathbf{i}, \varphi(\|\mathbf{i} - \mathbf{j}\|) > C \exp(-\theta\|\mathbf{i} - \mathbf{j}\|)\}$ (in the GSM case) depend on the mixing parameter θ .

For all $\mathbf{j} \in \mathcal{I}_n$, consider V'_j defined as previously for some $\theta' > 0$, not necessary equal to V_j . Then, let

$$\Sigma_{e,n}(\mathbf{j}) = \frac{1}{\hat{n}} \sum_{\mathbf{i}} r_{e,n}(Y_i) r_{e,n}(Y_i)^T \mathbf{I}_{V'_j}(\mathbf{i}) - \bar{X}(\mathbf{j}) \bar{X}^T(\mathbf{j})$$

with $\bar{X}(\mathbf{j}) = \frac{1}{\hat{n}} \sum_{\mathbf{i}} X_i \mathbf{I}_{V'_j}(\mathbf{i})$. Here again, the stationarity of the process ensures that $\Sigma_{e,n}(\mathbf{j}) \simeq \Sigma_{e,n}(\mathbf{k})$ for all sites \mathbf{j} and \mathbf{k} . Hence, an estimation of Σ_e is obtained by using any $\Sigma_{e,n}(\mathbf{j})$, or in an equivalent way, the median or the mean of the $\Sigma_{e,n}(\mathbf{j})$'s. It is the latest case that we consider here in our simulation study. Note also that the same procedure holds for the estimation of Σ .

Note that the choice of both V_j , the set of some nearest neighbors of \mathbf{j} , and V'_j 's is a difficult interesting problem. For our simulations we restrict ourselves to the case where the sets composed of an arbitrary fixed k_n number of nearest neighbours. The bandwidths are set using cross-validation techniques.

Finally the algorithm for estimating the spatial covariance of the inverse regression estimation is the following

1. Compute the optimal bandwidth, h_{opt} , by using cross-validation procedure.
2. For each $y_j \in \mathcal{I}_n$ take the set V_j of the k_n nearest neighbors and compute: $\sum_{\mathbf{i} \in V_j} K\left(\frac{y_j - Y_i}{h_n}\right)$, $\sum_{\mathbf{i} \in V_j} X_i K\left(\frac{y_j - Y_i}{h_n}\right)$, $\sum_{\mathbf{i} \in V_j} X_i$.
3. Choose e_n according to the assumptions of Theorem 1 and compute $r_{e,n}(y_j)$.
4. Compute $\Sigma_{e,n}$ based on step 2 and 3 with k'_n number nearest neighbors.

This algorithm is illustrated in the following simulations study.

Simulation study

Model 2. The data are generated from model:

$$Y_{i,j} = \exp(\beta_1^t X_{i,j}) + \sin(\pi(\beta_2^t X_{i,j})/2) + \varepsilon_{i,j} \quad (7)$$

where $1 \leq i, j \leq 26$ the β_i 's are the same as in **Model 1**, $(X_{i,j})$ is the process such that $X_{i,j} = A_{i,j}^2 \cdot W_{i,j} + B_{i,j} \cdot \mathbf{1}_9$, with $\mathbf{1}_9 = \underbrace{(1, \dots, 1)}_{9 \text{ times}}$, $B = GRF(0, 5, 7, 2)$, W being the process of the increments of a zero mean Brownian sheet in \mathbb{R}^9 , $\varepsilon = GRF(0, 1, 5, 1)$ and $A = D \sin\left(\frac{B+1}{20}\right)$ with $D_{i,j} = \frac{1}{26 \times 26} \sum_{1 \leq u, v \leq 26} \exp\left(-\frac{\|(i,j)-(u,v)\|}{a}\right)$.

Function D controls directly the spatial mixing condition even if using the Gaussian Random Fields also brings some spatial dependency. Namely, D corresponds to a mixing condition with $\chi(h) \rightarrow 0$ at exponential rate. We point out that the greater is a , the weaker is the spatial dependency.

Prediction for Model 2 with $a = 2$.

To get predictions, we have simulated **Model 2** with $1 \leq i, j \leq 36$. The initial sample has been divided into two samples according to a regular scheme: a training sample (of size 31×31) to estimate the EDR space and a test sample (size 335) to compute the prediction error. We have estimated the β_i 's obtained with $k_n = 10$ and $k'_n = 100$, we have used the kernel regression estimator of [10] and computed the prediction error based on the sample test. The coefficient of determination of the regression procedure is $R^2 \simeq 0.7$.

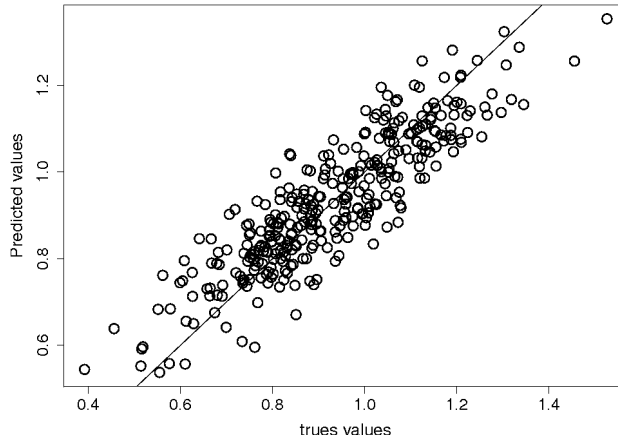


Fig. 1. Error of prediction of **Model 2** with $a = 2$: $R^2 \simeq 0.86$

4 Estimation of Model (1) in high dimensional setting

Here, we consider the case where $X \in \mathcal{E}$ is a high dimensional variable. Namely, we consider the following two cases.

4.1 The mapping, Φ is defined through a semi-metric

We deal in this part with the case where the space \mathcal{E} is endowed with a metric δ . Then, we consider the setting where the mapping Φ is such that:

$$\Phi(x) = \begin{cases} \mathcal{E} \rightarrow & \mathbb{R}^D \\ x \mapsto & (\delta(x_{cent_1}, x), \dots, \delta(x_{cent_D}, x)) \end{cases}$$

where $x_{cent_\ell}, \ell \in 1, \dots, D$ are some centralities of the distribution of the X_i 's to be defined. In the functional data analysis setting, x_{cent_ℓ} can be for example the mean function, the median curve, modals curves, depth functions,...

4.2 The mapping Φ is linear.

Let us consider the case where the space \mathcal{E} is endowed with an inner product. Then, we propose as function Φ , an operator of projection on some subspace $\mathcal{S} \subset \mathcal{E}$ spanned by the orthogonal system of vectors : u_i, \dots, u_D where the u_i 's are known.

References

1. Anselin, L. and Florax, R.J.G.M. *New Directions in Spatial Econometrics*, Springer, Berlin (1995).
2. Biau, G. and Cadre, B. Nonparametric Spatial Prediction, *Statistical inference for Stochastic Processes*, 7, 327–349 (2004).
3. Hallin, M., Lu, Z., and Tran, L. T. Local linear spatial regression. *Ann. statist.*, 32(6), 2469-2500 (2004).
4. Cressie, N.A.C. *Statistics for spatial Data*, Wiley Series in Probability and Mathematical Statistics, New-York (1991).
5. Dabo-Niang, S. and Yao, A.F. Kernel regression estimation for continuous spatial processes. *Math. method. stat.*, 16, 298–317 (2007).
6. Guyon, X. *Random fields on a network - modeling, statistics, and applications*. New-York: Springer (1995).
7. Hallin, M., Lu, and Tran, L.T. Local linear spatial regression, *Annal of Statist.*, 32(6), 2469–2500 (2004).
8. Hastie, T. J., and Tibshirani, R. Generalized additive models (with discussion). *Statist. sci.*, 1, 297-318 (1986).
9. Li, K. C. Sliced inverse regression for dimension reduction, with discussions. *J. amer. statist. assoc.*, 86, 316-342 (1991).
10. Lu, Z., and Chen, X. Spatial kernel regression estimation: Weak consistency. *Stat. proba. lett*, 68, 125-136 (2004).

11. Tran, L.T.,. Kernel density estimation on random fields. *J.Multivariate Anal.* 34, 37-53 (1990).
12. Ripley, B. *Spatial statistics*. New-York: Wiley (1981).
13. Zhu, L.Z., and Fang, TK. Asymptotics for kernel estimate of sliced inverse regression. *Ann. statist.*, 24, 1053-1068 (1996).

On classifying coherent/incoherent short texts

Anca Dinu

University of Bucharest, Faculty of Foreign Languages and Literatures, Center for Computational Linguistics

Email: anca_d_dinu@yahoo.com

Abstract: In this article we propose a quantitative approach to a relatively new problem: categorizing text as pragmatically correct or pragmatically incorrect (forcing the notion, coherent/incoherent). The typical text categorization criterions comprise categorization by topic, by style (genre classification, authorship identification), by expressed opinion (opinion mining, sentiment classification), etc. Very few approaches consider the problem of categorizing text by degree of coherence. One example of application of text categorization by its coherence is creating a spam filter for personal e-mail accounts able to cope with one of the new strategies adopted by spammers. This strategy consists of encoding the real message as picture (impossible to directly analyze and reject by the text oriented classical filters) and accompanying it by a text especially designed to surpass the filter.

An important question for automatically categorizing texts into coherent and incoherent is: are there features that can be extracted from these texts and be successfully used to categorize them? We propose a quantitative approach that relies on the use of ratios between morphological categories from the texts as discriminant features. We use supervised machine learning techniques on a small corpus of English e-mail messages and let the algorithms extract important features from all the pos ratios. The results are encouraging.

1 Introduction.

In this article we propose a quantitative approach to a relatively new problem: categorizing text as pragmatically correct or pragmatically incorrect (forcing the notion, we will refer to this categories as coherent and incoherent). The typical text categorization criterions comprise categorization by topic, by style (genre classification, authorship identification), by expressed opinion (opinion mining, sentiment classification), etc. Very few approaches consider the problem of categorizing text by degree of coherence, as in (Miller, 2003). One example of application of text categorization by its coherence is creating a spam filter for personal e-mail accounts able to cope with one of the new strategies adopted by spammers. This strategy consists of encoding the real message as picture (impossible to directly analyze and reject by the text oriented classical filters) and accompanying it by a text especially designed to surpass the filter. For human subjects, the text in the picture is easily comprehensible, as opposed to the accompanying text, which is only recognizable as either syntactically incorrect (collection of words), or semantically incorrect, or pragmatically incorrect i.e. incoherent (collection of proverbs or texts obtained by putting together phrases or paragraphs from different text). On the other hand, for classical spam filters, which usually relay on algorithms that use as features content words (based on the frequencies of the words commonly used in spam messages), the picture offers no information and the accompanying text may pass as valid (because it contains content word usually not present in spam messages). As a result, such messages are

typically sent by the spam filter into the Inbox, instead of the Bulk folder. The role of this e-mail messages is double: to surpass the spam filter so that get to be read by the owner of the account and, second and more important, if they are manually labeled as spam messages, they untrain the classical spam filter due to their content words which do not usually appear in spam messages. Thus, after the spam filter sees enough such messages labeled as spams, it eventually cannot make the difference any more between spam and normal messages. An important question for automatically categorizing texts into coherent and incoherent is: are there features that can be extracted from these texts and be successfully used to categorize them? We propose a quantitative approach that relies on the use of ratios between morphological categories from the texts as discriminant features. We supposed that these ratios are not completely random in coherent text. The goal of our experiment is to automatically classify e-mail messages into two classes: coherent messages, to go to Inbox and incoherent messages (good candidates for Bulk folder). We used a number of supervised machine learning techniques on a small corpus of English e-mail messages and let the algorithms to extract important features from all the pos ratios ; The results are encouraging: the best performing technique used in our experiment has a leave one out (l.o.o.) accuracy of 85.48%.

2 The corpus.

We manually built a small English e-mail messages corpus comprising 110 messages: 55 negative (incoherent) and 55 positive (coherent). The 55 negative messages were manually selected from a large list of personal spam messages. There are three categories of specially designed text for surpassing the spam filter: syntactically incorrect, semantically incorrect and pragmatically incorrect. In this article we focus on the last category, so we only included into the 55 negative examples the pragmatically incorrect messages (most of them being collections of proverbs or phrases randomly chosen from different texts and assembled together). We reproduce one negative and one positive examples in Appendix 1. As positive messages we selected coherent messages from two sources: Enron corpus (<http://www.cs.cmu.edu/enron/>) and personal e-mail messages, trying not to have a too homogenous collection of e-mail messages. All 110 e-mail messages are genuine, with no human intervention into their text.

3 Categorization experiments and results.

To produce the set of features, we tagged each text using the set of tags from Penn Tree Bank. We considered that this set of tags is too detailed; for the purpose of this experiment we do not need all tags, so we only took in consideration 12 representative parts of speech: we eliminated the punctuation tags and we mapped different subclasses of pos into a single unifying pos (for example all subclasses of adverbs were mapped into a single class: the adverbs, all singular and plural

common nouns were mapped into a single class: common nouns, etc). We give here the mapping table we used:

Pos	Label	Pos	Label	Pos	Label
EX	1	VBZ	3	RBS	7
NN	1	MD	4	PRP	8
NNS	1	PDT	5	PRP\$	8
NNP	2	DT	5	CC	9
NNPS	2	JJ	6	CD	10
VB	3	JJR	6	IN	11
VBD	3	JJS	6	TO	11
VBG	3	RB	7	WDT	12
VBN	3	RBR	7	WP	12
VBP	3	RBS	7	WP\$	12

For the task of tagging we used Maximal Entropy Part of Speech Tagger (Ratnaparkhi, 1996) because it is free to use and because it has a high reported accuracy of 96.43%.

We computed pos frequencies for each of the texts from the training set (both from the positive – coherent and from the negative - incoherent examples). We normalized them (divided all the frequencies to the total number of tagged words in each text), to neutralize the fact that the texts had different lengths. We then computed all possible 66 ratios between all tags. We also added a small artificial quantity (equal to 0.001) to all the frequencies before computing the ratios, to guard against division by zero. These 66 values become the features on which we trained the 3 out of 5 types of machines we employed (the other two needed no such pre-processing). Because of the relative small number of examples in our experiment, we used leave one out cross validation, which is considered an almost unbiased estimator of the generalization error. Leave one out technique consists of holding each example out, training on all the other examples and testing on all examples.

The first and the simplest technique we used was the linear regression (Duda et al., 2001), not for its accuracy as classifier, but because, being a linear method, allows us to analyze the importance of each feature and so determine some of the most prominent features for our experiment of categorizing coherent/ incoherent texts.

For this experiment we used the pre-processed data as described above. Its l.o.o accuracy was of 68.18%, which we used further as baseline for next experiments.

We ordered the 66 features (pos ratios) in decreasing order of their coefficients computed by performing regression. The top 5 features that contribute the most to the discrimination of the texts are very interesting from a linguistic point of view:

- the ratio between modal auxiliary verbs and adverbs, representing 17.71% of all feature weights;
- the ratio between the pre-determiner (such as all, this, such, etc) and adverbs, representing 14.6% of all feature weights;

- the ratio between pre-determiner and conjunction, representing 9.92% of all feature weights;
- the ratio between common nouns and conjunctions, representing 7.37% of all feature weights;
- the ratio between modal verbs and conjunctions, representing 7.25% of all feature weights.

These top 5 features accounted for 56.85% of data variation. The first ratio may be explained by the inherent strong correlation between verbs and adverbs. The presence of conjunction in 3 out of the top 5 ratios confirms the natural intuition that conjunction is an important element w.r.t. the coherence of a text. Also, the presence of the pre-determiners in the top 5 ratios may be related to the important role coreference plays in the coherence of texts.

As we said, we used the linear regression to analyze the importance of different features in the discrimination process and as baseline for state of the art machine learning techniques. We tested two kernel methods (v support vector machine and Kernel Fisher discriminant), both with linear and polynomial kernel.

Kernel-based learning algorithms work by embedding the data into a feature space (a Hilbert space), and searching for linear relations in that space. The embedding is performed implicitly, that is by specifying the inner product between each pair of points rather than by giving their coordinates explicitly.

$$\max_w \frac{(\mu_w^+ - \mu_w^-)^2}{(\sigma_w^+)^2 + (\sigma_w^-)^2 + \lambda \|w\|^2}$$

The kernel function captures the intuitive notion of similarity between objects in a specific domain and can be any function defined on the respective domain that is symmetric and positive definite. Details about SVM and KFD can be found in (Taylor and Cristianini, 2004).

The v support vector classifier with linear kernel ($k(x, y) = \langle x, y \rangle$) was trained, as in the case of regression, using the pre-processed 66 features, exactly the same features used for linear regression. The parameter v was chosen out of nine tries, from 0.1 to 0.9, the best performance for the SVC being achieved for $v = 0:3$. The l.o.o. accuracy for the best performing v parameter was 78.18%, with 10% higher than the baseline.

The Kernel Fisher discriminant with linear kernel was trained on preprocessed data as it was the case with the regression and v support vector classifier. Its l.o.o. accuracy was 75.46 %, with 7.28 % higher than the baseline. The flexibility of the kernel methods allow us to directly use the pos frequencies, without computing any pos ratios. That is, the polynomial kernel implicitly relies on the inner product of all features, so there is no further need to compute their ratios in advance.

The support vector machine with polynomial kernel was trained directly on the data, needing no computation of ratios. The kernel function we used is:

$$k(x, y) = (\langle x, y \rangle + 1)^2.$$

Its l.o.o. accuracy for the best performing $v = 0:4$ parameter was 81.81 %, with 13.63% higher than the baseline.

The Kernel Fisher discriminant with polynomial kernel was trained directly on the data, needing no ratios. Its l.o.o. accuracy was 85.46 %, with 17.28 % higher than the baseline. We summarized these results in the next table.

The best performance was achieved by the Kernel Fisher discriminant with polynomial kernel.

Learning method type	Accuracy
Regression (baseline)	68.18%
linear Support Vector Classifier	78.18%
quadratic Support Vector Machine	81.81%
linear Kernel Fisher discriminant	75.46%
polynomial Kernel Fisher discriminant	85.46%

4 Conclusions.

The best l.o.o. accuracy we obtained, i.e. 85.48% is a good accuracy because there are inherent errors, transmitted from the part of speech tagger and perhaps from the subjective human classification into the two classes (coherent/incoherent text) used as the training set. Also using only the frequencies of the parts of speech in the texts disregards many other important feature for text coherence.

5 Further works.

It would be interesting to compare our quantitative approach to some qualitative techniques related to text coherence, such as latent semantic analysis (Dumais et al., 1988) or lexical chains(Hirst and St.-Onge, 1997).

Also, it would be useful to train the machine to have an error as small as possible for positive examples (coherent texts sent into Bulk folder), even if the error for negative examples would be bigger (incoherent texts sent into Inbox).

6 Acknowledgements.

This work was supported by CNCSIS –UEFISCSU, project number PNII – IDEI 228/2007.

References

1. Chih-Chung Chang and Chih-Jen Lin. 2001. LIBSVM: a library for support vector machines. Software available at <http://www.csie.ntu.edu.tw/~cjlin/libsvm>.
2. John S. Taylor and Nello Cristianini. 2004. Kernel Methods for Pattern Analysis. Cambridge University Press, New York, NY, USA.
3. Duda, R.O., Hart, P.E., Stork, D.G. 2001. Pattern Classification (2nd ed.). Wiley- Interscience Publication.

4. Susan T. Dumais, George W. Furnas, Thomas K. Landauer, Scott Deerwester, and Richard Harshman. 1988. Using Latent Semantic Analysis to improve access to textual information. In *Human Factors in Computing Systems, CHI'88 Conference Proceedings* (Washington, D.C.), pages 281- 285, New York, May. ACM.
5. Hirst, Graeme and David St.-Onge. 1997. Lexical chains as representation of context for the detection and correction of malapropisms. In Christiane Fellbaum, editor, *Wordnet: An electronic lexical database and some of its applications*. MIT Press, Cambridge, pages 305- 332.
6. T. Miller. 2004. Essay Assessment with Latent Semantic Analysis. *Journal of Educational Computing Research* 28.
7. Adwait Ratnaparkhi. 1996. A Maximum Entropy Part- Of-Speech Tagger. In *Proceedings of the Empirical Methods in NLP Conference*, University of Pennsylvania A.J.F.

6 Appendix 1

We reproduce here in order:

- a positive example of a coherent e-mail message;
- a negative example of an incoherent e-mail message;

"I will be getting back to the website some time this week. Thank you for updating the info on the need analysis page. If you haven't done it yet, please look at Paula's page to check what remains to be done for your language. Remember that your deadline for sending me your final report forms as explained in Prague is Nov.15. I hope Mario can give you some details on how to go about filling in the various pages. Concerning the Wikipedia entry for Euromobil in all 9 languages, we agreed in Prague that it was indeed a good idea. I haven't been able to deal with it yet, but I saved the revised PL text and I hope to have some time shortly to do it. I hope those of you who haven't done it yet can do it also. Best, Jeannine"

"No one will ever think of looking for you in there. A job applicant challenged the interviewer to an arm wrestle. I am fascinated by fire. I did not object to the object. Your first-aid kit contains two pints of coffee with an I.V. hookup. And you can travel to any other part of the building without difficulty. Interviewee wore a alkman, explaining that she could listen to the interviewer and the music at the same time. You can outlast the Energizer bunny. Dancing around in a threatening manner until you have dispatched their predecessors. I know who is responsible for most of my troubles I have no difficulty in starting or holding my bowel movement. People get dizzy just watching you. Candidate said he never finished high school because he was kidnapped and kept in a closet in Mexico."

A rank based multi-classifier system in text categorization

Liviu P. Dinu

University of Bucharest
Faculty of Mathematics and Computer Science
Academiei 14, RO-0010014, Bucharest, Romania
(e-mail: ldinu@funinf.cs.unibuc.ro)

Abstract. In this paper we show that Rank Distance Aggregation can improve ensemble classifier precision in the classical text categorization task by presenting a series of experiments done on a 20 class newsgroup corpus, with a single correct class per document. We aggregate four established document classification methods (TF-IDF, Probabilistic Indexing, Naive Bayes and KNN) in different training scenarios, and compare these results.

Keywords: text categorization, rank distance categorization, Reuters database.

1 Introduction

The problem of combining classifiers has been intensively studied in the last period and it is a clear idea that "*together are stronger*" [5]. The domains where classifier scheme were introduced and applied vary a lot : bioinformatics (the sequence analysis problem), document classification, document image analysis, biometric recognition (personal identification based on various physical attributes such as iris, face, fingerprint) or speech recognition are few of them [6], [7], [8]. A typical combination schema consists of a set of individual classifiers and a combiner which combines the results of the individual classifiers to make the final decision. In many situations, the results of individual classifiers are *rankings* (an ordered list of objects). Every ranking can be considered as being produced by applying an ordering criterion to a given set of objects. The situation of ordering several objects, and, consequently, obtaining a ranking is encountered in many situation: an electoral process, where the ordering criterion between the participants is straightforward: the number of votes they have gained; the results of a football tournament, where the criterion is the number of points obtained by each team at the end of the tournament, etc. However, it is not the general case to have very simple methods to decide which is the ordering criterion, and, as a consequence, which is the ranking; to support this, we mention situations like: selecting documents based on multiple criteria, building search engines for the WEB [Dwork et al., 2001] or finding the author of a given text. Examples of multi-criteria selection arise when trying to choose a product from a database of products, such as travel plans or restaurants (users might rank

restaurants based on several different criteria like cuisine, driving distance, ambiance, star-rating, etc.) Other situations when we combine rankings are the cases when we take decisions based on subjective or sensorial criteria (e.g. perceptions). Especially when working with perceptions, but not only, we face the situation to operate with rankings of objects where the essential information is not given by the numerical value of some parameter of each object, but by the position the object occupies in the ranking, like movies or music tops (according to a natural hierarchical order, in which on the first place we find the most important element, on the second place the next one and on the last position the least important element). In all these situations we have to combine two or more rankings, which has been ordered by using different criteria, in order to make a decision. We deal with the so-called: *rank aggregation problem*.

In this paper we use a combining ranking schema based on the *rank distance* and show that this ensemble is superior to performances of individual classifiers.

2 Motivation

The issue of using multiple classification methods together to form a better classifier is a well researched problem and appears in a wealth of classical Machine Learning scenarios. We mention here some of the benefits of using more than one classifier: learning more complex decision boundaries (e.g. more than circles or lines); theoretical advantage shown for some combining methods (e.g. boosting); many classifiers already implemented, showing different accuracies.

The fields of Pattern Recognition and Machine Learning have reached a point where many approaches are available for all the usual stages of a categorization project. That is, for most of the real world applications, many feature extraction techniques have been proposed, tested and theoretically analyzed, which has lead to methodologies for data analysis being exported to different applications and projects. With diverse feature selection methods, extensive testing of many classifiers was possible.

Many feature extraction techniques do exist for nearly all applications. Many classifiers readily available, so which is "the best" featureclassifier pair? We have two options:

- choose wisely (but don't optimize for one dataset);
- use more than one pair, thus combine different features with different classifiers.

Most of the time though, more than one classifier–feature pair have proven "the best" precision or recall, and the nature of the supervised generalization problem has made choosing a clear cut winner, at least per application, particularly difficult.

3 Rank distance categorization

Usual ensemble methods put a considerable degree of emphasis on the numerical values outputted by different classifiers for each category. In theoretical settings they are processed and used as probabilities or as confidences. Different normalizing schemes are usually employed, After these steps the resulting values decide, in a fixed way, one winning class.

Our method discards these values and transforms the classifier outputs into rankings of class labels. This information is thereafter ignored, to the extent given by the positions in the rankings and the ranking lengths. Then we compute the rankings that are closest to all the base classifiers' outputs in terms of the rank-distance [1]. A set of rankings with this property is called the Rank Distance Aggregation of the original rankings. In the single correct class setting we simply take a vote among the aggregate rankings and output that class. If a tie between 2 or more classes appears, we select one at random, with equal probability. This is the usual voting fixed combiner on top of the aggregation set, instead of the base classifier outputs.

3.1 Formal definition

A ranking is an ordered list of labels and can be viewed as the result of applying an ordering criterion to a set of objects.

Definition 1. Given two partial rankings σ and τ over the same universe \mathcal{U} , we define the rank-distance between them as:

$$\Delta(\sigma, \tau) = \sum_{x \in \sigma \cup \tau} |\text{ord}(\sigma, x) - \text{ord}(\tau, x)|.$$

Theorem 1. [1] Δ is a distance function.

The motivation behind using orders instead of ranking positions is based on the intuition that ranking differences on the highly ranked objects should have a larger impact on the overall distance than disagreements on the lower ranked objects. Secondly, the length of the ranking is not discounted. This complies with the intuition that longer rankings are produced by more thorough criteria, although it puts extra pressure on base rankings; this means longer hierarchy must be justified, with the benefit of gaining extra expressivity.

Computing the rank-distance (RD) of two rankings is straight-forward and linear in the number of objects in the two rankings. This number is small in many practical applications, much lower than the total number of universe objects ($n = \#\mathcal{U}$). When implemented as random access arrays indexed by the universe objects, the rank-distance computation has complexity $\mathcal{O}(n)$ in the worst case.

3.2 Rank Aggregation

In a selection process rankings are issued for a common decision problem, therefore a ranking that “combines” all the original (base) rankings is required. One commonsense solution is finding a ranking that is as close as possible to all the particular rankings. Apart from many paradoxes of different aggregation methods, this problem is NP-hard for most non-trivial distances.

Formally, the result of all the individually considered selection criteria is a finite collection of, not necessarily different, (partial) rankings, that we will call a ranking multiset $\mathcal{T} = \{\tau_1, \tau_2, \dots, \tau_k\}$. When aggregating \mathcal{T} into a single ranking we are looking for a σ with a minimal rank distance to all the rankings of the multiset; since Δ takes only positive values, we have to minimize the sum:

$$\Delta(\sigma, \mathcal{T}) = \sum_{\tau \in \mathcal{T}} \Delta(\sigma, \tau).$$

Definition 2. Let $\mathcal{T} = \{\tau_1, \tau_2, \dots, \tau_k\}$ be a multiset of rankings over object universe \mathcal{U} . A rank-distance aggregation (RDA) of \mathcal{T} is a ranking σ (over the same universe \mathcal{U}) that minimizes $\Delta(\sigma, \mathcal{T})$. We denote the set of RD aggregations by $agr(\mathcal{T})$.

A partition of the set $agr(\mathcal{T})$ by ranking length will give an effective means of computation.

Definition 3. Let $1 \leq t \leq \#\mathcal{U}$ and \mathcal{T} a multiset of rankings over \mathcal{U} . A partial ranking τ of length t that minimizes $\Delta(\tau, \mathcal{T})$ among all other rankings of length t is said to be a t -aggregation of multiset \mathcal{T} .

Obviously, for any $1 \leq t \leq \#\mathcal{U}$ there exists at least one t -aggregation σ , with an associated minimal distance $d_t = \Delta(\sigma, \mathcal{T})$. To compute $agr(\mathcal{T})$ it is sufficient to compute the minimal distance:

$$d_{min} = \min_{1 \leq t \leq \#\mathcal{U}} \{d_1, d_2, \dots, d_{\#\mathcal{U}}\},$$

and the set of indices:

$$D = \{s | d_s = d_{min}, 1 \leq s \leq \#\mathcal{U}\}.$$

Also, for any s -aggregation $\sigma \in agr(\mathcal{T})$, all other s -aggregations are in $agr(\mathcal{T})$, since, for a fixed integer s , all other s -aggregations have (by definition) the same minimal distance to \mathcal{T} as σ . We can now summarize this approach:

Algorithm 1 Let $\mathcal{T} = \{\tau_1, \tau_2, \dots, \tau_k\}$
 1: for $t = 1$ to $\#\mathcal{U}$ then
 2: compute a t -aggregation of \mathcal{T} , namely π_t ;
 3: end

- 4: let $d_{min} = \min_{1 \leq s \leq \#\mathcal{U}} \Delta(\pi_s, \mathcal{T});$
- 5: for all t such that $\Delta(\pi_t, \mathcal{T}) = d_{min}$ then
- 6: compute and output all the t -aggregations of $\mathcal{T};$
- 7: end

Computing the closest t -aggregation to \mathcal{T} in line 2 is equivalent to finding one solution for a certain assignment problem / minimal weight bipartite perfect matching, which has complexity $\mathcal{O}(n^3)$, where n is the number of individual objects mentioned in at least one of the rankings. Line 6 is equivalent to enumerating all minimal weight perfect matchings in a certain bipartite graph. Therefore, the total time needed is $\mathcal{O}((2x + 2)n^4)$, where x is the number of existing aggregate rankings (i.e. rankings with the minimal RD to the base set). See [2] for further details.

Example 1. Let \mathcal{T} be the following multiset of rankings over the universe of objects $\mathcal{U} = \{1, 2, 3, 4\}$:

$$\mathcal{T} = \{(1 > 2 > 3), (3 > 4), (1 > 3 > 2 > 4)\}.$$

The RDA of \mathcal{T} is the set:

$$agr(\mathcal{T}) = \{(1 > 2 > 3), (1 > 3 > 4), (1 > 3 > 2 > 4)\}.$$

Notice that all the 3&4-aggregations are present in $agr(\mathcal{T})$. The 1&2-aggregations have larger distances to \mathcal{T} , so all are excluded. Also important to note is that $agr(\mathcal{T})$ is not necessarily a subset of \mathcal{T} , a desirable rationality condition for an aggregation method, known as “absence of dictator”. Other rationality conditions verified by the rank-distance aggregation are Pareto optimality, reasonableness, stability, loyalty, inversion and free order [1].

3.3 Rank distance categorization

Now we can formally introduce *Rank Distance Categorization* (RDC) method.

Let d be a pattern, $C = \{c_1, c_2, \dots, c_m\}$ be a set of all m possible categories of d , and l_1, l_2, \dots, l_n be n classifiers.

Each classifier gives a ranking of classes; let $\mathcal{L} = L_1, L_2, \dots, L_n$ be the multiset of the individual rankings obtained by applying the previous n classifiers.

Let $agr(\mathcal{L}) = \{A_1, A_2, \dots, A_k\}$ be the aggregation of the multiset \mathcal{L} .

Definition 4. The class of the object predicted by the RDC method is the one that occupies most frequently the first position in the rankings A_1, \dots, A_k .

Example 2. Set the following sequence of 5 rankings: $\mathcal{L} = \{(1 > 2 > 3), (1 > 2 > 3), (3 > 1 > 2), (2 > 3 > 1), (2 > 3 > 1)\}$.

We have: $agr(\mathcal{L}) = \{(1 > 2 > 3), (2 > 1 > 3), (2 > 3 > 1)\}$. So, the class predicted by RDC method is the class 2.

In other words, RDC is a voting method on rank distance aggregations.

Classifiers	2pc	5pc	10pc
TFIDF	<u>79.23</u>	70.46	93.10
PRIND	42.56	56.76	71.30
KNN	71.90	74.86	75.36
NBAYES	75.23	76.26	92.53
Voting on RDA	76.23	77.06	91.86

Fig. 1. Precision(%). **Underlined** is the maximum, **bold** is everything closer than 0.50% to the maximum.

4 Experiments in text categorization

We chose to conduct our experiments with fixed combining rules on top of the *libbow* library [9], available on most Unix systems, including Linux, Solaris, SUNOS, Irix and HPUX. We used the categorization tool *rainbow* and the *20_newsgroups* corpus, both provided by the library’s development team. The corpus consists of 20,000 newsgroup articles, uniformly distributed across 20 classes. The *rainbow* text classification tool supports Naive Bayes, TFIDF/Rocchio, Probabilistic Indexing and K-nearest neighbor, 4 established text categorization methods, with well known favorable settings and shortcomings, which also provide reliable results under certain conditions.

For our purposes, the universe objects are these 20 assignable classes, and the classifier outputs are transformed into rankings of class labels. There is a “pruning” phase, where values outputted by the classifiers for each document–class pair are rescaled per document and sorted in descending order. The most probable class is put first on the ranking. After that, only values which make up 60% or more of the previous class’ probability are added to the resulting ranking. This method is empirically consistent with the requirement that longer rankings are produced only when justified by the underlying criterion. The actual aggregation is done locally, on the 4 rankings available for each test document. The number of involved objects is much smaller than 20, usually less than 5 classes are competing for the first place. This fact makes the aggregation problem computationally trivial by today’s resources, such that fast and parallel aggregation for thousands of documents is possible in a very short time.

The number of training documents, as well as how representative they are statistically, are very important parameters for supervised categorization methods in general, with severe performance penalties. This means that, in many real life situations, much less information is available to these methods than required for descent classification precision. To be fair, we have chosen 7 training settings. Each setting consists of N random documents per class for training the classifiers (on the same documents), and 500 documents (per class) for testing, where:

$$N \in \{2, 5, 10, 20, 50, 100, 500\}.$$

Classifiers	20pc	50pc	100pc	500pc
TFIDF	<u>92.83</u>	91.53	91.63	91.76
PRIND	77.19	82.86	83.86	86.86
KNN	81.83	89.16	89.83	88.96
NBAYES	91.63	91.19	91.03	92.00
Voting on RDA	<u>92.66</u>	<u>92.56</u>	<u>92.16</u>	<u>92.40</u>

Fig. 2. Precision(%). **Underlined** is the maximum, **bold** is everything closer than 0.50% to the maximum.

These settings are consistent with the Reuters-21578 collection, which is challenging also because of the large number of under-sampled classes, and the more than 90 topics.

As shown in figure 1, if the number of training documents is relatively small, the base classifiers produce unreliable results, some more than others. In this scenario some of the base classifiers overtake the aggregations, as expected. Aggregating in these settings is also referenced in the literature as unbalanced classifier fusion.

On the other hand, if the training set is sufficiently large (or if special care is taken in the training process), the aggregations usually do better than the individual classifiers, as seen in figure 2. In this case Voting on RDA outperforms the other fixed fusion rules in all 4 training scenarios. What is remarkable is that Voting on RDA manages to outperform all the other methods, although there is significant precision fluctuations in the base classifiers over the 4 different scenarios, suggesting increased reliability. Interestingly enough, voting on RDA outperforms the individual classifiers, by as much as 0.64% which means 33 additional documents classified correctly. In an application that requires extreme precision, like person identification in security application, this is significant, since false positives can result in unauthorized access by coincidence or fake credentials, like fake fingerprints.

5 Conclusions and future works

This article presents a series of experiments with text categorization methods, realized with the rank-distance aggregation set. The categorization task (on the *20_newsgroup* corpus) features 20 assignable classes and 10.000 documents for testing (500 per class). We use the *rainbow* Unix document classification tool to output the results of 4 different text categorization methods, and we compare these results with Voting on the Rank Distance Aggregation set. The results demonstrates superior precision o RDC over all the fixed rules tested. In a future works we want to compare the RDC method with other combining schema regarding their performances on the same database.

Acknowledgements Research supported by CNCSIS, PNII-Idei, project 228/2007.

References

1. Dinu, L. P. On the classification and aggregation of hierarchies with diferent constitutive elements. *Fundamenta Informaticae*, vol. 55, no. 1, 39-50, 2002.
2. Dinu, L. P. and F.Manea. An efficient approach for the rank aggregation problem. *Theoretical Computer Science*, vol. 359, no. 1, 455-461, 2006.
3. Dinu, L. P. and M. Popescu. A multi-criteria decision method based on rank distance. *Fundamenta Informaticae*, vol. 86, no. 1-2, 79-91, 2008.
4. Dwork, C., Kumar, R., Naor, M. and Sivakumar, D., 2001. Rank aggregation methods for the web. *Proc. of the 10th International WWW Conference*, 613-622.
5. Kittler, J., M. Hatef, R.P.W. Duin, and J. Matas, 1998. *On Combining Classifiers*, IEEE Transactions on Pattern Analysis and Machine Intelligence, vol. 20, no. 3, 226-239.
6. Ho, T.K., J. Hull and S. Srihari, 1994. *Decision Combination in Multiple Classifier Systems*, IEEE Transactions on Pattern Analysis and Machine Intelligence, vol. 16, no 1, pp. 66-75.
7. Jain, A.K., R.P.W. Duin, and J. Mao, 2000. *Statistical Pattern Recognition: A Review*, IEEE Transactions on Pattern Analysis and Machine Intelligence, vol. 22, no. 1, 4-37.
8. Liu, C.L. 2005. *Classifier combination basedon confidence transformation*, Pattern Recognition 38, 11-28.
9. Andrew Kachites McCallum, Bow: A toolkit for statistical language modeling, text retrieval, classification and clustering. <http://www.cs.cmu.edu/~mccallum/bow>, 1996.

Comparing Interval-Valued Variables Using s_{LC} Coefficient

Isabel Pinto Doria, Georges Le Calvé and Helena Bacelar-Nicolau

LEAD, Faculty of Psychology and CEAUL, University of Lisbon
Lisboa, Portugal

Email: irpdoria@fp.ul.pt

Société Française de Statistique, France

Email: g.lecalve@free.fr

LEAD, Faculty of Psychology and CEAUL, University of Lisbon
Lisboa, Portugal

Email: hbacelar@fpce.ul.pt

Abstract: s_{LC} coefficient is a similarity index between variables proposed by Georges Le Calvé (1977), based on Daniels (1944) and Lerman's (1973) coefficients. In this paper we present the s_{LC} coefficient generalized to compare interval-valued variables, using real data presented by Guru, Kiranagi and Nagabhusan (2004). This symbolic data refers to the minimum and maximum temperatures registered during the twelve months of a certain year in twenty cities. By means of hierarchical cluster analysis and principal component analysis applied directly to the similarity matrix obtained with the generalized coefficient s_{LC} , we visualize the similarity between the twelve months of the year described by their interval [minimum, maximum] temperatures on each city. This approach allows the visualization of the data proximity structure, being highly consistent with previous knowledge about the data.

Keywords: Interval-valued variables, Similarity coefficient, Hierarchical cluster analysis, Principal component analysis, Symbolic data.

1. Introduction

The s_{LC} coefficient is a similarity index between variables proposed by Georges Le Calvé (1977), based on Daniels (1944) and Lerman's (1973) coefficients. Here the generalized coefficient s_{LC} is used to compare interval-valued variables (Doria, 2008).

As we know, in the context of Symbolic Data Analysis (e.g., Bock and Diday, 2000), in a symbolic data matrix, lines correspond to symbolic objects (SO 's) whereas columns correspond to symbolic variables, which may take not just one value, as usual, but several values that can be weighted and linked by logical rules and taxonomies. Interval-valued data appear when the observed values of the variables are intervals from the set of real numbers R . This type of data often arises in practical situations, such as the recording of monthly interval temperatures in twenty cities during the twelve months of the year (Guru et al., 2004). The twelve

months interval-valued temperatures in these cities are compared here using the generalized similarity coefficient s_{LC} . In addition, by means of hierarchical cluster analysis (HCA) and principal component analysis (PCA) models applied directly to the similarity matrix obtained with the generalized coefficient s_{LC} , we visualize the similarity between the twelve months of the year described by their interval [minimum, maximum] temperatures registered on these cities.

2. The generalized similarity coefficient s_{LC}

The similarity coefficients between variables s , s_{LC} and P_L were inspired on an idea originally advanced by Daniels (1944), later developed by Lerman (1973) and generalized by Le Calvé (1977). In this approach, each variable is associated with a score matrix, whose definition depends on the nature of the initial variable, as well as on the nature of the variable with which it is to be compared. The basic coefficient, s , is defined as the scalar product between the score matrices; the s_{LC} coefficient is the standardized coefficient s , under a certain reference hypothesis; and P_L coefficient corresponds to the probabilistic coefficient. Recently, coefficients s , s_{LC} and P_L were generalized to the comparison of interval-valued variables, among other symbolic variables (Doria, 2008).

Definition of the S , S_{LC} and P_L coefficients (Le Calvé, 1977): A probabilistic similarity coefficient between variables X , Y , designated by P_L , is defined by the probability of S_{LC} being smaller than s_{LC} : $P_L(x,y) = P(S_{LC} \leq s_{LC}(x,y)) = \Phi(s_{LC}(x,y))$. The random variable S_{LC} is the standardised similarity, $S_{LC} = (S_{X,Y}(w) - \mu) / \sigma$, and $S_{X,Y}(\theta, \theta') = \langle \theta X \theta^t, \theta' Y \theta'^t \rangle$, $\forall w \in (\theta, \theta')$, considering the set of all permutations couples, $\Omega = \Theta(I) \times \Theta(I)$ defined on I , provided with a probability measure uniformly distributed. P_L is the probability distribution function of that standardised similarity being observed. Under very general conditions about the score matrices, the random variable S_{LC} has asymptotic standard normal distribution, the coefficients s_{LC} and s are the actual values of the random variables S_{LC} and S , respectively, and Φ denotes the standard normal distribution function.

Let us consider a three-way data matrix $M(x_{ij}, x^{ij})$, ($i=1, \dots, n$ entities; $j=1, \dots, p$ interval-valued variables).

Definition of the score (Doria, 2008): The *score* of the interval-valued variable X_j is defined as follows

$$x_{i i'} = H(A, B) = \max_{a \in A} \left\{ \min_{b \in B} \{d(a, b)\} \right\}, \text{ if } i \neq i'$$

$$x_{ii} = 0$$

In which $A = [x_{ij}, x^{ij}]$, $B = [x_{i'j}, x^{i'j}]$ and $H(.,.)$ indicates the non-symmetric dissimilarity of Hausdorff between the interval values given by entities i and i' . We consider that $d(a,b)$ represents the Euclidean distance between a and b .

The score matrix defined is a dissimilarity matrix. If we compare interval-valued variables with other type of variables whose score matrices are similarity matrices, we consider the affine transformation: $S_H(A,B) = \max H(A,B) - H(A,B)$.

3 Comparing interval-valued variables using real data: Results

The data we have analysed refers to the minimum and maximum temperatures registered during the twelve months of a certain year in twenty cities considered very similar by the observers: Amsterdam, Athens, Copenhagen, Frankfurt, Geneva, Lisbon, London, Madrid, Moscow, Munich, New York, Paris, Rome, St. Francisco, Seoul, Stockholm, Tokyo, Toronto, Vienna, Zurich (Guru et al., 2004). The data is registered in a tridimensional matrix $M(20 \times 12 \times 2)$. Figure 1 illustrates the temperature distributions during the year in those cities. Our main goal is to compare the months of the year, taking in account the information about their interval temperatures, $[min, max]$, registered in those cities and represent them graphically.

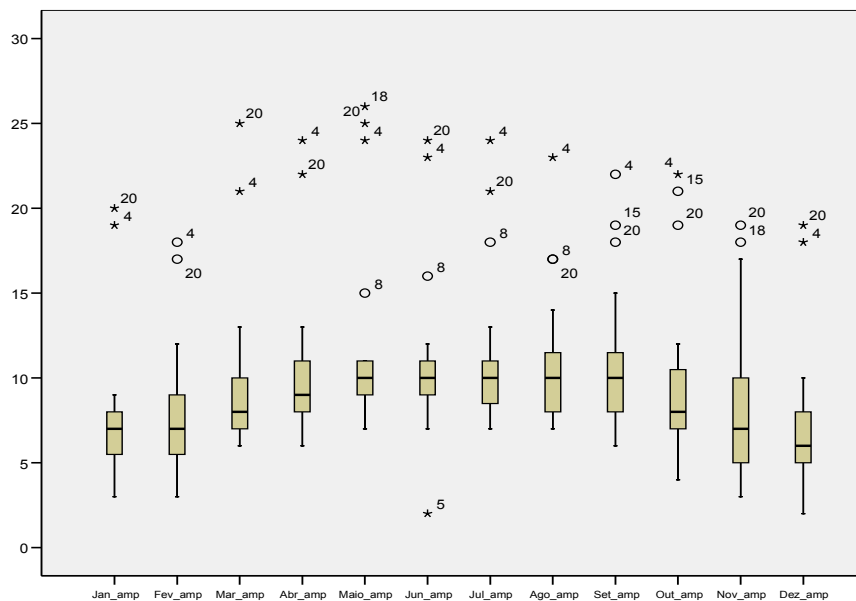


Fig. 1. Boxplots of the temperatures range distributions registered during the year in several cities. *Outliers* are marked with the data city codes: 4.Frankfurt, 5.Genebra, 8.Madrid, 15.Seoul, 18.Toronto and 20.Zurich.

The comparison between the variables was achieved using the generalized similarity coefficient s_{LC} and the similarity matrix S_{LC} (12x12) was obtained (Doria, 2008).

To represent S_{LC} matrix we have used data analysis techniques:

- Principal component analysis of this similarity table. The results are in Table 1, Figure 2 and Figure 3.

Similarity matrix S_{LC} is positive semi-definite. The 1st component is a general component that explains 67.6% of the data variability. The 1st component plane has a strong percentage of explained inertia associated to it (85.1% of total inertia explained).

Table 1. Results obtained with the P.C.A. of the similarity matrix S_{LC}

Axes	Units inertia (eigenvalue)	Percentage of explained inertia	Cumulate percentage of explained inertia
1	69.62	67.6	67.6
2	18.01	17.5	85.1
3	5.28	5.1	90.2

Similarity matrix S_{LC} is positive semi-definite. The 1st component is a general component that explains 67.6% of the data variability. The 1st component plane has a strong percentage of explained inertia associated to it (85.1% of total inertia explained).

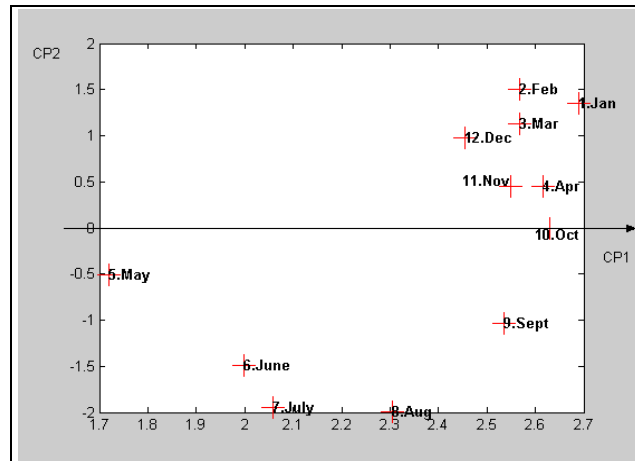


Fig. 2. Plot of the 1st component plane obtained with the P.C.A. of the similarity matrix S_{LC} .

The 2nd component, that explains 17.5% of total inertia, is the factor that opposes Summer (months with higher temperatures) to Winter (months with lower temperatures). In the 1st component plane we observe several associations: the warmer months (June, July, August), the colder months (December, January, February, March, November, April) and the milder months (October, September), but May is far from the other months because his peculiar temperatures range behaviour (e.g., Figure 1).

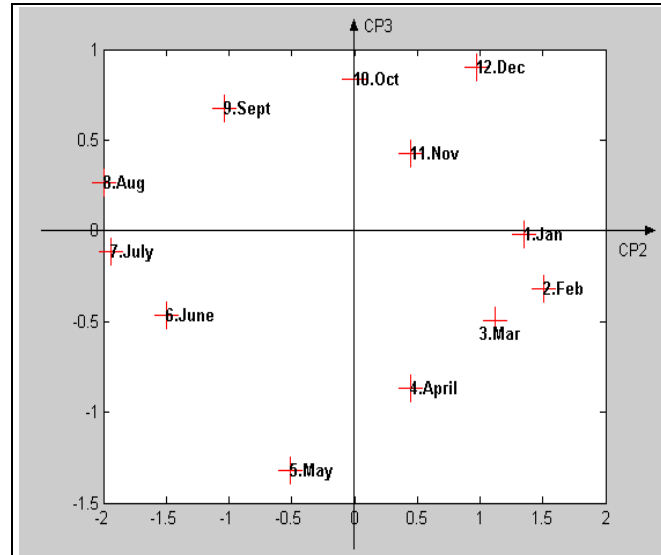


Fig. 3. Plot of the component plane (2, 3) obtained with the P.C.A. of the similarity matrix S_{LC} .

While the 3rd component only explains 5.1% of total inertia, this component is important as it represents the range of temperatures observed: it opposes May (with greater range of temperatures) to December (with smaller range of temperatures). The natural circular disposition of the months is also noticed.

- Hierarchical cluster analysis with complete linkage (Table 2, Figure 4).

Table 2: Results obtained with hierarchical cluster analysis (s_{LC} +*Complete Linkage*): the best clusters in conformity with the “level statistics” criterion (Lerman, 1970); Bacelar-Nicolau, 1972, 1980)

Algorithm:	Results: Partition obtained on the k^{th} level	Statistic: STAT(k)
Coefficient s_{LC}	Complete Link {Jan, Feb, Mar, Apr, Nov, Dec, Sep, Oct} {May}	STAT(9) 6.2377
3	5.28 {Jun, Jul, Aug}	

The hierarchy of partitions, and in particular the partition obtained at the 9th dendrogram's level with the HCA's algorithm ($s_{LC}+Complete Linkage$), are consistent with the factorial space composed by the first three components:
 Cluster 1={January, February, March, April, November, December, September, October}, Cluster 2={May}, Cluster 3={June, July, August}.

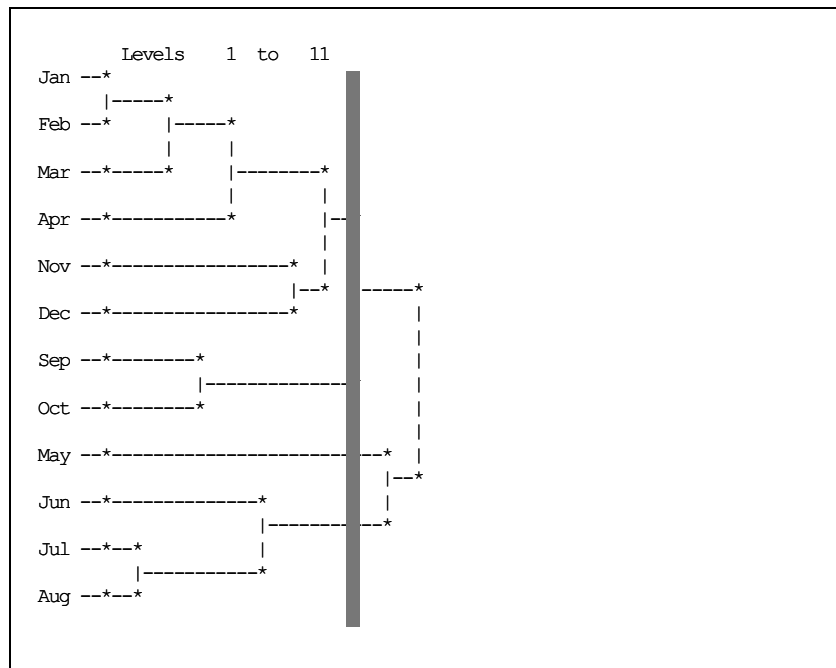


Fig.4. Dendrogram obtained with hierarchical cluster analysis ($s_{LC}+Complete Linkage$). The most relevant clusters are obtained at 9th level in conformity with the “level statistics” criterion (Lerman, 1970; Bacelar-Nicolau, 1972, 1980), $STAT(9)=6.2377$.

4 Conclusions

The similarity coefficients s , s_{LC} and P_L (Le Calvé, 1977) can be easily generalized as they are general by definition. The selection of Hausdorff distance to define the score matrix associated to interval-valued variables showed to be appropriated. With this type of data it's preferable to use the s_{LC} coefficient. The results showed that the s_{LC} coefficient accounted, not only the minimum and maximum values of

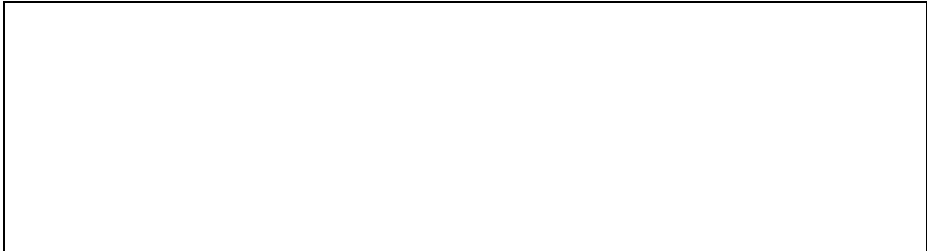
the interval, but also its range and represent well the monthly temperatures across seasons.

It can be concluded that this approach allows the visualization of the data proximity structure, being highly consistent with previous knowledge about the data.

References

1. Bacelar-Nicolau, H., *Analyse d'un Algorithme de Classification*. Thèse de 3^{ème} cycle, Université Pierre et Marie Curie, Paris (1972).
2. Bacelar-Nicolau, H., *Contribuições ao Estudo dos Coeficientes de Comparação em Análise Classificatória*. Tese de doutoramento, Faculdade de Ciências da Universidade de Lisboa, Lisboa (1980).
3. Bock, H.-H. and Diday, E. (Eds.) *Analysis of Symbolic Data: Exploratory Methods for Extracting Statistical Information from Complex Data*. Springer-Verlag, Berlin/Heidelberg (2000).
4. Daniels, H.E., The relation between measures of correlation in the universe of sample permutations. *Biometrika* **33**, 129-135 (1944).
5. Doria, I., *Representações Euclidianas de Dados: Uma Abordagem Para Variáveis Heterogéneas*. Tese de doutoramento, Faculdade de Medicina da Universidade de Lisboa, Lisboa (2008).
6. Guru, D.S., Kiranagi, B.B. and Nagabhushan, P., Multivalued type proximity measure and concept of mutual similarity value useful for clustering symbolic patterns. *Pattern Recognition Letters* **25**, 10, 1203-1213 (2004).
7. Le Calvé, G., Un indice de similarité pour des variables de type quelconque. *Revue Statistique et Analyse des Données* **01/02**, 39-47 (1977).
8. Lerman, I.C., *Sur l'Analyse des Données Préalable à une Classification Automatique. Proposition d'une Nouvelle Mesure de Similarité*. MSH, rapport 32 (8^e. année) (1970).
9. Lerman, I.C., *Étude Distributionnelle de Statistiques de Proximité entre Structures Algébriques Finies de Même Type. Application à la Classification Automatique*. Cahiers du Bureau Universitaire de Recherche Opérationnelle, n. 19. Institut de Statistique de l'Université de Paris, Paris (1973).

SMTDA 2010: Stochastic Modeling Techniques and Data Analysis
International Conference, *Chania, Crete, Greece, 8 - 11 June 2010*



Neural networks for nonlinear stochastic systems modeling

Ayachi ERRACHDI*, Ihsen SAAD, and Mohamed BENREJEB

Abstract—In this paper, an on-line algorithm using an adaptive learning rate is proposed for the modeling of the multivariable nonlinear stochastic systems. Different cases of Signal -to- Noise Ratio (SNR) are taken to show the effectiveness of this algorithm. The development of an adaptive learning rate is based on the analysis of the convergence of the conventional gradient descent method for the neural networks. A comparative study between the application of a neural networks using a variable and fixed learning rate for multivariable nonlinear stochastic systems is treated. The effectiveness of the proposed algorithm applied to the modeling of behavior of nonlinear dynamic stochastic systems is demonstrated by simulation experiments. The results of simulation showed that the use of neural networks with an adaptive learning rate is more interesting than a fixed learning rate. Two types of non linear stochastic systems are taken.

Key words — multivariable system, nonlinear, stochastic, neural networks, modeling, learning rate.

I. INTRODUCTION

MODELING nonlinear systems by Neural Networks (NN) has been the subject of much research over the past decade because of the ability of learning, generalization and approximation that have these networks [1]-[4]. Indeed, this approach provides an effective solution through which large classes of nonlinear systems can be modeled without a precise mathematical description. Identification is the process of determining the dynamic model of a system from measurements inputs / outputs. Often, the measured output of system is tainted by the noise. This is due either to the effect of disturbances acting at different parts of the process, either to measurement parts of the process, either to measurement noise. These disturbances introduce errors in the identification of model parameters. Among the parameters of the NN, there is the fixed learning rate. The research of the suitable learning rate represents a major disadvantage which can slow down the

phase of training. The adaptive training algorithm of a nonlinear single-variable system is studied in [5].

In this paper, the adaptive training algorithm of a multivariable nonlinear stochastic system is used.

This paper is organized as follows: The second section contains the presentation of the neural modeling of the nonlinear multivariable stochastic systems. In the third section, the gradient descent method is developed. The fourth section treats the simulation of the nonlinear multivariable stochastic systems by the NN with a fixed learning rate. The necessity of the variation of the learning rate is seen on the level of the fifth section.

II. NEURAL NETWORKS FOR NONLINEAR STOCHASTIC SYSTEMS MODELING

In this section, the stages of the neural modeling of nonlinear systems are treated then the gradient descent method is presented which is used to minimize the function cost.

II.1. STAGES OF NEURAL NETWORKS MODELING

Some stages of neural modeling of a nonlinear system are detailed in [6]-[7]. In order to find the neural model, it must respect these steps like standardize and center all the input variables, choose the structure of a model, estimate the synaptic weights and validate the obtained model.

Various types of algorithms of training are used such as the gradient descent method, the conjugate gradient algorithm [8], the Levenberg-Marquardt method [9], the adaptive learning algorithms [10]-[11] and other modified algorithms [12]-[17].

II.2. PRINCIPLE OF NEURAL MODELING

In this part, the principle of dynamic neural modeling of the stochastic nonlinear multivariable systems is presented. This principle is presented by Fig. 1.

A nonlinear multivariable system given by the following form:

$$y(k+1) = f[y(k), \dots, y(k-ns+1), u(k), \dots, u(k-nu+1)]$$

with

f : unknown function of model process.

$U = [u_1(k) \quad u_2(k) \quad \dots \quad u_{nu}(k)]$, $(1 \times nu)$ being the input of the process,

$Y = [y_1(k) \quad y_2(k) \quad \dots \quad y_{ns}(k)]^T$, $(ns \times 1)$ being the output of the process,

Manuscript submitted January 27, 2010.

Ayachi ERRACHDI, is Research Unit on Automatic (LARA), Department of Electrical Engineering, National School of Engineers of Tunis, BP37 1e Belvédère, Tunis 1002, Tunisia (corresponding author to provide phone: +216 97291979; e-mail: errachdi_ayachi@yahoo.fr).

Ihsen SAAD, He is now with the Department of Electric, National Engineering School of Sousse, Tunisia (e-mail: ihsen.saad@enit.rnu.tn)

Mohamed BENREJEB is with the Electrical Engineering Department, National Engineering School of Tunis, Tunisia (e-mail: mohamed.benrejeb@enit.rnu.tn).

* Corresponding Author Email Address: errachdi_ayachi@yahoo.fr

$Yr = [yr_1(k) \quad yr_2(k) \quad \dots \quad yr_{ns}(k)]^T$, $(ns \times 1)$ being the output of the NN,

$$E = [e_1(k) \quad e_2(k) \quad \dots \quad e_{ns}(k)]^T, (ns \times 1)$$

$e_i(k) = y_i(k) - yr_i(k)$: error between the i -th measured output and the i -th neural output,

x : the neural input vector, $(t \times 1)$, $(t = nu + ns)$,

ncc : number of nodes of the hidden layer.

W : synaptic weights of the input layer towards the hidden layer, size $(ncc \times t)$

Z : synaptic weights of the hidden layer towards the output layer, size $(ns \times ncc)$

s : activation function of all nodes.

η : learning rate.

λ : a scaling coefficient used to expand the range of NN output.

TDL: tapped delay line block

The output of the l -th hidden node $(l = 1, \dots, ncc)$:

$$net_l = \sum_{j=1}^t w_{lj} x_j = w_l x \quad (01)$$

$s(net_l)$: output of the l -th node of hidden layer,

The i -th neural output $(i = 1, \dots, ns)$ is given by the following equation:

$$yr_i(k+1) = \lambda s \left(\sum_{l=1}^{ncc} s \left(\sum_{j=1}^t w_{lj} x_j \right) z_{il} \right) \quad (02)$$

$$yr_i(k+1) = \lambda s \left(\sum_{l=1}^{ncc} s(net_l) z_{il} \right) \quad (03)$$

Finally, the compact form is defined as

$$Yr(k+1) = \lambda s \left[Z^T S(Wx) \right] \quad (04)$$

with

$$x = [x_j]^T \in R^{t \times 1}; j = 1, \dots, t$$

$$Z = [z_{il}]^T \in R^{ns \times ncc}; i = 1, \dots, ns \text{ and } l = 1, \dots, ncc$$

$$W = [w_{lj}] \in R^{ncc \times t}; l = 1, \dots, ncc \text{ and } j = 1, \dots, t$$

$$S(Wx) = [s(net_l)]^T \in R^{ncc \times 1}; l = 1, \dots, ncc$$

To see the influence of the noise to modeling, we act on the SNR . This report/ratio measures the correspondence between the real exit and the estimated exit, the equation of the SNR is as follows:

$$SNR_j = \frac{\frac{1}{N} \sum_{i=0}^N (y_j(i) - \bar{y}_j)^2}{\frac{1}{N} \sum_{i=0}^N (v_j(i) - \bar{v}_j)^2} \quad (05)$$

with

$v(i)$: noise of measurement of symmetric terminal

$$\delta, v(i) \in [-\delta, +\delta],$$

N : numbers of measurement,

\bar{y} : output average value,

\bar{v} : noise average value.

To see the influence of the noise to modeling, we act on the signal mean squared error mse .

$$mse(e_i) = \frac{1}{N} \sum_{i=0}^N (e_i)^2 \quad (06)$$

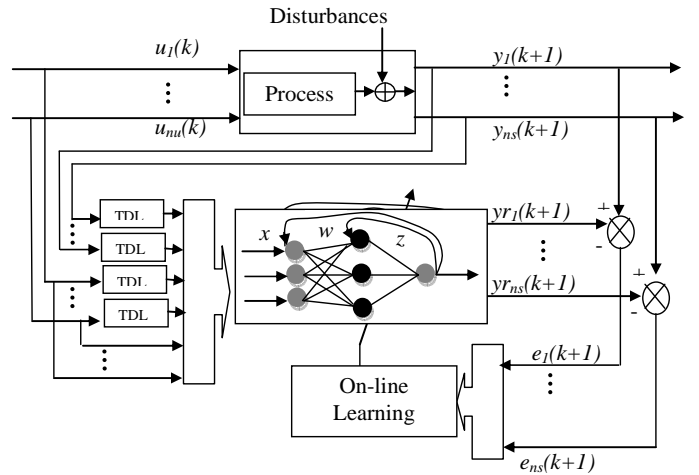


Fig.1. Principle of the neural modeling of the multivariable system

III. PRINCIPLE OF GRADIENT DESCENT METHOD

The principle of neural identification given for the single-variable systems [6] remains also usable for the case of the multivariable systems.

The principle is to minimize the i -th criterion such as:

$$J_i(k) = \frac{1}{2} (e_i(k))^2 = \frac{1}{2} [y_i(k) - yr_i(k)]^2 \quad (07)$$

To find the variation of the synaptic weights of the hidden layer towards the output layer, and the variation of the synaptic weights of the input layer towards the hidden layer the equations (3), (4), (7) and the theory of [1] are used, we find then:

$$z_{il}(k) = z_{il}(k-1) + \eta_i \lambda s'(net_i) S(Wx) e_i(k) \quad (08)$$

$$w_{lj}(k) = w_{lj}(k-1) + \eta_l \lambda s'(net_l) S'(Wx) z_{il} x^T e_i(k) \quad (09)$$

with $(i = 1, \dots, ns)$

In these expressions, η_i ($i = 1, \dots, ns$) is a positive constant value which represents the learning rate ($0 \leq \eta_i \leq 1$) and $S'(Wx)$ represents Jacobian matrix of $S(Wx)$.

$$S'(Wx) = \text{diag} \left[s' \left(\sum_{j=1}^l w_{lj} x_j \right) \right] \in \mathbb{R}^{ncc \times 1}; l = 1, \dots, ncc \quad (10)$$

with

$$s' \left(\sum_{j=1}^l w_{lj} x_j \right) = \frac{\partial s \left(\sum_{j=1}^l w_{lj} x_j \right)}{\partial \left(\sum_{j=1}^l w_{lj} x_j \right)}, l = 1, \dots, ncc.$$

IV. SIMULATION OF MULTIVARIABLE NONLINEAR STOCHASTIC SYSTEMS ($SNR = 5$)

In this section, two types of stochastic nonlinear multivariable systems with 2 dimensions ($ne = 2, ns = 2$) are presented with ($SNR = 5$).

The system (S1) and (S2) are defined respectively by the following equations:

$$(S1) \begin{cases} y_1(k+1) = \left[\begin{array}{l} 0.3y_1(k) + 0.6y_1(k-1) + 0.6\sin(\pi u_1(k)) + \\ 0.3\sin(3\pi u_1(k)) + 0.1\sin(5\pi u_1(k)) + v_1(k) \end{array} \right] \\ y_2(k+1) = \left[\begin{array}{l} 0.3y_2(k) + 0.6y_2(k-1) + 0.8\sin(2y_2(k)) + \\ 1.2u_1(k) + v_2(k) \end{array} \right] \end{cases} \quad (11)$$

$$(S2) \begin{cases} y_1(k+1) = \frac{0.8y_1^3(k) + u_1^2(k)u_2(k)}{2 + y_2^2(k)} + v_1(k) \\ y_2(k+1) = \left[\begin{array}{l} \frac{y_1(k) - y_1(k)y_2(k)}{2 + y_2^2(k)} + \\ \frac{(u_1(k) - 0.5)(u_2(k) + 0.8)}{2 + y_2^2(k)} + v_2(k) \end{array} \right] \end{cases} \quad (12)$$

with v_1 and v_2 are a random signal but u_1 and u_2 are the input of the systems considered defined by:

$$u_1(k) = \sin\left(\frac{2\pi k}{250}\right) \quad (13)$$

$$u_2(k) = \sin\left(\frac{2k\pi}{25}\right) \quad (14)$$

The system (S2) is strongly nonlinear compared to (S1). The input u_1 and u_2 are presented in the Fig. 2.

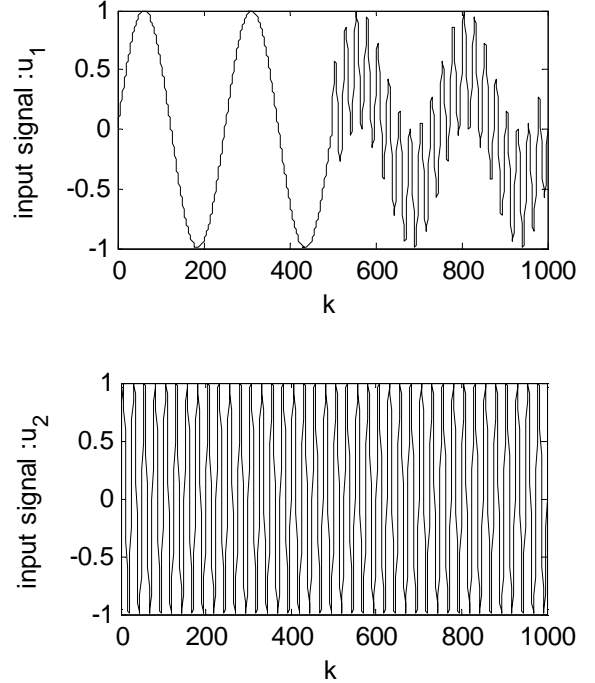


Fig. 2. Input signals of the nonlinear system

IV.1. SIMULATION RESULTS OF SYSTEM (S1)

A dynamic Neural Networks (NN) is used to simulate a multivariable system (S1) which defined by the equation (11).

Fig. 3 presents the evolution of the real output and the NN output of the system (S1).

Fig. 4 presents the prediction error between the real output and the NN output.

The results obtained, present that for a fixed learning rate $\eta_1 = 0.32$, the NN output yr_1 follows the measured output y_1 with an error of prediction $e_1 = 0.0720$ and that yr_2 follows the measured output y_2 with an error of prediction $e_2 = 0.0601$ whose learning rate is $\eta_2 = 0.27$

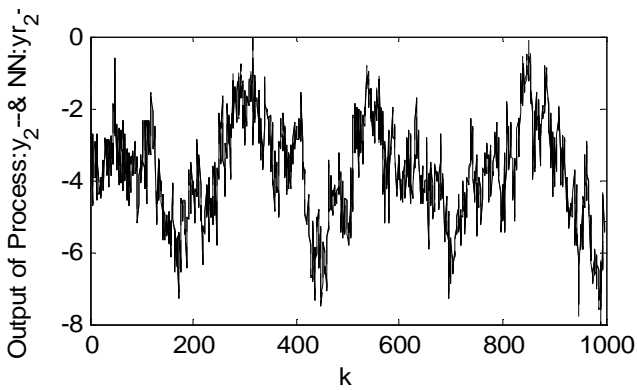
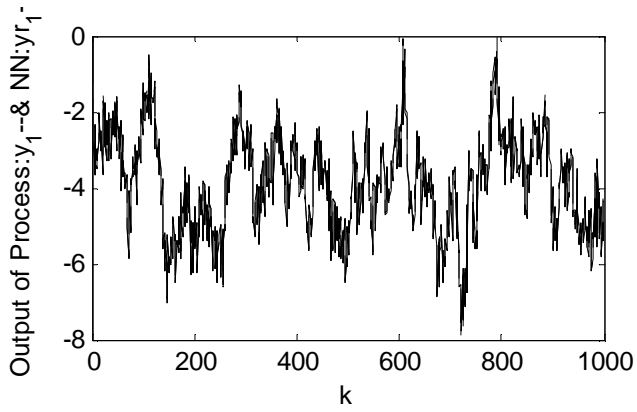


Fig. 3. Output of Process and NN of system (S1) using a fixed learning rate

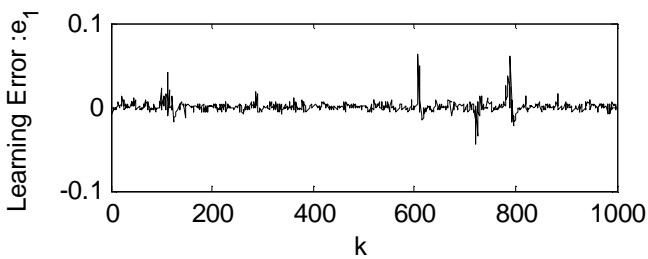
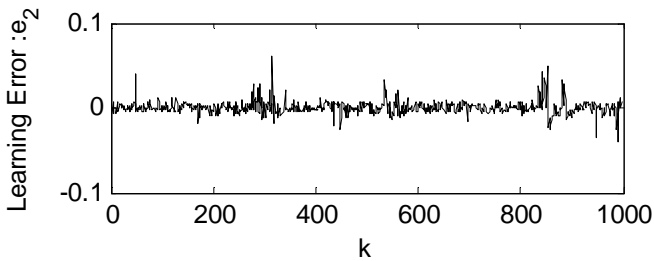


Fig. 4. Learning Error between the Output of Process and NN

IV.2. SIMULATION RESULTS OF SYSTEM (S2)

In this example, the input signals presented by Fig. 2.

Fig. 5 presents the evolution of the real output and the NN output of the system (S2) defined by the equation (12).

Fig. 6 presents the prediction error between the real output and the NN output.

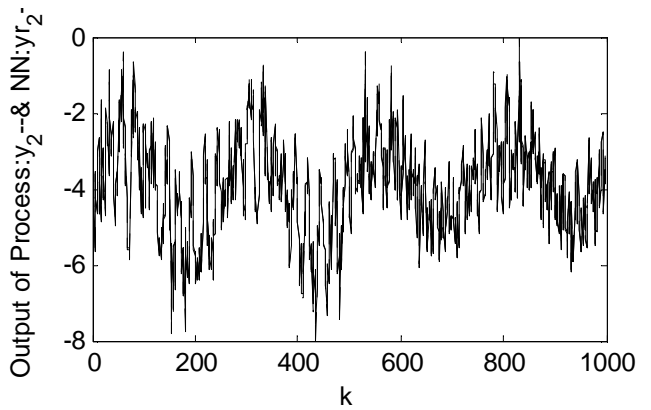
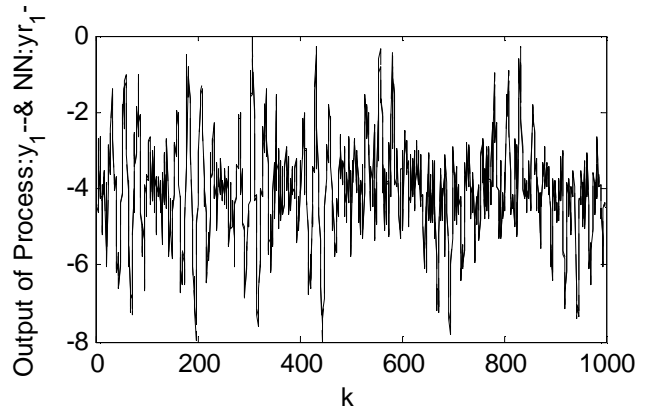


Fig. 5. Output of Process and NN of system (S2) using a fixed learning rate

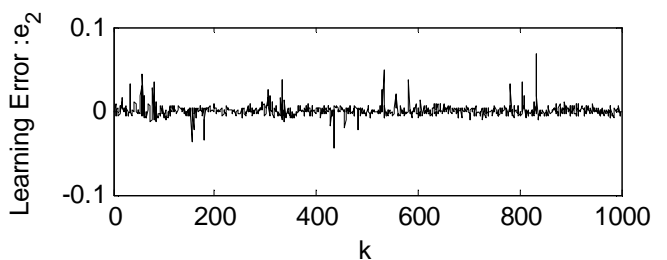
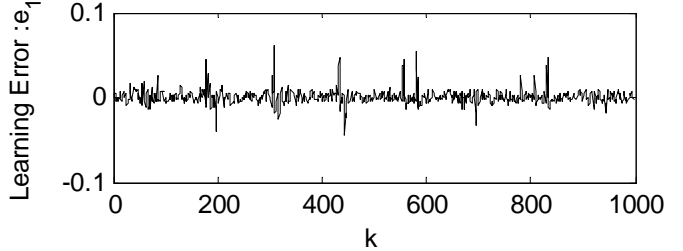


Fig. 6. Learning Error between the Output of Process and NN

The results obtained, present that for a fixed learning rate $\eta_1 = 0.3$, the NN output yr_1 follows the measured output y_1 with an error of prediction $e_1 = 0.0650$ and that yr_2 follows the measured output y_2 with an error of prediction $e_2 = 0.0670$ whose learning rate is $\eta_2 = 0.25$.

We took three cases of SNR (5,10 and 20) to show the influence of disturbance modeling. The results obtained are presented in table 1 for the first system and in table 2 for the second system.

TABLE 1
DIFFERENT CASES OF SNR

SNR	5	10	20
$mse(e_1)$	7.6115e-005	6.6792e-005	5.6480e-005
$mse(e_2)$	7.4588e-005	6.6434e-005	4.2051e-005

TABLE 2
DIFFERENT CASES OF SNR

SNR	5	10	20
$mse(e_1)$	8.6986e-005	7.7050e-005	5.9475e-005
$mse(e_2)$	8.6886e-005	7.5627e-005	5.2788e-005

In both tables, when the SNR increases the $mse(e_i)$ decrease, it is due under the presence of disturbance in the system.

In this section, the simulation of the two systems (S1 and S2) is carried out using a fixed learning rate. To find the suitable learning rate it is necessary to carry out several tests by keeping the condition that $(0 \leq \eta_i \leq 1)$. This research of the learning rate can slow down the phase of training. To cure this disadvantage and in order to accelerate the phase of training, a variable learning rate is used.

V. ADAPTIVE LEARNING RATE

The need for using a variable learning rate is to have a fast training.

For $(i=1, \dots, ns)$, we have:

$$e_i(k+1) - e_i(k) = y_i(k+1) - yr_i(k+1) - y_i(k) + yr_i(k) \quad (15)$$

we suppose that

$$\Delta y_i(k+1) = y_i(k+1) - y_i(k) \quad (16)$$

and

$$\Delta yr_i(k+1) = yr_i(k+1) - yr_i(k) \quad (17)$$

by application of [5]

$$\|\Delta y_i(k+1)\| \ll \|\Delta yr_i(k+1)\| \quad (18)$$

then

$$e_i(k+1) - e_i(k) \approx -\Delta yr_i(k+1) = -\lambda \Delta s(net_l) \quad (19)$$

$$e_i(k+1) - e_i(k) = -\lambda^2 \eta_i s'^2(net_l) * \left[S^T(W_x)S(W_x) + z_{il}^T S'(W_x)S'(W_x)z_{il}x^T x \right] * e_i(k) \quad (20)$$

So we find that

$$e_i(k+1) - e_i(k) = -\eta_i \xi_i(k) e_i(k) \quad (21)$$

with

$$\xi_i(k) = \lambda^2 s'^2(net_l) * \left[S^T(W_x)S(W_x) + z_{il}^T S'(W_x)S'(W_x)z_{il}x^T x \right] \quad (22)$$

from where

$$e_i(k+1) \approx [1 - \eta_i \xi_i(k)] e_i(k) \quad (23)$$

To ensure convergence, i.e., $\lim_{k \rightarrow \infty} e_i(k) = 0$ it is necessary that $\|e_i(k)\| < 1$ is satisfied.

This condition proves that $0 < \eta_i < 2\xi_i^{-1}(k)$. For that and in order to have a variable learning rate is necessary that for $(l=1, \dots, ncc)$ and $(i=1, \dots, ns)$:

$$\eta_i = \xi_i^{-1}(k) \quad (24)$$

$$\eta_i = 1 / (\lambda^2 s'^2(\sum_{j=1}^t w_{lj}x_j) * \left[S^T(W_x)S(W_x) + z_{il}^T S'(W_x)S'(W_x)z_{il}x^T x \right]) \quad (25)$$

We find that the learning rate η_i depends on the neural input vector x , depends on w_{lj} and depends on z_{il} . The variations of the synaptic weights of the hidden layer towards the output layer and of the input layer towards the hidden layer are presented respectively:

$$\begin{aligned} \Delta z_{il} &= \eta_i \lambda s'(\sum_{j=1}^t w_{lj}x_j) S(W_x) e_i(k) \\ &= \frac{S(W_x) e_i(k)}{\lambda s'(net_l) \left[S^T(W_x)S(W_x) + z_{il}^T S'(W_x)S'(W_x)z_{il}x^T x \right]} \quad (26) \end{aligned}$$

$$\begin{aligned} \Delta w_{lj} &= \eta_i \lambda s'(\sum_{j=1}^t w_{lj}x_j) S'(W_x) z_{il} x^T e_i(k) \\ &= \frac{S'(W_x) z_{il} x^T e_i(k)}{\lambda s'(net_l) \left[S^T(W_x)S(W_x) + z_{il}^T S'(W_x)S'(W_x)z_{il}x^T x \right]} \quad (27) \end{aligned}$$

Finally the update of the synaptic weights of the hidden

layer towards the output layer according to the variable learning rate is in the following way:

$$z_{il}(k) = z_{il}(k-1) + \frac{S(Wx)e_i(k)}{\lambda s'(net_l) \left[S^T(Wx)S(Wx) + z_{il}^T S'(Wx)S'(Wx)z_{il} x^T x \right]} \quad (28)$$

like for the synaptic weights of the input layer towards the hidden layer:

$$w_{lj}(k) = w_{lj}(k-1) + \frac{S'(Wx)z_{il} x^T e_i(k)}{\lambda s'(net_l) \left[S^T(Wx)S(Wx) + z_{il}^T S'(Wx)S'(Wx)z_{il} x^T x \right]} \quad (29)$$

V.1. SIMULATION RESULTS OF SYSTEM (S1) (SNR = 5)

Fig. 7 presents the evolution of the NN output and the real output of the system (S1).

Fig. 8 presents the prediction error between the real output and the neural output.

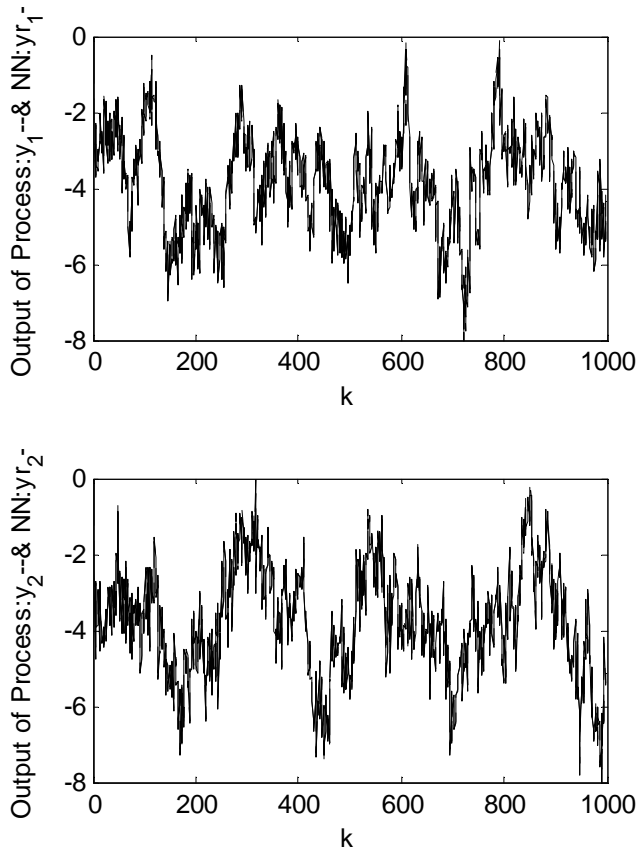


Fig. 7. Output of Process and NN of system (S1) using a variable learning rate

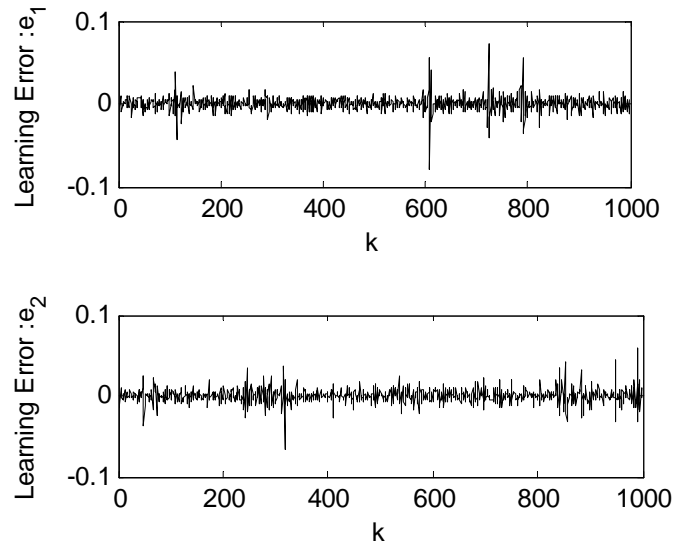


Fig. 8. Learning Error between the Output of Process and NN

The results obtained present that for an adaptive learning rate, the neural output yr_1 follows the measured output y_1 with an error of prediction $e_1 = 0.0634$ and that yr_2 follows the measured output y_2 with an error of prediction $e_2 = 0.0588$

V.1. Simulation results of system (S2) (SNR = 5)

Fig. 9 presents the evolution of the real output and the estimated output of the system (S2).

Fig. 10 presents the errors of the predictions between the real output and the neuronal output.

Fig. 11 and 12 present the evolution of the squared error in two case; fixed and adaptive learning rates.

The results obtained, concerning system (S2), present that for an adaptive learning rate, the neural output yr_1 follows the measured output y_1 with an error of prediction $e_1 = 0.0539$ and that yr_2 follows the measured output y_2 with an error of prediction $e_2 = 0.0668$.

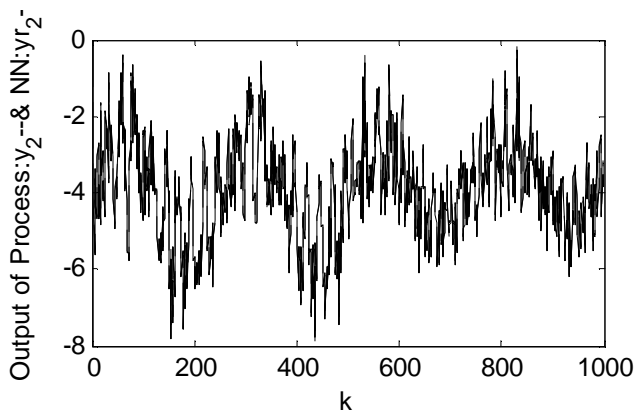
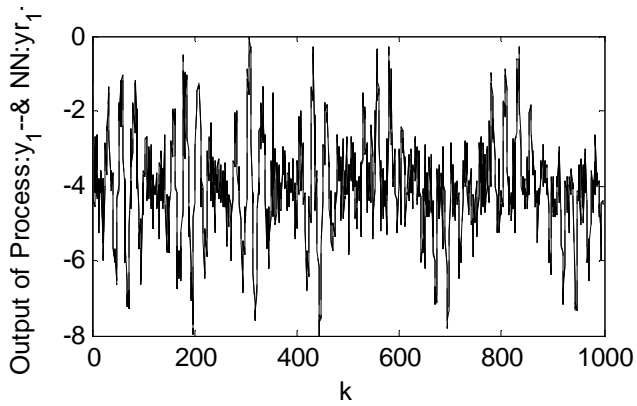


Fig. 9. Output of Process and NN of system (S2) using a variable learning rate

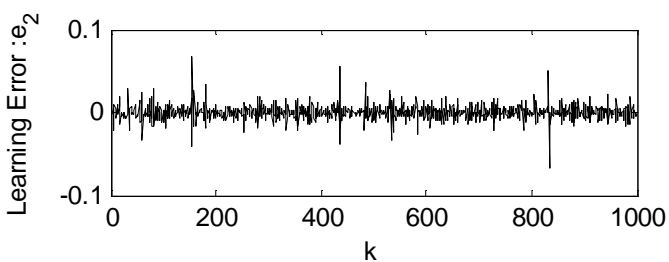
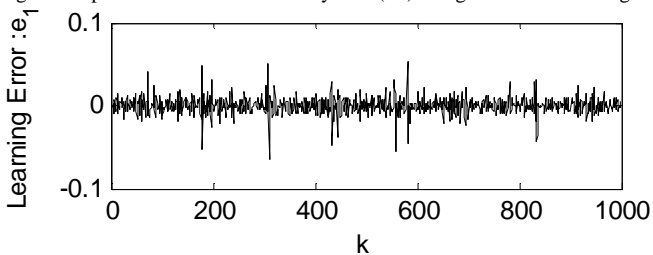


Fig. 10. Learning Error between the Output of Process and NN

The variable learning rate avoids the divergence of the training, so it provided an acceptable quality of training.

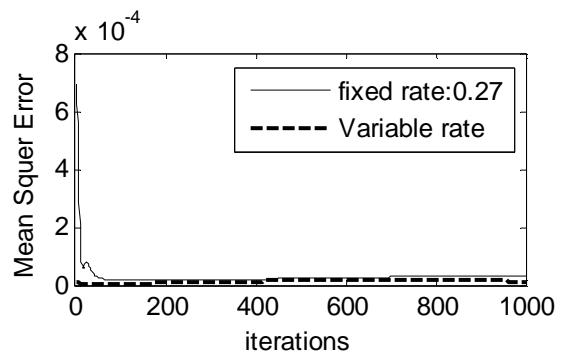
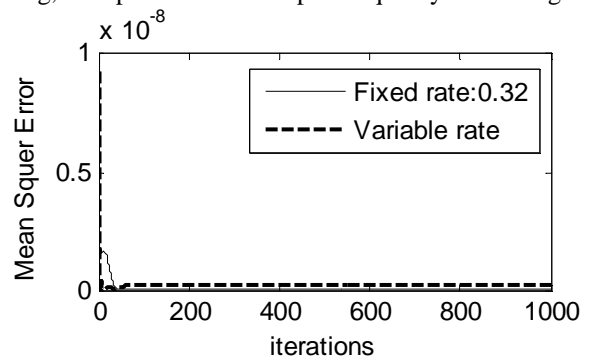


Fig. 11. Evolution of the Mean Squared Error of (S1)

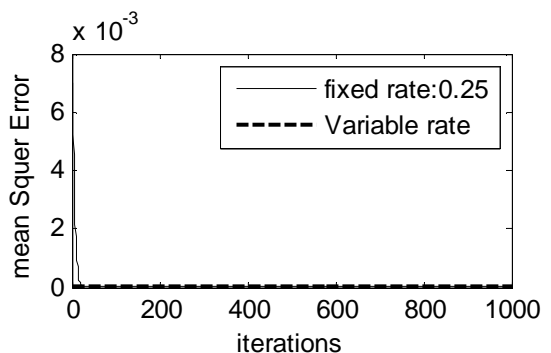
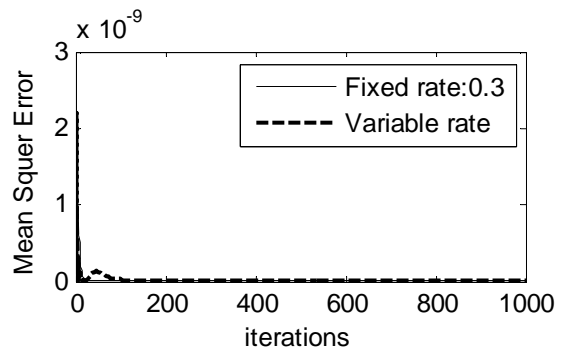


Fig. 12. Evolution of the Mean Squared Error of (S2)

The results obtained presented in Fig (11 and 12) showing that, when a variable learning rate is used, the convergence of the squared error is very fast that when a fixed learning rate is used.

The results obtained when used an adaptive learning rate are better than using a fixed learning rate.

The dynamic NN present a significant power in the simulation of the multivariable stochastic systems which have strong non-linearity.

The results obtained are presented in table 3 for the first system and in table 4 for the second system.

TABLE 3
DIFFERENT CASES OF SNR

SNR	5	10	20
$mse(e_1)$	5.9068e-005	5.1520e-005	3.9321e-005
$mse(e_2)$	6.5014e-005	5.5524e-005	4.3109e-005

TABLE 4
DIFFERENT CASES OF SNR

SNR	5	10	20
$mse(e_1)$	7.4020e-005	6.3687e-005	6.3348e-005
$mse(e_2)$	7.8639e-005	4.6019e-005	4.5375e-005

In both tables, when the SNR increases the $mse(e_i)$ decrease, it is due under the presence of disturbance in the system.

The values obtained by $mse(e_i)$ in tables 3 and 4 are lower compared to $mse(e_i)$ calculated in tables 1 and 2, that explains the variable rate adjusts with changes in examples.

VI. CONCLUSION

A new on-line variable rate learning algorithm for multivariable nonlinear stochastic systems is proposed. This algorithm is applied with success. It shows much better performance in terms of the learning speed and the reduced training error. This algorithm is a solution to avoid the search for such fixed training rate which presents a disadvantage at the level the phase of training. The variable rate learning algorithm does not require any experimentation for the selection of an appropriate value of the learning rate. Different cases of SNR are discussed to test, on the one hand, the power of the NN for modeling and on the other hand to see the performances of this algorithm. The obtained results showed that the neural network using a variable training rate is very powerful to model every multivariable nonlinear stochastic system. These results confirm the validity and suitability of the algorithms proposed.

REFERENCES

[1] K. Kara «Application des réseaux de neurones à l'identification des systèmes non linéaires» Thèse de Magister, Université de Constantine 1995.
 [2] K.S. Narendra «Neural networks for identification and control» Center of systems, Yale University 1998.

[3] S.R. Chu, R. Shoureshi, N. Tenorio «Neural networks for system identification» IEEE Control system Magazine, Vol. 10, N°. 3, pp 31-35, 1990.
 [4] S. Chen S.A. Billings «Neural networks for nonlinear system modeling and identification» Int. Journal, Vol. 56, N°. 2, pp. 319-346, 1992.
 [5] D. Sha, B. Bajic «On-line variable learning rate BP algorithm for multilayer feedforward neural networks» In Development and Practice of Artificial Intelligence Techniques, IAAMSAD, South Africa, pp 51-58, 1999.
 [6] G. Dreyfus, J-M. Martinez, M. Samuelides, M. Gordon, F. Badran, S. Thira, L. Héroult «Réseaux de neurones : méthodologie et applications» Eyrolles, 2004.
 [7] P. Borne, M. Benrejeb, J. Haggege «Les réseaux de neurones: présentations et applications» Editions Technip, 2007.
 [8] R.P. Brent «Fast training algorithms for Multilayer neural nets» IEEE Trans on neural networks, Vol. 2, N°. 3, pp. 346-354, 1991.
 [9] R.A. Jacobs «Increase rates of convergence through learning rate adaptation» Neural Networks, Vol. 1, pp. 295-307, 1988.
 [10] D.C. Park, M.A. El-Sharkawi, R.J. Marks II «An adaptively trained neural network» IEEE Trans on Neural Networks, Vol. 2, N°. 3, pp. 334-345, 1991.
 [11] P. Saratchandran «Dynamic programming approach to optimal weight selection in multilayer neural networks» IEEE Trans on Neural Networks, Vol. 2, N°. 4, pp. 465-467, 1991.
 [12] M.A. Sartori, P.J. Antsaklis «A simple method to derive bounds on the size and to train multilayer neural networks» IEEE Trans on Neural Networks, Vol. 2, N°. 4, pp. 467-471, 1991.
 [13] S. Shah, F. Palmieri, M. Datum «Optimal filtering algorithms for fast learning in feedforward neural networks» Neural Networks, Vol. 5, N°. 5, pp. 779-787, 1992.
 [14] C.M. Bishop «Curvature-driven smoothing: a learning algorithm for feedforward networks» IEEE trans on Neural Networks, Vol. 4, N°. 5, pp. 882-884, 1993.
 [15] A. Back, E. Wan, S. Lawrence, A.C. Tsou «A unifying view of some training algorithms for multilayer perceptrons with FIR filter synapses» Neural Networks for Signal processing 4, IEEE Press, pp. 146-154, 1995.
 [16] C.S. Chen «Dynamic structure adaptive neural fuzzy control for MIMO uncertain nonlinear systems», Information sciences 179, 2676-2688, 2009.
 [17] D. Sha «A new neural networks based adaptive model predictive control for unknown multiple variable no-linear systems», Int. J. Advanced Mechatronic Systems, Vol. 1, N°. 2, pp 146-155, 2008.

Uncertainty of random variables

Zdeněk Fabián

Institute of Computer Science
Academy of Sciences of the Czech republic
Pod vodárenskou věží 2, Praha 8
(e-mail: zdenek@cs.cas.cz)

Abstract. New characteristics of continuous random variables introduced in [4]-[6] are generalized for discrete random variables. It makes possible to introduce uncertainty function of random variable and compare its mean value with the Shannon entropy.

Keywords: scalar score, information, entropy.

1 Introduction

Let X be a discrete random variable with probability mass function $f(k)$, $k = 0, 1, \dots, n$. From the times of the Shannon's discovery, the uncertainty of X before the experiment or information contained in a realization x of X after the experiment is expressed, for any k , as $U(k) = \log(1/f(k))$. If the result of an experiment is more or less expected, uncertainty is low, whereas an unexpected result with low probability $f(k)$ carries a great amount of uncertainty. The mean value of this "uncertainty function" is the entropy

$$H(X) = EU(k) = \sum_{k=0}^n \log(1/f(k)) f(k) = \sum_{k=0}^n -f(k) \log f(k). \quad (1)$$

Let X be a continuous random variable with support set $\mathcal{X} = (a, b) \subseteq \mathbb{R}$, distribution F and density f . The analogy of the Shannon entropy for continuous random variables is the differential entropy

$$h(X) = E \log(1/f(x)) = \int_{\mathcal{X}} -\log f(x) f(x) dx. \quad (2)$$

Since $U(x) = \log(1/f(x))$ can be negative in certain range of parameters practically for any parametric distribution, it can be hardly considered to be an "uncertainty function". Even the mean value EU can be negative, too. This is the reason that statisticians prefer the Fisher information. However, Fisher information relates to the parameters of parametric distributions. The generalization presented in [2] is meaningful for distributions with support \mathbb{R} only.

In [3]-[5] we introduced to a given regular continuous distribution F a scalar function $S(x)$, called now the scalar score. It appeared that $S^2(x)$

can be considered as expressing information contained in observation x in the given model. In the present paper we briefly describe the scalar score and introduce an uncertainty function based on $S^2(x)$. In the last section we generalize concept of the scalar score for discrete distributions and show a relation between the mean uncertainty and the Shannon entropy.

2 Scalar score

As an important function of a distribution G with support \mathbb{R} and density g we identified, using lesson drawn from [6], the *score function*

$$T_G(y) = -\frac{1}{g(y)} \frac{d}{dy} g(y). \quad (3)$$

Value ET_G^2 is the generalized Fisher information introduced in [2].

Let $\eta : \mathcal{X} \rightarrow \mathbb{R}$ be a suitable mapping. As an important function describing the transformed distribution on $\mathcal{X} \neq \mathbb{R}$,

$$F(x) = G(\eta(x)), \quad x \in \mathcal{X}, \quad (4)$$

was suggested in [4] the transformed score function of G ,

$$T(x) = T_G(\eta(x)). \quad (5)$$

From (3) and (4) we obtain

$$T(x) = -\frac{1}{f(x)} \frac{d}{dx} \left(\frac{1}{\eta'(x)} f(x) \right), \quad (6)$$

where $\eta'(x) = d\eta(x)/dx$ is the Jacobian of the transformation.

For a comparison of properties of function (6) of different distributions, it turned out to be necessary to use one concrete $\eta : \mathcal{X} \rightarrow \mathbb{R}$ for all distributions with a given support. According the principle of parsimony, that one providing the simplest mathematical forms of (6) for a large amount of commonly used distributions should be used. According [7] and [5], η was defined as

$$\eta(x) = \begin{cases} x & \text{if } \mathcal{X} = \mathbb{R} \\ \log(x - a) & \text{if } \mathcal{X} = (a, \infty) \\ \log \frac{(x - a)}{(b - x)} & \text{if } \mathcal{X} = (a, b). \end{cases} \quad (7)$$

Function (6) with η given by (7) is called the *transformation-based score* or shortly the *t-score*.

Under mild regularity condition, the transformation-based score is a unique description of distributions, expressing the relative change of a “basic component” of the density of the model (the density divided by Jacobian of the transformation) with respect to the probability density.

T-scores of some distributions are well-known functions. The t-score of the standard normal distribution is $T(x) = x$. The t-score of a location distribution with support \mathbb{R} and location parameter μ (expressing the location of the maximum of the density) is the score function

$$T_G(y - \mu) = \frac{\partial}{\partial \mu} \log g(y - \mu). \tag{8}$$

The log-location distributions [8] are distributions transformed from \mathbb{R} into $\mathcal{X} = (0, \infty)$ by $\eta(x) = \log(x)$ with “transformed location” parameter $\tau = \exp(\mu)$. By [4], Theorem 1, it holds for them that

$$S(x; \tau) \equiv \eta'(\tau)T(x; \tau) = \frac{\partial}{\partial \tau} \log f(x; \tau), \tag{9}$$

which is the likelihood score for τ .

It is easy to see using (8) and (5) that $T(\tau; \tau) = 0$. Moreover, the value $ES^2 = \int_{\mathcal{X}} S(x; \tau)^2 f(x) dx$ is the Fisher information for τ .

Our basic notions, parameter τ and inference function S of log-location distributions, were generalized for arbitrary distribution as follows:

As the most important point of the distribution, expressing its central tendency, was identified, instead of τ , the zero of the t-score, the solution x^* of equation

$$T(x) = 0,$$

called the *t-mean*. The t-mean is actually the transformed mode (the maximum of the density) of the prototype. It is an easily manipulated number which is not far from the mean of light-tailed distributions, being a reasonable “center” of heavy-tailed and skewed distributions.

Function (9) was generalized by using the t-mean instead of τ by

$$S(x) = \eta'(x^*)T(x). \tag{10}$$

We call it a *scalar score of distribution F*. Scalar scores of parametric distributions $S(x; \theta) = \eta'(x^*)T(x; \theta)$ were suggested as inference functions for adapting the data to the assumed parametric model. For a given x , $S(x)$ describes the sensitivity of the t-mean to the value x . Function $S(x, \theta)$ as a function of θ is the “likelihood score for x^* ” either x^* is a parameter of the distribution or not.

The sample mean and sample variance of distributions with probability densities approaching to zero too slowly (the heavy tailed distributions) are not relevant characteristics of the data since the integrals defining the moments can be infinite. It follows from (3) that if $g(y) = O(e^{-y})$ if $y \rightarrow \pm\infty$ then $T_G(y) = O(1)$. Since (7) retains the properties of t-scores on boundaries of the support, the scalar scores of heavy-tailed distributions are bounded.

Function $S^2(x)$ attains its minimum at x^* (proof: the density of (4) is $f(x) = g(\eta(x))\eta'(x)$). The term $\eta'(x)$ is common to all distributions with the

given support and does not carry any information about X . The first term is minimal if $\frac{d}{dx}g(\eta(x)) = \frac{d}{dx}(f(x)/\eta'(x)) = 0$, which gives $T(x) = 0$ by (6). Further, $S^2(x)$ increases from x^* quickly/slowly if S is unbounded/bounded. Under the usual regularity conditions ES^2 is finite and means information. We thus insist that function $S^2(x)$ could play the role of the Fisher information function of continuous random variables, giving a relative information contained in observation x , small if the distribution is heavy-tailed, being vast if x is an outlier in a model which not “expect” an occurrence of outlying observations.

Since $\eta'(x^*) \neq 0$ and $ES^2 > 0$, the *score variance*

$$\omega^2 = \frac{1}{ES^2} = \frac{1}{[\eta'(x^*)]^2 ET^2(\theta)} \tag{11}$$

is finite. The score variance of distributions with $\mathcal{X} = (0, \infty)$, $\omega^2 = (x^*)^2/ET^2$, is proportional to the square of the t-mean, which is in agreement with σ^2 of light-tailed distributions (see Table 2, where we denoted $s = 1/c$. The value σ^2 of the Weibull distribution is an approximation for low s).

Distribution	exponential	gamma	Weibull	lognormal
σ^2	τ^2	α/γ^2	$\frac{\pi^2}{6}\tau^2s^2$	$\tau^2e^{s^2}(e^{s^2} - 1)$
ω^2	τ^2	α/γ^2	τ^2s^2	τ^2s^2

Table 1. Ordinary and score variance of light-tailed distributions

The score variance of heavy-tailed distributions, however, is a new quantity. The left panel of Fig. 1 compares ω and σ of the beta-prime distribution for $q = p$, where ω^2 is given in Table 2 below and $\sigma^2 = \frac{p(p+1)}{(q-1)(q-2)}$. The ordinary σ blows up at $q = 2$.

The score variance of distributions with support $\mathcal{X} = (-b, b)$ is $\omega^2 = \frac{b^2}{16ET^2}$. For the uniform distribution with $f(x) = \frac{1}{2b}$ thus $\omega^2 = \frac{3b^2}{4}$, whereas the ordinary $\sigma^2 = \frac{b^2}{3}$. The right panel of Fig. 1 shows σ and $\omega = (\frac{2p+1}{p^2})^{1/2}$ of the beta distribution, $q = p$. Measure ω assigns large values to U-shaped distributions with $p < 1$.

3 Uncertainty function

Definition 1. Let X be random variable with distribution F with support set \mathcal{X} . Denote by f its density, T the t-score and x^* the t-mean. Let η be given by (7) and S be the scalar score given by (10). Define the uncertainty function of X by

$$U(x) = \frac{S^2(x)}{(ES^2)^2}. \tag{12}$$

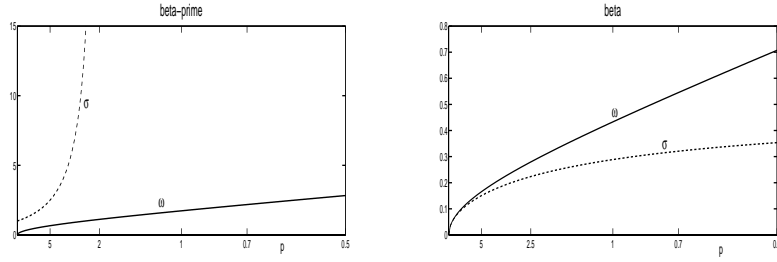


Fig. 1. σ and ω of the beta-prime and beta distributions as functions of p .

The uncertainty function is defined by such a way that the mean uncertainty equals to the score variance, $EU = \omega^2$. $U(x)$ can be determined also from relation

$$U(x) = \omega^2 \frac{T^2(x)}{ET^2}, \tag{13}$$

equivalent to (12). Table 2 and Fig. 2 shows uncertainty functions of some currently used distributions.

F	\mathcal{X}	$f(x)$	$T(x)$	ω^2	$U(x)$
normal	\mathbb{R}	$\frac{1}{\sqrt{2\pi}\sigma} e^{-\frac{1}{2}(\frac{x-\mu}{\sigma})^2}$	$\frac{1}{\sigma} \frac{x-\mu}{\sigma}$	σ^2	$(x - \mu)^2$
Cauchy	\mathbb{R}	$\frac{1}{\pi\sigma(1+(\frac{x-\mu}{\sigma})^2)}$	$\frac{1}{\sigma} \frac{2\frac{x-\mu}{\sigma}}{1+(\frac{x-\mu}{\sigma})^2}$	$2\sigma^2$	$\frac{16(x-\mu)^2}{(1+(\frac{x-\mu}{\sigma})^2)^2}$
lognormal	$(0, \infty)$	$\frac{c}{\sqrt{2\pi}x} e^{-\frac{1}{2}\log^2(\frac{x}{\tau})^c}$	$c \log(\frac{x}{\tau})^c$	$\frac{\tau^2}{c^2}$	$\frac{\tau^2}{c^2} \log^2(\frac{x}{\tau})^c$
Weibull	$(0, \infty)$	$\frac{c}{x} (\frac{x}{\tau})^c e^{-(x/\tau)^c}$	$c[(\frac{x}{\tau})^c - 1]$	$\frac{\tau^2}{c^2}$	$\frac{\tau^2}{c^2} [(\frac{x}{\tau})^c - 1]^2$
gamma	$(0, \infty)$	$\frac{\gamma^\alpha}{x\Gamma(\alpha)} x^\alpha e^{-\gamma x}$	$\gamma x - \alpha$	$\frac{\alpha}{\gamma^2}$	$(x - \alpha/\gamma)^2$
log-logistic	$(0, \infty)$	$\frac{c}{x} \frac{(x/\tau)^c}{[(x/\tau)^c + 1]^2}$	$c \frac{(x/\tau)^c - 1}{(x/\tau)^c + 1}$	$\frac{3\tau^2}{c^2}$	$\frac{9\tau^2}{c^2} \frac{[(x/\tau)^c - 1]^2}{[(x/\tau)^c + 1]^2}$
Pareto	(a, ∞)	ca^c/x^{c+1}	$c - \frac{a(c+1)}{x}$	$\frac{a^2(c+2)}{c^3}$	$\frac{a^2(c+2)^2}{c^2} \left(1 - \frac{a(c+1)}{cx}\right)^2$
beta-prime	$(0, \infty)$	$\frac{1}{B(p,q)} \frac{x^{p-1}}{(x+1)^{p+q}}$	$\frac{qx-p}{x+1}$	$\frac{p(p+q+1)}{q^3}$	$\frac{(p+q+1)^2}{q^2} \frac{(x-p/q)^2}{(x+1)^2}$
beta	$(0, 1)$	$\frac{x^{p-1}(1-x)^{q-1}}{B(p,q)}$	$(p+q)x - p$	$\frac{pq(p+q+1)}{(p+q)^4}$	$\frac{(p+q+1)^2}{(p+q)^2} \left(x - \frac{p}{p+q}\right)^2$

Table 2. Uncertainty functions of some distributions.

Denote the square root of the mean uncertainty ω^2 by $\omega(X)$. Instead of the differential entropy $h(X)$, the positive values $e^{h(X)}$ are sometimes studied (see [2]). Table 3 shows a close relation between $\omega(X)$ and $e^{h(X)}$ of distributions with support \mathbb{R} . The correspondence between $\omega(X)$ and $e^{h(X)}$ of distributions with support $\mathcal{X} \neq \mathbb{R}$ is less apparent, but they have, generally, a similar behavior. As an example, the left panel of Fig. 3 shows $e^{h(X)}$ and $\sqrt{2\pi}\omega(X)$ as functions of parameter α of the gamma distribution.

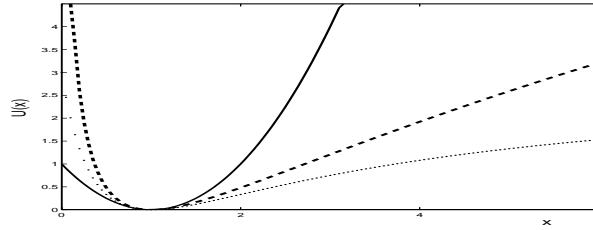


Fig. 2. Uncertainty functions of gamma (full line), lognormal (dashed line) and log-logistic (dotted line) distributions.

F	$f(x)$	$e^{h(X)}$	$\omega(X)$
normal	$\frac{1}{\sqrt{2\pi}\sigma} e^{-\frac{1}{2}\left(\frac{x-\mu}{\sigma}\right)^2}$	$\sqrt{2\pi}e\sigma$	σ
Cauchy	$\frac{1}{\pi\sigma(1+(x/\sigma)^2)}$	$4\pi\sigma$	2σ
gamma	$\frac{\gamma^\alpha}{\Gamma(\alpha)} x^{\alpha-1} e^{-\gamma x}$	$\frac{\Gamma(\alpha)}{\gamma} e^{((1-\alpha)\psi(\alpha)+\alpha)}$	$\sqrt{\alpha}/\gamma$
Weibull	$\frac{c}{\tau} x^{c-1} e^{-\frac{x^c}{\tau}}$	$\frac{\tau^{1/c}}{c} e^{(c-1)\epsilon/c+1}$	$\frac{\tau^{1/c}}{c}$
Pareto	ca^c/x^{c+1}	$\frac{a}{c} e^{(1+1/c)}$	$\frac{a}{c} \frac{\sqrt{c+2}}{\sqrt{c}}$
power	cx^{c-1}	$\frac{1}{c} e^{(1-1/c)}$	$\frac{\sqrt{c(c+2)}}{(c+1)^2}$

Table 3. Comparison of $e^{h(X)}$ and $\omega(X)$ for some distributions.

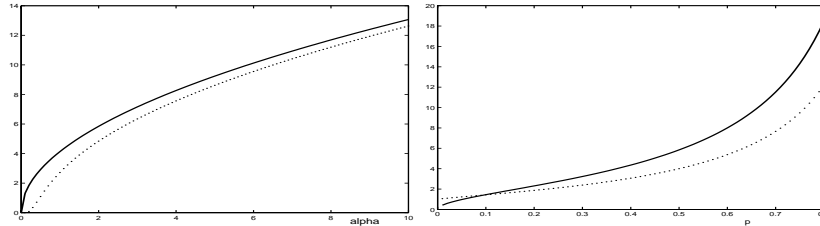


Fig. 3. $\sqrt{2\pi}e\omega(X)$ (full line) and $e^{h(X)}$ (dotted line) of gamma distribution as function of α (left) and of geometric distribution as function of p (right).

4 Uncertainty function of discrete random variables

In the last section we generalize the concept of the t-score for discrete distributions and show that the logarithm of the mean uncertainty has similar behavior as Shannon entropy.

Let a random variable takes on values $k = 0, 1, 2, \dots$ with probabilities $f(k)$. As an analogy with distributions with support $\mathcal{X} = (0, \infty)$, for which $1/\eta'(x) = x$, the t-score of the discrete distribution can be determined by replacing in formula (6) the derivatives by differences,

$$T(k) = -\frac{1}{f(k)}[(k+1)f(k+1) - kf(k)] = k - (k+1)\frac{f(k+1)}{f(k)}. \quad (14)$$

Example 4.1. *Geometric distribution* has probability mass function $f(k) = (1-p)p^k$. By (14), $T(k) = k(1-p) - p$. The t-mean $k^* = \frac{p}{1-p}$ equals the mean, and, since $ET^2 = p$, $\omega^2 = (k^*)^2/ET^2 = p/(1-p)^2$, which is the ordinary variance. The uncertainty function is, by (13),

$$U(k) = \frac{\omega^2}{ET^2}T^2(k) = \left(k - \frac{p}{1-p}\right)^2.$$

Functions of p , $e^{H(X)}$, where $H(X) = -\log p - \frac{p}{1-p} \log p$ and $\sqrt{2\pi e}\omega(X)$ of the geometric distribution are similar (right panel of Fig. 3).

Example 4.2. *Poisson distribution* has probability mass function $f(k) = \frac{e^{-\lambda}\lambda^k}{k!}$. By (14), $T(k) = k - \lambda$, $x^* = \omega^2 = \lambda$ and

$$U(k) = (k - \lambda)^2.$$

Let n be a fixed number and random variable X takes on values $k = 0, 1, 2, \dots, n$ with probabilities $f(k)$. As an analogy with distributions with finite interval support $\mathcal{X} = (0, n)$, for which $1/\eta'(x) = x(n-x)/n$, the t-score of the discrete distribution can be written as

$$T(x) = \frac{1}{f(x)} \frac{d}{dx} \left[-\frac{x(n-x)}{n} f(x) \right]. \quad (15)$$

If we approximate (15) by symmetric differences, we obtain

$$T(k) = -1 + \frac{2k}{n} - \frac{k(n-k)}{2nf(k)} [f(k+1) - f(k-1)] \quad (16)$$

for $k = 1, \dots, n-1$, with $T(0) = -1$ and $T(n) = 1$. The score variance is then

$$\omega^2 = \frac{[k^*(n-k^*)]^2}{n^2ET^2}. \quad (17)$$

Example 4.3. *Discrete uniform distribution* has probabilities $f(k) = \frac{1}{n+1}$. Its t-score is $T(k) = 2k/n - 1$ so that $x^* = n/2$ equals the mean. The t-score moment is $ET^2 = 2(2n+1)/3n - 1$. For large n , $ET^2 \doteq 1/3$. The score variance is $\omega^2 = \frac{n^2}{2^4ET^2}$ and the uncertainty function

$$U(k) = \frac{(k - n/2)^2}{4[(2n+1)/3n - 1]^2}.$$

For large n , $U(k) \doteq \frac{9}{4}(k - n/2)^2$. The uncertainty function of the continuous uniform distribution on $0, 1$ is $U(x) = \frac{9}{4}(x - 1/2)^2$.

Example 4.4. *Binomial distribution* has mass probability function $f(k) = \binom{n}{k} p^k (1-p)^{n-k}$. By (16), its t-score is

$$T(k) = -1 + \frac{2k}{n} - \frac{k(n-k)}{2n} \left[\frac{(n-k)p}{(k+1)(1-p)} - \frac{k(1-p)}{(n-k+1)p} \right].$$

Using (13), (17), numerical solutions of equation $T(x) = 0$ and the direct computation of $\frac{1}{n+1} \sum_{k=0}^n T^2(k)$, we obtained a plot of uncertainty function for $n = 10$ and $p = 0.5$ (left panel of Fig. 4), and the comparison of functions of p , the square root of the mean uncertainty $\omega(X)$ multiplied by term $\sqrt{2\pi}e$ with $e^{H(X)}$ (right panel of Fig.4). In this case, the mean uncertainty seems to be a better tool for distinguishing values of p as the Shannon entropy.

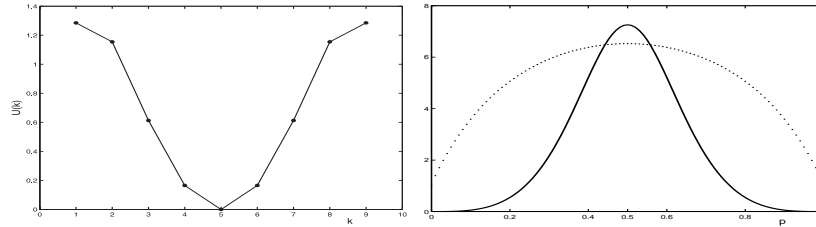


Fig. 4. Binomial distribution, $n = 10, p = 0.5$. Left: Uncertainty function, right: $\sqrt{2\pi}e\omega(X)$ (full line) and $e^{H(X)}$ (dotted line).

Acknowledgements. The research presented in the paper was supported by grant ME 949 "Analysis of negative impacts on driver attention" of The Ministry of Education, Youth and Sports of the Czech Republic.

References

1. Balakrishnan, N., and Nevzorov, V. B., *A Primer on Statistical Distributions*, Wiley, Hoboken (2003).
2. Cover, T. M., and Thomas, J.A., *Elements of Information Theory*, Wiley, Hoboken (1991).
3. Fabián, Z., "Information and entropy of continuous random variables", *IEEE Trans. of Information Theory* 43, 1080–1084, (1997).
4. Fabián, Z., "Induced cores and their use in robust parametric estimation", *Communication in Statistics, Theory Methods* 30, 537-556 (2001).
5. Fabián, Z., "New measures of central tendency and variability of continuous distributions". *Communication in Statistics, Theory Methods* 37, 159–174 (2008).
6. Hampel, F. R., Rousseeuw, P. J., Ronchetti, E. M. and Stahel, W. A. *Robust Statistic. The Approach Based on Influence Functions*, Wiley, New York (1986).
7. Johnson, N. L., "Systems of frequency curves generated by methods of translations". *Biometrika* 36: 149–176 (1949).
8. Lawless J. F., *Statistical models and methods for lifetime data*, Wiley, New York (2003).

Coefficient of Variation: Connecting Sampling with some Increasing Distribution Models

Dr FARMAKIS Nicolas
Aristotle University of Thessaloniki
Dept of Mathematics
farmakis@math.auth.gr

Abstract

A new use of Coefficient of Variation (C_v) is presented in order to define Distribution Models via Sampling. The interesting case of the simply increasing continuous probability distribution functions (pdf) is studied and the suitably obtained model is presented. A first level checking via sampling and graphs (e.g. histogram) is taking place in order to examine if we have an increasing or no model to be defined. After this using the idea of C_v and some polynomial forms the model is defined. In order to examine if the model is a well approximating one we check the correspondence of the sample data to the expected outputs from the model, by a Chi-square test. So the obtained model becomes a self checked one. The presented distribution models are polynomial and they so they have a real exponent $k > -1$. The value $k = -1$ seems to be a kind of an absolute zero point for the exponent of the polynomial pdf. The polynomial form of pdf is an approximation to the really existing pdf with more complicated form. This idea was also used in Farmakis (2003) for the symmetric continuous distributions (scd).

Key Words & phrases: Sampling, Distribution Models, Coefficient of Variation.

1. Introduction

The Coefficient of Variation (C_v) is a very well known and useful concept for the statisticians. A new idea from the early 2003 is to use C_v in order to check and manipulate distributions and their behavior. In other words the recently emerging new use of C_v is for the definition and the scaling of the symmetric continuous distributions (scd) by the help of sampling, Farmakis (2003). Basic tool is the probability density function (pdf) of the random variables and we approximately state it via sampling processes and using the concept of C_v too.

Definition: For any random Variable X , with only positive values, the Coefficient of Variation is the unit free rate given by

$$C_v = \frac{\sqrt{\text{Var}X}}{EX} \quad (1.1)$$

where $EX = \frac{1}{N} \sum_{i=1}^N X_i$ is the Mean Value of X and $\text{Var}X = EX^2 - (EX)^2$ its Variance.

It is well known that, for every random variable (r.v.) X , we can have any parameter like EX , $VarX$ and C_vX from its pdf. If the r.v. X is continuous, then it is sufficient to have to do with an integrable pdf. An integrable kind of pdf is always a pdf with polynomial form.

The new idea of this paper is to approximate the pdf of a random variable (rv) X with a k -degree polynomial form using sample data, beyond the case of symmetric pdf included in Farmakis (2003). Especially we deal with the Increasing pdf.

First of all we face the case of an increasing pdf in the interval $[0, b]$ in paragraph 2. Some illustrative Examples will be given in paragraph 3. A short discussion takes place in the frame of the last paragraph 4.

Here we give the form of mean value of a continuous rv X with pdf $f(x)$:

$$EX = \int_{-\infty}^{\infty} x \cdot f(x) \cdot dx \quad (1.2)$$

Obviously the pdf $f(x)$ is a non negative function of X with the basic property:

$$\int_{-\infty}^{\infty} f(x) \cdot dx = 1 \quad (1.3)$$

2. On the Increasing form of pdf

2.1 Theoretical point of view

Suppose we have a rv X with pdf approximable by the next polynomial function:

$$f(x) = \begin{cases} h \cdot \left(\frac{x}{b}\right)^k & x \in [0, b], \\ 0 & x \notin [0, b] \end{cases}, \quad h = \frac{k+1}{b}, \quad k \neq -1 \quad (2.1)$$

Trying to have the basic statistical parameters of X we have:

$$EX = \int_{-\infty}^{\infty} x \cdot f(x) \cdot dx = \int_0^b h \cdot x \cdot \left(\frac{x}{b}\right)^k = \dots = h \cdot \frac{x^{k+2}}{b^k \cdot (k+2)} \Big|_0^b = \frac{k+1}{k+2} \cdot b. \quad (2.2)$$

Also

$$EX^2 = \int_{-\infty}^{\infty} x^2 \cdot f(x) \cdot dx = \int_0^b h \cdot x^2 \cdot \left(\frac{x}{b}\right)^k = \dots = h \cdot \frac{x^{k+3}}{b^k \cdot (k+3)} \Big|_0^b = \frac{k+1}{k+3} \cdot b^2$$

and of course

$$VarX = \frac{k+1}{k+3} \cdot b^2 - \left(\frac{k+1}{k+2} \cdot b\right)^2 = \dots = \frac{b^2 \cdot (k+1)}{(k+3) \cdot (k+2)^2}. \quad (2.3)$$

From (1.1), (2.2) and (2.3) we obtain

$$C_v = \sqrt{\frac{1}{(k+1) \cdot (k+3)}} \quad (2.4)$$

i.e. the C_vX is straightforward connected with the degree k of pdf in (2.1). It is very important to note that C_vX is not depended on the parameter b (range).

For our convenience we adopt the form

$$C_v = \sqrt{\frac{I}{\lambda}} \quad \text{or} \quad \lambda = C_v^{-2} \quad (2.5)$$

From (2.4) and (2.5) we have the solution

$$k(\lambda) = -2 + \sqrt{1 + \lambda} \quad (2.6)$$

with rejection of the other root of (2.4)-(2.5).

Note 2.1: We can also express the adoption in (2.5) by the form of $\lambda = \frac{(EX)^2}{VarX} = C_v^{-2}$.

The next Table 2.1 with some values for C_v , λ and k will be helpful to see some cases of pdf (of integral values for λ):

Table 2.1

C_v	$\lambda = C_v^{-2}$	$k = -2 + \sqrt{1 + \lambda}$	Remarks
???	0	Tends to -1	$k \neq -1$
1	1	$-2 + \sqrt{2}$	
0.7071	2	$-2 + \sqrt{3}$	
0.5774	3	0	Uniform Distribution
0.5000	4	$-2 + \sqrt{5}$	
0.4472	5	$-2 + \sqrt{6}$	
0.4082	6	$-2 + \sqrt{7}$	
0.3780	7	$-2 + \sqrt{8}$	
0.3536	8	1	Linearity
0.3333	9	$-2 + \sqrt{10}$	
0.3162	10	$-2 + \sqrt{11}$	

If a r.v X has the value λ we can adopt the notation X_λ and so we can imagine the series $(X_\lambda)_{\lambda \in \mathbb{N}}$ of increasing pdf with the exponent k given by (2.6), see also in Farmakis (2003).

This is the theoretic point of view of the approximation of an increasing pdf via a polynomial form of degree k .

2.2 Applied point of view

We study a r.v. X . For this we get a sample of size n and we classify and put the data in a table and construct the suitable histogram, in order to have a view of the increasing nature of the pdf. If it is so, then we try to approximate the mean value, the variance and the coefficient of variation of X , from the sampling data and via their estimators: \bar{x} , s^2 , \hat{C}_v , respectively and the suitable quantity λ . From this we obtain the value of k and we calculate the coefficient h . So the polynomial model for the approximating pdf is ready (see (2.1)). From the obtained pdf we calculate the numbers n_r' of the expected observations for the suitable spaces of $[0, b]$ checking in parallel if they have a good fitting to the observed cases via the sample. We use of course Chi-Square test. If the least sample value of data x_{min} is not equal to zero, then we have to transform the data via $X - X_{min}$ and follow on. For more details, it is useful

to see the interesting examples in the paragraph 3. For the best reliability of this method, always a size of sample $n > 50$ is needed, Farmakis (2003).

3. Applications of the increasing form of pdf

We give some illustrative examples for some continuous random variables defined in $[0, b]$ as an increasing function.

Example 3.1: A sample of $n=140$ nodes (sites) was studied for the duration of the customer's visit and we have found the results included to the next table of data distributed in 7 spaces with wideness $w=4$ min. Calculate the parameters $\bar{x}, s^2, s, \hat{C}_v$. After this establish the formula of pdf for the r.v. X ="duration".

Table 3.1

Real Time Spaces	$X-X_{min}$ Spaces	Centers: x'_i	n_i	N_i	$x'_i = (x_i - m)/w$	$n_i \cdot x'_i$	$n_i \cdot x'^2_i$
[24 – 28]	[00 – 04]	02	2	2	-3	-6	18
[28 – 32]	[04 – 08]	06	8	10	-2	-16	32
[32 – 36]	[08 – 12]	10	15	24	-1	-15	15
[36 – 40]	[12 – 16]	14	20	44	0	0	0
[40 – 44]	[16 – 20]	18	25	70	1	25	25
[44 – 48]	[20 – 24]	22	30	102	2	60	120
[48 – 52]	[24 – 28]	26	40	140	3	120	360
Totals			140			T₁= 168	T₂= 570

Answer: The data are in the first four columns of Table 3.1. We have filled up the next columns of this table. The fifth column stands for the cumulative frequencies of the nodes. The parameter m on the title of the 5th is the temporary mean value for the sample and as usually is taken to be one middle standing value. Here $m=14$ is adopted. The parameter $w=4$ is the size of the seven spaces of the range of the time $R=b=28$ ($=52-24$).

The sample mean value is given as $\bar{x} = m + w \cdot \frac{T_1}{n} = 14 + 4 \cdot \frac{168}{140} = 18.8$ min

The sample variance is given as

$$s^2 = \frac{w^2}{n-1} \cdot \left(T_2 - \frac{T_1^2}{n} \right) = \frac{16}{139} \cdot \left(570 - \frac{168^2}{140} \right) = 42.4058$$

and the standard deviation is $s = \sqrt{s^2} = \sqrt{42.4058} = 6.5120$ min .

Thus the sample coefficient of variation is the unit free quantity

$$\hat{C}_v = \frac{s}{\bar{x}} = \frac{6.5120}{18.80} = 0.3464 . \quad (3.1)$$

Now the road is open to calculate the exponent k of the formula (2.1) via the (2.5) and (2.6), in order to obtain the formula (2.1) of pdf:

From (3.1) and (2.5) we get $\lambda = \hat{C}_v^{-2} = 0.3464^{-2} = 8.3338$,

from (2.6) we get $k(\lambda) = -2 + \sqrt{1 + \lambda} = -2 + \sqrt{1 + 8.3338} = 1.0551$

and from (2.1) we have $h = \frac{k+1}{b} = \frac{2.0551}{28} = 0.073396$.

Thus the pdf formula is given by

$$f(x) = \begin{cases} 0.073396 \cdot \left(\frac{x}{28}\right)^{1.0551} & x \in [0, 28] \\ 0 & x \notin [0, 28] \end{cases} \quad (3.2)$$

Now it is the moment to check the reliability of the method via the next test shown in the Table 3.2. The very-very little value of Chi-squared is a very good proof for the “good fitting” of the “observed” to the “theoretic” values n_i and n'_i respectively.

Table 3.2

Real Time Spaces	$X-X_{min}$ Spaces	Centers: x'_i	n_i	N_i	$n'_i = f(x_i) \cdot 140$ Theoretic	$\frac{(n_i - n'_i)^2}{n'}$
[24 – 28)	[00 – 04)	02	2	2	2.5	0.1000
[28 – 32)	[04 – 08)	06	8	10	8.1	0.0012
[32 – 36)	[08 – 12)	10	15	24	13.9	0.0871
[36 – 40)	[12 – 16)	14	20	44	19.8	0.0020
[40 – 44)	[16 – 20)	18	25	70	25.8	0.0248
[44 – 48)	[20 – 24)	22	30	102	31.9	0.1132
[48 – 52]	[24 – 28]	26	40	140	38.0	0.1053
Totals			140		140.0	$\chi^2 = 0.4336$

Example 3.2: Suppose we face the same sample of Example 3.1 but now the observed frequencies are in the exactly inverse order than in example 3.1, as we see in the 4th column of the next Table 3.3. Of course it is again $n=140$ nodes and the data were distributed in 7 spaces with wideness $w=4$ min. Calculate the parameters $\bar{x}, s^2, s, \hat{C}_v$. After this establish the formula of pdf for the r.v. $X=$ “duration”.

Table 3.3

Real Time Spaces	$X-X_{min}$ Spaces	Centers: x'_i	n_i	N_i	$x'_i = (x_i - m)/w$	$n_i \cdot x'_i$	$n_i \cdot x'^2_i$
[24 – 28)	[00 – 04)	02	40	40	-3	-120	360
[28 – 32)	[04 – 08)	06	30	70	-2	-60	120
[32 – 36)	[08 – 12)	10	25	95	-1	-25	25
[36 – 40)	[12 – 16)	14	20	115	0	0	0
[40 – 44)	[16 – 20)	18	15	130	1	15	15
[44 – 48)	[20 – 24)	22	8	138	2	16	32
[48 – 52]	[24 – 28]	26	2	140	3	6	18
Totals			140			T₁=-168	T₂= 570

Answer: The data are in the first four columns of Table 3.3. We have filled up the next columns of this table. The fifth column stands for the cumulative frequencies of the nodes. The parameter m on the title of the 5th is the temporary mean value for the sample and as usually is taken to be one middle standing value. Here $m=14$ is adopted. The parameter $w=4$ is the size of the seven spaces of the range of the weight $R=b=28$ ($=52-24$). For the present case we have the same data but now the frequencies

seem to come out from decreasing pdf than an increasing one, as we pass from space to space of the duration.

The sample mean value is given as $\bar{x} = m + w \cdot \frac{T_1}{n} = 14 + 4 \cdot \frac{-168}{140} = 9.2 \text{ min}$

The sample variance is given as

$$s^2 = \frac{w^2}{n-1} \cdot \left(T_2 - \frac{T_1^2}{n} \right) = \frac{16}{139} \cdot \left(570 - \frac{(-168)^2}{140} \right) = 42.4058$$

and the standard deviation is $s = \sqrt{s^2} = \sqrt{42.4058} = 6.5120 \text{ min}$.

Thus the sample coefficient of variation is the unit free quantity

$$\hat{C}_v = \frac{s}{\bar{x}} = \frac{6.5120}{9.20} = 0.7078. \quad (3.3)$$

Now the road is open to calculate the exponent k of the formula (2.1) via the (2.5) and (2.6) and to get the formula (2.1) of pdf:

From (3.1) and (2.5) we get $\lambda = \hat{C}_v^{-2} = 0.7078^{-2} = 1.9961$,

from (2.6) we get $k(\lambda) = -2 + \sqrt{1 + \lambda} = -2 + \sqrt{1 + 1.9961} = -0.2691$

and from (2.1) we have $h = \frac{k+1}{b} = \frac{0.7309}{28} = 0.026104$.

Thus the pdf formula is given by

$$f(x) = \begin{cases} 0.026104 \cdot \left(\frac{x}{28} \right)^{-0.2691} & x \in [0, 28] \\ 0 & x \notin [0, 28] \end{cases} \quad (3.4)$$

Now it is again the moment to check the reliability of the method via the next test shown in the Table 3.4. The very big value of Chi-squared is a very good proof for the “non good fitting” of the “observed” to the “theoretic” values n_i and n'_i respectively, with a value of $p < 0.005$.

Table 3.4

Real Time Spaces	$X - X_{min}$ Spaces	Centers: x'_i	n_i	N_i	$n'_i = f(x_i) \cdot 140$ Theoretic	$\frac{(n_i - n'_i)^2}{n'}$
[24 – 28)	[00 – 04)	02	40	40	33.8	1.1373
[28 – 32)	[04 – 08)	06	30	70	22.3	2.6587
[32 – 36)	[08 – 12)	10	25	95	19.3	1.6834
[36 – 40)	[12 – 16)	14	20	115	17.6	0.3273
[40 – 44)	[16 – 20)	18	15	130	16.5	0.1364
[44 – 48)	[20 – 24)	22	8	138	15.6	3.7026
[48 – 52]	[24 – 28]	26	2	140	14.9	11.1685
Totals			140		140.0	$\chi^2 = 20.8142$

Example 3.3: A sample of $n=249$ students worked on the internet and they make citation on the number of pages they had visited per week. X = number of pages cited by the students (Node=Student). The results are included to the next table of data could be seen as continuous data via the very big number of pages per student. The data are distributed in 6 spaces with wideness $w=500$ pages. Calculate the

parameters $\bar{x}, s^2, s, \hat{C}_v$. After this establish the formula of pdf for the r.v. $X = \text{"number of pages"}$.

Table 3.5

Number of pages	Centers: x'_i	n_i	N_i	$x'_i = (x_i - m)/w$	$n_i \cdot x'_i$	$n_i \cdot x'^2_i$
[0000 – 0500)	0250	3	3	-3	-9	27
[0500 – 1000)	0750	17	20	-2	-34	68
[1000 – 1500)	1250	32	52	-1	-32	32
[1500 – 2000)	1750	47	99	0	0	0
[2000 – 2500)	2250	66	165	1	66	66
[2500 – 3000)	2750	84	249	2	168	336
Totals		249			T₁= 159	T₂= 529

Answer: The data are in the first three columns of Table 3.1. We have filled up the next columns of this table. The fourth column stands for the cumulative frequencies of the nodes. The parameter m on the title of the 5th is the temporary mean value for the sample and as usually is taken to be one middle standing value. Here $m=1750$ is adopted. The parameter $w=500$ is the size of the six spaces of the range of the time $R=b=3000$.

The sample mean value is given as $\bar{x} = m + w \cdot \frac{T_1}{n} = 1750 + 500 \cdot \frac{159}{249} = 2069.28 \text{ pages}$

The sample variance is given as

$$s^2 = \frac{w^2}{n-1} \cdot \left(T_2 - \frac{T_1^2}{n} \right) = \frac{500^2}{248} \cdot \left(529 - \frac{159^2}{249} \right) = 430917.22$$

and the standard deviation is $s = \sqrt{s^2} = \sqrt{430917.22} = 656.44 \text{ pages}$.

Thus the sample coefficient of variation is the unit free quantity

$$\hat{C}_v = \frac{s}{\bar{x}} = \frac{656.44}{2069.28} = 0.3172. \quad (3.5)$$

Now the road is open to calculate the exponent k of the formula (2.1) via the (2.5) and (2.6) and to get the formula (2.1) of pdf:

From (3.5) and (2.5) we get $\lambda = \hat{C}_v^{-2} = 0.3172^{-2} = 9.9388$,

from (2.6) we get $k(\lambda) = -2 + \sqrt{1 + \lambda} = -2 + \sqrt{1 + 9.9388} = 1.3073$

and from (2.1) we have $h = \frac{k+1}{b} = \frac{2.3073}{3000} = 0.000769$.

Thus the pdf formula is given by

$$f(x) = \begin{cases} 0.000769 \cdot \left(\frac{x}{3000} \right)^{1.3073} & x \in [0, 3000] \\ 0 & x \notin [0, 3000] \end{cases} \quad (3.6)$$

Now it is the moment to check the reliability of the method via the next Chi-squared test by the help of the next Table 3.6. The very-very little value of Chi-squared is a very good proof for the “good fitting” of the “observed” to the “theoretic” values n_i and n'_i respectively. We found again a little value, the $X^2 = 0.4520$.

Table 3.6

Real Time Spaces	Centers: x'_i	n_i	N_i	$n'_i = f(x_i) \cdot 140$ Theoretic	$\frac{(n_i - n'_i)^2}{n'}$
[0000 – 0500)	0250	3	3	4.0	0.2500
[0500 – 1000)	0750	17	20	15.7	0.1076
[1000 – 1500)	1250	32	52	30.6	0.0641
[1500 – 2000)	1750	47	99	47.4	0.0034
[2000 – 2500)	2250	66	165	65.8	0.0006
[2500 – 3000)	2750	84	249	85.5	0.0263
Totals		249		249.0	$X^2 = 0.4520$

4. Discussing about the increasing form of pdf

We have already dealt with the theoretic point of view and with the applications of the increasing pdf as they can be detected on Tables 3.1 till 3.4. The source results coming out from comparison of the two tables 3.2 and 3.4 is that:

1st) *If and only if the pdf is an increasing one, then the formula (2.1) extracted from the sample data can describe the distribution of the r.v. X. This is an obvious result come out via the Chi-squared test of a very good significance level, i.e. the suitable p-value is vanishing. This result has been enforced by the example 3.3 where from a sample of size n=249 units and a pdf of increasing nature we have that the formula (2.1) takes its natural form of (3.6).*

2nd) *The forms (3.2), (3.4) and (3.6) are estimations at a point. The best estimation could be given by a confidence interval for $k(\lambda)$ in order to see if some expected value for k stands inside this interval, e.g. someone could be curious if in example 3.1 we have $k(\lambda)=1$. This means that if there is a question if $k=1$ or any information that it is probably $k=1$ we can state: “If there is a confidence interval (c.i.) of (at least 95%) including the value $k=1$, then we say that we have not enough information to restrict the hypothesis (H_0) which states that $k=1$ ”. For more details see Farmakis (2003), Sachs (1984). Let us note again that $k=1$ means that we have a pdf with a linear form of expression.*

3rd) *There is a natural infimum for the parameter k. This is $k=-1$ and it behaviors as an absolute zero. So the parameter k (or better the $k+1$ one) becomes a ratio variable for the increasing distribution, as it is for also proved for the symmetric distributions, Farmakis (2003).*

4th) *As a resume we give the next Table 4.1 with the basic formulae of the symmetric distributions, Farmakis (2003), and of the increasing distribution of the present paper.*

We note once again that in all we have write here and in Farmakis (2003) the value of the parameter λ is immediately connected with the concept of C_V by the formula:

$$\lambda = C_v^{-2} = \frac{(EX)^2}{\text{Var}X}. \quad (4.1)$$

We try in the most of the cases to imagine that it is $\lambda=1,2,3,4,\dots$, since the value $\lambda=0$ must be avoided because is a source of problems for the basic parameter, the exponent k . So the set of the increasing pdf can be seen as classified and scaled by the series $(X_\lambda)_{\lambda \in \mathbb{N}}$, see also Farmakis (2003).

Table 4.1

(I) Symmetric Distributions	(II) Increasing Distributions
$f(x) = \begin{cases} h \cdot (x-a)^k & x \in [a, \frac{a+b}{2}] \\ h \cdot (b-x)^k & x \in [\frac{a+b}{2}, b] \\ 0 & x \notin [a, b] \end{cases}$	$f(x) = \begin{cases} h \cdot \left(\frac{x}{b}\right)^k & x \in [0, b] \\ 0 & x \notin [0, b] \end{cases}$
$k = \frac{-5 + \sqrt{1 + 8\lambda}}{2}$	$k = -2 + \sqrt{1 + \lambda}$
$h = \frac{2^k \cdot (k+1)}{(b-a)^{k+1}}, k \neq -1$	$h = \frac{k+1}{b}$

REFERENCES

- FARMAKIS N.** (2001) “*Statistics, Theory in Brief-Exercises*”, A & P Christodoulidi, Thessaloniki, 2001 (in Greek).
- FARMAKIS N.** (2003) “Estimation of Coefficient of Variation: Scaling of Symmetric Continuous Distributions”, *Statistics in Transition*, **Vol. 6**, Nr 1, pp 83-96.
- FARMAKIS N.** (2007) “*Introduction to Sampling*”, Ed. A & P Christodoulidi, Thessaloniki, 2007 (in Greek).
- JOHNSON, N. L. & WELCH, B. L.** (1940), “Applications of the non-central distribution”, *Biometrika*, **Vol. 31**, p 362-389.
- LEVY, P. S. & LAMESHOW, S.** (1991) “*Sampling of Populations: Methods and Applications*”, John Wiley & Sons, Inc. New York.
- SACHS, L.** (1984) *Applied Statistics*, Springer-Verlang Inc, New York.

Dynamic routing combined to forecast the behavior of traffic in the city of São Paulo using Neuro Fuzzy Network

Ricardo Pinto Ferreira, Carlos Affonso and Renato José Sassi

Nove de Julho University, São Paulo, Brazil

Email: kasparov@uninove.edu.br

Nove de Julho University, São Paulo, Brazil

Email: carlos.affonso@ajato.com.br

Nove de Julho University, São Paulo, Brazil

Email: sassi@uninove.br

Abstract: The challenge of getting and keeping customers drives the development of new ways to meet the consumption needs of increasingly tends to micro-segmentation of product and consumer market. The new consumption habits of Brazilians have brought new prospects for consumption. The objective of this paper is to propose the development of a dynamic routing system supported by the behavior of urban traffic in the city of São Paulo using Neuro Fuzzy Network. The methodology of this paper consists in the capture of relevant events that interfere with the flow of traffic of the city of São Paulo and implementation of a fuzzy neural network trained with these events to the behavior of traffic. The system offers three levels of hierarchical routing is possible to consider not only the basic factors of routing, but also external factors that directly influence the flow of traffic and the disruption which may be avoided in large cities, through openings in the path (dynamic routing). Predicting the behavior of traffic represents the strategic level routing, dynamic routing is the tactical level and routing algorithms to the operational level. This paper will not be discussed the operational level.

Keywords: The behavior of traffic, Dynamic Routing, Neuro Fuzzy Network.

1 Introduction

The new consumption habits of Brazilians brought to market products with a life cycle shorter consequently increasing volumes of items collected and distributed every day by Today (2009).

An important aspect for maximum efficiency in transportation is the definition of the routes of the collections or deliveries. This setting determines the path that a vehicle will travel to complete the requirements of transport services. Bowersox et al., (2006).

The Vehicle Routing Problem (VRP) has been studied with much interest within the last three to four decades. The majority of these works focus on the static and deterministic cases of vehicle routing in which all information is known at the time of the planning of the routes. In most real-life applications though, dynamic information occurs parallel to the routes being carried out. Larsen (2001).

The problem of vehicle routing is to determine vehicle routes that minimize the total cost of attendance, each of which starting and ending in the warehouse or on the vehicle, ensuring

that each point is visited exactly once and the demand on any route does not exceed capacity of the vehicle that meets. When the definition of the routes involves not only spatial or geographical aspects, but also time, such as restrictions on hours of service points to be visited, the problems are then referred to as routing and scheduling. Cunha (1997).

In urban areas it is possible to give up some advantage as the minimum distance to obtain shorter shift. Ballou (1993). The proposed dynamic routing deviations from regions with lower traffic flow time offering other alternative routes that minimize the waiting time (unproductive).

The traffic chaos witnessed in the city of São Paulo is formed by several notable events recorded during the day and directly affect the flow of traffic, congestion impede the efficiency of urban transport and cause significant damage. Notable occurrences are instances highlighted by the Operations Center of the Society of Traffic Engineering, which interfere or may modify the conditions of flow and safety of city traffic. CET (2009).

A vehicle stops on a busy route immediately causes a reduction in the speed of vehicles that route. The consequence is the change in traffic flow on streets perpendicular or parallel, there is the momentary chaos. In cities without adequate planning as São Paulo, chaos may even become permanent. Pena (2004).

A fuzzy neural network was developed using an artificial neural network architecture Multilayer perceptrons (MLP) with backpropagation algorithm. Data were collected notable occurrences of traffic in the metropolitan region of São Paulo in December 16, 2009.

2 The hierarchy of routing

Through the three-level hierarchical routing is possible to consider not only the basic factors of routing (routing algorithms) as well as external factors, such episodes have a direct influence on service levels in large cities (dynamic routing) that represents the tactical level of routing. The prediction of the behavior of traffic represents the strategic level of routing. The Figure 1 illustrates the proposed hierarchy for routing supported by three levels. Ferreira et al., (2010).

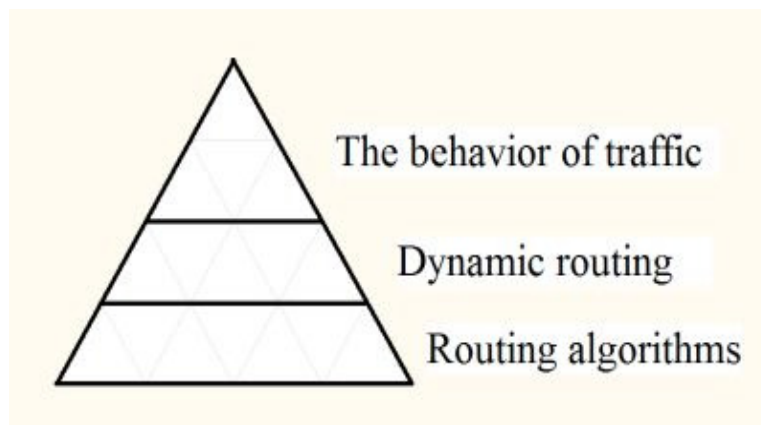


Fig. 1. Hierarchy routing. Source: Ferreira et al., (2010)

3 The Dynamic Routing

The static routes do not allow to optimize the entire path of the vehicle and urban areas are fertile in events that directly influence the time and travel distance so the time lost in traffic, and increase the cost of travel, provides better combustion of. Ferreira and Sassi (2009).

With dynamic routing, deliveries continue to occur and, after interruption, the previously congested pocket can usually be treated without prejudice to all points of delivery or pickup. Figures 2, 3 and 4 illustrate a step-by-example in changing the route during a break on the road where they were held up deliveries of supplies and other items already in the initial route amended without prejudice to other customers, so just stopping the vehicle takes deliveries in the semi-arc missed in the initial route.

Figure 2 (A) shows the path to the barren pocket of distribution (blue line) points to be served (green dot) and the initial planned route (red line). Figure 2 (B) shows the interruption of the path within the range of distribution schedule.

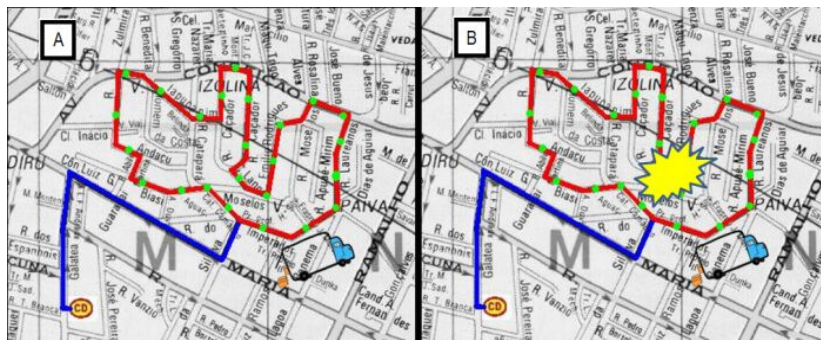


Fig. 2. Bag distribution (A and B). Source: Authors

Figure 3 (C) shows the alternative route (yellow line) that enables delivery of the same pocket of distribution continues to be made. Figure 3 (D) shows the end of the interruption and customers that have not been met.

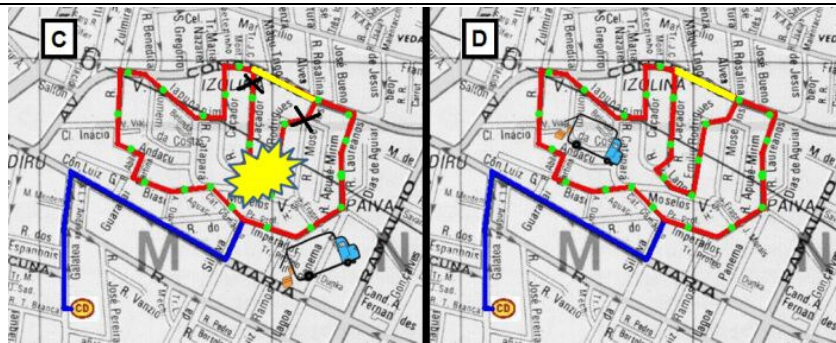


Fig. 3. Bag distribution (C and D). Source: Authors

Figure 4 (E) shows the new alternative route (yellow line) that will serve customers in the semi-arc missed in the initial programming.

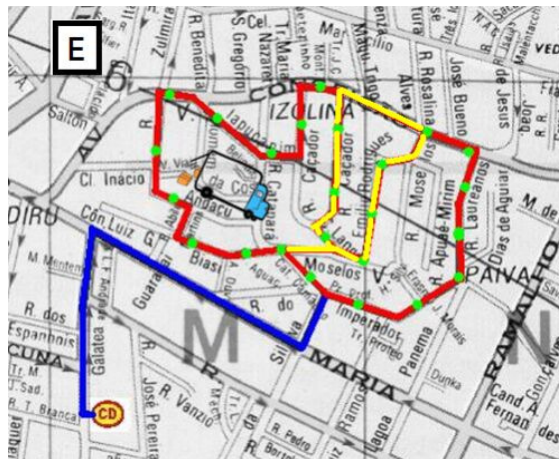


Fig. 4. Bag distribution (E). Source: Authors

The dynamic routing in this paper represents the tactical level of routing, as seen in section 2.

4 Fuzzy neural network to predict the behavior of urban traffic

We use the concept of fuzzy logic as the mathematical tools necessary for the treatment of algebraic and logical operations performed in the universe of fuzzy sets. Passino and Yurkovich (1998). The concepts of fuzzy logic can be used to

translate in mathematical terms the inaccurate information expressed by a set of linguistic variables.

Be used the nomenclature of Fuzzy sets defining them as a class of objects of continuous variables. Such sets are characterized by membership functions which indicate for each element a degree of membership from 0 to 1. Nicoletti and Camargo (2004). The concepts of intersection, union, complement, convexity, etc.. are extended to such sets, and various properties of these notions in the context of fuzzy sets are established by Zadeh (1965).

The artificial neural networks are models inspired by brain structure with the objective to simulate human behavior as learning, association, generalization and abstraction. Haykin (1999). These models consist of simple processing units called artificial neurons, which calculate mathematical functions.

The Artificial Neural Networks and Fuzzy Logic have been widely applied to many problems including identification, prediction, classification and control. However, both techniques have limitations, but put them together in a single model (network) can overcome these limitations. Gomide et al., (1998).

The Neuro Fuzzy networks have emerged as a promising tool, because they bring the benefits of neural networks and fuzzy logic, where the learning and computational power of neural networks, and capacity for representation and reasoning of fuzzy logic are combined. Gomide et al., (1998).

Currently, there is great interest in neural network models to solve unconventional problems in recent years the artificial neural networks have emerged as a viable alternative with many applications. A Neuro Fuzzy network was developed using Multilayer perceptrons (MLP) architecture with backpropagation for learning algorithm.

As a programming language was used Scilab 5.1, according to the advantages pointed out in (<http://www.scilab.org/>.) Are also available in this language computer packages (toolboxes) specially designed for fuzzy logic and neural networks as a metric to verify the validity of the network, the average error was established as the difference between the value returned by the network and the output of the database. Data were collected notable occurrences of traffic in the metropolitan region of São Paulo on December 16, 2009 in order to obtain the impact of such occurrences in the flow of traffic through relevant events on the behavior of traffic, these parameters have been converted through Fuzzy sets. Figure 5 shows the types of occurrences that were used in the fuzzy neural network.

Notable Occurrences	
1. Accident victim	9. Manifestations
2. Flooding	10. Occurrence involving dangerous
3. Trampling	11. Occurrence involving dangerous goods
4. Truck broken	12. Bus asset towards
5. Defect in the network of trolleybus	13. Falling Tree
6. Lack of electricity	14. Light off
7. Fire	15. Light flagged
8. Fire Vehicle	16. Vehicle excess

Fig. 5. Notable Occurrences. Source: Adapted from CET (2009)

Figure 6 illustrates the results of the behavior of real traffic, the blue line represents the actual behavior of December 16, 2009, the green line represents the lower middle and red line represents the upper middle-hours. The graph shows the slow rate of slow transit logged every 30 minutes, Monday through Friday, at the time of 7h to 20h and the lines indicating the lower and higher. CET (2009) and Ferreira et al., (2010).

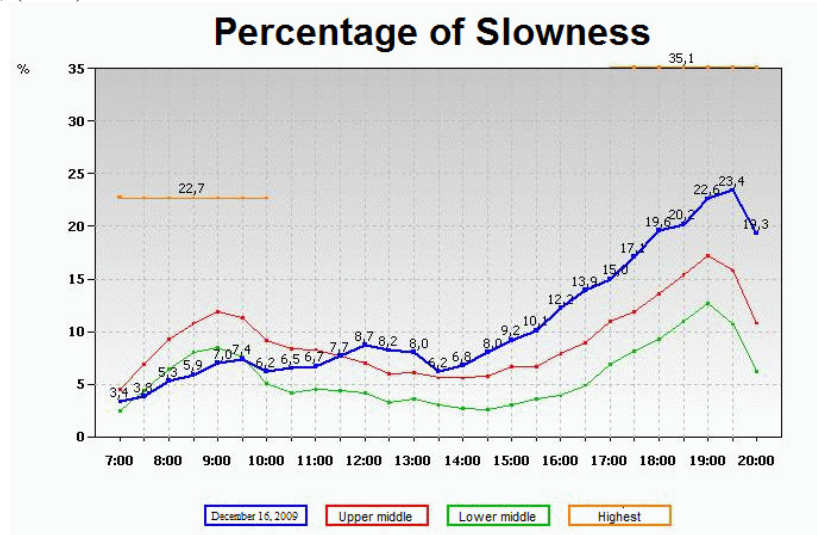


Fig. 6. Behavior observed in December 16, 2009. Source: CET (2009)

Figure 7 illustrates the results obtained by fuzzy neural network compared to the captured CET in December 16, 2009.

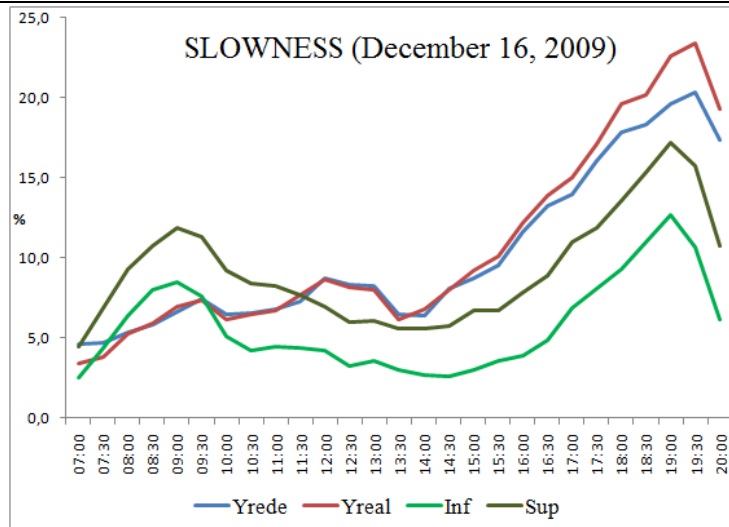


Fig. 7. Behavior calculated by the fuzzy neural network. Source: Authors

With the initial results it appears that the network was a reasonable outcome of the proposed problem and can assist in decision making about the time windows that should be avoided and that exhibit the behavior above the norm.

5 Conclusion

Predicting the behavior of traffic can be an excellent tool to help decision making before the routing so as to enable the steps of physical distribution with greater effectiveness and productivity. With the ability to predict the fluctuations of traffic flow you can choose the best windows in order to avoid times when traffic forecasting point to levels that undermine the slow service. The combined routing dynamic traffic forecasting can increase significantly the efficiency of routing in large cities. The static routes do not allow improving the whole route of the vehicle so that all customers are met within the estimated time window. Diversions intelligent aimed at reducing time in transit, even if distance is a little bigger, and there is a saving time and fuel, it is concluded that the prediction of traffic and routing dynamics are innovative alternatives to routing. The aim is to continue with this early work using other data samples collected on different days of the week, in different months and days with atypical of the city of São Paulo to get new results using the fuzzy neural network. The dynamic routing will also be studied in order to set the possible integration of the three levels of routing as proposed in the paper. In future studies is the prospect of using Rough Neuro Fuzzy Network to try to better resolution of the problem proposed.

References

1. BALLOU, R. H. Logística Empresarial: transportes, administração de materiais e distribuição física. Tradução de Hugo T. Y. Yoshizaki. São Paulo: Atlas (1993).
2. BOWERSOX, D. J., CLOSS, D. J., COOPER, M. B. Gestão Logística de Cadeia de Suprimentos. Porto Alegre: Bookman (2006).
3. CET - Companhia de Engenharia de Tráfego, <http://www.cetsp.com.br> (2009).
4. CUNHA, C. B. Aspectos Práticos da Aplicação de Modelos de Roteirização de Veículos a Problemas Reais. Departamento de Engenharia de transportes Escola Politécnica da Universidade de São Paulo (1997).
5. FERREIRA, R. P.; AFFONSO, C.; SASSI, R. J. Roteirização dinâmica de veículos combinada à Previsão do comportamento do tráfego urbano utilizando uma rede neuro fuzzy. In: IV Workshop de Tecnologia Adaptativa - WTA 2010 (2010).
6. FERREIRA, R. P.; SASSI, R. J. Dynamic Routing of Vehicles. XLI Simpósio Brasileiro de Pesquisa Operacional. Porto Seguro (2009).
7. GOMIDE, F., FIGUEIREDO, M. PEDRYCZ, W., A neural Fuzzy network: Structure and learning, Fuzzy Logic and Its Applications, Information Sciences and Intelligent Systems, Bien, Z. and Min, K., Kluwer Academic Publishers, Netherlands, pp. 177-186 (1998).
8. HAYKIN, S. Neural Networks: A Comprehensive Foundation. New York: Willey & Sons (1999).
9. LARSEN, A. The Dynamic Vehicle Routing Problem. Ph.D. thesis – Department of Mathematical Modelling (IMM) at the Technical University of Denmark, Lyngby (2001).
10. NICOLETTI, M. C., CAMARGO, H.A. Fundamentos da Teoria de Conjuntos Fuzzy, Edusfscar (2004).
11. PASSINO, K.M.; YURKOVICH, S. Fuzzy Control, Addison Wesley Longman, Inc (1998).
12. PENA, F. Biografias em fractais: múltiplas identidades em redes flexíveis e inesgotáveis. Revista Fronteiras – estudos midiáticos, Vol. VI n. 1, p. 82 - jan/jun. (2004).
13. TODAY Logistics & Supply Chain. São Paulo: Cecilia Borges, Ano III, n. 38 (2009).
14. ZADEH, L.A, Fuzzy Sets, Information and Control, v8. P338-353 (1965).

NEW INSIGHTS FOR RECURSIVE RESIDUALS

James M Freeman

Manchester Business School
University of Manchester
Booth Street West
Manchester, M15 6PB, UK
(e-mail: jim.freeman@mbs.ac.uk)

Abstract: The role of recursive residuals in the validation of linear models is well-recognised. Furthermore, their contribution to quality control and change point analysis has become increasingly valued. A new procedure for deriving recursive residuals – assuming data observations are time-ordered - is now presented and its theoretical efficacy established. Relevant results are illustrated across a number of real-life data applications.

Keywords: Influence, Leverage, Outliers

1 Introduction

Residual analysis is a vital aspect of any linear modelling application. In the past, residuals have proven an effective tool for dealing with a wide variety of modelling issues, including problems of structural change, serial correlation of errors, functional misspecification, heteroscedasticity, outliers, influence and leverage - amongst others. Corresponding tests have been developed in relation to various types of residuals – most recently, recursive residuals which can be shown to have important theoretical advantages over more common alternatives.

Kianifard and Swallow (1996) provide a comprehensive review of recursive residuals, their properties and usage. Most recently, a series of novel formulations for generating recursive residuals was offered by Goldolphin (2009). In contrast, Hamilton (1991) shows how conventional regression diagnostics can be modified to good effect using recursive residuals.

The paper introduces a new procedure for computing recursive residuals. Formulae for deriving the latter it is shown can be greatly simplified by exploiting longstanding algebraic identities from the field (Plackett, 1950) ,(Pollock, 1999). Relevant details of the computations are provided in the next section. In section 3, the technique is illustrated for a number of relevant data sets from the literature.

2 Analysis

Traditionally a linear regression model is formulated:

$$Y = X\beta + \varepsilon$$

where $Y = (y_1, \dots, y_n)'$ is an $n \times 1$ vector of values of the response variable, $\beta = (\beta_1, \dots, \beta_p)'$ is a $p \times 1$ vector of unknown fixed parameters, $X = (x_1', \dots, x_n')$ is an $n \times p$ matrix of explanatory variable values such that $\text{rank}(X) = p$ and $\varepsilon = (\varepsilon_1, \dots, \varepsilon_n)'$ is an $n \times 1$ vector of independent normal random variables with mean zero and unknown fixed variance σ^2 .

Ordinary least squares (OLS) residuals can be written:

$$e = Y - X \hat{\beta} \text{ where } \hat{\beta} = (X'X)^{-1} X'Y$$

Partitioning the data into the first $j-1$ cases and the last $n-j+1$ cases, then if X_{j-1} is the $(j-1) \times p$ matrix corresponding to the first $j-1$ rows of X where $j-1 \geq p$ and $(X'_{j-1}X_{j-1})^{-1}$ can be assumed non-singular,

then β can be estimated by $\hat{\beta}_{j-1} = (X'_{j-1}X_{j-1})^{-1} X'_{j-1}Y_{j-1}$ where Y_{j-1} is the vector consisting of the first $j-1$ elements of Y . We refer to this regression model based on the first $j-1$ cases as regression $j-1$.

If $S_j = (Y_j - X_j \hat{\beta}_j)'(Y_j - X_j \hat{\beta}_j)$ then it can be shown $S_j = S_{j-1} + w_j^2$ (Brown et al, 1975) where

the j th recursive residual, w_j can be written:

$$w_j = \frac{y_j - x'_j \hat{\beta}_{j-1}}{\{1 + x'_j (X'_{j-1}X_{j-1})^{-1} x_j\}^{1/2}}$$

or equivalently
$$\frac{v_j}{(1 + h_{jj(j-1)})^{1/2}} \quad j = p+1, \dots, n \quad (1)$$

where - adapting Hawkin's (1991) - notation

$$h_{jk(i)} = x_j (X_i X_i)^{-1} x_k$$

The numerator of (1) - which can be described as the predicted residual of case j using regression $j-1$ - can alternatively be expressed as:

$$\begin{aligned} v_j &= y_j - x'_j \hat{\beta}_{j-1} = y_j - x'_j \hat{\beta}_j + x'_j (\hat{\beta}_j - \hat{\beta}_{j-1}) \\ &= u_j + x'_j (\hat{\beta}_j - \hat{\beta}_{j-1}) \end{aligned} \quad (2)$$

where $u_j = y_j - x'_j \hat{\beta}_j$ is the OLS residual of the last case in regression j .

Now since

$$X'_{j-1}X_{j-1} \hat{\beta}_{j-1} + x_j y_j = X'_j Y_j = X'_j X_j \hat{\beta}_j = (X'_{j-1}X_{j-1} + x_j x'_j) \hat{\beta}_j \quad (3)$$

it follows:

$$(X'_{j-1}X_{j-1})(\hat{\beta}_j - \hat{\beta}_{j-1}) = x_j (y_j - x'_j \hat{\beta}_j)$$

and hence

$$\hat{\beta}_j - \hat{\beta}_{j-1} = (X'_{j-1}X_{j-1})^{-1}x_j(y_j - x'_j\beta_j)$$

Substituting for $\hat{\beta}_j - \hat{\beta}_{j-1}$ in (2) we have:

$$y_j - x'_j\hat{\beta}_{j-1} = y_j - x'_j\hat{\beta}_j + x'_j(X'_{j-1}X_{j-1})^{-1}x_j(y_j - x'_j\hat{\beta}_j) = (y_j - x'_j\hat{\beta}_j)(1 + x'_j(X'_{j-1}X_{j-1})^{-1}x_j)$$

$$\text{i.e.} \quad v_j = u_j(1 + h_{jj(j-1)}) = u_j \frac{v_j^2}{w_j^2} \quad (4)$$

which, following rearrangement, yields

$$w_j^2 = u_j v_j \quad (5)$$

2.1 Properties

When β is constant, Brown et al (1975) show that the recursive residuals w_j ($j \geq p+1, \dots, n$) are i.i.d $N(0, \sigma^2)$.

In contrast, it is known (Kianifard and Swallow, 1996) that the u_j errors are correlated with unequal variances according to the non-diagonal covariance matrix: $\sigma^2(I - x'_j(X'_jX_j)^{-1}x_j)$; similarly for the v_j terms which share the alternative covariance matrix: $\sigma^2(I + x'_j(X'_{j-1}X_{j-1})^{-1}x_j)$

By virtue of (5) it is evident that

$$\text{Sgn}(u_j) = \text{Sgn}(v_j) = \text{Sgn}(w_j)$$

Similarly from (4) it can be deduced that:

$$|u_j| \leq |w_j| \leq |v_j|$$

2.2 Leverage

Adapting a rule by Hoaglin & Welch (1978), Hawkins (1991) defines a case having “high leverage” as one where:

$$h_{jj(j)} > \frac{2p}{j} \quad (6)$$

Now since (Farebrother, 1978)

$$h_{jj(j)} = 1 - \frac{u_j^2}{w_j^2} \text{ it follows } \frac{u_j^2}{w_j^2} < 1 - \frac{2p}{j}$$

and thus from (5)
$$\frac{u_j}{v_j} < 1 - \frac{2p}{j}$$

Hence inequality (6) can alternatively expressed:

$$v_j > \frac{u_j}{(1 - \frac{2p}{j})} \quad (7)$$

3 Applications

3.1 Rousseeuw and Leroy's data (1987)

Rousseeuw and Leroy's data relate to the total number (tens of millions) of international calls from Belgium for the years 1950 – 1973. From late 1963 till early 1970, observations are inconsistently recorded in minutes of these calls. Thus, whereas data for 1964-69 can be thought of as ‘totally contaminated’ those for 1963 and 1970 are only ‘partially’ so.

Following Kianifard & Swallow (1996), Table 1 presents u_j , v_j and w_j residuals ($j = 4,4, \dots, 24$) for the dataset. Clearly for the years 1953-1957 the latter values are relatively consistent and small. After 1957 however they appear to undergo a step change. This lasts until 1962 after which they rise again very precipitately. By 1963 the increase is some three- or four-fold in line with the partial contamination of the data for that year. However, for 1964-1969, corresponding to the period when the full contamination occurred, the increase is by a further factor of 13 or more. Interestingly, from 1970-1973 the residuals become negative and in absolute value terms start to decline as bad data are progressively filtered from the calculations. Kianifard and Swallow (1996) show that recursive residuals are much more sensitive to the data's features than their standardised or studentised counterparts, significant values of the latter being obtained only for the year 1969. In contrast, w_j are found to be significant for the years 1958-1959, 1963-1966 and 1970-1971. Figure 1 which plots parameter estimates for regression j by j reveals that the pronounced changes in u_j and v_j – and hence w_j – found in Table 1 are primarily due to shifts in the intercept parameter.

Year-1949	u_j	v_j	w_j
4	0.03	0.10	0.05
5	0.02	0.06	0.03
6	0.02	0.04	0.02
7	0.02	0.04	0.03
8	0.01	0.02	0.02
9	0.08	0.13	0.10
10	0.09	0.14	0.12
11	0.11	0.16	0.13

12	0.11	0.16	0.13
13	0.10	0.14	0.12
14	0.38	0.51	0.44
15	7.61	10.04	8.74
16	5.98	7.75	6.81
17	5.68	7.24	6.42
18	5.33	6.70	5.98
19	5.50	6.83	6.13
20	6.19	7.60	6.86
21	-9.65	-11.73	-10.64
22	-10.30	-12.41	-11.30
23	-8.97	-10.71	-9.80
24	-7.90	-9.36	-8.60

Table 1. Residuals u_j , v_j and w_j residuals by j (= year -1949)

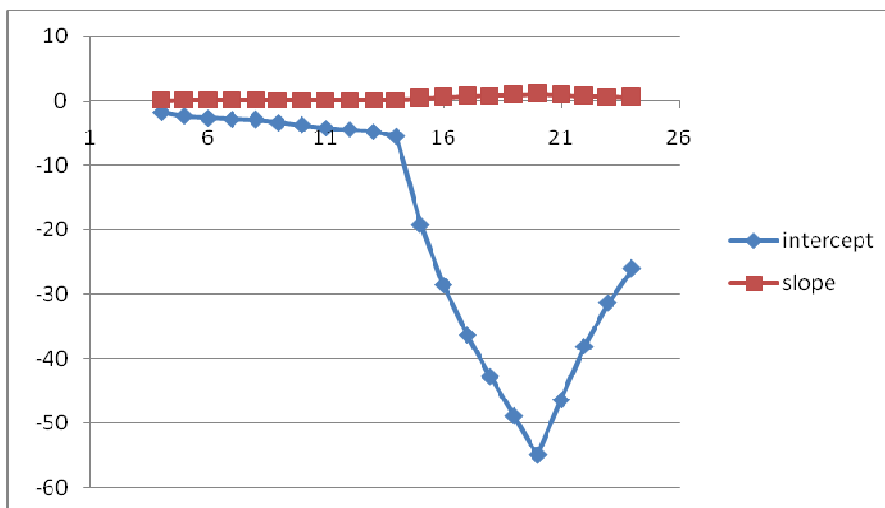


Fig. 1. Estimated intercept and slope for regression j ($j = 4, 5, \dots, 24$)

In addition, the graph of v_j versus u_j ($j = 4, 5, \dots, 24$) shown in Figure 2 highlights the existence of three distinct regimes mirroring those in Kianifard and Swallow's original scattergram of the data.

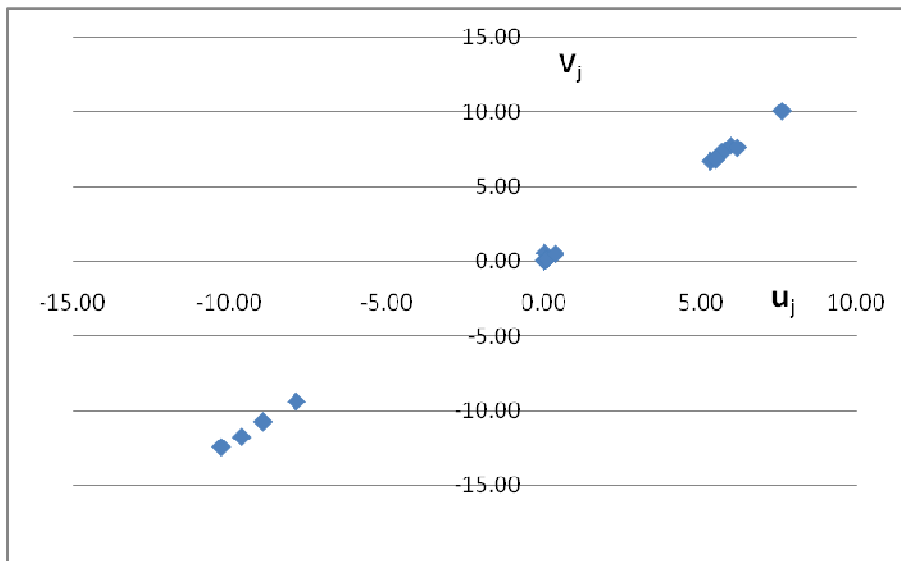


Fig. 2. Plot of v_j versus u_j ($j = 4, 5, \dots, 24$)

Note that whereas cases 1950-1952 were used as the basis set for the residuals covered in both Table 1 and Figures 1 - 2, cases 1971-1973 form the basis set for those plotted in Figure 3. Consistent with Figure 1, years 1963 ($j = 14$) and 1969 ($j = 20$) are highlighted here as those where change occurred and as Figure 4 confirms, shifts in intercept value seem once again to be the explanation for this.

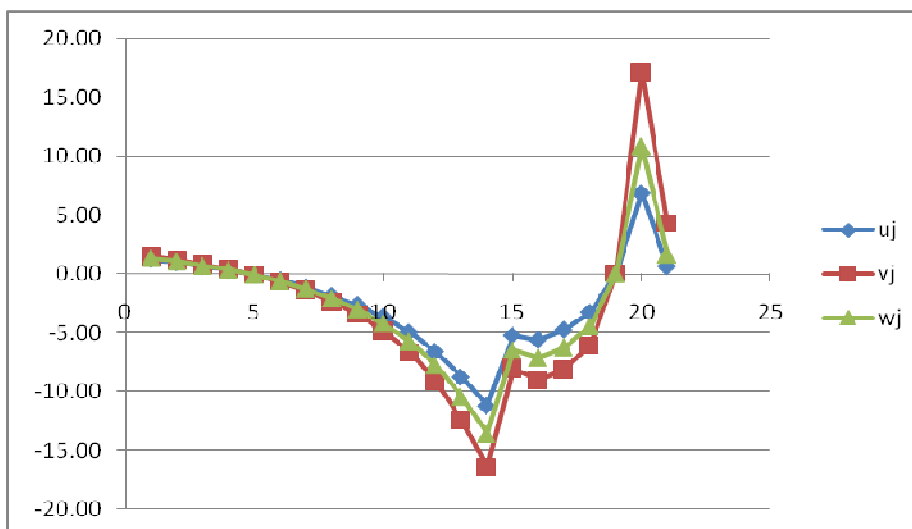


Fig. 3 Plot of residuals u_j , v_j and w_j ($j = 1, 2, \dots, 21$)

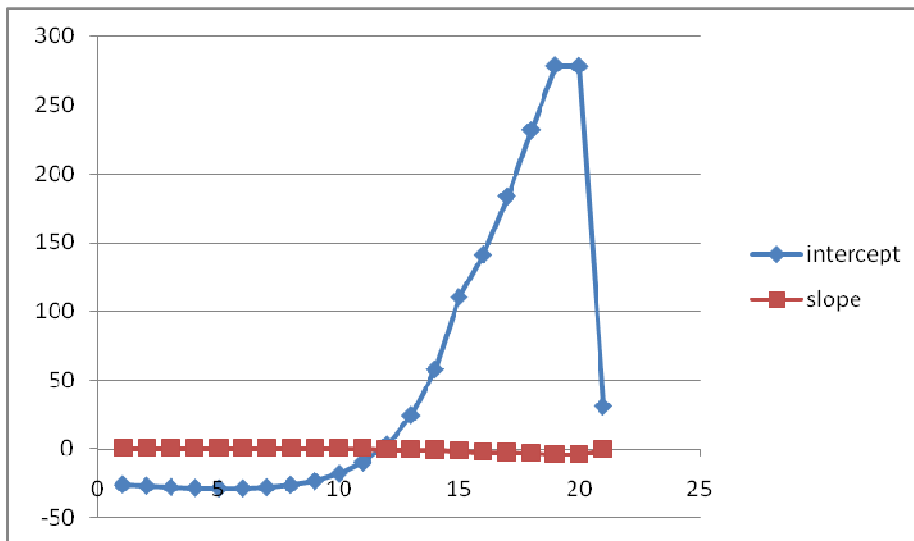


Fig. 4. Estimated intercept and slope for regression j ($j = 1, 2, \dots, 21$)

3.2 Montgomery and Peck's data (1982)

Data collected by Montgomery and Peck (see Hawkins, 1991) concern the three variables:

Y , the time taken to service a vending machine, X_1 , the number of items stocked by the machine and X_2 , the distance travelled to reach it. Though cases were not explicitly time-ordered, Hawkins argues reasonably that they might well be so. Residuals u_j , v_j and w_j – using the first four cases as the basis set for the calculations - are plotted in Figure 5, extreme values of w_j occurring for $j = 9$ and $j = 20$. Correspondingly, when residuals are calculated using the last four cases as the basis set w_j , can again be found to be maximised at $j = 9$. In both his backward and forward analyses Hawkins deduces that case 9 has high leverage. Similarly in his backward analysis, case 20 is identified as 'marginally outlying'.

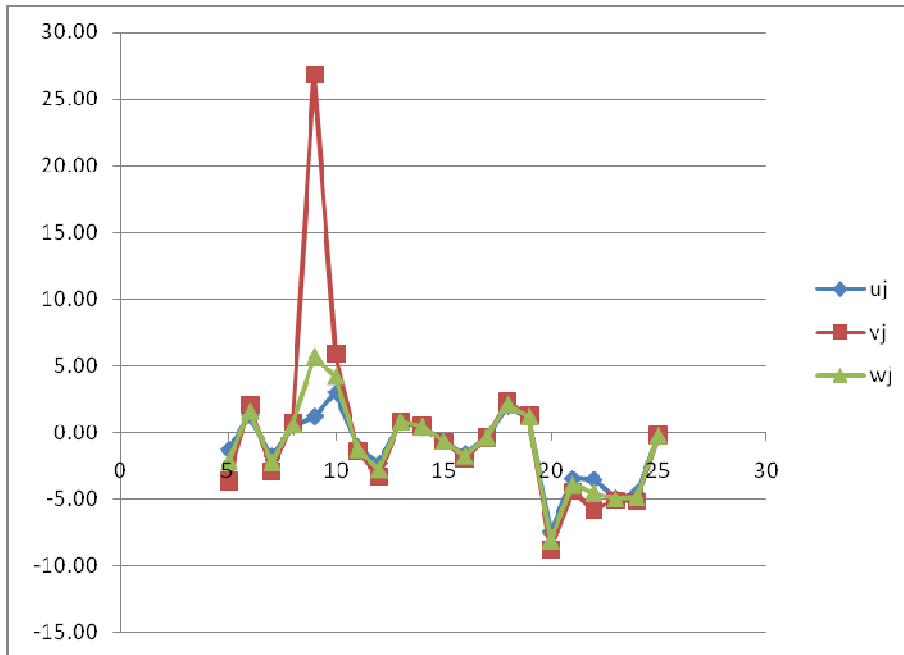


Fig. 5 Plot of residuals u_j , v_j and w_j ($j = 5, 6, \dots, 25$)

These different types of discordancy are represented quite differently in the plot of v_j by u_j in Figure 6. As with Figure 2 earlier the points here follow a roughly linear pattern but in keeping with inequality (7) that for case 9 is much higher than the pattern would suggest. Case 20 on the other hand conforms to the pattern but has a u_j value markedly lower than that for the other points.

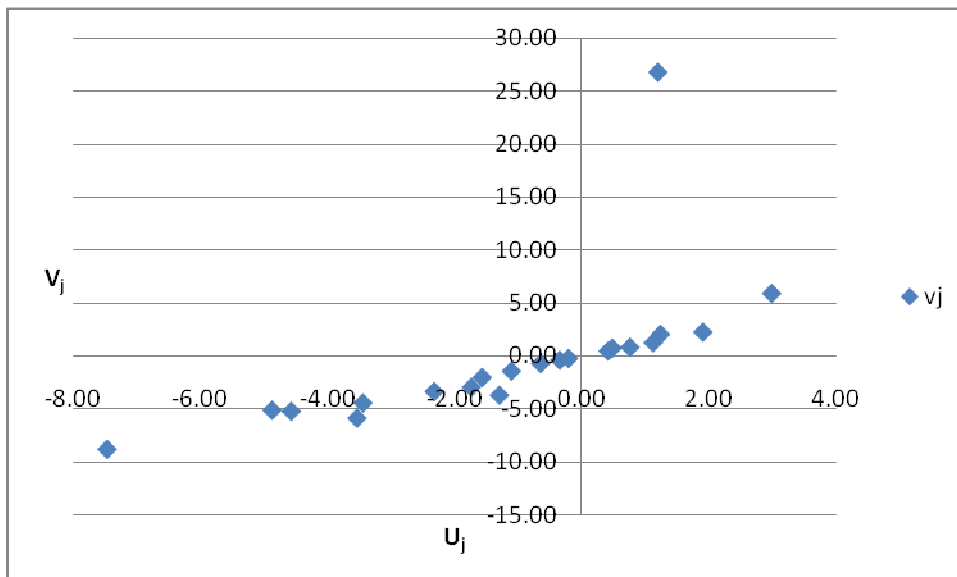


Fig. 6. Plot of v_j versus u_j ($j = 5, 6, \dots, 25$)

3 Conclusions

Various alternative formulae exist for computing recursive residuals. Supplementing these we have established that the j th recursive residual ($j = p+1, p+2, \dots, n$) can be simply found by taking the harmonic mean of the OLS residual of the last case in regression j and the predicted residual for case j using regression $j-1$. This elegant result is associated with a number of simple mathematical identities which allow existing tests – for example, that for leverage - to be productively re-interpreted. As several contrasting examples show, valuable new insights then become possible.

References

- R.L. Brown, J. Durbin and J.M. Evans. Techniques for testing the constancy of regression relationships over time. *J. Roy. Statist. Soc. Ser. B* 37 149-192. 1975
- D.R. Cox. Contribution to Brown. R.L. et al, 1975. *J. Roy. Statist. Soc. Ser. B* 37. 163-164. 1975.
- R.W. Farebrother. An historical note on recursive residuals. *J. Roy. Statist. Soc. Ser. B* 40 (3) 373-375. 1978.
- J.S. Galpin and D.M. Hawkins. The use of recursive residuals in checking model fit in linear regression. *Amer. Statist.* 38. 94-105. 1984.
- D.M. Hawkins. Diagnostics for use with regression recursive residuals. *Technometrics* 33, 221-234. 1991.
- A. Hedayat and D.S. Robson, Independent stepwise residuals for testing homoscedasticity. *J. Amer. Statist. Assoc.* 65, 1573-1581. 1970.
- D.C. Hoaglin and R. Welsch. The Hat Matrix in Regression and ANOVA. *Amer. Statist.* 33. 17-22. 1978.
- F. Kianifard and W.H. Swallow..A review of the development and application of recursive residuals in linear models. *J. Amer. Statist. Assoc.* 91, 391-400. 1996.
- J.A Nelder,, Contribution to Brown, R.L., Durbin.J., Evans.J.M. 1975. *J. Roy. Statist. Soc. Ser. B* 37,182-183. 1975.
- R.L. Plackett. Some theorems in least squares. *Biometrika* 37, 149-157. 1950.
- D.S.G. Pollock. *A handbook of time-series analysis, signal processing and dynamics*. London. 1999.
- P.J. Rousseeuw and A.M. Leroy. *Robust Regression and Outlier Detection*. New York. John Wiley. 1987.
- P.K Sen. Invariance principles for recursive residuals. *Ann. Statist.* 10, 307-312. 1982.
- J.H. Wright. A new test for structural stability based on recursive residuals. *Oxford Bull.Econ.Statist.* 61, 109-119. 1999.

Optimal Design of Smoothing Spline Curves with Equality and Inequality Constraints

Hiroyuki Fujioka¹ and Hiroyuki Kano²

¹ Department of System Management, Fukuoka Institute of Technology
3-30-1, Wajiro-higashi, Higashi-ku, Fukuoka 811-0295 Japan
(e-mail: fujioka@fit.ac.jp)

² School of Science and Engineering, Tokyo Denki University
Hatoyama, Hiki-gun, Saitama 350-0394, Japan
(e-mail: kano@mail.dendai.ac.jp)

Abstract. In this paper, we consider the problem for designing of optimal smoothing spline curves with equality and/or inequality constraints. The splines are constituted employing normalized uniform B-splines as the basis functions. Then various types of constraints are formulated as linear function of the so-called control points, and the problem is reduced to convex quadratic programming problem. The performance is examined by some numerical examples.

Keywords: B-splines, optimal smoothing splines, equality/inequality constraint, quadratic programming.

1 Introduction

The problems of constructing curves for a given set of discrete observational data may arise in many applications of science and engineering. For such problems, a commonly-used way is to use interpolating and approximating methods using spline functions. Thus splines have been studied extensively (e.g. [1–3]).

In addition to traditional approximating or interpolating splines, there are a large class of problems where we need to impose various constraints on splines – such as monotone smoothing splines [4], interval interpolation splines [5], etc. Employing B-splines approach, the authors have developed a method for designing smoothing splines with constraints over interval or at isolated points, and the construction of the spline then becomes a quadratic programming problem [6].

This paper is a continuation of our studies on the optimal design of constrained spline curves based on B-spline approach in [6]. We here develop the generalized design method so that the multiple curves can be designed simultaneously with equality and/or inequality constraints. Such a design method may be useful in many applications, e.g. estimation of probability density functions [7] and trajectory planning for robotic motions [8], etc. The performance is examined by some numerical example.

This paper is organized as follows. In Section 2, we briefly review B-splines and design methods of optimal splines. Then in Section 3, we show how various types of constraints on splines can be formulated and solved. We examine the performances

of the proposed method by numerical example in Section 4. Concluding remarks are given in Section 5.

We summarize some of the symbols that will be used throughout the paper: \otimes denotes the Kronecker product, and 'vec' the vec-function, i.e. for a matrix $A = [a_1 \ a_2 \ \cdots \ a_n] \in \mathbf{R}^{m \times n}$ with $a_i \in \mathbf{R}^m$, $\text{vec } A = [a_1^T \ a_2^T \ \cdots \ a_n^T]^T \in \mathbf{R}^{mn}$ (see e.g. [9]).

2 Optimal Smoothing Splines

Let $x(t) \in \mathbf{R}^p$ ($p \geq 1$) be vectorized spline curves defined by $x(t) = [x_1(t) \ x_2(t) \ \cdots \ x_p(t)]^T$. Then arbitrary spline curves $x(t)$ of degree k in an interval $\mathcal{D} = [t_0, t_m] \subset \mathbf{R}$ can be represented as

$$x(t) = \sum_{i=-k}^{m-1} \tau_i B_k(\alpha(t - t_i)) \quad (1)$$

by an appropriate choice of the weighting coefficient vector $\tau_i = [\tau_{1,i}, \tau_{2,i}, \dots, \tau_{p,i}]^T \in \mathbf{R}^p$ called control points [3]. Here, $B_k(t)$ is a normalized, uniform B-spline function of degree k , m is an integer, and $\alpha(> 0)$ is a constant for scaling the interval between equally-spaced knot points t_i with $t_{i+1} - t_i = \frac{1}{\alpha}$. It is noted that employing a higher degree k of B-splines in (1) yields splines $x(t)$ of higher degree and thus allows us to design more complex curves. Also, for fixed k and the interval $[t_0, t_m]$, increasing the parameter α (i.e. smaller knot points spacing) gives us more flexibility of spline design since m (equivalently the number of control points) increases.

2.1 Normalized Uniform B-Splines

Normalized uniform B-spline $B_k(t)$ of degree k is defined by

$$B_k(t) = \begin{cases} N_{k-j,k}(t-j) & j \leq t < j+1, \quad j = 0, 1, \dots, k \\ 0 & t < 0 \text{ or } t \geq k+1, \end{cases} \quad (2)$$

and the basis elements $N_{j,k}(t)$ ($j = 0, 1, \dots, k$), $0 \leq t \leq 1$ are obtained recursively by the following algorithm:

Algorithm 1 Let $N_{0,0}(t) \equiv 1$ and, for $i = 1, 2, \dots, k$, compute

$$\begin{cases} N_{0,i}(t) = \frac{1-t}{i} N_{0,i-1}(t) \\ N_{j,i}(t) = \frac{i-j+t}{i} N_{j-1,i-1}(t) + \frac{1+j-t}{i} N_{j,i-1}(t), \quad j = 1, \dots, i-1 \\ N_{i,i}(t) = \frac{t}{i} N_{i-1,i-1}(t). \end{cases} \quad (3)$$

Thus, $B_k(t)$ is a piece-wise polynomial of degree k with integer knot points and is $k-1$ times continuously differentiable. It is noted that $B_k(t)$ for $k = 0, 1, 2, \dots$ is normalized in the sense of $\sum_{j=0}^k N_{j,k}(t) = 1$, $0 \leq t \leq 1$.

For the sake of later reference, we introduce $(k+1)$ -dimensional vectors $N_k(t)$ and $h_k(t)$ as

$$N_k(t) = [N_{0,k}(t) N_{1,k}(t) \cdots N_{k,k}(t)]^T \quad (4)$$

$$h_k(t) = [t^k t^{k-1} \cdots 1]^T. \quad (5)$$

Then $N_k(t)$ is written as

$$N_k(t) = S_k h_k(t), \quad (6)$$

where $S_k \in \mathbf{R}^{(k+1) \times (k+1)}$ is a matrix whose i -th row consists of the coefficients of polynomial $N_{i-1,k}(t)$.

2.2 Optimal Smoothing Splines

The control point vector $\tau_i \in \mathbf{R}^p$ ($p \geq 1$) in (1) are typically determined by the theory of smoothing splines (see, e.g. [10] for details). Suppose that we are given a set of data

$$\{(s_i, d_i) : s_i \in [t_0, t_m], d_i \in \mathbf{R}^p, i = 1, 2, \dots, N\}, \quad (7)$$

and let $\tau \in \mathbf{R}^{p \times M}$ ($M = m + k$) be the weight matrix defined by

$$\tau = [\tau_{i,j}]_{i=1, j=-k}^{i=p, j=m-1}. \quad (8)$$

Then a standard problem is to find such a τ minimizing the cost function

$$J(\tau) = \int_{t_0}^{t_m} \|x^{(2)}(t)\|_{\Lambda}^2 dt + \sum_{i=1}^N \|x(s_i) - d_i\|_{W_i}^2, \quad (9)$$

where $\|z\|_S^2 = z^T S z$, $\Lambda = \text{diag}\{\lambda_1, \lambda_2, \dots, \lambda_p\} \in \mathbf{R}^{p \times p}$ with smoothing parameter $\lambda_i (> 0)$, $\forall i$, and $W_i = W_i^T \in \mathbf{R}^{p \times p}$ satisfies $I_3 \geq W_i \geq 0$, $\forall i$.

Letting $\hat{\tau} \in \mathbf{R}^{pM}$ be the vec-function of $\tau \in \mathbf{R}^{p \times M}$, i.e. $\hat{\tau} = \text{vec } \tau$, the cost function $J(\tau)$ can be rewritten as a quadratic function $J(\hat{\tau})$ in terms of $\hat{\tau}$,

$$J(\hat{\tau}) = \hat{\tau}^T G_N \hat{\tau} - 2\hat{\tau}^T g_N + \text{const}. \quad (10)$$

with

$$G_N = Q \otimes \Lambda + \sum_{i=1}^N (b(s_i) b^T(s_i)) \otimes W_i \quad (11)$$

$$g_N = \sum_{i=1}^N b(s_i) \otimes W_i d_i. \quad (12)$$

Here $Q \in \mathbf{R}^{M \times M}$ is a Gramian defined by

$$Q = \int_{t_0}^{t_m} \frac{d^2 b(t)}{dt^2} \frac{d^2 b^T(t)}{dt^2} dt \quad (13)$$

with $b(t) = [B_k(\alpha(t - t_{-k})) B_k(\alpha(t - t_{-k+1})) \cdots B_k(\alpha(t - t_{m-1}))]^T$. Note that G_N in (11) is positive-semidefinite, i.e. $G_N \geq 0$, since $\Lambda > 0$, $Q \geq 0$, $b(s_i) b^T(s_i) \geq 0$ and $W_i \geq 0$. Hence $J(\hat{\tau})$ in (10) is convex in $\hat{\tau}$. Thus, if there are no constraints, the optimal solution is given as a solution of linear algebraic equations $G_N \hat{\tau} = g_N$.

3 Optimal Splines with Constraints

There are various types of constraints on splines $x(t)$, $t \in [t_0, t_m]$, e.g. those for $x(t)$ for some interval of t , for equality and/or inequality, etc. Here we first develop basic formula for expressing the constraints.

Since each element of $x(t)$ in (1), i.e. $x_q(t)$, $q = 1, 2, \dots, p$, is a piece-wise polynomial of degree k , we examine the polynomial in each interval $[t_j, t_{j+1})$ for $j = 0, 1, \dots, m-1$. By focusing on the interval $[t_j, t_{j+1})$, $x_q(t)$ is written as

$$x_q(t) = \sum_{i=-k+j}^j \tau_{q,i} B_k(\alpha(t-t_i)). \quad (14)$$

Using (2), we then get

$$x_q(t) = \sum_{i=0}^k \tau_{q,j-k+i} N_{i,k}(\alpha(t-t_j)), \quad t \in [t_j, t_{j+1}), \quad (15)$$

and it depends on only the $k+1$ weights $\tau_{q,j-k}, \tau_{q,j-k+1}, \dots, \tau_{q,j}$. Moreover, by introducing a new variable u ,

$$u = \alpha(t-t_j), \quad (16)$$

the interval $[t_j, t_{j+1})$ in t is normalized to $[0, 1)$ in u , and we may write $x_q(t)$ as $\hat{x}_q(u)$,

$$\hat{x}_q(u) = \sum_{i=0}^k \tau_{q,j-k+i} N_{i,k}(u), \quad u \in [0, 1). \quad (17)$$

Letting $\tau_{(j)}^q = [\tau_{q,j-k}, \tau_{q,j-k+1}, \dots, \tau_{q,j}]^T \in \mathbf{R}^{k+1}$ and using (6), we may rewrite $\hat{x}_q(u)$ in (17) as $\hat{x}_q(u) = N_k^T(u) \tau_{(j)}^q$ and hence

$$x_q(t) = N_k^T(u) \tau_{(j)}^q. \quad (18)$$

Now we are in a position to derive various types of constraints on $x(t)$. For the sake of simplicity, we consider the case of cubic splines, i.e. $k = 3$.

3.1 Constraints over Knot Point Intervals

We first consider the cases of constraints over knot point intervals. As example, we consider an inequality constraint as

$$x_q(t) \geq c_q \quad \forall t \in [t_j, t_{j+1}] \quad (19)$$

for a constant c_q , $q = 1, 2, \dots, p$ of $c = [c_1, c_2, \dots, c_p]^T \in \mathbf{R}^p$. Note that this inequality ' \geq ' may readily be replaced with ' \leq ' and equality ' $=$ '.

The constraint in (19) may be realized by imposing the condition $\tau_{q,i} \geq c_q$ for $i = j-3, j-2, j-1, j$, or in terms of the control point vector $\hat{\tau}$ as

$$(E_j \otimes v_q)^T \hat{\tau} \geq c_q \cdot \mathbf{1}_4, \quad (20)$$

where $\mathbf{1}_4 = [1 \ 1 \ 1 \ 1]^T \in \mathbf{R}^4$, $E_j = [0_{4,j} \ I_4 \ 0_{4,M-j-4}]^T \in \mathbf{R}^{M \times 4}$ and $v_q = [0_{q-1}^T \ 1 \ 0_{p-q}^T]^T \in \mathbf{R}^p$. This is because, if $\tau_{q,i} \geq c_q$ holds, we have from (15)-(17),

$$\begin{aligned} x_q(t) &= \hat{x}_q(u) = \sum_{i=0}^3 \tau_{q,j-3+i} N_{i,3}(u) \\ &\geq \sum_{i=0}^3 c_q N_{i,3}(u) = c_q \sum_{i=0}^3 N_{i,3}(u) = c_q \quad \forall t \in [t_j, t_{j+1}), \end{aligned} \quad (21)$$

since $N_{i,3}(u) \geq 0 \forall u \in [0, 1]$.

The above arguments can be easily extended to larger knot point interval $[t_j, t_l]$ for some $l (> j)$.

3.2 Constraints on Integral Values

Next we consider the case of an equality or inequality constraint on the value of integral $\int_{t_0}^{t_m} x_q(t) dt$. From (16), (17) and (18), we get

$$\int_{t_0}^{t_m} x_q(t) dt = \sum_{j=0}^{m-1} \int_{t_j}^{t_{j+1}} x_q(t) dt = \frac{1}{\alpha} \sum_{j=0}^{m-1} \int_0^1 \hat{x}_q(u) du = \frac{1}{\alpha} \sum_{j=0}^{m-1} (\tau_{(j)}^q)^T \int_0^1 N_3(u) du. \quad (22)$$

Noting that $N_3(u) = [N_{0,3}(u), N_{1,3}(u), N_{2,3}(u), N_{3,3}(u)]^T$ and $\tau_{(j)}^q = [\tau_{q,j-3}, \tau_{q,j-2}, \tau_{q,j-1}, \tau_{q,j}]^T$, we obtain

$$\begin{aligned} \alpha \int_{t_0}^{t_m} x_q(t) dt &= \sum_{j=-3}^{-1} \tau_{q,j} \sum_{i=0}^{j+3} \int_0^1 N_{i,3}(u) du + \sum_{j=0}^{m-4} \tau_{q,j} \sum_{i=0}^3 \int_0^1 N_{i,3}(u) du \\ &\quad + \sum_{j=m-3}^{m-1} \tau_{q,j} \sum_{i=j-m+4}^3 \int_0^1 N_{i,3}(u) du. \end{aligned}$$

Here, using (6) and (5), we get

$$\int_0^1 N_3(u) du = \frac{1}{24} [1 \ 11 \ 11 \ 1]^T. \quad (23)$$

From the above two equations, it can be shown that the integral value $\int_{t_0}^{t_m} x_q(t) dt$ is expressed as a linear function in $\hat{\tau}$,

$$\int_{t_0}^{t_m} x_q(t) dt = (a \otimes v_q)^T \hat{\tau}, \quad (24)$$

where $a \in \mathbf{R}^M$ is given by

$$a = \frac{1}{24\alpha} [1 \ 12 \ 23 \ 24 \ \cdots \ 24 \ 23 \ 12 \ 1]^T. \quad (25)$$

Replacing v_q in (24) with I_p , the integral value $\int_{t_0}^{t_m} x(t) dt$ can be obtained as a linear function in $\hat{\tau}$, hence $\int_{t_0}^{t_m} x(t) dt = (a \otimes I_p)^T \hat{\tau}$.

3.3 Constrained Splines

As the foregoing development indicates, we can expect that a fairly large number of constrained spline problems may be treated in the above settings. The formulation is simple and is very well fit for numerical solutions as quadratic programming problems. Namely, the optimal smoothing splines are obtained by minimizing the convex quadratic cost $J(\hat{\tau})$ as shown in (10), whereas a number of constraints on the splines may be expressed as linear constraints on $\hat{\tau}$, either equality or inequality or both. A general form of problems is

$$\min_{\hat{\tau} \in \mathbf{R}^{pM}} J(\hat{\tau}) = \frac{1}{2} \hat{\tau}^T G \hat{\tau} + g^T \hat{\tau} \quad (26)$$

subject to the constraints of the form

$$A \hat{\tau} = d, f_1 \leq E \hat{\tau} \leq f_2, h_1 \leq \hat{\tau} \leq h_2, \quad (27)$$

for some matrices and vectors of appropriate dimensions. A very efficient numerical algorithm is available for this purpose [11].

4 Numerical Examples

We examine the design method presented in the previous sections numerically. We here approximate a probability density function from the histogram of random samples for the case of cubic splines, i.e. $k = 3$ and $p = 1$. Figure 1 shows the histogram of 100 ($= N_s$) Gaussian random numbers with zero mean and unit standard deviation. We approximate the density function in the interval $[t_0, t_m] = [-5, +5]$. The data (s_i, d_i) , $i = 1, 2, \dots, N$ in (7) is then generated as follows. First, s_i 's are taken as the center of each bins in the histogram as $s_1 = -5$, $s_2 = -4, \dots, s_{11} = 5$, and hence the number of data is $N = 11$. The data d_i is then obtained by rescaling the histogram, say H_i , $i = 1, 2, \dots, 11$, so that the area covered by the histogram over

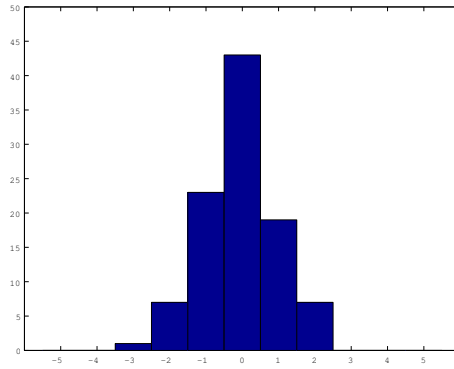


Fig. 1. Histogram of 100 Gaussian random numbers

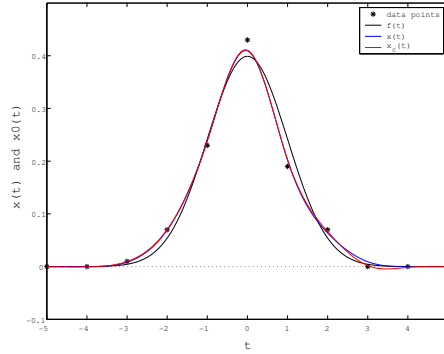


Fig. 2. Data points (*), constrained and unconstrained smoothing splines $x(t)$ and $x_0(t)$, resp.) for histogram from Gaussian probability density function $f(t)$.

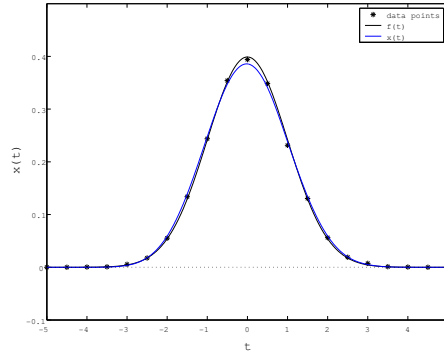


Fig. 3. Data points (*), constrained smoothing splines $x(t)$ for the case of 10000 samples, 21 bins ($N = 21$) and $m = 20$ for histogram from Gaussian probability density function $f(t)$.

$[t_0, t_m]$ is normalized to one, yielding $d_i = H_i/100$. Note that, in general, the histogram is scaled as $d_i = H_i/S$ with $S = N_s \frac{t_m - t_0}{N-1}$, and the pair (s_i, d_i) can be used for reconstructing probability density functions.

With $k = 3, \alpha = 1$ and $m = 10$ in (1), an optimal smoothing spline $x(t)(= x_1(t))$ is computed based on the criterion (9) with $\Lambda(= \lambda_1) = 0.001$ and $W_i = 1/N$. Obviously, we impose the equality and inequality constraints

$$\int_{t_0}^{t_m} x(t) dt = 1, \quad x(t) \geq 0 \quad \forall t \in [t_0, t_m], \quad (28)$$

using the formulation described in Section 3. The results are shown in Figure 2, where the data points (s_i, d_i) are shown by asterisks *, and the Gaussian probability density function $f(t)$ and the designed spline $x(t)$ are plotted in black and blue solid lines respectively. Also we showed in red solid line an optimal smoothing spline $x_0(t)$ obtained without the constraints (28). We see that the curve $x(t)$ closely approximates the Gaussian curve while maintaining the above constraint on density functions, which is not the case with the curve $x_0(t)$.

Obviously, we expect that, as the numbers of samples, bins and basis functions increase, the approximation improves. In fact we obtained the results as shown in Figure 3 for the case of 10000 random samples, $N = 21$ and $m = 20$.

5 Concluding Remarks

We developed a method for designing optimal smoothing splines with equality and/or inequality constraints. The splines are constituted employing normalized uniform B-splines as the basis functions, and hence the central issue is to determine an optimal matrix τ of the so-called control points. Such an approach enables us to express various types of constraints as linear function of $\hat{\tau}(= \text{vec } \tau)$, including those on the spline $x(t)$ and its elements, their integral. The design problem becomes a convex quadratic programming problem in $\hat{\tau}$, where very efficient numerical algorithms are available. We examined the performances of the design method by numerical example with equality and inequality constraints. To conclude, the developed method is effective as well as very useful for various types of problems.

References

1. G. Wahba, *Spline models for observational data*, CBMS-NSF Regional Conference Series in Applied Mathematics, 59, Society for Industrial and Applied Mathematics (SIAM), Philadelphia, PA (1990).
2. Z. Zhang, J. Tomlinson, and C. F. Martin, Splines and linear control theory. *Acta Appl. Math.*, 49, no. 1, 1–34 (1997).
3. C. de Boor, *A practical guide to splines*, Revised Edition, Springer-Verlag, New York (2001).
4. M. Egerstedt and C. F. Martin, Optimal control and monotone smoothing splines. New trends in nonlinear dynamics and control, and their applications, 279–294, Lecture Notes in Control and Inform. Sci., 295, Springer, Berlin (2003).
5. C.F. Martin, S. Sun and M. Egerstedt, Optimal control, statistics and path planning. Computation and control, VI (Bozeman, MT, 1998). *Math. Comput. Modelling*, 33, no. 1-3, 237–253 (2001).
6. H. Kano, H. Fujioka, and C. F. Martin, Optimal Smoothing and Interpolating Splines with Constraints, *Proc. of the 46th IEEE Conference on Decision and Control*, 3011-3016, New Orleans, LA, USA, Dec. 12-14 (2007).
7. R. Dias, Density estimation via hybrid splines, *J. of Statistical Computation and Simulation*, 60, Issue 4, 277-293 (1998).
8. J. Z. Kolter and A. Y. Ng, Task-Space Trajectories via Cubic Spline Optimization, *Proc. of the 2009 Int. Conf. on Robotics and Automation*, 1675-1682, Kobe, Japan, May 12-17 (2009).
9. P. Lancaster and M. Tismenetsky, *The Theory of Matrices*, Second Edition, Academic Press (1985).
10. H. Kano, H. Nakata, and C. F. Martin, Optimal Curve Fitting and Smoothing Using Normalized Uniform B-Splines : A tool for studying complex systems, *Applied Mathematics and Computation*, 169, no.1, 96-128 (2005).
11. J. Nocedal and S. Wright, *Numerical Optimization*, Second Edition, Springer (2006).

Patient pathway prognostication using the extended mixture distribution survival tree based analysis

Lalit Garg¹, Sally McClean¹, Maria Barton¹, Brian Meenan² and Ken Fullerton³

¹School of Computing and Information Engineering, University of Ulster, Coleraine, UK
Email: {garg-l, si.mcclean, m.barton}@ulster.uk

²School of Engineering, University of Ulster, Jordanstown, UK
Email: bj.meenan@ulster.ac.uk

³College of Medicine and Health Sciences, Queen's University, Belfast, UK
Email: ken.fullerton@belfasttrust.hscni.net

Abstract: Mixture distribution survival trees are constructed by approximating different nodes in the tree by distinct types of mixture distributions to achieve more improvement in the likelihood function and thus the improved within node homogeneity. In our previous work (Garg et al. 2009), we proposed a mixture distribution survival tree based method (where tree nodes were approximated using Gaussian mixture distributions and phase type distributions) for determining clinically meaningful patient groups from a given dataset of patients' length of stay where partitioning was based on covariates representing patient characteristics such as gender, age at the time of admission, and primary diagnosis code. This paper extends this approach to patient pathway prognostication i.e. for determining importance and effects of various input covariates such as gender, age at the time of admission and primary diagnosis code on patients' hospital length of stay and to examine the relationship between length of stay in hospital and or treatment outcome. An application of this approach is illustrated using 5 year retrospective data of patients admitted to Belfast City Hospital with a diagnosis of stroke (hemorrhagic stroke, cerebral infarction, transient ischaemic attack TIA, and stroke unspecified).

Keywords: Stochastic modeling, Survival tree, Length of stay modelling, Prognostication, Clustering, Gaussian mixture distributions, Phase type distributions

1 Introduction

Mixture distribution survival trees are special type of survival trees, which are constructed by approximating different nodes in the tree by distinct types of mixture distributions to achieve more improvement in the likelihood function and thus the improved within node homogeneity. Survival trees can be used as a powerful method for partitioning survival data into clinically meaningful patient groups for prognostication, i.e., for determining importance, effects of various input covariates (such as a patient's characteristics) and their influence on output measures such as patients' survival, their expected length of stay, discharge destination, or treatment outcome (Davis and Anderson 1989, Gao et al. 2004). In our previous work (Garg et al. 2009), we proposed a mixture distribution survival tree based method where tree nodes were approximated using Gaussian mixture distributions and phase type distributions, for into homogeneous groups with respect to their length of stay (LOS) where partitioning was based on covariates

representing patient characteristics such as gender, age at the time of admission and primary diagnosis code. This paper extends this approach to patient pathway prognostication i.e. for determining importance and effects of various input covariates such as gender, age at the time of admission and primary diagnosis code on patients' hospital length of stay and to examine the relationship between length of stay in hospital and treatment outcome.

An application of the approach to patient pathway prognostication is illustrated using 5 years' retrospective data (Barton et al. 2009) for 1985 patients admitted between January 2003 and December 2007 to the Belfast City Hospital with a diagnosis of stroke (hemorrhagic stroke, cerebral infarction, transient ischaemic attack TIA, and stroke unspecified). All patients were discharged between January 9th, 2003 and March 11th 2008. No information that identified individual patients was supplied. Patients were aged between 24 years and 101 years. Patient's lengths of stay range from is 0 days (admitted and discharge on the same day) to 1425 days, mean LOS 29.01 days with 52.84 days standard deviation (Barton et al. 2009).

2 Mixture distribution survival tree construction

A survival tree can be constructed by recursively splitting nodes into daughter nodes by one of the covariates based on some splitting criteria either maximizing either within node homogeneity or between node separation (Gao et al., 2004). Each daughter node is approximated by both GMD and C-PhD with different set of components. We used splitting criteria to maximize within node homogeneity expressed in terms of Akaike Information criterion (AIC) (Akaike, 1974).

$$AIC = -2*\text{Log likelihood}+2*df.$$

Where df is the number of free parameters to be estimated. For nodes modeled by n component (phase) Coxian phase type distribution (C-PhD), $df = 2*n-1$ and for a node modeled by m component Gaussian mixture distribution (GMD), $df = 2*m-1$.

A split with minimum value of AIC is selected. If at a node, there is no split providing positive improvement in the AIC, the node is designated as a terminal node.

We used three covariates gender, age at the time of admission and type of stroke diagnosed. The covariate 'age' has value 'old' for those aged 70 or over and it has value 'young' for those aged below 70 years. Based on the primary ICD-10 diagnosis code (World Health Organisation, 2007), patients can have any of the four values (hemorrhagic stroke, cerebral infarction, transient ischaemic attack TIA, and other strokes) for the covariate 'stroke diagnosed'.

Figure 1 is the schematic representation of the final mixture distribution survival tree for the length of stay data on stroke patients from the Belfast City Hospital. The resulting tree has 12 terminal nodes. A node with 'P' is modeled by C-PhD while a node with 'G' is modeled by GMD, i.e., node 9, node 17 and node 19 are modeled by GMDs and all other nodes root node (node 1), node 2, node 3, node 4, node 5, node 6, node 7, node 8, node 10, node 11, node 12, node 13, node 14, node

15, node 16, node 18, node 20 and node 21 are modeled by C-PhDs. Nodes of the tree and possible splits of these nodes are listed in Table 1. Bold faced covariates were selected for splitting the parent node. Nodes which are better fitted by GMD are having AIC shaded yellow. The AIC of root node was 16825.6 and new total AIC of all the terminal nodes of the survival tree is 16397.92 with 427.68 total improvement in AIC.

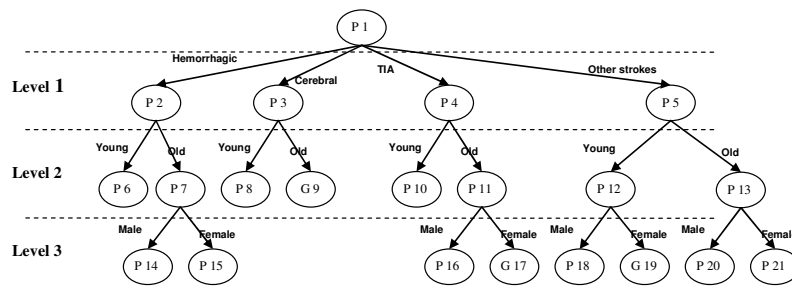


Fig. 1. Mixture distribution survival tree for the length of stay data on stroke patients from the Belfast City Hospital

3 Pathway prognostication using the mixture distribution survival tree

Using the results in Table 1, we can examine the relationship between age, gender, diagnosis and LOS. For convenience the tree is divided in to three levels. At level 1, it is seen that the most significant split is by the covariate ‘stroke diagnosed’ (improvement in AIC = 306.2), i.e., there was most significant difference among different stroke diagnosis groups. This can also be verified by the mean length of stay for each split (see Table 1) Such as patients with a diagnosis of TIA (transient ischemic attack) were most likely to have a shorter length of stay (mean LOS 9.31), while patients with a diagnosis of cerebral infarction were least likely to have shorter length of stay (mean LOS 36.66). The second best split at level 1 is the covariate ‘age’ (improvement in AIC = 127.2). Young patients were most likely to have a shorter length of stay (mean LOS 19.26) while old patients were less likely to have shorter length of stay (mean LOS 33.48). The other covariate ‘gender’ also provided a significant split (improvement in AIC = 10.3); however, it was least significant among the three covariates.

At level 2, for all nodes, the covariate ‘age’ provided the most significant split while the covariate ‘gender’ did not provide significant splits for the group of patients with diagnosis cerebral infarction and for the group of patients with diagnosis TIA. For example, among patients with TIA, young patients were most likely to have a shorter length of stay (mean LOS 5.84) while old patients were likely to have relatively longer length of stay (mean LOS 11.77).

At level 3, for all but one group of young patients (young patients with diagnosis of other strokes), the covariate gender did not provide prognostically significant splits. While at level 3, for groups of old patients with stroke diagnosis

hemorrhagic stroke, TIA and other strokes (node 7, node 11 and node 13) the covariate gender provided prognostically significant splits). For the group of old patients with cerebral infarction (node 9) the covariate gender split is not prognostically significant.

Table 1. Mixture distribution survival Tree construction (Nodes and possible splits)

Node	Covariate	Covariate value	Number of patients	Mean LoS	Standard deviation (LoS)	Coxian-phase type distribution			Gaussian mixture distribution			Improvement in AIC
						Loglikelihood (L _{max})	Number of phases	AIC	Loglikelihood	Number of phases	AIC	
All	Complete dataset	Root node	1985	29.0106	52.8382	-8407.8007	3	16825.60	-8481.625	10	17021.25	-
Level 1												
1 (Root node)	Gender	Male	933	26.5938	44.0575	-3859.8125	2	7725.625	-3897.236	7	7834.478	10.2825
		Female	1052	31.154	59.4698	-4539.8469	3	9089.694	-4569.59	9	9191.18	
	Age	Young	624	19.2564	39.1523	-2316.974	2	4639.948	-2342.454	7	4724.9	127.159
		Old	1361	33.4827	57.4932	-6024.2472	3	12058.49	-6047.846	9	12147.7	
	Diagnosis	Hemorrhagic	154	33.6039	56.4456	-659.05019	3	1328.1	-665.5723	6	1365.14	
		Cerebral	655	36.6611	47.6753	-2973.8941	4	5961.788	-2980.867	6	5995.73	306.1832
TIA		425	9.31294	19.9516	-1298.6262	2	2603.252	-1316.503	6	2667		
Other	751	32.5433	65.0453	-3310.1386	2	6626.277	-3297.443	8	6640.89			
Level 2												
2 Hemorrhagic	Gender	Male	80	28.2	52.09832	-317.63202	4	649.2640	-328.0819	4	678.1638	12.50299
		Female	74	39.4459	60.254	-328.16667	3	666.3333	-329.4363	6	692.873	
	Age	Young	50	24.56	55.117	-173.39875	4	360.7975	-187.3508	3	390.702	15.65113
		Old	104	37.9519	56.561	-468.82587	4	951.6517	-477.7462	4	977.492	
3 Cerebral	Gender	Male	302	33.70860	49.8833	-1334.898	4	2683.796	-1339.464	5	2706.93	-2.395836
		Female	353	39.18697	45.5501	-1635.194	3	3280.388	-1639.346	5	3306.69	
	Age	Young	194	24.0670	42.4506	-785.3629	3	1580.726	-793.676	5	1615.35	35.8404
		Old	461	41.961	48.787	-2173.9068	2	4353.814	-2158.611	5	4345.22	
4 TIA	Gender	Male	207	8.7005	22.6817	-607.9547	2	1221.909	-637.5377	4	1297.08	-1.20391
		Female	218	9.8945	16.9366	-686.27346	3	1382.547	-690.5091	5	1409.02	
	Age	Young	176	5.83523	11.1641	-455.8639	2	917.7278	-465.3673	4	952.735	24.78144
		Old	249	11.7711	24.0154	-827.3716	2	1660.743	-823.7194	8	1693.44	
5 Other strokes	Gender	Male	344	30.7413	43.4091	-1490.577	4	2995.154	-1490.229	6	3014.46	8.886526
		Female	407	34.0663	78.7981	-1808.118	2	3622.237	-1864.211	3	3744.42	
	Age	Young	204	24.9608	43.76126	-818.1347	4	1650.269	-819.1983	6	1672.4	36.23604
		Old	547	35.3711	71.1697	-2466.8858	2	4939.772	-2543.835	3	5103.67	
Level 3												
6 Hemorrhagic Young	Gender	Male	29	30.5172	69.1114	-108.83289	2	223.6658	-105.682	4	233.364	-9.21382
		Female	21	16.3333	22.8126	-70.172765	2	146.3455	-74.17359	3	164.347	
7 Hemorrhagic Old	Gender	Male	51	26.8823	39.2027	-211.39224	4	436.7845	-211.0736	4	444.147	2.30463
		Female	53	48.6038	67.5821	-253.2813	2	512.5626	-245.9886	7	531.977	
8 Cerebral Young	Gender	Male	104	24.6731	49.2715	-420.88798	2	847.776	-427.2601	4	876.52	-3.15333
		Female	90	23.36667	32.9415	-361.0516	4	736.1032	-364.2716	4	750.543	
9 Cerebral Old	Gender	Male	198	38.4545	49.6696	-903.58419	4	1821.168	-903.381	4	1828.76	-0.62756
		Female	263	44.6008	47.9429	-1259.34	2	2524.681	-1251.528	6	2537.06	
10 TIA Young	Gender	Male	88	5.7386	11.3263	-224.74588	2	455.4918	-232.5108	3	481.022	-5.52344
		Female	88	5.9318	10.9988	-230.8797	2	467.7595	-231.1457	4	484.291	
11 TIA Old	Gender	Male	119	10.8908	28.0847	-377.7327	2	761.4654	-401.7215	3	819.443	2.615394
		Female	130	12.5769	19.5270	-444.56883	4	903.1377	-437.3312	4	896.662	
12 Other strokes Young	Gender	Male	119	30.1092	52.7719	-493.3325	3	996.665	-486.2055	6	1006.41	
		Female	85	17.7529	24.6624	-322.7928	3	655.5857	-318.6695	3	653.339	0.265422
13 Other strokes Old	Gender	Male	225	31.0756	37.52	-987.5257	4	1989.051	-991.5326	4	2005.07	3.802914
		Female	322	38.3727	87.1713	-1470.4587	2	2946.917	-1517.217	3	3050.43	

4 The extended mixture distribution survival tree construction

This mixture distribution survival tree method can be extended to examine the relationship between the treatment outcome and patients' length of stay distribution and their interrelationship with patient characteristics by further partitioning each group of patients (determined using mixture distribution survival tree method above) into subgroups with more homogeneous patient pathways by covariate 'treatment outcome'. Although the information about the treatment outcome is not available at the time of admission, we can assign the probability to each treatment outcome using cohort analysis. The covariate 'treatment outcome' can have any of the two values death or discharge from the hospital.

Table 1. Extended mixture distribution survival Tree construction (Nodes and possible splits)

Node	Treatment outcome	Number of patients	Mean LoS	Standard deviation (LoS)	Coxian-phase type distribution			Gaussian mixture distribution			P/D	Improvement in AIC
					Loglikelihood (Lmax)	Number of phases	AIC	Loglikelihood (Lmax)	Number of phases	AIC		
6 Hemorrhagic Young	All	50	24.56	55.1170	-173.398747	4	360.797494	-187.3508	3	390.7016	P	
	Death	17	16.41176	40.62462	-45.164673	2	96.329346	-49.46814	3	114.93628	P	
	Discharge	33	28.75758	60.8346	-132.664452	2	271.328904	-124.2443	5	276.4886	P	-6.860756
14 Hemorrhagic Old Male	All	51	26.88235	39.2027	-211.392242	4	436.784484	-211.0736	4	444.1472	P	
	Death	21	10.90476	14.72576	-66.370745	2	138.74149	-69.28119	4	160.56238	P	
	Discharge	27	31.88889	38.8476	-120.480944	1	242.961888	-136.397712	3	288.795424	P	55.081106
15 Hemorrhagic old Female	All	53	48.6038	67.5821	-253.281317	2	512.562634	-245.9886	7	531.9772	P	
	Death	27	24.14815	35.46903	-107.557149	2	221.114298	-102.7218	4	227.4436	P	
	Discharge	26	74	82.08438	-137.905682	1	277.811364	-138.2828	2	286.5656	P	13.636972
8 Cerebral Young	All	194	24.067	42.4506	-785.362917	3	1580.72583	-793.676	5	1615.352	P	
	Death	14	21.28571	35.22464	-52.239817	2	110.479634	-52.89346	2	115.78692	P	
	Discharge	180	24.28333	42.83745	-754.162206	1	1510.32441	-741.9413	4	1505.8826	G	-35.6364
9 Cerebral Old	All	461	41.961	48.787	-2173.906849	2	4353.8137	-2158.611	5	4345.222	G	
	Death	112	35.66071	46.40227	-506.937452	3	1023.8749	-505.356	6	1044.712	P	
	Discharge	349	43.9828	49.35776	-1663.94776	2	3333.89552	-1646.572	6	3327.144	G	-5.796904
10 TIA Young	All	176	5.83523	11.1641	-455.863901	2	917.727802	-465.3673	4	952.7346	P	
	Death	2	57.5	12.5	-9.379398	2	24.758796	-7.889334	1	19.778668	G	
	Discharge	174	5.24138	9.656117	-439.511915	2	885.02383	-447.4886	5	922.9772	P	12.925304
16 TIA Old Male	All	119	10.8908	28.0847	-377.732704	2	761.4654	-401.7215	3	819.443	P	
	Death	6	21	21.11871	-24.267131	1	50.534262	-21.9243	2	53.8486	P	
	Discharge	113	10.354	28.3061	-351.428756	2	708.85751	-373.1814	3	762.3628	P	2.073634
17 TIA Old Female	All	130	12.3769	19.5270	-444.56883	4	903.13766	-437.3312	4	896.6624	P	
	Death	5	48	32.98484	-24.356002	1	50.712004	-24.57493	1	53.14986	P	
	Discharge	125	11.16	17.344691	-416.933111	2	839.86622	-410.8084	5	849.6168	P	12.559434
18 Other strokes Young Male	All	119	30.1092	52.7719	-493.332527	3	996.66505	-486.2055	6	1006.411	P	
	Death	11	34.4545	33.29036	-49.936044	1	101.87209	-47.59397	2	105.18794	P	
	Discharge	108	29.66667	54.34628	-441.546035	4	897.09207	-434.9861	6	903.9722	P	-2.299104
19 Other strokes Young Female	All	85	17.7529	24.6624	-322.792848	3	655.5857	-318.6695	3	653.339	G	
	Death	11	6.090909	6.273386	-30.874764	1	63.749528	-35.8078	1	75.6156	P	
	Discharge	74	19.48649	25.87613	-287.535163	3	585.070326	-290.6527	3	597.3054	P	4.519146
20 Other strokes Old Male	All	225	31.0756	37.52	-987.525677	4	1989.0514	-991.5326	4	2005.0652	P	
	Death	53	37.79245	46.98388	-245.501788	1	493.00358	-245.7851	3	507.5702	P	
	Discharge	172	29.00581	33.81026	-741.08819	4	1496.176	-742.574	4	1507.148	P	-0.128602
21 Other strokes Old Female	All	322	38.3727	87.1713	-1470.458696	2	2946.9174	-1517.217	3	3050.434	P	
	Death	89	44.21348	151.97	-395.257131	2	796.51426	-385.6987	5	799.3974	P	
	Discharge	233	36.14163	40.76418	-1062.77177	3	2135.5435	-1064.076	4	2150.152	P	14.859584

Each terminal node of the survival tree of Figure 1 is further partitioned into daughter nodes by the covariate 'treatment outcome'. We grow the tree if the split

maximizes node homogeneity by minimizing the value of AIC and if at a node, there is no split providing significant improvement in AIC, the node is designated as a terminal node.

Figure 2 is the schematic representation of the extended mixture distribution survival tree for the length of stay data on stroke patients from the Belfast City Hospital. The resulting tree now has 19 terminal nodes. Only two terminal nodes (node 9 and node 26) are approximated by GMD and all other terminal nodes are approximated by C-PhD. Table 2 lists terminal nodes of the survival tree of figure 1, and possible splits of these nodes by the covariate ‘treatment outcome’. Bold faced splits were selected for splitting the parent node. Parent nodes are represented by pale blue rows with treatment outcome “all”. The column P/G specifies which distribution among C-PhD and GMD provides better fit. The total improvement in AIC is 115.655 and the new AIC of all the terminal nodes is 16282.27.

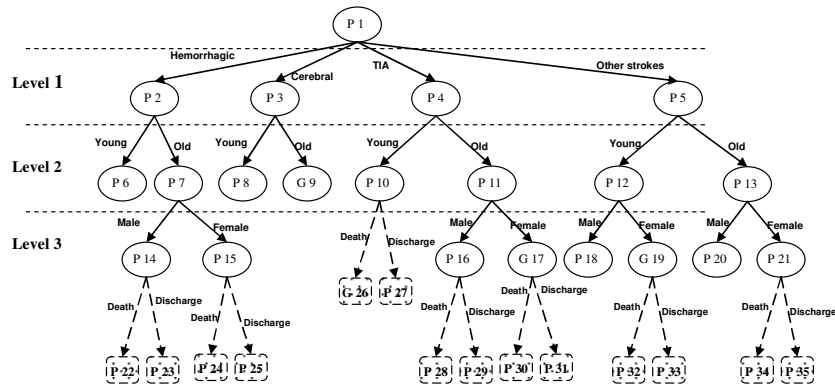


Fig. 2. Extended mixture distribution survival tree for the length of stay data on stroke patients from the Belfast City Hospital

5 Pathway prognostication using the extended mixture distribution survival tree

The extended mixture distribution survival tree method can effectively be used to examine the relationship between LOS and treatment outcome at discharge and their interrelation with patient characteristics such as age, gender and diagnosis.

The extended mixture distribution survival tree clusters the length of stay data into 19 clinically meaningful patient groups, each representing a distinct patient pathway within the system. We can see that in seven patient groups (i.e., the terminal nodes in Figure 1), the covariate ‘treatment outcome’ has prognostic significance, i.e., patients with different treatment outcomes follow different patient pathways, while, there is homogeneity among patient pathways followed by the other five patient groups. The treatment outcome is prognostically most significant among the group of old male patients diagnosed with Hemorrhagic stroke. This also reflects with the difference in mean LOS. Among this group of

patients, those are expected to discharge are likely to have longer length of stay (mean LOS 31.9) than those die in the course of their treatment (mean LOS 10.9). The Treatment outcome has prognostic significance for all groups of female patients while it has prognostic significance in only two groups of male patients (node 14 and node 16). All young patients with Hemorrhagic stroke followed homogeneous patient pathways. Treatment outcome does not have prognostic significance among all groups of patients diagnosed with cerebral infraction, while treatment outcome is prognostically significant in all groups of patients with TIA. Patients diagnosed with TIA and discharged from hospital are more likely to have shorter length of stay (mean LOS 5.24, 10.35, 11.16 respectively for node 27, node 29 and node 31) than those patients with TIA who died in the hospital (mean LOS 57.5, 21 and 48 respectively for node 26, node 28 and node 30).

6 Conclusion

Mixture distribution survival tree have advantage of achieving the improved within node homogeneity. Therefore, mixture distribution survival tree based analysis is a more effective method for prognostication of survival data and for clustering survival data into groups of patients following homogeneous patient pathways. It is a powerful method for determining the relationship between input covariates and outcome measures and their interrelations. It provides better understanding of heterogeneity of patient pathways stratified by covariates representing patient characteristics such as age, gender, diagnosis and outcome measures such as treatment outcome, destination at discharge. We can also use the model to estimate the length of stay of a patient based on his/her characteristics (age, gender, diagnosis) available at the time of admission. We can extend this approach by further growing the tree by partitioning the terminal nodes into subgroups with more homogeneous patient pathways based on covariates representing outcome measures. Although the information about the treatment outcome is not available at the time of admission, we can assign the probability to each treatment outcome using cohort analysis. This information can be used for estimating bed requirements for each group of patients (following homogeneous patient pathways) and capacity planning for the whole care system. As future work we will also assess the use of other mixture distributions in order to achieve further improvement in within node homogeneity. Presently we are developing application of our model for capacity planning in a stroke care unit.

References

1. Garg, L., McClean, S. I., Meenan, B. J., El-Darzi, E. and Millard, P. H., Clustering patient length of stay using mixtures of Gaussian models and phase type distributions. *The 22nd IEEE Symposium on Computer-Based Medical Systems (CBMS 2009)*, Albuquerque, New Mexico, USA, August 3-4, 2009, pp. 1-7, doi:10.1109/CBMS.2009.5255245 (2009).
2. Davis R. and Anderson J., Exponential Survival Trees, *Statistics in Medicine*, 8, 947-962 (1989).

3. Gao F., Manatunga A. K. and Chen S., Identification of prognostic factors with multivariate survival data, *Computational Statistics & Data Analysis*, 45, 813-824 (2004).
4. Barton M., McClean S. I., Garg L., Fullerton K., Modelling Stroke Patient Pathways using Survival Analysis and Simulation Modelling, *The XIII International Conference on Applied Stochastic Models and Data Analysis*, Vilnius, Lithuania, June 30 - July 3, 2009, 370-373 (2009).
5. Akaike H., A new look at the statistical model identification, *IEEE Transactions on Automatic Control*, 19(6), 716 – 723 (1974).
6. World Health Organisation, International Statistical Classification of Diseases and Related Health Problems, *Tenth Revision – ICD-10, second edition*, WHO: Geneva (2007).

On the use of Neural Networks in Statistical Shape Analysis

Stefan Giebel¹, Jens-Peter Schenk², Jang Schiltz¹

¹ Luxembourg School of Finance
University of Luxembourg, Luxembourg
(e-mail: Jang.Schiltz@uni.lu)

² Pädiatrische Radiologie
Universitätsklinik Heidelberg, Heidelberg, Deutschland
(e-mail: Jens-peter.Schenk@med.uni-heidelberg.de)

Abstract. There are different kinds of tumours that can appear in childhood: nephroblastoma, clear cell sarcoma, neuroblastoma etc. The chosen therapy depends upon the diagnosis of the radiologist which is done with the help of MRI (Magnetic resonance images). Our research is the first mathematical approach on MRI of renal tumours (n=80). We are using transversal, frontal and sagittal images and compare their potential for differentiation of the different kind of tumours by use of Statistical Shape Analysis. We determine the key points or three dimensional landmarks of the renal tumours by using the edges of the platonic body (C60). Furthermore we use a combination of Neural Networks and Statistical Shape Analysis to consider all kinds of linear transformations and compare the results to the one obtained by the traditional test of Ziezold test for the determination and differentiation of the mean shape.

Keywords: Neural Networks, Statistical Shape Analysis, Mean Shape, Renal tumours.

1 Introduction

In a wide variety of disciplines it is of great practical importance to measure, describe and compare the shapes of objects. In general terms, the shape of an object, data set, or image can be defined as the total of all information that is invariant under translations, rotation and isotropic rescaling. The field of shape analysis involves hence methods for the study of the shape of objects where location, rotation and scale can be removed. The two- or more dimensional objects are summarised according to key points called landmarks. This approach provides an objective methodology for classification whereas even today in many applications the decision for classifying according to the appearance seems at most intuitive.

Interest in shape analysis began in 1977. D.G. Kendall[7] published a note in which he introduced a new representation of shapes as elements of complex projective spaces. K.V. Mardia[10] on the other hand investigated the distribution of the shapes of triangles generated by certain point processes, and in particular considered whether towns in a plain are spread regularly with

equal distances between neighbouring towns. The full details of this elegant theory which contains interesting areas of research for both probabilists and statisticians were published by D. Kendall[8] and F. Bookstein[1]. The details of the theory and further developments can be found in the textbooks by C.G. Small[14] and I.L. Dryden & K.V. Mardia[4].

The renal tumour is limited by spleen or liver, the rest of the kidney, the spine and retroperitoneal vessels. In Giebel(2007)[2] it was shown that every landmark has another meaning for differentiating the tumours. Giebel et al. [3] showed that none of the landmarks has a special influence for the determination of the mean shape according to the test of Ziezold (2003)[17].

In this paper, the edges of the platonic body (C60) define the landmarks. We use a combination of Neural Networks and Statistical Shape Analysis and compare the results to the one obtained by the traditional test of Ziezold test for the determination and differentiation of the mean shape.

2 Wilms' tumours

Nephroblastoma (Wilms' tumour)[15] is the typical tumour of the kidneys appearing in childhood. Therapy is organised in therapy-optimizing studies of the Society of Paediatric Oncology and Haematology (SIOP). Indication of preoperative chemotherapy is based on radiological findings. The preferred radiological methods are sonography and MRI. Both methods avoid radiation exposure, which is of great importance in childhood. Preoperative chemotherapy is performed without prior biopsy[12].

Information of the images of magnetic resonance tomography, especially the renal origin of a tumour and the mass effect with displacement of other organs, is needed for diagnosis. Next to nephroblastomas other tumours of the retro peritoneum exist, which are difficult to differentiate [13]. Renal tumours in childhood are classified into three stages of malignancy (I, II, III). Typical Wilms tumors mostly belong in stage II. In stage II different subtypes of nephroblastoma tissue exist[6].

In our sample of tumours, four different types of retroperitoneal tumours are represented: nephroblastoma, neuroblastoma, clear cell carcinoma, and renal cell carcinoma. Renal cell carcinomas are very rare in childhood. They represent the typical tumours of adult patients. They have no high sensitivity for chemotherapy. Clear cell sarcomas are very rare in childhood and are characterised by high malignancy. Neuroblastomas are the typical tumours of the sympathetic nervous system and suprarenal glands. Infiltration of the kidney is possible.

The tumour grows with encasement of vessels. Because of the high importance of radiological diagnosis for therapy, it is of great interest to find markers for a good differentiation of tumours. MRI produces 2D-images. From the two dimensional data a three dimensional object has to be computed. Image 1 shows an example of the raw data.

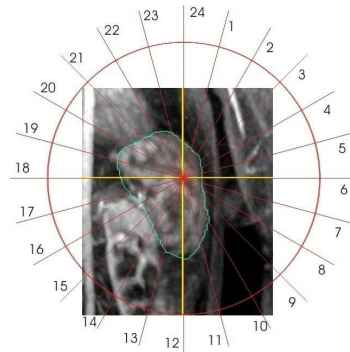


Fig. 1. 2D-image of the tumour

3 Mean Shape

To compare the standardised and centred sets of landmarks, we have to define the mean shape of all the objects and a distance function which allows us to evaluate how "near" every object is from this mean shape.

The term "mean" is here used in the sense of Fréchet (1948)[5]. If X denotes a random variable defined on a probability space $(\Omega, \mathcal{F}, \mathcal{P})$ with values in a metric space (Ξ, d) , an element $m \in \Xi$ is called a mean of $x_1, x_2, \dots, x_k \in \Xi$ if

$$\sum_{j=1}^k d(x_j, m)^2 = \inf_{\alpha \in \Xi} \sum_{j=1}^k d(x_j, \alpha)^2. \tag{1}$$

That means that the "mean shape" is defined as the shape that guarantees the smallest possible variance for a group of objects. For computing the mean shape we use the algorithm of Ziezold (1994)[16].

In the special case of oncology there is no theoretical medical reason to select a specific group of landmarks for differentiation. All landmarks in this research have thus to be selected by an explorative procedure.

The test of Ziezold (1994)[16] is a statistical test which allows to determine if a given object belongs to a set of objects defined by their mean shape. We have used this test to see if given Wilm's tumours can be differentiated from the mean shape of the neuroblastomas and vice versa.

4 Elements of neural networks

Neural networks have been developed originally in order to understand the cognitive processes. Nowadays there are a lot of applications of neural networks as a mathematical method in various quite different disciplines. The term "neural networks" points to the model of a nerve cell, the neuron,

and the cognitive processes carried and driven by the network of interacting neurons. A neuron perceives chemical and physical excitement from the environment by its dendrites. The neuron is processing this incoming data and sending the information to other neurons via axons and synapses. McCulloch and Pitts implemented the biological processes of a nerve cell for the first time in a mathematical way [9]. Nerve cells have to access and process incoming data in order to evaluate target information. Therefore the corresponding neural networks are called supervised neural networks.

An unsupervised neural network has no target and is similar to a cluster algorithm. The data consist of n variables x_1, \dots, x_n on binary scale. For data processing, the i th variable x_i is weighted with w_i . Normalised with $|w_i| \leq 1$, multiplication of x_i with w_i determines the relevance of x_i for a target y . The value w_i reflects the correlation between the input variable and the target, the sign indicating the direction of the influence of the input variable on the target. Weighting the input variables for a target variable is similar to discriminant analysis. The critical quantity for the neuron is the weighted sum of input variables

$$q := \sum_{i=1}^n w_i \cdot x_i = w_1 \cdot x_1 + \dots + w_n \cdot x_n \quad . \quad (2)$$

For a target y with binary scale, a threshold S is needed. Crossing the threshold yields 1 and falling below the threshold yields 0. Hence the activation function F can be written as

$$F(q) = \begin{cases} 1, & \text{if } x > S \\ 0, & \text{if } x \leq S \end{cases} \quad (3)$$

In comparison to discriminant analysis, for neural networks the threshold S has to be assigned, depending on properties of the target; it can not be derived from the data in a straightforward manner. Neural networks usually include no assumption about the data, they are a purely numerical method.

With the input (2) of the activation function, we obtain $y = F(q)$ as

$$y = 1, \quad \text{if } \sum_{i=1}^n w_i \cdot x_i > S$$

$$y = 0, \quad \text{if } \sum_{i=1}^n w_i \cdot x_i \leq S$$

Multi-layer neural networks are able to solve all logical functions for separating groups.

5 Multi-layer perceptrons

In general a given target may be reached only up to a certain error. Given a certain measure $E(\tilde{y}, y)$ for the distance between the given target state y

and the state \tilde{y} computed by the neural network, the learning of the neural network corresponds to the minimisation of $E(\tilde{y}, y)$. The following training algorithm is inspired by Rumelhart, Hinton and Williams [11]. The total error measure over all states of a given layer is defined as

$$E_{total}(\tilde{y}, y) := \frac{1}{2} \sum_{k=1}^N (\tilde{y}_k - y_k)^2 \quad . \quad (4)$$

It will be used below to reset the weights in each layer of the neural network.

The processed state \tilde{y} of the neural network is computed by the following steps.

First the critical parameter for the first layer is computed from n weighted input values as $\sum_{i=1}^n w_i \cdot x_i$. We consider a hidden output layer with m neurons. For $j = 1, \dots, m$, let g_j be the activation function of the j -th neuron of the hidden layer, with an activation value of h_j , given as

$$h_j = g_j \left(\sum_{i=1}^n w_i \cdot x_i \right) \quad . \quad (5)$$

Usually for all neurons of a given layer a common activation function $g = g_1, \dots, g_m$, e.g. a sigmoid function, is used.

Next, the output of the previous (hidden) layer becomes the input of the next layer, and the activation proceeds analogously to the previous layer. Let f be the activation function of the pre-final (here the second) output layer. Then the pre-final critical value is

$$q = f \left(\sum_{j=1}^m u_j \cdot h_j \right) \quad . \quad (6)$$

Finally, the pre-final critical value q is interpreted by a final activation function F yielding

$$\tilde{y} = F(q) \quad (7)$$

as a final state value computed from the neural network with the given weights of the input variables from input and hidden layers. Now the neural network performs a training step by modifying the weights of all input layers. The learning mechanism the weights is determined by the target distance measure

$$E = \frac{1}{2} \sum_{i=1}^n (y^i - \tilde{y}^i)^2 \quad .$$

The weights of both layers are changed according to the steepest descent, i.e.

$$\Delta w_i = \frac{\partial E}{\partial w_i} \quad (8)$$

$$\Delta u_j = \frac{\partial E}{\partial u_j} \quad (9)$$

With a learning rate α , which should be adapted to the data, the weights are changed as follows:

$$w_i^{new} = w_i^{old} - \alpha \cdot \Delta w_i \quad (10)$$

$$u_j^{new} = u_j^{old} - \alpha \cdot \Delta u_j \quad (11)$$

The necessary number of iterations depends on the requirements imposed by the data, the user, and the discipline.

For simplicity, we consider now an 1-layer perceptron network, which is sufficient for our purpose of minimising the variance. Every landmark is weighted in every direction.

$$\sum_{j=1}^k d(x_j, m)^2 = \inf_{\alpha \in \Xi} \sum_{j=1}^k d(x_j, \alpha)^2. \quad (12)$$

In contrast to the former application of neural networks we are using a metric function instead of a binary variable. The difference between the weighted objects and the approximated mean shape is used instead of the difference between the reality and the approximation E .

6 Results

To get 3D landmarks we construct a three dimensional object of the tumour from the 2D MRI. Then we take the intersection between the surface of the tumour and the vectors going from the centre to the edges of the platonic body C60 as landmarks as is shown in figure 2.

Minimising the variance in one of the groups does not lead always to an

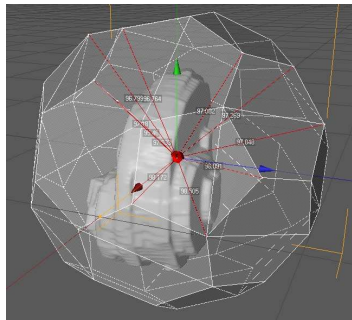


Fig. 2. 3D-Landmarks as cut points between the edge of a platonic body and the surface of the tumor

optimal differentiation between the different types of tumors. The neuronal network uses in fact a different metric to minimising the variance. Every

landmark is weighted in every direction. For a sample of 74 comparable tumors (69 nephroblastoma and 5 neuroblastoma) the u_0 -values are computed for comparing our nephroblastomas to the mean shape of neuroblastomas.

The range of the u_0 -values computed by the MLP lies between 0 and 188. If use the the test of Ziezold[16] with the Euclidean distance instead of the distance applied in MLP, we get an u_0 -value of 112. For a randomised sample ($n = 1000$), we get a p -value of 0.080.

If we compare our neuroblastomas to the mean shape of nephroblastomas, we get an u_0 value of 72 with a p -value of 0.116 in a randomised sample ($n = 1000$).

Figure 3 shows the mean shape of the nephroblastomas (red) and of the neuroblastomas (green).

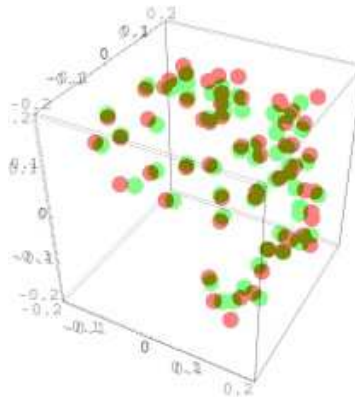


Fig. 3. Mean Shape: Red: 60 landmarks of the mean shape of the nephroblastoma, Green: 60 landmarks of the mean shape of the neuroblastoma

7 Conclusion

The neuroblastoma can be differentiated quite well from the mean shape of the nephroblastoma, especially if we use the Euclidian distance as metric. Shape Analysis is useful to make a decision in spite of different size, location etc. The test used for differentiating the existing kind of tumours does not need any assumptions in regard to distributions and the size of the sample. For improving our results we will try to use appropriate non-Euclidean transformations in the neural networks. A possible approach is to use a supervised 2-layer neural network with weighted landmarks. We will minimise the variance to estimate a "mean shape" in one of the groups instead of minimising

the mistake between output and reality. Indeed, we have seen that a small variance does not always allow an optimal differentiation between the groups. Not every transformation leads to a better differentiation of tumours. If the size or location of tumours plays a role in differentiation, it could be wrong to centre or standardise the objects.

References

1. Bookstein, F.L., "Size and shape spaces for landmark data in two dimensions", *Statistic Sciences* 1, 181-242 (1986).
2. Giebel, S., *Statistical Analysis of the shape of renal tumors in childhood*, Diploma thesis, University of Kassel (2007).
3. Giebel, S., Schiltz, J., and Schenk, J.P., "Application of Statistical Shape Analysis on renal tumours in 3D" *Bulletin de la Société des Sciences Médicales du Grand-Duché du Luxembourg* to appear (2010).
4. Dryden, I.L., and Mardia, K.V., *Statistical Shape Analysis* Wiley, Chichester (1998).
5. Fréchet, M., "Les éléments aléatoires de nature quelconque dans un espace distancié", *Annales de l'Institut Henri Poincaré*, 10, 215-310 (1948).
6. Graf, N., *Urologe A* 43:421 (2003).
7. Kendall, D.G., "The diffusion of shape", *Adv. Appl. Probab.* 9 (1977)
8. Kendall, D.G., "Shape manifolds, Procrustean metrics and complex projective spaces", *Bulletin of the London Mathematical Society*, 16, 81-121 (1984).
9. McCulloch, W.S., and Pitts, W., "A logical calculus of the idea immanent in neural nets", *Bulletin of Mathematical Biophysics*, 115-137 (1943).
10. Mardia, K.V., "Mahalanobis distance and angles", In: Krishnaiah, P.R. (ed) *Multivariate Analysis IV*, 495-511, North Holland, Amsterdam (1977).
11. Rumelhart, D.E., Hinton, G.E., and Williams, R.J., *Learning internal representation by error propagation*, 318-362 (1986).
12. Schenk, J.P, *Fortschr. Röntgenstr.* 178:38 (2006).
13. Schenk, J.P, *Eur. Radiol.* 18:683 (2008).
14. Small, C. G., *The Statistical Theory of Shape*, Springer-Verlag, New York (1996).
15. Wilms, M., *Die Mischgeschwülste der Niere*, Verlag von Arthur Georgi, Leipzig, 1-90 (1889).
16. Ziezold, H., "Mean Figures and Mean Shapes Applied to Biological Figure and Shape Distributions in the Plane", *Biometrical Journal* 36, 491-510 (1994).
17. Ziezold, H., "Independence of Landmarks of Shapes", *Mathematische Schriften Kassel*, Heft 03 (2003).

Ensemble Methods of Appropriate Capacity for Multi-Class Support Vector Machines

Yann Guermeur

LORIA-CNRS
Campus Scientifique, BP 239
54506 Vandœuvre-lès-Nancy Cedex, France
(e-mail: Yann.Guermeur@loria.fr)

Abstract. Roughly speaking, there is one single model of pattern recognition support vector machine (SVM), with variants of lower popularity. On the contrary, among the different multi-class SVMs (M-SVMs) published, none is clearly favoured. Although several comparative studies between M-SVMs and decomposition methods have been reported, no attention had been paid so far to the combination of those models. We investigate the combination of M-SVMs with low capacity linear ensemble methods that estimate the class posterior probabilities.

Keywords: Ensemble methods, M-SVMs, Capacity control.

1 Introduction

Most of the statistical models developed for pattern recognition are based on a principle that does not change fundamentally with the number of categories. Things are more complex in the case of SVMs. Those machines were initially devised to compute dichotomies [2], and the first articles dealing with their use for polytomy computation report results obtained with decomposition methods [10]. M-SVMs were introduced later [11]. Since then, a few M-SVMs have been proposed and evaluated, with the attention of the community focusing on four models exhibiting distinct properties. Several comparative studies between M-SVMs and decomposition methods have established that in practice, each model has its advantages and drawbacks (see for instance [7]). The behaviours observed are different, in accordance with what was predicted by the theory. To the best of our knowledge, nobody has tried so far to take benefit of that phenomenon by combining different M-SVMs. To fill this void, we deal with the combination of M-SVMs subject to two constraints: the sample complexity of the *combiners* must be low, to avoid overfitting, and the outputs must be class posterior probability estimates.

We propose to combine the post-processed outputs of M-SVMs with linear ensemble methods which differ with respect to their objective function. They satisfy the aforementioned constraints and experimental results illustrate their potential. The organization of the paper is as follows. Section 2 provides a general introduction to the M-SVMs and characterizes the four main models. Section 3 deals with the description and statistical analysis of

the linear combiners. Experimental results are exposed in Section 4, and we draw conclusions in Section 5. For lack of space, simple proofs are omitted.

2 Multi-class SVMs

We consider discrimination problems where \mathcal{X} is the description space and $\mathcal{Y} = \llbracket 1, Q \rrbracket$ is the set of categories. M-SVMs are kernel machines: they operate on a class of functions induced by a positive semidefinite function/kernel [1]. Let κ be a kernel on \mathcal{X}^2 and let $(\mathbf{H}_\kappa, \langle \cdot, \cdot \rangle_{\mathbf{H}_\kappa})$ be the RKHS spanned by κ [1]. Let $\bar{\mathcal{H}} = (\mathbf{H}_\kappa, \langle \cdot, \cdot \rangle_{\mathbf{H}_\kappa})^Q$ and $\mathcal{H} = ((\mathbf{H}_\kappa, \langle \cdot, \cdot \rangle_{\mathbf{H}_\kappa}) + \{1\})^Q$. By construction, \mathcal{H} is the class of vector-valued functions $h = (h_k)_{1 \leq k \leq Q}$ on \mathcal{X} such that:

$$\forall k \in \llbracket 1, Q \rrbracket, \quad h_k(\cdot) = \sum_{i=1}^{m_k} \beta_{ik} \kappa(x_{ik}, \cdot) + b_k$$

where the x_{ik} are elements of \mathcal{X} (the β_{ik} and b_k are scalars), as well as the limits of these functions as the sets $\{x_{ik} : 1 \leq i \leq m_k\}$ become dense in \mathcal{X} , in the norm induced by $\langle \cdot, \cdot \rangle_{\mathbf{H}_\kappa}$. It springs from Mercer's theorem [1] that there exists a map Φ from \mathcal{X} into a Hilbert space $(E_{\Phi(\mathcal{X})}, \langle \cdot, \cdot \rangle)$ such that \mathcal{H} defines a multivariate affine model on $\Phi(\mathcal{X})$. Functions h can then be rewritten as

$$h(\cdot) = (\langle w_k, \cdot \rangle + b_k)_{1 \leq k \leq Q}$$

where the vectors w_k belong to $E_{\Phi(\mathcal{X})}$. $\bar{\mathcal{H}}$ can then be seen as a multivariate linear model on $\Phi(\mathcal{X})$, endowed with a norm $\|\cdot\|_{\bar{\mathcal{H}}}$ given by:

$$\forall \bar{h} \in \bar{\mathcal{H}}, \quad \|\bar{h}\|_{\bar{\mathcal{H}}} = \sqrt{\sum_{k=1}^Q \|\bar{h}_k\|_{\mathbf{H}_\kappa}^2} = \sqrt{\sum_{k=1}^Q \|w_k\|^2} = \sqrt{\sum_{k=1}^Q \langle w_k, w_k \rangle}.$$

Definition 1 (M-SVM). Let $((x_i, y_i))_{1 \leq i \leq m} \in (\mathcal{X} \times \llbracket 1, Q \rrbracket)^m$ and $\lambda \in \mathbb{R}_+^*$. A Q -category M-SVM is a classifier obtained by minimizing over the hyperplane $\sum_{k=1}^Q h_k = 0$ of \mathcal{H} a penalized convexified empirical risk of the form:

$$J_{\text{M-SVM}}(h) = \|\xi_{\text{M-SVM}}\|_{\text{M-SVM}}^p + \lambda \|\bar{h}\|_{\bar{\mathcal{H}}}^2$$

where $\xi_{\text{M-SVM}}$ is a vector of slack variables associated with the constraints of good classification, which are linear, and $\|\cdot\|_{\text{M-SVM}}$ is either the ℓ_1 norm ($p = 1$) or the norm induced by a symmetric positive definite matrix ($p = 2$).

In chronological order, the four main M-SVMs are the machines of Weston and Watkins (WW) [11], Crammer and Singer (CS) [3], and Lee, Lin and Wahba (LLW) [8], and the M-SVM² [6]. Their characteristics are summarized in Table 1 (in the sequel, when no confusion is possible, the subscript identifying the machine, i.e., instantiating M-SVM, is omitted).

M-SVM	$\xi_{\text{M-SVM}}$ (constraints of good classification)	$\ \cdot\ _{\text{M-SVM}}$	p
WW	$\forall i \in [1, m], \forall k \in [1, Q] \setminus \{y_i\}, \begin{cases} h_{y_i}(x_i) - h_k(x_i) \geq 1 - \xi_{ik} \\ \xi_{ik} \geq 0 \end{cases}$	ℓ_1	1
CS	$\forall i \in [1, m], \forall k \in [1, Q] \setminus \{y_i\}, h_{y_i}(x_i) - h_k(x_i) \geq 1 - \xi_i$ $\forall k \in [1, Q], b_k = 0, \forall i \in [1, m], \xi_i \geq 0$	ℓ_1	1
LLW	$\forall i \in [1, m], \forall k \in [1, Q] \setminus \{y_i\}, \begin{cases} h_k(x_i) \leq -\frac{1}{Q-1} + \xi_{ik} \\ \xi_{ik} \geq 0 \end{cases}$	ℓ_1	1
M-SVM ²	$\forall i \in [1, m], \forall k \in [1, Q] \setminus \{y_i\}, h_k(x_i) \leq -\frac{1}{Q-1} + \xi_{ik}$	M	2

Table 1. Specifications of the four main M-SVMs

While the CS-M-SVM has one slack variable per training example, the other three have $Q - 1$. In that second case, ξ is the vector of \mathbb{R}^{Qm} whose component of index $(i - 1)Q + k$ is ξ_{ik} , with the ξ_{iy_i} being equal to 0. The matrix M is such that the quadratic form $\xi^T M \xi$ defining $\|\xi_{\text{M-SVM}^2}\|_{\text{M-SVM}^2}^2$ is given by $\xi^T M \xi = \sum_{i=1}^m \sum_{j=1}^m \sum_{k=1}^Q \sum_{l=1}^Q \delta_{i,j} (\delta_{k,l} + 1) \xi_{ik} \xi_{jl}$, where δ is the Kronecker symbol. The following observations illustrate the differences between these machines. The implementation of the training algorithm of the CS-M-SVM is the easiest one, the LLW-M-SVM was the first M-SVM with a Fisher consistent loss and the M-SVM² is the first soft margin M-SVM for which a generalized radius-margin bound applies.

3 Linear ensemble methods

We make the hypothesis that N classifiers $g^{(j)} = \left(g_k^{(j)}\right)_{1 \leq k \leq Q}$, ($1 \leq j \leq N$), are available to perform the classification task of interest. For all n in \mathbb{N}^* , let U_n be the polytope given by: $U_n = \left\{u = (u_p)_{1 \leq p \leq n} \in \mathbb{R}_+^n : \sum_{p=1}^n u_p = 1\right\}$. The outputs of the classifiers are supposed to be nonnegative and sum to one, i.e., to belong to U_Q . We first describe the ensemble methods considered, and then characterize their sample complexity as a function of N and Q .

3.1 Class of functions and training algorithms

Let \tilde{g} be the function from \mathcal{X} to U_Q^N obtained by appending the component functions of the N classifiers $g^{(j)}$: $g_k^{(j)}$ is its component function of index $(j - 1)Q + k$.

Definition 2 (multivariate linear model). We consider the multivariate linear model parameterized by the matrix $B \in \mathcal{M}_{Q,NQ}(\mathbb{R})$ such that

$$\forall x \in \mathcal{X}, \bar{g}(x) = (\bar{g}_k(x))_{1 \leq k \leq Q} = B\tilde{g}(x)$$

$$\text{s.t. } \forall u \in U_Q^N, Bu \in U_Q.$$

The transposes of the rows of B are denoted β_k , so that $\bar{g}_k(x) = \beta_k^T \tilde{g}(x)$, and $\beta = (\beta_k)_{1 \leq k \leq Q} \in \mathbb{R}^{NQ^2}$. The general term of B is written with three indices, i.e., β_{kjl} (β_{kjl} is the component of β_k of index $(j-1)Q + l$). Let $d_m = \{(x_i, y_i) : 1 \leq i \leq m\}$ be a training set. Let t_k denote the *one of Q coding* of category k : $t_k = (\delta_{k,l})_{1 \leq l \leq Q}$. We consider combiners obtained by solving convex programming problems of the form:

Problem 1 (Linear ensemble methods).

$$\begin{aligned} \min_B \sum_{i=1}^m \ell_{\text{LEM}}(t_{y_i}, B\tilde{g}(x_i)) \\ \text{s.t. } \forall u \in U_Q^N, \quad Bu \in U_Q \end{aligned}$$

where the loss function ℓ_{LEM} is convex.

Proposition 1 makes the optimization computationally tractable.

Proposition 1. *Irrespective of the nature of ℓ_{LEM} , there is an optimal solution of Problem 1 which belongs to the polytope $V_{N,Q}$ given by:*

$$\begin{cases} \beta \in \mathbb{R}_+^{NQ^2} \\ \forall j \in \llbracket 1, N \rrbracket, \forall l \in \llbracket 1, Q-1 \rrbracket, \sum_{k=1}^Q (\beta_{kjl} - \beta_{kjQ}) = 0 \\ \sum_{k=1}^Q \sum_{j=1}^N \beta_{kjQ} = 1 \end{cases} .$$

We focus on two natural choices for ℓ_{LEM} that give rise to class posterior probability estimates: the quadratic loss and the cross-entropy loss. Let \tilde{G} be the matrix of $\mathcal{M}_{m,NQ}(\mathbb{R})$ whose rows are the vectors $\tilde{g}(x_i)^T$. Let I_Q denote the identity matrix of size Q and \otimes the Kronecker product. For all k in $\llbracket 1, Q \rrbracket$, let $Y_k = (\delta_{y_i,k})_{1 \leq i \leq m}$ and let $Y = (Y_k)_{1 \leq k \leq Q} \in \{0, 1\}^{Qm}$. The objective function (empirical risk) corresponding to the quadratic loss is:

$$J_{\text{Quad}}(\bar{g}) = \frac{1}{2} \beta^T \left\{ I_Q \otimes (\tilde{G}^T \tilde{G}) \right\} \beta - \left\{ Y^T (I_Q \otimes \tilde{G}) \right\} \beta.$$

The standard expression of the cross-entropy loss ℓ_{CE} is:

$$\forall (x, y) \in \mathcal{X} \times \mathcal{Y}, \quad \ell_{\text{CE}}(t_y, \bar{g}(x)) = - \sum_{k=1}^Q \{ \delta_{y,k} \ln(\bar{g}_k(x)) + (1 - \delta_{y,k}) \ln(1 - \bar{g}_k(x)) \}.$$

This loss function can be used here since $U_Q \subset [0, 1]^Q$. We take benefit of the fact that the component functions sum to one to substitute to ℓ_{CE} a simplified expression, so that the objective function becomes

$$J_{\text{CE}}(\bar{g}) = - \sum_{i=1}^m \sum_{k=1}^Q \delta_{y_i,k} \ln \left(\frac{\beta_k^T \tilde{g}_k(x_i)}{\delta_{y_i,k}} \right).$$

It is well known that the combination of the one of Q coding of the desired outputs with these two loss functions leads to the selection of a function that generates estimates of the class posterior probabilities (see [9] for a proof).

3.2 Sample complexity of the linear ensemble methods

For $\beta \in V_{N,Q}$, let $g_\beta = (g_{\beta,k})_{1 \leq k \leq Q}$ be the function from U_Q^N to U_Q such that $g_\beta(u) = (\beta_k^T u)_{1 \leq k \leq Q}$. Let $\mathcal{G}_\beta = \{g_\beta : \beta \in V_{N,Q}\}$. We identify the capacity of the combiners with that of \mathcal{G}_β . In [4], we proved that for large margin multi-category classifiers, the appropriate generalizations of the Vapnik-Chervonenkis dimension are the γ - Ψ -dimensions. Their use involves the application of margin operators. Here, a suitable γ - Ψ -dimension is an extension of the Natarajan dimension and the operator needed is the Δ one.

Definition 3 (Δ operator). Let \mathcal{G} be a class of functions from \mathcal{X} to \mathbb{R}^Q .

$$\forall g \in \mathcal{G}, \forall x \in \mathcal{X}, \Delta g(x) = (\Delta g_k(x))_{1 \leq k \leq Q} = \frac{1}{2} \left(g_k(x) - \max_{l \neq k} g_l(x) \right)_{1 \leq k \leq Q}.$$

For the sake of simplicity, Δg_k is used in place of $(\Delta g)_k$. Let $\Delta \mathcal{G} = \{\Delta g : g \in \mathcal{G}\}$.

Definition 4 (Natarajan dimension with margin γ). Let \mathcal{G} be defined as above. For $\gamma \in \mathbb{R}_+^*$, $s_n = \{x_i : 1 \leq i \leq n\} \subset \mathcal{X}$ is said to be γ - N -shattered by $\Delta \mathcal{G}$ if there is a set $I(s_n) = \{(i_1(x_i), i_2(x_i)) : 1 \leq i \leq n\}$ of couples of integers satisfying $1 \leq i_1(x_i) < i_2(x_i) \leq Q$ and a vector $v_b = (b_i)$ in \mathbb{R}^n such that, for each vector $v_y = (y_i)$ in $\{-1, 1\}^n$, there is g_y in \mathcal{G} satisfying

$$\forall i \in \llbracket 1, n \rrbracket, \begin{cases} \text{if } y_i = 1, \Delta g_{y, i_1(x_i)}(x_i) - b_i \geq \gamma \\ \text{if } y_i = -1, \Delta g_{y, i_2(x_i)}(x_i) + b_i \geq \gamma \end{cases}.$$

The *Natarajan dimension with margin γ* of $\Delta \mathcal{G}$, $N\text{-dim}(\Delta \mathcal{G}, \gamma)$, is the maximal cardinality of a subset of \mathcal{X} γ - N -shattered by $\Delta \mathcal{G}$, if this maximum exists, and $+\infty$ otherwise.

An upper bound on $N\text{-dim}(\Delta \mathcal{G}_\beta, \gamma)$ is provided by Theorem 1.

Theorem 1.

$$\forall \gamma \in \mathbb{R}_+^*, N\text{-dim}(\Delta \mathcal{G}_\beta, \gamma) \leq \binom{Q}{2} \frac{NQ}{4\gamma^2}. \quad (1)$$

The proof of Theorem 1 is based on two lemmas.

Lemma 1. *Let $\gamma \in \mathbb{R}_+^*$ and $n \in \mathbb{N}^*$. If $s_n = \{u_i : 1 \leq i \leq n\} \subset U_Q^N$ is γ - N -shattered by $\Delta \mathcal{G}_\beta$, then there exists a subset s_p of s_n of cardinality $p = \left\lceil \frac{n}{\binom{Q}{2}} \right\rceil$ such that for every partition of s_p into two subsets $s_{p,1}$ and $s_{p,2}$,*

$$\left\| \sum_{u_i \in s_{p,1}} u_i - \sum_{u_i \in s_{p,2}} u_i \right\|_2 \geq \frac{2p}{\sqrt{Q}} \gamma. \quad (2)$$

Proof. Let $(I(s_n), v_b)$ witness the γ -N-shattering of s_n by $\Delta\mathcal{G}_\beta$. According to the pigeonhole principle, there is at least one couple of indices (k_1, k_2) such that there are at least p points in s_n for which $(i_1(u_i), i_2(u_i))$ is (k_1, k_2) . For the sake of simplicity, the points in s_n are reordered in such a way that the p first of them exhibit this property. The corresponding subset of s_n is denoted s_p . This means that for all vector $v_y = (y_i)$ in $\{-1, 1\}^n$, there is a function g_{β_y} in \mathcal{G}_β characterized by the vector $\beta_y = (\beta_{y,k})_{1 \leq k \leq Q} \in V_{N,Q}$ such that:

$$\forall i \in \llbracket 1, p \rrbracket, \begin{cases} \text{if } y_i = 1, \Delta g_{\beta_y, k_1}(u_i) - b_i \geq \gamma \\ \text{if } y_i = -1, \Delta g_{\beta_y, k_2}(u_i) + b_i \geq \gamma \end{cases}.$$

By definition of \mathcal{G}_β and the margin operator Δ , this implies:

$$\forall i \in \llbracket 1, p \rrbracket, \begin{cases} \text{if } y_i = 1, \frac{1}{2} \left(\beta_{y, k_1}^T u_i - \beta_{y, k_2}^T u_i \right) - b_i \geq \gamma \\ \text{if } y_i = -1, \frac{1}{2} \left(\beta_{y, k_2}^T u_i - \beta_{y, k_1}^T u_i \right) + b_i \geq \gamma \end{cases}. \quad (3)$$

Consider now any partition of s_p into two subsets $s_{p,1}$ and $s_{p,2}$. Consider any vector v_y in $\{-1, 1\}^n$ such that $y_i = 1$ if $u_i \in s_{p,1}$ and $y_i = -1$ if $u_i \in s_{p,2}$. It results from (3) that there exists g_{β_y} in \mathcal{G}_β such that:

$$\frac{1}{2} (\beta_{y, k_1} - \beta_{y, k_2})^T \left(\sum_{u_i \in s_{p,1}} u_i - \sum_{u_i \in s_{p,2}} u_i \right) - \sum_{u_i \in s_{p,1}} b_i + \sum_{u_i \in s_{p,2}} b_i \geq p\gamma.$$

Conversely, consider any vector v_y such that $y_i = -1$ if $u_i \in s_{p,1}$ and $y_i = 1$ if $u_i \in s_{p,2}$. There exists g_{β_y} in \mathcal{G}_β such that:

$$\frac{1}{2} (\beta_{y, k_2} - \beta_{y, k_1})^T \left(\sum_{u_i \in s_{p,1}} u_i - \sum_{u_i \in s_{p,2}} u_i \right) + \sum_{u_i \in s_{p,1}} b_i - \sum_{u_i \in s_{p,2}} b_i \geq p\gamma.$$

Thus, whatever the sign of $\sum_{u_i \in s_{p,1}} b_i - \sum_{u_i \in s_{p,2}} b_i$ is, by application of the Cauchy-Schwarz inequality, there is a vector β_y in $V_{N,Q}$ such that:

$$\frac{1}{2} \|\beta_{y, k_1} - \beta_{y, k_2}\|_2 \left\| \sum_{u_i \in s_{p,1}} u_i - \sum_{u_i \in s_{p,2}} u_i \right\|_2 \geq p\gamma. \quad (4)$$

For $\beta \in V_{N,Q}$, $\max_{1 \leq k \neq l \leq Q} \|\beta_k - \beta_l\|_2$ is reached when one of the vectors is the null vector and the other one concentrates all the mass on as few components as possible. A situation of this kind is obtained by choosing any couple (k_0, j_0) in $\llbracket 1, Q \rrbracket \times \llbracket 1, N \rrbracket$ and defining the vector β as follows

$$\forall k \in \llbracket 1, Q \rrbracket, \forall j \in \llbracket 1, N \rrbracket, \forall l \in \llbracket 1, Q \rrbracket, \beta_{kjl} = \delta_{k_0, k} \delta_{j_0, j}.$$

In that case, for all k in $\llbracket 1, Q \rrbracket \setminus \{k_0\}$, $\|\beta_{k_0} - \beta_k\|_2 = \sqrt{Q}$. Thus, $\|\beta_{y, k_1} - \beta_{y, k_2}\|_2 \leq \sqrt{Q}$, and a substitution in (4) concludes the proof.

Lemma 2. For all $n \in \mathbb{N}^*$, all subset $s_n = \{u_i : 1 \leq i \leq n\}$ of U_Q^N can be partitioned into two subsets s_1 and s_2 satisfying

$$\left\| \sum_{u_i \in s_1} u_i - \sum_{u_i \in s_2} u_i \right\|_2 \leq \sqrt{Nn}. \quad (5)$$

Proof. Let $\sigma = (\sigma_i)_{1 \leq i \leq n}$ be a Rademacher sequence: the σ_i are i.i.d. Bernoulli random variables with parameter $p = \frac{1}{2}$. $\forall (i, j) \in \llbracket 1, n \rrbracket^2$, $\mathbb{E}_\sigma [\sigma_i \sigma_j] = \delta_{i,j}$.

$$\mathbb{E}_\sigma \left\| \sum_{i=1}^n \sigma_i u_i \right\|_2^2 = \sum_{i=1}^n \sum_{j=1}^n u_i^T u_j \mathbb{E}_\sigma [\sigma_i \sigma_j] = \sum_{i=1}^n \|u_i\|_2^2 \leq n \max_{u \in U_Q^N} \|u\|_2^2.$$

The points of U_Q^N whose ℓ_2 -norm is maximum are its vertices. The value of their ℓ_2 -norm is \sqrt{N} . Thus, $\mathbb{E}_\sigma \left\| \sum_{i=1}^n \sigma_i u_i \right\|_2^2 \leq Nn$. This implies that there exists a vector $v = (v_i)_{1 \leq i \leq n} \in \{-1, 1\}^n$ such that $\left\| \sum_{i=1}^n v_i u_i \right\|_2 \leq \sqrt{Nn}$. Setting $s_1 = \{u_i \in s_n : v_i = 1\}$ and $s_2 = s_n \setminus s_1$ then concludes the proof.

With Lemmas 1 and 2 at hand, the proof of Theorem 1 is straightforward.

Proof. Let $s_n = \{u_i : 1 \leq i \leq n\}$ be a subset of U_Q^N γ -N-shattered by $\Delta \mathcal{G}_\beta$. According to Lemma 1, there is at least a subset s_p of s_n of cardinality

$$p = \left\lceil \frac{n}{\binom{Q}{2}} \right\rceil$$

satisfying (2) for all its partitions into two subsets $s_{p,1}$ and $s_{p,2}$. Since, according to Lemma 2, there is at least one of these partitions for which (5) holds true, $\frac{2p}{\sqrt{Q}}\gamma \leq \sqrt{Np}$, which implies (1) since $n \leq \binom{Q}{2}p$.

4 Experimental results

The problem considered is protein secondary structure prediction. It consists in assigning to each residue of a protein sequence its conformational state: α -helix, β -strand or coil ($Q = 3$). The four main M-SVMs and the two combiners resulting from using the quadratic and cross-entropy losses are assessed on the P1096 data set [5]. The experimental protocol differs from the one used in [5] in two respects. The outputs of the M-SVMs are normalized:

$$\forall j \in \llbracket 1, 4 \rrbracket, \forall k \in \llbracket 1, 3 \rrbracket, g_k^{(j)}(\cdot) = \frac{\exp\left(h_k^{(j)}(\cdot)\right)}{\sum_{l=1}^3 \exp\left(h_l^{(j)}(\cdot)\right)}$$

and an additional level of cross-validation is introduced so as to train the M-SVMs and the combiners on different data. Table 2 summarizes the results obtained. Prediction accuracy is described by means of three standard measures giving complementary indications: the recognition rate Q_3 , Matthews' correlation coefficients $C_{\alpha/\beta/\text{coil}}$, and the segment overlap measure Sov.

The comparison of the performance of the M-SVMs considered individually and in the framework of a combination shows a gain induced by the combination which is statistically significant with confidence at least 0.95.

	WW	CS	LLW	M-SVM ²	Combiner Quad	Combiner CE
Q_3	66.9	66.5	66.7	66.7	67.7	67.6
C_α	0.52	0.50	0.51	0.51	0.54	0.54
C_β	0.42	0.40	0.40	0.42	0.44	0.43
C_{coil}	0.46	0.44	0.46	0.44	0.47	0.48
Sov	56.0	55.7	56.2	56.0	58.1	57.9

Table 2. Relative prediction accuracy of the M-SVMs and the linear combiners on the 1096 sequences (268575 residues) of the P1096 data set

5 Conclusions and ongoing research

We have introduced linear combiners for M-SVMs. Their low sample complexity should prevent them from overfitting and they provide estimates of the class posterior probabilities. We are currently performing a large scale study of their performance, focusing on the quality of these estimates, used to derive emission probabilities in a hidden Markov model.

References

1. A. Berline and C. Thomas-Agnan. *Reproducing Kernel Hilbert Spaces in Probability and Statistics*. Kluwer Academic Publishers, Boston, 2004.
2. B.E. Boser, I.M. Guyon, and V.N. Vapnik. A training algorithm for optimal margin classifiers. In *COLT'92*, pages 144–152, 1992.
3. K. Crammer and Y. Singer. On the algorithmic implementation of multiclass kernel-based vector machines. *Journal of Machine Learning Research*, 2:265–292, 2001.
4. Y. Guermeur. Sample complexity of classifiers taking values in \mathbb{R}^Q , application to multi-class SVMs. *Communications in Statistics*, 39(3):543–557, 2010.
5. Y. Guermeur, A. Lifchitz, and R. Vert. A kernel for protein secondary structure prediction. In B. Schölkopf, K. Tsuda, and J.-P. Vert, editors, *Kernel Methods in Computational Biology*, chapter 9, pages 193–206. The MIT Press, 2004.
6. Y. Guermeur and E. Monfrini. A quadratic loss multi-class SVM for which a radius-margin bound applies. *Informatica*. (conditionally accepted).
7. C.-W. Hsu and C.-J. Lin. A comparison of methods for multi-class support vector machines. *IEEE Transactions on Neural Networks*, 13(2):415–425, 2002.
8. Y. Lee, Y. Lin, and G. Wahba. Multicategory support vector machines: Theory and application to the classification of microarray data and satellite radiance data. *Journal of the American Statistical Association*, 99(465):67–81, 2004.
9. M.D. Richard and R.P. Lippmann. Neural network classifiers estimate Bayesian *a posteriori* probabilities. *Neural Computation*, 3(4):461–483, 1991.
10. B. Schölkopf, C. Burges, and V. Vapnik. Extracting support data for a given task. In *KDD'95*, pages 252–257, 1995.
11. J. Weston and C. Watkins. Multi-class support vector machines. Technical Report CSD-TR-98-04, Royal Holloway, University of London, Department of Computer Science, 1998.

Analysis of the salary trajectories in Luxembourg : a finite mixture model approach

Jean-Daniel Guigou¹, Bruno Lovat², Jang Schiltz¹

¹ Luxembourg School of Finance
University of Luxembourg, Luxembourg
(e-mail: jang.schiltz@uni.lu)

² Université de Nancy II
Nancy, France
(e-mail: bruno.lovat@univ-nancy2.fr)

Abstract. We analyse the salaries of about 700.000 employees who worked in Luxembourg between 1940 and 2006 with the aim of detecting groups of typical salary trajectories with respect to some covariants like sex, workstatus, residentship and nationality. We use the proc traj SAS procedure from Bobby L. Jones to classify the workers and descriptive statistical methods like the CHAID procedure or multinomial logistic regression to get a characterisation with respect to the covariants of the different groups.

Keywords: Finite mixture models, Salary trajectories, CHAID, Multinomial logistic regression, Proc-Traj procedure, Economic modeling.

1 Introduction

Knowing the salary structure in a country is of great importance for a host of economic applications, for instance for an analysis of its pension system. We highlight the evolution of salaries in Luxembourg. To this end, we use the recent statistical group based trajectory model of D. Nagin [8]. We estimate model parameters from a single database, provided by the general social security inspection office (IGSS) and containing annual salaries of all wage earners in the Luxembourg private sector. As a result we divide up the population into nine groups, each with its own mean salary trajectory in time and its relative weight in society.

In a second part of the paper we give a socioeconomic description of the nine groups and address the question of the prediction of group membership for a given individual. These kind of results are of great interest for insurance companies and banks who like to know the evolution of the career of their customers to be better able to advise them on the possibilities of money investments in a pension fund for instance.

2 A statistical method based on clustering

Longitudinal data are the empirical basis of research on various subjects in the social sciences and in medicine. The common statistical aim of these various application fields is the modelisation of the evolution of an age or time based phenomenon. In the 1990s, the generalized mixed model assuming a normal distribution of unobserved heterogeneity [1] (Bryk and Raudenbush 1992), latent growth curves modeling (Muthén 1989 [7]) and the nonparametric mixture model, based on a discrete distribution of heterogeneity (Jones, Nagin and Roeder 2001 [5]) have emerged. We choose this variation of the generalized mixed model because of the growing interest in this approach to answer questions about atypical subpopulations (see Eggleston, Laub and Sampson 2004 [3]).

The SAS procedure Proc Traj, programmed by Daniel Nagin and Bobby Jones [5], allows to estimate the parameters of a semiparametric mixture model for longitudinal data that are either normal (censored) distributed or follow a Poisson or Bernoulli distribution. The subgroup trajectories can be modeled by polynomials up to the fourth degree. The procedure enables to calculate the posterior probability of group membership in terms of risk factors that are stable in time. Moreover, time-dependent covariates can influence the trajectories and cause different effects in different subgroups.

Nagin's nonparametric mixed model [8] starts from a set of individual trajectories and tries to divide the population into a number of homogeneous sub-populations and to estimate a mean trajectory for each of these sub-populations.

Consider a statistical variable Y defined on a population of size N . Let $Y_i = y_{i1}, y_{i2}, \dots, y_{iT}$ denote a longitudinal sequence of measurements on individual i over T periods.

Let $P(Y_i)$ denote the probability of Y_i . The purpose of the analysis is to find r trajectories of a given type, in general polynomials of degree 4, $P(t) = \beta_0 + \beta_1 t + \beta_2 t^2 + \beta_3 t^3 + \beta_4 t^4$. Let $P^j(Y_i)$ denote the probability of obtaining the observed data for individual i given membership in group j and π_j the probability of an individual chosen at random to belong to the group number j .

We try to estimate a set of parameters $\Omega = \{\beta_0^j, \beta_1^j, \beta_2^j, \beta_3^j, \beta_4^j, \pi_j; j = 1, \dots, r\}$ which maximises the probability of Y_i . The ideal number of groups r is also an outcome of the analysis. For a given group, conditional independence is assumed for the sequential realisations of the elements of Y_i, y_{it} , over the T periods of measurement. The likelihood L of the sample is then given by

$$L = \frac{1}{\sigma} \prod_{i=1}^N \sum_{j=1}^r \pi_j \prod_{t=1}^T \phi \left(\frac{y_{it} - \beta^j x_{it}}{\sigma} \right),$$

where ϕ denotes the density function of the standard normal distribution. These equations are too complicated to hope to obtain an algebraic solution.

Bobby L. Jones (Carnegie Mellon University) has programmed a SAS procedure based on a quasi-Newtonian maximum search method (Dennis, Gay & Welsch 1981[2]). The estimated standard deviations are obtained by inverting the observed information matrix.

Nagin's model also allows to determine to which group a given individual belongs. The posterior probability $P(j/Y_i)$ for an individual i to belong to group number j is indeed given by the Bayes theorem:

$$P(j/Y_i) = \frac{P(Y_i/j)\hat{\pi}_j}{\sum_{j=1}^r P(Y_i/j)\hat{\pi}_j}$$

A large posterior probability estimate for a small group requires that Y_i be so strongly consistent with the small group that $P(Y_i/j)$ for that group is very large in comparison to its companion probabilities for the big groups (Nagin 2005).

3 The IGSS database

The analysis relies on a file containing the salaries of all employees of the private sector in Luxembourg. The data cover the period from 1940 to 2006. Since the file contains the careers of those started to work from the beginning of the forties onwards, it is not complete during the first years, but becomes so gradually. In particular it includes all the employees of the private sector in Luxembourg from the beginning of the seventies till 2006.

This file originates from the General Inspectorate of Social Security (IGSS). The main variables are the net annual taxable salary, measured in constant euros (2006 euros), sex, age at first employment, residence and nationality (Luxembourg national living in Luxembourg, foreigner living in Luxembourg and commuters) and the type of employment contract (blue or white collar worker). Initially, the file consisted of about 7 000 000 lines showing the salaries of some 718 054 workers. Many careers are incomplete for many reasons. Moreover, for immigrant workers, we know only the part of their careers made in Luxembourg and know nothing about what they have done in their country of origin. Finally, the percentage of employees who quit prematurely with a disability pension or take pre-retirement or quit early for family reasons (women stopping work or interrupting their work to look after their children for example) is around 50 per cent. The domestic employment (which includes the commuters working in Luxembourg) has experienced strong growth since the mid-eighties, with an average increase of 3.5% annually and an increase of more than 110 000 jobs between 1986 and 2001 (compared to 20 000 jobs in the period 1975-1985) (Source: STATEC). The development of the financial and the growing needs of the public sector are key drivers of this evolution. Today, the services sector represents more than three-quarters of total employment. These changes are not without consequences in terms of professional status, so that changes in careers before

the 80s are necessarily significantly different from those of twenty-five years. We have therefore decided to pay interest careers of individuals who began working in Luxembourg between 1982 and 1986 and who have worked for at least 20 years. The final file used for our analysis includes data from 22 203 employees and private workers. Note that in Luxembourg, the maximum contribution ceiling on pension insurance is 5 times the minimum wage, or 7 577 (Euro 2006) per month. Wages in our data are also limited by that number.

4 The mean salary trajectories in Luxembourg

We used the SAS procedure Proc Traj, programmed by Daniel Nagin and Bobby Jones, to determine the mean salary trajectories of 22 203 people who began working between 1982 and 1987 in the private sector in Luxembourg and who worked for at least twenty years.

We established the trajectories for models with between 4 and 20 groups. As the salary trajectories form more or less a continuum in the continuous functions from [1000, 4000] with values in the interval [1200, 7577], the BIC adjustment criterion for determining the ideal number of groups is not well suited. Indeed, BIC increases with the number of groups. This is quite normal, since it just shows that if one assumes more groups, one can necessarily represent reality with more details. On the other hand, one creates smaller groups and an explanatory model more complicated to use. After discussion with the IGSS, we decided to retain a 9 groups solution, for it gives a good representation of the career development in Luxembourg. Solutions with more groups add essentially parallel paths to those present in our model.

To test the stability of trajectories in time, we also established the trajectories for the first 15 years of the careers (careers starting between 1985 and 1992) and for full career of 40 years (careers starting between 1960 and 1967). The trajectories of the first 15 years are very close to the first 15 years of trajectories of 20-year careers. The sizes of the groups vary between 2 and 6% compared to the ones we found and the changes are due to gains or losses to groups with similar salaries. Since moreover the macroeconomic situation has not changed dramatically during the last twenty years, we are fairly confident that the trajectories remain valid, except in cases of severe economic shock that could certainly change the situation completely. The only thing that might change over the coming years is the percentage of commuters in the different groups. Since the total number of employees increased faster than the population can do this percentage will continue to grow in all groups. The trajectories of the complete careers are also quite similar to ours, except that they show a clear decline of the wages during the steel crisis for the trajectories representing the high wages.

Figure 1 below shows the average salary trajectories in our 9 groups.

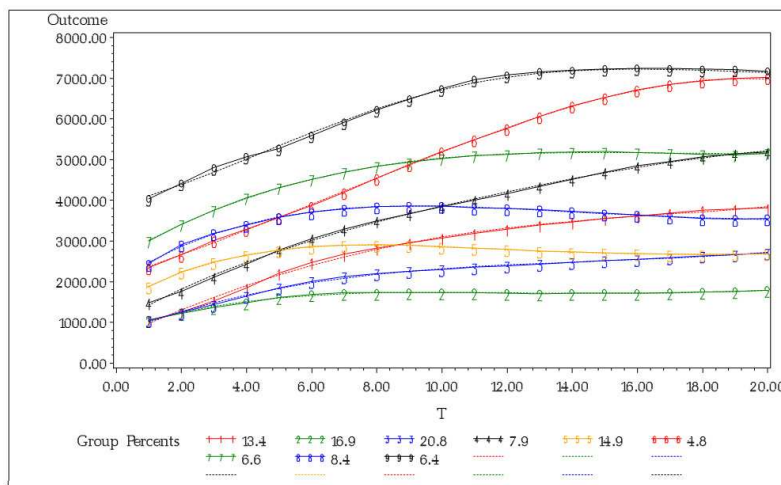


Fig. 1. Salary trajectories of the 9 groups

5 Partition of the labour force

We have investigated the nine groups obtained here above by means of numerous data analysis techniques in order to get a description of each of them. The details of the undertaken tasks can be found in [4]. Summerising our results, we can conclude that the different group trajectories are differentiated mainly by two factors: the starting salary, strongly related to the age at first employment (and therefore to the academic degree) of the employee and the dynamics of his career. There are actually three different types of dynamics: Groups 2, 5 and 8 show “flat” careers, meaning that people from these groups have almost no increase in their salary after the first five years of their career; groups 3 and 7 show a “normal” salary increase of about one per cent per year and groups 1, 4 and 6 show “dynamic” careers, in which wages increase much over time. The ninth group of trajectories is somewhat apart, since it contains the high salaries that exceed the ceiling of 7 577 contained in our data set. Taking this limitations into account, their path resembles that of the normal dynamics. Another interesting discovery is that in most of the groups workers of Luxembourg nationality have, on average, a more dynamic career than foreign workers and commuters. A difference between men and women can also be shown, but only in the groups with lower salaries. Due to lack of information, it is unfortunately impossible to give a more detailed socioeconomic descriptions of the nine groups. We hope to get more variables about the population in our dataset in the future to be able to obtain a better characterisation of the nine groups.

6 Group membership predictions

Bayes' formula allows to compute the probability of individual i to belong to group number j . It gives the possibility to classify correctly almost all persons, without any ambiguity about group membership. In analysing our full sample, we find indeed an average probability of belonging to one of the groups varying between 92.41 % (group 3) and 99.23 % (group 9). The median probability varies even between 99.12 % (group 3) and 100 % (groups 6 and 9). The practical disadvantage of the Bayes' formula is that we need the salaries of the first twenty years of the career. Hence, it is just useful for people who have already completed more than half of it. Analysing the distribution of salaries in the different groups, we find that in many groups the first three to five years show a relatively high dispersion usually paired with a bi- or even trimodal distribution. After the first years however the salary distribution becomes a normal law with a fairly low dispersion. Figure 2 shows the distribution of the salaries in the first twenty years of their career for the people belonging to group 1. It should hence be possible to correctly

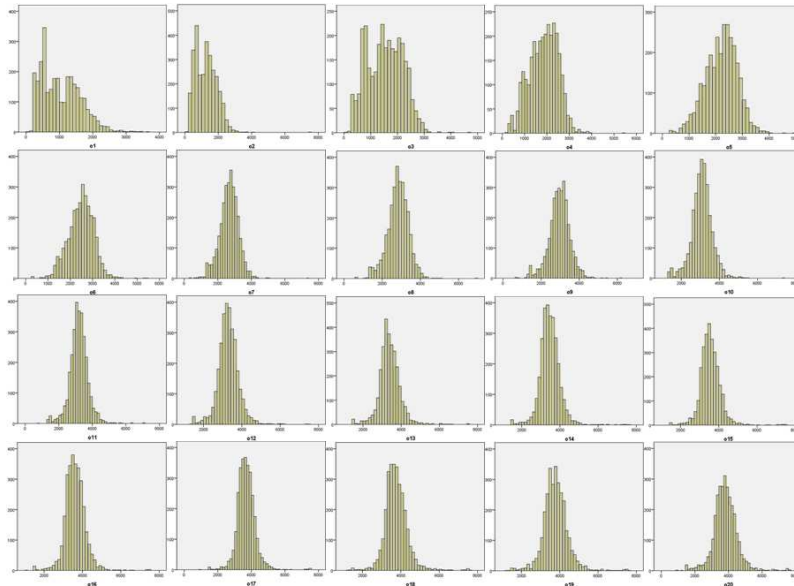


Fig. 2. Salary evolution during the 20 first year of the career for group 1

predict the group membership if we know the salaries of the first years of the career plus some socioeconomic information. That's what we will try in the sequel.

We tried to predict membership of a given person to one of the nine groups by means two statistical classification methods, the CHAID algorithm (Chi-

squared Automatic Interaction Detector) and multinomial logistic regression. The CHAID algorithm is a technique of decision tree type, published in 1980 by Gordon V. Kass citeKass. It can be used to detect interactions between variables or for prediction purposes. Its a mainly visual and easily interpretable method.

Trying to predict group membership of the entire sample using only the variable “sex”, “status”, “nationality and residence” and “age at first job in Luxembourg” gives a very bad result. Only 38.3 % of the individuals are correctly classified. The only group that is correctly predicted is group 9 (72.1 %). Moreover, we observe that classification faults are done to the benefit of nearly all groups.

If we consider the socioeconomic variables and the first 6 years of salary, the CHAID algorithm can correctly classify 54 % of the individuals. Groups 2 (63.3 %), 3 (63.9 %), 5 (59.5 %) and 7 (57.6 %) are fairly well predicted, the allocation to the group 9 starts to be good (89.3 %). The second method we

Classification										
Observed	Predicted									Percent Correct
	1	2	3	4	5	6	7	8	9	
1	1056	228	996	240	458	3	0	2	0	35,4%
2	94	2366	1164	22	90	3	0	1	0	63,3%
3	407	978	2954	37	246	1	0	0	0	63,9%
4	356	90	95	860	186	2	31	122	2	49,3%
5	351	26	184	437	1957	3	83	236	14	59,5%
6	27	93	12	184	17	21	432	192	77	2,0%
7	1	0	0	72	1	8	839	164	371	57,6%
8	22	12	0	487	205	12	367	657	104	35,2%
9	0	3	0	2	2	8	131	5	1256	89,3%
Overall Percentage	10,4%	17,1%	24,4%	10,6%	14,3%	,3%	8,5%	6,2%	8,2%	54,0%

Growing Method: CHAID
 Dependent Variable: group

Fig. 3. Results of the CHAID procedure with 6 years of salary

used for classification is the multinomial logistic regression. The results are quite similar to those discussed above. Trying to predict group membership of the entire sample using only the variable “sex”, “status”, “nationality and residence” and “age at first job in Luxembourg” gives a very bad result. Only 35.0 % of people are correctly classified and group 9 is the only correctly predicted group (61.8 %). The pseudo R-square of Cox and Snell, which gives the percentage of the total variability explained by the model is 0.563.

If we consider the socioeconomic variables and the first 6 years of salary, the multinomial logistic regression correctly classifies 53.9% of individuals and the pseudo R-square of Cox and Snell is 0.851, which is a fairly good result. Groups 2 (61.1%), 3 (59.7%), 5 (68.9%) are fairly well predicted, the allocation to the group 9 begins to be good (85.9%).

Classification										
Observed	Predicted									Percent Correct
	1	2	3	4	5	6	7	8	9	
1	1124	185	925	345	397	4	0	3	0	37,7%
2	132	2285	1204	24	91	0	0	4	0	61,1%
3	622	998	2761	30	212	0	0	0	0	59,7%
4	333	43	111	651	334	159	2	111	1	37,3%
5	233	20	162	324	2268	45	35	194	10	68,9%
6	14	19	71	134	57	275	322	126	37	26,1%
7	1	0	0	14	15	189	698	306	233	47,9%
8	3	1	3	142	600	169	224	676	48	36,2%
9	0	0	0	0	4	8	181	5	1209	85,9%
Overall Percentage	11,1%	16,0%	23,6%	7,5%	17,9%	3,8%	6,6%	6,4%	6,9%	53,9%

Fig. 4. Results of the multinomial logistic regression with 6 years of salary

7 Conclusion

We have established a classification of the careers in the private sector in Luxembourg into nine groups by means of Nagin's semiparametric mixture model and given a socioeconomic description of the groups. He have seen that the problem of the correct classification of a person in one of nine groups of salary trajectories is a rather complex problem. Considering only the socioeconomic variables, the results are very bad. Add a few years of salary greatly improves the situation and can give a correct result. For the future we try to get some additional socioeconomic variables and to program a classification software that will achieve a good result by combining these variables with the first years of salary.

References

1. Bryk, A.S., *Hierarchical linear models*, Sage, Newbury Park, CA (1992).
2. Dennis, J.E., Gay, D.M., and Welsch R.E., "An Adaptive Nonlinear Least-Squares Algorithm", *ACM Transactions on Mathematical Software* 7,348-383 (1981).
3. Eggleston, E.P., Laub, J.H., and Sampson, R.J., "On the Robustness and Validity of Groups", *Journal of Quantitative Criminology* 20-1, 37-42 (2004).
4. Guigou, J.D., Lovat, B., and Schiltz, J., *Les retraites au Luxembourg: modélisation et évaluation d'un système diversifié avec répartition et capitalisation*, Technical report, 112 pages (2010).
5. Jones, B.L., Nagin, D.S., and Roder, K., "A SAS procedure based on mixture models for estimating developmental trajectories", *Sociological Methods and Research* 29, 374-393 (2001).
6. Kass, G.V., "An Exploratory Technique for Investigating Large Quantities of Categorical Data", *Journal of Applied Statistics* 29-2, 119-127 (1980).
7. Muthén, B.O., "Latent Variable Modeling in Heterogeneous Populations", *Psychometrika* 54-4, 557-585 (1989).
8. Nagin, D.S., *Group-Based Modeling od Development*, Harvard University Press, Cambridge, Massachusetts (2005).

Aesthetic Considerations in Algorithmic and Generative Composition

Dr Kerry L. Hagan

Digital Media and Arts Research Centre (DMARC), University of Limerick,
Limerick, Ireland
Email: kerry.hagan@ul.ie

Abstract: Models of chance operations, random equations, stochastic processes, and chaos systems have inspired composers as historical as Wolfgang Amadeus Mozart. As these models advance and new processes are discovered or defined, composers continue to find new inspirations for musical composition. Yet, the relative artistic merits of some of these works are limited. This paper explores the application of extra-musical processes to the sonic arts and proposes aesthetic considerations from the point of view of the artist. The scope of the discussion is limited primarily to music composition based on mathematical models. Musical examples demonstrate possibilities for working successfully with algorithmic and generative processes in sound, from formal decisions to synthesis.

Keywords: Algorithmic and generative composition, aesthetics, random and stochastic processes, chaos systems, sound synthesis

1. Introduction

In many ways, the Western classical music tradition is steeped in numerical methods. Numbers define musical intervals, which then form systems in the earliest examples of Western counterpoint. Numerical systems identify chords and harmonies within the Western tonal (as opposed to contrapuntal) system, as well. Classically trained musicians continue to learn these systems and to express the music theory of Western classical systems in these methods.

Although there are the odd examples of musical numerical games emerging from history (e.g., Mozart's "Musical Games"), numerical systems came to the fore in the 20th century with the serializing of musical attributes such as pitch, duration, and timbre. The Second Viennese School freed music from the Western system of dissonance, consonance, and tonal center, allowing set operations to determine musical content through numeric representations of the twelve equal-tempered pitches in Western music.

Once the numbers of music were freed from the harmonic system, composers could look beyond the simple set operations of the Second Viennese

Hagan, K. L.

School into other sources of numerical patterns, systems, rules, and models. With the advent of computers and ultimately computer music, it seems hardly surprising that composition with any kind of numerical system would become more commonplace. And, once audio itself was digitized, the numbers representing music - sound itself, in fact - expanded beyond the restrictions of Western music notation of pitch and duration.

Despite this, the application of extra-musical models and systems to the numbers of sound and music is relatively new to music-making. As a result, composers are still exploring the true potential of using scientific or mathematical models to provide numbers to translate to music. The results can be surprising and occasionally dissatisfying. This paper seeks to address some arenas where pieces can fail to achieve the promise suggested by scientific or mathematical inspirations. Thus, this paper is a qualitative study of musical practices with extra-musical numbers.

In order to make useful formalizations of musical practice through qualitative assessment, the domain of practice must be defined and limited to a particular mode of artistic work. Specifically, this paper deals with what many composers call algorithmic music or generative music. Furthermore, the music addressed is intended to be experienced as music is experienced in the Western classical tradition, not as a scientific display or as a functional part of another entity. In most cases, this requires music to be experienced in the concert hall paradigm. Finally, there are many numerical systems, patterns, and models that can create the data needed for translation to musical ideas. This paper deals specifically with music drawing on algorithms or processes borrowed from mathematics and science. So, firstly, this paper defines the music by the historical context, intended reception, audience, and compositional methods.

Secondly, to draw conclusions of the effectiveness of a musical strategy pre-supposes a system of judgment, a basis on which music is to be compared. It is unethical to apply all systems of judgment to all systems of music. Therefore, this paper then defines the means by which a work is judged to be successful and, more importantly, how the musical experience is then critiqued.

Based on the constraints of compositional domain, the categories of human/model/computer interaction, and a critical system of comparisons, this paper then proposes some crucial questions and considerations a composer can make when creating algorithmic or generative music. Ultimately, this paper offers some conclusions regarding successful practice. However, it does not do so to set requirements or rules for good music, only to identify similarities between successful examples of algorithmic and generative composition.

2. What is Algorithmic and Generative Composition?

Perhaps the trickiest navigation on which this paper is based is the definition of the domain it is examining. Musicians are not scientists, and the vocabulary they use shifts and crosses meanings and often implies methods of practice that may seem entirely independent of the name given. Therefore, it is not enough to simply say this paper addresses algorithmic and generative composition.

Here the phrase “algorithmic and generative composition” includes many labels practitioners use to be more specific about their musical approach. For the most part, this music requires the use of computers for its generation; though, technically, there are early examples of these compositions that were calculated by hand or on very primitive machines. This phrase is also used to include the sub-domains of computer synthesis and computer-assisted composition. However, one may prefer to reserve the word algorithmic for certain types of compositional process, where the word algorithm is more precisely defined by the field of computer science. For this reason, generative composition is also included in order to accommodate a means of creating music with processes that may not fall within the more carefully circumscribed definition of algorithm.

2.1. Auditory Display vs. Musical Work

There is currently a multi-disciplinary practice arising from the field of data visualization, where sonic specialists and scientists work together to enhance graphical data visualization with the multi-modality and sensory advantages of hearing. The International Community for Auditory Display, or ICAD, is focused on bringing the advantages of a listening environment to the visual representations of large or complex data sets.

Though some of the auditory displays result in surprising or even somewhat pleasant sounds, the primary purpose of these examples is functional and even scientific. There is little room (in fact, it would be detrimental) for the specialists to alter outcomes for aesthetic purposes. Furthermore, the issues and concerns of these examples address scientific or mathematical problems, not the dilemmas faced by the contemporary musical artist working from the Western history of art- and music-making.

2.2. Sound Art vs. Composition

Finally, there are arenas of music-making that extend from other domains of artistic expression, including the visual arts and theatre. Although algorithmic and generative techniques have been applied in these circumstances, it is important to specify that this paper deals with the most normative and traditional definition of composition.

Unlike works where the artistic aims are beyond the sound alone (e.g., visual support, theatrical/narrative goals, political art, socio-historical

Hagan, K. L.

commentary), composers of these works intend them to be experienced and attended to in the concert hall paradigm. That is not to say that conclusions or discussions offered here cannot apply to these domains. Simply: to come to some conclusions, it is necessary to exclude the exceptions, however interesting, at the start.

The concert hall paradigm assumes the context of the Western classical tradition musical performance, and any experimentation within that paradigm relates to the presuppositions of the tradition. The paradigm expects a degree of scrutiny and attendance to sonic detail. It assumes that a work has a consistent identity, even if unique performances of that work may differ. A work within the concert hall paradigm will have a fixed duration, and the audience is expected to attend to the piece in its entirety without distraction.

Works that occur in gallery spaces, for example, that are continuous and ongoing and expect the audience to wander through at unexpected and uncontrollable intervals do not fall into this category of composition. Other works that function as background material, either to visual media, theatre performance, a narrative, or even a commercial environment, do not exist within the concert hall paradigm.

To summarize: this paper addresses algorithmic and generative music, which includes any systems from the strictly algorithmic to more open-ended generative processes. More importantly, it presupposes an artistic or aesthetic endeavor and not simply the act of demonstrating data for informational purposes. Finally, it is meant to be experienced within the concert hall paradigm, which relies on a general type of audience within certain traditional conventions including concerts and/or sound recordings associated with Western classical music performance.

Some of the composers who have works falling into these categories include Lejaren Hiller, Iannis Xenakis, Brian Ferneyhough, David Cope, Eduardo Reck Miranda, Julio d'Escrivan, and Hans Tutschku.

2.3. Exception to a common (mis)understanding

There is an unspoken understanding among some composers that “algorithmic composition” results in a specific style of music within the field of computer music. Perhaps this exists because some composers engaging in “automatic composition” have used the phrase “algorithmic composition” synonymously. The result of some pieces, though called music, approaches scientific auditory display and often does not withstand musical scrutiny. Many composers who may rely on mathematical or numerical systems will deny their inclusion in the field of algorithmic and generative music on this basis alone. The use of the phrase in this paper supposes, perhaps naïvely, that this connotative definition can be overlooked for the greater issue at hand. Even the author puts aside her usual

reservations and is including her own work as algorithmic composition in this case.

3. What is “successful”?

Given that the domain represented in this discussion is algorithmic and generative composition within the concert hall paradigm, then the metric for the relative success or failure of a work can be determined by the genre itself. There are works throughout history whose success is measured by endurance, impact, innovation, or similar features. These works are accepted as part of a canon in a tradition, perhaps what Goehr [4] would call a musical museum, despite any individual’s personal preference for these works.

This paper will review some of these canonic works and some newer examples that, nonetheless, offer examples of musical success to some degree. The newer works were chosen by positive answers to:

- Does the work stand on its own without recourse to scientific or extra-musical explanation?
- Does the work withstand intense and attentive musical scrutiny?

Additionally, this paper will comment on the published methodologies of composers self-identified as algorithmic composers.

In the following examples, there appears to be three main aspects that determine the relative success of an algorithmic composition. Firstly, there is a correlation between successful works and the degree to which the composer intervenes, influences, adds to, or shapes the composition. Alternately, successful works can also be the result of human performer intervention, e.g., algorithmic compositions performed on acoustic instruments by experienced performers.

Secondly, works that tend to stand without the aid of explanation or background have complex mapping paradigms of the data to musical parameters. Again, there is a correspondence between the success of a work and the obfuscation of the underlying process.

The third characteristic of a successful work is whether or not care has been taken in orchestration or design of timbre. At the same time, timbral considerations are intricately linked to decisions made by the composer in instrumentation and mapping. For this reason, timbre may not be considered as a third aspect. However, its immediate effect on the reception of the work makes it necessary to address it separately.

Hagan, K. L.

3.1. *Human Intervention*

Perhaps the most telling evidence of the need for human intervention comes from the evident bias against the term algorithmic composition since it can mean automatic composition (without human intervention), as mentioned earlier. Many composers who may rely on mathematical or numerical systems will deny their inclusion in the field of algorithmic and generative music on this basis alone.

History tends to support this bias in musical examples. A very compelling example comes from a work that is often regarded to be musically weak but is nonetheless historically important. Namely, *Analogique A + B* (1959) by Iannis Xenakis demonstrates very clearly that composer intervention and further human performance and interpretation result in more successful outcomes. In two parts, *Analogique A* and *Analogique B*, Xenakis implements the same Markov process in different media. One utilizes short, electronic sine tones arranged and recorded on tape. The other is translated into quantized notes according to Western music notation and scored for strings. Although the process is the same, the electronic version allows Xenakis greater freedom in both pitch and duration, since sounds could be arbitrarily generated. However, it is the string version that was more successful as a musical work.

In many cases, limiting material to a musical scale can reduce the complexity and interest of a governing algorithm. Yet, paradoxically, the acoustic version (*Analogique A*) is a stronger work. The first impression may be that the more familiar and acoustic timbre of the strings makes the version more successful. Yet, taken on its own, *Analogique B* does provide a rich timbral experience, as Xenakis' method of composition is a precursor to the common practice of granular synthesis today. Rather, the effect that human performance, hence human intervention, of the given musical material is far more salient than the sound source.

In a musicological investigation, a fully automated version of *Analogique B* was created using current software that was unavailable to Xenakis. The experiment attempted to show that newer technologies facilitate the philosophies and aesthetics of Xenakis [6]. The result of the program was surprising; rather than demonstrating the benefit of technology, it revealed that Xenakis made subjective decisions while piecing together the electronic sounds. So, as *Analogique A* was stronger than *Analogique B* as a result of the human interpretation in performance, the original *Analogique B* was stronger than the computer-generated version because all vestiges of human intervention were removed in the latter.

There is strong precedent for composer intervention (or interference, depending on the point of view) within algorithmic composition. Composers such as Di Scipio [3], Ariza [1], Gogins [5], and Xenakis [8] refer to integrating their feedback into systems, trial and error methods of fine-tuning systems, or

Aesthetic Considerations in Algorithmic and Generative Composition

“bending” by the composer in the process of writing algorithmic music. Essentially, the composer can make crucial decisions at various stages of the composition. For some interactive systems, composers make subjective judgment calls and guide algorithms. In other cases, composers will tweak systems several times before getting the musical material they need. And, whether the composer is “fudging” the output of a system or perturbing a steady state, composers will interfere and introduce error into the output of an algorithmic system. The resulting complexity of these composers’ works, especially the musicality of them, makes the case for composer intervention.

3.2. Complexity of mapping

The second, obvious attribute contributing to the success or failure of a work is the complexity of the mapping of the system or data output to the musical parameters. To accurately measure complexity is to pursue a study beyond the scope of this paper. Additionally, most composers do not publish their processes to the degree to which it would be necessary to quantify the complexity of their individual mapping. However, by looking at common student practices compared to those of established composers, the extreme ends of the spectrum can be identified.

Students learning the practice of algorithmic composition must learn a variety of skills relevant to the multi-disciplinary field. For example, they may need to learn the mathematics behind a particular equation or iterated function. They may then need to learn computer science skills that enable them to realize the mathematics in an environment that can lead to music or sound production. Finally, they must learn the art of composing and music-making, which is inherently a critical and subjective domain learned and advanced only by continual practice. To some degree, it is this last aspect that students cannot learn quickly, though some may have better natural instincts than others. Therefore, it is this final objective that students fail to realize in their short careers as students. As a result, student works in the algorithmic domain may show advanced understanding of scientific or mathematical systems and may exhibit sophisticated implementation of the systems in programming environments. Yet, students tend to fail dramatically in making music from these skills.

The fundamental difference between the student work and the established composer is the way the algorithms are translated into music. A student does not have the experience or depth of musical understanding to do much more than the most straightforward mapping of data to sound. For example, a two-dimensional system may be very simply translated into pitch and duration values, or pitch and instrument assignment.

Unfortunately, the use of MIDI led many early algorithmic composers to realize their ideas in this simple way. The resulting works have a primitive

Hagan, K. L.

quality and quickly lose any interest or novelty. In some cases, the mapping of output to musical parameter was so simple and the music was so automatic, that the results would be more accurately described as auditory display.

The fundamental problem with this note-based approach to algorithmic composition is that it is inherently simple. Despite the complexity of the stochastic or chaotic system, the output is directly mapped to obvious musical qualities, making the reception unchallenging and less engaging. Though the systems exhibit compelling qualities, the results fall flat when translated to the temporal domain in the form of sound.

More seasoned composers searched for a way to complicate the relationship of the systems to output. For example, Bidlack [2] utilized a note-based approach to algorithmic composition realized in MIDI. In order to complicate the mapping while working within the same constraints, Bidlack implemented multi-dimensional systems (Lorenz and Hénon-Heiles) so that the third and fourth dimensions could be utilized for duration and loudness in addition to pitch. Additionally, it appears that Bidlack chose timbres without recourse to a deterministic system, an example of composer intervention.

However, even more successful works exhibited a complexity of mapping to the degree that any sign of the original algorithm is hidden beneath the immediacy of musical material. The listener hears music, not an algorithm. Complex patterns may emerge or dissipate, but they seemingly follow an internal musicality, not deterministic rules.

One example, *Olivine Trees* (1994) by Eduardo Miranda, demonstrates that complexity of the application of the algorithm can be manufactured not simply by the number of dimensions or parameters the algorithm controls, but by the time scale on which it is controlled. Miranda uses cellular automata to control grains of sound (reminiscent of the Xenakis example above). In his own description, Miranda likens the blending of these small grains to that of impressionistic painting [7]. The composer is inspired by the artistic potential of the system and reflects it in a sophisticated approach to implementation. In addition to CA, Miranda uses other processes and composers' tools to further influence the sound of the piece. In this sense, Miranda not only obfuscates his mapping, but he introduces a free reign of composerly intervention.

3.3. The Importance of Timbre

From the first works of electroacoustic music composition, timbre was the primary material of music. Pitch, rhythm, loudness, silence – these were the brushes, but timbre was the paint. The fascination with electroacoustic means of making music was the palette it provided.

As more composers began working with the new tools, new foci entered the domain of practice. As a result, later music relied less on timbre as its primary

Aesthetic Considerations in Algorithmic and Generative Composition

material. This was especially true for algorithmic composers whose primary material was the system or algorithm itself.

Yet, this attitude has been a detriment to the field of algorithmic composition. Timbre is an immediate attribute that anyone can perceive, regardless of his or her musical sophistication. It does not take a musical education to be aware of badly synthesized sounds, nor to grow fatigued with poor orchestration. Therefore, the most successful algorithmic compositions are examples of excellent instrumental or sound design choices.

It is difficult to address the timbre problem without addressing the human factor or the complexity question. Therefore, timbre can really be seen as a consequence of those aspects.

For example, if human intervention happens at the performance stage, i.e., live instrumentalists realize a work, then timbre is a consequence of the acoustic instruments. As a result, it has the richness, variety, and familiarity these instruments have in the culture. Likewise, if the mapping of a system is to the microsound level or to sound synthesis, then the complexity and interest of the system used is mapped into timbre, resulting in rich and interesting sounds.

However, since timbre is the immediate attribute first perceived in a work, it warrants separate consideration. Recognizable timbres can improve or ruin a work. In the case of works by Lejaren Hiller, notably the *Quartet No. 6 for Strings* (1973), the natural instrument timbres performed by live humans create music that stands on its own, regardless of its algorithmic roots. Hiller augments his timbral possibilities with the extended playing techniques developed in the 20th century. In comparison, much more algorithmically complex works that were realized with MIDI and commercial synthesizers now sound dated and awkward.

In the earlier examples, both Xenakis and Miranda synthesize complex timbres through algorithmic processes applied to granular synthesis. However, there are many different ways in which algorithmic processes can enhance timbre. Chaos and stochastic systems have enhanced spectral (frequency domain) synthesis as well as physical modeling synthesis methods. These systems applied to acoustic science in this way are effective tools for sound design.

This aspect is an extension of the notion of complexity; an algorithm applied to the microsound of digital synthesis is rarely perceptible in its original form. Rather, algorithmic systems generate interesting and complex timbres in and of themselves, without immediate recognition.

Hagan, K. L.

4. Conclusion

Given a restricted domain of music that is made using algorithms and/or generative processes, it is possible to identify three aesthetic considerations common to the most successful works of the genre.

First, an algorithmic or generative system is rarely sufficient on its own. In the most enduring examples, the composers had significant input to the musical material, reserving some musical parameters for subjective judgment and development. Additionally, many influential composers intervened and modified their systems, either by perturbing them or by bending the outcomes.

Secondly, the systems used must be mapped complexly to musical parameters. Though it is not always the case, this usually means that the algorithms are not easily detected or identified.

Works that fail to reach these first two points, namely employ a lack of human intervention and simplistic mapping systems, create results similar to scientific, auditory display. Though informative in its own right and occasionally interesting sonically, this rarely withstands aesthetic scrutiny.

Thirdly, and intricately dependent on the first two points, the choice of timbre in an algorithmic work plays a significant and immediate role in the relative success of a work. Timbre is dependent on the first two points, because in one possible instantiation, acoustic instruments realize musical material generated by systems. In this case, human performative interpretation fundamentally changes the reception of a work. In some other cases, systems operated on the microsound level, the level of sound synthesis. This complex mapping of system to musical parameter often results in rich, varied, and interesting timbres. However, timbre can be the result of many other compositional decisions. And, its impact in the reception of a work is quite large. Therefore, it requires separate consideration.

Pieces that were used as examples include works by Iannis Xenakis, Lejaren Hiller, and Eduardo Reck Miranda, while the methodologies published by Rick Bidlack, Agostino Di Scipio, Christopher Ariza, and Michael Gogins supported these conclusions.

5. References

- [1] C. Ariza, Automata Bending: Applications of Dynamic Mutation and Dynamic Rules in Modular One-Dimensional Cellular Automata. *Computer Music Journal*, 31: 29-49, 2007.

Aesthetic Considerations in Algorithmic and Generative Composition

- [2] R. Bidlack, Chaotic Systems as Simple (But Complex) Compositional Algorithms. *Computer Music Journal*, 16: 22-47, 1992.
- [3] A. Di Scipio, On Different Approaches to Computer Music as Different Models of Compositional Design. *Perspectives of New Music*, 33: 360-402, 1995.
- [4] L. Goehr, *The Imaginary Museum of Musical Works: An Essay in the Philosophy of Music*. Oxford: Clarendon Press, 1992.
- [5] M. Gogins, Iterated Functions Systems Music. *Computer Music Journal*, 14: 40-48, 1991.
- [6] K. Hagan, *Genetic Analysis of Xenakis' Analogique B*, in *Electroacoustic Music Society*. 2005: Montreal, Canada.
- [7] E.R. Miranda and J.A. Biles, eds. *Evolutionary Computer Music*. 2007, Springer-Verlag: London.
- [8] I. Xenakis, *Formalized Music: Thought and Mathematics in Composition*. Revised ed. Harmonologia Series No. 6. Stuyvesant, NY: Pendragon Press, 1992.

Trends in Moving-Seasonal Time Series of Temperature and Precipitation Time Series in the Czech Republic

Karel Helman

Department of Statistics and Probability, University of Economics, Prague, Czech Republic
Department of Climatology, Czech Hydrometeorological Institute, Prague, Czech Republic
Email: helmank@vse.cz, karel.helman@chmi.cz

Abstract: This paper focuses on time series of the selected climatology elements measured in the Czech Republic territory. It represents a continuation of some previous author's works. The paper concentrates on the past developments. It aims to give a well-founded view on the seasonality development in selected time series. There are two main objectives of the paper. First, the construction of time series composed of moving-seasonal factors calculated from the input time series. Second, the calculation of trends included in the moving-seasonal time series.

Keywords: seasonality, trends, climatology, time series, Czech Republic

1 Introduction

The so-called moving-seasonal time series construction methodology of climatology time series in the Czech Republic was thoroughly described in Helman (2008). Here, only its main features are pointed out.

First, we have to distinguish between input time series and derived time series. The input time series are represented by monthly time series of average temperatures (in degrees Celsius) and precipitation amounts (in millimetres) from 44 measurement stations in the Czech Republic (i.e. 88 time series altogether) in the period between 1961 and 2008. The detailed description of measurement stations geography can be found in Helman (2009). The elevation of the selected measurement stations ranges from 158 metres above sea level (Doksany station) to 1322 metres above sea level (Lysá hora station). The southernmost station is that of Lednice (48°47'34"), the northernmost station is Bedřichov (50°48'54"). The Czech Republic "far west" region is represented by the station in the town of Aš (12°10'47") and the easternmost station is located at Lysá hora (18°26'52"). The input data were gained from the database of the Czech Hydrometeorological Institute CLIDATA. Other valuable information about this rich source of data, as well as additional references to resources in English, can be found e.g. in Helman (2006).

Employing a combination of standard statistical methods, we use these input time series for the construction of derived time series that we call "moving-seasonal"

time series. At the final stage of this work we analyse possible statistical significance of linear trends included in the moving-seasonal time series.

2 The Construction of Moving-Seasonal Time Series: Methodology

The first step is splitting the input time series into a certain number of parts. The main objective is to decide how to set up the combination of the length of the moving interval (part) in years (*LMI*) with the size of the movement in years (*SM*). For example, the selection of *LMI* = 5 and *SM* = 3 will split the time series beginning in the year 1775 into a sequence of the following time series: 1775–1779, 1778–1782, 1781–1785, etc. Reasons for the combination set-up of *LMI* = 10 and *SM* = 1 consistent with this work were given in Helman (2009).

The second step is the calculation of seasonal factors for each calendar month (twelve readings) for each particular time interval defined by *LMI* and *SM*. This calculation is done on the assumption of the additive decomposition of the time series analysed, which can be generally expressed as:

$$y_t = T_t + S_t + C_t + \varepsilon_t,$$

where y_t is the value of an indicator that is to be modelled in time t , T_t is a trend component, S_t is a seasonal component, C_t is a cycle component and ε_t is a random (error) component. For more precise description, see again Helman (2008), where an explanation of presuming additive instead of multiplicative decomposition can also be found. Average seasonal factors are given by the equation

$$\bar{s}_j = \frac{1}{m} \sum_{i=1}^m (y_{ij} - T_{ij}), \quad j = 1, 2, \dots, r,$$

where i indicates an ordinal number of years, m is the number of years, j represents the sequence of particular periods within a year, r is the number of partial periods within a year ($r = 12$ for monthly time series), y_{ij} is the value of input time series and T_{ij} quantities are an estimate of the trend component (most often obtained by an application of moving averages). These average seasonal factors do not meet the requirement that their total within each year equals zero – we will adjust them by proper standardization:

$$\hat{s}_j = \bar{s}_j - \frac{\sum_{k=1}^r \bar{s}_k}{r}.$$

For the sake of simplicity, we will call these values “seasonal factors”. These seasonal factors can be interpreted in the same units as the values in the analyzed time series.

The third and the last step in constructing the moving-seasonal time series consists in selecting seasonal factor values from each time interval for each particular

calendar month, twelve moving-seasonal time series arising for every measurement station.

3 The Construction of Moving-Seasonal Time Series: Results

1056 moving-seasonal time series in total (44 measurement stations, 12 months and two climatology elements) were constructed for analytical purposes. Furthermore, many graphs on the basis of two criteria were drawn, the following two criteria having been applied:

- 1) a comparison of seasonality developments according to the measurement stations' location ("spatial comparison" based on the branch offices of the Czech Hydrometeorological Institute that can be found at portal.chmi.cz¹); 168 graphs (12 calendar months, seven branch offices, two climatology elements);
- 2) a comparison of seasonality developments according to the measurement stations elevation ("elevation comparison"); 192 graphs (12 calendar months, eight² groups of the measurement stations, two climatology elements).

As an example of these graphs, see Figures 1 and 2 (some comments will be given below).

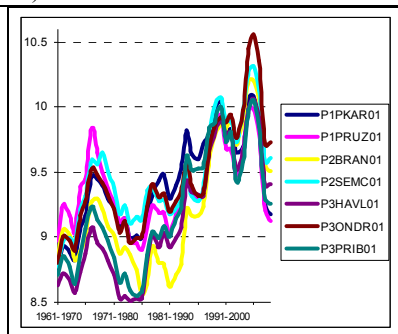


Fig. 1. Moving-seasonal time series, Praha branch office (P),

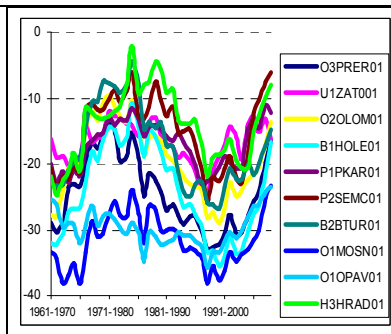


Fig. 2. Moving-seasonal time series, elevation 200-299,

¹ http://portalh.chmi.cz/http://portal.chmi.cz/portal/dt?menu=JSPTabContainer/P5_0_O_nas&last=false

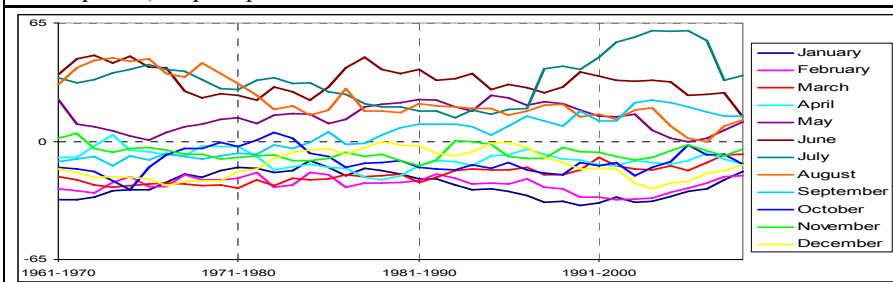
² Elevation below 200 metres (3 stations), 200-299 m (10), 300-399 m (7), 400-499 m (10), 500-599 m (3), 600-699 m (3), 700-799 m (5) and above 800 m (3).

temperature, August

precipitation, January

To understand properly the information involved in the moving-seasonal time series, it is necessary to bear in mind that these time series represent only the development of the seasonal component. This means that they tell us nothing at all about the other components and they may be used, for instance, as a supplement to the trend analysis. It is also important to remember that each single value of the moving-seasonal time series refers to a ten-year period of time, so it is rather contentious to speak about random fluctuations when analysing these particular series (their values should be considered as somehow “solid”).

All 12 moving-seasonal time series corresponding to 12 months for precipitation measured at Holešov station can be seen in Figure 3. In order to read this graph properly it is important to become aware of the fact that a total of these 12 time series for each time period (i.e. in each point on the x -axis) is zero (seasonal factors within each ten-year period counteract their mutual effects). It has also to be considered whether a particular moving-seasonal time series (a period/month in this case) is above or below zero on the y -axis. The value of a moving-seasonal time series equalling zero (on the y -axis) indicates that a corresponding calendar month was about the average among other months in a certain period of time (x -axis). In this sense of the word, it is shown in Figure 3 that June, August, July and May were the above-average months in the period between 1961 and 2008. The below-average months were December, March, February and January³. The remaining months – November, April, September and October (having crossed the zero-line on the y -axis) can perhaps be marked as the average months (strictly speaking, they were above-average in some phases of the whole 1961 – 2008 period and below-average in others). Noteworthy developments can be seen, for example, in the September series: at the beginning of the 1961 – 2008 period, September was the 6th driest month, at the end, however, it became the 2nd wettest month. Again, this is valid only in comparison with other months (time periods in particular) and shows nothing about absolute value (nor its development) of precipitation measured.



³ January not for the complete period 1961 – 2008.

Fig. 3. Moving-seasonal time series, precipitation, Holešov

Trends in moving-seasonal time series will be dealt with below. It is clear now that the positive trend in above-average months shows strengthening of the seasonal component on the one hand, and the positive trend in below-average months, on the other hand, testifies to the seasonal component's weakening. Alternatively, the negative trend in above-average months shows the seasonal component's weakening. The seasonal component strengthens, on the contrary, when it appears in below-average months.

Thus, in Figure 1, for example, we can see the positive (linear) trend of temperatures (Praha branch office) in August. This is an above-average month (positive values on the y -axis) which – together with the positive trend – indicates strengthening of the seasonal component in average monthly temperatures time series. In Figure 2, neither positive nor negative (linear) trend can be seen. In addition, there is another type of trend (an oscillation wave) observable in all the measurement stations.

4 Trends in Moving-Seasonal Time Series: Temperature

Table 1 shows the statistics of linear trends in temperature moving-seasonal time series. Before we make some comments on the findings, we will summarize the basic facts once again:

- 1) in this work, the period between 1961 and 2008 is being analysed,
- 2) moving-seasonal time series reflect development trends in the input time series seasonal component, and thus the trends in moving-seasonal time series show nothing about those in input time series,
- 3) the negative/positive linear trend in above-average months denotes an opposite effect on the negative/positive linear trend in below-average months.

Table 1. Trends in moving-seasonal time series, temperature

SMTDA 2010: Stochastic Modeling Techniques and Data Analysis
 International Conference, Chania, Crete, Greece, 8 - 11 June 2010

Trends in moving-seasonal time series for temperature	Below-average months			Above-average months		
	December	January	February	June	July	August
number of significant linear trends $\alpha = 5\%$	18	18	1	5	19	44
number of significant linear trends $\alpha = 10\%$	22	25	5	9	24	44
number of positive directions	4	44	23	25	33	44
number of negative directions	40	0	21	19	11	0
Average directions according to elevation (metres above sea level)						
<200 (3 stations)	-0.021	0.026	-0.003	-0.001	0.006	0.027
200-299 (10 stations)	-0.023	0.017	0.002	-0.003	0.012	0.030
300-399 (7 stations)	-0.015	0.021	0.005	-0.004	0.006	0.025
400-499 (10 stations)	-0.014	0.017	-0.003	-0.001	0.004	0.025
500-599 (3 stations)	-0.030	0.014	-0.008	0.001	0.014	0.036
600-699 (3 stations)	-0.011	0.018	0.003	-0.006	0.005	0.024
700-799 (5 stations)	-0.019	0.014	0.003	-0.003	0.004	0.030
>800 (3 stations)	-0.001	0.019	0.008	-0.003	0.007	0.032
Average directions according to location (branch offices from the east to the west)						
Ostrava (O, 9 stations)	-0.022	0.018	0.000	0.000	0.019	0.032
Brno (B, 8 stations)	-0.028	0.013	-0.003	0.003	0.012	0.037
Hradec Králové (H, 3 stations)	-0.022	0.015	-0.002	0.002	0.009	0.031
Praha (P, 7 stations)	-0.015	0.022	0.001	-0.004	0.003	0.027
České Budějovice (C, 4 stations)	-0.005	0.014	0.003	-0.002	0.000	0.025
Ústí nad Labem (U, 6 stations)	-0.013	0.026	0.003	-0.010	0.002	0.023
Pižetň (L, 7 stations)	-0.010	0.015	0.006	-0.005	-0.003	0.020

Three above-average (warm) months and three below-average (cold) months were selected. Unambiguous results were obtained in August; all 44 moving-seasonal time series contained statistically significant positive trends. This means that August was getting warmer (in comparison with other months within each year) during the monitored period. Moreover, this effect seems to be a little stronger in the east of the Czech Republic than in the west.

January statistics represent other conclusive results as all 44 time series showed positive linear trends but only 25 were statistically significant at $\alpha = 10\%$. Still, we can say that January tended to be less below-average in the course of time. Nevertheless, neither the connection with elevation nor with a location was found.

No conclusions⁴ for February and June can be made; only a few statistically significant linear trends were found and the distribution of positive and negative trends is almost even.

No relationship between linear trends in temperature moving-seasonal time series and the elevation of measurement stations can be detected either.

The analysis of temperature moving-seasonal time series with linear trends leads us to the following conclusion. The monthly seasonality (year cycle) of average temperature time series changed in the period 1961 – 2008. According to the research findings, the extent of this change is affected by the location (east

⁴ Collective for all measurement stations.

vs. west) of particular measurement stations. (Further follow-up analysis is, however, necessary.)

5 Trends in Moving-Seasonal Time Series: Precipitation

Table 2 shows the statistics of linear trends in precipitation moving-seasonal time series. The structure of this table is almost the same as that of Table 1. The only difference is that March (instead of December) was chosen as a representative of below-average months.

Table 2. Trends in moving-seasonal time series, precipitation

Trends in moving-seasonal time series for precipitation	Below-average months			Above-average months		
	January	February	March	June	July	August
number of significant linear trends $\alpha = 5\%$	11	23	44	31	28	31
number of significant linear trends $\alpha = 10\%$	15	27	44	32	28	32
number of positive directions	21	24	44	5	39	10
number of negative directions	23	20	0	39	5	34
Average directions according to elevation (metres above sea level)						
<200 (3 stations)	-0.087	-0.045	0.194	-0.123	0.622	-0.045
200-299 (10 stations)	-0.058	-0.071	0.261	-0.239	0.378	-0.542
300-399 (7 stations)	0.048	0.041	0.435	-0.408	0.343	-0.230
400-499 (10 stations)	-0.009	0.022	0.334	-0.125	0.423	-0.151
500-599 (3 stations)	-0.114	-0.039	0.468	-0.443	0.523	-0.139
600-699 (3 stations)	0.163	0.210	0.756	-0.547	0.480	-0.258
700-799 (5 stations)	0.010	0.070	0.584	-0.354	0.470	-0.417
>800 (3 stations)	0.032	0.276	0.699	-0.747	0.248	-0.869
Average directions according to location (branch offices from the east to the west)						
Ostrava (O, 9 stations)	-0.035	0.014	0.464	-0.429	0.056	-0.822
Brno (B, 8 stations)	-0.196	-0.203	0.319	-0.284	0.369	-0.155
Hradec Králové (H, 3 stations)	0.007	0.090	0.573	-0.450	0.873	-0.590
Praha (P, 7 stations)	-0.056	0.099	0.310	-0.256	0.724	-0.195
České Budějovice (C, 4 stations)	0.101	0.100	0.610	-0.591	0.338	0.071
Ústí nad Labem (U, 6 stations)	0.114	0.191	0.457	-0.315	0.609	-0.176
Píseň (L, 7 stations)	0.126	0.048	0.354	-0.043	0.320	-0.286

Unambiguous results in the area of precipitation moving-seasonal time series were obtained in the March series. Distinctive, statistically significant positive linear trends in all forty-four moving-seasonal time series were detected. This shows that monthly precipitation sums in March were becoming less below-average in comparison with other months in each year during the period 1961 – 2008. This trend tends to be a little stronger for higher elevations.

Convincing results were achieved in June measurements as well. 31 linear trends were statistically significant at 5% level and 39 linear trends were negative. This can be interpreted as weakening of the seasonal component (i.e. decrease in monthly precipitation sums in comparison with other months) in June in each year throughout the period. If we presumed hypothetically that no change in the seasonal component during the remaining ten months would take place (it is

impossible, though; see Table 2), this change in June moving-seasonal time series would correspond to the change in March moving-seasonal time series. The June results again tend to be more distinctive with rising elevation.

No conclusions can be drawn from the development of the seasonal component in January and February as only a small number of statistically significant trends were detected, negative and positive trends being almost evenly distributed.

No relationship between linear trends in precipitation moving-seasonal time series and the location of measurement stations can be seen either.

The analysis of precipitation moving-seasonal time series with linear trends leads us to the following conclusion. The monthly seasonality (year cycle) of precipitation sums time series changed in the period 1961 – 2008. According to the research findings, the extent of this change is affected by the elevation of particular measurement stations. (Further follow-up analysis is, however, necessary.)

6 Conclusions

Average monthly temperatures and precipitation sums time series for the period 1961 – 2008 taken from 44 measurement stations in the Czech Republic were used as the input time series for the construction of moving-seasonal time series. A total of 1056 moving-seasonal time series were constructed. Having divided them according to two criteria – the elevation (eight groups) and location of measurement stations (seven groups), 360 graphs were made.

Linear trends for the constructed moving-seasonal time series were calculated, giving some interesting results.

The end results for temperature moving-seasonal time series are as follows. The monthly seasonality (year cycle) of average monthly temperatures time series changed considerably in the period 1961 – 2008 (a lot of statistically significant linear trends were found). Among the months presented here, the most distinctive changes were recorded in January and August. Some facts, proving that the extent of this change was affected by the location (east vs. west) of measuring stations, were also found.

A relevant conclusion also follows from the analysis of precipitation moving-seasonal time series. The monthly seasonality (year cycle) of precipitation sums time series changed in the period 1961 – 2008 as well. Among the months presented in this work, the most distinctive changes were identified in March and June. Some data, showing that the extent of this change was affected by the elevation of measuring stations, were also found.

This paper was supported by the grant project of Internal Grant Agency of the University of Economics, Prague, No. F4/21/2010.

References

1. Helman, K., Analysis of seasonality in selected climatology element time series in the Czech Republic. Wrocław 15.09.2008 – 18.09.2008. In: *Quality of Life Improvement through Social Cohesion*. Wrocław: Department of Statistics, 43–65 (2008).
2. Helman, K., Analýza vývoje sezónnosti vybraných srážkových časových řad v České republice pro období 1961 - 2008. Praha 17.09.2009 - 18.09.2009. In: *Mezinárodní statisticko-ekonomické dny na VŠE [CD-ROM]*. Praha (2009).
3. Helman, K., Analýza meteorologických časových řad s využitím databáze ČHMÚ CLIDATA. Praha 23.02.2006. In: *Sborník prací účastníků vědeckého semináře doktorandského studia Fakulty informatiky a statistiky VŠE v Praze*. Praha : Oeconomica, 158–166 (2006).

A semi-Markov regime switching extension of the Vasicek model

Julien S. Hunt¹ and Pierre Devolder²

¹ Université Catholique de Louvain, Institut de statistique, Voie du roman pays 20, B-1348 Louvain-La-Neuve (e-Mail: julien.hunt@uclouvain.be)

² Université Catholique de Louvain, Institut des sciences actuarielles, Voie du roman pays 20, B-1348 Louvain-La-Neuve (e-Mail: pierre.devolder@uclouvain.be)

Abstract. We briefly recall some essential notions on interest rates and zero-coupon bonds. We then define a sound mathematical framework to study a model of the short rate in which the parameters are allowed to vary according to an underlying semi-Markov process. We give some properties of the short rate in our model. We follow by studying the notion of risk-neutral martingale measures in this context. Finally, we discuss the pricing of interest-rate derivatives. In particular, we show that the price of a zero-coupon bond has to satisfy a system of integro-differential equations that is influenced both by the market price of risk and by the market price of regime switch risk.

Keywords: Semi-Markov, Regime-switching, Vasicek model, Interest rates, Marked point processes, Semimartingales, Martingale measures, Integro-PDE.

1 Introduction

Modelling the uncertainty about the future behavior of interest rates has become a very active topic of research. Some classical continuous-time models include the Vasicek model (see Vasicek [15]), the Hull and White model (see Hull and White [8]) or the CIR model (See Cox *et al.* [2]).

Regime switching models of interest rates have gained some interest in the literature. The idea is to model the fact that the economic environment is not constant through time and that this should be reflected in the model via a change of the value of the parameters. Some papers that deal with this are Landén [11] and Wu and Zeng [16].

Most of the existing literature focuses on homogeneous Markov switching models. However, many authors have shown that markets exhibit some characteristics that are not well captured by homogeneous Markov switching models (let us cite Hong and Li [7], Easley and O'Hara [5] and [6], Diebold and Rudebusch [3] and Durland and McCurdy [4]). An interesting extension that better fits the data is the class of semi-Markov regime switching models. These are flexible and more general than homogeneous Markov models. Our

paper deals with such a model, specifically a semi-Markov switching extension of the Vasicek model of the short rate of interest. The aim is to provide a sound mathematical framework for this model and to derive equations that allow to price interest-rate derivatives in this framework.

2 Basic notation

We consider a financial market defined on a probability space $(\Omega, \mathcal{F}, \mathbb{P})$ carrying a filtration \mathcal{F}_t and a brownian motion W . We suppose that it is defined for all times $t \in [0, T]$.

We recall some notions about interest rate theory (see Björk [1] for more on this subject).

Definition 1. A zero coupon bond with maturity T (also called a T-bond) is a contract which guarantees the holder a payment of one unit of currency at time T . We denote by $p(t, T)$ the price of a T-bond a time t . We suppose that $p(t, T)$ is a strictly positive adapted process for all $t \in [0, T]$.

Definition 2. The instantaneous forward rate with maturity T contracted at t is defined by

$$f(t, T) = -\frac{\partial \log p(t, T)}{\partial T}$$

Definition 3. The instantaneous short rate at time t is defined by

$$r(t) = f(t, t)$$

Our paper will provide a model for the evolution of the short rate r_t . For the moment, we simply assume that r_t is adapted to the filtration \mathcal{F}_t . Given the short rate, the money account process or risk free asset (that will serve as numeraire) is defined by

$$B_t = \exp \left\{ \int_0^t r(s) ds \right\}$$

This allows us to introduce risk neutral martingale measures that will be useful in the pricing of interest rate derivatives.

Definition 4. A risk neutral martingale measure will be a measure \mathbb{P}^* equivalent to \mathbb{P} and such that for every T , the quantity

$$\frac{p(t, T)}{B_t}$$

is a \mathbb{P}^* -martingale.

3 Semi-Markov regime switching model

We define the set $E \subset \mathbb{R}$ by $E = \{1, \dots, m\}$ for a fixed $m \in \mathbb{N}$ and we define \mathcal{E} as the sigma-algebra of all the parts of E .

For each $n \in \mathbb{N}$, let (X_n, T_n) be a pair of random variables taking values in $E \times \mathbb{R}^+$. We suppose that the process $(X, T) = \{X_n, T_n; n \geq 0\}$ is a homogeneous Markov renewal process with state space E . The associated semi-Markov kernel is denoted by $Q_{ij}(t)$. We denote by P the transition matrix of the embedded Markov chain.

Remark 1. Given the number of states is finite, the number of jumps in a finite time interval is almost surely finite (for a proof see Pyke [13]).

We impose some regularity conditions on the Markov renewal process:

- No fictitious transitions are allowed i.e. $P_{ii} = 0$.
- No instantaneous transitions are allowed i.e. $Q_{ij}(0) = 0$.
- All states in E "communicate" at all times i.e. $Q_{ij}(t) > 0, \forall t > 0$.

Definition 5. Let us define s_t by

$$s_t := \sup(n \geq 0 : T_n \leq t)$$

with $n \in \mathbb{N}$ and $t \in \mathbb{R}^+$ and Y_t as

$$Y_t := X_{s_t}$$

Process Y is called a semi-Markov process with kernel Q .

Definition 6. We define \mathcal{F}_t as the completed filtration generated by process Y_t and W_t i.e., $\mathcal{F}_t = \sigma(Y_s, W_s, N, N \in \mathcal{N}, s \leq t)$ where \mathcal{N} is the collection of all null sets.

The aim is to use Y with the usual tools of stochastic calculus. A step in that direction is made with the following result.

Lemma 1. Y_t is a semimartingale.

Proof. It is easy to show that Y is an adapted càdlàg finite variation process.

We denote the set of all possible jumps of Y by Z i.e. $Z = \{z_{ij} = i - j; i, j \in E, i \neq j\}$. Given there are m states, the set Z comprises $m(m - 1)$

elements. Let Z_n denote the size of the n^{th} jump of Y . The jump measure of Y is the random integer-valued measure μ on $(0, \infty) \times Z$ defined by

$$\mu = \sum_{n=1}^{\infty} \mathbb{1}_{(T_n, Z_n)}$$

We can write

$$Y_t = Y_0 + \int_0^t \int_Z z \mu(ds, dz)$$

This can be written as

$$Y_t = Y_0 + \sum_{z_{ij} \in Z} z_{ij} N_t(z_{ij})$$

where

$$N_t(z_{ij}) = \sum_{n \geq 1} \mathbb{1}_{\{T_n \leq t\}} \mathbb{1}_{\{Z_n = z_{ij}\}}$$

Proposition 1. *The \mathbb{P} -compensator associated with the jump measure μ is given by*

$$\nu(ds, \{z_{ij}\}) = \lambda_s(z_{ij}) ds \quad (1)$$

where the intensity $\lambda_s(z_{ij})$ is defined as

$$\lambda_s(z_{ij}) = \sum_{n \geq 0} \mathbb{1}_{\{T_n < s \leq T_{n+1}\}} \frac{P_{j,i} g(j, i, t - T_n)}{1 - \sum_{i \neq j} Q_{j,i}(t - T_n)} \mathbb{1}_{\{X_n = j\}}$$

where $g(j, i, t - T_n)$ is the density of the waiting time distribution between state j and i calculated at time $t - T_n$.

Proof. This follows from the general theory of marked point processes and properties of semi-Markov processes (for more details see [12]).

Remark 2. It follows that the intensity associated with process $N_t(z_{ij})$ is simply $\lambda_t(z_{ij})$.

We introduce the backward recurrence time K_t . This process represents the time continuously spent in a state since the last regime switch. We can write

$$K_t = t - T_{N_t(Z)} = t - \sum_{z_{ij} \in Z} \int_0^t K_{s-} dN_s(z_{ij})$$

We now turn to our model of the short rate. Under \mathbb{P} , the short rate is supposed to have the following dynamics:

$$dr_t = (a(Y_t) - b(Y_t)r_t)dt + \sigma(Y_t)dW_t \quad (2)$$

where we define $a(Y_t)$, $b(Y_t)$ and $\sigma(Y_t)$ by

$$\begin{aligned} a(Y_t) &= \sum_{i=1}^m a_i \mathbb{1}_{\{Y_t=i\}} \\ b(Y_t) &= \sum_{i=1}^m b_i \mathbb{1}_{\{Y_t=i\}} \\ \sigma(Y_t) &= \sum_{i=1}^m \sigma_i \mathbb{1}_{\{Y_t=i\}} \end{aligned}$$

for some given constants (a_1, \dots, a_m) , (b_1, \dots, b_m) and $(\sigma_1, \dots, \sigma_m)$ (all the σ_i 's are strictly positive).

Proposition 2. *Equation 2 is well defined.*

Proof. The proof is exactly similar to that in Hunt [9], proposition 3.

Remark 3. Equation 2 is an extension of the well-known Vasicek model (see Vasicek [15]) where we allow for the parameters of the model to switch between different states and the switching is controlled by a semi-Markov process Y .

In the classical Vasicek model, r_t is a mean-reverting process. In our setting, we have

Proposition 3. *For $T_n \leq t < T_{n+1}$, $r_t | \mathcal{F}_{T_n} \sim N(\mu, \sigma^2)$ where*

$$\begin{aligned} \mu &= r_{T_n} e^{-b(Y_{T_n})(t-T_n)} + \frac{a(Y_{T_n})}{b(Y_{T_n})} (1 - e^{-b(Y_{T_n})(t-T_n)}) \\ \sigma^2 &= \frac{\sigma^2(Y_{T_n})}{2b(Y_{T_n})} (1 - e^{-2b(Y_{T_n})(t-T_n)}) \end{aligned}$$

Proof. This is a direct application of Itô's formula and of the properties of semi-Markov processes.

Remark 4. Proposition 3 tells us that for $T_n \leq t < T_{n+1}$, r_t starts in r_{T_n} but moves away from this value as time goes by and that the process tends to locally mean revert around value $\frac{a(Y_{T_n})}{b(Y_{T_n})}$ until the next jump.

4 Martingale measures and derivative pricing

Let N_t represent the multivariate point process ($m(m-1)$ -dimensional) whose components are given by $(N_t(z_{ij}))_{z_{ij} \in Z}$. Let λ_t be the multivariate intensity associated to process N_t whose components are given by $(\lambda_t(z_{ij}))_{z_{ij} \in Z}$.

We discuss the existence of risk neutral measures by following this version of the Girsanov theorem.

Theorem 1. *Let θ be a progressively measurable process such that*

$$\int_0^t \theta_s^2 ds < \infty$$

Consider the multivariate point process N_t previously defined with $(\mathbb{P}, \mathcal{F}_t)$ -intensity λ_t . Consider a predictable multivariate process $(\psi_t(z_{ij}))_{z_{ij} \in Z}$ such that \mathbb{P} -a.s. and for $t \in [0, T]$

$$\sum_{z_{ij} \in Z} \int_0^t \psi_s(z_{ij}) \lambda_s(z_{ij}) ds < \infty$$

Define the process L by:

$$L_t = \exp \left\{ -\frac{1}{2} \int_0^t \theta_s^2 ds + \int_0^t \theta_s dW_s \right\} \prod_{z_{ij} \in Z} \left[\exp \left\{ \int_0^t (1 - \psi_s(z_{ij})) \lambda_s(z_{ij}) ds \right\} \prod_{n=1}^{N_t(z_{ij})} \psi_{T_n}(z_{ij}) \right]$$

And suppose that for all finite t :

$$\mathbb{E}^{\mathbb{P}}[L_t] = 1$$

Define a probability measure \mathbb{Q} on \mathcal{F} by

$$d\mathbb{Q} = L_t d\mathbb{P}$$

Then, every measure \mathbb{Q} equivalent to \mathbb{P} has the structure above. Furthermore, let $W_t^{\mathbb{Q}}$ be defined as

$$dW_t^{\mathbb{Q}} = dW_t - \theta_t dt$$

then $W_t^{\mathbb{Q}}$ is a \mathbb{Q} -brownian motion. We denote by $N_t^{\mathbb{Q}}$ the multivariate point process N_t whose \mathbb{Q} -intensity given by $\lambda_t^{\mathbb{Q}}(z_{ij}) := (\psi_t(z_{ij}) \lambda_t(z_{ij}))_{z_{ij} \in Z}$.

Proof. For a proof see [10].

It follows from theorem 1 that under any risk neutral measure \mathbb{Q} , we have the following dynamics for processes r_t , Y_t and K_t :

$$\begin{aligned} dr_t &= (a(Y_t) + \theta_t \sigma(Y_t) - b(Y_t) r_t) dt + \sigma(Y_t) dW_t^{\mathbb{Q}} & (3) \\ Y_t &= Y_0 + \sum_{z_{ij} \in Z} z_{ij} N_t^{\mathbb{Q}}(z_{ij}) \\ K_t &= t - \sum_{z_{ij} \in Z} \int_0^t K_{s-} dN_s^{\mathbb{Q}}(z_{ij}) \end{aligned}$$

Specifying a risk neutral measure requires the knowledge of θ , the market price of risk but also the $m(m-1)$ other parameters i.e. the $\psi_t(z_{ij})$'s. These represent the market price of regime switch risks for jumps from state j to state i .

Remark 5. It is clear from equation 3 and proposition 3 that the distribution of $r_t|\mathcal{F}_{T_n}$ under \mathbb{Q} is the same as that in proposition 3 with $a(Y_{T_n})$ replaced by $a(Y_{T_n}) + \theta_{T_n} \sigma(Y_{T_n})$.

Suppose a measure \mathbb{Q} has been chosen. As far as pricing is concerned, it is well known that the price P_t at time t of a contingent claim whose payoff is given by an \mathcal{F}_T measurable square integrable random variable H is given by

$$P_t = \mathbb{E}^{\mathbb{Q}}[e^{-\int_t^T r_s ds} H | \mathcal{F}_t] \tag{4}$$

Remark 6. Equation 4 implies that we treat Y_t as an observable variable as argued in Silvestrov and Stenberg [14].

The process (r_t, Y_t) does not -in general- satisfy the Markov property but process (r_t, Y_t, K_t) does and so we can write:

$$P_t = \mathbb{E}^{\mathbb{Q}}[e^{-\int_t^T r_s ds} H | r_t, Y_t, K_t]$$

In particular the price of a zero-coupon T -bond is given by

$$P_t = \mathbb{E}^{\mathbb{Q}}[e^{-\int_t^T r_s ds} | r_t, Y_t, K_t] = f(t, r, y, k)$$

This leads to the following result

Theorem 2. *The price $f(t, r, y, k)$ of a zero-coupon bond is given by the solution to the following system of integro-differential equations (one for each possible state i)*

$$r f = \mathcal{L}f + \mathcal{S}f \quad \forall (t, r, k) \in [0, T] \times \mathbb{R}_0^+ \times \mathbb{R}_0^+$$

where (with the subscript on f indicating the partial derivatives)

$$\begin{aligned} \mathcal{L}f &= f_t(t, r, i, k) + f_k(t, r, i, k) + (a(i) + \theta\sigma(i) - b(i)r)f_r(t, r, i, k) + \frac{1}{2}f_{rr}(t, r, i, k)\sigma^2(i) \\ \mathcal{S}f &= \sum_{j \neq i} (f(t, r, j, 0) - f(t, r, i, k))\lambda_t^{\mathbb{Q}}(z_{ji}) \end{aligned}$$

with boundary condition:

$$f(T, r, i, k) = 1 \quad \forall i \in E \forall r, k \in \mathbb{R}_0^+$$

Proof. This follows from Feynman-Kac theory and the fact that (r_t, Y_t, K_t) is a Markov process.

Remark 7. In theorem 2, we clearly see the impact of the market price of risk and the market prices of regime switch risk on the price of a zero-coupon bond.

References

1. Björk T. ; *Arbitrage theory in continuous time*; Oxford university press, Oxford (1998).
2. Cox J.C., Ingersoll Jr.J.E., Ross S.A.; "A theory of the term structure of interest rates", *Econometrica*, 53: 385-408 (1985).
3. Diebold F., Rudebusch G.; "A nonparametric investigation of duration dependence in the American business cycle", *Journal of Political Economy*, 98: 596-616 (1990).
4. Durland J., McCurdy T.; "Duration dependent transitions in a Markov model of U.S. GNP growth", *Journal of Business and Economics Statistics*, 12: 279-288 (1994).
5. Easley D., O'Hara M.; "Price, trade size and information in securities markets", *Journal of Financial Economics*, 19: 69-90 (1987)
6. Easley D., O'Hara M.; "Time and the process of security price adjustment", *Journal of Finance*, 47: 577-605 (1992).
7. Hong Y., Li H.; "Nonparametric specification testing for continuous-time models with applications to term structure of interest rates", *Review of Financial Studies*, 18: 37-84 (2005).
8. Hull J., White A.; "Pricing interest-rate derivative securities", *Review of Financial Studies*, 3: 573-592 (1990).
9. Hunt J.S.; "Equivalent local martingale measures and market incompleteness in a continuous-time semi-Markov regime switching model", *Discussion paper, Institute of statistics, Université Catholique de Louvain*, DP 0924 (2009).
10. Jacod J., Shiryaev A.N.; *Limit theorems for stochastic processes*, Springer-Verlag, Berlin (1987).
11. Landén C.; "Bond pricing in a hidden Markov model of the short rate"; *Finance and Stochastics*, 4: 371-389 (2000).
12. Prigent J.-L.; "Option pricing with a general marked point process"; *Mathematics of Operations Research*, 26 (1): 50-66 (2001).
13. Pyke R.; "Markov renewal processes: definitions and preliminary properties"; *The Annals of Mathematical Statistics*, 32 (4): 1231-1242 (1961).
14. Silvestrov D., Stenberg F. ; "A pricing process with stochastic volatility controlled by a semi-Markov process"; *Communications in Statistics: theory and methods*, 33 (3): 591-608 (2004).
15. Vasicek O. ; "An equilibrium characterisation of the term-structure"; *Journal Of Financial Economics*, 5: 177-188 (1977).
16. Wu S., Zeng Y.; "The term structure of interest rates under regime shifts and jumps"; *Economics Letters*, 93: 215-221 (2006).